Copyright fib, all rights reserved. This PDF copy of fib Bulletin 24 is intended for use and/or distribution only by National Member Groups of fib.

3.3 Displacement-based procedures for seismic assessment

3.3.1 The displacement-based detailed assessment procedure in the New Zealand draft guidelines

3.3.1.1 Background and overview of displacement-based design, assessment and retrofit

Several recent studies (Moehle, 1992, Calvi and Pavese, 1995, Kowalsky *et al.*, 1995) have introduced the concept of 'displacement-based design' (DBD) as a logical and rational alternative to the currently used 'force-based design'. In this approach, a structure is designed for a target deformation criterion, whilst strength and stiffness become end-products of the design (or redesign) procedure. Since capacity design requires control on the deformational demand and supply at dissipative zones, it blends perfectly with displacement- (or, more generally, deformation-) based design. Such an approach to seismic design clearly requires a higher level of control over the local behaviour of members and their global effect on the seismic response of a structure.

A displacement-based assessment methodology has been proposed by Priestley (1995, 1997). It follows the procedure in the flow chart of Fig. 3-1. Strength in both flexure and shear, as well as inelastic rotation capacity are firstly evaluated. The strength is used to determine the base shear capacity (V_b) and failure mechanism. For the evaluation of the latter, Priestley & Calvi (1991) proposed a sway potential index S_p, based on the comparison of the flexural capacities of beams and columns at all joints at a given storey level. Rotation capacity in the expected plastic hinge of the members may be computed from moment-curvature analyses or simplified expressions in the literature and is used to determine the deformation capacity of the member. A check on the shear strength is required to assess the possibility of the development of a flexural failure mode; otherwise shear failure controls the deformation capacity of a member. The latter enables calculation of the storey drift capacity, which, together with the expected failure mechanism is used to evaluate the yield and ultimate displacement capacity of the structure (Δ_y and Δ_u) and its displacement ductility (μ_Δ). To this end, inelastic pushover analysis or more simple expressions in (Priestley, 1997) may be used.

To complete the assessment procedure, the displacement demand (Δ_d) needs to be determined. This is accomplished by considering the dynamic characteristics of the substitute system in terms of effective period and equivalent damping (e.g. Borzi *et al.*, 1998) and the displacement spectra (e.g. Bommer et al., 1998). The ratio Δ_u / Δ_d is then used to assess the seismic risk associated with the structure, as conceptually shown in Fig. 3-2. The annual probability of the displacement ratio being exceeded (p), considered as the true risk to the public (Priestley, 1997) is employed here. If the value of p is lower than the specified target value, the structure does not need retrofittig. Otherwise, structural intervention is required.

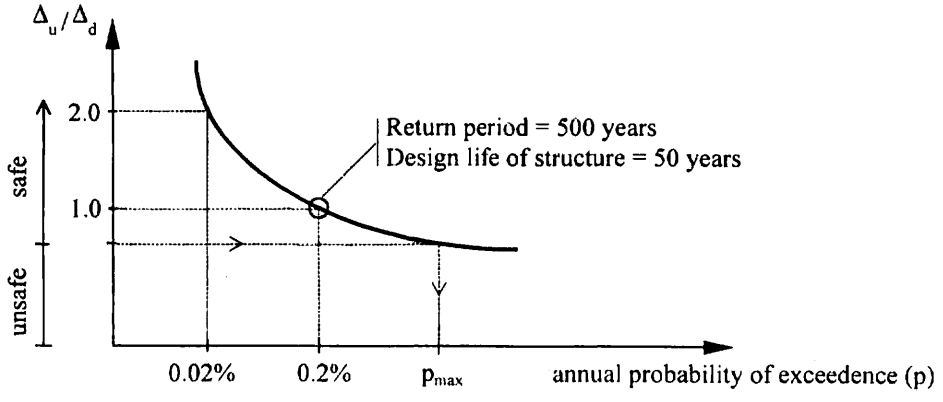

Fig. 3-2: Relationship between annual probability of exceedence and displacement ratio (from CEB, 1997)

The three parameters governing displacement-based design (DBD) and assessment according to Priestley (1995, 1997) are period, equivalent damping and global displacement. Period (T_{eff}) is the secant value at the target displacement; hence it becomes a function of the stiffness (herein defined as the secant stiffness at yield), strength and maximum displacement. The equivalent damping (ξ) is a function of the level of ductility, for it is mainly contributed to by hysteretic energy dissipation. If separate control of stiffness, strength and ductility is

Copyright fib, all rights reserved. This PDF copy of fib Bulletin 24 is intended for use and/or distribution only by National Member Groups of fib.

afforded to the designer (in a displacement-based assessment leading to strengthening redesign), then more than one solution to achieve the target DBD objective is availed of. Hence, selective intervention techniques, described in great detail in Chapter 5 of the report, blend well with displacement-based approaches. Such an intervention philosophy is conceptually described in Fig. 3-3. The original structure may have a supply-demand displacement ratio (Δ_u/Δ_d, where Δ_u is the displacement capacity of the structure and Δ_d represents the displacement demand) that does not meet the target safety requirements. The three intervention scenarios present different solutions to address such a situation, either by targeting the elastic stiffness of the structure (K_y), its strength (F_y) or its ductility (μ). Which solution is more economical and feasible depends on the case being studied, considering both the structure characteristics and the displacement spectra for different damping levels. Whilst an increase in the level of equivalent damping will decrease the displacement demand, changes in the effective period of vibration of the structure may or may not be beneficial, depending on the spectrum shape and location of the initial T_{eff}.

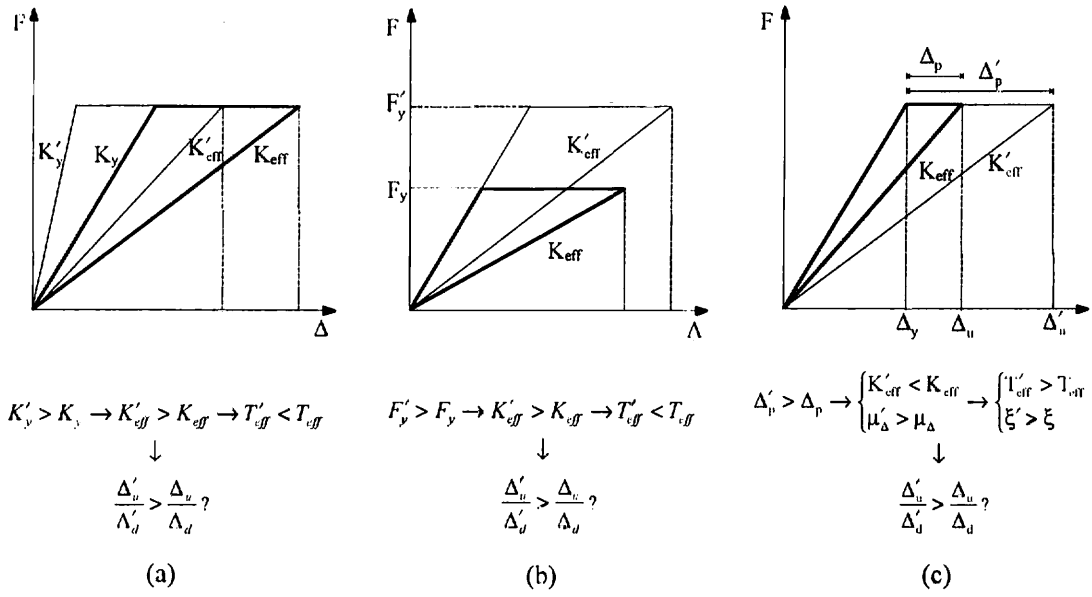

Fig. 3-3: Variation in DBD design parameters due to selective intervention: (a) stiffness; (b) strength; (c) ductility.

3.3.1.2 The steps of the displacement-based assessment procedure

The displacement-based approach for assessment of RC structures in the NZ draft Guidelines follows Priestley (1995, 1997). Instead of the elastic stiffnes and the global displacement ductility factor of the SDOF system and the inelastic acceleration spectrum of the force-based procedure, it uses the secant stiffnes to peak displacement of the SDOF system, a damping value consistent with this displacement and a damping-dependent displacement spectrum. It is considered more rational and generally produces less conservative results.

In the following the steps of the procedure for RC frames are described.

(1) Step 1: Capacities of members and joints; likely failure modes and location of plastic hinges.

Step 1 of the displacement-based approach in the NZ draft Guidelines consists of identification of the likely failure mechanism and is essentially identical to Step 1 of the force-based procedure. Identification of the potential for soft-storey formation is important for Step 3 of the displacement-based approach.

(2) Step 2: Member deformation capacities

Step 2 comprises calculation of deformation supplies at potential plastic hinges, in terms of the associated plastic rotation capacities: $\theta_{pl,u}=L_{pl}(\varphi_u-\varphi_y)$ (cf. Step 5 of the force-based approach). The possible limitation of plastic rotation capacity due to reduction of the shear

Copyright fib, all rights reserved. This PDF copy of fib Bulletin 24 is intended for use and/or distribution only by National Member Groups of fib.

strength, V_u, to the point that it becomes controlling is also recognised, as in Step 5 of the forced-based approach. It is noted that plastic hinge rotations computed in this way reflect mainly flexural deformations and do not fully capture the effects of shear deformations and bar slippage from their anchorage zone beyond the member end.

(3) Step 3: Global deformation capacity

Step 3 of the procedure estimates the global displacement capacity of the structure, as this is determined by deformation capacity of its members. This may be accomplished through a pushover analysis in the horizontal direction of interest. The outcome of the pushover analysis is the (work-equivalent) lateral displacement of the structure at attainment of the deformation capacity at one or more locations therein. The equivalent lateral displacement, δ_e, may be taken such that the work produced through it by the resultant of the lateral forces, ΣF_i (i.e. the base shear), is equal to the work of the forces F_i acting on the corresponding nodal displacements δ_i: $\delta_e=\Sigma F_i\delta_i/\Sigma F_i$. For an approximately inverted triangular heightwise pattern of δ_i, it is convenient to think of δ_e as the lateral displacement at the point of application of the resultant force ΣF_i at a height h_{ef} from the base of the structure. The values of δ_e: a) at peak force or at ultimate, δ_u, and b) at yielding, δ_y, both determined as described above in Step 5 of the force-based approach, give the available displacement ductility factor: $\mu_\delta=\delta_u/\delta_y$.

It is noteworthy that the "pushover" analyses possibly used in Step 3 of the NZ displacement-based approach and in Step 2 of the force-based one differ only in what we want to get out of them: the value of the ultimate base shear from the latter, versus that of the corresponding equivalent lateral displacement at ultimate, δ_u, from the former.

For structures which have a simple configuration and are symmetric in plan, the NZ draft Guidelines suggest simple expressions for the conversion of the plastic rotation capacity, $\theta_{pl,u}$, of the controlling plastic hinges into an ultimate value for the equivalent lateral δ_u, and for the displacement ductilty factor, μ_δ, of the structure, depending on its most likely plastic mechanism. These expressions are developed on the basis of the observation that the displacement at the height h_{ef} of application of the resultant ΣF_i of lateral forces can be expressed as: $\delta_u=\delta_{pl,u}+\delta_y$ (implying: $\mu_\delta=1+\delta_{pl,u}/\delta_y$), with $\delta_{pl,u}$ denoting the plastic part of the ultimate displacement. The value of $\delta_{pl,u}$ is determined from a postulated heightwise pattern of the plastic lateral displacements, considered to hold when the controlling plastic hinges reach their plastic rotation capacity, $\theta_{pl,u}$:

1) If a beam-sway mechanism is expected, which is always accompanied by rotations at the base of all bottom-storey vertical elements (be it due to plastic hinging there or to the compliance of the foundation soil), then in all likehood the most critical storey is the bottom storey. At ultimate deformation the plastic part of the drift ratio in that storey is equal to the plastic rotation capacity of its elements, $\theta_{pl,u}$, and represents the maximum storey plastic drift throughout the structure. In dual structures dominated by shear walls, or in frame structures with a number of storeys, n_{st}, up to 4, the heightwise pattern of plastic lateral displacements may be considered as inverted triangular, implying: $\delta_{pl,u}\approx h_{ef}\theta_{pl,u}=2/3H\theta_{pl,u}$. In frames with n_{st} greater than 4, the plastic part of the storey drift may be considered to decrease from the base to the top. If this reduction is parabolic, then $h_{ef}\approx 5H/8$ and $\delta_{pl,u}\approx 0.5\theta_{pl,u}h_{ef}$. So the NZ draft Guidelines recommend:

- For dual structures dominated by the walls, or for frame structures with $n_{st}\leq 4$:

$$\delta_{pl,u}=0.64H\theta_{pl,u},\ \mu_\delta=1+0.64H\theta_{pl,u}/\delta_y \tag{3-14}$$

- For highrise frames ($n_{st}\geq 20$):

$$\delta_{pl,u}=0.44H\theta_{pl,u},\ \mu_\delta=1+0.44H\theta_{pl,u}/\delta_y \tag{3-15}$$

- For frames with $4\leq n_{st}\leq 20$:

$$\delta_{pl,u}=[0.64-0.0125(n_{st}-4)]H\theta_{pl,u},\ \mu_\delta=1+[0.64-0.0125(n_{st}-4)]\ H\theta_{pl,u}/\delta_y \tag{3-16}$$

The first case above may be extended to buildings expected to develop a beam-sway mechanism not throughout the total height H of the building but from a height h_i above the base up to the top (meaning that at ultimate the part of the building up to a height h_i

Copyright fib, all rights reserved. This PDF copy of fib Bulletin 24 is intended for use and/or distribution only by National Member Groups of fib.

from the base remains elastic). In such buildings the term $H\theta_{pl,u}$ in eq. (3-14) should be multiplied by $(1-h_i/H)^2(1+0.5h_i/H)$.

2) If a soft-storey is expected to develop at a storey which starts at a height h_i from the base (h_i=0 at the bottom storey), plastic deformations are assumed to take place only in that storey, which at ultimate develops a plastic drift ratio equal to $\theta_{pl,u}$. Above that storey plastic horizontal displacements are equal to $\theta_{pl,u}$ times the height of the soft storey, h_{st}. We have then:

$$\delta_{pl,u}=h_{st}\theta_{pl,u}(1-h_i/H)^2, \qquad \mu_\delta=1+h_{st}\theta_{pl,u}(1-h_i/H)^2/\delta_y \tag{3-17}$$

For comparison of eq. (3-17) with eqs. (3-14)-(3-16), for a building with constant storey height the value: $h_{st}=H/n_{st}$ may be used in eq. (3-17).

The value of $\theta_{pl,u}$ in eqs. (3-14)-(3-17) may be taken equal to the mean value of $L_{pl}(\varphi_u-\varphi_y)$ at the base of the vertical elements of the most critical storey - i.e. of the soft-storey in eq. (3-17), or of the lowest storey in the beam-sway mechanism for eqs. (3-14)-(3-16). In the special case that, instead of a plastic hinge, a "fixed-end-rotation" develops at the base of the vertical elements due to foundation compliance, the value of $\theta_{pl,u}$, may be taken equal to the mean value of $L_{pl}(\varphi_u-\varphi_y)$ at the tops of the columns of the soft storey for eq. (3-17) or at the ends of the beams of the bottom storey for eqs. (3-15) and (3-16), or to the minimum storey-average value of $L_{pl}(\varphi_u-\varphi_y)$ among all the storeys of the plastic mechanism for eq. (3-14). Obviously the contribution of the "fixed-end-rotation" at the base to the value of δ_y at global yielding should be included.

(4) Step 4: Estimation of displacement demand.

In Step 4 the displacement demand due to the seismic action is estimated. To this end the NZ draft Guidelines adopt the Shibata and Sozen (1976) "substitute structure" approach, as outlined in 3.3.1.1: the peak value of the equivalent lateral displacement of the structure is estimated from the elastic response spectrum entered at a period corresponding to the secant lateral stiffness at peak response and at a value of damping ξ which is a function of the ductility factor, μ_δ. As the peak displacement response is equal to μ_δ times the yield displacement, δ_y, and the corresponding force is approximately equal to the yield value V_y of the base shear (or to $[p(\mu_\delta-1)+1]V_y$ for non-zero hardening ratio p), the secant stiffness at peak response is equal to the elastic lateral stiffness $K_{el}=V_y/\delta_y$ times $1/\mu_\delta$ (or times $[p(\mu_\delta-1)+1]/\mu_\delta$ for $p\neq 0$). So the period of the "substitute structure" is equal to: $T=2\pi\sqrt{(M/K_{el})\mu_\delta/(p(\mu_\delta-1)+1)}\approx T_{el}\sqrt{\mu_\delta}$, with: $T_{el}=2\pi\sqrt{M/K_{el}}$ denoting the fundamental period of the elastic structure with cracked member stiffnesses. According to Shibata and Sozen (1976) the damping factor, ξ, is:

$$\xi\,(\%)=2+20\left(1-1/\sqrt{\mu_\delta}\right) \tag{3-18}$$

For $\mu_\delta\geq 4$, the value of ξ may be taken independent of μ_δ in the range 20%-25%. It is reminded that the elastic spectra for $\xi\neq 5\%$ are taken in the NZ draft Guidelines equal to the 5%-damped ones times $\sqrt{7/(\xi+2)}$. For ξ between 20% and 25% the value of this reduction factor is between 0.5 and 0.55.

The displacement demand is determined either directly from an elastic displacement spectrum or by multipling the elastic spectral acceleration by $(T/2\pi)^2$. It is worth mentioning that: a) as the cracked member stiffnesses used for the calculation of the elastic period T_{el} may be in the order of one-quarter of those of uncracked members and b) as the effective period of the "substitute structure" $T=T_{el}\sqrt{\mu_\delta}$ may be much longer than T_{el}, the final value of T may end up at the tail of the acceleration spectrum, i.e. in a region which is poorly represented by the usual code spectra. The assessment concludes with a comparison of the demand value of the equivalent lateral displacement from Step 4, to the supply value of $\mu_\delta\delta_y$ from Step 3.

Copyright fib, all rights reserved. This PDF copy of fib Bulletin 24 is intended for use and/or distribution only by National Member Groups of fib.

3.3.2 The 1997 NEHRP Guidelines and the 2000 ASCE Prestandard for seismic rehabilitation

3.3.2.1 Introduction

Despite their title, the NEHRP "Guidelines for the Seismic Rehabilitation of Buildings" (ATC, 1997a, and b, commonly known as FEMA 273/274, and their follow-up ASCE "Prestandard for the Seismic Rehabilitation of Buildings" (ASCE, 2000, commonly known as FEMA 356) put little emphasis on rehabilitation and more on assessment. They are essentially comprehensive State-of-the-Art documents on rational quantitative seismic assessment of existing buildings of concrete, steel or cast iron, masonry and timber construction.

As far as retrofitting is concerned, these documents list the various possible strengthening techniques for members or structures, without giving details for their application or proportioning. The retrofitted building has to go through the same seismic assessment procedure as the unretrofitted one and has to fulfil the verification criteria that the unretrofitted building failed to satisfy.

The coverage of: a) performance objectives and requirements, b) the Seismic Hazard and c) modelling and analysis in the 1997 NEHRP Guidelines for rehabilitation is more complete than in the corresponding NEHRP document for new structures (BSSC 2001), and may indeed form the basis for a future comprehensive code-type document for both new and existing buildings. These broad and ground-breaking State-of-the-Art documents have already exerted a profound influence on worldwide code-writing efforts and - as a matter of fact - of engineering practice, both for existing and for new structures.

An extensive programme of trial application of the 1997 NEHRP guidelines by design firms to real buildings, presented in FEMA report 343, provided valuable feedback regarding the user-friendliness, the technical completeness, cost-effectiveness, etc. of the guidelines. Three RC frame buildings, five RC shear wall buldings and three RC buildings with masonry infills were included in the trial application. Conclusions of the trial applications formed the basis for the revision of the NEHRP Guidelines and their upgrade into ASCE prestandard (ASCE 2000). This (pre)standard is intended to be applicable throughout the US, for adoption and enforcement by the pertinent code officials in any directed (mandatory) seismic rehabilitation programme, or for reference by owners in voluntary rehabilitation projects.

The review herein of recent US developments in seismic assessment is based mainly on the most recent document, namely the ASCE prestandard (ASCE, 2000). In the following the relevant FEMA documents will be collectively termed: "Seismic rehabilitation guidelines and prestandard".

Prior to being subjected to a full assessment according to the seismic rehabilitation guidelines and prestandard, it is recommended that a building goes through the first two tiers (or levels) of the preliminary seismic evaluation procedure of FEMA 310 (ASCE 1998, ASCE 2001), for the identification of its seismic deficiencies. This recent document, which is also currently upgraded into an ASCE draft standard, is also overviewed herein in 3.3.3. Seismic assessment according to FEMA 310 is qualitative or simplified quantitative (in that seismic analysis of the full building is either not required or done with simpler procedures). It aims at the identification of the seismic deficiencies of the building, as well as at screening out those buildings which clearly have sufficient strength to render any further consideration for retrofitting unnecessary. It is noteworthy that the acceptance (i.e. verification) criteria in (ASCE 1998, 2001) apply only to the existing building and its members, whereas those of FEMA 273 (ATC 1997a) and 356 (ASCE 2000) apply uniformly to the as-built existing members, to the retrofitted members and to the new ones which may be added for strengthening. To reduce the number of buildings identified as deficient and in need of retrofitting, the acceptance criteria in (ASCE 1998, 2001) are generally less stringent than the corresponding criteria in FEMA 273 or 356. As a result, buildings assessed per FEMA 273 or 356 as marginally deficient, may be assessed as seismically adequate according to (ASCE 1998, 2001).

3.3.2.2 Classification of elements and of modes of behaviour

According to the seismic rehabilitation guidelines and prestandard, and unlike what is typically done for new structures, all building elements (termed components) deemed important for earthquake resistance (including, e.g., masonry infills) are included in the analysis model. Moreover their available capacity is fully used to the benefit of the seismic

Copyright fib, all rights reserved. This PDF copy of fib Bulletin 24 is intended for use and/or distribution only by National Member Groups of fib.

resistance of the structure, if appropriate. To this end structural and non-structural components are classified as "primary" or "secondary". The structure can rely on its "primary" components for its earthquake resistance and stability against collapse, regardless of any cyclic degradation in their strength and stiffness. For "secondary" components, what matters is only their gravity-load bearing capacity under the maximum displacements or deformations induced by the earthquake. It is noted that the distinction between "primary" and "secondary" components is essentially equivalent to that of members which belong to the lateral force resisting system, or not, traditionally made in US codes for earthquake-resistant design of new buildings. The new terminology has already been adopted by other international codes, such as Eurocode 8, for both new and existing buildings.

Verification criteria for the "primary" and the "secondary" components are typically defined in terms of the corresponding peak seismic deformation supplies and demands. The deformation supplies specified by the seismic rehabilitation guidelines and prestandard are more liberal (less conservative) for the "secondary" components than for the "primary" ones. The engineer is free to assign a structural component to the class of "primary" or to that of the "secondary" ones, provided that this component is appropriately considered in the analysis and satisfies the corresponding capacity-demand verification criteria. The engineer may also re-classify some components as secondary in the evaluation, to benefit from the less demanding criteria for them, provided that their low and unreliable stiffness and strength under cyclic loading is appropriately recognised in the model. Non-structural components, such as masonry infills, which account for a significant part (more than 10%) of the global lateral stiffness, can only qualify as "primary" components, since they play no role in the support of gravity loads and hence cannot be classified as "secondary".

The evaluation of existing building components and the verification of new or modified ones in the rehabilitated structure are based on a capacity-demand comparison in terms of either deformations or forces, if in the particular mode of behaviour examined (i.e. in flexure, in shear, axial load, etc.) the component is characterised as "deformation-" or "force-controlled" respectively. Primary components with an available displacement (or chord rotation) ductility factor less than 2, or secondary ones which shed their load abruptly after ultimate strength, are considered as force-controlled. As force-controlled are classified: the primary beams, columns and joints (but not the primary walls) in shear, and the primary columns for bond and splicing or against very high axial compression (axial load ratio ν greater than 0.7, or columns supporting discontinuous shear walls). All other modes of behaviour are classified as deformation-controlled. This is a generalisation of the distinction between "ductile" and "brittle" elements and behaviour modes, with implications for the verification formats and criteria.

3.3.2.3 Performance requirements

In the spirit of performance based seismic engineering, introduced in the first half of the '90s by the famous Vision 2000 document (SEAOC, 1995), performance requirements are expressed in terms of "Performance Objectives", i.e. of (typically more than one) combinations of "Performance Levels" (Limit States which determine the required component capacity) at specified "Seismic Hazard" levels (which determine the component demands).

A generic and very detailed presentation of performance levels and objectives for seismic assessment and retrofit has been made in Chapter 2, Section 2.4, of this report. For convenience, the definitions of the key structural performance levels used in the FEMA 273/356 documents are repeated here: At the "Life Safety" (LS) level the structure is stable with considerable reserve capacity (e.g. against aftershocks), while non-structural damage is controlled. At the "Collapse Prevention" (CP) level the structure is barely standing and any kind of damage other than collapse is acceptable. Finally, at the "Immediate Occupancy" (IO) level the building may return to normal occupancy after minor repair.

In the US, Seismic Hazard is typically defined in terms of the 475-year earthquake (10% exceedance probability in 50 years) and the "Maximum Considered Earthquake" (1.5 times the characteristic event of known major faults, or, where no such faults can be identified, the 2500-year earthquake, i.e. the one with 2% exceedance probability in 50 years). Two-thirds of the Maximum considered Earthquake may be used instead of the 475-year event. An "Occasional" earthquake is also defined, with a mean return period of 225 years and 20% exceedance probability in 50 years.

Copyright fib, all rights reserved. This PDF copy of fib Bulletin 24 is intended for use and/or distribution only by National Member Groups of fib.

An (existing or rehabilitated) structure of ordinary importance normally has to meet the "Immediate Occupancy" performance level under the "Occasional" earthquake, the "Life Safety" performance level under the 475-year event and the "Collapse Prevention" performance level under the Maximum Considered Eartquake. The importance and criticality of the building, or the owner himself, may dictate a higher "Performance Objective", e.g. meeting the "Immediate Occupancy" and the "Life Safety" objectives under the 475-year and the 2500-year earthquakes respectively. Alternatively, to avoid retrofitting or to reduce retrofitting costs, the owner may limit the "performance objective" to fulfilment of the "Life Safety" performance level under the 475-year earthquake, without "Collapse Prevention" under the 2500-year event.

Explicit verification of the components of the (existing or retrofitted) structure at all selected performance levels is required. At the "Collapse Prevention" level member deformation capacities are taken at ultimate strength for "primary" components, or at ultimate deformation for "secondary" ones. At the "Life Safety" level, member deformation capacities are reduced by a (safety) factor of 4/3 over those applying at "Collapse Prevention". As noted in 3.3.2.6, if "secondary" components are included in the analysis, with models that account realistically for the degradation of their behaviour and of their properties with large cyclic deformations, then the deformation capacity of "primary" components may be taken at the same level as in "secondary" components, i.e. at ultimate deformation at the "Collapse Prevention" performance level, or at 3/4 of that deformation at the "Life Safety" level.

It is reminded that current seismic design codes for ordinary new buildings require verification of structural components only at the "Life Safety" performance level. If the associated verification criteria are satisfied, it is presumed that, due to: a) the hierarchy of strengths and failure modes achieved through the application of capacity design, and b) the seismically favourable configuration typically achieved through proper conceptual design and the structural regularity promoted by current codes, a new earthquake-resistant structure possesses the necessary safety against "Collapse Prevention" under earthquakes much stronger than the one for which the "Life Safety" performance level has been verified. Existing structures do not have these safeguards built-in by design, and hence need to be explicitly verified for the "Collapse Prevention" performance level under the corresponding "Hazard Level".

3.3.2.4 Seismic analysis procedures

In the seismic rehabilitation guidelines and prestandard, the horizontal components of the seismic action are defined in terms of uniform-hazard 5%-damped elastic response spectra, specified through the values of spectral acceleration and spectral pseudovelocity in the acceleration- and in the velocity-controlled ranges, after correction for the effect of subsoil conditions. Member deformation demands for these horizontal components may be determined either by <u>linear</u> or by <u>nonlinear</u> analysis, <u>static</u> or <u>dynamic</u>.

Linear analyses basically employ the equal displacement rule (which states that peak response displacements in the 5%-damped linear and in the nonlinear system are about equal) to estimate peak structural displacement demands, with possible correction through empirical coefficients for short-period and P-Δ effects (hence the method of estimation of inelastic displacements employed in the FEMA 273/356 documents is often called the "Coefficient Method"). For example, the correction for short-period effects is essentially based on eq. (3-13) by Vidic et al (1994). These corrections are normally unimportant and not essential for RC structures. The equal displacement rule, with similar corrections on the displacements (per eq. (3-13)), is also employed in the nonlinear static analysis to estimate the peak displacement demand at roof level. For buildings with more than two storeys and with fundamental period less than 1 sec, displacement estimates obtained from linear (equivalent) static analysis are reduced by 10% or 20% in frame or wall buildings, respectively, to account more realistically for the mass participation in the fundamental mode.

The linear static analysis is performed with a heightwise variation of floor accelerations between inverted triangular (for $T \leq 1$ sec) and parabolic (for $T \geq 2.5$ sec).

The nonlinear dynamic procedure employs time-historey analysis of the response to a suite of (at least three, but preferably at least seven) spectrum-compatible horizontal motion components. The time-historeys of these components may be fully artificial, or may emulate historic motions as far as phasing, duration and intensity function are concerned.

All four types of analysis procedures should: a) account for both senses of action of each

Copyright fib, all rights reserved. This PDF copy of fib Bulletin 24 is intended for use and/or distribution only by National Member Groups of fib.

horizontal component, b) be performed preferably in 3D and c) take into account multi-directional component effects (with simultaneous excitation in both horizontal directions for time-historey analyses, or through the 1:0.3 or SRSS combination rules in the other cases), diaphragm non-rigidity, the unfavourable effects of natural and accidental torsion, soil compliance (including nonlinearity and uplift) and P-Δ effects. The elastic stiffness of RC members should include the effects of flexural and shear cracking and of reinforcement slippage or pull-out from the anchorage zones, as well as participation of a large effective flange width in compression and tension. Indicative values of this flange width given in the seismic rehabilitation guidelines and prestandard, around 50% of the stiffness of the uncracked gross section, are considered as unrealistically high, possibly leading to understimation of displacements and of member deformation demands.

(1) Applicability conditions for analysis procedures

Linear analysis is permitted only if the nonlinearity of the response is limited and uniformly distributed throughout the structure. Namely this type of analysis is allowed if: a) the linearly estimated force demands no-where exceed capacities by more than a factor of 2 (i.e. inelastic action and expected damage is very limited), b) the demand-capacity-ratio (DCR) on one side of a storey is not greater than 150% of the value of that ratio on the other side of the plan (torsionally balanced strength) and c) the storey-average DCR value does not vary from storey to storey by more than 25% (weak storey effects).

If higher mode effects are unimportant (i.e. if: a) the height is less than 30m, b) plan dimensions vary from storey to storey by less than 10% and c) the interstorey drift ratio differs from one side of the plan to the opposite or from one storey to the next by less than 50%) linear analysis may be (equivalent) static. Otherwise it should be modal, of the response spectrum type, with CQC (complete quadratic combination) of peak modal responses.

Unfortunately the limitations for the application of the linear elastic analysis are not only very stringent but also such that their fulfillment can be checked only after the analysis has been completed. The same applies to the selection between its (equivalent) static and modal versions.

The above material-wide limitations of the seismic rehabilitation guidelines and prestandard for the application of the four possible analysis procedures imply that for cast-in-place RC buildings without masonry infills the most appropriate analysis procedure is the following:

- For low- or medium-rise buildings, expected to develop limited inelastic action and damage at the performance level of interest, linear analysis may be used, static if the building is regular in plan and elevation, dynamic if it is not.
- For tall buildings expected to develop limited inelastic action and damage at the performance level of interest, linear dynamic (modal) analysis should be used.
- For any building - other than those of the case below - expected to develop significant inelastic action and damage at the performance level of interest, nonlinear static (pushover) analysis should be used.
- For tall heightwise irregular buildings, expected to develop significant inelastic action and damage at the performance level of interest, nonlinear dynamic analysis should be used.
- For infilled RC frames only nonlinear static analysis is recommended as appropriate.
- For precast buildings, including those with tilt-up construction and shear walls for earthquake resistance, only static analysis is considered appropriate. The static analysis needs to be nonlinear only in irregular precast buildings expected to develop significant inelastic action and damage at the performance level of interest.

(2) Modelling of "secondary" components

The contribution of "secondary" components to lateral strength and stiffness is neglected in linear analyses. This means that these elements are modeled with negligible stiffness against lateral loads, but with realistic strength and stiffness against gravity loads and in a manner permitting determination of their earthquake-induced deformations and of their impact on gravity load capacity (For vertical elements, for example, their axial stiffness is assembled in the Stiffness Matrix but their flexural one is not; during the element state-determination phase however, their real flexural stiffness is considered). However in linear analysis the real contribution to lateral stiffness of all elements designated as "secondary"

Copyright fib, all rights reserved. This PDF copy of fib Bulletin 24 is intended for use and/or distribution only by National Member Groups of fib.

cannot account for more than 20% of the total stiffness. Moreover, the conditions for regularity of the planwise and the heightwise distribution of strength and stiffness, to be fulfilled for the linear elastic analysis to be used, need to be satisfied both when the "secondary" components are considered and when they are neglected in the model. Unless fulfillment of this condition is obvious, its verification requires performing the linear analysis with all "secondary" components included in the model with realistic stiffnesses.

In the nonlinear analyses, instead, "secondary" elements are included in the model with their realistic (but degrading) strength and stiffness. No upper limit is set on their contribution to the global lateral stiffness. It is noted, though, that due to the degradation of the strength of "secondary" components with cyclic deformations, the slope of the global force-displacement relation of the structure may become negative, increasing the dynamic P-Δ effects. This increase in P-Δ effects is automatically accounted for during a nonlinear dynamic analysis. If the nonlinear static analysis is applied instead, these effects are approximated through multiplication of the seismic displacement demands from the elastic response spectrum by an additional correction factor. The value of this factor exceeds unity by an amount which increases in proportion to: a) the mean (negative) slope of the global force-displacement curve, b) the difference between the elastic base shear demand and the base shear strength of the building, and c) its fundamental frequency.

The resistance and stiffness of "secondary" components against lateral forces, as well as the post-ultimate-strength drop of the resistance of "primary" components, may be neglected in a nonlinear static analysis, but not in a nonlinear dynamic one. In that case deformation demands on "primary" components from the nonlinear static analysis should satisfy more stringent criteria (cf. second paragraph from the end in Sect. 3.3.2.6). "Primary" elements not meeting these more stringent criteria may be classified then as "secondary", provided that this reclassification will not change the regularity characterisation of the building.

(3) Nonlinear analysis procedures

The nonlinear static analysis is of the "pushover" type. Two patterns of lateral load variation with height should be considered. In the first pattern, response accelerations are either taken as heightwise uniform, or are continuously adapted - during the analysis - to the heightwise variation of storey displacements. In the second pattern, two options are given for the floor accelerations: The first is to compute them through SRSS-combination of modal accelerations from the modes which account for at least 90% of the total mass (this choice is mandatory if the first mode period exceeds 1sec). In the second option, if the 1st- mode participating mass is more than 75% of the total, floor accelerations may follow the heightwise pattern used in the linear static analysis; otherwise they should follow that of the accelerations in the fundamental mode. Nevertheless, as with its prescribed lateral load pattern(s) the nonlinear static procedure cannot capture well higher-mode effects at the member deformation level, if the first mode base shear from a linear modal analysis is less than 1/1.3 of the total base shear due to all modes accounting for at least 90% of the total mass, the nonlinear static analysis needs to be accompanied by a linear dynamic (modal) one, with the acceptance criteria of the latter relaxed (i.e. the capacities increased) by one-third.

The point on the base-shear vs. roof-displacement curve to which the structure is driven by the earthquake is determined from the 5%-damped elastic spectrum entered at a period: $T = 2\pi\sqrt{M/K_{el}}$. This period is based on the secant stiffness K_{el} at 60% of the base shear at global yielding of the structure (corner of the bilinear approximation of the base shear-roof drift curve). The afore-mentioned correction factors for lack of validity of the equal displacement rule are applied to the displacement demand from the spectrum (except for the correction for the first mode participating mass applied to the displacement demand of the linear static analysis). The so-computed SDOF displacement demand is converted to a top displacement, through multiplication by a factor increasing from 1.0 to 1.5 when going from single-storey to multistorey buildings. Member internal forces and deformations due to the earthquake represented by the spectrum are those corresponding to this (corrected) displacement demand in the pushover analysis.

One- or two-component lumped inelasticity models can be used for the RC members in the nonlinear analyses. A multilinear relationship between the end moment and the corresponding deformation measure (chord rotation, plastic hinge rotation or curvature), with the first corner point at yielding and the second at ultimate strength, suffices for the

Copyright fib, all rights reserved. This PDF copy of fib Bulletin 24 is intended for use and/or distribution only by National Member Groups of fib.

description of monotonic loading. In columns and shear walls this relationship needs to take into account the effect of axial load on yield and ultimate strength and, if possible, on stiffness. In beams, the potential for plastic hinge formation at intermediate points along the span due to gravity loads needs to be investigated a-priori (e.g., from the moment diagrams of the transversely loaded beam with the two ends considered yielding in opposite bending), in order to decompose the beam into smaller elements with intermediate nodes at the potential plastic hinge locations.

Unlike the other analysis methods, which are described in FEMA 273 and 356 in enough detail to enable review and checking of the seismic assessment and of the retrofit design by engineers of the level of checking ordinary designs of new buildings, the nonlinear dynamic analysis procedure is described only in general terms, as its application and review requires special qualifications and expertise. For nonlinear dynamic analysis, member models need to be supplied with simple and numerically stable, yet realistic, hysteresis rules. Takeda-type, modified-Clough and similar models (Takeda et al 1970, Otani, 1974, Saiidi and Sozen, 1979) are most appropriate for this purpose.

In addition to the appropriate hysteresis models, a seismic assessment based on nonlinear dynamic analysis requires peer third-party review and site-specific spectra for the definition of the seismic input. This latter requirement is for uniformity of the accuracy and the reliability across the entire evaluation process. For the same reason reliable "as-built" material and geometric data need to be supplied as input to any nonlinear analysis, static or dynamic. If as-built information is considered incomplete, the evaluation is penalised, first, by allowing only linear analysis and, second, by reducing component capacities by 25% over those inferred from either the available documentation and in-situ and lab measurements (as mean or m-σ values), or from very low default values given in the seismic rehabilitation guidelines and prestandard for cases in which no strength tests are performed.

Apart from the requirement for exhaustive and costly data collection and the lack of widely available nonlinear analysis software, there are significant benefits and incentives for the engineer in choosing a more sophisticated analysis procedure (e.g. a nonlinear instead of a linear, a dynamic instead of a static), because the more sophisticated and accurate an analysis procedure, the less conservative its results are. As an important example, in a linear analysis forces in force-controlled elements and modes of behaviour (e.g. the shear force in a beam, column or joint) are significantly overestimated. To reduce conservatism, if these forces depend, through equilibrium, on yielding components or zones (as the shear in a beam, column or joint depends on the yield moments of the end sections of the component), their computed values can be empirically reduced by dividing by the lower DCR (demand-capacity-ratio) among all elements connected to the force-controlled component. (For simplicity, this reduction factor may be taken equal to 2.0 in high seismicity regions, or to 1.5 and 1.0 in intermediate or low seismicity regions, respectively). The reduction by the lower DCR factor is also applied to load effects derived for the foundation (e.g. overturning moments) from linear analysis.

(4) Alternative determination of demand for pushover analysis: The "Capacity Spectrum" method in ATC-40.

In an effort parallel to that which led to the "1997 NEHRP Guidelines for the Seismic Rehabilitation of Buildings", a document focusing on concrete buildings was produced for ATC (ATC, 1996). As it has been disseminated earlier, this document – widely known as ATC-40 - has been used extensively by design professionals and software developers for seismic assessment and retrofit design.

The ATC-40 approach differs from that of the 1997 NEHRP Guidelines mainly in the way the global inelastic displacement demand is estimated and compared to capacity. Instead of the so-called "Coefficient Method" of the 1997 NEHRP Guidelines (based on the equal displacement rule with possible correction through empirical coefficients for short-period and P-Δ effects), ATC-40 employs Freeman's "Capacity Spectrum Method" (Freeman, 1978). In this later approach global lateral force capacity and seismic demand are both presented through separate global force-displacement diagrams, and visually compared by presenting both diagrams on the same plot. In this respect the term "Capacity Spectrum" may be considered as a misnomer, as neither demand nor capacity is plotted as a function of period. The term may have derived from the presentation of seismic demand in the form of a plot of spectral acceleration vs. spectral displacement of a highly-damped SDOF oscillator (the so-

Copyright fib, all rights reserved. This PDF copy of fib Bulletin 24 is intended for use and/or distribution only by National Member Groups of fib.

called Acceleration-Displacement-Response-Spectrum, or ADRS, format), where the slope of radial lines is inversely proportional to the square of the period, T. The capacity curve is derived from a nonlinear static (pushover) analysis of the structure. The stage in the lateral force response where the "Performance Level" of interest is attained in one or more components of the structure, corresponds to a single point on the capacity curve, to be compared then with the seismic demand point.

The way in which the seismic demand point is determined has become a matter of considerable controversy in recent years. In the "Coefficient Method" of the 1997 NEHRP Guidelines the seismic demand point is located on the 5%-damped ADRS curve, at a the "target-displacement" derived from the equal displacement rule with possible corrections coefficients for short-period and P-Δ effects. In the ATC-40 approach, as well as in its original source (Freeman, 1978), the seismic demand point is identified with the intersection of the capacity curve with that ADRS demand curve which corresponds to a value of the equivalent viscous damping consistent with the global ductility demand represented by the location of that point on the capacity curve. Implicit in such a determination of the demand is the use of a period T for the equivalent linear SDOF system corresponding to the global secant stiffness at the intersection with the capacity curve. This is similar to the Shibata and Sozen (1976) "substitute structure" approach, outlined in Section 3.3.1.1 and in (4) of 3.3.1.2 as the basis of the displacement-based assessment procedure of the New Zealand draft guidelines (see also eq. (3-18) for the Shibata and Sozen, 1976, relationship between the equivalent viscous damping ratio and the global ductility ratio).

The above approach in ATC-40 for the determination of seismic demand has been questioned in recent years as lacking a physical basis and as producing inaccurate or biased results, compared to those of nonlinear time-history analysis (see, e.g., Krawinkler, 1994, Chpra and Goel, 2000a, 2000b, 2001, Chopra et al, 2001). An attractive alternative, that retains the visual appeal of the "Capacity Spectrum" while increasing accuracy and reliability of the demand predictions, has been proposed in Fajfar (1999, 2000). This alternative consists essentially in recasting the N2 method (Fajfar and Fischinger, 1988) in the "Capacity Spectrum" format, with replacement of the highly-damped elastic spectra (per Shibata and Sozen, 1976) as a means for describing demand, by an inelastic spectrum based on the Vidic et al (1994) q-μ-T relationship (cf. eq. (3-13)).

Several examples of application of the ATC-40 and of the N2-based versions of the "Capacity Spectrum" approach are given in the case studies of Chapter 7. The reader is referred to those case studies for examples of assessment in the form of "Capacity Spectra".

3.3.2.5 Data collection for material properties and condition assessment

The requirements of FEMA 273 (ATC 1997a, b) for collection of information about the as-built structure and its materials were onerous. More specifically, FEMA 273 required that complete geometric and material data are available, either: a) from as-built construction documents, confirmed through sporadic in-situ tests and exposure of reinforcement, as well as by lab tests, or b) through an extensive and comprehensive campaign of such in-situ and lab tests and measurements. The trial application of FEMA 273 to 43 real buildings, reported in FEMA 343 (BSSC, 1999), shows that the benefits from an exhaustive collection of data regarding the as-built structure do not warrant its cost. As a result FEMA 356 (ASCE, 2000) has reduced considerably the data collection requirements of FEMA 273. According to the new thinking, the information readily available from drawings and documents about the as-built structure and its materials may be supplemented for the purposes of assessment of the building and of the design of the retrofitting, with certain hypotheses about missing data. To the extent necessary, these hypotheses may be confirmed (or revised) through in-situ and laboratory measurements at the final stage of the design of the retrofitting. If the building is so deficient that it is decided to resist fully the seismic action through new elements (e.g. through new shear walls), there is little sense in conducting an exhaustive data collection campaign about the as-built structure.

More specifically, according to the update of FEMA 273 in FEMA 356, if: a) the objective of the rehabilitation is the normal one (termed in FEMA 273 and 356 "basic"), i.e. "Life Safety" and "Collapse Prevention" under the 475-year and 2500-year earthquakes, respectively, and b) the analysis is linear elastic (static or dynamic), in-situ measurements are not needed. Resort may be made instead to the construction drawings and to a visual survey of a representative percentage of the "primary" components (of 20% of the "primary"

Copyright fib, all rights reserved. This PDF copy of fib Bulletin 24 is intended for use and/or distribution only by National Member Groups of fib.

components in each storey, or of 40% in the presence of significant damage or deterioration). If the construction drawings are incomplete or missing, the in-situ collection (or confirmation) of data regarding the geometry of the structural system should include exposure of the reinforcement in at least three components for each type of component (preferably at or near connections). If this is not sufficient for development of a clear idea on how the components were reinforced and detailed, further exposure of reinforcement may be necessary. When construction documents are not available, (conservative) default values may be assumed for material properties on the basis of the prevailing practice at the time of construction. A capacity reduction factor equal to 0.75 is applied to member resistances calculated on the basis of such (incomplete) information.

If the information above is supplemented with laboratory test results on material samples, the afore-mentioned capacity reduction factor of 0.75 is not applied to member resistances and a nonlinear analysis procedure may be used, provided that the normal ("basic") rehabilitation objective is selected. If the grades of materials specified for the building are known, testing of three concrete cores for the entire building is sufficient for this purpose. If the concrete grade specified is not known, the minimum number of concrete cores is six. If the steel grade specified is not known, at least two steel coupons should be tested in tension.

The information quoted in the previous paragraph suffices also for an "enhanced" rehabilitation objective, including, e.g., fulfilment of the "Life Safety" performance level under the 2500-year earthquake and of the "Immediate Occupancy" one after the 475-year event. In that case, however, the 0.75 capacity reduction factor is applied on member resistances. In order to be allowed to use a capacity reduction factor of 1.0 for an "enhanced" rehabilitation objective, the engineer should confirm the materials specified and the test results available in the documents of the original construction, through testing: a) of at least six concrete cores for the entire building and of at least three cores for each type of "primary" component, and b) of at least three steel coupons. If the available documents do not include concrete test results at the time of construction, the minimum number of concrete cores is three per storey, or per 300m^3 of concrete, or per 1000m^2 of floor plan area, whichever is most critical. If the concrete specified for the original construction is not known, the minimum number of cores is doubled. If the steel specified is not known, at least six tension coupons should be tested per 3 storeys for each type of "primary" component. If the period of construction provides some clue for the steel grade used, the number of coupon tests may be reduced by half. Finally, if available construction drawing are incomplete, then, in order to be allowed to use a capacity reduction factor equal to 1.0, the engineer should expose the reinforcement in at least three locations per type of "primary" component, or in more, if this exposure leaves doubts about the type of reinforcement and the detailing of members.

3.3.2.6 Verification criteria for members

For force-controlled components the verification or acceptance criteria consist in comparison of the force demand due to the seismic action and the simultaneous quasi-permanent gravity loads, with the lower characteristic value of the corresponding capacity (calculated on the basis of m-σ material strengths).

The verification of deformation-controlled components employs expected, rather than lower-characteristic, values of the capacities. Moreover, for reasons of convenience and familiarity of the potential users with the format, if linear analysis has been applied member forces are used in the verification instead of deformations, with member resistances (capacities) multiplied by an m-factor, defined as the ratio of the elastic internal force at the deformation limit to the strength capacity of the member. The m-factor resembles the familiar displacement ductility factor μ of the member and may be considered as a local (member) behaviour factor q.

In both types of verification, for linear analysis the force capacities of existing components are reduced by 25% if as-built information is incomplete or unreliable.

Tables 3-1 to 3-3 give the plastic rotation capacities, $\theta_{pl,u}$, of RC beams, columns and walls according to the seismic rehabilitation guidelines and prestandard. They also give – in the columns labelled (FEMA) 356 – the values of the local behaviour factor m not to be exceeded by "primary" or "secondary" components, depending on the target performance level (: IO for "Immediate Occupancy", LS for "Life Safety", CP for "Collapse Prevention"). Values of the m-factor listed under the heading (FEMA) 310 are taken from the seismic evaluation handbook and draft standard (FEMA 310 and ASCE, 2001).

Copyright fib, all rights reserved. This PDF copy of fib Bulletin 24 is intended for use and/or distribution only by National Member Groups of fib.

Flexure critical (: $M_u<L_sV_u$) with: a) in pl. hinge: hoop spacing $s_h \leq d/3$ & no laps; and b) $V_w \geq 3/4M_u/L_s$													
ω-ω'	$\frac{M_u}{L_s\sqrt{f_c}b_wd}$ (MN, m)	$\theta_{pl,m}$ (%)	$\theta_{pl,u}$ (%)	m, Primary component					m, Secondary component				
				IO		LS		CP	IO		LS		CP
FEMA report:				356	310	356	310	356	356	310	356	310	356
≤0	≤0.25	2.5	5.0	3	3	6	8	7	3	3	6	8	10
0-0.2	≤0.25	↕	↕	↕	3	↕	8	↕	↕	3	↕	8	↕
≥0.2	≤0.25	2.0	3.0	2	1.5	3	2.5	4	2	1.5	3	3	5
≤0	≥0.5	2.0	4.0	2	2.5	3	4	4	2	2.5	3	4	5
0-0.2	≥0.5	↕	↕	2	2.5	↕	4	↕	2	2.5	↕	4	↕
≥0.2	≥0.5	1.5	2.0	2	1.5	2	2.5	3	2	1.5	2	3	4
Flexure critical with: a) in pl. hinge: $s_h>d/3$ or laps; or b) $V_w<3/4M_u/L_s$													
≤0	≤0.25	2.0	3.0	2	1.5	3	2.5	4	2	1.5	3	3	5
0-0.2	≤0.25	↕	↕	2	1.5	3	2.5	↕	2	1.5	3	3	↕
≥0.2	≤0.25	1.0	1.5	2	1.5	3	2.5	3	2	1.5	3	3	4
≤0	≥0.5	1.0	1.5	1.25	1.5	2	2.5	3	1.25	1.5	2	3	4
0-0.2	≥0.5	↕	↕	1.25	1.5	2	2.5	↕	1.25	1.5	2	3	↕
≥0.2	≥0.5	0.5	1.0	1.25	1.5	2	2.5	2	1.25	1.5	2	3	3
Shear critical ($M_u>L_sV_u$) or with bond failure in the span													
$s_h< d/2$		0.3	2.0	1.25	1.5	1.5	2.0	1.75	1.25	2.5	3	3.5	4
$s_h> d/2$		0.3	1.0	1.25	1.5	1.5	2.0	1.75	1.25	2.5	2	3.5	3
Beams with bond failure in joint													
		1.5	3.0	2.0	-	2	-	3		-	3	-	4

Table 3-1: Plastic rotation at ultimate strength, $\theta_{pl,m}$, and at ultimate deformation, $\theta_{pl,u}$, and local behaviour factors m for beams

The seismic rehabilitation guidelines and draft standard give limiting values of the member plastic hinge rotation demands at various performance levels as fractions of the plastic rotation capacity (ultimate value of the plastic rotation), $\theta_{pl,u}$, or of the plastic hinge rotation at ultimate strength (i.e. at maximum resistance), $\theta_{pl,m}$. The values of $\theta_{pl,m}$ and $\theta_{pl,u}$ are listed in the 3rd and 4th column of Tables 3-1 to 3-3. Deformation limits are defined on the basis of these values as follows:

- At the "Collapse Prevention" performance level (CP), the limit to the plastic hinge rotation demand is equal to $\theta_{pl,m}$ (but not greater than $0.75\theta_{pl,u}$) for "primary" components and to $\theta_{pl,u}$ for "secondary" ones.
- At the "Life Safety" performance level, the limit to the plastic hinge rotation demand is taken as 75% of that at "Collapse Prevention" (i.e. a safety margin of 4/3 on plastic hinge rotations).
- At the "Immediate Occupancy" performance level the limiting plastic hinge rotation is that causing visible member damage, but not greater than $0.5\theta_{pl,m}$ (which is rarely controlling).

The values of the local behaviour factor m listed in Tables 3-1 to 3-3 are 75% of the value of the rotation ductility factor corresponding to the above limiting values of plastic hinge rotation, i.e. of 1 plus the ratio of the limiting value to the rotation at yield, (θ_{pl}/θ_y+1). The yield rotation implicit in the m-values in Tables 3-1 to 3-3 are about 0.5% for beams or columns, or approximately 0.25% for walls. As the plastic component of the chord rotation of the shear span is approximately the same as the plastic hinge rotation at the member end, the member chord rotation at yield is implicitly taken equal to the values of 0.5% and 0.25% quoted above. In general these values are on the low side of experimentally measured chord rotations at yield. This difference may not be on the safe side, if member models in the analysis employ an (elastic) stiffness up to the yield point which is closer to reality. Nonetheless, the 0.75 factor applied on (θ_{pl}/θ_y+1) for the calculation of the m-factors – which may be considered as a penalty for the use of the less accurate linear analysis – partly compensates for the low implicit values of θ_y, as effectively it increases these values by 4/3.

Copyright fib, all rights reserved. This PDF copy of fib Bulletin 24 is intended for use and/or distribution only by National Member Groups of fib.

Flexure critical (: $M_u<L_sV_u$) with: a) in pl. hinge: hoop spacing $s_h \le d/3$ & no laps; and b) $V_w \ge 3/4 M_u/L_s$													
ω-ω'	$\frac{M_u}{L_s\sqrt{f_c}b_w d}$ (M N, m)	$\theta_{pl,m}$ (%)	$\theta_{pl,u}$ (%)	M, Primary component IO		LS		CP	m, Secondary component IO		LS		CP
FEMA report:				356	310	356	310	356	356	310	356	310	356
≤0.1	≤0.25	2.0	3.0	2	3	3	5	4	2	3	4	5	5
0.1-0.4	≤0.25	↕	↕	↕	↕	↕	↕	↕	↕	↕	↕	↕	↕
≥0.4	≤0.25	1.5	2.5	1.25	1.5	2	2	3	1.25	1.5	3	2	4
≤0.1	≥0.5	1.6	2.4	2	3	2.4	5	3.2	2	3	3.2	5	4
0.1-0.4	≥0.5	↕	↕	↕	↕	↕	↕	↕	↕	↕	↕	↕	↕
≥0.4	≥0.5	1.2	2.0	1.25	1.5	1.6	2	2.4	1.25	1.5	2.4	2	3.2
Flexure critical with: a) in pl. hinge: $s_h>d/3$ or laps; or b) $V_w<3/4M_u/L_s$													
≤0.1	≤0.25	0.6	1.5	2	1.5	2	2.5	3	2	2	2	3	3
0.1-0.4	≤0.25	↕	↕	↕	↕	↕	↕	↕	↕	↕	↕	↕	↕
≥0.4	≤0.25	0.3	1.0	1.25	1.5	1.5	1.5	2	1.25	1.5	1.5	1.5	2
≤0.1	≥0.5	0.5	1.2	2	1.5	1.6	1.5	2.4	2	2	1.6	3	2.4
0.1-0.4	≥0.5	↕	↕	↕	↕	↕	↕	↕	↕	↕	↕	↕	↕
≥0.4	≥0.5	0.2	0.8	1.25	1.5	1.5	1.5	1.75	1.25	1.5	1	1.5	1.6
Shear critical ($M_u>L_sV_u$) or with bond failure in the span													
$s_h<d/2$ or $v\le0.1$		-	-	-	-	-	-	-	-	-	2	-	3
$s_h>d/2$ & $v>0.1$		-	-	-	-	-	-	-	-	-	1.5	-	2
Beams with bond failure in joint													
$s_h\le d/2$		1.0	2.0	1.25	-	1.5	-	1.75	1.25	-	3	-	4
$s_h<d/2$		0	1.0	1.0	-	1	-	1	1	-	2	-	3
Columns with $v>0.7$													
$s_h\le d/3$ & $V_w\ge3/4M_u/L_s$		1.5	2.5	1	-	1	-	2	1	-	2	-	2
$s_h>d/3$ or $V_w<3/4M_u/L_s$		0	0	1	-	1	-	1	1	-	1	-	1

Table 3-2: Plastic rotation at ultimate strength, $\theta_{pl,m}$, and at ultimate deformation, $\theta_{pl,u}$, and local behaviour factors m for columns

Flexure critical. In boundary elements: $\omega_w\ge0.12$, $\omega_{wx}\ge0.3(A_c/A_o-0.1)$													
ω-ω'+ν	$\frac{M_u}{L_s\sqrt{f_c}b_w d}$ (MN, m)	$\theta_{pl,m}$ (%)	$\theta_{pl,u}$ (%)	m, Primary component IO		LS		CP	m, Secondary component IO		LS		CP
FEMA report:				356	310	356	310	356	356	310	356	310	356
≤0.1	≤0.25	1.5	2.0	2	3	4	5	6	2	3	6	6	8
0.1-0.25	≤0.25	↕	↕	↕	↕	↕	↕	↕	↕	↕	↕	↕	↕
≥0.25	≤0.25	0.9	1.2	1.5	1.5	3	3	4	1.5	1.5	4	4	6
≤0.1	≥0.5	1.0	1.5	2	3	3	5	4	2	3	4	6	6
0.1-0.25	≥0.5	↕	↕	↕	↕	↕	↕	↕	↕	↕	↕	↕	↕
≥0.25	≥0.5	0.5	1.0	1.25	1.5	2	3	2.5	1.25	1.5	2.5	4	4
Flexure critical with: a) in pl. hinge: $s_h>d/3$ or laps; or b) $V_w<3/4M_u/L_s$													
≤0.1	≤0.25	0.8	1.5	2	2	2.5	3	4	2	2	4	4	6
0.1-0.25	≤0.25	↕	↕	↕	↕	↕	↕	↕	↕	↕	↕	↕	↕
≥0.25	≤0.25	0.3	0.5	1.25	1.5	1.5	2	2	1.25	1.5	2	2.5	3
≤0.1	≥0.5	0.6	1.0	1.5	2	2	3	2.5	1.5	2	2.5	4	4
0.1-0.25	≥0.5	↕	↕	↕	↕	↕	↕	↕	↕	↕	↕	↕	↕
≥0.25	≥0.5	0.2	0.4	1.25	1.5	1.5	2	1.75	1.25	1.5	1.5	2.5	2
Shear critical ($M_u>L_sV_u$) or with bond failure in the span													
		NA	NA	2	1.5	2	2.5	3	2	2	2	3	3

Table 3-3: Plastic rotation at ultimate strength, $\theta_{pl,m}$, and at ultimate deformation, $\theta_{pl,u}$, and local behaviour factors m for walls

Copyright fib, all rights reserved. This PDF copy of fib Bulletin 24 is intended for use and/or distribution only by National Member Groups of fib.

The ultimate plastic hinge rotations specified in the seismic rehabilitation guidelines and prestandard are compared here to experimental values from 828 flexure-controlled cyclic tests to failure, on components with or without seismic detailing. In those tests the ratio of yield moment, M_y, to shear span, L_s, is less than the calculated shear strength of the specimen, even after subsequent reduction of shear strength due to cyclic inelastic flexural deformations (expressed through the displacement ductility ratio $\mu_\delta=\theta_u/\theta_y$). FEMA 273 and 356 give values of the ultimate plastic rotation θ_{pl} (which is approximately equal to the total minus the implied yield rotation of 0.005rad in beams or columns, or of 0.0025rad in walls). So for the 828

		$\theta_{uexp}/\theta_{uFEMA}$		$\theta_{plexp}/\theta_{plFEMA}$			$\theta_{uexp}/\theta_{uFEMA}$		$\theta_{plexp}/\theta_{plFEMA}$			$\theta_{uexp}/\theta_{uFEMA}$		$\theta_{plexp}/\theta_{plFEMA}$	
ω-ω'+ν	$V/bd\sqrt{f_c}$ (MN, m) < 0.25					$V/bd\sqrt{f_c}$ (MN, m): 0.25 ÷ 0.5					$V/bd\sqrt{f_c}$ (MN, m) > 0.5				
	n	m	m-σ	m	m-σ	n	m	m-σ	m	m-σ	n	m	m-σ	m	m-σ
BEAMS	conforming stirrups : YES														
<0.0															
0.00-0.25	40	1.25	0.78	1.32	0.91	12	1.28	0.96	1.49	1.15	4	0.72	0.46	0.84	0.61
0.25-0.50	3	3.13	2.95	2.68	2.53										
>0.50															
	conforming stirrups: NO														
<0.0															
0.00-0.25	1	1.28	1.28	1.05	1.05										
>0.25															
COLUMNS	conforming stirrups : YES														
<0.1	3	2.54	1.50	2.36	1.48	52	1.44	0.86	1.43	0.94	98	1.31	0.55	1.34	0.69
0.10-0.25	8	1.43	0.84	1.51	1.00	89	1.48	0.96	1.68	1.12	95	1.14	0.54	1.32	0.69
0.25-0.40	24	1.54	0.53	1.61	0.75	30	1.40	0.37	1.46	0.53	29	1.17	0.37	1.22	0.60
>0.4	14	1.07	0.34	1.15	0.52	26	1.19	0.12	1.16	0.26	3	1.47	0.55	1.50	0.71
	conforming stirrups: NO														
<0.1	8	3.97	3.05	3.48	2.54	39	2.74	1.21	2.48	1.27	27	2.75	0.98	2.48	1.05
0.10-0.25	9	1.57	0.34	1.65	0.75	16	2.27	1.35	2.23	1.31	24	1.51	0.54	1.53	0.72
0.25-0.40	15	1.20	0.51	1.50	0.94	22	1.93	0.66	1.83	0.77	5	1.93	0.95	1.82	1.15
>0.4	11	2.90	1.36	2.49	1.45	4	0.98	0.57	1.06	0.85	5	0.99	0.47	1.17	0.81
WALLS	conforming stirrups : YES														
<0.1	15	0.78	0.35	0.86	0.50	22	1.11	0.59	1.19	0.73	26	0.71	0.50	0.86	0.67
0.10-0.175	3	0.83	0.52	0.86	0.52						6	0.65	0.34	0.69	0.48
0.175-0.25	1	1.73	1.73	1.61	1.61						4	1.00	0.64	1.10	0.64
>0.25						1	0.73	0.73	0.85	0.85					
	conforming stirrups: NO														
<0.1	1	0.52	0.52	0.45	0.45										
>0.1															
Diagonally reinforced	33	1.62	0.82	1.57	0.87										

Note: For beams and columns, "conforming" stirrups means closed stirrups at spacing s_h less than d/3 and resisting at least 75% of the shear force, $V=M_u/L_s$. For walls, it means presence of well-confined boundary elements.

Table 3-4 Statistics of the ratio of experimental ultimate total or plastic (chord) rotation, θ_u or θ_{pl}, to values suggested by FEMA 273 and FEMA 356 (m=mean; σ=standard deviation, n=number of tests)

Copyright fib, all rights reserved. This PDF copy of fib Bulletin 24 is intended for use and/or distribution only by National Member Groups of fib.

cyclic tests to failure Table 3-4 presents separately: a) the ratio of the plastic part, θ_{pl}, of the experimental ultimate chord rotation (total rotation θ_u minus the experimental value of θ_y) to the ultimate plastic hinge rotation in FEMA 356; and b) the ratio of the experimental ultimate chord rotation, θ_u, to the sum of the FEMA 356 plastic rotation, plus an implied yield rotation of 0.005 rad for beams and columns or of 0.0025 rad for walls.

For beams or columns with well-detailed and closely spaced transverse reinforcement (termed "conforming" in Table 3-4), the FEMA values are on average conservative, but not overly so. For columns with poorly detailed or widely spaced transverse reinforcement, the FEMA values are on average very conservative. If the values in FEMA 356 are meant to be mean (m) minus one standard deviation (σ) bounds, then they lie on the unsafe side for well-detailed members, but are closer to reality for poorly detailed beams and columns. For walls, the FEMA values are on the low side, especially if they are meant to represent m-σ values. For diagonally reinforced members, for which test results are available only for well detailed specimens, the FEMA values are on the high side at the level of the mean and slightly unsafe at the m-σ level. The difference may be partly due to the axial load on some of the test specimens, while the FEMA values are quoted for diagonally reinforced coupling beams.

If the FEMA values are meant to represent a m-σ bound, the use of plastic rotations, θ_{pl}, instead of total ultimate rotations, θ_u, makes the FEMA values more consistent with the available data and offers an advantage.

If "secondary" components are not neglected in the analysis but considered with realistic (strength- and stiffness-degrading) models, the limiting or "acceptable" deformations of "primary" components are taken to be the same as in the "secondary" ones, i.e. they are limited by the value of $\theta_{pl,u}$, rather than by that of $\theta_{pl,m}$. If the seismic shear force in "primary" columns, V_S, computed from nonlinear analysis exceeds the concrete contribution to shear strength, V_c, (including the effect of column axial force and displacement ductility demand on V_c), then the column limiting deformation is taken equal to the deformation at which V_c becomes equal to V_S, if the building is assessed at the "Collapse Prevention" performance level, or at 75% of that deformation if assessment is at the "Life Safety" level.

It is noted that verification of the "Collapse Prevention" performance level at the member level alone may lead to very conservative assessments, as redundant structures may survive the loss of one or more of their members without global or even collapse.

3.3.2.7 Masonry infilled RC structures

The seismic rehabilitation guidelines and draft standard do not allow an assessment at the "Collapse Prevention" performance level to count on masonry infills; at that level they require the bare structure to sustain the seismic action after postulated collapse of the infills. Nevertheless, in recognition of the good performance of infilled structures in past earthquakes, the contribution of any infills to strength and stiffness is fully accounted for the "Life Safety" and the "Immediate Occupancy" levels.

In linear analysis procedures infill panels are modelled as diagonal struts, with width and axial stiffness according to Mainstone (1971). Panels with openings are modelled with multiple struts through two opposite corners of the panel and the corners of the openings. Models of the post-ultimate force-deformation behaviour of the struts, for use in nonlinear analyses, need to be fitted to the results of detailed F.E. calculations. Simple expressions for the stiffness, strength and other properties of infill panels with openings are lacking. This is a serious obstacle to the application of nonlinear analysis (which, in its static version, is the most appropriate analysis procedure for this case) to infilled RC structures.

RC members of masonry-infilled structures are modelled and verified as in bare structures, except those around infill panels. Those members may be considered in the analysis as one-dimensional struts or ties and may be verified as deformation-controlled components, by comparing their axial strains (or their axial forces in linear analysis) to strain values which, unless limited due to poorly confined or short splices, are quite high and easy to be fulfilled.

Shear strain (i.e. storey drift) limits are set also for the infill panels themselves at the "Life Safety" performance level. These limits correspond more to infill ultimate strength than to ultimate deformation and are very conservative, as the confinement of infill panels by the surrounding frame allows attainment of very large post-ultimate deformations with little loss in resistance. If the shear strength of the RC structure is about the same as the total shear resistance of the infill panels, the ultimate shear deformation (storey drift ratio) is taken equal

Copyright fib, all rights reserved. This PDF copy of fib Bulletin 24 is intended for use and/or distribution only by National Member Groups of fib.

to 0.8% if the panel is square, or to values by 25% higher or lower, if the length-to-height aspect ratio is equal to 0.5 or 2.0, respectively. As stronger frames offer better confinement and are affected less by a possible loss of infill strength, the above-mentioned infill ultimate deformations are increased or reduced, respectively, by 50% if the global shear strength of the frame exceeds, or is lower than, the aggregate infill strength by more than 30%.

At the "Life Safety" performance level, infill panels are checked against approximately 75% of the infill ultimate deformations above. At the "Collapse Prevention" level they are neglected and for "Immediate Occupancy" they are required not to exceed ultimate strength (m=1).

If a linear analysis procedure is used, infill panels are verified at the "Life Safety" performance level through comparison of their shear strength to the corresponding shear force from the analysis, divided by the value of (the local behaviour factor) m of the infill panel. This value is equal the ratio of the above "acceptable" shear strain of the infill panel at the "Life Safety" performance level, to a shear strain at infill cracking of 0.11%.

The shear strength of an infill panel without openings is taken equal to its horizontal cross-sectional area times the shear strength of bed joints, estimated from in-situ tests or taken equal to conservative default values (0.19MPa, 0.14MPa and 0.09MPa for good-, fair- and poor-quality fully-grouted masonry in running bond, or 60% of these values otherwise).

In recognition of the possibility of local damage in weak RC members surrounding overly strong infills, if the masonry shear strength exceeds 0.35MPa (i.e. 2.5 times the default value for fair- quality fully-grouted masonry in running bond), RC beams and columns surrounding the panel are required to resist, in a force-controlled manner in bending and shear, the infill strut force computed from the analysis (divided by the infill m-factor, if it comes from a linear analysis). This strut force is considered to act not concentrically on the joint but displaced from its face in the direction of the RC member by the strut width according to Mainstone (1971). Alternatively, and if it is more favourable, the length of the beam or column falling within the width of this eccentrically acting strut, is checked in shear as a "captive" member, against a shear force demand equal to the sum of the flexural capacities at its ends divided by its length.

3.3.2.8 Conclusions from the trial application of the NEHRP Guidelines.

The pilot application of the 1997 NEHRP Guidelines in FEMA 273/274 for the seismic assessment and retrofit design of 43 real buildings (eleven of which were concrete buildings) is overviewed in BSSC (1999). Through this application, valuable conclusions were reached regarding the user-friendliness and operationality, the cost-effectiveness and the technical soundness of the Guidelines in each one of the three phases of: a) data collection on material properties, etc., for the as-built structure; b) seismic assessment and design of the retrofitting; and c) execution of the retrofitting.

In all 43 buildings studied in BSSC (1999) the seismic assessment and the design of the retrofitting were also performed following current prevailing US practice. Such practice follows either: a) the special (but conventional, i.e. force-based) codes for seismic assessment and rehabilitation available in some States of the USA, or b) codes for new buildings, appropriately interpreted and adapted for existing buildings (e.g., with lower lateral force requirements, or disregarding certain provisions on structural configuration and regularity, etc.). Two of the 11 concrete buildings (and three out of the 43) were assigned to two engineering firms each. Seven of the 43 building (but only one the 7 being a concrete building) were subjected to two analysis procedures (linear - typically static - and nonlinear static), while three others were analysed with three procedures (linear static, nonlinear static and nonlinear dynamic).

The most important conclusions drawn from the trial application of the 1997 NEHRP Guidelines are summarized below.

Engineers who applied the NEHRP Guidelines found them transparent and technically rational and sound. They commented, though, that casting the 1997 NEHRP Guidelines in a more code-like format and language would improve clarity and user-friendliness. They also encountered difficulties in applying the nonlinear analysis procedures, static or dynamic, due to the lack of reliable and user-friendly software. It should be noted, though, that since the time of these trial applications, the nonlinear static ("pushover") analysis capability has been added to quite a few commercial software packages, notably following the FEMA 273 specifications for lateral load distribution, etc.

Copyright fib, all rights reserved. This PDF copy of fib Bulletin 24 is intended for use and/or distribution only by National Member Groups of fib.

The amount of data collection and material testing required by FEMA 273 in order to allow: a) the use of a capacity factor reduction with a value of 1.0, rather than of 0.75, on component resistances and b) application of nonlinear analysis procedures, was considered onerous and not worthwhile. This finding has led to relaxation of the data collection and material testing requirements in FEMA 356 (ASCE, 2000).

Assessment and retrofit design costs were found to be higher when applying the 1997 NEHRP Guidelines instead of the prevailing current US practice. The cost differential depends strongly on the method of analysis. On average for the 43 buildings the additional cost from the application of the 1997 NEHRP Guidelines is 25%, 70% or 100% of that of current practice, if the linear (equivalent) static, linear (modal) dynamic, or nonlinear static ("pushover") analysis is applied. Nonetheless, the savings in direct construction costs achieved through the less conservative but more sophisticated analysis procedures more than offset the additional design cost. On average for the 43 buildings direct construction cost resulting from the application of the 1997 NEHRP Guidelines exceeds by 70%, or by 18%, the construction cost from prevailing current practice, if the analysis procedure is linear static or linear dynamic, respectively, but is by 7% lower than prevailing practice when the nonlinear static procedure is applied. (It is reminded that prevailing practice in the US also uses linear analysis, typically static, but with a global q-factor, the value of which reflects the feeling of the engineer about the energy dissipation capacity, redundancy and toughness of the existing building). It should be noted, though, that the 1997 NEHRP Guidelines increase retrofit costs not so much due to the more systematic and complete identification and correction of building deficiencies, but mainly due: a) to the inherent conservatism of load effects from linear analysis for the assessment of the foundation and b) to the higher Seismic Hazard levels considered.

Differences in construction cost between the application of the 1997 NEHRP Guidelines and current practice are significantly reduced for the 11 concrete buildings. (Although the number of these building is not large enough to allow reaching conclusions of general validity). In the three concrete frame buildings considered, the 1997 NEHRP Guidelines gave on average 4% less direct retrofitting cost than current US practice. In the five concrete wall buildings they gave a retrofitting cost which was on average 46% higher, whereas in the three infilled frame buildings they gave on average 16% less retrofitting cost (the largest cost differential in favour of the 1997 NEHRP Guidelines among the 43 buildings, possibly due to the fact that these Guidelines take into account, at least partly, the beneficial effects of infills). The differences in construction cost relative to the averages for all construction materials may be partly due to the analysis procedure applied: the (more conservative) linear static procedure was used for 60% of the 43 buildings and of the five concrete wall buildings, as opposed to 50% or one-third of the concrete frame buildings with or without infills, respectively.

The cost-effectiveness of the 1997 NEHRP Guidelines becomes evident if the direct cost of the retrofitting derived from them is compared to the statistical data on seismic retrofit costs for the same type of building and region in the US reported in FEMA 156 (Hart, 1994). The average retrofit cost of the three concrete frame buildings was at the lower 25%-fractile of the FEMA 156 distribution of costs for this type of buildings; the average retrofit cost of the five concrete wall buildings was close to the average cost for that type of buildings according to FEMA 156; the average retrofit cost for the three buildings with infilled concrete frames was well below the lower 25% fractile of the corresponding range in FEMA 156.

Last but not least, in those cases where the assessment and retrofit design of the same building was done independently by two design firms, retrofit cost diffentials of up to 300% were found between the two firms. This finding shows that the judgement and experience of the design engineer may overshadow other factors, including the codes or guidelines used for the assessment and retrofitting.

The findings of the trial application of the NEHRP Guidelines provided the main basis for their revision into the ASCE prestandard FEMA 356 (ASCE, 2000).

3.3.3 The 1998 ASCE Prestandard for seismic evaluation of buildings

3.3.3.1 Introduction

Within the framework of the US effort and documents towards mitigating the seismic risk posed by existing substandard buildings, the Federal Emergency Management Agency (FEMA) issued in 1998 as FEMA Report 310 the "Handbook for the Seismic Evaluation

Copyright fib, all rights reserved. This PDF copy of fib Bulletin 24 is intended for use and/or distribution only by National Member Groups of fib.

Buildings (ASCE, 1998). That document has been prepared by ASCE and currently has the status of a prestandard. It replaces FEMA Report 178: "NEHRP Handbook for Seismic Evaluation of Existing Buildings" as a more technically up-to-date document in line with the philosophy and the procedures of the ground-breaking FEMA 273/274 and 356 Guidelines and Prestandard for Seismic Rehabilitation of Buildings. Currently ASCE is working towards producing an ASCE Standard on the basis of the FEMA 310 ASCE pre-Standard, indended to replace both FEMA 178 and 310 documents. The latest development (in late 2001) was the 4th-ballot version of the ASCE draft standard (ASCE, 2001). As there are some differences between this version and the FEMA 310 "Prestandard", the present overview is based on the provisions of the 4th-ballot version of the ASCE draft Standard. Collectively this document will be termed "Seismic evaluation draft Standard".

The draft Standard for seismic evaluation seems to represent an effort to bridge the gap between the empirical and narrow-scope rapid screening procedures prescribed in the older FEMA documents 154 and 155 ("Rapid Visual Screening of Buildings for Potential Seismic Hazards") and the advanced and elaborate analytical procedures of the Seismic Rehabilitation Guidelines and Prestandard (FEMA 273/274 and 356).

The procedures in the "Seismic Evaluation draft Standard" are addressed to potentially vulnerable buildings (possibly characterized as such after a rapid screening, like the visual one of FEMA documents 154/155). They aim at identifying those buildings which are in real need of a more in-depth evaluation and possibly rehabilitation according to FEMA 273/274 and 356. This is pursued through a multistage approach, structured at three levels or "Tiers": 1, 2 and 3. As in the 1977/1990 Guidelines of the Japan Building Disaster Prevention Association, individual buildings are supposed to be filtered throught the three tiers of evaluation, starting from Tier 1, to screen out those buildings which are not deficient and do not need seismic retrofit.

The difference between the three tiers of the Seismic Evaluation draft Standard is much larger than that exhibited by the three levels of the Japanese Guidelines. Tier 1 is a qualitative screening phase with very little calculations; Tier 2 is normally a phase of analytical evaluation using methods familiar to most practicing engineers, while Tier 3 is a very detailed evaluation phase, with procedures characterized by sophistication and analytical accuracy similar to that of the advanced procedures foreseen in the Guidelines and Prestandard for Seismic Rehabilitation (FEMA 273/274 and 356). As a matter of fact the description of the Tier 3 evaluation procedure in the Seismic Evaluation draft Standard is limited to reference to the Rehabilitation Guidelines and Prestandard, with the only difference being that seismic action effects (e.g. forces) determined according to that latter document may be reduced by 25% for the purposes of evaluation. This reduction of seismic action effects - which does not apply for the retrofit design, in case it is decided at the end of the evaluation to proceed to seismic retrofitting – amounts essentially to removing a perceived conservatism in the design of new buildings or of retrofit measures and granting the "benefit of the doubt" to buildings evaluated as marginally deficient, in view of the high economic burden of seismic retrofitting to individual owners and to the society as a whole. This difference of 25% in seismic action effects is also reflected in the acceptance criteria foreseen for concrete members in the analytical evaluation according to the Tier 2 procedure.

Another important difference with the Rehabilitation Guidelines and Prestandard (FEMA 273/274 and 356) lies in the "Performance Objective" adopted in the Seismic Evaluation draft Standard: Unlike the versatility offered by FEMA 273/274 and 356 in the adoption of various possible "Performance Objectives" consisting of two to four combinations of "Performance Level" ("Operational", Immediate Occupancy", "Life Safety" and "Collapse Prevention") and "Hazard Level" ("Frequent", "Occasional", "Rare", "Very rare" earthquake), in all three tiers of the Seismic Evaluation draft Standard the Performance Objective consists of a single combination of the "Rare" earthquake (defined as two-thirds of the "very rare" – Maximum Considered Earthquake and equivalent to the 475-year earthquake of probabilistic Seismic Hazard analyses) with the "Life-Safety" (for ordinary buildings and occupancies) or the "Immediate Occupancy" (for safety-critical or essential facilities) performance level.

For certain combinations of seismic hazard, performance level, type of structural system and number of storeys, a positive outcome of a Tier 1 evaluation cannot be used to characterize a building as seismically adequate. For these combinations of conditions a complete Tier 2 analytical evaluation of the building is required; then the Tier 1 evaluation may be omitted or used only to gain for insight regarding the deficiencies of the building. The

Copyright fib, all rights reserved. This PDF copy of fib Bulletin 24 is intended for use and/or distribution only by National Member Groups of fib.

conditions under which a full Tier 2 evaluation is necessary are the following:

a) In "low seismicity" regions – defined as those with a 5%-damped spectral acceleration at 1 sec period, S_{a1}, and an Effective Peak Acceleration (EPA) both less than 0.067g - and evaluation for the "Immediate Occupancy" performance level: RC frame buildings (infilled or not) of 3 storeys or more and shear wall buildings of 5 storeys or more.
b) In "high seismicity" regions – defined as those where either S_{a1} or EPA exceed 0.2g – and evaluation at the "Immediate Occupancy" performance level: all RC shear wall and frame buildings (infilled or not) of 4 storeys or more. If evaluation is at the "Life Safety" performance level: all RC frame buildings with masonry infills and 3 or more storeys and all shear wall buildings or frame building without masonry infills and 7 or more storeys.
c) In the intermediate case of "moderate seismicity", if evaluation is at the "Immediate Occupancy" performance level: shear wall buildings with 5 storeys or more and all framed buildings. If evaluation is at the "Life-Safety" performance level, all RC buildings of 7 storeys or more.

The following sections provide a bried overview of the procedures in the Seismic Evaluation draft Standard for Tier 1 or Tier 2 evaluation.

3.3.3.2 Evaluation (Screening) at Tier (Level) 1

Evaluation at the first (Tier 1) level is based on checklists for compliance or not of the building. Three types of structural checklists are provided: a) A special one for regions of "low seismicity" and evaluation at the "Life Safety" performance level; b) a "Basic Structural" checklist for all other combinations of seismicity and of desired performance level, and c) a "Supplemental Structural" checklist which applies in addition to the "Basic" one, always in regions of "high seismicity" but only for evaluation at the "Immediate Occupancy" performance level in those of "moderate seismicity". It is noted that a "Geologic Site Hazard and Geotechnical" and a "Basic Nonstructural" checklist apply also along with the "Basic Structural" checklist. A "Supplemental Nonstructural" checklist exists as well for evaluation at the "Immediate Occupancy" level in "moderate" or "high" seismicty regions.

The "Special Checklist" for "low seismicty" regions is limited to a check of:

- Existence of a complete load path from the masses to the foundation;
- The anchorage of exterior walls in the out-of-plane direction; and
- The possibility of foundation movements endangering structural integrity.

The "Basic Structural" Checklist includes some generally applicable checks, plus some special ones for each predominant type of structural system. The general checks are:

- The existence of a complete load path (as above).
- The structural connection of mezzanines to the lateral-load-resisting system, or their independent bracing.
- The following issues of structural configuration:
  - presence of a "weak storey" (shear strength less than 80% of that of adjacent ones);
  - presence of a "soft-storey" (lateral stiffness less than 70% of that of the storey above or below, or 80% of the mean lateral stiffness of three consecutive storeys above or below);
  - differences in plan dimension from one storey to the next exceeding 30%;
  - vertical elements not continuing to the foundation;
  - differences in storey masses exceeding 50% from one storey to the next;
  - centres of mass and stiffness in a storey which are apart by more than 20% of the storey plan dimension;
  - lack of redundancy, identified with less than two vertical planes of framing or shear walls in each horizontal direction, or with less than two bays per frame if evaluation is at the "Life Safety" performance level, or less than three if it is at the "Immediate Occupancy" one.

In the checks of stiffness regularity, the storey stiffness may be considered as inversely proportional to the product of the square of the storey height and the sum of the average column and beam flexibilities in the storey (defined as the length-to-moment-of-inertia ratio of the column or the beam).

The basic structural checklist includes special checks depending on the type of structural system:

- In shear wall and RC frame buildings without masonry infills, the average shear stress

Copyright fib, all rights reserved. This PDF copy of fib Bulletin 24 is intended for use and/or distribution only by National Member Groups of fib.

in columns and walls should not exceed the contribution of concrete to shear strength, V_c/b_wd, or 0.7MPa, whichever is less. In this check the average shear stress demand is estimated by dividing the elastic base shear by the total cross-sectional area of vertical elements – assuming that exterior columns undertake half the shear force of similar interior ones – divided by an available behaviour factor q, taken equal to 2 for framed and to 4 for wall buildings evaluated at the "Life Safety" performance level; the corresponding values for "Immediate Occupancy" are 1.3 and 2.0. For frame buildings with masonry infills this check refers to the infills and is based on an assumed available q-factor of 1.5. The shear stress limit is 0.5MPa for reinforced masonry or for concrete masonry units and 0.2MPa for clay units.

- In non-infilled RC frames, a check that the value of the normalized axial load, $\nu=N/A_cf_c$, in exterior columns does not exceed 0.1 under the quasi-permanent gravity loads considered to apply simultaneously with the earthquake, or 0.3 under the earthquake alone. Axial force at the base of exterior columns is estimated as the ratio of the elastic overturning moment (elastic base shear times 2/3 of the building height) to the total number of exterior columns on one side and the length of the building parallel to the earthquake direction, divided by the available column local behaviour factor m, taken equal to 2 for evaluation at the "Life Safety" level or to 1.3 for evaluation at the "Immediate Occupancy" one.
- In shear wall buildings, walls should have a steel ratio of at least 0.15% in the vertical direction and 0.25% in the horizontal, and a bar spacing of not less than 450mm. Moreover, the frame system in such buildings - neglected against seismic actions as "secondary elements" – should be capable of sustaining the full gravity loads without the walls.
- Non-infilled frame buildings and shear wall buildings with flexible diaphragms should be not closer than 4% of the (shorter) building height from adjacent buildings, in order to avoid pounding or to reduce its consequences.

Supplemental Structural Checklists for "high seismicity" regions or for the "Immediate Occupancy" performance level in "moderate seismicity" ones, include a few general conditions for buildings with stiff diaphragms namely: a) a lateral-force-resisting system without flat slabs as "primary elements"; and b) "secondary elements" that can resist the shear force calculated for them on the basis of capacity-design considerations (from the flexural capacities of their end sections) if evaluation is at the "Life-Safety" performance level, or with ductile detailing if it is at the "Immediate Occupancy" level. For the diaphragms themselves the conditions include a ban on split-level floors and – only if evaluation is at the "Immediate Occupancy" level – the provision of adequate and well anchored reinforcement next to large openings and at re-entrant corners.

The special Supplemental Structural checklists for different structural systems include:

For RC frames without infills:

- A limit on the use and level of prestressing.
- A ban on columns with slenderness ratio, L/h, less than half of the storey average value for the "Life Safety" performance level, or less than 75% of that value for the "Immediate Occupancy" one.
- Shear resistance in all columns not less than their capacity-design shear force.
- Fulfillment of the strong column-weak beam condition at all joints, with an overstrength factor of 1.2 on beam flexural capacities.
- Two continuous bars at top and bottom of beams and 25% of beam support reinforcement continuing throughout the span.
- Lap splices of at least 35 bar diameters in columns evaluated at the "Life Safety" level, or of at least 50 bar diameters at the "Immediate Occupancy" one, closed by stirrups at 8 bar diameter centres; no lap splices in beam plastic hinge regions or at the outer quarters of the beam span.
- Ties within joints at less than 8 bar diameters centres.
- For evaluation at "Immediate Occupancy", eccentricity of beam axis with respect to that of columns less than 20% of the column width and stirrups with 135°-hooks.

For RC frames with masonry infills the special conditions refer to the out-of-plane stability of infills and to avoidance of captive columns. They include:

- A slenderness limit, L/t, of 9.0 for evaluation at the "Life Safety" level in "high seismicity" regions, of 8.0 for evaluation at the "Immediate Occupancy" level in these

Copyright fib, all rights reserved. This PDF copy of fib Bulletin 24 is intended for use and/or distribution only by National Member Groups of fib.

regions, or of 13 in "moderate seismicity ones".

- A ban on "cavity construction" of walls. (Two independent wythes).
- The requirement of infills continuous to the beam soffit and to both columns surrounding the infill panel.

For shear wall buildings, on top of a condition on the reinforcement of coupling beams above staircases, special requirements apply only for evaluation at the "Immediate Occupancy" level. They include:

- An upper limit of 4.0 on the wall aspect ratio, H/l_w, to limit overturning moments.
- A requirement for well confined boundary elements in walls with H/l_w above 2.0.
- A limit on wall thickness of 100mm or 4% of the unsupported (e.g. storey) height.

Material properties do not need to be inferred from construction documents or tests on samples: default strengths of 14MPa for concrete, 230MPa for steel, 7MPa for masonry in compression and 0.14MPa for shear in bed joints of masonry walls may be used. Non-destructive examination of a sample of elements and their connections is also sufficient for the evaluation of the condition of materials and components.

3.3.3.3 Analytical Evaluation at Tier 2

The analytical evaluation at Tier (level 2) normally needs to be supported by more detailed information on material properties. Although no material sampling and testing is required, information on materials needs to be sought from drawings and construction documents (including tests at the time of construction) and from codes applying at that time.

Normally a "Full building Tier 2 evaluation" is performed. It consists of linear elastic analysis, static or (modal response spectrum) dynamic, following the rules specified for these analysis procedures in FEMA 273/274/356. These rules include considering the effects of natural and of storey accidental torsion (5% of the building plan), the latter amplified by the square of the ratio of the maximum drift on the perimeter of the storey to 1.2 times the average storey drift, if this ratio exceeds 1.0. Analysis results are compared to capacities as in FEMA 273/274/356. For deformation-controlled (ductile) components the check is against the expected strength (1.25 times the nominal, without capacity reduction or material safety factors) times a local behaviour factor m, which assumes values (see Tables 3-1 to 3-3) which are normally higher than those specified by FEMA 273/274/356 for seismic rehabilitation projects. Force-controlled (brittle) components are checked with their nominal (design) strength against capacity-design action-effects, or against conservative estimates of these effects estimated as in FEMA 273/274/356. The foundation is checked in terms of forces, with a local behaviour factor m of 1.5 for the "Immediate Occupancy" level, or of 3.0 for the "Life Safety" one, accounting, among others, for the effect of uplift on forces transmitted to the foundation.

Lateral forces to be used in the linear analysis are based on natural periods calculated from mechanics (from the Rayleigh quotient for static analysis, or from the solution of the eigenvalue problem for a modal response spectrum one). This is unlike the Tier 1 evaluation, where empirical formulas are used for the fundamental period, when its estimation is needed for the rapid numerical checks.

If the building does not fall in the categories listed at the end of the Introduction Section as requiring a full Tier 2 evaluation, then the evaluation at Tier 2 may address only the deficiencies identified during the Tier 1 screening. The deficiencies that may be handled in this may and the necessary course of action are the following:

- For a "weak-storey" situation: the capacity of the storey to resist the elastic shear with a postulated storey behaviour factor m of 2 is checked.
- For vertical elements not continued to the foundation: the diaphragm is checked for its adequacy as an alternative load path and the columns beneath the discontinued element for their capacity against the effects of the overturning moment.
- Adjacent buildings closer than 4% of the shortest building height: the drifts due to the design earthquake are calculated through linear analysis, those of the adjacent building are estimated, the two drifts are combined with the SRSS rule and the outcome is compared to the gap between the two buildings.
- If the frames considered as "secondary members" in shear wall buildings cannot take alone the full gravity load: the gravity load capacity of the shear walls is checked.
- "Secondary elements" that cannot resist the capacity-design shear for the "Life-Safety" performance level, or do not have ductile detailing for the "Immediate Occupancy"

Copyright fib, all rights reserved. This PDF copy of fib Bulletin 24 is intended for use and/or distribution only by National Member Groups of fib.

one, are explicitly checked for their capacity against the calculated seismic demands with the local behaviour factors m listed in Table.

All other deficiency types require a complete linear analysis of the system and a detailed check of all structural elements using the m-factors in Tables 3-1 to 3-3. If there are irregularities of storey mass, geometry or stiffness ("soft storey") exceeding the limits quoted above for Tier 1 evaluation, modal response spectrum analysis is required. If the distance between the storey mass and stiffness centers is more than 20% of the storey plan dimension, the analysis should take into account the natural and the amplified accidental eccentricity. In general, analysis results may be used to check only the elements identified as deficient in the Tier 1 "Basic" or "Supplemental Structural" checklists: a) the columns, walls or infills not satisfying the rough shear or axial stress checks or the wall minimum reinforcement; b) the frame columns identified as short or as not resisting the capacity design shear (to be checked now as force-controlled components); c) the columns identified as weaker than the beams, or the entire storey containing such columns (in both cases checked with a postulated m-factor of 2); d) the flexural capacity of several sections along the span of beams without the minimum required continuous reinforcement (checked now with m=1); e) elements with deficient lap splices (checked with appropriately reduced m-values); f) joints without ties for their (empirically estimated) resistance against shear forces from the analysis.

Failure to satisfy the slenderness limits or the ban on cavity masonry construction of masonry infills included in the "Supplemental Structural" checklists of infilled frame buildings, signals directly the need for a Tier 3 evaluation.

3.3.4 The draft EN version of Eurocode 8, Part 3

3.3.4.1 Introduction

The June 2002 draft-EN of Part 3 of Eurocode 8: "Strengthening and repair of buildings" (CEN, 2002b) has opted for a displacement-based approach, along the main lines of the NEHRP "Guidelines for the Seismic Rehabilitation of Buildings" (ATC, 1997a, b) and of the ASCE "Prestandard for the Seismic Rehabilitation of Buildings" (ASCE, 2000). Similarly to the ENV (CEN, 1996), the EN version covers only the detailed assessment of individual buildings and the design of their retrofitting: preliminary evaluation procedures, as per (ASCE, 2001), or as in Tier 1 of the 1977/1990 Guidelines of the Japan Building Disaster Prevention Association, or in the "initial evaluation procedure" of the 2002 NZ draft Guidelines, are not included.

3.3.4.1 Performance requirements

Three "Performance Levels" (termed, in the European tradition, "Limit States") are introduced:

- The "Near Collapse" (NC) level, corresponding to the "Collapse Prevention" level of the 1997 NEHRP Guidelines and the 2000 ASCE Prestandard.
- The "Significant Damage" (SD) level, corresponding to the "Life Safety" level of the NEHRP Guidelines and the ASCE Prestandard and to the single performance level for which new structures are designed according to most current seismic design codes.
- The "Damage Limitation" (DL) level, corresponding to the "Immediate Occupancy" level of the NEHRP Guidelines and the ASCE Prestandard.

Within the spirit that prevails in the Eurocodes for national determination in all safety-related issues, the "Seismic Hazard" levels for which the three "Performance Levels" above will be required, are specified by competent National Authorities. For ordinary buildings, the recommendation in Part 3 of Eurocode 8 is for a 225yr. (20% in 50 years), a 475yr (10% in 50 years) and a 2475yr. (2% in 50 years) earthquake, for the DL, the SD and the NC "Limit State", respectively. National Authorities will also decide on whether all three "Performance Levels" above will be verified under the corresponding "Seismic Hazard" level, or whether a more limited verification will suffice. Reliability or performance differentiation of essential or large occupancy buildings from ordinary ones is effected through adjustment of their "seismic hazard" level, by multiplying the seismic action with the "importance factor" as in new buildings.

The distinction between elements which are, or are not considered as part of the lateral-force-resisting system ("primary" vs. "secondary" elements) is made as in the 1997 NEHRP Guidelines and the 2000 ASCE Prestandard, with the "secondary" elements collectively

Copyright fib, all rights reserved. This PDF copy of fib Bulletin 24 is intended for use and/or distribution only by National Member Groups of fib.

accounting for not more than 15% of total lateral stiffness and being distributed regularly and uniformly in plan and elevation, so that they don't change the regularity classification of the system. Components characterised in the 1997 NEHRP Guidelines and the 2000 ASCE Prestandard as "deformation-" or "force-controlled", are termed here "ductile" and "brittle" elements, respectively

At the "Damage Limitation" (DL) level, primary components are required to remain elastic (below yielding). At the "Significant Damage" (SD) level, the deformations (chord rotations) of "ductile" components are limited to a certain fraction (75%) of their ultimate deformation capacity, while the force response of "brittle" components is required to remain below a conservative estimate (i.e. a value computed on the basis of partial safety factors) of their force resistance. Finally, at the "Near Collapse" (NC) level "ductile" components are required to remain below their ultimate deformation capacity and "brittle" components below their ultimate strength.

3.3.4.2 Analysis methods

The four methods of analysis foreseen in the June 2002 draft-EN of Part 3 of Eurocode 8 are the same as in the 1997 NEHRP Guidelines and the 2000 ASCE Prestandard. For the definition of the seismic action they all use the 5%-damped response spectrum, or the quantities of interest derived therefrom (namely the target displacement for nonlinear static analysis, acceleration time-histories for nonlinear dynamic analysis).

Linear analysis, static or dynamic, may be used only if it results in internal force demands that nowhere exceed twice the associated (force) capacities. (This should always be the case at the "Damage Limitation" performance level). Moreover, linear static analysis (termed "lateral force procedure") may be applied instead of linear dynamic (modal response spectrum) analysis, if the effects of higher modes are not significant, i.e. only when:

- In both horizontal directions the fundamental period is less than 2 sec and 4 times the transition period T_c between the constant-acceleration and the constant-velocity regions of the spectrum.
- There are no significant irregularities in elevation, i.e. if:
  - The lateral force-resisting systems are continuous to the top of the – relevant part of the – building.
  - Storey mass and stiffness is constant or reduces gradually and smoothly to the top.
  - Individual setbacks are less than 20% of the underlying storey if they are provided symmetrically on both sides of the building, or 10% if they are unsymmetrical, etc.
  - In frame buildings, there is smooth variation of overstrength of the individual storeys relative to the prescribed strength.

When linear analysis is applied, internal forces in "brittle" components are estimated in a "Capacity-design" fashion, i.e. on the basis of equilibrium assuming that "ductile" components delivering force to them develop their overstrength force capacities (except where they don't yield according to the linear analysis, in which case the force demands therefrom are considered to apply at the corresponding locations).

Except as mentioned in the paragraph above, the rules for linear or nonlinear analysis are the same as for new buildings (CEN, 2002a). These rules are biefly reviewed here, for completeness.

Linear static ("lateral force") analysis may use empirical expressions for the fundamental period ($T_1=0.075H^{3/4}$ for RC frames, $T_1=0.05H^{3/4}$ for RC wall buildings, with H=height from base in m). A period calculated from mechanics – e.g. via the Rayleigh quotient – may be used instead (as preferred in European practice), without limiting the outcome relative to the empirical value. If the fundamental period is less than twice the transition period T_c between the acceleration and the velocity-controlled spectral ranges, in buildings with more than two storeys the total lateral force may be reduced by 15% - to account for the difference between the 1st mode mass and the total. The total lateral force is distributed to the storeys following a 1st mode pattern of response accelerations, which may be taken as inverted triangular.

In the response spectrum analysis modal contributions are combined by rigorous application of the SRSS or CQC rules, i.e. at the level of the final seismic action effects of interest (internal forces, displacements, etc.).

Pushover analyses should be performed under two lateral load patterns: one

Copyright fib, all rights reserved. This PDF copy of fib Bulletin 24 is intended for use and/or distribution only by National Member Groups of fib.

corresponding to uniform lateral accelerations and another similar to the lateral forces used in linear static (lateral force) analysis, if applicable, or derived from a modal response spectrum one. The target displacement for pushover analysis is derived according to the N2 procedure by Fajfar and Fischinger (1988).

Nonlinear response-history analysis should use as input at least three artificial, recorded, or simulated records (or pairs of different records, for analysis in 3D), the mean elastic spectrum of which in the period range from $2T_1$ to $0.2T_1$ should not fall below the target spectrum by more than 10%. The results of nonlinear dynamic analyses are averaged, if at least seven such analyses are performed; otherwise the most unfavourable results in the analyses performed are used.

In buildings which are regular in plan, two independent 2D models may be used for the analysis of the response to the two horizontal components of the seismic action. A building may be identified as regular-in-plan, prior to any analysis, if it has:

- Rigid diaphragms, nearly rectangular in plan (re-entrant corners reducing floor area by not more than 5% each), with aspect ratio less than 4.
- Eccentricity between the storey centres of mass and stiffness less than 30% of the corresponding torsional radius (square root of ratio of torsional to lateral stiffness, with stiffness parameters estimated in most cases from the moments of inertia of vertical elements).
- Torsional radius less than the radius of gyration of the floor plan.

Two separate 2D models may also be used for buildings of ordinary importance with: a) height less than 10m; b) storey centres of mass and stiffness approximately on (two) vertical lines; and c) in both horizontal directions torsional radius not less than the SRSS of the radius of gyration of the floor in plan and of the projection of the eccentricity between centers of mass and stiffness in that direction. If conditions a) and b) are fulfilled, but not condition c), then two separate 2D models may still be used, provided that all seismic action effects from the 2D analyses are increased by 25%.

Regardless of whether they are computed via a single 3D or two separate 2D models, seismic action effects due to the individual horizontal components are combined through the SRSS rule, or via the 1:0.3 rule. Maximum values of action effects estimated individually through the SRSS rule may be conservatively assumed to take place at the same time. More accurate and less conservative rules may be introduced at the national level for estimation of the likely simultaneous values of action effects due to the different components of the seismic action. In buildings regular in plan, with independent lateral-force-resisting systems in the two directions consisting solely of walls, the effects of the two horizontal components do not need to be combined.

Accidental eccentricity is taken equal to 5% of the perpendicular plan dimension, without amplification due to torsional-lateral coupling. For linear analysis, its effects may be calculated statically, by applying storey torsional moments to a 3D structural model, even when the modal response spectrum method is used for the analysis of the response to the two horizontal components. The effects of accidental eccentricity may be accounted for in a simpler and conservative way by amplifying the results of the – linear static or dynamic, or nonlinear static – analysis for each horizontal component by $1+0.6x/L$, with x denoting distance of the element of interest from the centre in plan and L the plan dimension, both normal to the direction of the seismic action. In structures regular in plan and analysed with two separate 2D models, the factor 0.6 is replaced by 1.2. Amplification of eccentricities between centres of mass and stiffness is not required.

The elastic stiffness used in linear analysis should be the secant stiffness to yielding; it may be taken as half of the uncracked stiffness of the gross concrete section. Nonlinear analysis may use this value as pre-yield stiffness (pre- and post cracking stiffnesses may be considered also, if so-desired), and may neglect the effect of strain hardening on post-yield stiffness. (Post-yield stiffness should be taken negative, if significant strength degradation develops).

The requirement on hysteresis rules to be used in nonlinear response-history analysis is just to reflect realistically energy dissipation within the expected range of displacement amplitudes. Nonlinear element models should be based on mean values of material properties, which are higher than nominal values.

For linear analysis global displacements are generally calculated on the basis of the equal displacement rule. Allowance is made for more accurate calculation, including the q-μ-T

Copyright fib, all rights reserved. This PDF copy of fib Bulletin 24 is intended for use and/or distribution only by National Member Groups of fib.

relation by Vidic et al, 1994, given for the target displacement for pushover analysis. Interstorey drifts δ determined thereafter are used for the estimation of P-Δ effects as a ratio to 1st-order ones. If the ratio $\theta=P\delta/Vh$ exceeds 0.1 in any storey, 1st-order analysis results are divided by $1-\theta$.

3.3.4.4 Information for the assessment

Similarly to the NEHRP "Guidelines for the Seismic Rehabilitation of Buildings" (ATC, 1997a, b) and the ASCE "Prestandard for the Seismic Rehabilitation of Buildings" (ASCE, 2000), depending on the amount and reliability of the information available for the as-built structure, the partial safety factors used in the calculation of member capacities are adjusted and limitation on the analysis method to be applied are posed.

The reference case regarding the available information is that of "normal knowledge". It entails knowledge for the structural geometry and the amount and detailing of its reinforcement, which is sufficient for building a detailed structural model for either linear or nonlinear analysis. It includes knowledge of member lengths, cross-sectional dimensions and reinforcement from original construction drawings, confirmed through in-situ spot checks. Material properties are derived either from the original specifications and construction drawings, spot-verified in situ, or through limited in situ sampling and tests. For this level of knowledge either linear or nonlinear analysis may be used; the values adopted for the partial safety factors are those used for the design of new structures.

The case of "limited knowledge" involves information sufficient for building a structural model only for linear analysis. It corresponds to a situation in which original construction drawings and specifications are not available and recourse has to be made to in situ measurements of member lengths and cross-sectional dimensions (such information may also be available from original construction drawings and in-situ spot checks for confirmation). There is no information on the amount and detailing of the reinforcement or the originally specified materials. Knowledge of the applicable codes and the prevailing practice at the time of construction is used to base default assumptions for the materials employed and to estimate the amount of reinforcement from a simulation of the original design (to be confirmed through spot checks). This level of knowledge may support only linear analysis (implying that the structure assessed has sufficient force capacity to remain nearly elastic under all seismic action levels considered in the assessment). Increased values of partial safety factors are adopted, relative to those used for the design of new structures.

At the other extreme, the case of "full knowledge" includes knowledge of member lengths, cross-sectional dimensions and reinforcement either from a comprehensive and in depth survey of the structure and exposure of the reinforcement, or from detailed original construction drawings, confirmed through in-situ spot checks. Material properties are derived either from test reports at the time of construction, verified through sample checks in situ, or from a comprehensive and extensive campaign of in situ tests, material sampling and lab tests. For this level of knowledge linear or nonlinear analysis may be applied with a higher level of reliability and reduced values of the partial safety factors may be adopted, relative to those used in design of new structures.

3.3.4.5 Design of the retrofitting

Unlike the other regulatory-type documents overviewed herein, the June 2002 draft-EN of Part 3 of Eurocode 8 provides not only general guidance for the conceptual design of the retrofitting, but also detailed dimensioning rules for RC members strengthened through steel, FRP or concrete jackets, etc., including expressions for the resistance and the deformation of retrofitted elements at yielding and at ultimate deformation capacity. These expressions bear strong similarities with those given in Chapter 5 of the present report.

3.3.5 Alternative assessment on the basis of member chord rotations

3.3.5.1 Introduction

Another approach is presented here for displacement-based seismic assessment of RC buildings (Fardis, 1998a, 1998b, 2001, Panagiotakos et al, 2002). The method comprises estimation of peak inelastic chord rotation demands at the ends of RC members under the seismic action and comparison with the corresponding capacities. Chord rotation at member

Copyright fib, all rights reserved. This PDF copy of fib Bulletin 24 is intended for use and/or distribution only by National Member Groups of fib.

ends is a very convenient measure of both demand and capacity: in linear analysis, as well as in the simplest and most common element model for nonlinear analysis, namely the lumped inelasticity model, chord rotation is the primary output variable for member deformations; regarding capacity and its quantification, it is reminded that experimental data for deformations are typically available in the form of specimen tip deflection or drift ratio, i.e. essentially of chord rotation at the end where moment is maximum. The use of chord rotation, rather than of displacement ductility factor or plastic hinge rotation, bypasses estimation of deformations at yielding, thus avoiding one additional source of uncertainty.

For the estimation of both demands and capacities, best estimates (mean values) of the as-built material properties are used.

Mean or 95%-fractile values of seismic chord rotation demands, θ_{Em} and $\theta_{Ek,0.95}$, are estimated for the seismic action of interest, and compared with mean or 5%-fractile values of the chord-rotation capacity, θ_{um} and $\theta_{uk,0.05}$, with a safety factor, γ, depending on the target safety margin for the verification of the performance level of interest.

3.3.5.2 Estimation of seismic chord rotation demands at member ends

Estimation of chord rotation demands under the seismic action of interest is based on the fact that RC structures without masonry infills typically have an effective predominant period of response to strong ground motions in the velocity-controlled part of the response spectrum, where the equal displacement rule between elastic and inelastic SDOF systems applies well. Then member chord rotations may be estimated from a 5%-damped linear elastic analysis, either static with inverted triangular distribution of lateral forces, or modal response spectrum (dynamic). Results of such elastic analyses represent on average well the peak inelastic demands, θ_{Em}.

Alternatively, chord rotation demands may be estimated from a nonlinear static (pushover) analysis, carried up to a top (or a work-equivalent) displacement of the building given by the 5%-damped elastic spectrum at the fundamental period T_1. Either the top displacement δ_{top}, or a work-equivalent displacement, defined as $\delta_{eq} = \sum m_i \delta_i^2 / \sum m_i \delta_i$ (with δ_i denoting horizontal displacement of mass m_i), may be used to establish the correspondence between inelastic chord-rotation demands at member ends and the seismic action of interest, described via its elastic 5%-damped spectrum.

For these two approaches to yield good estimates of inelastic chord rotation demands, the structure should be considered in the analysis with member elastic rigidity equal to the secant rigidity of the RC member at yielding of both ends in antisymmetric bending, i.e. as:

$$EI = M_y L / 6\theta_y \tag{3-19}$$

In general four values of EI are computed in this way, considering positive or negative bending at each end, and averaged into a single EI-value. The yield moment M_y can be computed from first principles. The chord rotation θ_y at yielding is computed via eq. (5-2) of this report (quoted also in column 3 of Table 4-2), accounting for flexural and shear deformations and for bond slip of the bars. As noted in sections 5.3.3.4, 5.3.4.3 and 5.3.4.3 of this report, for RC members repaired through epoxy injection or strengthened with concrete jackets, the yield moment M_y and the chord rotation θ_y at yielding (and hence EI) may be obtained by applying multiplicative factors on the corresponding quantities computed as if the member were monolithic.

The above version of the equal displacement rule was developed by Panagiotakos and Fardis (1999) on the basis of about 1500 nonlinear dynamic analyses of several fairly regular bare RC frame or dual structures, from 3 to 12 storeys, designed to the ENV versions of Eurocodes 2 and 8 and to different combinations of peak ground acceleration and Ductility Class, as well as to different versions of capacity design of columns in bending. Peak inelastic chord rotations computed at member ends from these analyses were divided by the corresponding elastic values obtained from a linear static or modal response spectrum analysis using the 5%-damped elastic spectrum. The ratio of these values seems relatively insensitive to the details of the structural configuration (at least for fairly regular geometries) and to the intensity of ground motion (from the design earthquake to about twice that level). The

Copyright fib, all rights reserved. This PDF copy of fib Bulletin 24 is intended for use and/or distribution only by National Member Groups of fib.

inelastic-to-elastic chord rotation ratio depends systematically on the type of element (horizontal or vertical), its elevation in the structure and the type of elastic analysis procedure used. Table 3-5 presents means and 95%-fractiles of this ratio for chord rotations and displacements, top or equivalent (mean). If one wants to keep in mind only one representative value for the mean and one for the 95%-fractile, these values are 1.07 and 1.53 respectively for chord rotations, 0.97 and 1.12 for top drifts, or 1.03 and 1.34 respectively for mean drifts (roughly 1.0 and 1.5 for chord rotations, 1.0 and 1.25 for drifts).

	Beam chord rotation				Column or wall chord rotation				Displacement			
	Mean		95%-fractile		Mean		95%-fractile		Mean		95%-fractile	
	Stat.	Dyn.	Stat.	Dyn.	Stat.	Dyn.	Stat.	Dyn.	Stat.	Dyn.	Stat.	Dyn.
roof	1.2	1.25	1.85	1.7	1.15	1.0	1.9	1.65	0.85	1.02	1.04	1.21
base	1.0	1.2	1.35	1.65	0.9	0.85	1.1	1.05	-	-	-	-
mean	1.11	1.22	1.59	1.67	1.04	0.92	1.51	1.35	1.06	1.0	1.35	1.33

Table 3-5: Mean and 95%-fractile building-averages of inelastic-to-elastic chord rotation and drift ratio

Beams		Existing columns (assessment)				Upgraded columns (redesign)			
		Bottom		Top		Bottom		Top	
mean	95%-fract.	mean	95%-fract.	mean	95%-fract.	mean	95%-fract.	mean	95%-fract.
0.7	1.0	0.95	1.2	1.2	1.8	0.7	0.9	0.8	1.35

Table 3-6: Inelastic-to-elastic chord rotation ratio in open-ground-storey of partially infilled buildings

The conclusions above were derived for new RC structures, which typically satisfy the strong-column/weak beam rule of capacity design. Nevertheless, the nonlinear analyses on which these results were based exhibit plastic hinging and inelastic deformations both in columns and beams. For this reason the conclusion above (namely that an elastic analysis using the 5%-damped spectrum and the secant-to-yield stiffness of all members in antisymmetric bending, can be used to estimate member peak inelastic chord demands) is expected to hold also for existing structures without significant engineered earthquake resistance, under ground motions inducing overall ductility demands significantly higher than 1.0. It is also expected to hold even better for a retrofitted structure, which will have a more uniform distribution of inelasticity. Detailed numerical results may differ from those in Table 1, if there is strong tendency for concentration of inelasticity in a single storey. For such cases nonlinear static (pushover) analysis may be used, with target displacement (at the top or work-equivalent mean displacement) obtained from a linear-elastic 5%-damped analysis and the modification factors from the last four columns of Table 3-5.

Old RC buildings are often infilled in all storeys except the bottom one. Ground storey columns are normally not designed for the concentration of inelastic seismic deformations expected there. Several thousands nonlinear dynamic analyses of partially infilled multi-storey buildings led to the conclusion that peak inelastic chord rotations at the ends of ground storey beams and columns may be estimated from the 5%-damped spectrum and an equivalent static analysis of the elastic structure, with the infills in all infilled storeys modelled as rigid diagonal struts, by applying the factors of Table 3-6.

For single-storey planwise-regular RC structures, infilling reduces inelastic displacement demands without affecting much the predominant period of nonlinear response to strong motions. Chord rotations of RC members can be computed from an equivalent static elastic analysis of the bare structure, considering a higher damping ratio due to the infills (Fardis, 1996):

$$\xi(\%) = 5 + (2.5 + 5T_{fr} - 5T_{fr}^2)f_u \qquad (3\text{-}20)$$

In eq. (3-20) T_{fr} denotes the natural period of the bare frame with the secant stiffness of all its members in antisymmetric bending and f_u the total shear strength of the infills in the story, normalised by the base shear of a rigid structure with the same mass, ma_g (a_g=peak ground acceleration). The increase in damping can be effected by multiplying results obtained for 5%

Copyright fib, all rights reserved. This PDF copy of fib Bulletin 24 is intended for use and/or distribution only by National Member Groups of fib.

damping by $\sqrt{7/(2+\xi)}$. For structures with more (uniformly infilled) storeys, this procedure significantly overestimates peak inelastic chord rotations, especially in the upper storeys.

Nonlinear static (pushover) analysis may also be used for the estimation of chord rotation demands in fully or partially infilled RC buildings, including the members of an open ground storey. For improvement over the linear-elastic procedure described so far, the nonlinear static analysis should also include the infills as nonlinear diagonal compression struts. The target top displacement can still be estimated from the 5%-damped elastic spectrum according to the last four columns of Table 3-5.

The nonlinear static (pushover) analysis has an advantage over linear analysis, static or dynamic, as far as estimation of internal forces. Internal forces are important for the brittle (or force-controlled) failure modes and elements, e.g. in shear-critical members and beam-column joints. Moreover, the chord rotation capacity of columns or walls, as well as the value of their yield moment and effective stiffness, depend on their axial force N. If linear analysis is used for the estimation of deformation demands according to Tables 3-5, 3-6, internal forces for brittle failure modes should be estimated on the basis of the available member longitudinal reinforcement and of equilibrium, as in capacity design calculations.

3.3.5.3 Deformation capacity and verification of members and joints

At the "Immediate Occupancy" performance level, member chord rotation demands θ_E (mean or 95%-fractile values) should be compared to the corresponding mean chord rotation at yielding, given by eq. (5-2) of this report (quoted also in column 3 of Table 4-2).

At the "Life Safety" or the "Collapse Prevention" performance level, mean or 95%-fractile values of member chord rotation demands are compared to the corresponding - factored by γ - capacity, i.e. to the ultimate chord rotation, θ_u of the member under cyclic loading.

For flexure-controlled beams, columns or walls, eq. (4-6) or (5-12) of this report was fitted to the results of a very large database of monotonic or cyclic tests to failure. This expression should be applied with $a_{cyc} = 1$ (cyclic loading) and $a_{sl} = 1$ (slippage of bars in the anchorage zone beyond the member end).

For flexure-critical members without seismic detailing, the right-hand-side of eq. (4-6) or (5-12) should by multiplied by a correction factor k_u of 0.85.

The ultimate chord rotation given by eq. (4-6) or (5-12) (with the correction above for members without seismic detailing) is considered as an expected value and denoted by θ_{um}. Due to the large scatter, in the verification of chord rotations the lower characteristic value (5%-fractile) of the deformation capacity is used instead of θ_{um}. This 5%-fractile is equal to:

$$\theta_{uk,0.05}=0.4\theta_{um} \tag{3-21}$$

Then the verification of flexure-controlled members at the "Life Safety" or the "Collapse Prevention" performance level is:

$$\gamma\theta_{Ek,0.95}\leq\theta_{uk,0.05} \tag{3-22}$$

with γ: safety factor against exhaustion of member deformation capacity at the performance level of interest.

If the demand value θ_E is derived from a linear-elastic analysis, the modification factors for mean or 95% chord rotations from Tables 3-5, 3-6 should be applied to it. If derived from pushover analysis, it only needs to correspond to the mean or 95%-fractile value of top or equivalent (mean) drift, obtained by applying to the 5%-damped elastic displacement the multiplicative factors in the last columns of Table 3-5.

As noted in sections 5.3.3.4, 5.3.4.3 and 5.3.4.3 of this report, the procedure above may be applied also to RC members repaired through epoxy injection or strengthened with concrete jackets, by applying multiplicative factors on the member ultimate chord rotation computed through eq. (4-6) or (5-12) considering the member as monolithic.

The database from which eq. (4-6) or (5-12) for θ_u was derived includes elements with shear span ratio, M/Vh, as low as 1.5, but does not contain shear-critical members, in which

Copyright fib, all rights reserved. This PDF copy of fib Bulletin 24 is intended for use and/or distribution only by National Member Groups of fib.

sometime during the cyclic response the nominal flexural capacity M_u exceeds L_s times the nominal shear capacity, V_R, as this decreases with the cyclic flexural ductility ratio, $\mu_\theta=\theta/\theta_y$. The possibility of pre-emptive shear failure should be evaluated separately, as development of the chord rotation capacity θ_u at member ends presupposes that the member does not fail earlier in shear.

Assessment of members in shear is based on the verification that maximum shear force during the response, $V_{E,max}$, does not exceed shear capacity, V_R:

$$V_{E,max} \leq V_R \tag{3-23}$$

Eq. (4-13) or eq. (4-14) of this report provides V_R as a function of plastic chord rotation ductility demand, $\mu_\theta^{pl}=\theta^{pl}/\theta_y$, ($\theta^{pl}=\theta-\theta_y$) at the member end where shear is checked. These expressions were fitted to 154 cyclic tests, carried up to shear-controlled failure (some of which on specimens with old detailing). For the purposes of the verification through eq. (3-23), partial safety factors may be applied in the calculation of the value of V_R.

If the analysis is nonlinear static (pushover) the acting shear force $V_{E,max}$ is the "actual" value from the analysis, taking into account the simultaneously acting transverse loads, $g+\psi_2 q$ (for beams). Then shear can be checked at any step of the analysis, using the current values of V_E on one hand, and of $\mu_\theta^{pl}=(\theta-\theta_y)/\theta_y$ and N in eq. (4-13) or eq. (4-14) on the other. If the analysis is linear (static or dynamic), in the nonlinear regime $V_{E,max}$ and N are overestimated. Then $V_{E,max}$ at end i may be estimated as:

$$V_{E,max,i} \approx V_{g+\psi_2 q,oi} + \frac{M_{yi}^- + M_{yj}^+}{l_n} \tag{3-24}$$

In eq. (3-24) $V_{g+\psi 2q,oi}$ is the shear force at end i due to the simultaneously acting transverse loads, $g+\psi_2 q$, considering the member as simply-supported; l_n is the member clear length; M_{yi}^-, M_{yj}^+ the yield moments at ends i and j, considering for beams tension at the top at end i and at the bottom at j (in symmetrically reinforced columns or walls the value of M_y is independent of its sence of action).

In columns the shear resistance V_R and the values of M_{yi}, M_{yj}, in eq. (3-24) should be based on consistent values of the axial force N. As both the demand, $V_{E,max}$, and the supply, V_R, increase with N, it makes sense to neglect the fluctuation of N during the seismic response and to use in both places its value $N_{g+\psi 2q}$ due to gravity loads alone. The alternative would be to check eq. (3-24) for two extreme values of N: a) the value at the balance point of the M-N interaction diagram of the column (where the column yield moments, M_{yi} and M_{yj} and hence $V_{E,maxi}$, attain their maximum values) and b) the value N=0 for which the component of shear resistance due to N vanishes. This alternative makes sense for exterior columns, in which the fluctuation of the axial force during the seismic response is large. Another alternative for these columns is to base the calculation of M_{yi}, M_{yj} and V_R on the two extreme values of axial force resulting from the capacity design shears, $V_{E,max}$, of the beams framing into the column in all storeys above, computed according to eq. (3-24) but with a + or – sign on the 2nd term, depending on which side of the column the beam frames into, and on whether an unfavourable effect is produced or not. This alternative produces extreme results only in exterior columns and even more so in corner ones, where the beams framing into the column in the two horizontal directions should be taken to produce capacity design shears either both upwards or both downwards.

Slippage of beam or column bars within joints contributes with a fixed-end rotation to the chord rotation at member ends. In the proposed procedure this fixed-end rotation is taken into account directly: a) in the calculation of θ_y via eq. (5-2) of this report (reducing the member effective rigidity, $EI=M_yL/6\theta_y$) and b) in the increase in member chord rotation capacity by

Copyright fib, all rights reserved. This PDF copy of fib Bulletin 24 is intended for use and/or distribution only by National Member Groups of fib.

taking a_{sl} = 1.0 in the expression for the ultimate chord rotation, eq. (4-6) or (5-12). In addition to contributing to these effects, beam-column joints develop very high shear forces (and stresses) in their core, running the risk of preemptive shear failure. This is more so in existing RC buildings, which typically have no shear reinforcement in the core of beam-column joints. Such joints should be verified in shear and strengthened, if necessary.

In the proposed procedure the approach outlined previously in this chapter, namely eqs. (3-1) to (3-10) in (4) of 3.2.2.5, is applied for checking beam-column joints in shear. Joints satisfying eq. (3-9) do not need to be retrofitted. Nonetheless, placement of horizontal hoops in column jackets around the joint core to take the full horizontal joint shear, V_{jh}, will control any diagonal cracking that develops when the limit v_c of eq. (3-9) is exhausted. If, however, diagonal compression failure is identified through eq. (3-10), the (horizontal) dimensions of the joint will need to be increased, to reduce the value of v_j below the limit of eq. (3-10), without increasing the longitudinal reinforcement of the most critical (weakest) elements framing into the joint, to avoid increasing the joint shear force demand, V_{jh} or V_{jv}.

References

Aoyama, H., 1981, A method for the evaluation of the seismic capacity of existing reinforced concrete buildings in Japan, Bulletin of the New Zealand National Society for Earthquake Engineering, Vol. 14, No.3, 105-130.

ASCE, 1998. Handbook for the seismic evaluation of buildings – A prestandard. prepared by American Society of Civil Engineers for the Federal Emergency Management Agency (FEMA Report 310), Reston, Va.

ASCE, 2000. Prestandard for the seismic rehabilitation of buildings. Prepared by American Society of Civil Engineers for the Federal Emergency Management Agency (FEMA Report 356), Reston, Va.

ASCE, 2001. Seismic evaluation of existing buildings. ASCE draft Standard, 4th Ballot, American Society of Civil Engineers, Reston, Va.

Ascheim, M.A. and Moehle, J.P. 1992. Shear strength and deformability of RC bridge columns subjected to inelastic cyclic displacements. Univ. of California, Earthq. Engng. Res. Center, Rep. UCB/EERC-92/04, Berkeley, Ca.

ATC, 1997a. NEHRP Guidelines for the seismic rehabilitation of buildings. Applied Technology Council, for the Building Seismic Safety Council and the Federal Emergency Management Agency (FEMA Report 273), Washington, D.C.

ATC, 1997b. NEHRP Commentary on the guidelines for the seismic rehabilitation of buildings. Applied Technology Council, for the Building Seismic Safety Council and the Federal Emergency Management Agency (FEMA Report 274), Washington, D.C.

Bommer, J.J., Elnashai, A.S., Chlimintzas, C. and Lee, D., 1998. Review and development of spectra for displacement-based seismic design. Research Report ESEE/98-3, Engineering Seismology and Earthquake Engineering Section, Imperial College, London, UK.

Borzi, B., Elnashai, A.S., Faccioli, E., Calvi, G.M. and Bommer, J.J., 1998. Inelastic spectra and ductility-damping relationships for displacement-based seismic design. Research Report ESEE/98-4, Engineering Seismology and Earthquake Engineering Section (joint report with Politenico di Milano, Italy), Imperial College, London, UK.

BSSC, 1999. Case studies: An assessment of the NEHRP guidelines for the seismic rehabilitation of buildings. Prepared by the Building Seismic Safety Council for the Federal Emergency Management Agency (FEMA Report 343), Washington, D.C.

BSSC, 2001. NEHRP recommended provisions for seismic regulations for new buildings and other structures. 2000 Edition, Building Seismic Safety Council for the Federal Emergency Management Agency (FEMA Rep. 368, 369), Part 1: Provisions (FEMA Report 368) 374p; Part 2: Commentary (FEMA Report 369) p.444, Washington, D.C.

Calvi, G.M. and Pavese, A. 1995. Displacement based design of building structures. Proc. of the Fifth SECED Conference on European Seismic Design Practice, Chester, UK, edited by A.S. Elnashai, pp. 127-132, Balkema, Rotterdam.

CEB 1983. CEB Bulletin 162 - Assessment of concrete structures and design procedures for

Copyright fib, all rights reserved. This PDF copy of fib Bulletin 24 is intended for use and/or distribution only by National Member Groups of fib.

upgrading (Redesign). Comité Euro-International du Béton, Lausanne.
CEB, 1997. CEB Bulletin 236 - Seismic design of reinforced concrete structures, Chapter 6: Assessment of existing buildings. Comité Euro-International du Béton, Lausanne, pp. 159-204
CEN, 1996. European prestandard ENV 1998-1-4:1996: Eurocode 8: Design provisions for earthquake resistance of structures. Part 1-4: Strengthening and repair of buildings. Comite Europeen de Normalisation, Brusells.
CEN, 2002a. Draft European Standard prEN 1998-1: Eurocode 8: Design of structures for earthquake resistance. Part 1: General rules, seismic actions and rules for buildings. Revised Final Project Team Draft (preStage 49), Doc. CEN/TC250/SC8/N317, Comite Europeen de Normalisation, Brusells.
CEN, 2002b. Draft European Standard prEN 1998-3: Eurocode 8: Design of structures for earthquake resistance. Part 3: Strengthening and repair of buildings. Draft No.2. Doc. CEN/TC250/SC8/N306. Comite Europeen de Normalisation, Brusells.
Chopra, A.K. and Goel, R.K. 2000a. Capacity-demand diagram methods based on inelastic design spectrum. 12th World Conference on Earthquake Engineering, Paper No. 1612, Acapulco, Mexico.
Chopra, A.K. and Goel, R.K. 2000b. Evaluation of NSP to estimate seismic deformation: SDF systems. Journal of Structural Engineering, Vol. 126, No. 4. pp. 482-490.
Chopra, A.K. and Goel, R.K. 2001. Direct displacement-based design: use of inelastic vs. elastic design spectra. Earthquake Spectra, Vol. 17, No. 1, pp. 47-64.
Chopra, A.K., Goel, R.K. and Chintanapakdee, C. 2001. Statistics of SDF-system estimate of roof displacement for pushover analysis of buildings. PEER Report 2001/16, Pacific Earthquake Engineering Research Center, College of Engineering, University of California, Berkeley.
Fajfar, P. and Fischinger, M. 1988. N2 - a method for nonlinear seismic analysis of regular RC buildings. Proc. 9th World Conference in Earthquake Engineering, Tokyo-Kyoto, Vol. V, pp.111-116.
Fajfar, P. 1999. Capacity spectrum method based on inelastic demand spectra. Earthquake Engineering and Structural Dynamics, Vol. 28, pp.979-993.
Fajfar, P. 2000. A nonlinear analysis method for performance-based seismic design. Earthquake Spectra, Vol. 16, No. 3, pp.573-592.
Fardis, M.N. (editor). 1996. Experimental and numerical investigations on the seismic response of RC infilled frames and recommendations for code provisions, ECOEST/PREC8 Report No.6, Laboratorio Nacional de Engenharia Civil Publications, Lisbon, 199p.
Fardis, M.N. 1998a. Assessment of resistance of RC structures to lateral loads, Proceedings, Centro Internazionale di Aggiornamento Sperimentale-Scientifico, International Seminar "Evoluzione Nella Sperimentazione per le Costruzioni, Corinth (GR).
Fardis, M.N. 1998b. Seismic assessment and retrofit of R/C structures, Invited Lecture, Proc. 11th European Conference on Earthquake Engineering, Paris. .
Fardis, M.N. 2001. Displacement-based seismic assessment and retrofit of reinforced concrete buildings, Proc. 20th European Regional Earthquake Engineering Seminar, European Association of Earthquake Engineering, Sion (CH).
Freeman, S.A. 1978. Prediction of response of concrete buildings to severe earthquake motion. Douglas McHenry International Symposium on Concrete and Concrete Structures, ACI SP-55, American Concrete Institute, Detroit, MI. pp.589-605.
Hart, G. 1994. Typical costs for seismic rehabilitation of buildings, Volume 1: Summary. Prepared by G. Hart Consultant Group for the Federal Emergency Management Agency (FEMA Report 156), Washington D.C.
Hirosawa, M., Sugano, S. and Kaminosono, T., 1995, Essentials of current evaluation and retrofitting for existing and damaged buildings in Japan, Japan International Cooperation Agency, Tsukuba International Center, Tsukuba-shi, Ibaraki-ken.
Japan Building Disaster Prevention Association, 1977. Standard for evaluation of seismic capacity and guidelines for seismic retrofit design of existing reinforced concrete buildings. (in Japanese, revised in 1990).
Japan Building Disaster Prevention Association, 1996. Law for promotion of seismic srengthening of existing reinforced concrete structures and related commentary. (in Japanese).

Copyright fib, all rights reserved. This PDF copy of fib Bulletin 24 is intended for use and/or distribution only by National Member Groups of fib.

Krawinkler, H. 1994. New trends in seismic design methodology. Proc. 10th European Conference in Earthquake Engineering, Vienna, Vol. 2, Balkema, Rotterdam, pp.821-830.

Kowalsky, M.J., Priestley, M.J.N. and MacRae, G.A. 1995. Displacement-based design of RC bridge columns in seismic regions. Earthquake Engineering and Structural Dynamics, Vol. 24 No. 12, pp. 1623-1643.

Mainstone, R.J. 1971. On the stiffnesses and strengths of infilled frames. Proc. Institution of Civil Engineers, iv 7360s.

Moehle, J.P. 1992. Displacement-based design of RC structures subjected to earthquakes. Earthquake Spectra, Vol. 8, No.3, pp.403-428.

New Zealand National Society for Earthquake Engineering. 1996. The assessment and improvement of the structural performance of earthquake risk buildings. Draft for General Release.

New Zealand National Society for Earthquake Engineering. 2002. The assessment and improvement of the structural performance of earthquake risk buildings. Draft prepared for the NZ Building Industry Authority.

Otani, S. 1974. Inelastic analysis of R/C frame structures. J. Struct. Div., ASCE, Vol. 100, ST7, pp. 1433-1449.

Otani, S. and Kaminosono, T., 1999, Seismic retrofitting technology for reinforced concrete buildings in Japan, Proc. of U.Ersoy Symposium on Structural Engineering, Middle East Technical University, Ankara, pp. 59-80.

Otani, S., 2000, Seismic vulnerability evaluation methods in Japan, Proc. of Tubitak-World Bank Workshop on a Seismic Assessment and Retrofitting Strategy for Turkey, (U.Ersoy, ed.), Tubitak, Ankara.

Panagiotakos, T.B. and Fardis, M.N. 1999. Estimation of inelastic deformation demands in multistorey RC buildings, J. of Earthquake Engineering and Structural Dynamics, Vol.29, pp. 501-528.

Panagiotakos, T.B. Kosmopoulos, A.J. and Fardis, M.N. 2002. Displacement-based seismic assessment and retrofit of reinforced concrete buildings, Proc. 1st fib Congress, Paper No.W-177, Osaka.

Priestley, M.J.N. and Calvi, G.M. 1991. Towards a capacity design assessment procedure for reinforced concrete frames, Earthquake Spectra, Vol. 7, No. 3, pp.413-437.

Priestley, M.J.N.1997. Displacement-based seismic assessment of reinforced concrete buildings, J. of Earthquake Engineering, Vol. 1, No. 1, pp.157-192.

Saiidi, M. & Sozen, M.A. 1979. Simple and complex models for nonlinear seismic response of R/C structures, Civil Engrg Studies, Str. Res. Series No.465, Un. of Illinois, Urbana, Ill.

Shibata, A. and Sozen, M.A. 1976. Substitute-structure method for seismic design in R/C, J. of Structural Division, ASCE, January.

Takeda, T. Sozen, M.A. and Nielsen, N.N. 1970. R/C response to simulated earthquakes, J. of Struct. Div. ASCE, Vol. 96, ST12, pp. 2557-2573.

Vidic, T., Fajfar, P. and Fischinger, M., 1994. Consistent inelastic design spectra: strength and displacement. Earthquake Engineering and Structural Dynamics, V.23, pp.502-521.

Watanabe, F. and Sumi, A., 1998, Assessment of seismic performance and upgrading of building structures, Proc. 13th FIP Congress on "Challenges for Concrete in the next Millenium", (D. Stoelhorst & G.P.L. den Boer, eds.), Balkema, Rotterdam, pp. 851-864.

Copyright fib, all rights reserved. This PDF copy of fib Bulletin 24 is intended for use and/or distribution only by National Member Groups of fib.

4 Strength and deformation capacity of non-seismically detailed components

4.1 Introduction

This Chapter deals with reinforced concrete structural components that do not conform to modern standards for earthquake resistant detailing. Such components often comprise materials of substandard quality. For convenience such components are termed here "old-type" components. Depending on the global characteristics of the structural system and the imposed local deformation demand, poorly detailed elements may become the critical components during seismic excitation, as they generally possess inadequate resistance to reversed cyclic load. Experience from past earthquakes has repeatedly shown than when subjected to cyclic inelastic deformation reversals, old-type components undergo a fast deterioration and degradation of strength, failing in a brittle fashion with fatal consequences for the integrity of the structure as a whole.

The inventory of reinforced concrete structures that qualify under the classification of old-type is vast throughout seismic regions of the world. A major shift in international seismic design codes occurred in the early 1980's introducing the modern form of detailing with closed stirrups and proper reinforcement anchorage as a required practice. Structures designed prior to that point conform to a variety of earlier standards, as these evolved through the years from the post world-war era to the 1980's. Typical of reinforced-concrete design practice of that period is that member dimensioning was driven by considerations of allowable stresses, with little or no emphasis placed on the role of transverse reinforcement as a means of confinement. As evidenced in reconnaissance reports following the destructive earthquakes of the last 25 years worldwide the following are commonplace in older construction:

- Use of low reinforcement ratios (longitudinal and transverse).
- Insufficient details, particularly with regards to anchorage of transverse reinforcement.
- Low concrete strengths; non-uniform distribution of concrete quality throughout the structure, particularly in very old structures (due to concreting in field-mixed batches).
- Poor anchorage of reinforcement – smooth bars with end hooks, usually lower steel strengths.
- Insufficient lap-splice lengths and lap splices of column reinforcement just above the floor level.
- Discontinuous load paths (inadequate reinforcement in beam column joints, insufficient bar anchorages).
- Discontinuous reinforcement.
- Design (dimensioning) based on allowable stresses, with no consideration of capacity-based hierarchy of available strengths.
- Compounded effects due to corrosion of steel (either from carbonation or chlorides) and cracking / deterioration of concrete from exposure to climatic changes.

Of the published experimental evidence relatively few tests concern components representing former code practices. Even fewer were conducted under cyclic load histories that simulate earthquake effects. The general conclusion that may be deduced from the tests is that the monotonic envelope offers an overly optimistic view of the expected response of old-type components and should not be used as a reference in assessment. Note that in the absence of adequate confinement, both basic indices of performance, namely strength and deformation capacity (deformability) are affected dramatically by the cyclic nature of the seismic load, in that the various mechanisms that contribute to seismic resistance *do not degrade proportionately*. For example, mechanisms that rely on contributions from concrete in tension (diagonal tension failures) and steel in compression (limited by longitudinal steel buckling) are more susceptible to damage buildup that accompanies reversal of load.

Primary objective of this chapter is to quantify the relationship between design parameters and performance of reinforced concrete members that classify as old-type construction, under load conditions that simulate earthquake effects. Because of the complexity of the problem and the need for conservative estimates, lower bound curves are sought in quantifying a reliable measure of lateral load strength and deformability. This objective is pursued using various analytical approaches, but also by processing the available experimental evidence which was assembled in the form of a database of published tests; some, but not many, of the

Copyright fib, all rights reserved. This PDF copy of fib Bulletin 24 is intended for use and/or distribution only by National Member Groups of fib.

experiments concern components that may be characterized as "old-type" based on the criteria listed above. To address the large variety of combinations of variables, results of parametric analyses will also be considered.

4.2 Typical characteristics of older type construction

In assessing strength and deformation capacity of old-type components with analytical methods and empirical tools it is necessary to consider the systematic differences between former construction practices and the modern controlled conditions in the field and the laboratory. Differences concern all aspects of construction but three principal parameters prevail that characterize the structural product, namely, (a) material characteristics, (b) detailing practice, and (c) design principles relied upon for dimensioning (i.e., whether failure modes have been prioritized by design or not).

Another aspect is layout and discontinuities in stiffness and mass: up to the early 1960's, several codes required a minimal ratio of wall to floor area in each principal direction of the building ($0.002N_s$ where N_s the number of storeys), in addition to columns. Walls were lightly reinforced compared to modern standards, however, due to the use of small spans and masonry infills for room partitions, structures of the pre-60 period in their majority are rigid. For example, a typical six-storey building of that period would have 2x1.2% = 2.4% of the base floor in walls, which corresponds to a certain level of elastic lateral stiffness and yield strength. Based on damage statistics concerning several reinforced concrete buildings in Turkey, Gulkan and Sozen (1999) and Sozen (2001) have shown that the risk of seismic damage for buildings with such a high floor ratio of wall area is substantially reduced and becomes negligible for even higher ratios. Large wall area ratios control the seismic drift below the levels that would try the deformation capacity of poorly detailed structural members. Unfortunately, this conservatism gave way to greater freedom in terms of larger span widths, use of open ground storeys and larger open spaces without infills in the 1960's and 70's, a period when frame analysis capabilities under lateral load had improved while understanding of seismic detailing was still very poor. For this reason, structures built in that era appear to be the most susceptible of all other groups of engineered old construction, to earthquake-induced damage.

4.2.1 Material characteristics

Material properties in older type construction show greater variability, due to the more primitive methods of concreting used 50 years ago as compared to today (eg. field-mixed concrete batches vs. pumped ready-mix concrete). Specified strengths used in design of building structures were generally lower than today, in the range of 160 – 250 kg/cm^2 (mean values). The corresponding characteristic strengths (f_{ck}) adopted in modern Eurocodes (e.g. EC2) are in an approximately linear relationship with the strength values used before (considering the 8 MPa difference between characteristic and mean value). For example, C12 (Bn150 according to DIN 1045) is almost the same as B225 (nominal cubic strength of 225kg/cm^2), whereas C20 (Bn250) is slightly over B30.

Evaluation of older components should consider evidence of possible cracking, whereas from the appearance of the cracking patterns it should be investigated whether these suggest deterioration of the material structure due to deleterious phenomena (alkali-aggregate reaction-AAR, delayed ettringite formation-DEF) or they are evidence of structural distress (FEMA 273, 1997). In general, all expansive physicochemical processes (such as AAR or DEF) cause deterioration of the mechanical strength, particularly on mechanisms of resistance that rely on tension. However, assessing the global effects of these processes is neither straightforward nor unidirectional – the presence of steel reinforcement is known to delay or even stop the expansion, inducing second order clamping forces that - depending upon the boundary restraints - may even increase some strength parameters (Pantazopoulou and Thomas 2000).

Steel reinforcement varies in terms of quality (strength and ductility) and surface characteristics (smooth bars or G class in DIN488, and ribbed bars or class R in DIN488). In very old construction even bars of non-rectangular cross sections may be found. Based on published standards from the 1960s and 1970s, in several European countries steel reinforcement qualities were StI (f_{yk}=2200 kg/cm^2), StIII (f_{yk}=4200kg/cm^2), StIV (f_{yk}=5000

Copyright fib, all rights reserved. This PDF copy of fib Bulletin 24 is intended for use and/or distribution only by National Member Groups of fib.

kg/cm^2), or according to DIN 1045/1972 and DIN 488, BStI, BStIII and BStIV with characteristic yield strength / fracture strength of 22/34, 42/50, 50/55 kp/mm^2, respectively. Ribbed reinforcement was introduced in structural design in the 1960's, but in southern Europe smooth bars continued to be used up to the late 1970s in building structures. Related rib areas, f_R, and rib height h_r of ribbed bars in use in the 1960s and 1970s were, for $\Phi 6$: f_R=0.04, h_r=0.4, for $\Phi 8$: f_R =0.05, h_r=0.55, for $\Phi 10$: f_R=0.055, h_r=0.7 and for bar diameters above $\Phi 12$: f_R=0.065, $h_r \geq 0.8$. (Beton-Kalender, 1970).

Under normal circumstances and in the absence of the deleterious effects of corrosion, properties of steel reinforcement present much less variability than concrete. However, the likelihood of reinforcement corrosion ought to be assessed by careful evaluation because its effects on the mechanical properties of steel and on the steel to concrete bond are manifold. In the older-type low strength concretes, porosity is high, a characteristic that accelerates carbonation of the cover; steel corrosion due to carbonation is usually spread out over large lengths of the bar. In general, corrosion causes embrittlement of steel, loss of bar section (if of the pitting type, usually associated with chloride-induced corrosion) and cracking of the concrete cover with attendant losses of bond, whereas the intersitial layer of soft corrosion products between bar and the surrounding concrete acts as a bond breaker reducing friction even more, especially for bars with smaller rib heights.

Absent detailed experimental results from tests with smooth corroded bars, experiments conducted on ribbed bars are used to guide the assessment: Stanish et al. (1999), proposed the following expression for mean bond strength of corroded bars: $f_{b,corr}=(0.75-5.4\Delta\Phi/\Phi)\sqrt{f_c'}$ (MPa), where $\Delta\Phi$ represents the diameter depletion due to corrosion. Similarly, Rodriduez et al. (1994) related bond strength of corroded reinforcement to corrosion penetration depth x_{corr}, including the confining action that the stirrups provide: $f_{b,corr}=0.6f_{ctm}((c/d)+0.5)(1-\beta x_{corr}^{\mu})+(kA_{st}f_{yst}/sd)$, where β, μ and k are empirical constants, s the spacing of web reinforcement and d the effective cross-sectional depth. (The above expressions should be used with caution in assessment, because concrete strengths used in the reference tests are relatively high.)

4.2.2 Older – type detailing

In the presence of confinement many of the influences of material imperfections noted above are suppressed or attenuated, with the noted exception of bar section loss due to pitting corrosion. Basically, the quintessential difference in design between today and 30 years ago has been in the emphasis placed on transverse reinforcement as a means of confinement. In older codes stirrups were recommended: (a) for support of the longitudinal reinforcement against buckling, (b) to resist a small fraction of the design shear force and (c) for torsion. The German DIN 1045 reflects the spirit of the period: reinforcement placement was driven by the concern that principal reinforcement should cross every possible crack path. For this reason the designer was encouraged to bend the main bars, in order to provide for shear resistance of prismatic members. This practice was quite widespread in Europe and North America. A late example of this philosophy is illustrated in Fig. 4-1, showing the proposed arrangements for knee joint reinforcements. In that problem, it had already been shown experimentally long

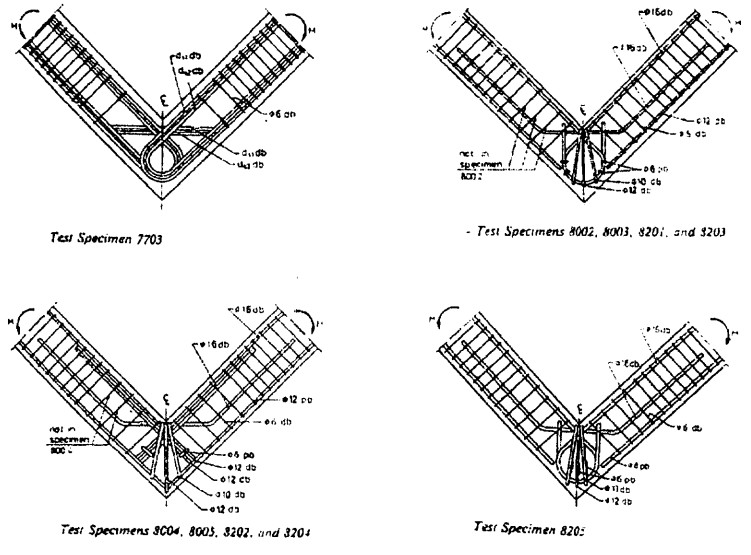

Fig. 4-1: Characteristic example of former detailing philosophy (from Skettrup et al. 1984)

Copyright fib, all rights reserved. This PDF copy of fib Bulletin 24 is intended for use and/or distribution only by National Member Groups of fib.

time ago that it was impossible to realize the design strength of the connection under monotonic and reversed loads with the accepted reinforcement details. The perpetual research effort of the 60's and early 70's was to improve the pattern of bending and anchoring the principal reinforcement in the joint, but yet, no consideration for stirrups is mentioned in the regulatory literature of the period as a solution to the problem.

(a) Some excerpts of the Beton-Kalender (1970), which is based on DIN 1045, are as follows:

Minimum tension reinforcement ratio in prismatic reinforced concrete elements was 0.4%; however this percentage was calculated over the *statically required* concrete section (SRCS) (this implies that smaller amounts were possible in very large sizes of concrete sections). Compression reinforcement was at most equal to the tension reinforcement. Minimum bar diameter allowed for longitudinal reinforcement was $\Phi 14$ for StI or StII and $\Phi 12$ for St III or StIV. Maximum distance between parallel longitudinal bars in compression elements was 300mm. The minimum number of bars in rectangular columns was four (with section dimension not exceeding 400 mm). Minimum cross section size was 200x200 mm, with the minimum percent of longitudinal column reinforcement controlled by the slenderness ratio of the column ($\rho_{s,min}$, the percentage of minimum longitudinal reinforcement over the SRCS, was interpolated between the limits $\rho_s \geq 0.5\%$ for $H/b_o \leq 5$ and $\rho_s \geq 0.8\%$ for $H/b_o \geq 10$, where H the centre to centre distance between successive floors, and $b_o = \min\{b,h\}$). The maximum value $\rho_{s,max}$ over the SRCS was 3% for low quality concrete or 6% for normal strength concrete, with the requirement that when maximum amounts are used, lap splices be welded. For circular columns: $1\% < \rho_s < 6\%$ of the core area, with the volumetric spiral ratio $\rho_{s,sp} < 3\rho_s$. Minimum stirrup size was $\Phi 5$ for separate bars or $\Phi 4$ for wire mesh. For columns, maximum stirrup spacing $s_{max} = \min\{b_o, 12\Phi_l\}$; for spirals, the step $s_{max} = \min\{80mm, D_c/5\}$.

The total area of shear reinforcement in a region with a moment gradient of $V=\Delta M/L_s$ is $A_{shear} = \Delta M/z \cdot \sigma_{al}$. This comprises contributions of the equivalent area of longitudinal bars bent at 45-60° with respect to the longitudinal axis, $A_l\sqrt{2}\cos\beta$ (β=0-15° respectively) and transverse stirrups having total leg area A_{st} per stirrup layer. The total amount $A_{shear} = A_l\sqrt{2}\cos\beta + A_{st} = A_{sl,1} + A_{sl,2}$, i.e. the total area of shear reinforcement A_{shear} equals the sum of tension longitudinal reinforcement at midspan ($A_{sl,1}$) and support ($A_{sl,2}$). In shear design stirrups were assumed to secure *interaction* between tension and compression zones in the cross-section. Section size was determined by the requirement that average shear stress over the cross section was below 16-18 kp/cm^2 (for B160-B225). The entire shear force would be resisted by bent bars and stirrups if average shear stress exceeded 6-7 kp/cm^2, in which case the maximum allowable spacing of stirrups was 150 mm. The general recommendation was that the larger component of shear force be resisted by bent bars rather than stirrups (stirrups were assigned to resist 25% to 50% of the allowable shear force only).

(b) Similarly, the design requirements of the 1963 ACI Code (ACI 318-63) were:

Minimum cross sectional dimension of load-carrying columns was $D_o \geq 10$ in. or $b_o = \min\{b, h\} \geq 8$ in., with minimum area $A_c \geq 96$ sq in. Statically effective area used for stress and minimum reinforcement calculations is taken as at least half the available A_c. Limits for column longitudinal reinforcement over A_c were: $1\% < \rho_s < 8\%$, with $\Phi_{l,min}$ = 5/8 in. At least six and four bars were required in circular and rectangular columns respectively.

Lateral ties in rectangular columns were at least $\Phi_{t,min}$ = 1/4 in. spaced at the minimum of $\{16\Phi_l, 48\Phi_t, b_o\}$. Volumetric ratio of spiral steel: $\rho_{s,sp} \geq 0.45(A_c/A_o - 1)f_c/f_y$. Every corner and alternate longitudianl bar had to be supported by the corner of a tie bent at an angle of at most 135°, and lateral distance between long. bars was ≤ 6 in. In beams, closed ties with $\Phi_{t,min}$ = 1/4 in. spaced at the min of $\{16\Phi_l, 48\Phi_t\}$ were required over the anchorage length of compression reinforcement. Shear reinforcement could comprise combination of stirrups and bent bars; concrete contribution was taken $1.1\sqrt{f_c}$ for working stress design and $2\varphi\sqrt{f_c}$ for ultimate strength design (capacity reduction factor φ=0.85). The corresponding maximum allowable stresses for an unreinforced section were $1.75\sqrt{f_c}$ and $3.5\varphi\sqrt{f_c}$. No one type of reinforcement was assumed to resist more than 2/3 of the total shear carried by all forms of web reinforcement (bent bars plus stirrups). For shear stress demands $\leq 3\sqrt{f_c}$ (allowable stress design) or $6\varphi\sqrt{f_c}$ (ultimate strength design), maximum spacing of

Copyright fib, all rights reserved. This PDF copy of fib Bulletin 24 is intended for use and/or distribution only by National Member Groups of fib.

shear reinforcement was d/2, whereas for higher demands maximum tie spacing was d/4 (demands were limited by $5\sqrt{f_c}$ in working stress design, or $10\varphi\sqrt{f_c}$ in ultimate stress design). Note that *when* shear reinforcement was required, the minimum amount was $\rho_{w,min} = A_{st}/sb = 0.0015$.

Spiral column reinforcement consisted of evenly spaced continuous spirals having a minimum diameter of 1/4 in. (or No. 4 gage wire), having centre to centre spacing $\leq D_c/6$ (where D_c the diameter of the core), and a clear spacing $\leq$ 3 in. The reinforcing spiral extended over the clear length of the column.

Minimum bearing wall thickness was 4% of the unsupported height or width, or 6 in. thick for the upper two storeys; 7 in. were required for taller walls. Minimum thickness for panel and enclosure walls was 4 in. Minimum reinforcement percentages in the horizontal and vertical directions were 0.0025 and 0.0015, having Φ_{min} =3/8 in. at a maximum spacing on centres of 18 in.

	DIN1045		ACI 318-63	
steel:	bottom-cast bars	top-cast bars	f_y=40-50-60 ksi, top cast	f_y=40-50-60 ksi, bottom cast
concrete	B160-B225-B300	B160-B225-B300		
f_{bo}	5-6-8 kp/cm^2	5-6-8 kp/cm^2	min{0.5f_{bR}, 0.16ksi}	min{0.5 f_{bR}, 0.16ksi}
f_{bR}	11-16-21 kp/cm^2	6-8-11 kp/cm^2	min{3.4$\sqrt{f_c}$/Φ, 0.35ksi}	min{4.8$\sqrt{f_c}$/Φ, 0.5ksi}
A_4	6Φ	12Φ	6 in	6 in
A_5	12Φ-10Φ-10Φ	24Φ-16Φ-12Φ	max{d,12Φ}$^{(1)}$	max{d,12Φ}$^{(1)}$
A_6	30Φ-25Φ-15Φ	60Φ-50Φ-30Φ	max{d, 1/16L}$^{(2)}$	max{d, L/16}$^{(2)}$
A_7	35Φ-30Φ-25Φ	65Φ-55Φ-40Φ	24Φ-30Φ-36Φ >12Φ	24Φ-30Φ-36Φ >12Φ

(1)measured from the point where the bar is no longer needed to resist flexural stress;
(2)measured from the point of inflection.

Table 4-1: Minimum requirements for anchorage and splicing of reinforcement

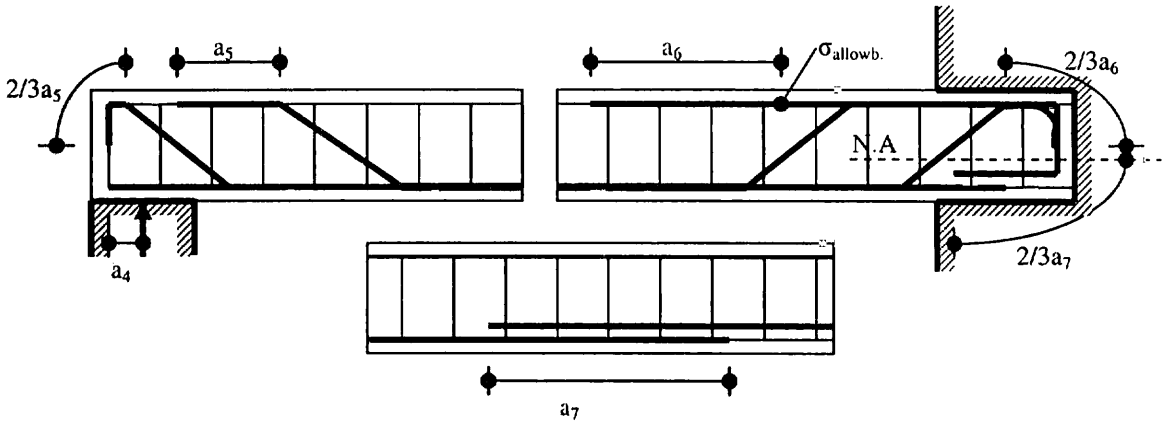

Fig. 4-2: Definition of terms in Table 4-1

(c) Reinforcement Anchorage

Old-type requirements for reinforcement anchorage are considered separately in this section, due to their quintessential importance on the behaviour of many different types of members. Relevant information is listed in Table 4-1 as per DIN1045 and ACI318-63, with reference to Fig. 4-2. According to DIN1045, tension reinforcement (smooth bars) was anchored with 180-hooks. Bottom tension reinforcement in beam spans should be extended to the supports or bent upwards, so that it be anchored in the compression zone of the member. Lap splices were discouraged for tension steel, but when unavoidable, they should be placed in regions of low tension, such as points of inflection, and should include 180°-hooks at the ends; required lap length was calculated from the allowable steel stress (1400, 1800, 2000 kp/cm^2 for each category of steel) and allowable bond stress as in Table 4-1. For ribbed reinforcement, hooks could be avoided if stirrups (unspecified amount) were used as an alternative in the lap or anchorage zone. Again, particular emphasis was placed on the

Copyright fib, all rights reserved. This PDF copy of fib Bulletin 24 is intended for use and/or distribution only by National Member Groups of fib.

requirement that all reinforcement be anchored in the compression zone of the member.

Similar to DIN1045, anchorage of tension reinforcement in the ACI318-63 specifications was also achieved by means of bending the bars across the web and anchoring them in the opposite face of the member. Reinforcement anchorage should occur in the compression zone of the member, unless either the minimum amount of stirrups required for shear was supplied in the region of the curtailment, unless shear stress was less half the permissible value, or the remaining bars provided double the area required for flexure or double the perimeter required for bond. The length of bar bent into a hook was considered effective in developing bond (standard hook extensions were 4Φ and 6Φ for 180° and 90° hooks, respectively). Critical sections for bond were supports, points of curtailment and points of inflection.

Lap splices were discouraged for bar-sizes larger than No.11 (35mm). Tension splices were designed to transfer the computed stress of the bar without exceeding 75% of the permissible bond values. Minimum tension splice lengths are given in Table 4-1; compression splices were 20Φ, 24Φ and 30Φ for $f_y \leq 50$ ksi (350 MPa), f_y=60 ksi (420 MPa), and f_y=75 ksi (520 MPa) respectively and $f_c \geq 3$ ksi (20 MPa). These values were increased by 30% for lower concrete strengths. Values for smooth bars were twice those for deformed bars. Offsetting of vertical compression reinforcement in columns was permitted at an angle 1:6. For splices in close proximity, the minimum amount of stirrups was also required (see the parts of sections (a) and (b) above which refer to shears).

4.3 Strength and deformation capacity of prismatic components

4.3.1 Problem definition

It may be easily concluded from the preceding that old-type components have sparse, small diameter stirrups meant to support compression reinforcement against buckling and to supply a small fraction only of shear resistance. Stirrups as a possible means of confinement of deformed bars was only used in lap-splices and points of curtailment of reinforcement in both the North American and the European practice, but not with mandatory emphasis, for they could be substituted by an increase in anchorage length or by the use of hooks. For members with *very low amounts* of confinement (maximum effective confining pressure less than 10% of f_c) the increase from the reference unconfined values of either strength or deformation capacities effected by the stirrups can be negligible, especially when considering the reversed cyclic nature of the seismic load. In any case, dependable rotation ductility factors in plastic hinge regions are unlikely to exceed the value of 2 for such lightly confined members. Note that for S400 steel and for every increase by 1% of the effective volumetric confining steel ratio, the maximum effective confining pressure increases by only 2 MPa.

In the case of assessment of existing concrete structures, it is probably most important to consider a lower bound for both strength and deformation capacity given the sparseness of confining reinforcement. Although assessment is done on a case by case basis, a consistent methodology of calculating the lower bounds is sought. In this regard, mechanistic models derivable from first principles are attractive, for they provide the user with a plausible explanation of physical behaviour. However, recent research has illustrated that such an approach may also be unconservative, for it may lead to vast overestimation of deformation capacity and residual strength, particularly when dealing with mechanisms that rely on concrete tension (Inel and Aschheim 2002).

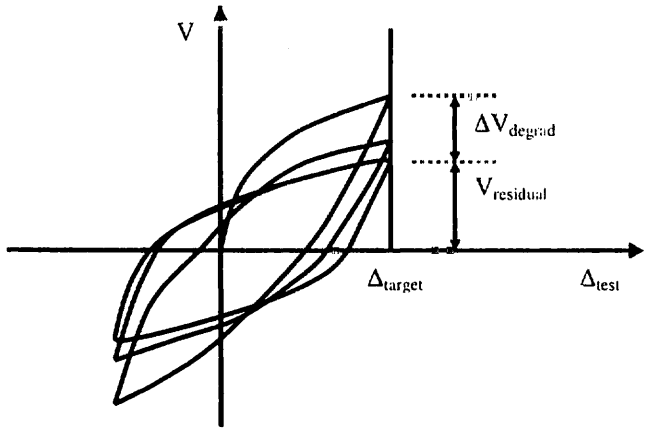

Fig.4-3: Definition of residual strength for assessment

An alternative to mechanistic models, empirical relations have been used to guide assessment, with the caution that the tests relied upon for extracting design relations be conducted under

Copyright fib, all rights reserved. This PDF copy of fib Bulletin 24 is intended for use and/or distribution only by National Member Groups of fib.

repeated complete reversals of load to simulate the degradation process that occurs during the earthquake. For example, residual strength values associated with a certain level of displacement capacity should preferably be obtained after the third complete reversal of load to the target displacement (Fig. 4-3). Both analytical and empirical approaches are considered in the remainder of this chapter.

4.3.2 Detailed calculation of strength and deformation capacity of prismatic old-type components

The question of systematically calculating an estimate of strength and deformation capacity of reinforced concrete elements under flexure-shear reversals with and without axial load has been at the centre of ongoing research activity worldwide. Several models have prevailed in the international literature (Park and Paulay 1975, Lehman et al. (1998), Panagiotakos and Fardis (2001), FEMA 273 (1997), Priestley et al. (1996)). The success of some of these models in reproducing experimental strength values is very good when flexural failures dominate the response, but their performance, as measured by the amount of scatter between experiment and analysis, deteriorates increasingly, when they are used to estimate shear capacity and the various indices of deformation (i.e., curvature, drift, displacement, or ductilities thereof). For example, although the mean ratio of estimated to measured deformation capacities obtained over a large number of specimens is around 1, the analytical estimations may differ from the experimental measurements by as much as 100%. To address this issue, Panagiotakos and Fardis (2001) have proposed the use of lower characteristic values for drift capacity, θ_{uk}, rather than the mean values, θ_{um}; based on regression analysis that they conducted on a database of a large number of tests the authors concluded that $\theta_{uk} = 0.55 \cdot \theta_{um}$ if cyclic response is considered. The 0.55 factor is reduced even further to 0.4, when considering monotonic test results.

Furthermore, it appears that no unique index of deformation capacity is invariant to member dimensions, so as to be used as a single measure of inelastic deformability (Inel and Aschheim 2002).

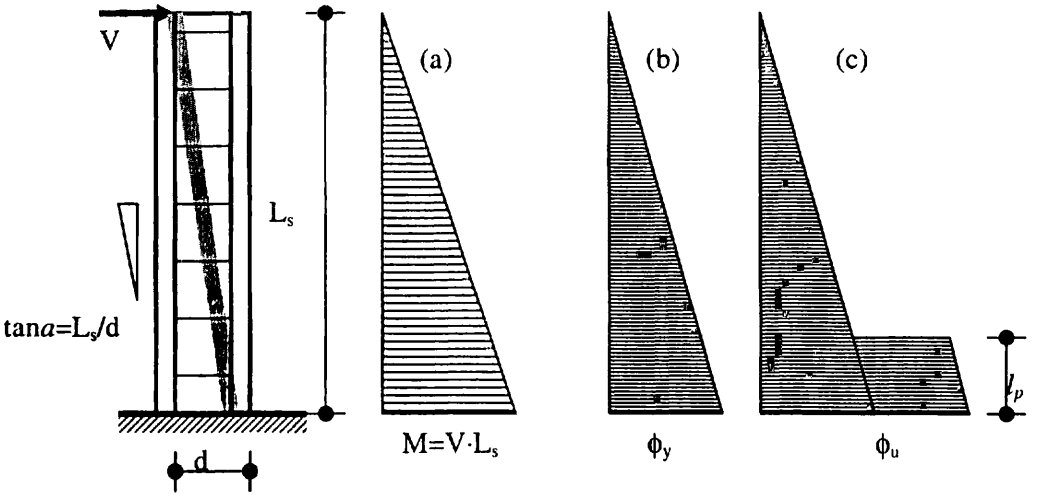

Fig. 4-4: Cantilever model used for definition of deformation indices

In most of the available models, deformation capacity at yielding and ultimate is computed using the lumped inelasticity cantilever – "stick model"– with a tip load, as shown in Fig. 4-4 a (exception to this is the empirical model in Fardis and Panagiotakos (2001). The length of the cantilever L_s corresponds to the shear span of an actual frame member under lateral sway; the aspect ratio of the member $L_s/d = M/Vd$ quantifies the slope of the diagonal compression strut through which compression forces are transferred to the support of the member. Larger angles signify a larger contribution of the compression zone in resisting shear. Inelastic activity is assumed to occur within an equivalent "plastic hinge length", l_p, whereas the segment of the member outside l_p is assumed to behave elastically. In the simplest form of the model, displacements are calculated from flexural curvatures assuming the curvature distributions of Fig. 4-4 b and 4-4 c, which correspond to development of

Copyright fib, all rights reserved. This PDF copy of fib Bulletin 24 is intended for use and/or distribution only by National Member Groups of fib.

yielding and post-yielding flexural strengths at the fixed support. In a bilinear envelope approximation of the force-displacement relationship, Fig. 4-4 c corresponds to development of the ultimate flexural strength of the member.

The relevance between the cantilever model and the actual circumstances of a prismatic reinforced concrete element subjected to strong ground motion effects is in the statics of the two systems as depicted in Fig. 4-5 (i.e., in the force boundary conditions). Note that to the extent that displacement boundary conditions could also matter in determining the actual response, these may not be simulated correctly by the stick-model (for example, the restrained extension of member length in indeterminate frame members as compared to the free extension of the cantilever model). The same difference exists between the isolated cantilever beam-column tests, and either the stick model and/or the actual circumstances in frame structures. In many isolated cantilever column tests the tip load is a "follower-force", i.e. its angle to the longitudinal axis of the member decreases with drift. Thus, in terms of cross-sectional resultants the tip force can be resolved into a pure shear and a tensile axial force that increases with the amount of drift, thereby forcing a more prevailing demand for pullout of reinforcement from the support than would actually occur in some practical cases.

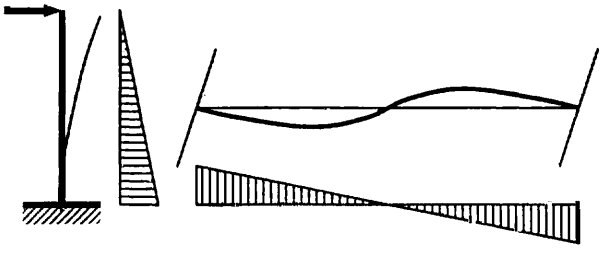

Fig. 4-5: Moment distribution of the two systems

Given these limitations of both tests and models, compounded by other uncertainties that relate to the rate of degradation of the various resistance mechanisms with reversal of load, it is justifiably difficult to estimate with accuracy indices of deformability. Deformation ductilities are further obscured by lack of a unique definition of deformation at yielding; instead, a variety of definitions have been used by individual investigators when interpreting test results to determine yielding. For qualitative purposes the various models listed in the literature for calculation of deformation capacities and strengths are reviewed herein.

4.3.3 Calculation of the length of plastic hinge, l_p

At the centre of controversy in defining deformation capacities is the quantitative definition of the plastic hinge length, which is rather elusive despite the mathematical convenience it offers. The physical definition of the plastic hinge length is illustrated in Fig. 4-4 c: considering the ultimate flexural strength developing at the support, it is the distance from the support over which the applied moment exceeds the yield moment. The established practice has been to take l_p=0.5d. Thom (1983) suggested the following expression for the plastic hinge length:

$$l_p = \frac{M_{max} - M_y}{M_{max}} \cdot L_s + c = \alpha L_s + c_t \qquad (4-1)$$

where c_t represents a correction for the tension shift effect which occurs due to diagonal cracking (crack spacing) and $\alpha=(f_u-f_y)/f_u$ the normalized strength increase from yield to ultimate of tension steel (in the model of Priestley et al. (1996), the corresponding α is 0.08, in the model of Panagiotakos and Fardis (2001), α=0.12, whereas Lehman et al. (1998) use the general expression for α, given by eq. (4-1)). The plastic rotation θ_p^f developing in the hinge due to flexure is $\theta_p^f = (\phi_u-\phi_y)l_p$; similarly, the plastic rotation due to pullout of reinforcement from the support is $\theta_p^{slip} = \theta_u^{slip} - \theta_y^{slip}$; the total plastic rotation is $\theta_p = \theta_p^f + \theta_p^{slip}$. With reference to Fig. 4-6 the corresponding terms are:

$$\theta_y^{slip} = \frac{\varepsilon_y l_{b,y}}{2}\frac{1}{z}; \quad \theta_u^{slip} = \theta_y^{slip} + \frac{(\varepsilon_u - \varepsilon_y)}{z}\frac{f_u - f_y}{f_u} L_{b,u}; \quad L_{b,y} = \frac{\Phi}{4}\frac{f_y}{f_{b,y}}; \quad l_{b,u} = \frac{\Phi}{4}\frac{f_u}{f_{b,u}} \qquad (4-2)$$

Copyright fib, all rights reserved. This PDF copy of fib Bulletin 24 is intended for use and/or distribution only by National Member Groups of fib.

where z the distance of the tension steel to centroid of the compression zone and f_b the uniform bond stress along the development length L_b. Substituting the ratios ε_y/z and ε_u/z by the yield and ultimate curvatures ϕ_y and ϕ_u, respectively, and the average bond stress at the ultimate, $f_{b,u}$ as a fraction of the corresponding bond stress value at yield of reinforcement, $f_{b,y}$, i.e.: $f_{b,u}=\lambda f_{b,y}$ the plastic rotation due to slip and the corresponding correction to the plastic hinge length l_p may be extracted (eq. (4-3) is written for $\lambda=1/1.2$; for other values of λ, the multiplier 1.2 would be replaced by $1/\lambda$):

$$\theta_p^{slip} = (\phi_u - \phi_y)\frac{\Phi}{4}\frac{1.2(f_u - f_y)}{f_{b,y}}\ ; \quad l_p = \alpha L_s + \frac{1.2(f_u - f_y)}{4 f_{b,y}}\Phi = \alpha L_s + \frac{1.2\alpha}{4(1-\alpha) f_{b,y}} f_y \Phi \qquad (4-3)$$

All the alternative proposals for l_p have the form of eq. (4-3); differences exist in defining the various constants, including the magnitude of the average bond stress $f_{b,y}$ mobilized over the development length upon yielding of the bar and the bond strength reduction factor λ:

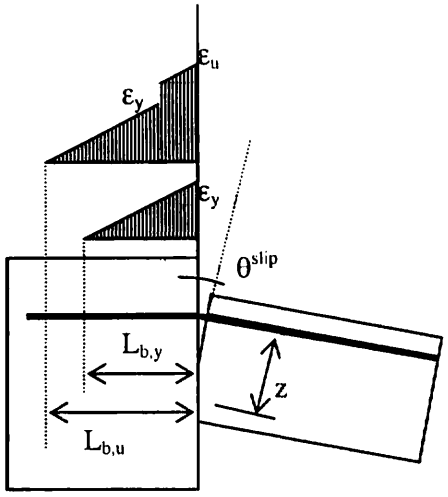

Fig. 4-6: Calculation of rotation due to pullout

Lehman et al. (1998):
$l_p=0.5\alpha L_s+1.2\alpha f_u\Phi/4f_{b,y}$, with $f_{b,y}=12\sqrt{f_c}$ (psi) = $1\sqrt{f_c}$ (MPa), and $1/\lambda=1.2$ (without the term (1-*a*) in the denominator).
Panagiotakos and Fardis (2001):
$l_p=0.12L_s + 0.0965f_y\Phi$ (ksi, in) or $l_p=0.12L_s + 0.014f_y\Phi$ (MPa, mm), with $\alpha=0.12$ (i.e. $f_{su}\approx1.15f_{sy}$). Assuming normal strength concrete with $\sqrt{f_c} \approx 5$ MPa, values for the other parameters that could fit the above are, $f_{b,y}=6\sqrt{f_c}$ (psi) = $0.5\sqrt{f_c}$ (MPa) and $\lambda\approx1$.
Priestley et al (1996):
$l_p=0.08L_s+0.15f_y\Phi$ (ksi, in), or $l_p=0.08L_s+0.022f_y\Phi$ (MPa, mm) with $\alpha=0.08$ (i.e. $f_{su}\approx1.1f_{sy}$). Again, assuming normal strength concrete with $\sqrt{f_c} \approx 5$ MPa, values for the other parameters that could fit the above are: $f_{b,y}=6\sqrt{f_c}$ (psi) = $0.5\sqrt{f_c}$ (MPa) and $\lambda=0.4$, $1/\lambda=2.5$.

An objection to the above proposals is that they refer to an advanced state of plastification of the member (displacement ductilities in excess of 4, beyond which the l_p reportedly tends to stabilize, Penelis and Kappos 1997). To organize the experimental scatter at lower ductility levels Kappos (1991) suggested the relationship: $l_p = l_{po}\,[(\mu_o-1)/3]\,1/2 \le l_{po}$ where l_{po} the plastic hinge length beyond displacement ductilities of 4.

4.3.4 Indices of deformation capacity of prismatic components

The deformation measures listed below refer to a bilinear envelope of the characteristic load-deformation curve, be it computed analytically or approximately fitted to experimental results. Note that the two characteristic points (yield and ultimate) are not defined uniquely. Usually, ranges of values are possible, according to various alternative definitions of the limiting conditions. However, once the yield and ultimate points are established, the following quantities are derived for a cantilever column:

(a) the sectional curvature and curvature ductility ratio at the critical section of the cantilever model, ϕ_y, ϕ_u, $\mu_\phi=\phi_u/\phi_y$. The plastic curvature capacity, assumed to be constant over the plastic hinge length is $\phi_{p,u}=\phi_u-\phi_y$.

(b) the tip displacement, tip plastic displacement and displacement ductility, Δ_y, $\Delta_u=\Delta_y+\Delta_{p,u}$, $\mu_\Delta=\Delta_u/\Delta_y$. Yield and ultimate displacements and results thereof may include contributions of flexural curvature, shear distortion and anchorage slip:

$$\Delta_y = \Delta_y^{flex} + \Delta_y^{shear} + \Delta_y^{slip} \quad ; \quad \Delta_u = \Delta_u^{flex} + \Delta_u^{shear} + \Delta_u^{slip} \qquad (4-4)$$

Copyright fib, all rights reserved. This PDF copy of fib Bulletin 24 is intended for use and/or distribution only by National Member Groups of fib.

(c) the total drift, estimated from the chord rotation of the cantilever by dividing the tip displacement with the shear span L_s, $\theta_y=\Delta_y/L_s$, $\theta_u=\Delta_u/L_s$. Being a non-dimensional quantity, drift is a more meaningful measure of deformation capacity than displacement.

(d) the plastic rotation capacity of the hinge, which equals approximately to the total drift minus the elastic contributions, $\theta_p=\Delta_p/(L_s-0.5l_p)$.

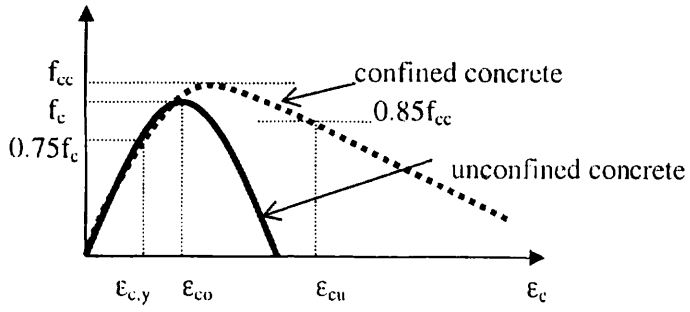

Fig. 4-7: Definition of limiting concrete strains

Of the above selection of deformability indices, no one alone can assess all aspects of member response. Each index is suitable for a different objective: μ_Δ best characterizes global response of the component, μ_ϕ could quantify local damage (Inel and Aschheim 2002). Also, using several indices identifies possible shortcomings in strengthening and repair procedures (e.g. controlling the displacements by adjusting the stiffness can increase the ductility demand, Inel and Aschheim, 2002). Calculation of the various deformation indices according with the different models is listed in Table 4-2. In most cases, computing the yield and ultimate curvatures is prerequisite to the application of the models. Some expressions for estimating these variables are given in Appendix 4 A, but the reader is cautioned that other models may also be found in the literature that produce reliable estimates of yield and ultimate curvatures of concrete members. To calculate the curvature at yield, ϕ_y, the limiting concrete strain that corresponds to either the onset of concrete nonlinearity or tension steel yielding (Fig. 4-7)[1], is divided by the corresponding depth of the compression zone, x_y. Ultimate curvature, ϕ_u, is calculated from the ultimate compressive strain that may be supported by the compression zone (by accounting for the confinement provided by the stirrups using a pertinent confinement model, see Appendix 4 A), divided by the corresponding depth of the compression zone, x_u.

$$\phi_y = \min\{\frac{f_y}{E_s}\cdot\frac{1}{d-x_y}, \frac{\varepsilon_{c,y}}{x_y}\},\ \text{where}, \varepsilon_{c,y} = 0.75\varepsilon_{co}\quad ;\quad \phi_u = \frac{\varepsilon_{c,u}}{x_u} \qquad (4-5)$$

Evidently, in defining all the above terms the emphasis is on flexural action. Even when other contributions to deflection are considered (such as deflection due to slip and shear distortion), the underlying assumption is that a robust flexural mechanism can develop. A hypothesis central to the mechanics of flexure in reinforced concrete is that deformations may be averaged over finite distances, so that the notion of strain and strain measurement, which forms the basis of it all, may be meaningfully defined and calculated. This averaging procedure requires uniform distribution of reinforcement, so as to provide for adequate crack control. This assumption, however, may not be necessarily valid for all old-type components. In these cases often failure has the appearance of localized fissures in concrete (few wide cracks), where resistance may be due to friction and interlocking of dislocated fragments of concrete. Lacking detailed models to reproduce this behaviour, the nonlinear continuum mechanics models in Table 4-2 are for now the only tools available for estimating the deformation capacity of old type components, with a possible error margin as high as 100%.

Eq. (4-6) quoted in column (3) of Table 4-2 is:

$$\theta_u = \beta_{st}(1-0.38a_{cyc})\left(1+\frac{a_{sl}}{1.7}\right)\left(1-\frac{3}{8}a_{wall}\right)\left(0.3^{\nu}\right)\left[\frac{\max(0.01,\omega')}{\max(0.01,\omega)}f_c\right]^{0.2}\left(\frac{L_s}{h}\right)^{0.425} 25^{CC}1.45^{100\rho_d} \qquad (4\text{-}6)$$

[1] In Fig. 4-7 it is assumed that onset of concrete nonlinearity occurs at a strain equal to 75% of the strain at peak stress, ε_{co} (eq. 4-5). In the model of Panagiotakos and Fardis this point is taken at 90% ε_{co}, to better fit test results on ϕ_y. The unconfined concrete stress-strain curve is modeled by a Hognestad-type parabola, so $\varepsilon_{co}=2f_c/E_{co}$.

Copyright fib, all rights reserved. This PDF copy of fib Bulletin 24 is intended for use and/or distribution only by National Member Groups of fib.

Deforma -tion Index	Stick-Model Mechanics	Lehman et al. (1998)	Panagiotakos & Fardis empirical model (2001)	Panagiotakos & Fardis, mechanics model (2001)	Priestley et al. (1996)
	(1)	(2)	(3)	(4)	(5)
$\Delta_{y,flex}$	$\phi_y L_s^2/3$	$\phi_y L_s^2/3$	$\phi_y L_s^2/3$	$\phi_y L_s^2/3$	$\phi_y(L_s+0.15 f_y \Phi)^2/3$
$\Delta_{y,shear}$	NA	$V_y L_s/0.4E_{c,sec}0.8A_g$	$0.0025L_s$	NA	$\Delta_{y,shear}^{concr} + \Delta_{y,shear}^{truss}$ (eq.4-7)
$\Delta_{y,slip}$ (eq. 4-4)	NA	$(\phi_y/2)f_y\Phi L_s/4f_{b,y}$	$L_s\varepsilon_y L_{b,y}/2(d-d') = \varepsilon_y f_y \Phi L_s/8f_{b,y}(d-d')$	NA	(was accounted for in $\Delta_{y,flex}$)
$f_{b,y}$	NA	$1\sqrt{f_c}$ (MPa)	$0.5\sqrt{f_c}$ (MPa)	$0.5\sqrt{f_c}$ (MPa)	$0.5\sqrt{f_c}$ (MPa)
θ_p	$(\phi_u-\phi_y)l_p$	$(\phi_u-\phi_y)l_p$	$\theta_u-(\Delta_y/L_s)$	$(\phi_u-\phi_y)l_p$	$(\phi_u-\phi_y)l_p$
θ_u	Δ_u/L_s	Δ_u/L_s	eq. (4-6)	Δ_u/L_s	Δ_u/L_s
Δ_p	$\theta_p(L_s-0.5l_p)$	$\theta_p(L_s-0.5l_p)$	$\Delta_u-\Delta_y$	$\theta_p(L_s-0.5l_p)$	$\theta_p(L_s-0.5l_p)$
Δ_u	$\Delta_y+\Delta_p$	$\Delta_y+\Delta_p$	$\theta_u \cdot L_s$	$\Delta_y+\Delta_p$	$\Delta_y+\Delta_p$
l_p	0.5d	$0.5\alpha L_s+1.2\alpha f_u\Phi/4f_{b,y}$	$0.12L_s+0.014f_y\Phi$	$0.12L_s+0.014f_y\Phi$	$0.08L_s+0.022f_y\Phi$

NA=not applicable

Table 4-2: Analytical definition of deformation components

In eq. (4-6) α_{sl} is a binary coefficient (0,1) to indicate if reinforcement pullout is possible or not, α_{wall} a binary coefficient (1,0) if the member is a wall or not, ν the axial load ratio ($N/A_c f_c$), $CC=k_e\rho_{s,st}f_{yst}/f_c$ (i.e. it is the effective normalized confining pressure provided by transverse reinforcement in the direction of lateral sway) and ρ_d the diagonal reinforcement ratio in diagonally reinforced members. ω, ω' are the mechanical ratios of the tension and compression longitudinal reinforcement (not including diagonal bars); for elements with distributed reinforcement between the two flanges, the entire vertical web reinforcement is included in the mechanical ratio of the tension steel. Coefficient a_{cyc} is a binary variable (0, 1) to account for the monotonic or cyclic nature of the load, whereas β_{st} accounts for the type of steel: 0.016 for ductile hot-rolled or heat-treated (tempcore) steel and 0.0105 for cold-worked steel. The value calculated from eq.(4-6) represents the mean value for rotation capacity (i.e. at 20% post-peak drop of lateral strength). The expression has been fitted to a database of the results of about 1100 monotonic or cyclic tests of RC beams, columns or walls up to flexure-controlled failure (excluding specimens with circular or hollow-circular sections). For assessment, the characteristic values may be used, corresponding to a 95% probability of exceedence by a random sample of the database (see section 4.2.2).

Since its original appearance (as in Table 4.2) the equation for the drift at yielding has been modified to account for the differences between the shear span L_s and the length of the member, H, over which the chord rotation is measured (typically $H=L_s$) (i.e. the term $\theta_y = \Delta_y/L_s = \phi_y L_s/3$ in Table 4-2 has been replaced by $\phi_y L_s(1-(H/3L_s))/2$).

Using the same database, the plastic rotation capacity, $\theta_p=\theta_u-\theta_y$, was obtained as follows:

$$\theta_p = \gamma_{st}(1-0.46a_{cyc})(1+0.6a_{sl})\left(1-\frac{3}{8}a_{wall}\right)\left(0.25^{\nu}\right)\left[\frac{\max(0.01,\omega')}{\max(0.01,\omega)}f_c\right]^{0.25}\left(\frac{L_s}{h}\right)^{0.4}25^{CC}1.55^{100\rho_d} \quad (4\text{-}6\text{ a})$$

where γ_{st} is 0.0125 for ductile hot-rolled or for heat-treated (tempcore) steels and 0.00575 for brittle cold-formed reinforcement.

Reportedly eqs. (4-6), (4-6 a) fit the data with a median of the ratio of experimental-to-predicted-value of 1.0 and a coefficient of variation of 47%.

Eqs. (4-6), (4-6 a) were applied to 27 cyclic tests in the literature on flexure-controlled specimens without seismic detailing ("old-type" components in the present terminology). For those specimens exponent CC was taken equal to 0, as the sparse stirrups were not closed with 135° hooks. It was found that both these equations overpredict deformation capacity by 15%. So, it has been proposed that for "old-type" components the right-hand-side of eqs. (4-6), (4-6 a) should be multipled by 0.85, in addition to taking CC=0. (See c) in 4.3.6).

The equations for the plastic hinge length were modified over the expression displayed in Table 4-2, for cyclic and monotonic load conditions respectively to f_y:MPa),

Copyright fib, all rights reserved. This PDF copy of fib Bulletin 24 is intended for use and/or distribution only by National Member Groups of fib.

$$l_{p,cy} = 0.08L_s + 0.0167a_{sl}d_b f_y \quad ; \quad l_{p,mon} = 0.18L_s + 0.025a_{sl}d_b f_y \qquad \text{(4-6 b)}$$

In the model of Priestley et al. (1996) the following terms are cited in Table 4-2 as eq. (4-7):

$$\Delta_{shear}^{concr} = \frac{2(V_c + V_N)}{0.4E_{sec}0.8A_c} \cdot L_s \cdot \frac{V_n}{V_y} \; ; \quad \Delta_{shear}^{truss} = \frac{V_s s}{E_s A_{st}(d-d')} \cdot L_s \cdot \frac{V_n}{V_y} \quad ; \quad V_c = 3.5\sqrt{f_c'}(0.8A_c) \quad f_c' \text{ in psi}$$

$$V_N = \frac{N(d-x)}{2L_s} \; ; \quad V_y = \frac{M_y}{L_s} \; ; \quad V_s = V_y - (V_c + V_N) \geq 0 \quad (\text{otherwise } \Delta_{shear}^{truss} = 0) \qquad (4-7)$$

Note that eq. (4-7) is derived from the assumption that, upon cracking of the concrete web due to diagonal tension, shear strength is represented by a Mörsch-type truss. As in the case of shear force resistance, the total shear displacement comprises contributions that result, (a) from shortening of the diagonal concrete compressive struts and (b) the elongation of the tension ties of the truss mechanism (Park and Paulay 1975, Thom 1983). These are calculated for each panel of the assumed truss model, and accumulate towards the tip of the cantilever (Fig. 4-8). The $0.4E_{sec}$ factor in eq. (4-7) represents the shear modulus G_c of uncracked concrete ($G_c = E_{sec}/2(1+\nu) = 0.4E_{sec}$) where the Poisson's ratio, ν, of concrete is taken as 0.25, Park and Paulay (1975). The term $0.8A_c$ represents the effective shear-area of the member, to account for the nonuniform distribution of shear stresses on the cross section, as prescribed by the Theory of Elasticity for shear. This approach has also been adopted by Lehman et al. (1998) (Table 4-2), in calculating the elastic component of shear distortion as well as in the FEMA 273 (1997) guidelines (Chapter 6 of that document). The second term in eq. (4-7), i.e., Δ_{shear}^{truss} represents the cumulative shear distortion resulting from the elongation of stirrups, Park and Paulay (1975), Thom (1983). Note that the above expressions are meaningful so long as the ratio $V_s/V_w \leq 1$ (shear taken by the stirrups, V_s, is less than the stirrup contribution to the shear strength, V_w - otherwise, the stirrups have yielded and hence shear failure has prevailed in the member). The Priestley et al. (1996) method departs from that of its predecessors (Park and Paulay (1975) and Thom (1983)) in that it includes a separate contribution to distortion due to axial compression. Distortion results from shortening of the end-to-end inclined compression strut, which is formed by the axial compressive load N of the member (the strut extends from the point of application of axial compression to the centroid of the compression zone at the critical section, Priestley at al. (1996).

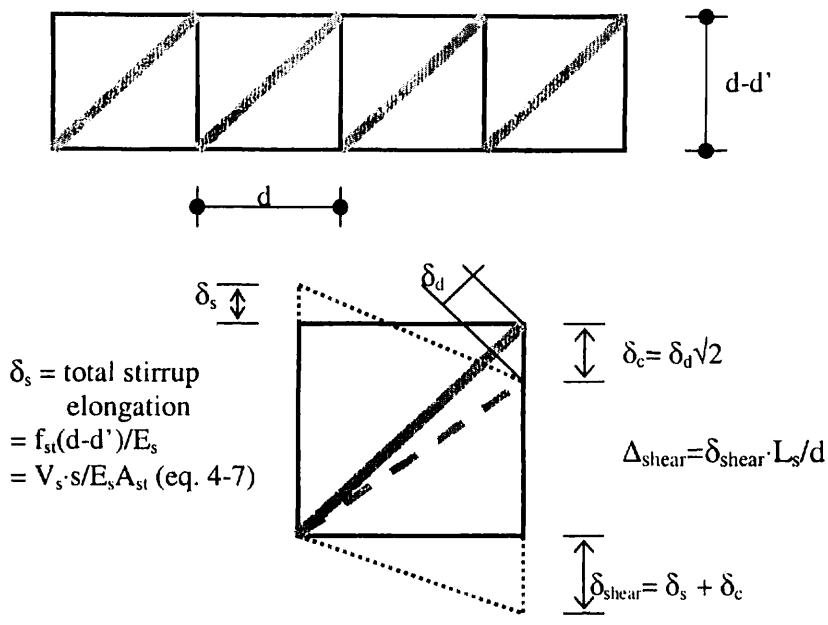

Fig. 4-8: Definition of the shear distortion terms (Park and Paulay (1975), Thom (1983))

4.3.5 Parametric investigations of analytical expressions for deformation capacity

Inel and Aschheim (2002) conducted parametric investigations using the available models so as to study the analytical trends. The reference element was a cantilever column with a 600

Copyright fib, all rights reserved. This PDF copy of fib Bulletin 24 is intended for use and/or distribution only by National Member Groups of fib.

mm square cross section, an aspect ratio of 4, loaded at the tip with a concentrated lateral load and a concentric axial force. Variables considered were the cross-section size (ranging from 300 mm to 1200 mm), the aspect ratio (ranging from 2 to 10), the amount of transverse reinforcement (as per the ATC-32 requirement, or 1/10 of that amount) and the normalized axial load ν (10% and 50% of $A_c f_c$, where f_c=28 MPa and f_y= 420 MPa). Longitudinal reinforcement ratio was 1.5% for all cases considered.

It was found that displacement ductility, plastic hinge rotation and ultimate drift capacities were insensitive to cross section size under constant aspect ratio (i.e. models are size-independent). All indices of deformation capacity (with the marked exception of the plastic hinge rotation capacity as estimated by the simple model l_p=0.5d), depend on aspect ratio, but different models can yield vastly different values of inelastic deformation measures. Aspect ratio had a particular influence on elastic contributions to peak displacement capacity and this could lead to a parametric dependency of ductility and drift on aspect ratio, particularly for lightly confined sections.

All models estimate a strong dependency of deformation indices on axial load ratio when confinement is poor, with a marked reduction of deformability as axial load ratio increases. In the presence of significant confinement, the estimated deformability is generally high and relatively insensitive to the axial load ratio. However, the discrepancy between the various models increases with increasing axial load ratio - the largest differences are observed in the inelastic component of total deformation capacity (plastic hinge rotation and drift capacity) and for high aspect ratios. The reverse result concerns the displacement ductility capacity (largest differences are observed for low aspect ratios).

From the analytical investigation it was concluded that, in general, the simple model l_p=0.5d tends to provide a lower bound estimate of plastic hinge rotation and drift for well-confined elements. The model of Lehman et al (1999) was found sensitive to the level of confinement and, for poor confinement, it was more conservative than the other models, particularly in the case of low axial load. This trend was reversed for well-confined members with a high axial load ratio, with the deformation capacity estimates of this model exceeding all others. Inel and Aschheim (2002) suggest this behaviour is due to the explicit dependency of plastic hinge length on axial load ratio. (Note this is the only model to relate l_p to $\nu=N/A_c f_c$, but the expression has been correlated only with tests conducted with axial load ratio ranging between 0% and 10%).

Displacement ductility estimates of the semi-empirical model by Panagiotakos and Fardis (2001) are higher than those of other models for poorly confined elements. Furthermore, results seem almost independent of aspect ratio, which is not quite in line with benchmark behaviour tests. It is suggested that this is due to a combination of low ultimate displacement capacity (l_p is small for low aspect ratios) and larger than usual estimates of the yield displacement.

4.3.6 Experimental data set

Experimental databases assembled from tests published in International Literature were also considered for evaluation of the model performance. Three such investigations are highlighted (Inel and Aschheim (2002), Syntzirma and Pantazopoulou (2002) and Panagiotakos and Fardis (2002)). Each database was assembled independently, using different criteria for including or excluding the various specimens. Of those, the database of Panagiotakos and Fardis (2002) has evolved from a large database that had been used previously in calibrating the empirical expressions of Panagiotakos and Fardis (2001) for yield and ultimate drift. A particular feature of the current state of the database is the inclusion of a new subset of specimens with old-type detailing.

(a) The Database Study of Inel and Aschheim (2002):

The experimental data considered here was obtained from *large-scale* tests of rectangular reinforced concrete columns subjected to quasi-static reversed cyclic lateral loading, with axial load ratios of varied intensities held constant throughout the tests. Criteria used were: (1) rectangular cross section with a minimum section size of 300 mm; (2) at least 8 longitudinal bars, each laterally supported by transverse reinforcement; and (3) aspect ratio $L_s/d \geq 2.5$. A total of 29 tests conformed with these criteria, with aspect ratios ranging between 2.86 and 4.83, $N/A_c f_c$ ranging between 0.1 and 0.77 (held constant throughout the test), f_c between 22

Copyright fib, all rights reserved. This PDF copy of fib Bulletin 24 is intended for use and/or distribution only by National Member Groups of fib.

and 47 MPa, longitudinal reinforcement ratio $1.5\% \leq \rho_c \leq 3.3\%$ with $430 \leq f_y \leq 510$ MPa, and a variety of transverse reinforcement arrangements.

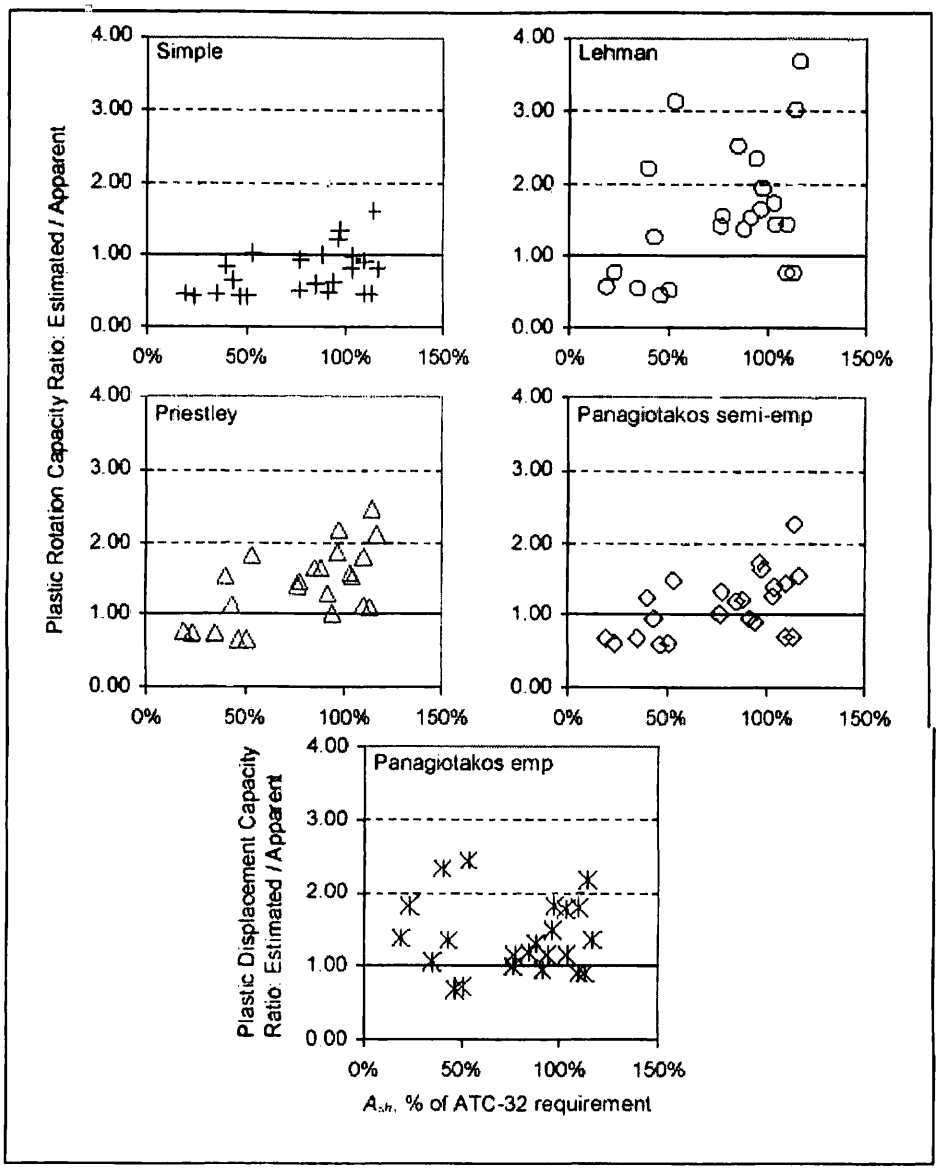

Fig. 4-9 b: Ratio of estimated to apparent plastic rotation capacities versus confinement of the retained specimens expressed as a percentage of the ATC-32 confinement requirement [From Inel and Aschheim 2002]

Experimental data was evaluated by identifying an envelope of the moment at the base of
Experimental data was evaluated by identifying an envelope of the moment at the base of
column that includes the applied lateral force and the contribution of the applied axial load. Specimens considered in the database had sufficient transverse reinforcement both within and outside the potential plastic hinge regions, so as to carry the maximum experimental shear developed during the tests. Thus, the inelastic deformation capacity of the specimens was expected to be limited by mechanisms associated with flexural deformation rather than shear strength decay. Shear strength capacities within and outside the potential plastic hinge regions of each specimen were calculated according to ATC-32 and the minimum value was taken as the calculated shear strength of each specimen. The shear demand was obtained from the experimental reports as $V_u = M_{max}/L_s$, where M_{max} is the maximum moment (including P-Δ contributions) developed during the test.

Calculated yield displacements showed large scatter compared to the experimental values,

Copyright fib, all rights reserved. This PDF copy of fib Bulletin 24 is intended for use and/or distribution only by National Member Groups of fib.

regardless of axial load magnitude and for all models. Results of the models by Lehman et al. (1998) and by Priestley et al. (1996) were similar and generally yielded lower estimates than the model by Panagiotakos and Fardis (2001), particularly in the case of small aspect ratios (due to the constant shear contribution term of the latter model).

The influence of axial load ratio on plastic rotation capacity was not clear in the presence of sufficient confinement (satisfying ATC-32 requirements). Actually, even columns with high axial load ratio could provide at least moderate deformation capacities when properly confined. Based on the experimental evidence, specimens with ATC-32 compliant transverse reinforcement achieved displacement ductility factors in excess of 6, plastic rotation capacities in excess of 0.04 rad, and drift capacities more than 4.5%.

Comparison between calculated and measured deformation capacities suggests that the analytical models can produce unconservative estimates of deformation capacity (Figures 4-9 a and 4-9 b) and generally tend to amplify the influence of transverse steel on deformation capacities (Fig. 4-9 b).

(b) The Database Study of Syntzirma and Pantazopoulou (2002):

A total of 500 tests on R.C. prismatic members were assembled into a database. Tests considered were conducted under combined reversed cyclic flexure/shear and axial load. Beams and columns with either symmetric or unsymmetric reinforcement arrangements were included. Reported failure patterns of the tests range from compression crushing to shear sliding. Since large shear demands may change the design of shear reinforcement from that required for normal stresses, whereas large shear distortions may drastically influence the buckling pattern of the reinforcement, non-shear-critical cases were distinguished in the analysis of the data, comparing the ultimate shear strength that the member attained during testing with the shear strength calculated according to the ACI Code (limit for a test to be considered as non critical in shear was: the applied maximum shear $V \leq 60\% V_u$). Experimental values for the deformation indices, such as yield and ultimate displacement or curvature were extracted from the published experimental envelopes unless otherwise specified by the respective investigators. Yielding was defined as the point marking a sharp change in the elastic stiffness, whereas ultimate deformation capacity was taken at a residual post-peak strength equal to 80% of the peak value. The geometry of the test specimens in the database, the amount and layout of the reinforcement, the concrete strength, the type of steel and the axial load, cover a very broad range (Table 4-3). In constructing the specimens a variety of volumetric ratios of confining reinforcement with different confining patterns were used (note that most of these tests would not classify as "old-type"). Transverse reinforcement was mainly grade 40 and grade 60 steel, and in many cases it did not exhibit a yield plateau. This is a weakness of the data set. In actual circumstances, transverse steel may exhibit a large post-yield strain range prior to strain hardening, that generally promotes core expansion and the subsequent deterioration of resistance at a much faster rate than hardening confining steel. To enable meaningful comparisons between different specimens, the confining effectiveness k_e of the various schemes was evaluated as described by Mander et al. (1988a) for rectangular sections.

$\nu = N/A_c f_c$	-0.18 to 0.86	Φ_l (mm)	9.51 to 31.75
s/Φ_l	1.58 to 15	f_y (MPa)	275 to 932
$\rho_{s,tr}$	0.3% to 5.9%	f_{yst} (MPa)	236 to 2050
s(mm)	22.7 to no stirrups	f_c (MPa)	14.3 to 130
ρ_c	0.8% to 6.0%	k_e	2.4% to 82.0%

Table 4- 3: Ranges of database parameters in Syntzirma and Pantazopoulou (2002)

Database values were compared against model estimates in Figs. 4-10 a, 4-10 b and 4-10 c (yield curvature, yield displacement and ultimate curvature, respectively). Calculated values are plotted on the y-axis, whereas measured values are on the x-axis. The numbers on the individual figure legends refer to the model used (columns in Table 4-2). The "a" and "b" designations imply that in calculating the respective Δ_y values, either measured or calculated

Copyright fib, all rights reserved. This PDF copy of fib Bulletin 24 is intended for use and/or distribution only by National Member Groups of fib.

yield curvatures had been used. The diagonal line represents the equal value case. Evidently, there is large scatter, confirming that in 50% of the cases most models produce unconservative results. Calculated yield curvature was under-estimated for a large number of tests. Apart from an apparent lack of correlation between analysis and experiment, this might imply that local curvature measurements are significantly affected by local slip and shear strain in the critical regions and should not necessarily be taken to reflect the actual state of deformation.

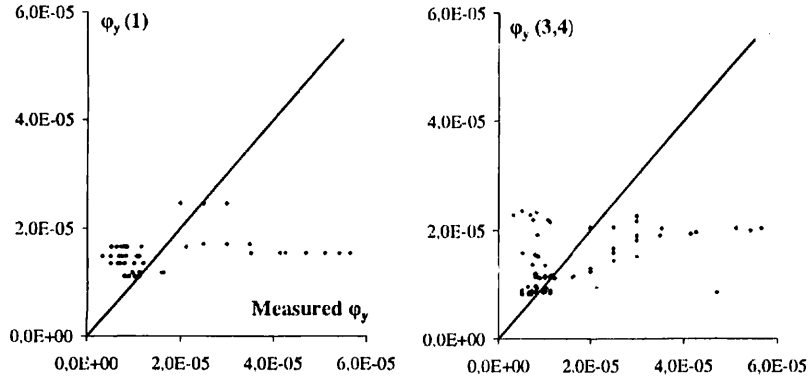

Fig. 4-10 a: Calculated vs. measured yield curvatures

From Fig. 4-10 b it is evident that the yield displacement calculated by the classical simple model (referred to as Model (1) in Table 4-2) underestimates the displacement when combined with a calculated value of yield curvature, but reproduces the mean when used with the experimental value of ϕ_y. This performance appears the best of all estimates when using experimental values of ϕ_y. Models (2) to (4) calculate reliable mean values for the yield displacement based on database results, however the scatter is as high as 100%. In terms of the ultimate curvature estimates (Fig. 4-10 c), the mean is reproduced by the classical model, although the scatter is still significant. All other models appear to significantly underestimate the mean, however, without effectively reducing the scatter over the simplistic approach.

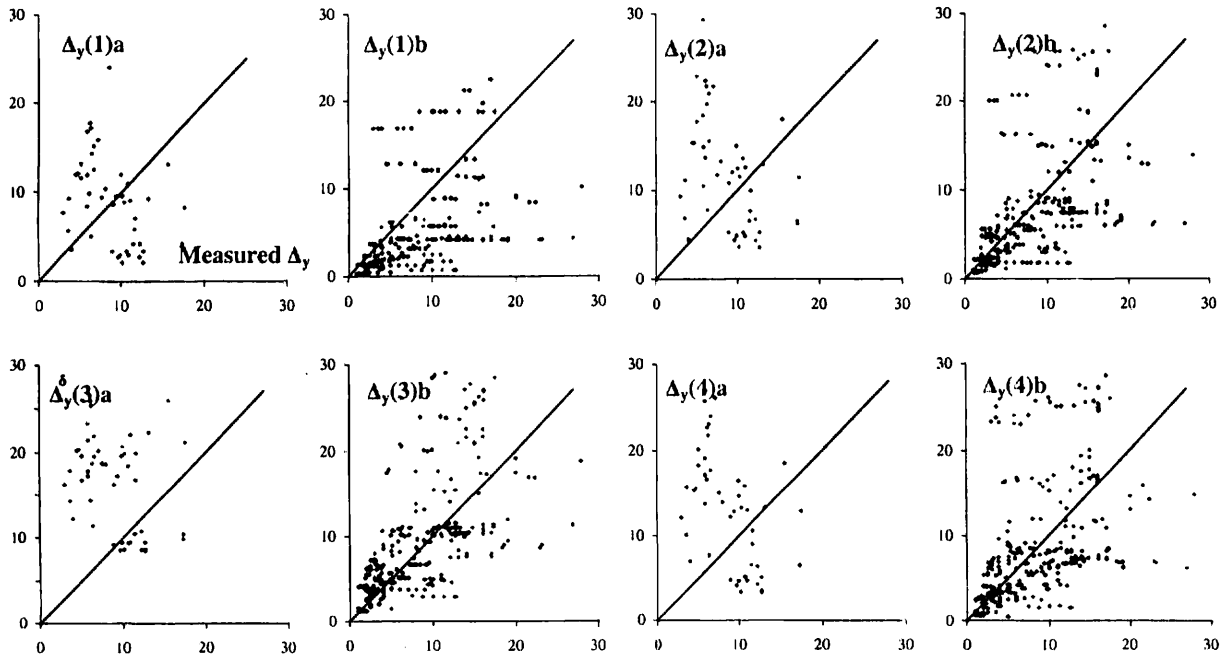

Fig. 4-10 b: Yield displacement according to the proposed models (Table 4-2). The "a" and "b" in the figure legends signify experimental and calculated values for the ϕ_y.

Copyright fib, all rights reserved. This PDF copy of fib Bulletin 24 is intended for use and/or distribution only by National Member Groups of fib.

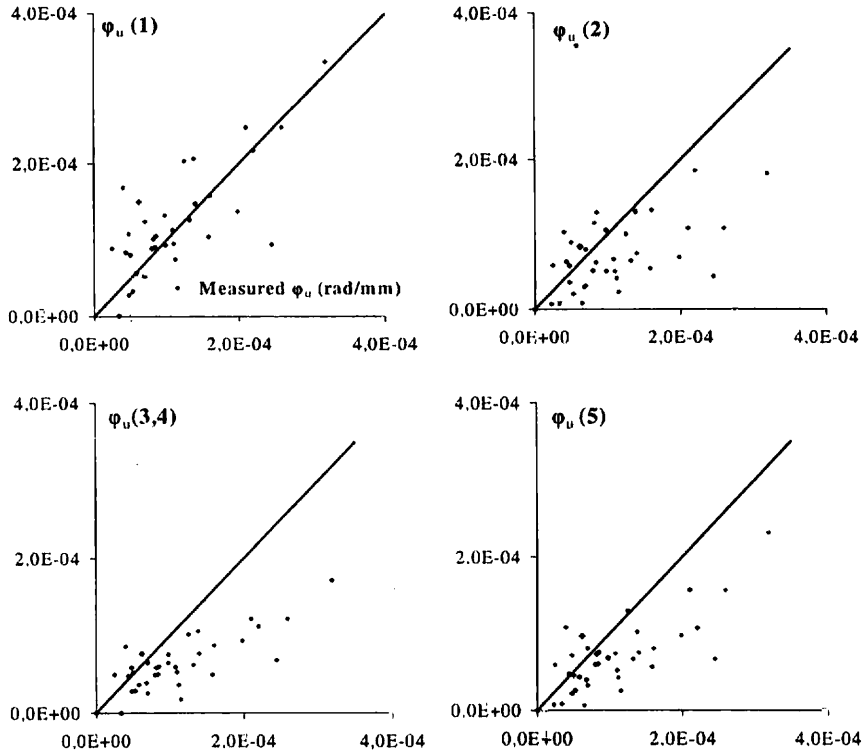

Fig. 4-10c: Ultimate curvature according to the proposed models. Note that the measured ultimate displacement has been used.

Quantity	data	mean	median	coef. of variation, %
$\theta_{u,exp}/\theta_{u,calc.eq.(4\text{-}6a)}$ "new" members monotonic	69	1.055	0.98	50.5
$\theta_{u,exp}/\theta_{u,\ calc.eq.(4\text{-}6a)}$ "new" members cyclic	786	1.04	1.00	42.5
$\theta_{u,exp}/\theta_{u,\ calc.eq.(4\text{-}6a)}$ "old" members monotonic	201	1.19	1.06	56.5
$\theta_{u,exp}/\theta_{u,\ calc.eq.(4\text{-}6a)}$ "old" members cyclic	27	0.81	0.85	42
$\theta_{u,exp}/\theta_{u,\ calc.eq.(4\text{-}6b)}$ "new" members monotonic	69	1.03	0.945	51
$\theta_{u,exp}/\theta_{u,\ calc.eq.(4\text{-}6b)}$ "new" members cyclic	786	1.04	1.00	43
$\theta_{u,exp}/\theta_{u,\ calc.eq.(4\text{-}6b)}$ "old" members monotonic	201	1.21	1.055	55.5
$\theta_{u,exp}/\theta_{u,\ calc.eq.(4\text{-}6b)}$ "old" members cyclic	27	0.84	0.85	41
$\theta_{u,exp}/\theta_{u,\ calc.eq.(4\text{-}6c,\ model\ 4)}$ "new" members monotonic	69	1.26	1.11	59
$\theta_{u,exp}/\theta_{u,\ calc.eq.(4\text{-}6c,\ model\ 4)}$ "new" members cyclic	786	1.21	1.00	77
$\theta_{u,exp}/\theta_{u,\ calc.eq.(4\text{-}6c,\ model\ 4)}$ "old" members monotonic	201	1.34	0.96	100
$\theta_{u,exp}/\theta_{u,\ calc.eq.(4\text{-}6c,\ model\ 4)}$ "old" members cyclic	27	1.68	1.72	43
$\theta_{u,exp}/\theta_{u,\ calc.eq.(4\text{-}6c,\ model\ 4)}$ "new" members monotonic	69	1.24	1.19	61
$\theta_{u,exp}/\theta_{u,\ calc.eq.(4\text{-}6c,\ model\ 4)}$ "new" members cyclic	786	1.23	1.02	73
$\theta_{u,exp}/\theta_{u,\ calc.eq.(4\text{-}6c,\ model\ 4)}$ "old" members monotonic	201	1.35	0.94	102
$\theta_{u,exp}/\theta_{u,\ calc.eq.(4\text{-}6c,\ model\ 4)}$ "old" members cyclic	27	1.80	2.00	43

Table 4-4: Mean, median and coefficient of variation of ratio of experimental-to-predicted quantities at ultimate deformation for flexure-controlled members with ("new") or without ("old") seismic detailing

(c) The Database Study of Panagiotakos and Fardis (2002).

The empirical or semi-empirical expressions proposed by the authors for θ_u (eqs. 4-6, 4-6 a, 4-6 b) were fitted to a large database of tests that covers a very wide range of values for the important design and response parameters. (For earthquake resistance and deformation capacity, these are: stirrup spacing and confining reinforcement ratio, axial load ratio, compression-to-tension reinforcement ratio, diagonal reinforcement ratio, shear span ratio,

Copyright fib, all rights reserved. This PDF copy of fib Bulletin 24 is intended for use and/or distribution only by National Member Groups of fib.

etc.). The motivating premise was that earthquake-resistant detailing or lack thereof would be reflected naturally and smoothly by the expressions fitted to such a broad database. To check whether this is indeed the case, a total of 201 monotonic test specimens were identified from the database as not intended for use in earthquake resistant construction. Most of these specimens derive from relatively old studies of the deformation capacity of flexural members for the purposes of moment redistribution under nonseismic loads. Examples are the studies by Bigaj and Walraven (1993), Bosco and Debernardi (1993), Burns and Siess (1962), Calvi et al (1993), Corley (1966), Ernst (1957), Mattock (1964), McCollister (1954), Ruiz and Winter (1969), Yamashiro and Siess (1962), etc. An additional 27 cyclic tests to flexure-controlled failure were drawn from recent investigations of deformation capacity of old-type RC members under cyclic loading (e.g. Abo-Shadi et al (2000), Aycardi et al (1994), etc.), or studies of the cyclic behaviour of such members before or after seismic retrofitting (e.g. Gomes and Appleton (1998), Fukuyama et al (1999), Furukawa et al (1996), Masuo (1999), Bousias et al (2002), Rodriguez and Park (1994), etc.). Note that this latter group of poorly-detailed specimens had not been included in the reference database of tests that had been used by Panagiotakos and Fardis (2002) for calibration of the analytical expressions for θ_y and θ_u. For these specimens the confinement effectiveness factor k_e in eq. (4-6 b) was set equal to zero, to reflect lack of proper stirrup-anchorage details.

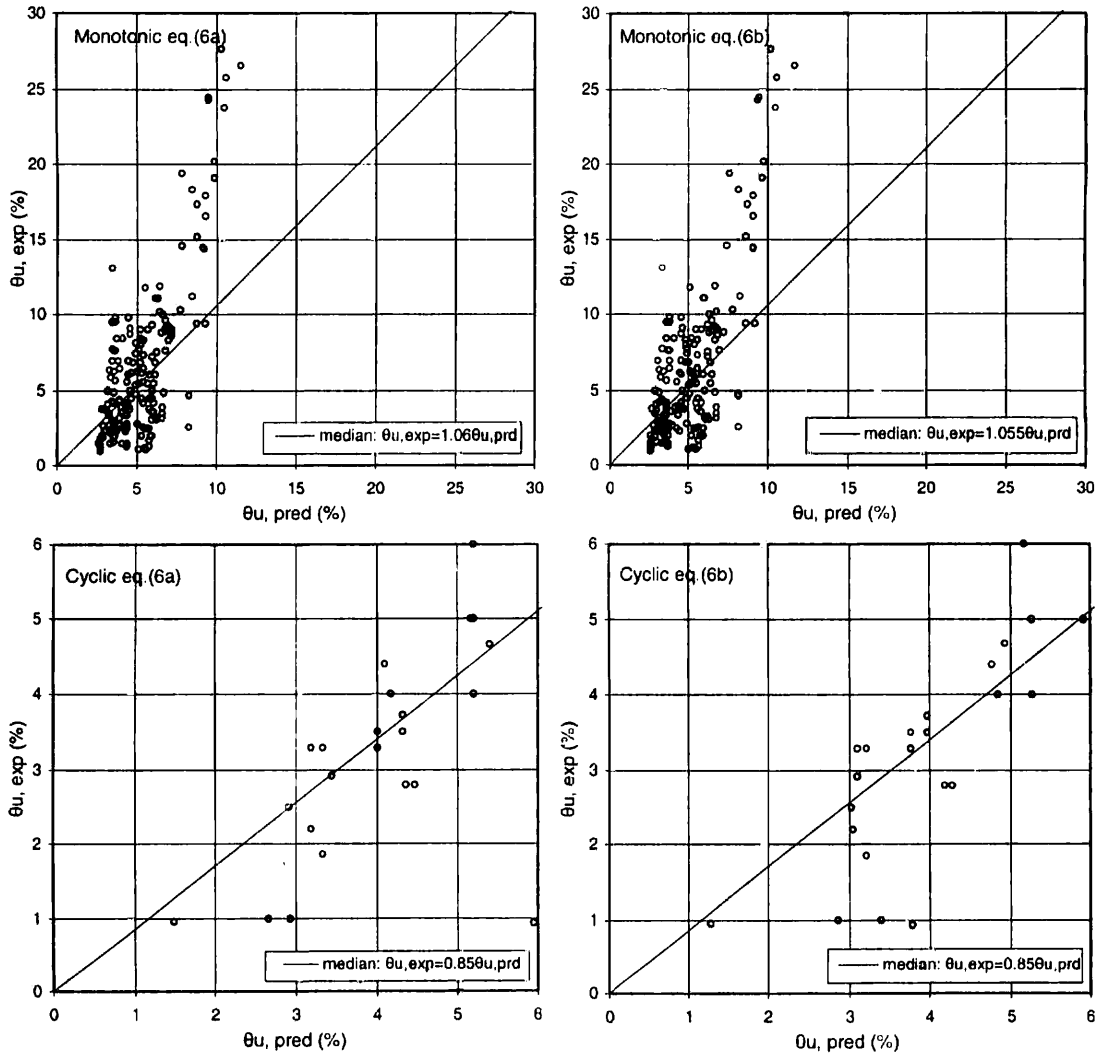

Fig. 4-11: Comparison of predictions of empirical expressions, Eqs. (4-6), (4-6 a) with results on specimens without seismic detailing ("old").

Calculated results of the empirical and the semi-empirical models of Panagiotakos and Fardis (2002) were compared with the experimental data separately for the monotonic and the cyclic tests, and separately for old-type and seismically-detailed members.

Copyright fib, all rights reserved. This PDF copy of fib Bulletin 24 is intended for use and/or distribution only by National Member Groups of fib.

As shown in Table 4-4, most of the specimens identified as having seismic detailing (termed "new") had been subjected to cyclic loading, whereas practically all non-seismically detailed specimens (termed "old") were tested monotonically. The empirical expressions, eqs. (4-6) and (4-6 a), overestimate the deformation capacity by about 15% in the few cyclic tests of non-seismically detailed members. Differences in model performance between old-type and new-type specimens are reflected in the statistics of the ratio of experimental to calculated values of θ_u listed in Table 4-4. Figures 4-11 and 4-12 compare the experimental data with the analytical estimates of the so-called empirical model (Model (3) in Table 4-2), as modified for "old" type components (eqs. (4-6 a) and (4-6 b)). The more fundamental semi-empirical alternative (Model (4) in Table 4-2 combined with eq. (4-6 c)) was also considered. Results were biased for the few cyclic tests on "old" members. The bias was much larger and in the opposite direction relative to that of the empirical model, with increased scatter.

It was concluded therefore that certain features of old-type members are not reflected through the mechanical and geometric design parameters that were selected to control either the underlying regression analyses, or the basic mechanics expressions. Clearly, these unidentified variables significantly influence the ultimate deformation capacity of old-type elements under cyclic loading. The present data may not be enough for the quantification of these effects. This is an issue requiring further work.

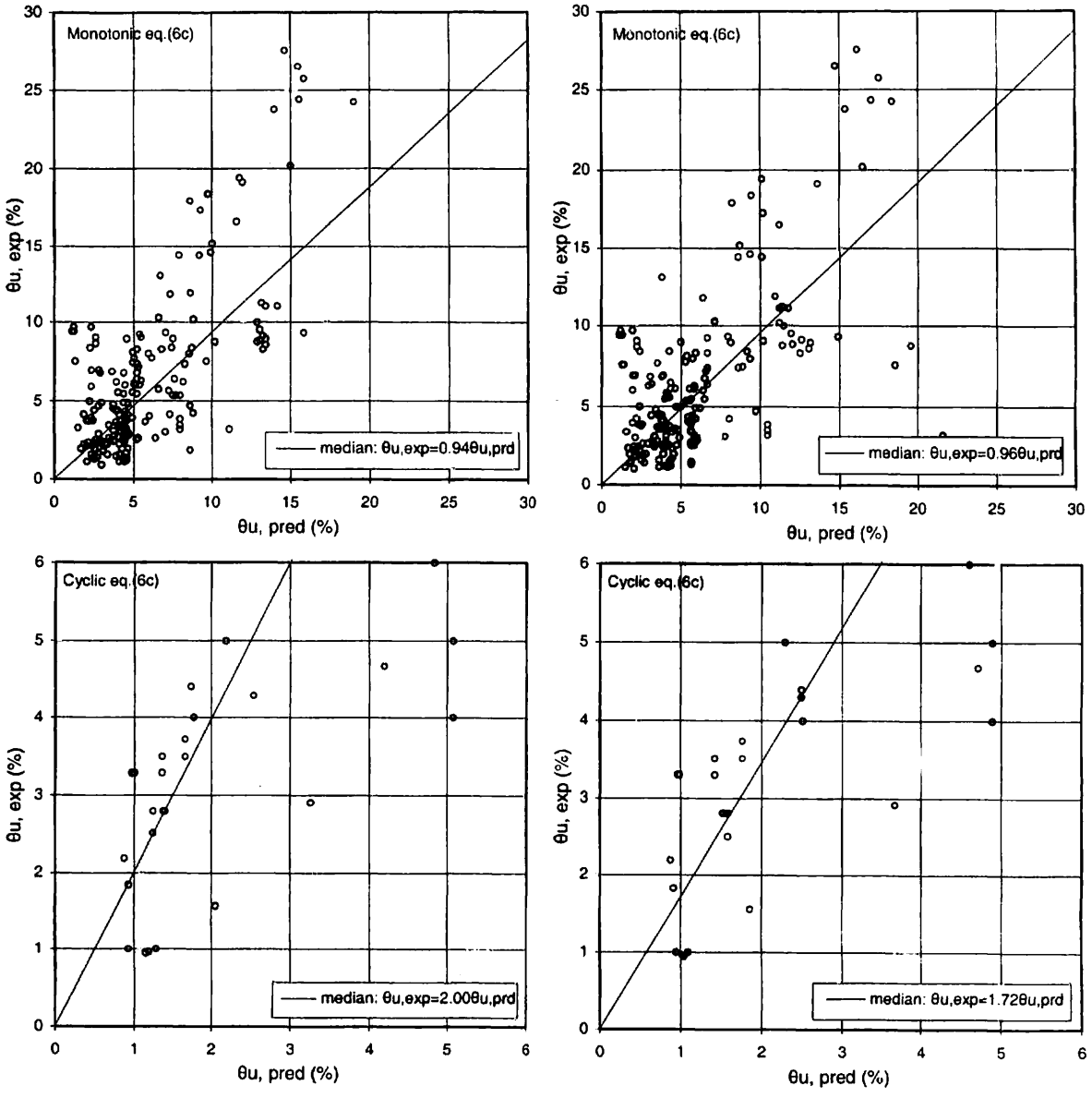

Fig. 4-12: Comparison of predictions of semi-empirical expressions (Model 4 in Table 4-2) combined with eqs. (4-6 b) for the length of plastic hinge, with results on specimens without seismic detailing ("old").

Copyright fib, all rights reserved. This PDF copy of fib Bulletin 24 is intended for use and/or distribution only by National Member Groups of fib.

4.4 Capacity-based prioritizing of strengths – localization of inelastic deformations

4.4.1 Introduction

In a deformation-based framework of assessment, a member is assumed to undergo a relative displacement of the end supports, consistent with the statics of Fig. 4-5. But the exact pattern of dependable deformations is not simply a matter of cross-sectional properties as Fig. 4-4 (b) and 4-4 (c) would imply. Whereas a moment-curvature analysis could suggest a sufficiently ductile behaviour up to a compressive strain level of 0.005 (this limit usually marks the onset of cover spalling near the critical section), for an effectively unconfined, lightly reinforced cross-section, the actual amount of displacement will be limited by other mechanisms of failure likely to prevail prior to development of full inelastic flexural action. (Note that typical conditions in unconfined reinforced concrete members include, spacing of hoops or stirrups in the critical region at $s \geq d/2$ or $s \geq 16d_{bl}$, with stirrup ends not properly anchored back into the core, whereas restraint against bar buckling by tying the bar at a tie corner is seldom available for intermediate bars). In the absence of closely spaced stirrups alternative failure mechanisms could be: diagonal tension failure of the web, buckling of compression reinforcement, disintegration of the compressive struts due to reversal of load and limited anchorage or lap-splice capacity of primary reinforcement.

The sequence in which these mechanisms will occur *uniquely* defines the deformation response of the member; therefore, the problem of assessing deformation capacity is rather complex and cannot easily be treated by closed form expressions. By prioritizing the dependable capacities of the alternative mechanisms of member behaviour, it is possible to determine the weak link of the member (e.g. a lap-splice failure). Once the strength of the weakest link is overcome, then that mechanism of behaviour becomes the fuse of the member response. Upon increase of the imposed end displacement, deformation is expected to localize in that fuse and hence, beyond that stage, all other forms of nonlinear behaviour are irrelevant.

Considering that localized deformations of any kind other than flexural (including pullout) may prove fatal for member integrity, it is natural to associate Δ_u and the corresponding value of ϕ_u, that are used in the expressions of Table 4-2, to the onset of localization. The limiting strength $V_{u,lim}$ is obtained from the requirement,

$$V_{u,\lim} = \min\{V_{flex}, V_{lap}, V_{shear}, V_{buckl}\} \qquad (4-8)$$

where, V_{flex}: shear force required to develop the flexural capacity at the support: $V_{flex}=M_u/L_s$

V_{lap}: shear force that may be sustained when the anchorage of reinforcement or lap splice reaches its capacity: $V_{lap}=M_{lap}/L_s$, M_{lap} being the moment sustained at the support at that instant.

V_{shear}: web shear strength

V_{buckl}: shear force sustained when compression reinforcement buckles at the critical section.

The terms of eq. (4-8) may be derived from first principles. One such approach is detailed in the following.

4.4.2 Calculation of flexural strength

The ideal flexural strength is meaningful only if it may be safely assumed that it is supported by all other mechanisms of behaviour (i.e., if $V_{flex} < \{V_{shear}, V_{lap}, V_{buckl}\}$). The bending moment sustained when the flexural reinforcement reaches yield for the first time is M_y^m and in a monotonic loading history the ultimate flexural resistance is M_u^m. Both M_y^m and M_u^m may be calculated from standard theory. Panagiotakos and Fardis (2001) have proposed analytical expressions for calculating M_y^m (given in Appendix 4 A) and M_u^m. The corresponding values of V_{flex} are, $V_{flex,y}^m = M_y^m/L_s$, $V_{flex,u}^m = M_u^m/L_s$.

The reduced flexural yield strength that may be sustained after cyclic reversal of load, ought to consider that the compression steel has yielded in tension in the preceding cycle (Thom 1983). At this point cracks will be still open in the compression zone; hence all the compressive force will be resisted by compression reinforcement. Only if this reinforcement

Copyright fib, all rights reserved. This PDF copy of fib Bulletin 24 is intended for use and/or distribution only by National Member Groups of fib.

yields in compression may the cracks close so that the concrete may contribute to compression resistance. For equal areas of top and bottom reinforcement the cyclic yield moment, M_y^c is $M_y^c=A_{s1}f_{ys}(d-d_2)$ (Thom 1983). For the same case, the ultimate cyclic moment theoretically is $A_{s1}f_{us}(d-d_2)$, but in the absence of confinement the maximum compressive strain, ε_{cu}, is not expected to exceed 0.005 (the cover spalling strain); it is therefore best to take $M_u^c=M_y^c$. For unequal areas of compression and tension reinforcement, $M_y^c=A_{s2}f_{ys}(d-d_2)$ and $M_u^c=A_{s2}f_{us}(d-d_2)+(A_{s1}-A_{s2})f_{us}z$ (the last term to be included if confinement is available).The corresponding values of V_{flex} are: $V_{flex,y}^c= M_y^c/L_s$, $V_{flex,u}^c= M_u^c/L_s$.

4.4.3 Calculation of shear strength

Based on recent tests it has become evident that shear strength of reinforced concrete degrades faster with cyclic load, for higher ratios of shear demand to shear supply. Wood and Sittipunt (1990) proposed a limit of 60% as a cutoff point in identifying shear failures from other types of failures when processing the experimental literature on walls. Thus, according to this proposal, a shear failure is likely to occur when $0.6V_{shear}< V_{flex}$, even if the nominal check prescribed by the code holds, namely that $V_{flex}<V_{shear}$. The reason why the traditional "capacity check" is not sufficient to preclude a shear failure is because the mechanisms of shear resistance in reinforced concrete break down with damage accumulation, as they depend either directly or indirectly on the ability of concrete to carry tension.

A variety of models have been proposed for the shear strength of reinforced concrete as a function of deformation (Ma et al. 2000, Priestley et al. 1996, Lehman et al. 1998, Martin-Perez and Pantazopoulou 1998, FEMA-273 1997, Moehle et al. 1999, 2001, Kowalsky and Priestley, 2000)). A working hypothesis for all models is that the shear strength of cracked reinforced concrete comprises a primary contribution, V_w, of web reinforcement (the tension ties of the Ritter-Mörsch truss analogy) and secondary contributions, V_c. These are attributed to other mechanisms of resistance that are mobilized through diagonal tension of the concrete web, i.e., the dowel action of longitudinal reinforcement spanning across cracks, the frictional interlock between cracked interfaces and reinforcement to concrete bond (tension-stiffening) along the bar between successive cracks. A point of difference between the various models is whether the contribution of axial compression to shear resistance (which is believed to delay opening and affect inclination of cracks) should be accounted for under V_c, or whether it should be added separately to highlight its significance as a distinct mechanism of resistance. The latter approach is adopted in the models developed at UC San Diego for circular columns by Priestley and his co-workers (e.g. Priestley et al. 1996, Kowalsky and Priestley, 2000). The most recent version of these models is that presented by Kowalsky and Priestley (2000) as "Revised UCSD model" (units: MN, m):

$$V_{shear}=\sqrt{f_c}k(\mu_\Delta)\min\left(1.5,\ \max\left(1,\ 3-\frac{L_s}{h}\right)\right)\min(1,\ 0.5+20\rho_{tot})(0.8A_g)+N\frac{h-x}{2L_s}+V_w \qquad (4\text{-}9a)$$

In eq. (4-9a) ρ_{tot} is the total ratio of longitudinal steel, A_g is taken equal to $\pi D^2/4$ (D= diameter of gross section), h is the depth of the cross-section (equal to the diameter D in circular sections), N the axial load (positive for compression), x the depth of the compression zone and L_s the shear span. $k(\mu_\Delta)$ is a coefficient equal to:

$$0.05 \le k(\mu_\Delta) \le 0.28,\ k(\mu_\Delta)=\frac{1.07-0.115\mu_\Delta}{3} \qquad (4\text{-}9b)$$

For rectangular sections Eq. (4-9a) has been applied with term $0.8A_g$ replaced by b_wd.

The contribution of transverse steel, V_w, is taken as:

$$V_w=\rho_w b_w z f_{yw}\cot\theta \quad \text{in rectangular sections,} \quad V_w=\frac{\pi}{2}\frac{A_{sw}}{s}f_{yw}(D-c-x)\cot\theta \quad \text{in circular} \qquad (4\text{-}9c)$$

with A_{sw} denoting the cross-sectional area of a circular hoop, s its spacing and c its concrete cover, ρ_w the ratio of transverse steel in members with rectangular section and $z\approx d-d'\approx 0.9d$ their internal lever arm. The inclination of compression struts θ is taken equal to 30° in the revised UCSD model.

Kowalsky and Priestley (2000) developed eqs. (4-9) on the basis of 18 circular columns that failed in shear after yielding in flexure. They compared also its predictions to the strength

Copyright fib, all rights reserved. This PDF copy of fib Bulletin 24 is intended for use and/or distribution only by National Member Groups of fib.

of 20 columns failing in shear from the beginning and of nine failing in flexure.

Syntzirma and Pantazopoulou (2001) tested the available shear strength model estimations against a large database of experimental results on prismatic R.C. members under reversed cyclic load. It was concluded from this study that no model could systematically reduce scatter between analytical and experimental values. However, one model that appeared to be mostly on the conservative side, was the one proposed by Moehle et al (2001). Another attractive aspect of that proposal was simplicity of form: nominal shear strength is calculated from truss and concrete contributions, but multiplied by a single reduction coefficient k that depends on the magnitude of imposed ductility demand. Through k, which operates on both the V_w and V_c terms, it is recognized that the truss component V_w is also affected by damage accumulation due to the tension-softening of the compressive struts that support the truss function (Vecchio and Collins 1986, Martin-Perez and Pantazopoulou 2001):

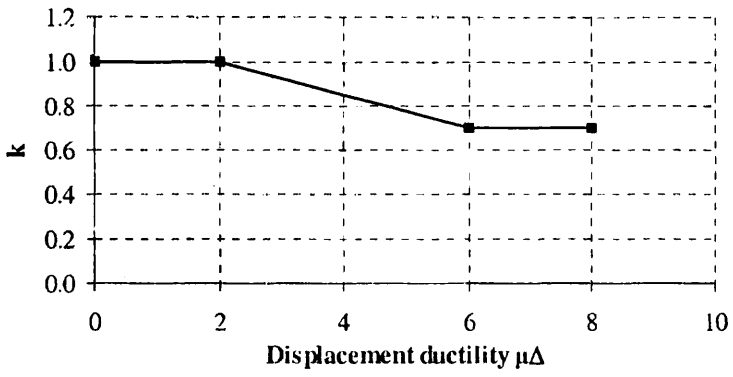

Fig. 4-13: Variation of reduction coefficient k as a function of displacement ductility demand

$$V_{shear} = k(V_w + V_c); \quad V_w = A_{st} f_{yst} \frac{d}{s}; \quad V_c = 0.5\sqrt{f_c'}\left(\frac{d}{L_s}\sqrt{1+\frac{N}{0.5\sqrt{f_c'}\cdot A_c}}\right)\cdot A_c \ (MPa) \quad (4-10a)$$

$$0.7 \le k(\mu_\Delta) \le 1.0, \quad k(\mu_\Delta) = 1.15 - 0.075\mu_\Delta \quad (4-10b)$$

The V_c term is the product of the principal tensile stress at diagonal cracking by the gross section area. The tensile strength of concrete is taken as $0.5\sqrt{f_c}$ (MPa) ($6\sqrt{f_c}$ in psi). Fig. 4-13 plots the proposed variation of k with displacement ductility demand; the reduced shear strength value is 70% of the initial value at a displacement ductility of 6.

This empirical model is consistent with theoretical investigations based on the diagonal compression field theory, which have shown that at a ductility of shear distortions in the order of 2 (yielding of shear reinforcement occurring in a range of shear distortion of 0.004-0.006), the total shear resistance is reduced to 75% of the initial value. Further reduction up to 30% of the peak value was estimated at a ductility of shear distortions of 3 or more (Tastani and Pantazopoulou 2001). (Note that ductility of shear distortions concerns the ratio of peak to yield shear strain in the plastic hinge region, γ_u/γ_y; therefore the total displacement ductility is much higher than these reference values).

Three aspects of shear behaviour of reinforced concrete are particularly relevant to old-type construction and need be highlighted:

(a) The truss action can only be counted for if ties are spaced close enough to secure that any diagonal crack (taken for simplicity at an angle of 45° to the longitudinal axis of the member) is crossed by at least one stirrup layer. Open or inadequately anchored stirrups may not be able to develop their full yield strength, if the critical section where

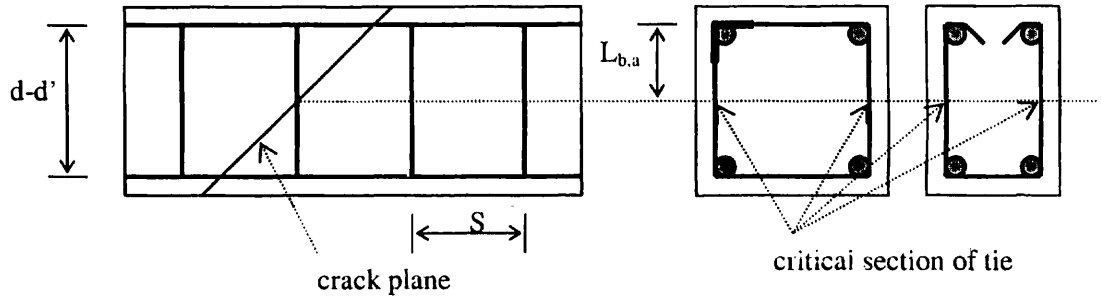

Figure 4-14: Calculation of the tie capacity based on tie anchorage conditions

Copyright fib, all rights reserved. This PDF copy of fib Bulletin 24 is intended for use and/or distribution only by National Member Groups of fib.

they cross the crack is very near to their anchorage (Fig. 4-14). In such cases, the V_w term in eq. (4-10a) ought to be computed for a stirrup stress equal to the value that the tie anchorage can support and not the ideal yield value f_{yst} as implied by eq. (4-9a). Thus, $f_{st}=f_{yst}\cdot L_{b,a}/0.7L_b$, where $L_{b,a}$ the available anchorage length of the tie measured from the point where it is intercepted by the crack to the end hook and L_b the standard straight anchorage length for the bar diameter of the ties considered (Fig. 4-14).

(b) It can be shown that shear distortion imposes a tensile strain on all reinforcements, the magnitude of which may be estimated from equilibrium and compatibility. If the axial stress force is low or negligible, the net stress in all longitudinal reinforcement may be tensile, particularly for low aspect ratios - high shear demands (Tastani and Pantazopoulou 2001). Based on the 45° truss model, the tensile strain increments resulting from shear action in the longitudinal and transverse directions may be taken approximately as:

$$\varepsilon_s = \frac{0.5V_s}{E_s A_s}\ ; \quad \varepsilon_{str} = \frac{0.5V_s}{E_s A_{str}} \qquad (4-11)$$

where V_s the shear force that is actually resisted by the stirrups (eq. 4-7). Indeed, considering these strain values as additive to the flexural strains, it is concluded that, unless the compression strains caused by flexure or axial load in the compression zone are very high, the compression reinforcement may carry a net tensile strain upon load reversal (i.e., a full reversal of load will not produce symmetric strains in tension and compression). This means that compression reinforcement is principally susceptible to sideways buckling as described in section 4.3.5. A simple assumption is that upon load reversal, if the normalized axial load is less than $(\rho_{s1}-\rho_{s2})f_y/f_c$, it should be assumed that the cracks remain open and therefore the V_c term should be taken zero. Hence, a modified version of eq. (4-10a) for calculating the V_c term in eq. (4-10) is as follows:

$$\text{if } \frac{N}{A_c\cdot f_c'} \geq (\rho_{s1}-\rho_{s2})\frac{f_y}{f_c'} \quad \Rightarrow V_c = 0.5\sqrt{f_c'}\cdot\left(\frac{d}{L_s}\sqrt{1+\frac{N}{0.5\sqrt{f_c'}\cdot A_c}}\right)\cdot A_c\ (MPa) \qquad (4-10c)$$

$$\text{otherwise,} \quad V_c = 0 \qquad (4-10d)$$

(c) Moehle et al. (2001) investigated the gravity load carrying capacity of damaged columns using a shear friction model. A motivating observation was that drift at column failure appears to be inversely related to the magnitude of axial load. With reference to Fig. 4-15, they derived from equilibrium considerations the following relationship between residual axial load capacity and stirrup forces:

$$N_{res} = A_{st} f_{st}\frac{d-d_2}{s}\tan a\left(\frac{1+\mu_f \tan a}{\tan a-\mu_f}\right) \quad ; \quad \text{where } \mu_f = 2(1-\frac{\theta}{0.08}) \qquad (4\text{-}12)$$

The angle a is the inclination of the critical crack plane to the horizontal (depending on the axial load it varies between 50° and 70°). The model is supported by relevant experimental evidence and is based on the formation of a sliding plane where frictional resistance develops. The column is supposed to have lost most of its lateral load resistance, thus the external force V shown in the figure is taken equal to zero. The coefficient of friction μ_f was related to the maximum lateral drift, θ, experienced by the column during lateral sway as prescribed by eq. (4-12); its range is between 2 and 0 (for 8% drift). For 2% drift, μ_f is 1.5, for 4% μ_f is 1. Corollary to this finding is that, if V_{shear} (from eq. (4-10)) controls the check prescribed by eq. (4-8), then the structure may be assumed to have reached a state of imminent collapse (since the stirrups will have reached their capacity according to eq. (4-10)). The relative magnitude of the tributary gravity load of each column, as compared to the N_{res} value given by eq. (4-12), determines whether the collapse also involves loss of gravity load carrying

Copyright fib, all rights reserved. This PDF copy of fib Bulletin 24 is intended for use and/or distribution only by National Member Groups of fib.

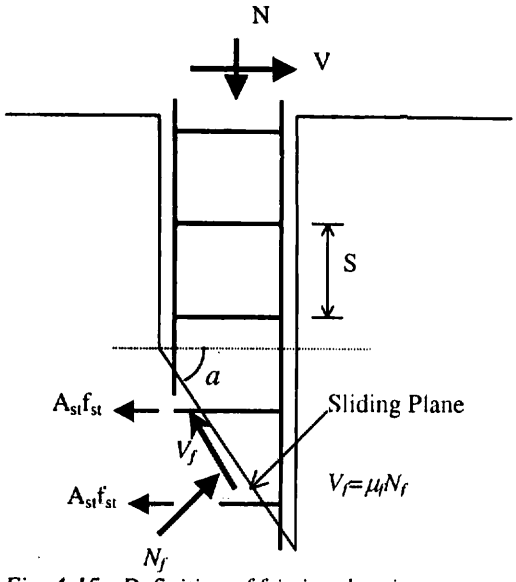

Fig. 4-15: Definition of frictional resistance along a sliding plane (from Moehle et al. 2001)

capacity. Note that eq. (4-12) is very sensitive to the value of a, yielding vastly different results for large changes in the angle. A lower bound stable solution is obtained for the entire range of values for μ_f, when a is taken between 65° and 70°.

Evaluation of Shear Resistance Using the Extended Panagiotakos and Fardis Database

The Panagiotakos and Fardis database of available cyclic test results was extended by Biskinis, et al (2003) with specimens failing in shear after yielding in flexure, with the aim of contributing to the effort of shear-strength assessment along the lines of previous work. The end result was a database of 154 cyclic tests considered to lead to shear-controlled failure after initial flexural yielding. The database includes 41 tests on columns with circular section and 113 tests with square or rectangular one. One specimen with circular section and 23 with rectangular are deemed representative of specimens without seismic detailing ("old" type of columns).

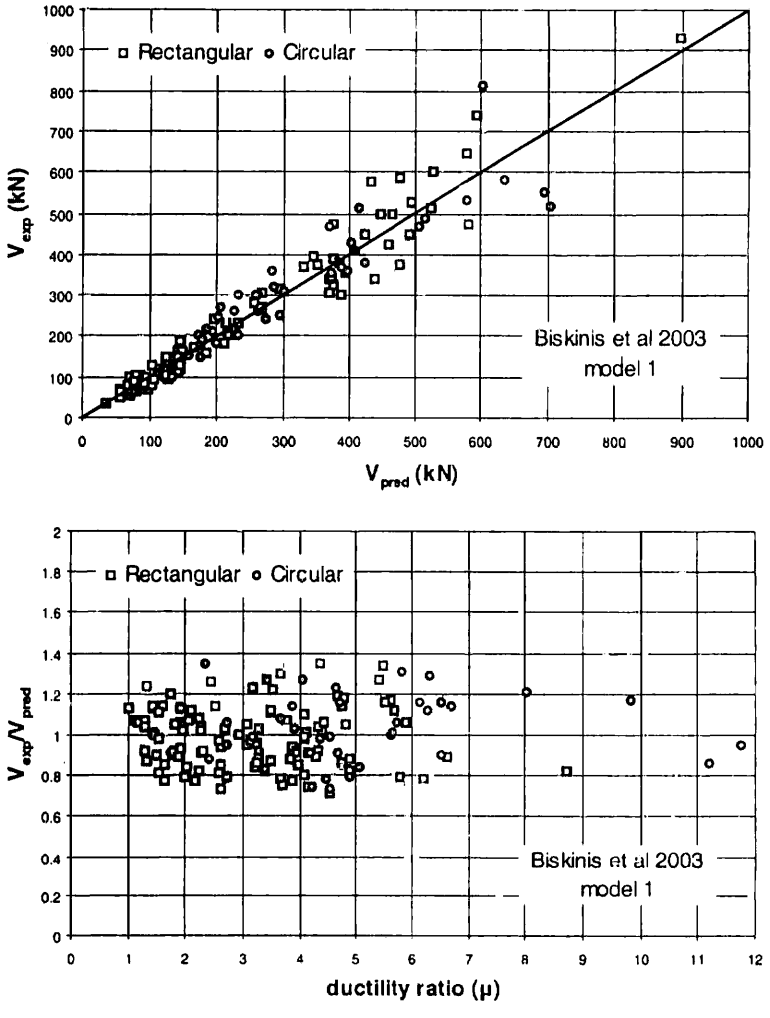

Fig. 4-16: Comparison of estimates of eq. (4-13) with experimental data

The 154 tests are included in the database on the basis of the following criteria:

- the observed failure mode – (shear or shear/flexure, after initial flexural yielding);
- an experimental yield moment which is not significantly less than the value estimated

Copyright fib, all rights reserved. This PDF copy of fib Bulletin 24 is intended for use and/or distribution only by National Member Groups of fib.

on the basis of first principles (to avoid tests in which yielding is controlled by shear);

- an experimental ultimate chord rotation not significantly exceeding the value calculated from the empirical equations for flexure-controlled members – eqs. (4-6 a), (4-6 b); and
- the estimates of previous models, namely those by Kowalsky and Priestley (2000) and Moehle et al (2001) for shear resistance as a function of the experimental value of μ_Δ, as compared to the experimental yield force.

The outcome is two expressions for V_{shear} in terms of μ_Δ; the first following the format of Kowalsky and Priestley (2000) and the other one that of Moehle et al (2001).

The first expression is (units: MN, m):

$$V_{shear} = \frac{h-x}{2L_s}\min(N, 0.55A_c f_c) + 0.16\max\left(0,\ 1-0.08\min\left(5, \mu_\Delta^{pl}\right)\right)\max(0.5, 100\rho_{tot})\left(1-0.16\min\left(5, \frac{L_s}{h}\right)\right)\sqrt{f_c}A_c + V_w \tag{4-13}$$

In eq. (4-13) V_w is taken according to eq. (4-9b) with the inclination of compression struts θ equal to 45° (as in the classical Ritter-Mörsch truss) and with (D-c-x) replaced by D for circular columns. μ_Δ^{pl} is the ratio of the plastic component of chord rotation at failure (total chord rotation minus value at yield) to the yield chord rotation θ_y calculated as per Table 4-2 (Model (3)), or from a similar expression for columns of circular section – with the 2nd term (shear distortion at yielding) replaced by 0.001.

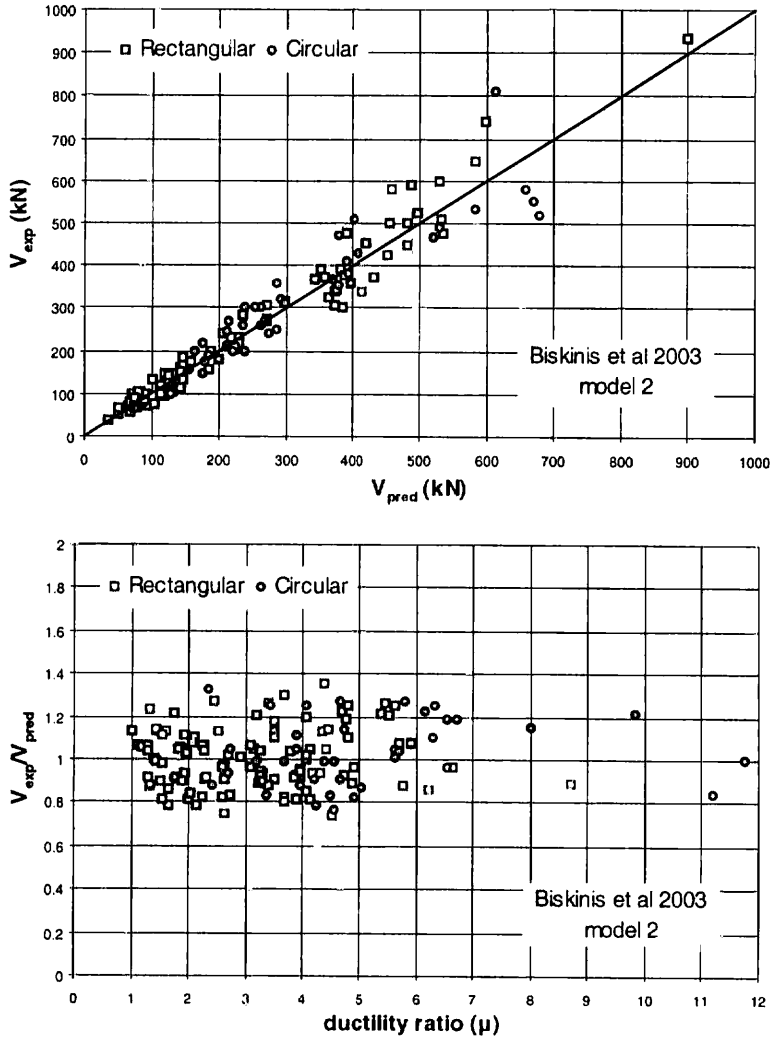

Fig. 4-17: Comparison of estimates of eq. (4-14) with experimental data

The reason for using the calculated value of θ_y as a normalising factor instead of the experimental one is two-fold: a) in practical applications the exact value of θ_y is not known a-priori and has to be predicted by some means; and b) to prevent parasitic experimental effects from affecting the result; this is the case with the flexibility of the base of the 24 cantilever

Copyright fib, all rights reserved. This PDF copy of fib Bulletin 24 is intended for use and/or distribution only by National Member Groups of fib.

specimens by Ang et al (1985), which may have artificially increased the pre-yield tip deflection but is believed to have affected very little post-yield deformations of the specimen.

Eq. (4-13) fits the data with a mean and median of the ratio of experimental to calculated values equal to 1.0 and a coefficient of variation of 15.3%. The median is also equal to 1.0 for the subsets of columns with circular or rectangular section, and for those with new or old-type detailing. It should be noted that in the 11 specimens by Sezen (2000) and Lynn et al (1996) the contribution of stirrups was reduced by half due to the 90° hooks of stirrups.

Fig. 4-16 compares the estimates of eq. (4-13) with the test results and shows the ratio of experimental to calculated shear as a function of $\mu_\Delta=\mu_\Delta^{pl}+1$.

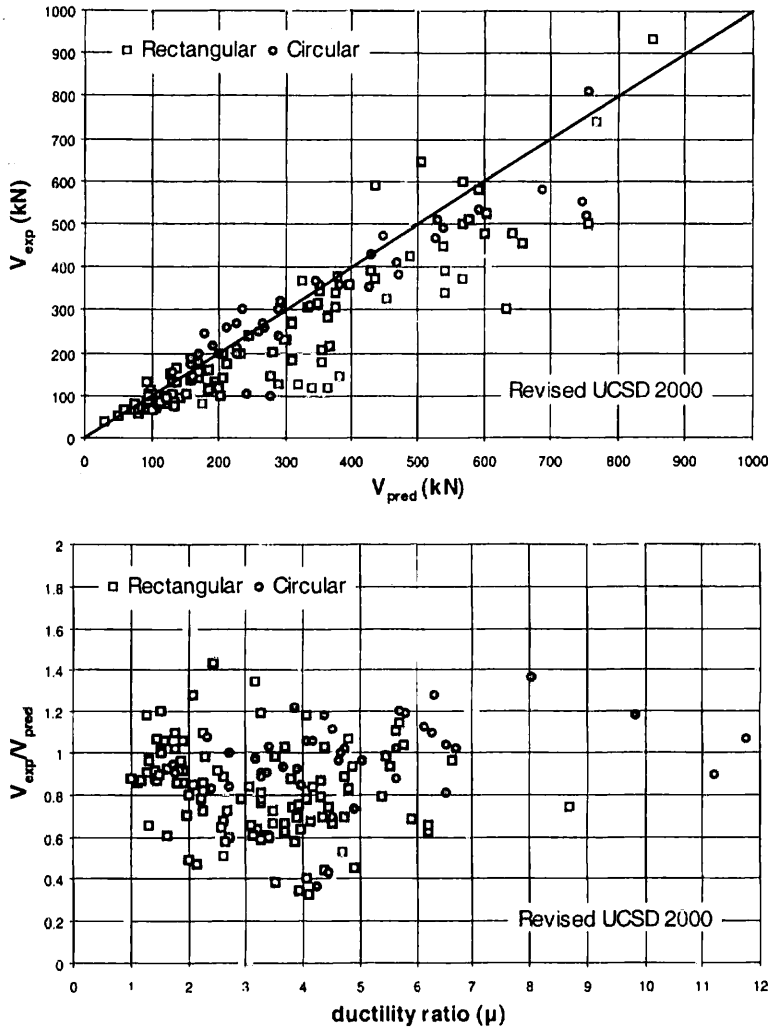

Fig. 4-18: Comparison of the model by Kowalsky and Priestley (2000), eq. (4-9a, b), with experimental data.

The second alternative is, following the format of Mochle et al (2001):

$$V_{shear}=\frac{h-x}{2L_s}\min(N,0.55A_cf_c)+0.16\max\left(0,1-0.055\min\left(5,\mu_\Delta^{pl}\right)\right)\left[\max(0.5,100\rho_{tot})\left(1-0.16\min\left(5,\frac{L_s}{h}\right)\right)\sqrt{f_c}A_c+V_w\right] \quad (4\text{-}14)$$

Eq. (4-14) fits the data with a mean and median of the ratio of experimental to predicted values of 1.0 and a coefficient of variation of 14% (lower than that achieved with eq. (4-13)). Again, the median is equal to 1.0 also for the subsets of columns with circular or rectangular section, and for those with new or old-type detailing (again with the contribution of stirrups with 90° hooks halved). Fig. 4-17 compares the predictions of eq. (4-14) with the test results and shows the ratio of experimental to predicted shear as a function of $\mu_\Delta=\mu_\Delta^{pl}+1$.

If the experimental value of μ_Δ^{pl} is used in eqs. (4-13), (4-14) (i.e. with the experimental yield chord rotation as normalizing factor, in the same way as eqs. (4-9) and (4-10) were developed and proposed), then average agreement with tests remains good, while the

Copyright fib, all rights reserved. This PDF copy of fib Bulletin 24 is intended for use and/or distribution only by National Member Groups of fib.

coefficient of variation of the ratio of experimental to predicted values decreases to 14.8% and 13.4% respectively (for eq. (4-13) though, the median of the ratio is 0.98; if factor 0.16 in the 2nd term of eq. (4-13) is replaced by 0.155, a median of 1.0 and a coefficient of variation of 15% are achieved).

The same 154 tests were used to evaluate previous proposals, namely those of Kowalsky and Priestley (2000), eq. (4-9 a, b), and of Moehle et al (2001), eq. (4-10 a, b). Comparison of test results with these models is presented in Figs 4-18 and 4-19.

The Kowalsky and Priestley (2000) proposal gives median value of the ratio of experimental to calculated results equal to 1.0 for circular columns or to 0.83 for rectangular sections (overall median of 0.88) and corresponding coefficients of variation of 20.1% and 26.1% (overall coefficient of variation 25.5%). The Moehle et al (2001) proposal gives median value of the ratio of experimental to calculated results equal to 1.0 for rectangular sections and 1.11 for circular ones (overall median of 1.05) and corresponding coefficients of variation of 26.3% and 17.2% (overall coefficient of variation 24.3%). In other words, both models provide good average agreement for the type of column to which it was fitted (as a matter of fact, the data used for the development of these two models are also included in the Biskinis et al, 2003 database), albeit with larger scatter than any of the two models by Biskinis et al, 2003. The fit for the other type of section is, however, worse.

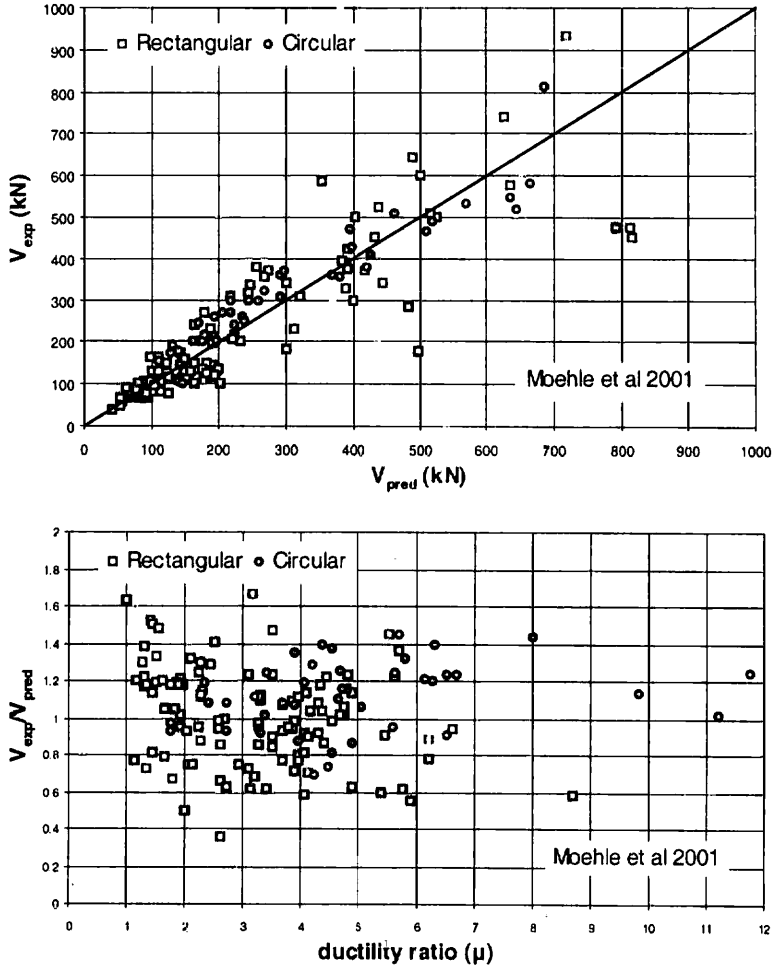

Fig. 4-19: Comparison of the model by Moehle et al (2001), eq. (4-10 a, b), with experimental data

4.4.4 Calculation of anchorage and lap-splice strength

Premature failure of a lap-splice or anchorage effectively limits the force developed in the reinforcing bar to a value lower than its axial strength. In old-type construction, common bond-related problems are owing to: (a) The practice of splicing the main column reinforcement just above the base of each floor (i.e., within a plastic hinge zone), but without special provisions for confinement through stirrups. (b) The use of smooth reinforcement, where anchorage capacity depends on frictional mechanisms mobilized along the anchored

Copyright fib, all rights reserved. This PDF copy of fib Bulletin 24 is intended for use and/or distribution only by National Member Groups of fib.

length. (c) The use of short embedment or lap lengths.

Both flexural bond and bond between lap-spliced bars need be considered. Note that flexural bond refers to the bond action resulting from variation of bar stress due to moment over the member length. Although not commonly checked for columns of moderate aspect ratio and longitudinal bar diameter, this action is particularly important for columns with relatively large-diameter longitudinal bars, small concrete cover and light transverse reinforcement. ACI 318-99 and EC2 present procedures for determining the minimum required lengths for straight bar anchorage and for lap–splices in new construction. The required lap lengths in regions of high stress exceed the required anchorage lengths, mainly to discourage use of laps in regions of high stress (ACI 408). According to Lynn et al (1998), tests demonstrate that strength for given length of lap–splice is essentially the same as that for the same length of straight bar anchorage (equal to only about 20 bar diameters). Therefore one view is that, in evaluating existing splices it is appropriate to use equations for straight anchorage length without code–specified modifications for lap–splices.

The force F_s, that a lap-splice or anchorage zone of length L_b may develop, may be taken equal to the total frictional force that develops on the bar lateral surface within the length L_b (Priestley et al. 1996). The frictional force is proportional to the normal clamping force, through the frictional constant μ_f (for concrete, μ_f is usually taken between 1 and 1.5). In the absence of stirrups in the lap region, the clamping pressure is only provided through the tensile resistance of the concrete cover, f_t, developing over a crack path of length p (Fig. 4-20). Therefore, the force that an unconfined lap splice may develop equals to: $F_s=p \cdot f_t \cdot L_b$, and the corresponding bar stress $f_s= p \cdot f_t \cdot L_b/A_b$, where A_b the cross sectional area of one lapped bar. Even if $f_s \geq f_y$, the actual strength that may be supported by the lap length without stirrups is likely to disintegrate upon load reversal. The region of the lap, being also in a plastic hinge region, will be located alternatingly in the compression and tension zone of the column cross section as the direction of the seismic force reverses. For axial compressive strains in excess of 0.0015-0.002, tensile cracks parallel to the direction of the compressive force are expected to occur (when axial compressive strain is in that range, the corresponding transverse strains are approximately half that value, i.e. Poisson's ratio near peak stress ≈ 0.5). Upon reversal of the load the lap region will try to develop tension force in the bar, but with the cover cracked, the clamping force will be diminished. Therefore, even if the theoretical flexural strength is reached once, upon the first cycle of loading to a full reversal response is expected to degrade rapidly. Priestley et al. (1996) proposed a methodology for determining the residual moment capacity of columns: (a) without any stirrups in the lapped region, and (b) with adequate amounts of stirrups. Interpolation between these two limits is proposed in order to assess the lap-splice strength of an existing component with some, but not adequate amount of transverse reinforcement.

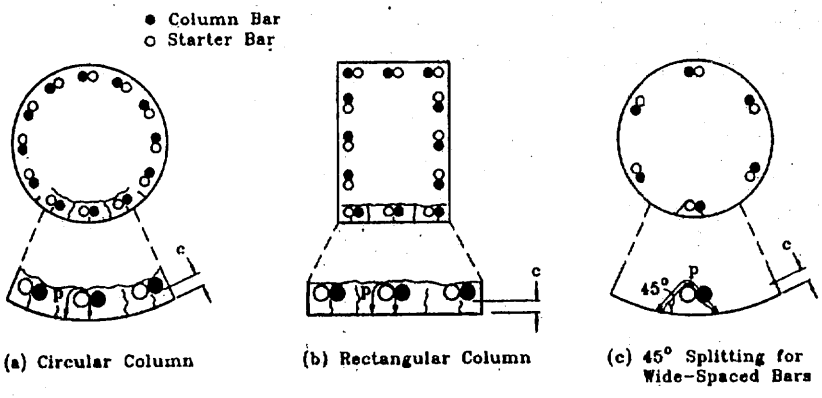

Fig. 4-20: Definition of crack path after Priestley et al (1996)

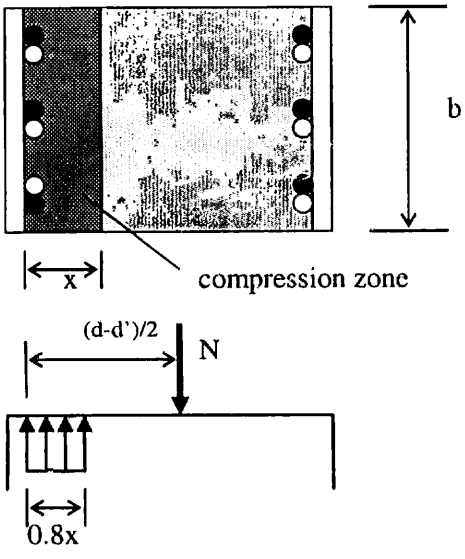

Fig. 4-21: Development of residual couple upon failure of unconfined lap-splices

Copyright fib, all rights reserved. This PDF copy of fib Bulletin 24 is intended for use and/or distribution only by National Member Groups of fib.

A similar approach is proposed in the FEMA 273 (1997) Commentary (Chapter 6) for anchorages. When the available length of embedment is not sufficient to develop the bar force, it is recommended that the clamping action of normal reinforcing bars is used in lieu of restraining action to support friction (for example, in the case of a beam-column joint where beam bars do not have adequate anchorage length into the joint, the stress in the adjacent longitudinal column bar determines the magnitude of clamping action: the higher the tension in the column bar, the lower is the clamping force on the beam bar (Moehle et al. 1994).

The following relationship (in lb, in) describes the reduction in beam bar anchorage capacity (stress), as a function of the column bar tension stress: $f_{s,beam}=120\sqrt{f_c}L_b(50000-f_{s,column})/\Phi \leq f_y$ (it is implicitly assumed that $f_{s,column}$ will be calculated from a column section moment analysis). Calvi et al. (2001) used the same model to evaluate the force developed in horizontal smooth beam bars anchored through a beam column joint from the compressive resultant in the compression zone of the adjacent column cross section, using the frictional force concept.

Limit (a): Residual flexural strength of a cross section without stirrups along the lap-length

In this case the contribution of the lapped reinforcement in the flexural behaviour of the cross-section is neglected. The residual flexural strength is due to the eccentricity - or lever arm - between resultant compressive forces on the cross section and the externally applied axial load (taken to act at the centroid of the section, Fig. 4-21). Hence, $F_s=0$, and

$$M_{res} = N \cdot \left(\frac{d-d_2}{2} - 0.4x \right) \quad ; \quad x = \frac{N}{0.85 f_c' b} \qquad (4-15)$$

Limit (b): Flexural strength of a cross section with stirrups along the lap length.

The maximum clamping force that stirrups may provide equals $A_{tr}f_{yst}L_b/s \cdot n$ where n the total number of bars restrained by the stirrups in the direction considered (Fig. 4-20). (For stirrups to be accounted for in this calculation, they should interrupt the crack path p mentioned in the preceding). Priestley et al. (1996) suggested a coefficient of friction equal to 1.4 when transverse reinforcement is used as a restrainer. Thus, the axial force supported by each lapped longitudinal bar equals: $F_s=(1.4A_{tr}f_{yst}L_b/s \cdot n)+(p \cdot f_t \cdot L_b)$ and the corresponding axial tension stress, $f_s=(1.4A_{tr}f_{yst}L_b/s \cdot n \cdot A_b)+(p \cdot f_t \cdot L_b/A_b) \geq f_y$, where the second term is to be ignored if the maximum axial compression strain exceeds 0.002. An alternative is to take the coefficient of friction equal to 1 (Lynn et al. 1998). By setting $f_s=f_u$, the required amount of transverse (stirrup) reinforcement $(A_{tr})_{req}$ may be obtained for the splice to develop its strength (if hooks are used, then a reduction factor of 0.7 ought to be used on the bar strength value that need be developed).

For all other cases between the two limits presented above (i.e. for values of $A_{tr}<A_{tr,req}$), it is direct to interpolate between $M_{res}(A_{tr}=0)$ and $M_n(A_{tr,req})$, by assuming a linear variation between flexural strength M_{lap} and the strength of tension lap-splices. The corresponding shear strength V_{lap} in eq. (4-8) is calculated from: $V_{lap}=M_{lap}/L_s$.

4.4.5 Calculation of strength of compression reinforcement

Instability of compression reinforcement always accompanies crushing of the concrete compression zone, as necessitated by compatibility of deformations (shortening) between the two components. Under monotonic load conditions, deformation capacity of the compressed zone of the member depends on the effectiveness of the confining reinforcement, because the confining pressure that may be mobilized uniquely determines the critical compression strain that the core may sustain without loss of integrity. Buckling of primary reinforcement reduces expected axial and flexural strength and ductility, causing very short plastic hinge lengths (some studies

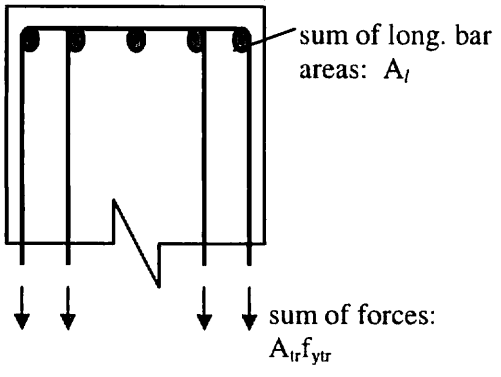

Fig. 4-22: Definition of terms in eq. (4-16)

Copyright fib, all rights reserved. This PDF copy of fib Bulletin 24 is intended for use and/or distribution only by National Member Groups of fib.

suggest hinge lengths even shorter than stirrup spacing, Albanesi et al. 2001, 2002). The resulting localization of deformations corresponds to doubling or even tripling the curvature ductility demands accompanied by brittle failure.

(a) In the absence of well anchored, stiff and closely spaced ties, elastic buckling may occur before the bar reaches yielding. The bar slenderness ratio (s/Φ) determines the buckling conditions: for a S400 compressed bar to yield in compression before it buckles, stiff ties must be spaced at $s/\Phi=35$; the corresponding ratio for S220 is 47. If the ties are very flexible, it is conservative to assume that the length of the buckled bar may extend over the entire length of the plastic hinge, which may encompass several tie spacings. In that case the axial compressive strain sustained by the bar is $\varepsilon_{s2}=\pi^2\Phi^2/4l_p^2\leq\varepsilon_y$. This is the upper limit in a moment-curvature calculation, defining the moment strength, M_{buckl}, of the cross section and the corresponding buckling shear force $V_{buckl}= M_{buckl}/L_s$. An approximate criterion is that, in order to avoid elastic buckling over several tie spacings, a restraint force of 1/16 of the yield capacity of the longitudinal bar would be required (i.e. the tie diameter would need be ¼ of the bar diameter, Priestley et al., 1996). For assessment, to establish whether buckling will occur over a single or multiple tie spacings the following check must be considered (Priestley et al. 1996):

$$k_o = \frac{A_{tr} f_{yst}}{s} \geq \frac{1}{16} A_l f_{yl} \frac{1}{6\Phi} \qquad (4-16)$$

where A_{tr} the total area of stirrup legs in the direction of restraint and A_l the total area of restrained compressed bars (Fig. 22). Alternatively, Albanesi and Biondi (1994) proposed that buckling is expected to occur over a single tie spacing if tie stiffness exceeds the limit

$$k_{cr} = \frac{\pi^4 EI}{l^3} \eta_{cr} \qquad (4-16\,a)$$

where E the longitudinal bar modulus, $l=(n_t+1)s$ being the number of stirrups involved in buckling and η_{cr} a nondimensional stiffness index equal to β/π^2, with $\beta=64$ or 26 in the case of equally spaced stirrups ($s=l/2$) or with different spacing $0.33l$ and $0.66l$, respectively. Depending on the configuration of stirrups the above limit may be expressed alternatively as a limit on tie to longitudinal bar diameter ratio.

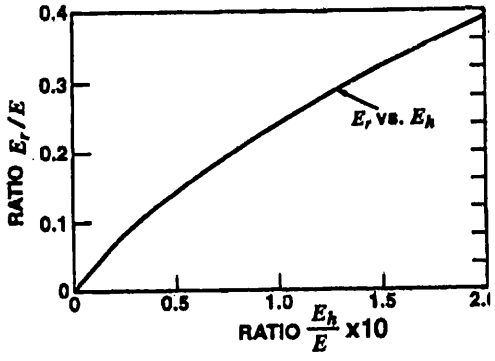

Fig. 4-23: Calculation of double modulus from tangent modulus (from Pantazopoulou 1998)

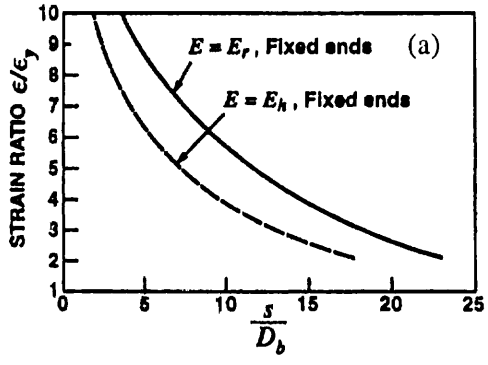

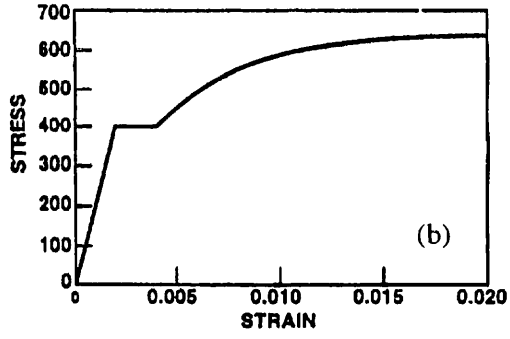

Fig. 4-24: (a) Normalized critical strain as a function of the s/Φ ratio. (b) Stress strain model used in deriving (a)

(b) Based on the works of Mau (1990), Monti and Nuti (1992), Watson et al. (1994) and

Copyright fib, all rights reserved. This PDF copy of fib Bulletin 24 is intended for use and/or distribution only by National Member Groups of fib.

others, tie spacing should not exceed 6Φ for the longitudinal bar to develop its *ultimate* strength, f_u, before buckling. This has been based on bars with significant amount of strain hardening (f_u=1.5f_y); closer tie spacing is required for lower amounts of strain hardening. The relationship between spacing of ties, modulus of elasticity and bar axial compressive stress is:

$$\frac{s}{\Phi} = 1.5\sqrt{\frac{E}{f_s}} \quad ; \quad E = 200\,GPa, if\ f_s \le f_y; \quad E = E_r, if\ f_s > f_y \qquad (4-17)$$

In eq. (4-17) E_r is the double modulus, i.e., a weighted average of the elastic and the strain hardening modulus E_h (tangent value). For easy reference the ratio of E_r/E, where E the elastic modulus of steel, is plotted against the ratio E_h/E in Fig. 4-23. (Here, the double modulus is considered to be an upper limit for the effective bar stiffness, whereas the tangent modulus provides a lower limit.) Given the tie spacing in a member with old-type detailing, the dependable axial compressive strain at which reinforcement is likely to buckle, ε_{buckl}, is calculated from (4-17), or may be obtained graphically as shown in Fig. 4-24 (a) different curves are obtained for different stress-strain relationships in the strain hardening region. The plot shown has been obtained from the steel stress-strain model shown in Fig. 4-24 (b). An equivalent to the lower limit mentioned in the preceding (eq. 4-16) for the distributed tie stiffness, $k = K/s$, has been derived from first principles as f_u^2/E_r for each restrained, longitudinal bar, where K the tie stiffness to extension in its plane of action (Pantazopoulou, 1998).

Note that the above relationships break down if E_h=0. For the bar to survive through the yield plateau region and to enter strain-hardening, the adjacent core must be effectively confined so as to enable load redistribution from the bar to the concrete once the bar looses stiffness as a consequence of buckling. The axial compressive strain that corresponds to the deformation capacity of the confined core is estimated from the normalized effective confining pressure in the direction of lateral sway, $k_e\rho_{s,st}f_{yst}/f_c$ using either of the following two expressions (Paulay and Priestley 1992, Imran and Pantazopoulou, 1996):

$$\varepsilon_{cu} = 0.004 + \frac{1.4\varepsilon_{su}\rho_{s,tr}f_{yst}}{f_{cc}} \qquad (4\text{-}18a)$$

$$\varepsilon_{cu} = \varepsilon_{cu}^{o}\left(1 + \frac{24.6k_e\rho_{s,st}f_{yst}}{f_c'}\right) \quad ; \quad 0.003 \le \varepsilon_{cu}^{o} \le 0.004 \qquad (4-18b)$$

where ε_{su} is the deformation capacity of the stirrup steel and ε_{cu}^{o} the deformation capacity of uniaxially loaded concrete (in the above, note the difference in the amount of transverse reinforcement used – in eq. (4-18 a), the volumetric ratio $\rho_{s,tr}$ is being used, whereas in the model of Imran and Pantazopoulou it is the ratio of shear reinforcement in the direction of sway, $\rho_{s,st}$). The critical compression strain in moment-curvature analysis should not exceed the limit ε_{crit}=min{ε_{buckl}, ε_{s2}}, where ε_{s2} the strain in the compression reinforcement when the maximum core strain reaches the limit given by eq. (4-18). If M_{buckl}^m is the monotonic moment strength value corresponding to a maximum compressive strain of ε_{crit} (either on the extreme fibre on in the centroid of the compression steel depending on the controlling minimum limit) then the corresponding shear V_{buckl}^m in eq. (4-8) is, $V_{buckl}^m = M_{buckl}^m/L_s$.

According to Albanesi and Biondi (1996) the post-elastic buckling may be triggered by a sudden change in the configuration of confinement associated with yielding of transverse reinforcement, which effectively increases the unsupported length of the bar. Therefore, the critical compression strain may be defined as the least of {ε_{buckl}, ε_k), where ε_k is the strain when actual tie stiffness reaches the limit value given by eq. (4-16a). Albanesi and Biondi (1996) state that the limit ε_k closely matches experimental data, while ε_{buckl} underestimates the ultimate concrete compressive strain.

(c) For closer spacing of ties, inelastic buckling occurs, involving extensive plastification of the longitudinal bar, but only after significant core expansion has occurred (confined concrete in the postpeak branch). In such cases the failure zone is extensive and buckling may spread over a large number of tie spacings (Pantazopoulou 1998).

Copyright fib, all rights reserved. This PDF copy of fib Bulletin 24 is intended for use and/or distribution only by National Member Groups of fib.

(d) Under reversed cyclic load, buckling of reinforcement may occur in many different ways, depending on the overall circumstances of the compression zone, including the load history. A bar in compression may have yielded in tension during the previous cycle. Whether cracks are open or closed depends on the amount of tensile strain, $\varepsilon_{s,t}$, sustained by the bar in the previous excursion (Fig. 4-25).

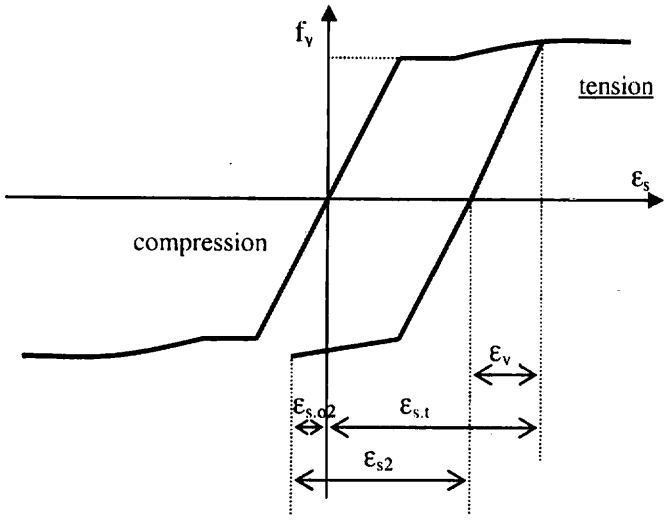

Fig. 4-25: Critical compression strain under cyclic load reversals

Note that in the presence of shear, additional tensile strains are expected on the cross section (Tastani and Pantazopoulou, 2001). Thus, full reversal of strains and closure of cracks in the compression zone may occur only in the presence of significant axial compression, or alternatively, if large plastic rotation develops in the plastic hinge from excessive pullout of the tensile reinforcement. Up until the cracks close the reinforcement is also susceptible to sideways buckling (Scribner et al, 1984). To preclude this possibility, the tie diameter must be at least half that of the longitudinal reinforcement, particularly if the longitudinal bar is restrained only by the flexural action of the tie (i.e., if it is not tied on a stirrup corner). If ε_c is the maximum compressive strain at the extreme fibre of the compression zone, the corresponding strain in the compressed bar is $\varepsilon_{s,o2}=(1-(d_2/x))\varepsilon_c$. But the strain (and corresponding stress) that must now be entered in Fig. 4-24 or eq. (4-17) to evaluate the likelihood of buckling is: $\varepsilon_{s2}=\varepsilon_{s,t}-\varepsilon_y+\varepsilon_c(1-d_2/x) \approx \phi \cdot d-\varepsilon_y$, where ϕ is the maximum sectional curvature experienced during the preceding cycle.

4.5 Empirical calculations of deformation capacity

Empirical relationships were extracted from an extensive database of column and beam tests with various confining arrangements, to quantify deformation capacity of reinforced concrete members (Pantazopoulou, 1998). These provide lower bounds (*characteristic values*) for: (a) The compressive strain of concentrically loaded confined concrete. (b) The displacement ductility capacity of prismatic members under combined moment-shear and axial load:

$$\varepsilon_{85} = 0.003 + 0.075(k_e \rho_{s,tr} f_{yst} / f_c' - 0.1) \geq 0.003 \quad (4\text{-}19)$$

$$\mu_{\Delta,80} = 1.3 + 12.4(k_e \rho_{s,tr} f_{yst} / f_c' - 0.1) \geq 1.3 \quad (4\text{-}20)$$

The subscripts $_{85}$ and $_{80}$ highlight that the respective deformation capacities are associated with a 15 and 20% drop of peak strength in the descending envelope of the experimental load-deformation curve, respectively (i.e., 15% loss of strength in the group of concentrically loaded specimens, and 20% loss of strength in the group of flexural members). The database was also used in Section 4.2.6 in testing the models of Table 4-2 and contained specimens with various volumetric ratios of confining reinforcement, having different confining patterns (different confinement effectiveness coefficients, k_e); (most specimens would not classify as "old-type", Syntzirma and Pantazopoulou 2001). As it is suggested by the form of the empirical relationships, confining reinforcement that yielded nominal confining pressures < $10\% f_c'$ were considered ineffective (e.g. old type construction). Thus, the constants 0.003 and 1.3 represent the axial strain and displacement ductility capacities of lightly reinforced members. Note that eq. (4-19) represents dependable axial compressive strain, obtained from tests with uniform strain distribution on the member cross-section.

Copyright fib, all rights reserved. This PDF copy of fib Bulletin 24 is intended for use and/or distribution only by National Member Groups of fib.

To reduce the conservatism implicit in eq. (4-19), the strain-gradient effects that occur in flexure may be considered in the same manner as in the EC2 design procedure (where ε_{cu} for concentric compression is 0.002, whereas for eccentric compression ε_{cu} is taken 0.0035). This increase by 50% of the values obtained by eq. (4-19) would result in a lower bound of compressive strain capacity for flexure equal to 0.0045, which corresponds to the strain at cover spalling observed in cyclic shear tests.

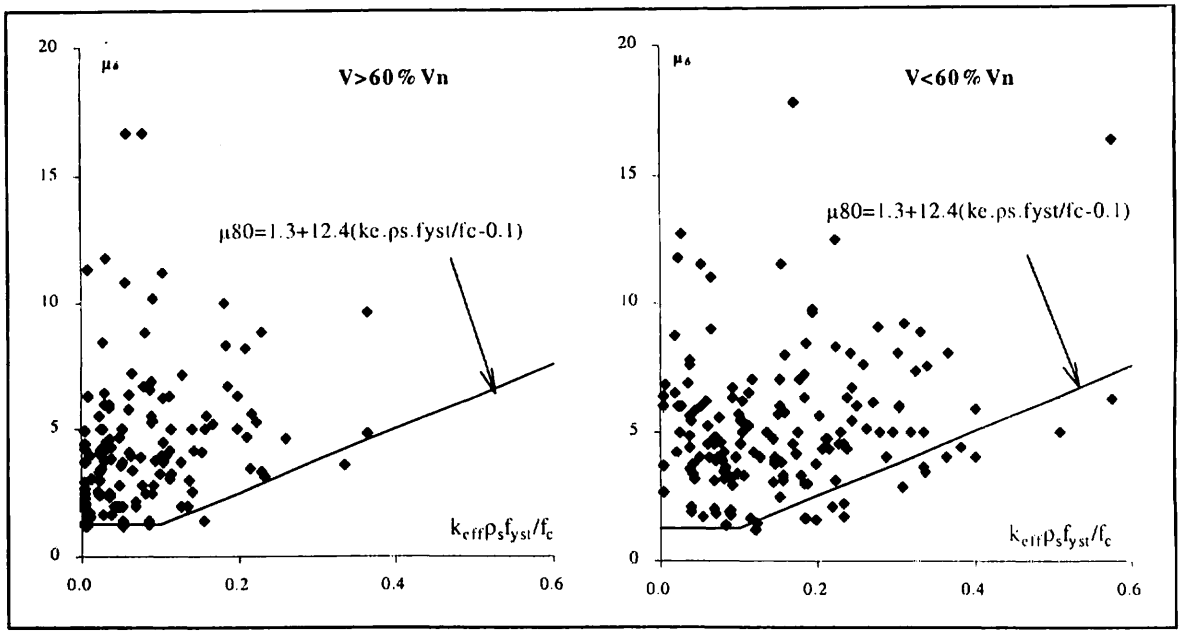

Figure 4-26: Fitting of eq.(4-20) to experimental data

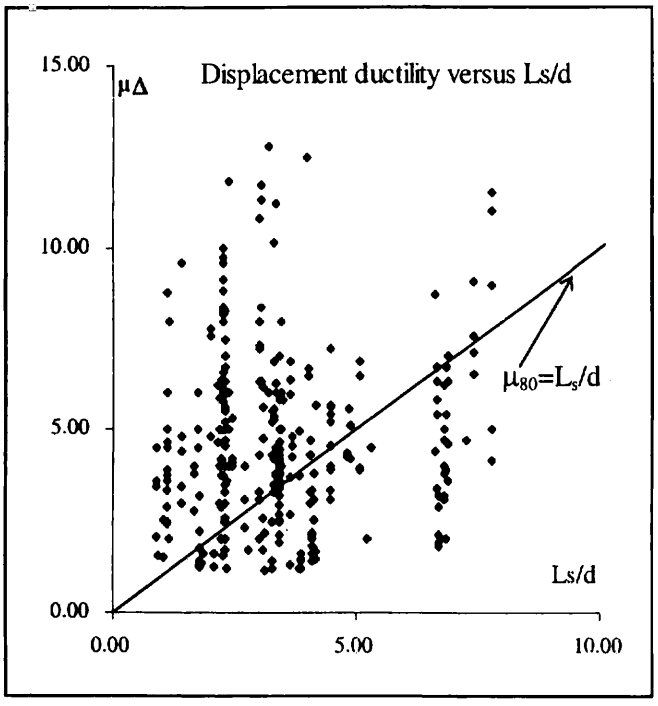

Fig. 4-27: Displacement ductility according to the Tassios and Moretti (2001) Model.

Displacement ductilities were calculated from ultimate (as defined in the preceding) and yield displacements; the latter was read off the force-displacement plots at the point where a sharp change in slope would occur, and is therefore somewhat subjective. A more consistent and meaningful index of deformability would have been curvature or curvature ductility; however this information was not available in most published experimental reports.

Tassios and Moretti (2001) performed a similar investigation to obtain lower bounds of deformation capacities of short (so-called captive) columns. It was concluded that confinement is not as effective in increasing displacement ductility of short columns as in conventional flexural concrete members, because the principal mode of action is the inclined strut from end to end, rather than the familiar truss model. Conservatively, the available displacement ductility may be taken equal to the aspect ratio i.e., $\mu_{80}=L_s/d$. Fig. 4-27 plots the proposed relationship for the complete database of tests assembled by Syntzirma and Pantazopoulou (2001); it appears that the proposed relationship corresponds to a mean approximation of the experimental trend.

Copyright fib, all rights reserved. This PDF copy of fib Bulletin 24 is intended for use and/or distribution only by National Member Groups of fib.

An alternative empirical model was proposed by the Japan Building Disaster Prevention Association (1977). According to this procedure, the flexural and shear capacities M_u and V_u need be computed first; flexural capacities are converted into associated shear forces, V_{flex}, assuming the point of inflection is at midspan. If $V_{flex} < V_u$, a flexural failure mode is considered as most likely and the corresponding element behaviour factor $q > 1.0$, otherwise q is taken as 1. For columns the available displacement ductility factor (corresponding to ultimate displacement at 20% loss of yield capacity) is estimated from the empirical relation:

$$\mu_\Delta = 10 \cdot \left(\frac{V_u}{V_{flex}} - 1 \right) - 30 \cdot \left(\frac{V_u}{b \cdot z \cdot f_c'} - 0.1 \right) - 2 \text{, when } 1 \le \mu_\Delta \le 5 \tag{4-21}$$

The last term (i.e. the –2) is omitted if the stirrup spacing s is less than 8 times the longitudinal bar diameter. The value of μ_Δ is limited between 1 and 5. From this value of μ_Δ the column behavior factor q is computed using the empirical relation:

$$q = \frac{(2 \cdot \mu_\Delta - 1)^{1/2}}{0.75 \cdot (1 + 0.05 \cdot \mu_\Delta)} \tag{4-22}$$

4.6 Behaviour of old-type beam-column joints

4.6.1 Introduction and background

Design provisions for dimensioning and detailing of beam-column joints were introduced relatively late in modern design codes (the first set of design requirements for joints were introduced in 1967 in the ACI 318-67 Code and in 1985 in the CEB Model Code for seismic design of concrete structures). Modern provisions regulate the joint-panel dimensions so as: (a) to ensure adequate development of beam and column bars passing through the joint; and (b) to limit the joint shear stress demand below allowable shear stress limits; thereby precluding the possibility of diagonal tension failure of the joint panel. In old-type reinforced concrete structures, built prior to the introduction of these provisions, monolithic beam-column connections were usually not designed for shear action unless they were knee-joints (i.e. joints at the roof of a frame building). It is noteworthy that most national codes still do not explicitly require any particular shear stress check at the joint, although today it is generally required that stirrups in the column critical zones adjacent to the connection be continued through the height of the joint. In older construction, column stirrups were usually discontinued within the joint for ease of construction, whereas the joint region usually served for anchorage of beam longitudinal reinforcement. In some cases reinforcement comprised smooth bars with the anchorage developed through semicircular hooks; 90^0 hooks were used mainly with ribbed bars, particularly for development of beam top reinforcement in the joint.

Preservation of gravity load carrying capacity and lateral load strength in reinforced concrete frame structures under earthquake action is linked to the integrity of the beam-column joints, since these elements are part of both the vertical and horizontal load path. Transfer of forces (shear, moment and axial loads) through the joints is necessary for the development of framing action. In a new design, ideally, the joint is dimensioned so as to sustain development of the flexural strengths of the adjacent frame elements at the joint faces, without significant degradation of bond along beam and column primary reinforcement. In an older design, where neither shear nor bond stress demands had been regulated, joint failures during earthquakes may be very brittle and are a common cause for excessive flexibility of the overall frame and a consequent loss of vertical load carrying capacity (Lehman 2002).

Stirrups, when provided, act as a mechanism of confinement, preserving the integrity of the diagonal compressive strut (or compression stress-field), through which concrete participates to the joint shear action, while also enabling sharp force gradients along the beam and column primary reinforcements through development of high bond stresses. In the absence of stirrups these response mechanisms become the weak link of joint action, for their sustainment relies on the limited tensile strength of the joint panel. For this reason, in the

Copyright fib, all rights reserved. This PDF copy of fib Bulletin 24 is intended for use and/or distribution only by National Member Groups of fib.

absence of confinement, joint failure can be very brittle, the magnitude and consequences of joint damage depending upon the overall circumstance of the connection:

From among the many variables influencing the extent of joint distress and failure type the most critical are:

- the bar size anchored through the joint (i.e., the magnitude of bond demand),
- the available joint reinforcement,
- the magnitude of joint shear stress,
- the magnitude of column axial load,
- the position of the joint – whether it belongs to a perimeter frame of the building or not,
- the flexural strengths of the beam and column elements framing to the joint (weakest link) and,
- the history of imposed lateral drift,
- and (to a lesser extent) the strength of concrete.

From a collective review of experimental evidence, particularly focussing on old-type joints, Lehman (2002) concluded that joint performance appears to be particularly sensitive to the magnitude of joint shear stress and drift history.

The above list of parameters has been evaluated in experimental literature with regards to the sequence of failure in the beam-column connection, where joint damage is associated with shear distortion or slip of primary reinforcement. Other, spurious failure modes possible in joints with unusual details are also likely and assessing the likelihood of their occurrence may not necessarily depend on the preceding list of design parameters. For example, some anchorage details common in old-type construction, such as hooked anchorages of primary reinforcement that is oriented orthogonal to free joint faces, have been reported to lead to localized failure modes that involve spalling of the frontal cone of joint cover and complete elimination of the anchorage strength. The ensuing rapid degradation of the joint panel endangers the vertical load carrying capacity of the overall frame (Calvi et al. 2001). By definition, exterior and knee-joints of this type are the most vulnerable.

Experimental studies of old-type beam-column connections report that collapse of complete structural components due to joint panel degradation may occur before any significant damage may take place in either beams or columns. Note that columns designed for gravity only are often considerably weaker than beams, possibly leading to formation of a soft storey mechanism. But considering the relatively low reinforcement percentage and axial force in the columns, considerable deformation capacity may be available in the column critical sections even in a soft storey frame. The consequence is that prior to the development of a flexure-shear hinge in the columns, joints of limited strength and/or deformation capacity may be reduced to function as shear hinges. Thus, in order to properly assess the likely hierarchy of failure and distribution of anticipated damage in an old-type frame connection, it is necessary to represent in the analytical model of the connection the joint flexibility resulting from joint shear function.

Calvi et al. (2001) discuss the possibility that the formation of joint shear hinges in old type frames may not always prove as detrimental as it is usually thought, depending on the ductility of the joint after attainment of joint strength. In a deformable joint of low shear strength, such as joints with poor anchorage capacity where response is dominated by reinforcement slip, redistribution of drift demands is expected to occur between the floors immediately above and below the joint, alleviating the consequences of a soft storey mechanism. Due to bond degradation, lower flexural moments are sustained by the column, with different equilibrium conditions prevailing in the connection than what would occur when assuming ideal bond conditions. On the other hand, joints combining low strength with low deformation capacity (e.g. joints with unfavourable reinforcement details, such as hooked primary reinforcement) are detrimental to the structure. Clearly, in properly assessing the implications of joint failure on structural response, a measure of the available joint deformation capacity is as important as joint strength.

In light of the preceding discussion it is evident that a design model is required for systematic and quantitative assessment of the basic response aspects of poorly detailed joints, namely strength, stiffness, deformation capacity and failure mode. Various modelling procedures for joints, quantifying the above properties, are available in international literature and are briefly reviewed in the following sections. A note of caution is, however, that some of these models may not be applicable to old-type connections, as they rely on homogenisation

Copyright fib, all rights reserved. This PDF copy of fib Bulletin 24 is intended for use and/or distribution only by National Member Groups of fib.

assumptions that could only be supported in the presence of adequate confining reinforcement (such as smearing of cracks and averaging of stresses and strains in the joint panel).

4.6.2 General classification of beam-column joints

By definition the joint is the column segment that also belongs to the beam at the intersection of the two members (Fig. 4-28). Depending upon the kinematic constraints imposed by the surrounding members, joints are classified as interior (cross-type), exterior (T-shaped) and corner or knee joints (L-shaped). In its latest draft recommendations, ASCE Committee 352 (Beam-Column Joints) (2001) further classified the joint types thereby specifying the corresponding joint shear strength depending upon the number of *free column faces in the joint region* (i.e. depending on whether the column is continued or discontinued above the joint). This is in recognition of the confining action and its beneficial effect on joint shear strength, imparted by members framing into the joint. For a given drift, both the imposed joint shear stress and the intrinsic joint shear strength are *highest* in interior and *lowest* in corner joints; however the basic parameter defining the corresponding design shear is the strength of anchorage of primary beam and column reinforcement through the joint.

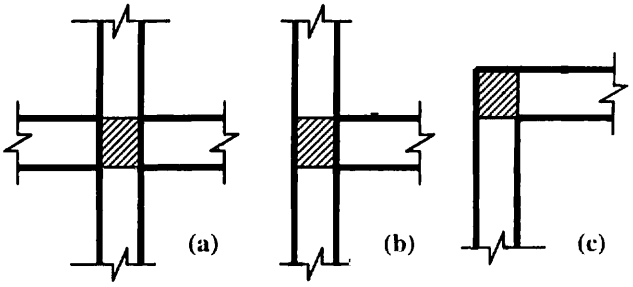

Fig. 4-28: Various types of beam-column joints. (a) interior, (b) exterior, (c) knee-joint

4.6.3 Calculation of nominal shear stress in the joint panel

Under lateral sway, flexural moments in frame members are distributed linearly between nodal points with the point of inflection (zero moment) approximately at midspan (actually, beam moments deviate from the linear distribution by the amount associated with gravity load distribution; however, the moment transfer at the connection cannot exceed the flexural capacity of the beams adjacent to the joint). Moments attain extreme values (of opposite sign) at the joint boundaries as illustrated in Fig. 4-29. The sign reversal from one joint face to the other is achieved by sharp moment gradients within the joint panel; the slope of the moment diagram within the joint dimension represents the corresponding joint shear force. It can be easily shown that joint shear V_j is several times greater than member shear acting in the adjacent beams and columns. Considering M_b^+ and M_b^- the beam moments adjacent to the joint, L the beam span and d_c the effective depth of the column cross section, then V_j is related to the beam shear V_b as:

$$V_j = \frac{M_b^+ + M_b^-}{d_c} = V_b \frac{L}{d_c} \tag{4-23}$$

The ratio L/d_c is about 10 for common older-type buildings (a beam span of approximately 4m and a column dimension of 0.4m). Therefore for this problem joint shear is about 10 times as large as the beam shear associated with flexural hinging on both sides of the joint. This magnitude highlights the vulnerability of the joint as a disturbed region (D-region) in the structure.

The shear force thus calculated represents the horizontal input to the joint, but the same method can be used as well to calculate the vertical joint shear force (by equilibrium of moments along the column). When normalized by area so as to obtain units of stress, the two results are the same, as required by equilibrium:

$$v_{zx} = v_{xz} = \frac{V_b L}{b d_c d_b} \tag{4-24}$$

Copyright fib, all rights reserved. This PDF copy of fib Bulletin 24 is intended for use and/or distribution only by National Member Groups of fib.

As it is unlikely that any portion of the member intersection region will be inert with regard to joint deformation and in order to simplify notation, stress calculation in eq. (4-24) was based on joint dimensions defined by the common volume of beam and column: $d_b d_c b$, where d_b the beam effective depth, d_c the column effective depth and b the least of beam and column widths (Bonacci and Wight, 1999). According to the ACI 1999 Code, the joint is a rectangular member with height equal to the beam sectional height, length equal to the column cross sectional height and width equal to the least of: (a) the average of column width and beam width, and (b) the beam width plus one half of the column section height.

Similarly in knee-joints (and tee-joints along the column axis) joint shear may be calculated from the moment gradient within the joint panel, with the exception that, in this case there is no moment reversal within the joint. Rather, moment may be taken zero at the free joint face in the direction of interest (Fig. 4-29). (More conservatively, moment should be taken as zero at the centroid of the outer layer of main reinforcement)

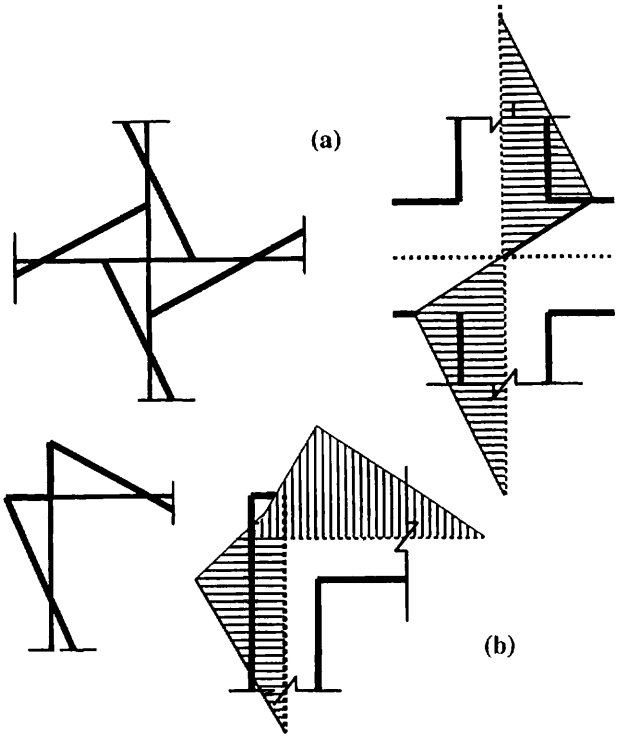

Fig. 4-29: Calculation of joint shear from moment gradient within the joint. (a) interior joints; (b) knee joints

$$V_j = M_b / d_c = V_b \, L / 2d_c \quad ; \quad v_{zx} = v_{xz} = \frac{0.5 V_b L}{b d_c d_b} \tag{4-25}$$

Evidently, by comparison of eqs. (4-23) and (4-25), knee joints are subject to approximately half the intensity of shear stress as compared to interior joints.

4.6.4 Nominal calculation of demand in beam column joints according to international codes

4.6.4.1 Calculation of shear demand

An alternative method for calculating joint shear to the one presented above is through equilibrium of forces acting on half of the joint considered as a free body, bounded by a cross section that passes through the joint centre as illustrated in Fig. 4-30. Depending on the location of the plastic hinge (in the beam or the column), the pertinent cross section is oriented in the horizontal or the vertical direction, respectively. For interior joints and assuming the plastic hinge is on the beam outside the joint, it follows from equilibrium that joint shear equals $V_j = C_c^+ + C_s^+ + T_s^- - V_c^o$, where C_c^+, C_s^+, T_s^- are the forces in the compression and tension zone of the beam cross sections adjacent to the joint, whereas V_c^o is the column shear above the joint (Fig. 4-30).

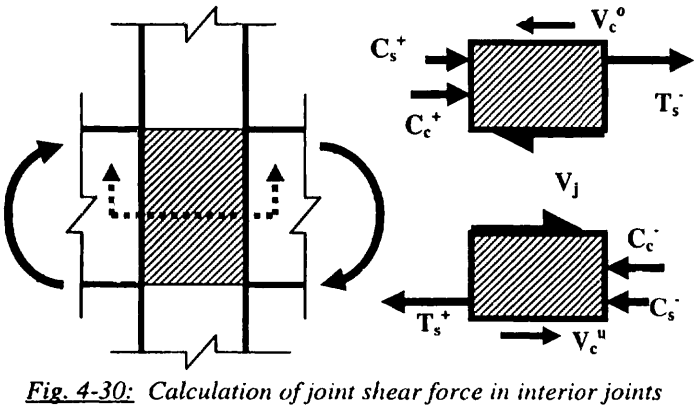

Fig. 4-30: Calculation of joint shear force in interior joints

In the absence of beam axial load (a common assumption for interior beam spans in frames) it follows from equilibrium of the beam cross

Copyright fib, all rights reserved. This PDF copy of fib Bulletin 24 is intended for use and/or distribution only by National Member Groups of fib.

section that $C_c^+ + C_s^+ = T_s^+$. If it is further assumed that tensile reinforcement in the plastic hinge regions adjacent to the joint has yielded, the joint shear may be expressed in terms of the areas of top and bottom beam reinforcement as follows:

$$V_j = T_s^+ + T_s^- - V_c = A_{s1} f_{yk} + A_{s2} f_{yk} - V_c \tag{4-26}$$

which, in units of stress may be written as:

$$v_{xz} = v_{zx} = (\rho_{s1} + \rho_{s2}) f_{yk} \frac{d_b}{d_c} - v_c \tag{4-27}$$

Some Codes require that flexural overstrength resulting from reinforcement strain hardening be accounted for in eq. (4-27) by factoring f_{yk} by 1.25 (introduced in the ACI-ASCE 352 Recommendations as early as 1976 and in the New Zealand Standard in 1982). Also important in estimating the demand on the joint is consideration of the slab participation on beam flexure (this was a requirement in the New Zealand Standard as early as 1982, but today this is included also in the ACI Code (1999) and in EC8 (1994).

In the case of knee joints it is also necessary to consider the member axial forces that may be resolved from the statics of the connection as shown in Fig. 4-31 (beam shear is in equilibrium with the column axial force and vice versa). The sign of shear force changes according with the direction of lateral sway; under closing moments (Fig. 4-31 b), the resultant axial forces in both beam and column are compressive, but they become tensile upon reversal of the moment direction (opening moments), thereby influencing unfavourably the flexural resistance of those members and severely taxing the anchorage of primary reinforcement. Using the model in Fig. 4-31, joint shear is obtained from:

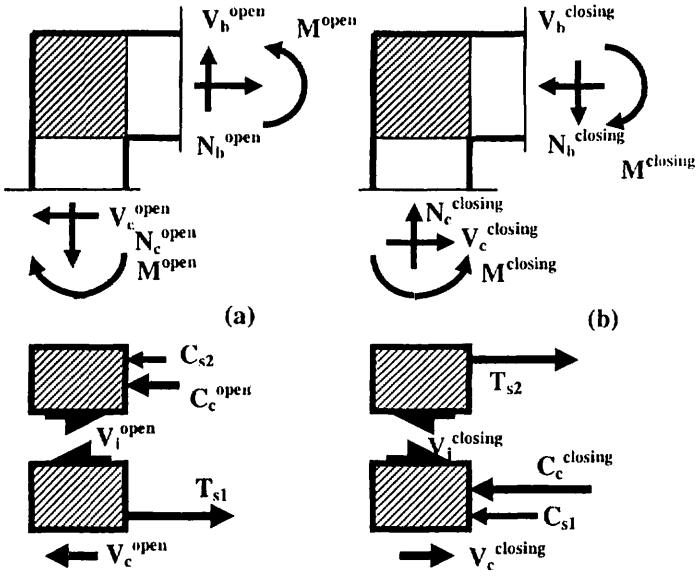

Fig. 4-31: Calculation of shear in knee-joints. (a) opening action, (b) closing action

$$V_j^{open} = C_c^{open} + C_{s2} = T_{s1} - V_c^{open} = A_{s1} f_{yk} - V_c^{open} \quad ; \quad v_{zx} = v_{xz} = \rho_{s1} f_{yk} \frac{d_b}{d_c} - v_c^{open} \tag{4-28}$$

$$V_j^{closing} = T_{s2} = A_{s2} f_{yk} \quad ; \quad v_{zx} = v_{xz} = \rho_{s2} f_{yk} \frac{d_b}{d_c} \tag{4-29}$$

where A_{s1}, A_{s2} are the areas of bottom and top beam reinforcement at the joint face, respectively. Evidently, from eqs. (4-28) and (4-29) it follows that the intensity of shear stress in the case of opening moments is lower than the corresponding value in the case of closing moments. Thus, joint shear failure is more likely under closing moments, whereas under opening the likely failure mode is related to diagonal tension cracking due to the flexural action occurring in the joint.

4.6.4.2 Nominal calculation of demand in the form of principal stresses in the joint

Some Codes specify resistance directly in terms of diagonal principal stresses in the joint. For verification purposes it is therefore essential that joint demand be also expressed along the same reference coordinates. In this regard, the stress tensor at the joint centre is defined from boundary forces, in terms of total average stresses as follows:

Copyright fib, all rights reserved. This PDF copy of fib Bulletin 24 is intended for use and/or distribution only by National Member Groups of fib.

$$\tilde{\sigma} = \begin{pmatrix} n_x & v_j & 0 \\ v_j & n_z & 0 \\ 0 & 0 & n_y \end{pmatrix} \tag{4-30}$$

In eq. (4-30), v_j is the joint shear stress input as calculated by one of the preceding methods. The diagonal terms are defined as follows: total normal stresses nx, nz and ny are taken equal to the average boundary stresses acting on joint faces, resulting from the permanent axial compression forces sustained by the adjacent members in the longitudinal (x), vertical (z) and transverse (y) directions, respectively (including the effects of prestressing after losses). Note that if a member (beam, column, or transverse beam) is discontinued past the joint, then the corresponding normal stress at the joint centre should be taken as one-half of the corresponding boundary stress value.

$$n_z = \frac{N_{jz}}{b_j d_c}; \quad n_x = \frac{N_{jx}}{b_j d_b}; \quad n_y = \frac{N_{jy}}{d_b d_c} \tag{4-31}$$

Principal stress values may be computed either as total stresses (concerning the reinforced concrete panel that represents the joint), or as concrete stresses (concerning only the concrete material of the panel).

The first approach follows directly from the definition of the total stress tensor, eq. (4-30):

$$\sigma_1 = \frac{n_z + n_x}{2} - \sqrt{\left(\frac{n_z - n_x}{2}\right) + v_j^2} \; ; \; \sigma_2 = \frac{n_z + n_x}{2} + \sqrt{\left(\frac{n_z - n_x}{2}\right) + v_j^2} \tag{4-32}$$

where σ_1 is the principal tensile stress and σ_2 the principal compressive stress.

The second option has been formulated by Pantazopoulou and Bonacci (1992, 1994): in that case, the average concrete stresses are obtained from the total normal stresses, by consideration of equilibrium in the reference frame of axes:

$$\sigma_x = \rho_{sx} f_x + n_x \; ; \; \sigma_z = \rho_{sz} f_z + n_z \; ; \; \sigma_y = \rho_{sy} f_y + n_y \tag{4-33}$$

where ρ_{sx}, ρ_{sz} and ρ_{sy} are the area ratios of reinforcement crossing a plane through the joint centre normal to the x, z, and y axes, respectively, and f_x, f_z, and f_y the corresponding reinforcement average stresses at the joint centre. Note that longitudinal reinforcement passing through the joint is accounted for in the corresponding area ratios at 50% efficiency (to account for yield penetration), unless a substantial axial compression was transmitted through the joint (Pantazopoulou and Bonacci, 1991). With the definition of normal concrete stress values given by eq. (4-33), principal stress values are given by:

$$\sigma_{1c} = \frac{\sigma_z + \sigma_x}{2} - \sqrt{\left(\frac{\sigma_z - \sigma_x}{2}\right) + v_j^2} \; ; \; \sigma_{2c} = \frac{\sigma_z + \sigma_x}{2} + \sqrt{\left(\frac{\sigma_z - \sigma_x}{2}\right) + v_j^2} \tag{4-34}$$

Prior to cracking, it may be assumed that the reinforcement action has not been mobilised and therefore its contribution in the equilibrium eqs (4-33) may be ignored; in that case, concrete stresses become coincident with total stresses, and thus, in setting limiting values for the cracking principal stress, the two approaches described by eqs. (4-34) and (4-32) produce identical results. After cracking has occurred, the principal tensile concrete stress σ_{1c} is set to zero. From this requirement, the failure shear stresses in the joint obtained from eq. (4-32) and (4-34) are no longer coincident.

4.6.5 Nominal resistance of beam column joints according to the international codes

Joint failure is an undesirable design option because it is difficult to repair and its implications are severe on the vertical load carrying capacity of the column. Therefore, one verification criterion is to ensure that joint shear resistance exceeds the demand as estimated by one of the two methods presented in the preceding. Joint strength is defined either directly

Copyright fib, all rights reserved. This PDF copy of fib Bulletin 24 is intended for use and/or distribution only by National Member Groups of fib.

in terms of nominal shear resistance (ACI 318-1999, EC8-2002), or indirectly, in terms of diagonal tension and compression principal failure stresses (CALTRANS 1999). In a new design, nominal shear resistance values are used as allowable stress limits, but the underlying premise remains that adequate detailing exists in the joint in the form of stirrups to preclude brittle shear failure or anchorage failure of the primary reinforcement. The objective in new designs is to ensure that inelastic action occurs outside the joint, preferably in the form of stable inelastic rotation of flexural plastic hinges in the adjacent beams (or columns in the case of bridges).

In assessment of existing structures, using the nominal shear resistance values may only serve as a plausible upper limit for monotonic joint shear strength, to be available only if the lower-strength, alternative spurious failure modes that could threaten joint integrity may be precluded. Furthermore, this resistance is to be sustainable under cyclic load only if adequate confinement is simultaneously present. Such spurious failure modes involve anchorage failures of unconfined smooth bars bent through or terminating with hooks in the joint, diagonal splitting failures due to complete lack of transverse reinforcement, instability due to offsetting of compressed reinforcement passing through the joint, lap splice failures in the column critical region directly above the joint, etc.

4.6.5.1 Joint shear resistance estimates – Historical review of the State of the Art

Because concrete shear failure is prioritised by design to involve diagonal tension cracking followed by yielding of transverse reinforcement (as opposed to compression crushing of concrete), shear stress limits are usually expressed as multiples of concrete tensile strength, in the same manner as is used to quantify bond resistance. Thus, the Eurocodes stress limits are related to $f_{ck}^{2/3}$ whereas in the ACI Code $f_{ck}^{1/2}$ is used instead.

Joint shear resistance values are largely empirical, having their origin in a small number of milestone beam-column connection tests under reversed cyclic load (Meinheit and Jirsa, 1976). Prior to that time, joints were only considered in the ACI Code in satisfying the requirements for development of beam reinforcement and were otherwise provided for as part of the column, a practice that is used in some codes even today. The first mention of a joint shear strength estimate was introduced in the ACI-ASCE Committee 352 recommendations in 1976. Based on the Meinheit and Jirsa experiments, the allowable joint shear stress was set at $1.67\sqrt{f_c}$ (stresses in MPa). The shear strength of the joint was assumed to comprise concrete and transverse steel contributions. For *type-2* joints (a classification adopted by ACI-ASCE 352 Recommendations for joints in earthquake resisting frames) the concrete contribution was limited by the assumed occurrence of diagonal tension failure to $0.29\sqrt{f_c}$ (in MPa). This bound was increased to approximately $0.42\sqrt{f_c}$ (in MPa) for joints confined by transverse beams, but was set to zero for joint subjected to a net tensile force (Pantazopoulou and Bonacci 1994). The difference between nominal joint shear stress input and the concrete contribution as defined above was used to estimate the required transverse steel, with the proviso that v_s was limited by an upper bound of $1.25\sqrt{f_c}$ (in MPa). The long time North American practice of offsetting longitudinal column bars in the joint was discouraged at the 1976 edition of the ACI-ASCE 352 Recommendations and was prohibited in the revised 1985 edition. No specific anchorage requirements for beam bars were given up to that point, but the designer was encouraged to use small diameter bars to reduce the amount of bond deterioration likely to occur under alternating inelastic deformation cycles (Pantazopoulou and Bonacci 1994).

The requirement to distribute column bars around the perimeter of the column cross section for improved confinement of the joint core was introduced in the 1985 edition of the ACI-ASCE 352 Recommendations. Other changes embodied in the 1985 edition were: (a) the requirement that the diameter of beam bars developed through the joint be limited to 1/20 of the column sectional dimension in the direction considered; (b) explicit requirement regarding the ratio of column flexural strength to probable beam flexural strength to encourage a strong column – weak beam connection behaviour; (c) recognition of the confining action of transverse beams by allowing that confining reinforcement in the joint which was the same as that in column critical regions be reduced by 50% when beams framed into all faces in the joint, and (d) scaling of allowable shear stress levels according with the type of joint (interior, exterior and corner joint) to 1.65, 1.25 and $1\sqrt{f_c}$ in MPa, respectively. This acknowledged the favourable influence of confinement on joint resistance (provided by transverse beams),

Copyright fib, all rights reserved. This PDF copy of fib Bulletin 24 is intended for use and/or distribution only by National Member Groups of fib.

which is owing to the restraint they present to dilation of the concrete core. According to ACI Committee 352 (2002) these values may be unconservative for connections where the column is discontinued above the joint (i.e., in top floor connections in buildings, or common bridge joints). Thus, for knee joints the recommended allowable shear stress value is $0.67\sqrt{f_c}$ in MPa, whereas for T joints the interpolated values of $1\sqrt{f_c}$ and $1.25\sqrt{f_c}$ are recommended (exterior and interior joints, respectively).

Similar levels for the allowable joint shear stress were established in the1982 edition of the New Zealand Standard ($1.5\sqrt{f_c}$ in MPa). Shear reinforcement (in both horizontal and vertical directions in the joint) were obtained by postulating a corner-to-corner diagonal failure plane across the joint core and assuming no concrete contribution unless significant axial compression was transmitted through the joint. Confinement reinforcement tied in directions normal to the plane of action so as to limit dilation of the joint core due to cracking was required. This confinement reinforcement was also computed as in the case of ACI-ASCE 352 Recommendations (1985) from column design requirements and was reduced by 50% in cases where beams framed in all faces of the joint to recognise the beneficial influence of transverse beams. To minimize deterioration of bond due to yield penetration, maximum beam bar diameters were limited to 1/25 and 1/35 of the column depth for 280 and 420 MPa steels, respectively. The allowable shear stress limits were modified in more recent proposals originating from New Zealand, to fractions of the uniaxial compressive concrete strength (0.2-$0.25f_c$) to recognise the role of the diagonal compression strut in resisting joint shear after diagonal tension cracking of the joint (Paulay 1989, Cheung et al. 1993, NZS3101:1995).

The first provisions of the AIJ (1988) regarding joints refer to the formation and sustenance of the diagonal compressive strut in the joint core as the primary mechanism of resistance. Key consideration is minimising the magnitude of bond demand in bars anchored through the joint, by increasing the column size and by reducing the beam bar diameters. Dimensioning of the joint is controlled by the limitation that bars anchored through the joint have diameter less than $f_y/3.2\sqrt{f_c}$ (in MPa), and by allowable joint shear stress limits of $0.25f_c$ for interior joints and two-thirds of that amount for exterior joints. Again, the allowable shear stress limit is expressed as a fraction of uniaxial compressive strength to recognize the role of the diagonal compression strut as the primary source of joint shear resistance. This of course is implicitly linked with the proviso that sufficient confinement exists in the joint (as in the column critical zones), so as to ensure that the diagonal compression strut is formed and sustained to large drifts (at least 1.5%) without the occurrence of alternative, premature failures.

The ENV versions of EC8 considered only two general classes for joints, those of interior and exterior joints, with allowable shear stress limits of 20 and $15\tau_{Rd}$, respectively. (In these limits, τ_{Rd} is design shear resistance, related to the characteristic compressive strength of concrete as: $\tau_{Rd}=0.25f_{ctd}=0.25f_{ctk}/\gamma_c=0.25\times0.3f_{ck}^{2/3}/\gamma_c=0.075f_{ck}^{2/3}/1.5$; hence: $20\tau_{Rd}=1.0f_{ck}^{2/3}$, $15\tau_{Rd}=0.75f_{ck}^{2/3}$).

4.6.5.2 Joint shear resistance estimates in terms of principal stress limits

Setting limits for the principal stress values in the joint (both compressive and tensile) is an alternative approach in design/assessment that is arguably more consistent with the underlying mechanics of the problem, as it illustrates in a transparent manner the influence of axial load acting on beams or columns on joint cracking and ultimate strength. This is especially true in the case of assessment of old-type structures, where it is not possible to prioritise stirrup yielding prior to crushing of the diagonal compression strut that forms from end to end in the joint, as many old-type connections completely lack shear reinforcement or possess inadequate amounts thereof. Therefore, diagonal tension cracking may be assumed to occur in the joint if the tensile principal stress exceeds the limit:

$$\sigma_1 = \frac{n_z + n_x}{2} - \sqrt{\left(\frac{n_z - n_x}{2}\right) + v_j^2} \le f_{ctk} = \begin{cases} 0.29\sqrt{f_c} & (ACI318,1999) \\ 0.3f_{ck}^{2/3} & (EC8) \end{cases} \qquad (4\text{-}35\ a)$$

Note that eq. (4-35 a) may also be expressed as a limit in the magnitude of joint shear stress, consistent with basic principles as:

Copyright fib, all rights reserved. This PDF copy of fib Bulletin 24 is intended for use and/or distribution only by National Member Groups of fib.

$$v_j = f_{ctk}\sqrt{\left(1+\frac{n_z}{f_{ctk}}\right)\cdot\left(1+\frac{n_x}{f_{ctk}}\right)} \tag{4-35 b}$$

In the absence of shear reinforcement, exceedance of the above limit corresponds to shear failure of the joint. As mentioned in Section 4.6.5(a), the 1976 ACI-ASCE 352 Recommendations proposed that for joints restrained on all faces by beams, a shear stress value as high as $0.42\sqrt{f_c}$ may be sustained by the concrete core alone, whereas for all other joints this limit was only $0.29\sqrt{f_c}$. Priestley et al. (1996) proposed using these limits in the assessment of substandard old-type connections provided that members framing into the joint remain elastic. If there is no axial load in the longitudinal (x) direction, as is the case in interior beam-column joints, eq. (4-35 a) simplifies further to:

$$\sigma_1 = \frac{n_z}{2} - \sqrt{\left(\frac{n_z}{2}\right)^2 + v_j^2}\ ;\ \Rightarrow\quad v_j = f_{ctk}\sqrt{\left(1+\frac{n_z}{f_{ctk}}\right)} \tag{4-36}$$

Using $k\sqrt{f_c}$ for the tensile strength of concrete, Park (1997) expressed the above limit (eq. (4-36)) for diagonal cracking of joints without transverse reinforcement in the joint region as:

$$v_j = k\sqrt{f_c'}\cdot\sqrt{1+\frac{n_z}{k\sqrt{f_c'}}} \tag{4-37}$$

For exterior joints with beam longitudinal bars that terminate as hooks into the joint, the recommended value for k is 0.4 (Park 1997). However, from comparisons with published experimental results, Lehman (2002) concluded that the above value may be overly conservative and proposed relaxing the limit for k to 0.6-0.7.

If reinforcement is present, so that formation of a diagonal strut and tie system is possible, the principal compressive stress may not exceed the crushing limit of concrete. Depending upon the manner of its definition (i.e. whether it is derived from total or from concrete stresses) the following two alternative design limits are suggested:

(a) Based on total stresses, (eq. (4-32) (Priestley et al. 1996, CALTRANS 2002):

$$\sigma_2 = \frac{n_z+n_x}{2} + \sqrt{\left(\frac{n_z-n_x}{2}\right)+v_j^2} \le \lambda_c f_{cd} = \begin{cases} 0.25 f_c' & (CALTRANS\ 2001) \\ 0.6(1-\frac{f_{ck}}{250})\cdot f_{cd} & (EC8,\ 2002) \end{cases} \tag{4-38}$$

(b) Based on concrete stresses (eq. (4-34) Pantazopoulou and Bonacci 1992, 1994):

Two possible scenarios are considered, depending on the type of failure that ensues after yielding of transverse reinforcement, namely yielding of vertical steel or concrete strut crushing. For these two cases, the limiting joint shear stress is obtained from eq. (4-34) for the principal compression stress σ_{2c}, as:

$$v_{j,ult} = \min\begin{cases} \sqrt{(\rho_{sx}f_y+n_x)\cdot(\rho_{sz}f_y+n_z)} \\ \sqrt{(\rho_{sx}f_y+n_x)\cdot(\lambda_c f_c'-\rho_{sx}f_y+n_x)} \end{cases} \tag{4-39}$$

In eq. (4-38) and (4-39), $\lambda_c \le 1$ considers the weakening influence of orthogonal tensile strains on the strength of the diagonal compressive strut, and for new construction may include a safety factor ϕ_c or γ_c of about 1.5 ($f_{cd}=f_{ck}/1.5$). (Based on the work by Vecchio and Collins (1986), a pertinent expression for λ_c without the safety factor is given as a function of the principal tensile strain: $\lambda_c=1/(0.8+0.34(\varepsilon_1/\varepsilon_{co})))$. The above limit of $\lambda_c f_c$ for the strut compressive strength, may be multiplied by a confinement effectiveness coefficient, $a_c=[1+2(n_y+\rho_{sy}f_{yd})] \le 1.5$, where ρ_{sy} the reinforcement ratio (closed stirrups) in the transverse direction of the joint panel (orthogonal to the plane of action of the joint).

Copyright fib, all rights reserved. This PDF copy of fib Bulletin 24 is intended for use and/or distribution only by National Member Groups of fib.

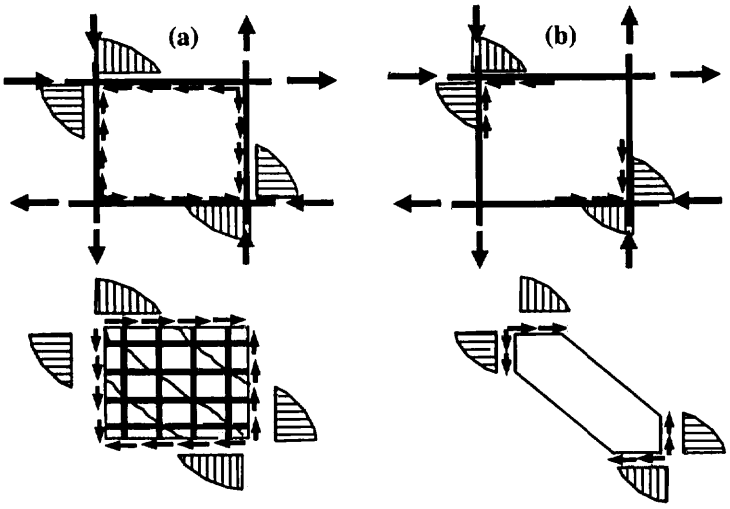

Fig. 4-32: Interior joint: (a) well detailed joint prior to loss of bond of primary reinforcement. (b) single strut action after loss of bond.

Eq. (4-38), having been derived without considering the favourable effects of reinforcement on joint shear resistance, is likely to be more appropriate for old-type joints lacking adequate amounts of transverse steel. But a general disclaimer as to the applicability of either of the above limits eqs. (4-38) and (4-39) in unreinforced joints may be appropriate at this point. Note that prerequisite to defining a stress tensor and to using the relevant coordinate transformations in order to obtain principal stresses, was the assumption that a homogeneous stress field acts in the joint. In the absence of reinforcement to secure adequate control of cracking, the homogenisation assumptions underlying the process of averaging stresses and strains are no longer valid, rendering both models above somewhat irrelevant to the problem of joint capacity assessment past the occurrence of diagonal cracking.

4.6.6 Interpretation of old-type joint behaviour

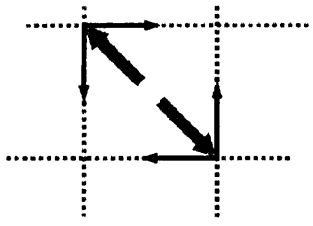

Fig. 4-33: Diagonal strut and ties (joint truss model)

It has been shown before that the same basic truss model qualitatively describes the behaviour of all joint types (Figs. 4-32, 4-33, Park and Paulay 1975). The truss comprises a *single* diagonal compressive strut (representing concrete) held in equilibrium by forces developed in the horizontal and vertical tension ties (representing the reinforcement). Failure of the truss may occur by crushing of the strut, by splitting of the nodal region, or by bond failure along the anchorage of a tie. Figs 4-32 and 4-34 a, 4-34 b illustrate the truss function in interior and knee joints – under closing and opening moments, respectively. If the primary reinforcement is smooth, then the truss model functions in its familiar form from early on, immediately upon formation of diagonal tension cracks. If primary reinforcement is deformed, then the truss mechanism consolidates at large drifts (Fig. 4-32 b), whereas early on, shear is introduced into the joint through bond along the beam and column bars and resistance is developed along several smaller struts (Fig. 4-32 a).

A significant feature of the truss model is that tension ties must be able to

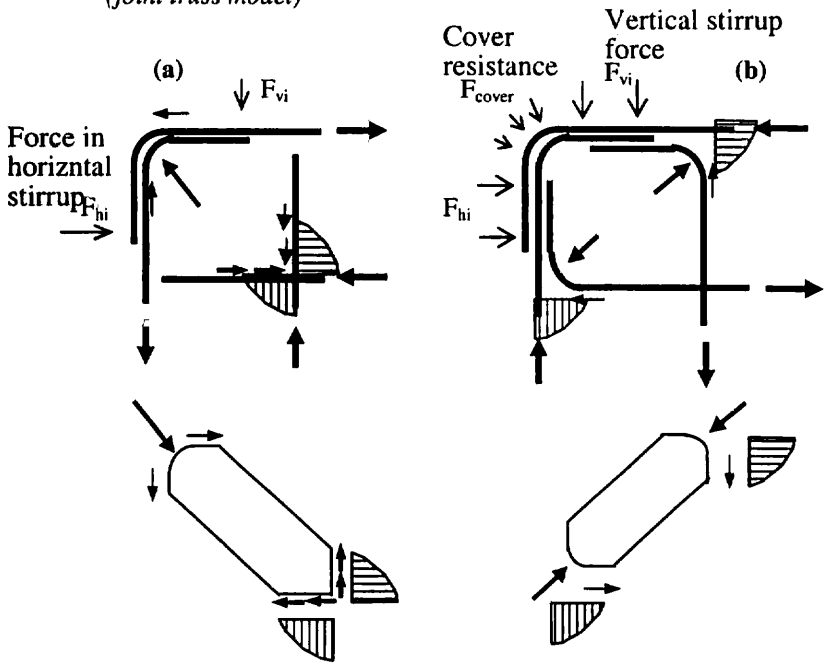

Fig. 4-34: Knee Joint: (a) Response under closing moments, (b) Response under opening moments

Copyright fib, all rights reserved. This PDF copy of fib Bulletin 24 is intended for use and/or distribution only by National Member Groups of fib.

develop their force (e.g. yield strength) up to the node of the truss, regardless of how good or bad the bond conditions might be along the straight part of the anchorage ahead of the node. This point has been highlighted in many joint shear experiments, the most illustrative being the case of the knee joint, which, of all connections, possesses the lowest redundancy. For isolated knee-joint components, it has been experimentally shown that the top cover of the joint with deformed bars will spall-off under cyclic load reversals, regardless of the moment strength ratio of the connection, with the top bar force being transferred all the way to the bent portion of the anchorage. This is observed even when a large number of vertical (inverted U-shaped) stirrups are placed in the joint to improve clamping of the beam top longitudinal bars (Wallace and McConnel, 1995). (An exception should be noted, however, regarding vertical stirrups, namely that the clamping action they provide improves anchorage of the bent part of the beam bars by suppressing the "lift-up and kick-out" mechanism shown in Fig. 4-35). Similar is the effect of horizontal joint stirrups on column bars that are bent and anchored into the joint (Fig. 4-34 b).

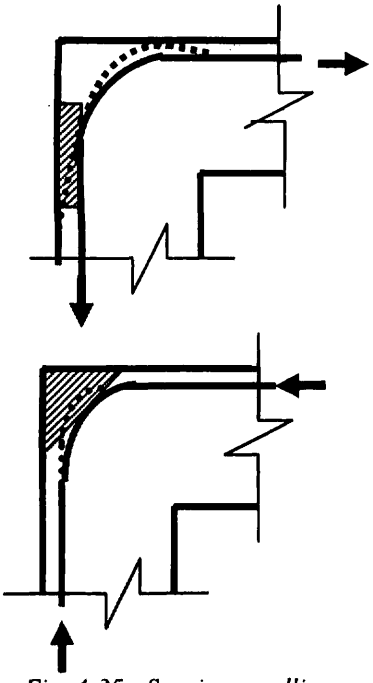

Fig. 4-35: Spurious spalling action of bent bars due to curvature changes under force

Accepting that the force of a tension tie in the joint truss model must be developed at the node, is equivalent to requiring that bond development occurs past that point. Depending on the available, details this is not always possible, particularly in the absence of stirrups or any other restraining mechanism. A variety of anchorage arrangements is possible (whether beam bars will be bent in or out of the joint, whether the length of the bent portion will extend into the column past the joint or not, whether column and beam bottom bars will end in hooks, etc.); most of those would result in vastly different strengths and connection deformation capacities, even if the nominal beam to column flexural strength ratio is kept the same. (As far as the tension tie force is concerned, it is also important whether beam or column bars will yield first, in the sense that the force magnitude of the tension tie and thereby the demand on the anchorage depends on the moment developed at the face of the joint).

Deformed bars acting as tension ties mobilize: (a) bond along the segment of the bar that is anchored through the truss node, (b) bearing action under the bent portion of the bar, and (c) bond along the length of the bar extension beyond the node. Smooth bars acting as tension ties rely on the bearing action under the bent portion in order to develop tension; the associated displacements are significant, whereas they are much smaller in the case of a deformed bar. Therefore, the type of detailing of primary reinforcement past the nodal point determines whether the joint will be able to develop its design strength, whether joint degradation will occur, as well as the magnitude of attendant deformations due to bar slip. Furthermore, the capacity of the truss nodal zone to support the diagonal strut and to anchor the tension ties is critically related to the amount of confinement provided to the node either by means of confining reinforcement, framing members or other details; these will assist the node to divert the forces from one path to the other without splitting. For example, when beam bars are bent away from the joint, as typical in old practice, no effective node point is provided for the development of an efficient compression strut mechanism, unless a significant amount of transverse column hoops is

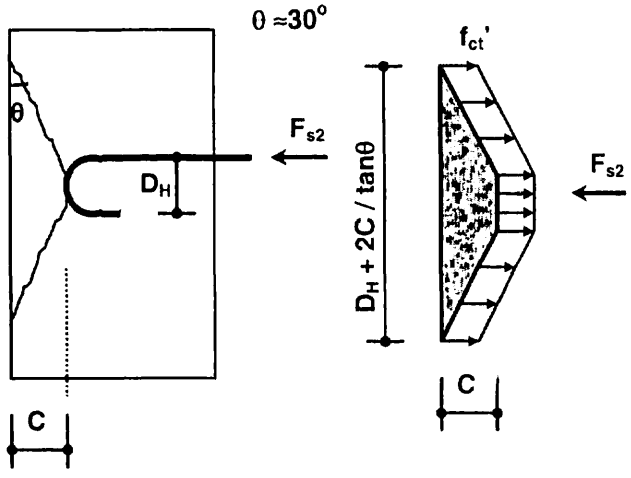

Fig. 4-36: Cone splitting failure of the cover in front of a hooked anchorage without stirrups

Copyright fib, all rights reserved. This PDF copy of fib Bulletin 24 is intended for use and/or distribution only by National Member Groups of fib.

placed immediately above the joint core (Priestley et al. 1996, Calvi et al. 2001).

Compressed smooth bars have as much resistance as the push off strength of the cone in front of the bar hook (Fig. 4-36). Therefore, $F_{s2}=0.26f_{ct}'C(R_H+2C/\tan\theta)^2$, where C is the cover over the hook and R_H the hook radius. (The angle of inclination of the crack plane from the vertical axis, θ, is taken about 30°). For example, for a cover over the hook of 30mm, a hook radius of 50mm and concrete tensile strength of 2 MPa, the compression force that may be sustained by the bar is 2.5 kN. This, for a Φ12 bar, corresponds to a compressive stress equal to just over 21 MPa. If stirrups parallel to the compressed bar are present in the joint, then the yield force of the stirrups crossing the diagonal splitting plane should be added to the cone pushout strength in determining the bearing capacity of compression reinforcement. (Similarly, the dowel strength of orthogonal bars crossing the splitting plane should also be accounted for in determining the cone pushout strength).

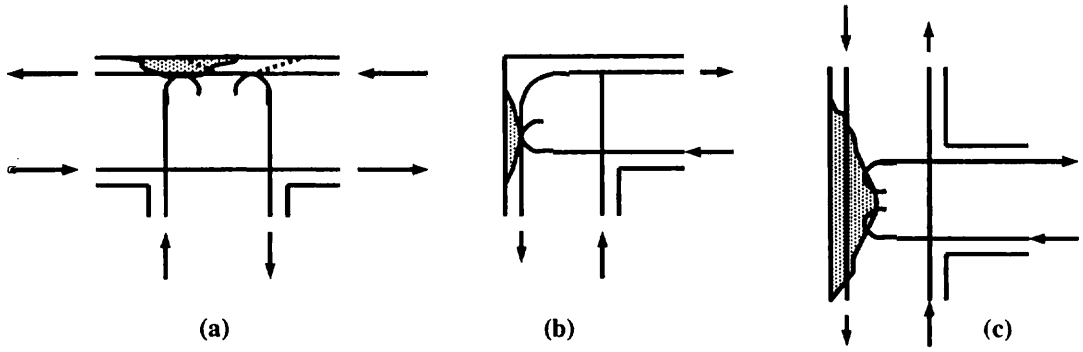

Fig. 4-37: Cone (wedge) splitting failures in various old-type joints

It is evident that exterior connections with smooth bars anchored within the joint panel with a hook oriented normal to a free face of the joint will inevitably mobilise the cone pushout failure mentioned in the preceding when the hooked bar is compressed (Fig. 4-37). Under cyclic loading, this process will occur early (at a low applied moment, according to the bar stress levels calculated in the preceding). Once the splitting plane forms, the bar slides freely when in compression, causing dramatic strength deterioration for the entire connection. Naturally, this response differs substantially from that of joints with modern detailing and cannot be quantified even roughly by the familiar models reported in the literature for beam-column joints. The margin of difference is illustrated in Fig. 4-38, which outlines the joint shear strength envelope as a function of shear distortion in joints having various degrees of boundary restraint.

Calvi et al. (2001) conducted experiments on various types of beam-column joints using scalled specimens having the reinforcement detail shown in Fig. 4-37. For T-joints they observed that joint cracking typically occured first under positive beam moment due to the reduction of axial force for this direction of response, whereas dilation and spalling of cover occurred in the reverse direction of bending. The shear degrading mechanisms (concrete wedges) in these specimens showed a particularly brittle behaviour with a sudden and severe joint shear strength reduction after first diagonal cracking. The combined action, at alternating half cycles of a concentrated compression force at the beam bar end-hook anchorage

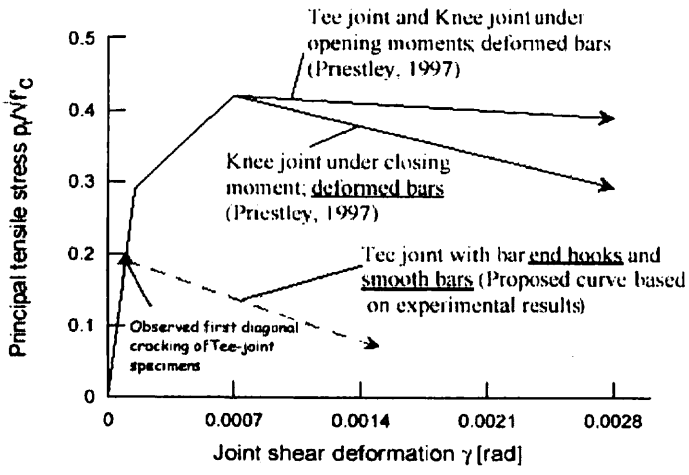

Fig. 4-38: Qualitative plot of shear strength vs. shear distortion envelope for various joint types (Calvi et al.2001).

Copyright fib, all rights reserved. This PDF copy of fib Bulletin 24 is intended for use and/or distribution only by National Member Groups of fib.

and of the diagonal compression strut within the joint region, inhibited any alternative sources of shear transfer in the joint region.

4.6.7 Definition of bond index (BI) as an assessment parameter

Damage reconnaissance reports from the performance of highway bridges during the Loma Prieta (1989) and Northridge (1995) earthquakes in California have highlighted several problems in older-type beam column joint construction attributable to excessive bond demand. Poor joint performance was marked by cover splitting over large diameter beam bars having small anchorage or lap lengths beyond the bent, and by lack of stirrups representative of bridge detailing practices of the 1960's and 70's. In addition, because design was geared towards elastic response (strength rather than ductility), large amounts of primary reinforcement were used without adequate stirrup confinement. In some failed joints, the closely spaced, large diameter main bars formed a plane of weakness leading to through-spalling of the cover layer. Concrete crushing under the main bar 90° bents caused splitting of the joints along a vertical plane (the crack plane run parallel to the plane of action of the joint between main bars). In many cases the effects of inadequate detailing were compounded by the low redundancy of the bridge frames.

Earlier analytical and experimental studies of interior and exterior beam column joints have highlighted the significance of bond demand as a measure of joint vulnerability (Kurose 1987, Bonacci and Pantazopoulou 1992). In the remainder, bond demand is quantified by a non-dimensional parameter known as Bond Index (B.I., Otani 1985, also Kitayama et al. 1991). The BI is defined as the mean bond demand along the total available anchorage length past the critical section, required to sustain yielding of the primary reinforcement at the critical section, normalized with respect to $\sqrt{f_c}$. By definition, BI is inversely proportional to the available anchorage length of the bar, therefore, larger values of BI suggest increased risk of anchorage failure:

$$BI = \frac{f_b}{\sqrt{f_c}} = \Phi \frac{f_{yk}}{4L_b\sqrt{f_c}} \tag{4-40}$$

where L_b is the total length of the bar from the point of entrance into the joint up to the end of the bar, Φ the bar diameter and f_{yk} the nominal yield strength.

Another dimension of the same problem prevails when considering that bond demand is related to joint shear stress; from eqs. (4-27), (4-29), and considering that bond demand depends on the total surface of all tension reinforcement, it may be shown that:

$$BI = \frac{V_j + V_c}{\pi \cdot \sum \Phi \cdot L_b \sqrt{f_c}} \tag{4-41}$$

for interior and knee joints (under opening moments) and

*

$$BI = \frac{V_j}{\pi \cdot \sum \Phi \cdot L_b \sqrt{f_c}} \tag{4-42}$$

for knee joints under closing moments. In the above, $\sum\Phi$ is the sum of all bar diameters that are part of the tension reinforcement.

From analysis of several published beam-column connection tests conducted under repeated deformation reversals it was concluded that values of BI in excess of 1.65, 0.85 and 0.5 (for 420 MPa steel and interior, exterior and knee joints respectively), were associated with anchorage failures of the primary reinforcement. As a rule, specimens having values of BI less than the above limits did not fail in the anchorage region, while sustaining rather high joint shear stresses. From eqs. (4-42), (4-43) it is evident that the bond demand is linearly related to the joint shear demand; thus, in order for the BI to maintain low values, whereas the

Copyright fib, all rights reserved. This PDF copy of fib Bulletin 24 is intended for use and/or distribution only by National Member Groups of fib.

joint sustains high shear stresses, it is essential that the available anchorage lengths are rather extensive. Such a practice is not common in neither new nor old construction; however this point has been proven experimentally in the knee-joint tests by Bai and Luo (1988).

Note that in beam-column cases with high BI values, reversal of loading accelerates and exacerbates the loss of bond in the lead-in length of the bar (i.e. along the straight portion of the bar anchorage). At large drifts, bond may be considered nonexistant in this segment, so that the bar force may be taken constant up to the point of the hook bent (i.e., up to the node of the equivalent strut and tie model depicted in Fig. 4-32). Therefore, development of the bar force occurs along the bent portion of the hook, as well as through bearing of the hook on concrete.

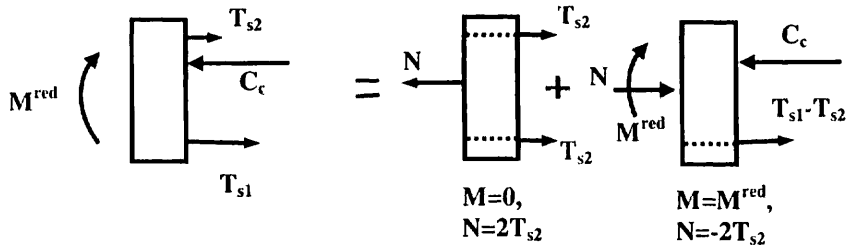

Fig. 4-39: Calculation of the reduced moment capacity, M^{red}, due to slip of primary reinforcement

A note of caution is called for at this point: in the context of a capacity based prioritising of failure, eq. (4-40) may lead to erroneously high values for the BI, as it presumes that tension yielding will occur in the beam reinforcement, therefore implying anchorage failure. However, in old-type reinforced concrete frames, occurrence of weak column-strong beam connections is not uncommon. If the plastic hinge forms in the column, with the beam reinforcement remaining elastic, then the actual bond demand may be much lower than the nominal value given by eq. (4-40). In this regard, eqs. (4-41) and (4-42) may be considered more general, because the joint shear can be calculated from the moment transfer occurring in the joint (eqs. (4-23)-(4-25)) without reference to the state of the adjacent members (i.e., whether yielding occurs or not and in which member it prevails).

Particularly relevant to the case of interior joints are the consequences of excessive bond demand on the moment transfer capacity of the connection: after few cycles of inelastic lateral drift, bond degradation may be so extensive, that the bond capacity of the bars within the joint no longer suffices to support reversal of stresses from one face of the joint to the next, as required by equilibrium (i.e, tension on one face, compression on the other face, Figs. 4-30, 4-33). More accurately stated, the problem is that under poor bond conditions, slip of the bars occurs within the joint, whereas the ideal anchorage point of tension reinforcement occurs in the adjacent span, outside the joint. Hence the "plane sections remaining plane" assumption used to calculate the flexural properties of the critical beam sections adjacent to the joint is no longer valid with regards to the reinforcement. The beam "compression" reinforcement on one face of the column may actually be in tension, leading to significant loss of flexural strength. (Moment capacity of the affected beam section equals that of a singly reinforced cross section, subjected to simultaneous axial compression equal to twice the amount of residual tension force carried by the compression reinforcement and having an effective area of tension steel reduced from the actual amount by as much as the area of compression reinforcement, Fig. 4-39). In this case the connection becomes a source of flexibility for the entire structure, impairing the total ductility and energy dissipation capacities of the system as a whole. The same behaviour occurs when bond conditions are intrinsically poor, such as for example in old-type connections with smooth primary reinforcement (Calvi et al. 2002). This particular problem is addressed in greater detail in the following Section (4.6.8).

At this point it is relevant to note that, due to the high shear forces acting on all members of the connection (in the plastic hinges in beams or columns and within the joint panel), and considering the familiar effect of shear causing tension on all reinforcement available in disturbed regions, it is practically very difficult for reinforcement to act as compression steel in the manner prescribed by a theoretical moment-frame analysis, even if the anchorage

Copyright fib, all rights reserved. This PDF copy of fib Bulletin 24 is intended for use and/or distribution only by National Member Groups of fib.

conditions were favourable (Vecchio and Collins 1986, Pantazopoulou and Bonacci 1994). It therefore remains an unresolved point whether compression reinforcement under any circumstances would ever attain the stress levels calculated from conventional flexural analysis of the beam critical sections.

Recognizing the significance of bond demand on joint performance, Priestley et al. (1996) link joint detailing requirements to successful development of the yield force of primary reinforcement in the joint panel. Using the shear friction model reviewed in Section 4.3, the anchorage capacity of a primary bar after the development of splitting cracks is obtained from the clamping action provided by orthogonal stirrups (or hoops). A tensile strain of 0.0015 is set as a limit to the transverse steel function, for beyond this strain level concrete dilation is considered too excessive to effectively support any frictional action. Therefore, the area of required transverse reinforcement is given from:

$$T_s = \mu A_{tr} f_{yst} \cdot n_{stirrups} \tag{4-43}$$

where T_s is the tension force in the adjacent critical section (overstrength value), to be developed in the joint, $n_{stirrups}$ is the number of stirrup layers crossing the bar, μ the coefficient of friction (taken as 1.5), A_{tr} the area of stirrup legs along one direction of restraint and f_{yst} the yield stress of stirrup reinforcement. According to Priestley et al (1996), as effective are solutions whereby the required stirrups calculated by eq. (4-43) are provided in various alternative schemes (either parallel or orthogonal to the bars being developed), so long as they confine the diagonal strut in the joint; this is valid even if stirrups are located outside the joint core, confining the region where the diagonal compression strut experiences a sharp change of direction.

4.6.8 Modeling anchorage forces along smooth bars

In modern construction, the use of deformed bars, combined with the practice of dimensioning the beam section depth as a multiple of the column bar diameter, usually regulates bond demand in the joint core within acceptable bounds. In old construction, where smooth bars had been used, friction along the concrete-bar interface is the only bond resistance mechanism available, known to supply low bond strength and fast decay upon load reversal. In assessment, the frictional model is used to describe and quantify the development capacity of reinforcement that has undergone bond deterioration through the joint core, both for smooth and deformed bars.

In the model originally proposed by Moehle et al. (1994) and adopted in the FEMA 273 and 356 document, the frictional force developed along the length of embeddment of a bar through the joint is related to the clamping action of normal reinforcing bars. For example, in the case of a beam column joint where beam bars do not have adequate anchorage length into the joint, the stress in the adjacent longitudinal column bar determines the magnitude of clamping action: the higher the tension in the column bar, the lower is the clamping force on the beam bar. The beam bar development capacity (in units of stress) is assumed linearly related to the column bar tension stress through the following empirical relation (also see Section 4.3):

$$f_s^{beam} = \frac{10\sqrt{f_c'} \cdot L_b}{\Phi} \cdot \left(350 - f_s^{column}\right) \le f_y \quad \text{(MPa)} \tag{4-44}$$

The column reinforcement stress, f_s^{column}, used in eq. (4-44) may be obtained from flexural analysis of the column section.

Using the frictional force concept, Calvi et al. (2001) evaluated the force that may be supported by the anchorage through the beam-column joint of horizontal smooth beam bars, from the compressive resultant in the compression zone of the adjacent column cross section. The same approach may also be used to evaluate the anchorage capacity of column longitudinal reinforcement through the joint. Here the problem appears to be in column reinforcing bar sections directly under the joint, having anchorage arrangements as depicted in Fig. 4-40. Whereas ideal anchorage conditions are secured by the hook in the bar segment above the joint, at the lower level compressed longitudinal column bars are actually in tension due to slip in the joint. Transverse compression to the column bars occurs within the joint,

Copyright fib, all rights reserved. This PDF copy of fib Bulletin 24 is intended for use and/or distribution only by National Member Groups of fib.

over a segment x_b that corresponds to the depth of compression zone of the adjacent beam. Hence, the maximum frictional force that may develop along the column longitudinal bar within the joint height equals:

$$N_f = \mu \cdot \sigma_c \cdot x_b \cdot \pi\Phi \tag{4-45}$$

where μ is the coefficient of friction and σ_c the average concrete compressive stress within the compression depth of the beam cross section. To yield the bar by frictional support only, N_f must exceed $F_y = f_y \pi \Phi^2/4$. Normalizing all terms of eq. (4-45) with F_y, the above simplifies to:

$$\frac{N_f}{F_y} = \frac{4\mu \cdot \sigma_c \cdot x_b}{f_y \Phi} = \frac{4\mu \cdot \alpha f_c' \cdot \xi_b d_b}{f_y \Phi} = 4\alpha\mu\xi_b \frac{d_b}{\Phi} \cdot \frac{f_c'}{f_y} = \beta \tag{4-46}$$

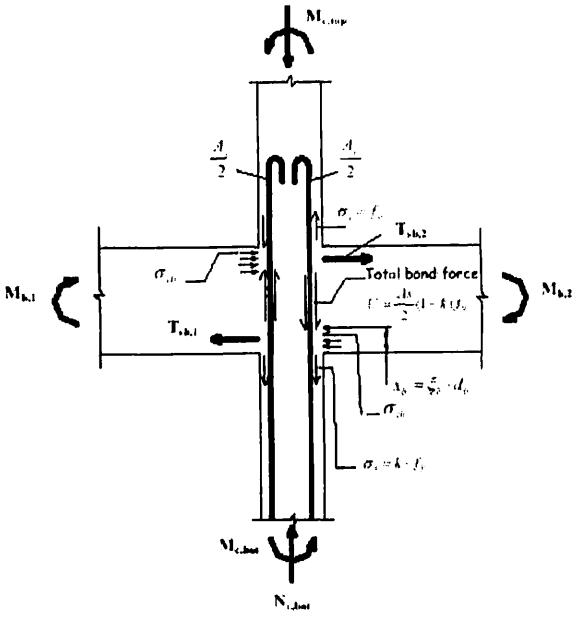

Fig. 4-40: Column bars anchored through the joint, terminating in hooks(Calvi et al. 2002)

Therefore, the corresponding bar force bellow the joint is $F_y - N_f = f_s \pi \Phi^2$, i.e., the residual bar stress is, $f_s = k f_y = \pi \Phi^2 f_y (1-\beta)$. It follows that $k = 1-\beta$. Coefficient k assumes a range of values depending on the bond conditions through the joint: the theoretical limit is k=-1, which corresponds to perfect bond conditions (not attainable in the critical region below the joint based on the mechanics of cracked reinforced concrete in shear, as discussed in the preceding). Depending on the degree of bond deterioration, coefficient k will attain positive values, the upper limit of k=1 corresponding to complete elimination of friction (for μ=0, β=0 from eq. (4-46), i.e., no bond is available).

The reduced moment capacity of the column section below the joint may be estimated if the axial load ratio is given and the bar force that can develop in the compression reinforcement is resolved as described in the preceding (Calvi et al. 2002, Hakuto et al. 1999). The consequences of the reduced effectiveness of compression steel were discussed in Section 4.6.7 and relate to loss of flexural resistance of the affected member cross section in the order of 20-30%. In this regard, neglecting reinforcement slip may prove unconservative; a conventional analysis of the column would suggest the section below the joint to be stronger than the one above the joint, due to the axial load increase in the section below the joint from the gravity force transfer of the diaphragm.

joint details	axial load ratio[2]	joint shear demand/supply ratio	interior joints: shear angle (radians)[3]			other joints: shear angle (radians)[3]		
			d	e	c	d	e	c
Conforming details[1]	≤0.1	≤1.2	0.015	0.03	0.2	0.01	0.02	0.2
	≤0.1	≥1.5					0.015	
	≥0.4	≤1.2		0.025			0.02	
	≥0.4	≥1.5		0.02			0.015	
Non-conforming details	≤0.1	≤1.2	0.005			0.005	0.01	
	≤0.1	≥1.5		0.015				
	≥0.4	≤1.2				0.0	0.0	0.0
	≥0.4	≥1.5						

[1]Conforming is a joint having closed and well-anchored hoops or stirrups, with spacing not exceeding one third of the column cross sectional dimension in the plane of action.
[2]Parameters are defined with reference to Fig. 4-41.

Table 4-5: Parameter values for the limit-state model adopted in the FEMA 273(1997) guidelines for assessment of existing beam-column joints.

Copyright fib, all rights reserved. This PDF copy of fib Bulletin 24 is intended for use and/or distribution only by National Member Groups of fib.

4.6.9 Limit state models for assessment of joint behaviour

Joint design according to the established codes of practice is centred on the estimation of demand and supply in terms of shear stress and bond. An intrinsic weakness in this approach is lack of emphasis on the magnitude of deformations that would be required to develop in the joint panel at the design limit state. Therefore it is truly not evident whether the amount of joint distortion associated to attainment of nominal strength in the joint can be realized, nor is the extent of corresponding damage in the joint explicitly stated. Yet, it is established from experimental results that the magnitude of joint deformation can serve as an indicator of performance of the connection as a whole, or of its individual components (Pantazopoulou and Bonacci 1994).

Assessing performance of existing (old-type) connections depends even more on definitions of acceptable damage levels. An established practice is to quantify damage in terms of critical joint drift due to distortion, associated with milestone events in the joint (such as cracking, yielding, concrete crushing, etc.). Therefore, a *limit-state* model for use in assessment of existing connections should reflect the dependence of strength on deformation and should represent the pattern of strength degradation with imposed drift, qualitatively at least. One such model, depicted in Fig. 4-41 is adopted in the FEMA 273/356 Guidelines for assessment of existing construction. The model parameters are listed in Table 4-5 for both "conforming" and "non-conforming" joints (i.e., joints having old-type reinforcement details, non-conforming to modern standards for earthquake-resistant construction).

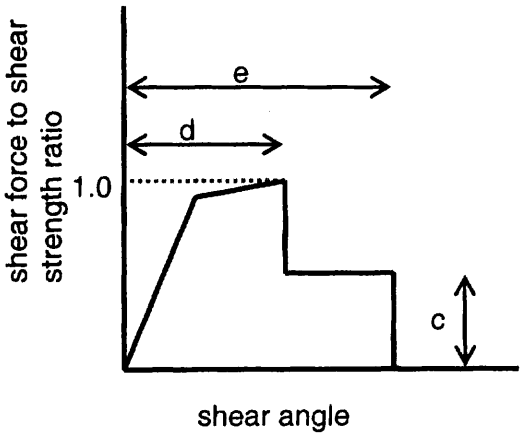

Fig. 4-41: Limit State model for beam-column joints

In the model, *d* represents the shear deformation angle at peak strength, taken as 0.005 for non-conforming joints in general, *e* is the shear distortion at the collapse level, taken as 0.01, whereas a higher value is allowed in interior joints. The residual strength ratio, *c*, is taken 0.2 in general and zero in the case of exterior joints with a high axial load.

An alternative limit state model for beam column joints, originally developed by Priestley et al. (1996), has been revised by Calvi et al. (2002) to include old-type joints with hooked anchorages, which, as discussed in Section 4.6.6, are susceptible to premature, spurious failure modes. The model, illustrated in Fig. 4-42, regulates joint strength as a function of drift. Note that it differs fundamentally from the model of Fig. 4-41, which is a component response curve (Fig. 4-41 plots the shear-stress vs. shear distortion envelope for the joint panel). Nominal strength of old-type joints is taken equal to the concrete contribution according with the ACI-ASCE 352 (1976) Recommendations (see Section 4.6.5(a)), i.e., $0.29\sqrt{f_c}$ (MPa) or $0.42\sqrt{f_c}$ (MPa), depending on the anchorage conditions of beam bars through the joint; this amount is sustained up to a joint drift of 0.75%. Strength degrades to $0.1\sqrt{f_c}$ (MPa) for a drift of 2% and is completely lost at 4% drift. According to Calvi

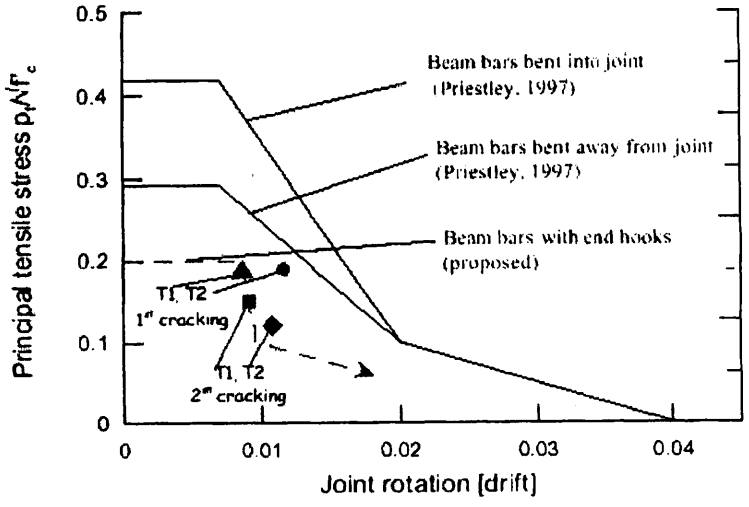

Fig. 4-42: Qualitative plot of shear strength vs. shear distortion envelope for T-joints (Calvi et al. 2001)

Copyright fib, all rights reserved. This PDF copy of fib Bulletin 24 is intended for use and/or distribution only by National Member Groups of fib.

et al. (2002), in the case of poorly detailed exterior joints with hooked anchorages, the reference strength value should be limited to $0.2\sqrt{f_c}$ (MPa) up to a drift of 1%, with sharp degradation ensuing at higher drift levels.

Lehman (2001) developed further the FEMA 273 limit-state model, seeking to express joint performance in terms of engineering parameters. The motivating research objective was to provide evaluation tools for estimating the effects of high drift demand on gravity load-carrying capacity of the column and the influence of column axial load magnitude on joint shear capacity.

To this end, Lehman (2001) examined analytical and experimental evidence from tests on connections representative of older detailing practices, in order to establish the influence of the main design parameters on joint strength and deformation capacity (such as axial load ratio, input shear, joint reinforcement, transverse beams, and slabs). From the results of the investigation it was concluded that the level of joint shear stress and the displacement history had the largest influence on connection behaviour. Of several alternative load histories that were examined, most severe strength degradation was observed in specimens subjected to three symmetric cycles of load at each drift level. Shear strength of joints without transverse reinforcement appeared to be determined by several factors, apart of concrete material strength and drift history, including beam bar yielding, column bar confinement and displacement history.

Damage as an indicator of performance, was most affected by the magnitude of input joint shear stress; maintaining shear stress levels below $\sqrt{f_c}$ (MPa) for both interior and exterior joints was an effective means of curbing excessive joint distortion, column slip, and beam bar pullout (Lehman 2002). Note that the shear stress limit set by the FEMA 273 (1997) Guidelines is $\sqrt{f_c}$, $0.83\sqrt{f_c}$, $0.67\sqrt{f_c}$, and $0.5\sqrt{f_c}$ (MPa) for interior and exterior joints with and without transverse beams, whereas the corresponding limit for knee joints is $0.33\sqrt{f_c}$ (the values listed are for non-conforming joints).These provisions are linked to joint shear reinforcement only (i.e. the strength values for all joint types, listed above, correspond to low volumetric transverse reinforcement ratio in the joint, $\rho_s<0.3\%$, whereas for higher reinforcement ratios allowable joint shear stress limits are increased by 33-50% for interior and by 100% for exterior and knee joints).

Confirming earlier studies by other investigators, Lehman (2002) reported that axial load had little effect on joint shear strength (at least in the case of exterior joints) and a profound influence on deformability (Bonacci and Pantazopoulou 1992). Maximum nominal joint shear stress occurred at a joint shear strain in the range of 0.0035-0.0045 for $n_v=0.1$, and in the range of 0.003-0.0035 for $n_v=0.25$. With reference to Fig. 4-41, the proposed values for parameters *d* and *e* were, 0.024 and 0.032 for $n_v=0.1$, and 0.015 and 0.025 for $n_v=0.25$, thus significantly greater than the corresponding values of Table 4-5 for non-conforming joints. Values for parameter *e* corresponded to 50% strength loss. Based on isolated beam-column connection tests, it was found that stiffness degradation caused a reduction in the axial load magnitude from its initial value, ranging between 10% and 25% towards the end of the test (this may not be necessarily relevant in real structures, where gravity load is statically determinate from the tributary area of any given column). Crack widths in the joint panel increased almost exponentially with drift magnitude.

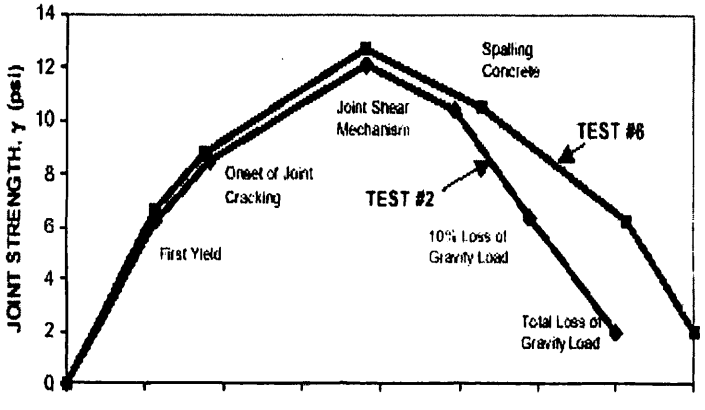

Fig. 4-43: Experimental curve defining performance limit states for joints (Pantelides et al. 2002)

Governing parameters that corresponded to milestone damage states were found to be: 1) drift, 2) joint crack width, and 3) joint shear strength. In a refined version of the limit-state model of Fig. 4-41, Pantelides et al. (2002) (also summarised by Lehman (2002)) proposed using five rather than three damage levels, so as to characterise the state of the joint panel by discrete values for the three salient parameters mentioned, as illustrated in Figures 4-43 and 4-44. In turn, these values may be

Copyright fib, all rights reserved. This PDF copy of fib Bulletin 24 is intended for use and/or distribution only by National Member Groups of fib.

interpreted with regards to engineering decisions as to the repairability of the joint:

- Level I: first yield (0.5%-0.75% drift),
- Level II: onset of joint cracking (0.5%-1% drift),
- Level III: formation of a joint shear mechanism (1.5-1.9% drift),
- Level IV: spalling of concrete (2.5% drift),
- Level V: total loss of gravity load (2.5-3.5% drift).

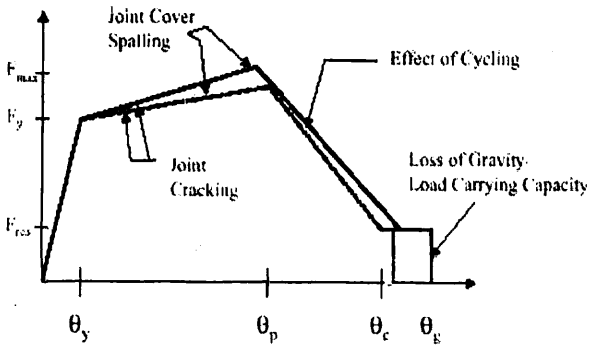

Fig. 4-44: Idealized Limit-State model for beam – column joints (Lehman 2002)

Therefore, with reference to Fig. 4-43 and 4-44, between the elastic limit and the plastic state, θ_y and θ_p, two damage levels are identified; injectable residual crack widths and joint spalling. The gravity load carrying capacity of the member is lost at drift levels exceeding θ_g.

Joint shear strain at yield (sudden slope change, θ_y in Fig. 4-44) appears to be in the order of 0.006-0.008 radians. This information is essential in applying the limit state model of either Fig. 4-41 or Fig. 4-44 in a performance-based context. It complements the FEMA 273 (1997) provisions for joint shear stress limits, in that no guidance was given originally in the Guidelines as to how to determine the initial joint stiffness, other than that the failure point is obtained from the yield point by a positive slope at 10% of the yield stiffness.

Ideally, the inelastic rotation values corresponding to the various performance levels in either of Figs. 4-41 and 4-44 ought to be specified in terms of drift history indices: This point, according to Lehman (2002), ought to be a driving objective in future analytical and experimental studies of old-type and modern beam-column joints.

4.6.10 Calculating deformations at milestone events of the limit-state model

A weakness in the limit-state models presented in the preceding is in the empiricism necessarily attached to milestone deformation or drift values. Whereas strength can be estimated through mechanistic models that reflect at least qualitatively the role of important design parameters on strength demand and supply, the corresponding deformation values are prescribed. Therefore the possible dependency of these response indices on component characteristics is lost in the process.

Of course, under no circumstances should one be misled to think that deformation estimates derived from rational mechanistic models necessarily carry a much greater level of confidence or accuracy as compared to the empirical values. Yet, closed form expressions for calculating θ_y, θ_p, and even θ_c and θ_g (Fig. 4-44) are valuable, despite their pitfalls, because they convey the underlying physical link between basic properties and resulting response. In this regard, the model formulated for beam-column joints by Pantazopoulou and Bonacci (1991) had already established a procedure for calculating stress and deformation of the joint throughout the range of response up to failure. The resulting response curve extended to the range of full inelastic joint action, it was therefore in itself a limit-state envelope. The model was subsequently complemented by Bonacci and Wight (1998) by including closed form expressions for the drift contributions of the various elements in the beam-column connection, including the joint. The importance of this point cannot be overemphasised, particularly because there exists a certain degree of ambiguity in international literature as to which deformation index is used in the limit state model. (For example, the x-coordinate in the models of Fig. 4-42 and 4-44 are different, the first being storey drift and the second being joint panel distortion).

Storey drift comprises contributions from deformations in beams and columns, rotation due to slip of reinforcement and joint panel distortion. Results from many beam-column connection tests have illustrated that joint distortion increases sharply after hoop yielding; restraint to joint volume growth is greatly diminished, leaving concrete susceptible to low

Copyright fib, all rights reserved. This PDF copy of fib Bulletin 24 is intended for use and/or distribution only by National Member Groups of fib.

cycle fatigue and rendering diagonal compression failure of the joint core the most likely event to follow. Upon hoop yielding the joint becomes a source of flexibility in the connection, effecting pronounced softening of the overall frame assembly under cyclic load (Pantazopoulou and Bonacci 1994, Bonacci and Wight 1998).

Prior to joint stirrup yielding, the joint is assumed elastic, therefore the joint shear strain may be determined from the joint shear force and the shear modulus of concrete (Bonacci and Wight, 1998):

$$\gamma_j = \frac{v_j}{G_j} = \frac{V_j}{G_j b_c h_c h_b} = \frac{2M_b / L}{G_j b_c h_c h_b} \tag{4-47}$$

The corresponding shear stiffness of the joint, $G_j = E_c/2(1+\nu)$, where E_c the secant modulus of concrete (corresponding to the level of compressive strain) and ν its Poisson ratio (a secant value may be used at the same level of strain). Joint shear strain, γ_j, contributes to storey lateral displacement by an amount Δ_j according to the following expression (Bonacci and Wight, 1998):

$$\Delta_j = \gamma_j H(1 - \frac{h_b}{H} - \frac{h_c}{L}) \tag{4-48}$$

To approximately calculate joint shear stress and effective modulus at the point of hoop yield the following procedure is used (Pantazopoulou and Bonacci 1991):

$$\begin{aligned} & v_j^{yield} = \frac{\rho_h f_{y,h}}{\tan\theta} \;;\; \varepsilon_h = \varepsilon_s^{yield} \; (\approx 0.002) \;;\; \varepsilon_v = \frac{1}{E_s \rho_v}(\frac{v_j^{yield}}{\tan\theta} - n_v) \;;\; \varepsilon_2 = \frac{\varepsilon_v - \varepsilon_h \tan^2\theta}{1-\tan^2\theta} \\ & \gamma_j^{yield} = \frac{2(\varepsilon_v - \varepsilon_2)}{\tan\theta} \;;\; G_j = \frac{v_j^{yield}}{\gamma_j^{yield}} \;;\; \tan^4\theta \cdot \frac{1+1/m_r\rho_h}{1+1/m_r\rho_v} + \tan^2\theta \cdot \frac{\varepsilon_h \cdot n_v / E_c}{(1+m_r\rho_v)m_r\rho_h} - 1 = 0 \end{aligned} \tag{4-49}$$

In the above, subscripts *h* and *v* correspond to the horizontal and vertical axes respectively; ε is strain, θ the angle of inclination of principal stresses (and strains) measured from the horizontal axis, m_r is the ratio E_s/E_c, where E_s the elastic modulus of steel and E_c the secant modulus of concrete (usually, for the conditions at hoop yielding it is taken as $2f_c/\varepsilon_{co}$, ε_{co} being the axial compressive strain at peak stress). Reinforcement area ratios, ρ_h and ρ_v, are calculated as prescribed in Section 4.6.4(b) (see also Pantazopoulou and Bonacci 1991).

After yielding of joint reinforcement the pattern of deformation in the joint changes dramatically. This occurs for values of shear distortion $\gamma_j > \gamma_j^{yield}$. The angle of principal stresses becomes: $\tan\theta = (\rho_h f_y + n_h)/v_j$.Equilibrium and compatibility equations in the joint panel may be solved, using as controlling parameter either the hoop strain, $\varepsilon_h > \varepsilon^{yield}$, the joint panel distortion, $\gamma_j > \gamma_j^{yield}$, or the joint shear stress, v_j. Average verical joint stress, σ_v, average principal compressive stress, σ_2, and hoop strain, ε_h, are obtained from the joint shear stress, v_j, as:

$$\begin{aligned} & \sigma_v = -\frac{v_j^2}{\rho_h f_y + n_h} \;;\; \sigma_2 = -\rho_h f_y - n_h - \frac{v_j^2}{\rho_h f_y + n_h} \;; \\ & \varepsilon_h = \frac{1+1/m_r\rho_v}{E_c[\rho_h f_y + n_h]^3} v_j^4 - \frac{n_v / E_c}{m_r \rho_v [\rho_h f_y + n_h]^2} v_j^2 - \frac{\rho_h f_y + n_h}{E_c} \end{aligned} \tag{4-50}$$

Therefore a dramatic increase occurs in the values of σ_v, σ_2, and ε_h for small increases in the value of joint shear after yielding of the hoops, since all other terms in eq. (4-50) but v_j remain constant after hoop yielding.The next event is expected to be either yielding of vertical reinforcement in the joint, or crushing of the diagonal compressive strut. Thus, joint shear strength is the minimum of the corresponding shear values associated with those two mechanisms of failure (eq. 4-39).

Shear distortion corresponding to the prevailing failure limit state is found from the basic compatibility requirement:

Copyright fib, all rights reserved. This PDF copy of fib Bulletin 24 is intended for use and/or distribution only by National Member Groups of fib.

$$\gamma_{j,max} = \frac{2(\varepsilon_1 - \varepsilon_h)}{\tan\theta} = 2(\varepsilon_1 - \varepsilon_v)\tan\theta \quad ; \quad \varepsilon_h + \varepsilon_v = \varepsilon_1 + \varepsilon_2 \tag{4-51}$$

where ε_h is found from eq. (4-50) for the corresponding value of shear strength (either $v_{j,max1}$ or $v_{j,max2}$), and the associated strain (either yield strain in the vertical steel, ε_v=0.002 or peak strain in the diagonal compressive principal direction, $\varepsilon_2=\alpha\varepsilon_{co}$). Because equilibrium and compatibility relations are valid throughout the range of response (i.e. eqs. (4-33)-(4-34) and (4-51)), the softening branch of the limit state model may be also approximated by solving the above set of equations for even higher values of shear strain $\gamma_j>\gamma_{j,max}$ (Bonacci and Pantazopoulou 1992), whereby in the absence of joint reinforcement, the post-peak branch is basically controlled by the behavior of concrete in compression past the peak point (Vecchio and Collins 1986).

4.6.11 Relevance of joint damage and collapse on global frame behaviour

In order to determine the consequences of joint damage and collapse on the seismic performance of existing frame systems with structural inadequacies typical of gravity load design, it is often necessary to explicitly model joint flexibility in the frame idealisation used in time-history or pushover analysis. In this regard, an equivalent moment-rotation spring has been traditionally used to simulate joint flexibility in inelastic frame finite-element analysis. The moment-rotation envelope of the spring may be derived directly from the limit state model, by consideration of the relationship between joint shear stress and moment transfer occurring in the connection (eq. (4-23)-(4-25). Thus, the vertical axis in the moment rotation envelope is obtained by multiplying the corresponding axis of the limit state model by the area of the joint and the column height, whereas there is one-to-one correspondence between the values in the rotation/deformation axis.

Joint shear damage can be assumed to correspond to the development of a "shear hinge", which is activated by shear behaviour and not by flexural behaviour. The post-elastic response of that hinge is not ductile, exhibiting the marked strength degradation pattern past the peak illustrated by the limit-state models of Figs. (4-41)-(4-44). In cases of assessment, the possibility that a shear hinge might develop ought to be considered. From analytical studies of old-type frames using this modelling procedure Calvi and co-workers demonstrated the following points (Calvi et al. 2002):

- Joint damage was found to relieve some of the rotation demand from the adjacent columns, in some cases even delaying the formation of a pure soft-storey mechanism, without amplifying the global displacement demands.
- The favourable effect on adjacent structural members (due to reduced demand) is obtained at the cost of increased deformation demand within the joint panel. However, the local ultimate joint deformation capacity could limit the benefits of a shear-hinge formation.

References:

AASHTO 1994. LRFD bridge design specifications. American Association of State Highway and Transportation Officials, Washington, D.C.

ACI 318-63 1963. ACI standard: building code requirements for reinforced concrete. American Concrete Institute, Detroit, Michigan, 141 pp.

ACI 318-99 & ACI 318R-99 1999. Building code requirements for structural concrete and commentary. American Concrete Institute, Farmington Hills, Michigan, 391 pp.

ACI-ASCE Committee 352 1976. Recommendations for design of beam-column joints in monolithic reinforced concrete structures. ACI Journal, Vol. 73, No. 7, pp. 375-393.

ACI-ASCE Committee 352 1985. Recommendations for design of beam-column joints in monolithic R.C. structures. ACI Structural J., Vol. 82, No. 3, pp. 266-283.

ACI-ASCE Committee 352 2001. Recommendations for design of beam-column joints in monolithic R.C. structures. Draft Report, in print.

AIJ 1988. Design guidelines for earthquake resistant RC buildings based on the ultimate strength concept. Architectural Institute of Japan, Tokyo, Japan.

Copyright fib, all rights reserved. This PDF copy of fib Bulletin 24 is intended for use and/or distribution only by National Member Groups of fib.

Albanesi S., and Biondi S. 1994. On longitudinal reinforcement buckling in flexural R.C. members subjected to strong inelastic loads. Proceedings, 10th European Conference on Earthquake Engineering, Vienna, A.A. Balkema, Rotterdam, Vol. 3, pp. 1613-1618.

Albanesi S., Biondi S., Cioppi F., and Massi D. 1996. The influence of reinforcement buckling on the ultimate response of R.C. elements: a comparison with seismic codes. Proceedings, 11th World Conference on Earthquake Engineering, Acapulco, paper No. 1061.

Albanesi T., Biondi S., and Nuti C. 2002. The influence of longitudinal reinforcement buckling in structural response. Proceedings, 12th European Conference on Earthquake Engineering, London, Paper No. 749.

Ang, B.G., Priestley, M.J.N. and Paulay, T. 1989, Seismic shear strength of circular reinforced concrete columns, ACI Structural J., Vol. 86, No. 1, pp.45-59.

Bai S. and Luo Y. 1988. Concrete frame corners. Proceedings, Pacific Concrete Conference, N. Zealand, pp. 157-168.

Beton-Kalender 1970. Taschenbuch für Beton- und Stahlbetonbau, sowie die verwandten Facher, W. Ernst & Sohn, Berlin-München.

Biskinis, D., Roupakias, G. and Fardis, M.N. 2003. Cyclic deformation capacity of shear-critical RC elements. Proceedings, *fib* Symposium: Concrete Structures in Seismic Regions. Athens

Bonacci J. F., and Wight J. K. 1996. Displacement based assessment of reinforced concrete frames in earthquakes. Proceedings, Mete Sozen Symposium: A Tribute from his Students, American Concrete Institute, ACI SP-162, No. 6, pp. 117-138.

Bonacci J., and Pantazopoulou S. 1993. Parametric investigation of joint mechanics. ACI Str. J., Vol. 90, No. 1, pp. 61-71.

Bresler B., and Gilbert G. H. 1961. Tie requirements for reinforced concrete columns. J. of the American Concrete Institute, Vol. 58, pp. 555-570.

Calvi G. M., Magenes G., and Pampanin S. 2002. Relevance of beam-column joint damage and collapse in RC frame assessment", J. of Earthquake Engineering, Imperial College Press, Vol. 6, No. 1, pp.75-100.

Cote P. A., and Wallace J. W. 1994. A study of RC knee-joints subjected to cyclic loading. Report No. CU/CEE-94/04, Dept. Civil Engrg., Clarkson University, Potsdam, NY, pp. 13699-5710.

DIN 1045, 1972. Beton- und Stahlbetonbau, Bemessung und Ausführung. Deutsches Institut für Normung, Berlin.

Eurocode 2, 1991. Design of concrete structures. Part 1: General rules and rules for buildings. European Committee for Standardisation, Brussels.

Eurocode 8, 1994. Design provisions for earthquake resistance of structures. European Committee for Standardisation, Brussels.

FEMA 273, 1997. NEHRP guidelines for the seismic rehabilitation of buildings. Report No. FEMA-273, Federal Emergency Management Agency, Washington D.C.

FEMA 274, 1997. NEHRP commentary on the guidelines for the seismic rehabilitation of buildings. Report No. FEMA-274, Federal Emergency Management Agency, Washington D.C.

Gülkan P., and Sozen M. 1999. Procedure for determining seismic vulnerability of building structures. ACI Structural J., Vol. 96, No. 3, pp. 336-342.

Hakuto S., Park R. and Tanaka H. 1999. Effect of deterioration of bond of beam bars passing through interior beam column joints on flexural strength and ductility. ACI Str. J., Vol. 96, No. 5.

Hakuto S., Park R., and Tanaka H. 2000. Seismic load tests on interior and exterior beam-column joints with substandard reinforcing details. ACI Str. J., Vol. 97, No. 1, pp. 11-25.

Imran I. and Pantazopoulou S. J. 1996. Experimental Study of Plain Concrete Under Triaxial Stress. ACI Mat. J., Vol. 93, No. 6, Nov.-Dec. 1996, pp. 589-601.

Inel M., and Aschheim M. 2002. Displacement-based strategies for the seismic design of short bridges considering embankment flexibility. MAE Center Report, University of Illinois at Urbana-Champaign, USA.

Kitayama K., Otani S. and Aoyama H. 1991. Development of design criteria for RC interior beam-column joints. Design of Beam-Column Joints for Seismic Resistance, ACI SP-123, American Concrete Institute, Detroit, Mich., pp. 97-123.

Copyright fib, all rights reserved. This PDF copy of fib Bulletin 24 is intended for use and/or distribution only by National Member Groups of fib.

Kowalsky, M.J. and Priestley, M.J.N. 2000. Improved analytical model for shear strength of circular reinforced concrete columns in seismic regions. ACI Structural J., Vol. 97, No. 3, pp.388-396.

Kurose Y. 1987. Recent studies on reinforced concrete beam-column joints in Japan. PMFSEL Report No. 87-8, Phil M. Ferguson Structural Engineering Laboratory, Department of Civil Engineering, The University of Texas at Austin, Austin, Tex..

Lehman D. 2002. State-of-the-Art review on exterior and interior beam column joints (Communicated by J. Moehle, from a 2002 PEER report)

Lehman D.E., Calderone, A.J. and Moehle, J. P. 1998. Behavior and design of slender columns subjected to lateral loading. 6th US National Conference on Earthquake Engineering, EERI, Seattle, Washington, May 31 June 04.

Lehman D.E., Lynn A.C., Aschheim M.A., Moehle J.P. 1996. Evaluation methods for reinforced concrete columns and connections. 11th World Conference On Earthquake Engineering, Paper No.673.

Luo Y. H., Durrani A. J., Bai S., and Yuan J. 1994. Study of reinforcing detail of tension bars in frame corner connections. ACI Structural J., Vol. 91, No. 4, pp. 486-496.

Lynn A., Moehle J.P., Mahin S., and Holmes W. 1996. Seismic evaluation of existing R.C. building columns. Nov., EERI, Oakland CA., Earthquake Spectra, Vol. 12, No. 4, pp. 715-739.

Ma R., Xiao Y., and Li K.N. 2000. Full – scale testing of a parking structure column retrofitted with carbon fiber reinforced composites. Construction and Building Materials, Elsevier Science, Vol. 14, pp. 63-71.

Mander J. B., Priestley M. J. N., and Park R. 1988. Theoretical stress-strain model for confined concrete. Journal of Structural Engineering, ASCE, Vol. 114, No. 8, pp.1804-1825.

Mander J. B., Priestley M. J. N., and Park R. 1988. Observed stress-strain behavior of confined concrete. J. of Structural Engineering, ASCE, Vol. 114, No. 8, pp. 1827-1849.

Martín-Pérez B., and Pantazopoulou S. J. 1998. Mechanics of concrete participation in cyclic shear resistance of RC. J. of Structural Engineering, ASCE, Vol. 124, No. 6, pp. 633-641.

Mau S. T. 1990. Effect of tie spacing on inelastic buckling of reinforcing bars. ACI Structural Journal, Vol. 87, No. 6, pp. 671-677.

McConnell S. W. and Wallace J. W. 1995. Behavior of RC beam-column knee joints subjected to reversed cyclic loading. Report No. CU/CEE-95/07, Dept. Civil Engrg., Clarkson University, Potsdam, NY.

Moehle J., Lynn A., Elwood K., Sezen H. 2001. Gravity load collapse of building frames during earthquakes. PEER Report: 2nd US-Japan Workshop on Performance-based Design Methodology for Reinforced Concrete Building Structures. Pacific Earthquake Engineering Research Center, Richmond, CA.

Moehle J.P., Roger Li Y., Lynn A., Browning J. 2000. Performance assessment for a reinforced concrete frame building. ACI SP-197. S.M. Uzumeri Symposium: Behavior and Design of Concrete Structures and Seismic Performance, American Concrete Institute, Detroit, MI.

Monti G., and Nuti C. 1992. Nonlinear cyclic behavior of reinforcing bars including buckling. J. of Structural Engineering, ASCE, Vol. 118, No. 12, pp. 3268-3284.

NZS 3101, 1982. Code of practice for the design of concrete structures – Vols. 1 and 2. (Standards Association of New Zealand, Wellington).

NZS 3101, 1995. Code of practice for the design of concrete structures – Vols. 1 and 2. (Standards Association of New Zealand, Wellington).

Otani S., Kitayama K., and Aoyama H. 1995. Beam bar bond stress and behaviour of reinforced concrete interior beam-column connections. Proceedings, 2nd US-NZ-Japan Seminar on Design of Reinforced Concrete Beam-Column Joints, Department of Architecture, University of Tokyo, Tokyo, Japan, pp. 1-40.

Pampanin S., Calvi G. M. and Moratti M. 2001. Seismic response of reinforced concrete beam column joints designed for gravity loads. ASCE Str. J., submitted for publication.

Panagiotakos T. and Fardis M. N. 2001. Deformation of R.C. members at yielding and ultimate", ACI Structural J., Vol. 98, No. 2, pp. 135-148.

Pantazopoulou S. J. and Bonacci J. F. 1991. Consideration of questions about beam-column joints, ACI Str. J., Vol. 89, No. 1, pp. 27-36.

Copyright fib, all rights reserved. This PDF copy of fib Bulletin 24 is intended for use and/or distribution only by National Member Groups of fib.

Pantazopoulou S. J. and Bonacci J. F. 1994. On earthquake resistant reinforced concrete frame connections. Vol. 21, No. 2, pp. 307-328.

Pantazopoulou S. J. and Thomas M.D.A. 2000. Mechanical behaviour of AAR-damaged R.C. members, Proceedings, 11th International Conference on AAR, Quebec, Canada.

Pantelides C., Clyde C. and Reaveley L.D. (2002). Performance-based evaluation of reinforced concrete building exterior joints for seismic excitation, Earthquake Spectra, Vol. 18, No. 3, EERI, Oakland CA, pp. 449-480.

Papia M. and Russo G. 1989. Compressive concrete strain at buckling of longitudinal reinforcement. J. of Structural Engineering, ASCE, Vol. 115, No. 12, pp. 382-397.

Park R., and Paulay T. 1975. Reinforced concrete structures. J. Wiley and Son, Inc., N. York, 769 pp.

Paulay T. and Priestley M. J. N. 1992. Seismic design of reinforced concrete and masonry buildings, J. Wiley and Sons Inc., New York.

Penelis G., and Kappos A. J. 1997. Earthquake-Resistant Concrete Structures, E&FN Spon, Chapman & Hall, London, UK, 572 pp.

Priestley M.J.N. 1997. Displacement – based seismic assessment of reinforced concrete buildings. Journal of Earthquake Engineering, Vol.1, No.1, pp.157-191.

Priestley M.J.N., Ranzo G., Benzoni G., and Kowalsky M. J. 1996. Yield displacements of circular bridge columns. Proceedings of the 4th Caltrans Seismic Research, California Department of Transportation Engineering Center, Sacramento, CA, July 9-11.

Priestley, M.J.N., Seible F., and Calvi M. 1996. Seismic design and retrofit of bridges. J. Wiley & Sons Inc., N. York.

Rodriguez J., Ortega L.M., and Casal J. 1997. Load carrying capacity of concrete structures with corroded reinforcement. Construction and Building Materials, Elsevier Science, Vol. 11, No. 4, pp. 239-248.

Rodriguez M. E., Botero J. and Villa J. 1999. Cyclic stress-strain behavior of reinforcing steel including the effect of buckling, ASCE J. of Structural Engineering, Vol. 125, No. 6, pp. 605-612.

Scribner C. F. 1986. Reinforcement buckling in reinforced concrete flexural members. Vol. 83, No. 6, pp. 966-973.

Sezen, H. 2000. Evaluation and testing of existing reinforced concrete columns. Report CE 299, Dept. of Civil and Environmental Engineering. Un. of California, Berkeley, CA

Skettrup E., Strabo J., Anderson N. H. and Brondum-Nielsen T. 1984. Concrete frame corners. ACI Structural J., Vol. 81, No. 6, pp. 587-593.

Sozen M. 2001. From Erzincan to Istanbul. Presentation given at the Greek-Turkish workshop on Seismic Assessment and Retrofit, January 2001, Athens, Greece.

Stanish K., R.D. Hooton, and Pantazopoulou, S. J. 1999. Corrosion effects on bond strength in reinforced concrete. ACI Structural J., Vol. 96, No. 6, pp. 915-921.

Suda K. and Masukawa J. 2000. Models for concrete spalling and reinforcement buckling of reinforced concrete. Proceedings, 12th World Conference on Earthquake Engineering, Auckland, New Zealand, Paper No. 1437.

Syntzirma D., and Pantazopoulou S. J. 2001. Strength assessment of reinforced concrete members in shear. Proceedings, 2nd National Greek Conference on Earthquake Engineering, EPPO, Thessaloniki, Volume B, November 2001, pp. 191-199.

Tassios T.P. and Moretti M. 2002. Modelling and Design of R.C. short columns. Proceedings, 4th Forum on Implications of Recent Earthquakes on Seismic Risk, Tokyo Institute of Technology, May 27-29, Tokyo Japan, Technical Report TIT/EERG 02-1, pp. 157-168.

Tastani S., and Pantazopoulou S. J. 2001. Shear strength degradation of reinforced concrete elements under cyclic loading. Proceedings, 2nd National Greek Conference on Earthquake Engineering, EPPO, Thessaloniki, Volume B, November 2001, pp. 267-275.

Thom C. W. 1983. The effects of inelastic shear on the seismic response of structures, PhD Thesis, University of Auckland, New Zealand 100 pp.

Vecchio F.J., and Collins M.P. 1986. The modified compression field theory for R.C. elements subjected to shear", ACI Structural J., Vol. 83, No. 2, pp. 219-231.

Copyright fib, all rights reserved. This PDF copy of fib Bulletin 24 is intended for use and/or distribution only by National Member Groups of fib.

APPENDIX 4.A:

Calculation of yield curvature and moment

Panagiotakos and Fardis (2001) defined the yield curvature φ_y as the point that marks onset of nonlinearity in the moment-curvature diagram (owing to either yielding of tension reinforcement or nonlinearity in concrete – for compressive strains exceeding 90% of the strain at peak stress of uni-axially loaded concrete):

$$\phi_y=\min\{\frac{f_{yk}}{E_s(1-\xi_y)d};\ \frac{\varepsilon_c}{\xi_y d}\approx\frac{1.8f_{ck}}{E_c\xi_y d}\} \qquad \text{(A4-1)}$$

The corresponding compression zone depth at yield, x_y, normalized with respect to d, is: $\xi_y=(\alpha^2A^2+2\alpha B)^{1/2}-\alpha A$, in which $\alpha=E_s/E_c$ and A, B are given by the following equations, depending on whether yielding is controlled by the tension steel or by nonlinearity in the compression zone:

$$A=\rho_{s1}+\rho_{s2}+\rho_v+\frac{N}{bdf_y},\quad B=\rho_{s1}+\rho_{s2}\delta_2+0{,}5\rho_v(1+\delta_2)+\frac{N}{bdf_y}\quad \text{(tension steel yielding)}$$

$$A=\rho_{s1}+\rho_{s2}+\rho_v-\frac{N}{1.8\alpha.8\alpha_c},\quad B=\rho_{s1}+\rho_{s2}\delta_2+0{,}5\rho_v(1+\delta_2)\ \text{(nonlinearity in the compression zone).}$$

where ρ_{s1} and ρ_{s2} the area ratios of tension and compression reinforcements, ρ_v the area ratio of distributed longitudinal reinforcement, $\delta_2=d_2/d$ (d_2 is the distance of the extreme compression fiber to the centroid of compression reinforcement), N the axial load (compression positive). Concrete Modulus of Elasticity is taken as $E_c=0.85x2{,}15x\cdot10^4(f_c/10)^{1/3}$.

The corresponding yield moment, M_y, was estimated by Panagiotakos and Fardis (2001) using the following expression:

$$\frac{M_y}{bd^3}=\varphi_y\left\{E_c\frac{\xi_y^2}{2}\left[0{,}5(1+\delta_2)-\frac{\xi_y}{3}\right]+\frac{E_s}{2}\left[(1-\xi_y)\rho_{s1}+(\xi_y-\delta_2)\rho_{s2}+\frac{\rho_v}{6}(1-\delta_2)\right](1-\delta_2)\right\} \qquad \text{(A.4.2)}$$

Similar is the calculation of the nominal flexural strength M_n (replacing ξ_y by ξ_u).

Calculation of ultimate strain capacity of confined concrete

A variety of expressions are available in international literature for calculating the ultimate strain capacity. Frequently used models are: the expression by Richart et al. (1928) modified to represent strain at 85% drop of peak strength and the model of Mander et al. (1988a) in its original or modified forms (the latter was proposed by Fardis and Panagiotakos, 2001).

Richart et al. (1928):

$$f'_{cc}=f'_c+4.1\sigma_{lat}\approx f'_c(1+2k_e\rho_{s,tr}\frac{f_{yst}}{f'_c});$$

$$\varepsilon_{cc,u}=\varepsilon^o_{cu}(1+5(\frac{f'_{cc}}{f'_c}-1))=\varepsilon^o_{cu}(1+10k_e\rho_{s,tr}\frac{f_{yst}}{f'_c})=\varepsilon^o_{cu}(1+20k_e\rho_{s,st}\frac{f_{yst}}{f'_c}) \qquad (A4-3)$$

Mander et al. (1988a):

$$f'_{cc}=f'_c\left(-1.254+2.254\sqrt{1+7.94\frac{0.5k_e\rho_{s,tr}f_{yst}}{f'_c}}-\frac{k_e\rho_s f_{yst}}{f'_c}\right);$$

Copyright fib, all rights reserved. This PDF copy of fib Bulletin 24 is intended for use and/or distribution only by National Member Groups of fib.

$$\varepsilon_{cc,u} = 0.004(=\varepsilon_{cu}^{o}) + 1.4\varepsilon_{su}\frac{\rho_{s,tr} f_{yst}}{f_{cc}'} \qquad \text{(A4-4)}$$

<u>Modified Model of Mander et al. (Fardis and Panagiotakos, 2001):</u>
From calibration of 277 flexural tests at the reported failure point, where the value of the failure curvature ϕ_u has been measured, best fit was obtained using the following expressions for failure stress and strain of confined concrete:

$$f_{cc}' = f_c'\left(1 + 3.7\left(\frac{0.5k_e\rho_{s,tr} f_{yst}}{f_c'}\right)^{0.87}\right); \quad \varepsilon_{cc,u} = 0.004 + 0.6\varepsilon_{su}\frac{\rho_{s,tr} f_{yst}}{f_{cc}'} \qquad \text{(A4-5)}$$

in which ε_{su} and $\rho_{s,tr}$ are the failure strain and volumetric ratio of confining steel. With this choice 277 test data on ϕ_u were fitted with a median for the ratio of predicted-to-experimental value of 0.99 and a coefficient of variation of 73% (the authors report this to be the best fit among various alternative calculations of $\varepsilon_{cc,u}$ in the literature).

Confinement effectiveness of stirrups (for rectangular sections)

The stirrup confinement effectiveness coefficient, k_e, is obtained according to Sheikh and Uzumeri (1978), also adopted in the CEB/FIP Model Code 90 and in Eurocode (prEN1992-1:2002), from the following expression (for rectangular sections):

$$k_e = \left(1 - \frac{s_h}{2b_c}\right)\left(1 - \frac{s_h}{2h_c}\right)\left(1 - \frac{\sum b_i^2}{6b_c h_c}\right) \qquad \text{(A4-6)}$$

with b_c, h_c denoting the width and depth of the confined core of the section, s_h the clear stirrup spacing and b_i the distances of successive longitudinal bars laterally restrained at stirrup corners or by 135°-hooks.

Depth of compression zone at ultimate

The normalized depth of compression zone at ultimate, ξ_u, may be estimated using interpolation, for a specified axial load ratio $N/A_c f_c$, from the following set of equations (Pantazopoulou 1998):

$$\text{if } N_{bal} < N < N_{max}, \quad \xi_u = \xi_{bal,u} + (1 - \xi_{bal,u})\frac{N - N_{bal}}{N_{max} - N_{bal}} \qquad (A4-7a)$$

$$\text{if } N_{min} < N < N_{bal}, \quad \xi_u = \delta_2 + (\xi_{bal,u} - \delta_2)\frac{N - N_{min}}{N_{bal} - N_{min}} \qquad (A4-7b)$$

The values of N_{min}, N_{bal}, and N_{max} correspond to characteristic values of the depth of compression zone for ε_{cu}=0.005, as follows:

$$\text{for } x = d_2, \Rightarrow \xi = \delta_2, \quad \frac{N_{min}}{A_c f_c'} = 0.72\delta_2 - \frac{f_y}{(1-\alpha)f_c'}[\rho_{s1} + \rho_v(1 - 2\delta_2)] \qquad \text{(A4-8 a)}$$

$$\text{for } x = x_{bal}, \Rightarrow \xi_{bal} = 0.64, \quad \frac{N_{bal}}{A_c f_c'} = (\rho_{s2} - \rho_{s1})\frac{f_y}{f_c'} + 0.462 + 0.275\rho_v\frac{f_y}{f_c'} \qquad \text{(A4-8 b)}$$

$$\text{for } x = d, \Rightarrow \xi = 1, \quad \frac{N_{max}}{A_c f_c'} = 0.85^2 + \frac{f_y}{f_c'}(\rho_{s2} + 0.8\rho_v) \qquad \text{(A4-8 c)}$$

Copyright fib, all rights reserved. This PDF copy of fib Bulletin 24 is intended for use and/or distribution only by National Member Groups of fib.

where a the strain hardening ratio of the reinforcement (a=(f_u-f_y)/f_u). With the depth of compression zone at ultimate, the corresponding ultimate curvature may be obtained, using the confined compression strain capacity according with eqs. (A4-3), (A4-4) or (4-18a), (4-18b):

$$\phi_u = \frac{\varepsilon_{cu}}{\xi_u d}; \quad \phi_p = \phi_u - \phi_y \qquad (A4-9)$$

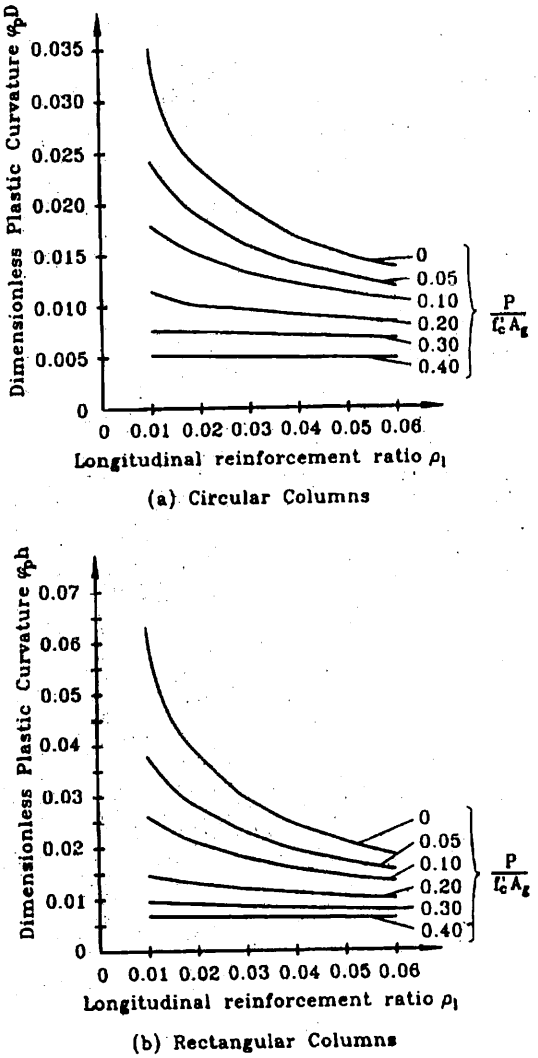

Fig. A4-1: Plastic curvature as a function of $N/A_g f_c'$ and ρ_l (from Priestley et al. 1996)

Direct calculation of yield and ultimate curvatures

Priestley et al. (1996) conducted parametric investigations of yield and plastic curvatures ϕ_y and ϕ_p, for poorly confined circular and rectangular column sections. Maximum compressive concrete strain was taken as ε_{cu}=0.005, because at that strain cover spalling is expected to occur in the plastic hinge region. For this value of maximum compressive strain, it is suggested that the nominal flexural strength be taken equal to the yield strength. Results show that the ultimate plastic curvature depends strongly on the axial load ratio, whereas the longitudinal reinforcement ratio has a less pronounced influence. Computed values are given in nondimensional format in Fig. A4-1; multiplying the ultimate plastic curvature ϕ_p by the plastic hinge length provides an estimate of ultimate plastic rotation, $\theta_{p,u}$. The values plotted in Fig. A4-1 have been calculated using a concrete strength f_c'=35 MPa, and a reinforcement yield strength of 300 MPa. Plastic curvature values for other material strengths may be obtained using a modified longitudinal reinforcement ratio, ρ_l^m, calculated as follows: $\rho_l^m=\rho_l(f_{ya}/300)(35/f_{ca})$ where the subscipt "a" denotes given (applied) values. Values obtained in this manner may be overestimates by as much as 15% for higher steel strengths, so a correction factor of 0.85 is pertinent in such cases.

Calculated yield curvatures were found to be insensitive to both axial load ratio and longitudinal steel ratio. The following expressions summarize the parametric results:

$$\phi_y D_o = 2.45\varepsilon_y \pm 15\% \quad \text{for circular column cross-sections} \qquad (A4.10)$$

$$\phi_y h = 2.14\varepsilon_y \pm 10\% \quad \text{for rectangular column cross-sections} \qquad (A4.11)$$

Similar expressions have been derived by Fardis and Panagiotakos (2001), through correlation with a large database of test results. The coefficients are slightly different from those of eqs. A4-10, A4-11, and are classified depending on the type of the member (beam or column).

Copyright fib, all rights reserved. This PDF copy of fib Bulletin 24 is intended for use and/or distribution only by National Member Groups of fib.

5 Seismic retrofitting techniques

5.1 Introduction

According to Chapter 1 *Introduction* repair is defined as reinstatement of the original characteristics; retrofit, rehabilitation or strengthening imply enhancement of one or more seismic response parameter. They often include addition of structural elements or a change of the structural system, whilst repair is restricted to the as-built system. Multiple-effect methods refer to established intervention methods which affect more than one response parameter, such as concrete jacketing. Selective-effect methods refer to the use of techniques and mechanisms to influence one response parameter at a time, with little or no effect on others.

The objective of undertaking remedial work in earthquake engineering is rather simple; achieving the simple objective is a matter of considerable complexity. The objective is to ensure that the modified seismic demand is less than the modified capacity. The main modification to the seismic demand (expressed as deformation or more commonly force) is the change in the design life of the structure. It could also be argued that the return period of the earthquake or the probability of being exceeded could be increased in recognition of the recent occurrence of an earthquake.

The decision as to the level of intervention is complex and is governed by technical as well as financial and social considerations. Some of the factors affecting intervention policy are:

- retrofit vs. replacement cost;
- relationship between level of strengthening and future impact of earthquake damage;
- retrofit materials and technology available;
- consequences of partial or total evacuation;
- duration of the retrofit operation;
- restrictions on surrounding space and outlook of the structure;
- social, political and/or historical significance;
- requirements of repeatability and reversibility of the intervention.

Ideally, intervention decisions are taken within a complete framework of cost-benefit and assessment of the effect of various options. Such a framework [FEMA, 1989] has been applied to several areas of the USA. The intervention programme also includes decisions on the level of intervention. These may be one of the following:

- restriction or change of use;
- partial demolition and/or mass reduction;
- local or global modification of elements and system;
- transformation of non-structural into structural components;
- modification of the structural system;
- member replacement;
- addition of a new lateral load resistance system;
- provision of supplementary damping;
- incorporation of passive or active vibration control devices.

It is emphasised that each structural intervention constitutes a special case for which one or more of the above provide the best solution. Therefore, generalisation of rules for application in retrofit strengthening is neither possible nor advisable.

5.2 Selection of the retrofit technique ("Retrofit strategy")

Section 2.3 of the report has given a broad overview of retrofit strategies and systems. The present section provides additional general information on retrofit, linking them with the outcome of the assessment and serving as an introduction to the rest of the chapter. It also focuses on certain aspects specific to retrofitting of concrete buildings.

The retrofit strategy should be guided by the results of a detailed (preferably displacement-based) assessment of the building. If the assessment has identified deformation capacity deficiencies in a few scattered components (member or joints), then a strategy of local modification of these components or joints is appropriate.

If the deficiencies are concentrated in one part of the structure, they may be due to an irregularity of the structural configuration: a weak storey or a torsionally unbalanced structure. Then retrofitting should address the irregularity through one or more of the following means:

Copyright fib, all rights reserved. This PDF copy of fib Bulletin 24 is intended for use and/or distribution only by National Member Groups of fib.

a) by strengthening some vertical elements (those of the weak storey or of the weak and flexible side of the building); b) by adding some new elements, which are strong and stiff enough to remove or overshadow the irregularity (new shear walls on the weak side of a torsionally unbalanced building; full-height shear walls to act as a stiff spine and suppress the column side-sway mechanism); or c) by removing material to weaken some elements (e.g. cutting steel bars, or coring concrete through the web of deep spandrel beams framing with weak columns, if this is acceptable for the gravity load resistance of beams). If the structural configuration in 3D is strongly irregular, vertical joints may even be introduced at selected locations in plan, to reduce the building into a set of structurally independent but regular units. Vertical elements should be provided in this case on both sides of each joint for independent support of the corresponding horizontal elements. The width of the joint should be enough to avoid pounding, especially if the parts separated by the seismic joint differ significantly in height and/or lateral stiffness.

If the assessment reveals a generalized deficiency throughout the building, a more radical intervention may be necessary, in the form of adding shear walls or bracing systems, or of upgrading most, if not all, existing elements, especially the vertical ones.

New shear walls or steel bracing systems protect the existing elements by reducing the global displacements under the "design" seismic action(s) to levels corresponding to the deformation capacities of the existing components (within the force- and strength-based philosophy and terminology, these new elements provide most of, if not all, the resistance to lateral loads). They represent a more cost-effective strategy than universal upgrading of the existing components, especially if disruption of occupancy and relocation of occupants to another building ("surge costs") and the demolition and replacement of partitions, architectural finishes and other non-structural components are taken into account. New shear walls, and sometimes the addition of bracing systems, may require, though, an intervention to the foundation system, which is normally a costly, disruptive and sometimes technically challenging operation. If interventions at the perimeter of the building are feasible, addition of shear walls or steel bracing at the facades should be favoured over general upgrading of (vertical) elements throughout the building, especially if occupancy needs to be continued during retrofitting.

Unless very specific and substantial deficiencies are identified in some beams, upgrading of existing components may be limited to vertical elements (columns and shear walls), possibly including their joints with the beams. Due to the monolithic connection of the beams with the slabs, upgrading a beam is technically more difficult than upgrading a column or wall. Moreover, experience from past earthquakes has shown that damage in beams is far less frequent than in columns and much less important for the global structural stability. Finally, the design of beams for gravity loads normally provides enough top reinforcement over the supports (supplemented by the slab bars within a sizable effective flange width) and substantial shear reinforcement in the form of stirrups closed at the critical bottom side. What is missing in such beams is continuity and anchorage of bottom bars over the supports and lack of deformation capacity of the bottom flange in compression. Nonetheless, recent tests have shown that bar pull-out in positive bending, if it occurs, only increases the lateral deformations of frames, while beam plastic hinging in negative bending does not always take place (El Attar et al, 1997, Bracci et al, 1995). After all, jacketing of the columns into which the beams frame, improves, albeit indirectly, the anchorage of beam bottom bars and the confinement of the bottom flange of the beam. Last but not least, the main hazard for existing buildings is posed by too much, rather than by too little, flexural strength capacity of the beams relative to the columns.

When seismic retrofitting is combined with architectural remodeling and/or a change in use, seismic upgrading is made easier if heavy finishes, partitions and claddings are replaced with lighter alternatives and heavy equipment or storage loads are removed, to reduce the total mass of the building and its global force and displacement demands (in the velocity-controlled region of the spectrum, where the effective fundamental period typically falls, forces and displacements are proportional to the square root of mass). For the same reason, but also to remove extreme irregularities in elevation, demolition of penthouses and upper storey setbacks is sometimes worth considering. If the deficiencies identified in the existing structure are marginal, reduction and removal of masses throughout the building or, in extreme cases, complete removal of the upper storey(s), may make seismic strengthening of the structural system unnecessary.

Copyright fib, all rights reserved. This PDF copy of fib Bulletin 24 is intended for use and/or distribution only by National Member Groups of fib.

Regardless of its type and extent, any retrofitting intervention should not impair the safety or the capacity of any part of the building in any respect, e.g. by introducing irregularities in plan or in elevation, by shifting the deformation demands to inadequate components or to other failure modes, etc. The engineer should make sure that by upgrading the flexural capacity of a component, he or she does not make it critical in shear, and that strengthening of beams does not shift plastic hinging to columns. He or she should also give very serious consideration to the consequences of discontinuing the strengthening, i.e. the new shear walls or bracing or the jacketing of existing strengthening columns, etc., at a certain storey: this may result in concentration of damage just above the level where strengthening was discontinued (for examples see Sugano, 1996 and Nakano, 1995).

Regardless of the particular retrofit strategy chosen, the engineer should check carefully the existing and the retrofitted structure for what is usually termed "continuity of the load path(s)". In other words he or she should ensure the safe transfer of inertia forces from the masses where they originate to the (primary) elements of the lateral-load-resisting system and from there to the foundation. This means that any connection within the floor system, between the floors and the lateral-load-resisting elements and between existing and new components, should be checked as force-controlled components for the maximum possible forces that they may be required to transfer. It should be kept in mind that peak inertia forces that may need to be transferred are proportional to peak floor accelerations and that global strengthening and stiffening of a structure for seismic retrofitting results in higher response accelerations at all floor levels in comparison to the non-retrofitted building. Even though they normally consist of a ductile material, such as steel, connectors and fasteners should be treated as force-controlled components and protected from yielding, because once they yield they are called to accommodate significant relative displacements of the components they connect within their limited size and hence they may soon exhaust their deformation capacity. Connections liable to be subjected to cycles of tension and compression may fracture under forces below their nominal tensile capacity, if they have suffered buckling or have been severely deformed in a previous compression half-cycle. It is also reminded that welded or bolted connections are inherently brittle and that steel parts in an existing connection which appears adequate in construction documents may have corroded in the mean time.

Connections between prefabricated elements, especially in diaphragms consisting of precast units, are potentially weak links in the load path. Thin and lightly reinforced toppings in precast floors or roofs may already be cracked over seams between the precast units, or may easily do so during the earthquake and then they may break open. It is difficult and not cost-effective to assure integrity of a precast floor or roof, topped or untopped, through retrofitting. Removal and replacement with a proper cast-in-place concrete floor or roof, monolithically connected to the vertical framing elements, should be preferred.

Cast-in-place slabs are normally considered to provide a continuous load path. One should be careful though with one-way slabs in old buildings, which may have very little reinforcement in the transverse (secondary) direction. If required to transfer tensile in-plane forces, such floor systems may break open through the points of the supporting beams where the analysis for gravity loads had given zero moment (longitudinal steel in old beam designs was proportioned without the shift rule and with very short anchorage lengths; therefore most of the longitudinal top and bottom bars were terminated near the inflection point, as predicted by the analysis for gravity-loads).

After this listing of general and principles governing selection of a seismic retrofit strategy and its implementation through the various alternative retrofitting techniques, a more detailed overview of the most commonly used among these techniques is presented in the next few sections. The application of base isolation and energy dissipation for seismic upgrading is not covered in this overview. These two techniques, or rather strategies, are best suited for seismic upgrading of existing bridges, for some configurations of which they represent by far the best solution. For existing buildings, however, these two strategies are not cost-effective. This is particularly so for base isolation, which essentially requires a double foundation system, i.e. one foundation for the superstructure above the isolation devices and another for the entire structure below the isolation system. Nevertheless, base isolation can offer not only safety to the building and its occupants under very strong and rare earthquakes, but also protection of building contents under any earthquake event. Therefore, for critical or important facilities required to remain operational during the design earthquake or to be available for immediate occupancy afterwards, isolation may be the most cost-effective strategy, provided that the

Copyright fib, all rights reserved. This PDF copy of fib Bulletin 24 is intended for use and/or distribution only by National Member Groups of fib.

existing building has low aspect ratio and large stiffness. At any rate, base isolation is a sophisticated and complex technique and its application requires not only specialized expertise but also, possibly, peer review of the design.

To become effective, an energy dissipation system requires development of significant lateral displacements. So it can only be used in flexible structures, as a supplement of another system which does not increase significantly the global stiffness: dissipation devices can be used in parallel to, or combined with base isolation devices, or can be inserted in the braces of a steel bracing system added to the existing structure for strengthening. However, in this latter case the displacements needed for activation of the dissipation system are not concentrated at the base (isolation) level but are distributed throughout the structure, and may cause significant damage to existing structural and non-structural components. This technique is also sophisticated and costly, but less than base isolation.

5.3 Modification of individual members: Multiple effects

5.3.1 Introduction

If deficiencies in a few components have been identified from the seismic assessment of the full building, then the engineer may opt for modification of only these components. Individual existing components may also be modified for improved earthquake resistance and/or deformation capacity, within the framework of a strategy of global measures for seismic upgrading, such as the addition of shear walls or of a steel bracing system. In such cases, modification of selected members may be deemed as necessary for a uniform and balanced planwise distribution of the lateral force resistance, or for removing member deficiencies in gravity load capacity, or simply to supplement the global upgrading measures.

Most retrofit techniques modify at the same time, by intention or unavoidably, more than one of the properties or parameters characterizing the response of the member: Its stiffness, its strength (force-resistance), its deformation capacity, its energy-dissipation capacity, etc. These are the techniques addressed in Section 4.3 of the report. Techniques that modify selectively and in a controlled manner only one parameter or property of the member, while not affecting the others, are described in Section 4.4.

As noted in Section 5.2, from the application point-of-view modification of vertical members (columns or walls) for the purposes of seismic retrofitting is much easier than that of horizontal members (beams or slabs). Moreover, vertical members are much more critical for earthquake resistance and stability of the building than horizontal members. For these two reasons, modification of vertical members for seismic retrofitting is far more common than that of horizontal components. Furthermore, strengthening of horizontal components is more of interest for gravity loads than for seismic actions, as it is often needed when a change in use increases design live loads (imposed or traffic loads). So the techniques for modification of horizontal members for strengthening purposes are covered in more general documents, which do not focus on seismic retrofitting. For all these reasons, the emphasis in the following is on modification of existing vertical concrete members, and of columns in particular, as modification of walls is normally harder and less necessary than that of columns.

Before treating in detail the application and design of the various means for modification of existing columns, for reasons of completeness the subject of repair of previous seismic damage without strengthening of the element is briefly addressed within this section. As nowadays earthquake-induced damage to a building almost invariably triggers upgrading of its deficient earthquake resistance through global seismic retrofitting, this subject is of interest only for those members of the damaged structure which are not included in the list of members to be upgraded, but are just restored to their pre-earthquake condition.

5.3.2 Properties and parameters of monolithic concrete members

The yardstick for the stiffness, strength and cyclic deformation capacity of components repaired or retrofitted with a concrete jacket, is the behaviour of a monolithic virgin member with the final cross-sectional dimensions and reinforcement of the modified member. For reference purposes the parameters chosen to model: a) the secant-to-yield stiffness; b) the yield strength; and c) the cyclic deformation capacity of monolithic concrete members are summarized below, along with the quantitative expressions chosen to describe these

Copyright fib, all rights reserved. This PDF copy of fib Bulletin 24 is intended for use and/or distribution only by National Member Groups of fib.

parameters in terms of the geometric and material properties of the member. These expressions have been developed for members which have: a) compression zone with constant width b (rectangular); and b) concentration of longitudinal reinforcement near the extreme tension and compression fibres, possibly with additional reinforcement uniformly distributed between these concentrations of longitudinal reinforcement (web reinforcement). This scope covers the vast majority of RC members in buildings; not covered are columns with circular cross-section or – in general - circular arrangement of the longitudinal reinforcement.

- The secant-to-yield stiffness of a RC member is expressed in terms of its effective rigidity over the shear span L_s=M/V:

$$EI_{eff} = \frac{M_y}{3\theta_y} L_s \tag{5-1}$$

where M_y and θ_y are the moment and the chord-rotation at yielding of the member end section. (It is reminded that the chord-rotation, i.e. the angle between the tangent to the axis at the yielding end and the chord connecting that end with the end of the shear span, i.e. the point of inflection, is equal to the member drift ratio, i.e. the deflection of the end of the shear span divided by L_s).

- The chord-rotation θ_y at yielding is computed through Eq. (5-2), accounting for flexural and shear deformations (1st and 2nd term) and for bond slip of bars (3rd term).

$$\theta_y = \phi_y \frac{L_s}{3} + 0.0025 + a_{sl} \frac{0.25\varepsilon_y d_b f_y}{(d-d')\sqrt{f_c}} \tag{5-2}$$

In Eq. (5-2), fitted to 1133 test results, ϕ_y is the yield curvature, computed from first principles as described below, f_y and f_c (in MPa) the strengths of steel and concrete, d_b the diameter of tension reinforcement, and d, d' the depth to the tension and compression reinforcement, respectively.

- If yielding of the section is signaled by yielding of tension steel, the yield curvature is:

$$\phi_y = \frac{f_y}{E_s(1-\xi_y)d} \tag{5-3}$$

whereas if it is due to nonlinearity of the concrete in compression, then:

$$\phi_y = \frac{\varepsilon_c}{\xi_y d} \approx \frac{1.8 f_c}{E_c \xi_y d} \tag{5-4}$$

The compression zone depth at yield, ξ_y, (normalised to d) is:

$$\xi_y = \left(\alpha^2 A^2 + 2\alpha B\right)^{1/2} - \alpha A \tag{5-5}$$

in which $\alpha = E_s/E_c$ and A and B are given by Eqs. (5-6) or (5-7), if section yielding is controlled by the tension steel or by the compression zone, respectively:

$$A = \rho + \rho' + \rho_v + \frac{N}{bdf_y}, \qquad B = \rho + \rho'\delta' + 0.5\rho_v(1+\delta') + \frac{N}{bdf_y} \tag{5-6}$$

$$A = \rho + \rho' + \rho_v - \frac{N}{\varepsilon_c E_s bd} \approx \rho + \rho' + \rho_v - \frac{N}{1.8\alpha bdf_c}, \quad B = \rho + \rho'\delta' + 0.5\rho_v(1+\delta') \tag{5-7}$$

In eqs. (5-6), (5-7) ρ, ρ' and ρ_v are the reinforcement ratios of the tension, the compression and the web reinforcement (all normalised to bd), δ'=d'/d, where d' is the distance of the centre of the compression reinforcement from the extreme compression fibres, b is the width of the compression zone and N the axial load (compression: positive). In this analysis the area of any diagonal bars times the cosine of their angle with respect to the member axis is added to the reinforcement area considered in calculating ρ and ρ'.

Copyright fib, all rights reserved. This PDF copy of fib Bulletin 24 is intended for use and/or distribution only by National Member Groups of fib.

The lower of the two values resulting from Eqs. (5-3), (5-4) is the yield curvature. Then the yield moment can be computed as:

$$\frac{M_y}{bd^3} = \phi_y \left\{ E_c \frac{\xi_y^2}{2}\left(0.5(1+\delta') - \frac{\xi_y}{3}\right) + \frac{E_s}{2}\left[(1-\xi_y)\rho + (\xi_y - \delta')\rho' + \frac{\rho_v}{6}(1-\delta')\right](1-\delta') \right\} \quad (5\text{-}8)$$

- The mean ultimate chord rotation of flexure-controlled RC members is:

$$\theta_u = \alpha_{st,w}(1-0.38a_{cyc})\left(1+\frac{a_{sl}}{1.7}\right)(1-0.375a_{wall})(0.3^{\nu})\left[\frac{\max(0.01,\omega')}{\max(0.01,\omega)} f_c\right]^{0.2}\left(\frac{L_s}{h}\right)^{0.425} 25^{\left(\alpha\rho_{sx}\frac{f_{yw}}{f_c}\right)}\left(1.45^{100\rho_d}\right) \quad (5\text{-}9)$$

in which:

$L_s/h=M/Vh$: shear span ratio at the member end;

ω, ω': mechanical reinforcement ratios, $\rho f_y/f_c$, of the tension and compression longitudinal reinforcement (not including any diagonal bars); in shear walls the entire vertical web reinforcement is included in the tension steel;

f_c: uniaxial concrete strength (MPa);

$\nu=N/bh_cf_c$: axial load ratio normalized to width b of the compression zone, section depth h and f_c;

$\rho_{sx}=(A_{sx}/b_ws_h)$: ratio of transverse steel parallel to the direction (x) of loading (s_h=stirrup spacing);

α: confinement effectiveness factor, equal to:

$$\alpha = \left(1-\frac{s_h}{2b_c}\right)\left(1-\frac{s_h}{2h_c}\right)\left(1-\frac{\sum b_i^2}{6b_ch_c}\right) \quad (5\text{-}10)$$

(b_c, h_c = dimensions of confined concrete core, b_i= distances of restrained longitudinal bars on the perimeter);

ρ_d: steel ratio of diagonal reinforcement (if any) in each diagonal direction;

a_{st}: coefficient for the steel of longitudinal bars, equal to 0.016 for ductile hot-rolled steel and for heat-treated (tempcore) steel, or to 0.0105 for brittle cold-worked steel;

a_{cyc}:zero-one variable for the type of loading, equal to 0 for monotonic and to 1 for cyclic loading with at least one full cycle at peak deformation;

a_{sl}: zero-one variable for the slip of longitudinal bars, equal to 1 if there is slippage of the longitudinal bars from their anchorage beyond the member end, or to 0 if there is not;

a_{wall}: coefficient, equal to 1.0 for shear walls or to 0 for beams or columns.

Eq. (5-9) was fitted by regression to the results of 1048 monotonic or cyclic tests to failure of flexure-controlled beam-, column- or wall-specimens. The ratio of experimental values to the predictions has a median of 1.0 and a coefficient of variation of 46%.

An alternative to Eq. (5-9) is:

$$\theta_u = \theta_y + \alpha_{st}(1-0.46a_{cyc})(1+0.6a_{sl})(1-0.375a_{wall})(0.25^{\nu})\left[\frac{\max(0.01,\omega)}{\max(0.01,\omega)} f_c\right]^{0.25}\left(\frac{L_s}{h}\right)^{0.4} 25^{\alpha\rho_{sx}\frac{f_{yw}}{f_c}} 1.55^{100\rho_d} \quad (5\text{-}11)$$

With θ_y computed via Eq. (5-2), coefficient α_{st} in Eq. (5-11) is equal to 0.0125 for ductile hot-rolled or for heat-treated (tempcore) steels and to 0.00575 for brittle cold-formed ones.

For seismic loading Eqs. (5-9) and (5-10) should be applied considering cyclic loading and including slippage of the reinforcement from its anchorage zones beyond the member ends.

- An alternative to the empirical expressions, Eqs (5-9), (5-11), is:

Copyright fib, all rights reserved. This PDF copy of fib Bulletin 24 is intended for use and/or distribution only by National Member Groups of fib.

$$\theta_u = \theta_y + (\phi_u - \phi_y) L_{pl} \left(1 - \frac{0.5 L_{pl}}{L_s}\right) \tag{5-12}$$

in which ϕ_u is the ultimate curvature and L_{pl} the plastic hinge length.

Section failure may take place either at the full section level, or at the level of the confined core after spalling of the unconfined concrete cover. For failure of the full section prior to spalling, the corresponding ultimate curvatures are:
For failure due to steel rupture at elongation equal to ε_{su}:

$$\phi_{su} = \frac{\varepsilon_{su}}{(1 - \xi_{su}) d} \tag{5-13}$$

At failure of the compression zone:

$$\phi_{cu} = \frac{\varepsilon_{cu}}{\xi_{cu} d} \tag{5-14}$$

ξ_{su} and ξ_{cu} in Eqs. (5-13), (5-14) are, respectively, the compression zone depth at steel rupture or failure of the compression zone, both normalised to d. ε_{cu} in Eq. (5-14) is the extreme compression fiber strain when the compression zone fails and sheds its load. For unconfined concrete ε_{cu} is approximately equal to 0.004.

Assuming a stress-strain law for unconfined concrete which rises parabolically up to a strain equal to ε_{co} ($\approx$0.002) and stays constant up to a strain of ε_{cu}, the plane-section assumption and equilibrium give for ξ_{su}:

$$\xi_{su} = \frac{(1-\delta')\left(\frac{N}{bdf_c} + \frac{\rho f_t}{f_c} - \omega' + \frac{\varepsilon_{co}}{3\varepsilon_{su}}\right) + \left(\frac{1+\delta'}{2}\right)\frac{\rho_v(f_y + f_t)}{f_c}}{(1-\delta')\left(1 + \frac{\varepsilon_{co}}{3\varepsilon_{su}}\right) + \frac{\rho_v(f_y + f_t)}{f_c}} \tag{5-15}$$

Steel rupture at elongation ε_{su} takes place prior to compression zone failure and controls the ultimate curvature, if:

$$\frac{N}{bdf_c} < \frac{\varepsilon_{cu} - \frac{\varepsilon_{co}}{3}}{\varepsilon_{cu} + \varepsilon_{su}} + \omega' - \frac{\rho f_t}{f_c} - \frac{\rho_v(f_y + f_t)}{f_c} \frac{\varepsilon_{su}(1+\delta') - \varepsilon_{cu}(1-\delta')}{(1-\delta')(\varepsilon_{su} + \varepsilon_{cu})} \tag{5-16}$$

For values of N/bdf_c greater than the right-hand-side of eq. (5-16), spalling of the concrete cover will occur and the moment of the section will drop (at least temporarily). This will take place with yielding of the tension steel if:

$$\frac{N}{bdf_c} \le \omega' - \omega - \frac{\delta'}{1-\delta'}\omega_v + \frac{\left(\varepsilon_{cu} - \frac{\varepsilon_{co}}{3}\right) + (\varepsilon_{cu} - \varepsilon_y)\frac{\omega_v}{(1-\delta')}}{\varepsilon_{cu} + \varepsilon_y} \tag{5-17}$$

with $\omega_v = \rho_v f_y / f_c$ denoting the mechanical ratio of web steel.

If Eq. (5-17) is satisfied, ξ_{cu}, for use in Eq. (5-14), is:

$$\xi_{cu} = \frac{(1-\delta')\left(\frac{N}{bdf_c} + \omega - \omega'\right) + (1+\delta')\omega_v}{(1-\delta')\left(1 - \frac{\varepsilon_{co}}{3\varepsilon_{cu}}\right) + 2\omega_v} \tag{5-18}$$

(if the numerator in Eq. (5-18) is close to zero, ρ may be multiplied by f_t instead of f_y).

Copyright fib, all rights reserved. This PDF copy of fib Bulletin 24 is intended for use and/or distribution only by National Member Groups of fib.

Otherwise ξ_{cu} is the positive root of the following equation:

$$\left[1-\frac{\varepsilon_{co}}{3\varepsilon_{cu}}-\frac{\omega_v}{2(1-\delta)}\frac{(\varepsilon_{cu}-\varepsilon_y)^2}{\varepsilon_{cu}\varepsilon_y}\right]\xi^2+\left[\omega+\omega\frac{\varepsilon_{cu}}{\varepsilon_y}-\frac{N}{bdf_c}+\frac{\omega_v}{(1-\delta)}\left(\frac{\varepsilon_{cu}}{\varepsilon_y}-\delta\right)\right]\xi-\left[\omega+\frac{\omega_v}{2(1-\delta)}\right]\frac{\varepsilon_{cu}}{\varepsilon_y}=0 \quad (5\text{-}19)$$

If Eq. (5-16) is satisfied, section failure will occur at $\phi_u=\phi_{su}$ according to Eqs. (5-13), (5-14). If it is not, attainment of ϕ_{cu} according to Eqs. (5-14), (5-17)-(5-19) does not necessarily signal failure. If the moment capacity of the confined section, determined on the basis of the strength f_{cc} and ultimate strain ε_{cc} of confined concrete and the dimensions b_c, d_c, d_c' of the confined core (d_c and d_c' result by subtracting from d or d' the sum of the cover and half the diameter of transverse reinforcement; b_c is obtained by subtracting double this sum) is not less than a fraction in the order of 80% of the capacity of the full but unconfined section, failure will ultimately occur at the lower of the two curvature values given by Eqs. (5-13) or (5-14), applied this time for the confined core (i.e., dimensions b, d and d' are replaced by b_c, d_c, d_c'; N, ρ, ρ' and ρ_v are normalized to b_cd_c instead of bd; and f_{cc}, ε_{cc} are used instead of f_c, ε_{cu}).

To summarize: If Eq. (5-16) is satisfied, ϕ_u is determined from Eqs. (5-13), (5-14). Otherwise the moment capacities of the full but unconfined section and of the confined core after spalling of the cover are computed and compared. If the capacity of the confined core is less than 80% of that of the unconfined section, ϕ_u is the lower of the two values determined either from Eqs. (5-13), (5-15), or from Eqs. (5-14), (5-17)-(5-19), applied in both cases for the confined core of the section.

This calculation of ϕ_u was applied to 277 tests for which measured values of ϕ_u are available, using three alternative confinement models:

- that of the CEB/FIP model code 1990 (CEB 1993), adopted also in Eurocode 8;
- the Mander model (Mander et al 1988), as simplified by Paulay and Pristley (1992) regarding calculation of the ultimate strain ε_{cu} of confined concrete:

$$\varepsilon_{cu}=0.004+1.4\varepsilon_{su}\frac{\rho_s f_{yw}}{f_{cc}} \quad (5\text{-}20)$$

in which ρ_s is the volumetric ratio of confining steel; and

- c) a model which adopts for the strength of confined concrete the expression:

$$f_{cc}=f_c\left(1+3.7\left(\frac{0.5\alpha\rho_s f_{yw}}{f_c}\right)^{0.87}\right) \quad (5\text{-}21)$$

and for ε_{cu} the following modification of the Mander model:

$$\varepsilon_{cu}=0.004+0.6\varepsilon_{su}\frac{\rho_s f_{yw}}{f_{cc}} \quad (5\text{-}22)$$

Coefficient α in Eq. (5-21) is the confinement efficiency factor from Eq. (5-10).

The last alternative, namely Eqs. (5-21) and (5-22), produces the best fit to the available test data on ϕ_u.

With ϕ_u computed in this way and ϕ_y from Eqs. (5-3) to (5-7), the following expressions for L_s provide the best fit to experimental data:

For cyclic loading:

$$L_{pl,cy,L_s}=0.08L_s+\frac{1}{60}a_{sl}d_b f_y \quad (5\text{-}23)$$

$$L_{pl,cy,h}=0.225h+\frac{1}{60}a_{sl}d_b f_y \quad (5\text{-}24)$$

Copyright fib, all rights reserved. This PDF copy of fib Bulletin 24 is intended for use and/or distribution only by National Member Groups of fib.

For monotonic loading:

$$L_{pl,mon,L_s} = 0.18L_s + 0.025a_{sl}d_b f_y \tag{5-25}$$

$$L_{pl,mon,h} = 0.8h + 0.025a_{sl}d_b f_y \tag{5-26}$$

in which f_y is in MPa and a_{sl} is the zero-one variable used in Eqs. (5-8), (5-9), (5-11) for absence or presence of bar pull-out from the anchorage zone beyond the section of maximum moment.

- The yield moment, M_y^*, the chord rotation, θ_y^*, and the ultimate chord rotation, θ_u^*, of repaired elements or members retrofitted with concrete jackets, is usually expressed as a fraction of the corresponding parameters, M_y, θ_y, θ_u, of a monolithic member with the same external dimensions and reinforcement, as follows:

$$M_y^* = k_m M_y \tag{5-27}$$

$$\theta_y^* = k_y \theta_y \tag{5-28}$$

$$\theta_u^* = k_u \theta_u \tag{5-29}$$

The values of the modification factors k_m, k_y, k_u are not far from 1.0.

5.3.3 Repaired RC members

A member may be chosen to be repaired - instead of repaired and also strengthened - if its damage is judged to be slight or moderate. A member with severe or heavy damage, consisting of significant disintegration of the concrete core inside the stirrups or ties, and/or buckled or fractured reinforcing bars, cannot be restored to effectively its initial strength and deformation capacity with simple repair means and in all likelihood will be chosen to be jacketed instead.

Commonly repair consists of one or more of the following measures:

- Injection of cracks (with epoxy or grout)
- Replacement of spalled or loose concrete
- Replacement of rebars.

One or more of these measures, as appropriate, are also applied to damaged members prior to retrofitting with concrete jackets or other techniques, the only differences being that in such cases fine cracks (in the order of 0.3 mm) do not need to be injected and that replacement of spalled or loose concrete may be effected with the cast-in-situ concrete or the shotcrete of the concrete jacket.

Some information about the technology of these measures is given below.

It is noted that there are some issues that cast doubt over the effectiveness and controllability of these techniques, especially for RC structures. In the case of epoxy resin injection, it is very difficult to ascertain the degree of penetration of the resin into the complex crack configurations resulting from cyclic loading. Therefore, the level of reinstatement of stiffness is uncertain [Elnashai and Salama, 1993]. Moreover, the displacement at which the repaired parts of the structural member start "picking-up" load is also uncertain.

5.3.3.1 Injection of cracks

This is the most widely used repair method for minor to medium size cracks in RC structures. Tests on low viscosity epoxies [Bertero *et al.*, 1980] have confirmed the feasibility of this technique, especially with regard to bond reinstatement.

Injection of cracks is normally considered worthwhile if crack width exceeds 0.2 to 0.3mm. Cracks with width from 0.1mm (or even less) to a few (2 or 3) mm may be injected with a usual low-viscosity epoxy. Medium-viscosity epoxies are used for larger crack widths, up to 5 or 6 mm. In the rare case of larger cracks, up to 20 mm wide, cement grout is the appropriate material for injection.

Copyright fib, all rights reserved. This PDF copy of fib Bulletin 24 is intended for use and/or distribution only by National Member Groups of fib.

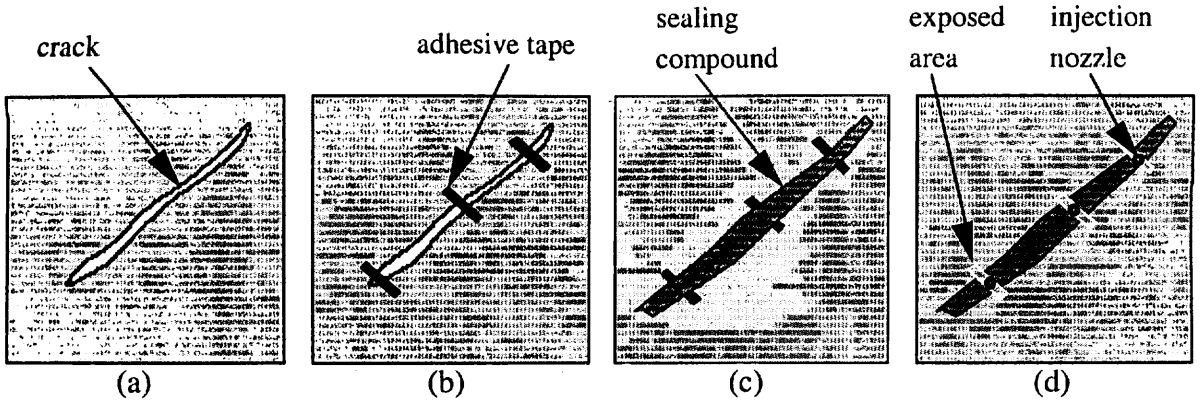

Fig. 5-1: Application of epoxy resin for crack repair

There are several variations on the method of application of this widely used system. A typical procedure is shown in Fig. 5-1. Loose material is removed from the cracks prior to injection. For the more usual case of epoxy injection, the surface trace of cracks is fully sealed with epoxy paste, leaving only surface-mounted plastic ports for the injection. The spacing of ports along the crack should be in the order of the distance that can be reached by the epoxy prior to hardening. (This distance depends on crack width and on the viscosity of the epoxy at the application temperature). In members thicker than this distance, ports at both surfaces should be provided along penetrating cracks.

The process comprises application of adhesive tapes across the crack at the intended locations of injection ports, staring from the bottom tip of the crack (b). A special sealing compound is then applied on top of the tape and the crack and this is left to set (c). The tape is then removed, thus exposing parts of the crack where injection nozzles are inserted and sealed (d). Thereafter, an epoxy mix is injected. Injection should start from the lowest level of the member where a crack appears; when the epoxy bleeds out from the next port, injection should stop and continue from the next port, after the previous port is sealed. Upon setting of the repair epoxy, the nozzles are bent and tied firmly. They can be cut flush and sealed with an epoxy patching compound prior to rendering of the affected member.

A similar procedure is used for cement grouts, except that injection pressure is lower by an order of magnitude.

The technique is widely used and is quite effective, provided that the travel path inside the crack is clear. It, however, requires specialist application and the materials used are rather expensive. The strength is usually reinstated, especially for under-reinforced members. The effect on stiffness is more uncertain. Injection has no effect on ductility of members failing in flexure.

5.3.3.2 Replacement of loose or spalled concrete

Loose concrete should be removed until sound concrete is reached. The concrete all around rebars which are exposed due to spalling or disintegration of concrete should be removed, until sufficient clearance is achieved for the repair mortar to surround the bar. Replacement material is normally an epoxy- or cement-based nonshrink grout mortar. For such repair materials, no epoxy-based bonding agent needs to be applied to the substrate.

Depending on the size and depth of spalling or of the loose concrete to be replaced, sand, pea-gravel or coarser aggregates may be used. The repair mortar is normally trowelled against the substrate or against the mortar placed in previous lifts. Formwork is normally not needed.

5.3.3.3 Replacement of rebars

If rebars have suffered significant buckling or fracture, a certain length of them has to be cut and replaced with a new piece of rebar, properly lap- or butt-welded to the two ends of the old bar.

Reference	Test	cyclic	h_w mm	L_s mm	b mm	h mm	d mm	$\rho_1=\rho_2$ %	ρ_v %	f_y MPa	f_{yv} MPa	ϕ_L mm	steel type	hoop legs	ϕ_h mm	s_h mm	f_{yw} MPa	f_c MPa	ν	θ_y %	θ_u %	M_y kNm	ϕ_y 1/m	ϕ_u 1/m
Kraetzig et al (1989)	S1.0S	No	1500	1500	300	300	260	0.670	0.440	514	514	16	2	2	8	80	514	88.0	0.00	1.30	4.4	93	-	-
Kraetzig et al (1989)	S2.0S	No	1500	1500	300	300	260	0.670	0.440	514	514	16	2	2	8	80	514	48.0	0.00	1.30	4.4	78	-	-
Kraetzig et al (1989)	S1.1S	Yes	1500	1500	300	300	260	0.670	0.440	514	514	16	2	2	8	80	514	88.0	0.00	1.80	5.8	97	-	-
Kraetzig et al (1989)	S1.2S	Yes	1500	1500	300	300	260	0.670	0.440	514	514	16	2	2	8	80	514	88.0	0.00	1.35	4.3	90	-	-
Kraetzig et al (1989)	S1.3S	Yes	1500	1500	300	300	260	0.670	0.440	514	514	16	2	2	8	80	514	60.0	0.00	1.40	3.3	98	-	-
Kraetzig et al (1989)	S1.6S	Yes	1500	1500	300	300	260	0.670	0.440	514	514	16	2	2	8	80	514	60.0	0.00	1.60	3.7	60	-	-
Kraetzig et al (1989)	S2.1S	Yes	1500	1500	300	300	260	0.670	0.440	514	514	16	2	2	8	80	514	48.0	0.00	1.35	4.4	82	-	-
Kraetzig et al (1989)	S2.2S	Yes	1500	1500	300	300	260	0.670	0.440	514	514	16	2	2	8	80	514	48.0	0.00	1.20	6.0	82	-	-
Kraetzig et al (1989)	S2.3S	Yes	1500	1500	300	300	260	0.670	0.440	514	514	16	2	2	8	80	514	60.0	0.00	1.30	3.7	68	-	-
Kraetzig et al (1989)	S3.2S	Yes	1500	1500	300	300	260	0.670	0.440	514	514	16	2	2	8	80	514	73.0	0.00	1.35	4.5	113	-	-
Kraetzig et al (1989)	S4.2S	Yes	1500	1500	300	300	260	0.670	0.440	514	514	16	2	2	8	80	514	75.0	0.00	1.30	4.4	102	-	-
Gomes, Appleton (1998)	P0R	Yes	1000	1000	200	200	180	0.565	0.000	480	0	12	1	2	6	150	480	74.0	0.05	0.85	6.8	30	0.0300	-
Gomes, Appleton (1998)	P1R	Yes	1000	1000	200	200	180	0.565	0.000	480	0	12	1	2	6	75	480	49.6	0.07	0.88	7.0	30	0.0300	-
Tasai (1992)	RFR15-1	Yes	750	375	250	250	220	0.640	0.000	324	0	13	2	2	6	150	324	77.8	0.20	0.40	>3.3	38	-	-
Tasai (1992)	RFR15-2	Yes	750	375	250	250	220	0.640	0.000	324	0	13	2	2	6	150	324	28.9	0.20	0.66	3.3	58	-	-
Tasai (1992)	RFR25-1	Yes	1250	625	250	250	220	0.640	0.000	324	0	13	2	2	6	150	324	77.8	0.20	1.00	>5.0	47	-	-
Tasai (1992)	RFR25-2	Yes	1250	625	250	250	220	0.640	0.000	324	0	13	2	2	6	150	324	28.9	0.20	0.64	3.3	53	-	-
Tasai (1992)		Yes	1000	500	250	250	220	1.060	0.000	459	0	13	2	2	6	45	459	35.2	0.00	0.60	>4.0	63	-	-
Ilya, Bertero (1980)	$SW7R_1$-1	Yes	1181	6622	254	2388	2261	0.374	0.135	510	586	19	1	4	5	21	483	40.8	0.07	0.40	4.8	5360	-	-
Ilya, Bertero (1980)	$SW7R_1$-2	Yes	2096	6622	254	2388	2261	0.374	0.135	510	586	19	1	4	5	21	483	40.8	0.07	0.50	4.0	5500	-	-
Ilya, Bertero (1980)	$SW7R_1$-3	Yes	3010	6622	254	2388	2261	0.374	0.135	510	586	19	1	4	5	21	483	40.8	0.07	0.50	3.9	5500	-	-
Ilya, Bertero (1980)	$SW8R_1$-1	Yes	1181	6622	254	2388	2261	0.374	0.135	510	586	19	1	4	5	21	483	40.8	0.07	0.45	5.1	5900	-	-
Ilya, Bertero (1980)	$SW8R_1$-2	Yes	2096	6622	254	2388	2261	0.374	0.135	510	586	19	1	4	5	21	483	40.8	0.07	0.45	5.0	5900	-	-
Ilya, Bertero (1980)	$SW8R_1$-3	Yes	3010	6622	254	2388	2261	0.374	0.135	510	586	19	1	4	5	21	483	40.8	0.07	0.45	4.9	5900	-	-
Wang et al. (1975)	SW1R-1	Yes	1181	4386	254	2388	2261	0.374	0.260	501	507	19	1	4	5	21	571	22.6	0.12	0.52	1.1	3728	0.0023	0.006
Wang et al. (1975)	SW1R-2	Yes	2096	4386	254	2388	2261	0.374	0.260	501	507	19	1	4	5	21	571	36.5	0.07	0.76	1.1	3728	0.0023	0.005
Wang et al. (1975)	SW1R-3	Yes	3010	4386	254	2388	2261	0.374	0.260	501	507	19	1	4	5	21	571	36.5	0.07	0.89	1.2	3728	0.0033	0.006
Wang et al. (1975)	SW2R-1	No	1181	4408	254	2388	2261	0.374	0.260	501	507	19	1	4	5	21	571	33.1	0.08	1.00	3.1	4473	0.0022	0.016
Wang et al. (1975)	SW2R-2	No	2096	4408	254	2388	2261	0.374	0.260	501	507	19	1	4	5	21	571	37.1	0.07	1.23	3.0	4473	0.0035	0.015
Wang et al. (1975)	SW2R-3	No	3010	4408	254	2388	2261	0.374	0.260	501	507	19	1	4	5	21	571	37.1	0.07	1.23	2.8	4473	0.0060	0.013
Fiorato et al (1983)	B5R	Yes	4572	4572	305	1905	1753	0.585	0.097	444	444	19	1	4	6	34	502	42.8	0.00	1.16	3.2	2847	-	-
Fiorato et al (1983)	B9R	Yes	4572	4572	305	1905	1753	0.585	0.097	429	429	19	1	4	6	34	462	51.8	0.00	1.00	3.9	3660	-	-
Fiorato et al (1983)	B11R	Yes	4572	4572	305	1905	1753	0.585	0.097	435	435	19	1	4	6	34	518	42.6	0.00	0.94	3.5	2908	-	-

Table 5-1: List of repaired and tested specimens (the first 18 are columns, the last 15 are walls)

Copyright fib, all rights reserved. This PDF copy of fib Bulletin 24 is intended for use and/or distribution only by National Member Groups of fib.

Copyright fib, all rights reserved. This PDF copy of fib Bulletin 24 is intended for use and/or distribution only by National Member Groups of fib.

5.3.3.4 Strength and deformations of repaired members

There are few cyclic test data in the literature on concrete specimens repaired and retested without strengthening, other than replacement of the crushed concrete with epoxy mortar, non-shrink concrete, fibre-reinforced concrete, etc. These materials typically have higher strength f_c than the original specimen.

These tests, summarized in Table 5-1, are the following:

1) 11 tests on simple cantilever columns by Krätzig et al (1989).
2) Two tests on simple cantilever columns by Gomes and Appleton (1998).
3) Five tests on double-ended cantilever columns by Tasai (1992).
4) Three tests on large cantilever shear walls by Fiorato et al (1983).
5) Four tests at UC Berkeley (Iliya and Bertero 1980 and Wang et al 1975) on three-storey shear walls. (Separate measurement are presented for the three storeys in the four wall tests, so each test is considered to give data for three test cases).

Eqs. (5-2) to (5-26) were applied to the 33 test cases for repaired specimens, considering them as monolithic and adopting the (normally higher) value of f_c of the repair concrete for the entire specimen. So this is the value of f_c given in Table 5-1.

All test cases provide data for the chord rotation and the moment at yielding, θ_y and M_y, and for the maximum chord rotation attained during the test. Except in three tests by Tasai (1992), failure was reached and the value of θ given in Table 5-1 is the ultimate chord rotation θ_u. The wall tests by Wang et al (1975) provide also curvature values at yield and ultimate, ϕ_y and ϕ_u respectively.

The conclusions of the comparison are summarized in Table 5-2; they are the following:

1) If monolithic behaviour of the repaired specimen is assumed, the yield moment and chord rotation, M_y and θ_y, are underpredicted by about 5% and 15% respectively, giving about 10% higher effective stiffness. Therefore for repaired columns the modification factors to be applied on M_y and θ_y in Eq. (5-27), (5-28) are k_m=1.05 (or practically 1.0) and k_y=1.15.

2) The ultimate chord rotation θ_u may be taken as 85% of that predicted assuming monolithic behaviour, according to Eqs. (5-9) or (5-11) ($k_u \approx 0.85$ in Eq. (5-29)). For one of the three specimens that did not fail, the empirical expressions, Eqs. (5-9), (5-11), were at the margin of failure, while the more rational alternative, Eq. (5-12)-(5-26), gave a small margin against failure. For the other two specimens the empirical expressions gave failure at a chord rotation somehow less than the value safely attained, whereas the more rational alternative predicted failure at a much lower chord rotation.

Quantity	No. of data	Mean	Median	Coef. of variation (%)
$M_{y,exp}/M_{y,pred.eq(5-8)}$	33	1.04	1.05	24
$\theta_{y,exp}/\theta_{y,pred.eq(5-2)}$	33	1.34	1.13	41
$(M_{y,exp}L_s/3\theta_{y,exp.})/(M_{y,pred.}L_s/3\theta_{y,pred.})$	33	0.89	0.88	41
$\theta_{u,exp}/\theta_{u,pred.eq(5-9)}$	30	0.95	0.87	45
$\theta_{u,exp}/\theta_{u,pred.eq(5-11)}$	30	0.91	0.83	44
$\theta_{u,exp}/\theta_{u,pred.eq(5-12)-(5-26)}$	30	1.34	0.97	74

Table 5-2: Mean, median and coef. of variation of ratio of experimental to-predicted quantities, assuming monolithic member. Repaired specimens

5.3.4 Concrete jackets

5.3.4.1 Introduction

Owing to their cost-effectiveness, concrete jackets have been, over the past two to three decades, by far the most widely-used technique for seismic upgrading of existing concrete members. This cost-effectiveness is due to several reasons:

- The familiarity of engineers and of the construction industry alike with the field application of structural concrete: It is emphasized that retrofitting, especially when it refers to modification of existing components, does not lend itself to even partial prefabrication in shop; it is reminded in this connection that reinforced concrete is the prime structural material for field fabrication and application.

Copyright fib, all rights reserved. This PDF copy of fib Bulletin 24 is intended for use and/or distribution only by National Member Groups of fib.

- The suitability of concrete jacketing for simultaneous repair of serious seismic damage, involving local or more extensive concrete crushing, or even buckling of bars and fracture of stirrups; the reasons being that: a) replacement of the crushed concrete is done in the same operation as casting or shotcreting of the jacket and b) full restoration of buckled or fractured bars may not be absolutely necessary, if such reinforcement is replaced by the new reinforcement of the jacket. The importance of this factor was even larger in the past, as only recent years have seen seismic retrofitting projects not been triggered by seismic damage.
- The versatility of reinforced concrete and its ability to adopt to almost any desired shape, including that needed in order to fully encapsulate existing concrete members and joints and provide structural continuity between different components (e.g., between a joint and the adjoining members, or between members in adjacent storeys).
- The ability of a concrete jacket to have, through the appropriate reinforcement, multiple effects: such a jacket is the only means to enhance at the same time: a) the stiffness of a member, b) its flexural resistance, c) its shear strength, d) its deformation capacity, and e) the anchorage and continuity of reinforcement in anchorage or splicing zones. The first two effects are due to the increased cross-sectional dimensions and the added longitudinal reinforcement, which – most importantly and unlike other retrofit techniques of individual members – can easily extend beyond the member end into and through joint regions. For the other three effects, although the added concrete is also a factor, the main contributor is the added transverse reinforcement (acting both against shear and as confining and antibuckling reinforcement).

From the technical point of view the multiple effectiveness of concrete jackets is what mainly differentiates them from the other techniques of seismic retrofitting individual concrete members, which, in principle, cannot readily extend beyond the member end and into joint regions. For this reason, other techniques are used mainly to enhance some or all of the properties listed under (a) and (c) to (e) in 1) above, but normally not the flexural strength (item (b) above).

Concrete jackets have certain drawbacks in comparison to other member retrofit techniques: 1) They considerably increase member cross sectional dimensions, which may be a serious drawback in the case of columns or walls in buildings where floor area is at a premium. 2) They are worse than any other technique as far as magnitude and length of disruption of occupancy, production of dust and debris (especially if shotcrete is used instead of cast-in-situ concrete), noise pollution and health and safety of workers are concerned. As there is a tendency for increasing importance of all these factors or issues where concrete jackets are at disadvantage relative to competing techniques, described also in the following, the balance may soon turn against concrete jackets, despite their present and future advantage in direct construction costs.

5.3.4.2 Configuration, detailing and construction of concrete jackets

Jacketing of columns and walls is typically done with an overlay of cast-in-situ concrete or of shotcrete. The jacket can accommodate longitudinal and transverse reinforcement to increase the member flexural and shear strength, enhance the deformation capacity (through confinement and antibuckling action) and improve the strength of deficient lap splices. Concrete jacketing of columns for increased flexural strength is a convenient and common means for conversion of weak-column/strong-beam frames into strong-column/weak-beam ones.

For the increase of flexural strength, longitudinal reinforcement should be continued to the storeys above and below, through holes or slots in the slab. To avoid perforating the beams on all sides of the cross-section into which a beam frames into the column jacket, reinforcement continued through the slab needs to be concentrated near the corners of the new section, often in bundles. (To avoid bond problems, bundling of bars concentrated near the corners of the jacket should be avoided, if feasible). Anchorage into a footing or foundation element of jacket longitudinal reinforcement intended for increased column flexural capacity may be achieved either: a) by increasing the size of the footing or foundation element to accommodate anchorage of the jacket bars (possibly increasing at the same time capacity of the footing or foundation element to meet the increased demands from the jacketed column), or b) by fastening (e.g. through adhesives) starter bars in vertical holes drilled in the footing and lap-

Copyright fib, all rights reserved. This PDF copy of fib Bulletin 24 is intended for use and/or distribution only by National Member Groups of fib.

splicing to them the jacket vertical reinforcement outside the plastic hinge region at the bottom of the retrofitted column.

In order to provide adequate cover of the new reinforcement and to allow placement of the ties, the concrete overlay should be at least 75mm to 100mm. For this range of thickness shotcrete is most convenient. Thicker overlays will have to be cast-in-place and formwork is needed for the construction of the jacket. Then the concrete is cast from the top, through holes and slots in the slab.

A closed perimeter tie is placed around the longitudinal bars of the jacket, to provide shear strength, restraint of longitudinal bars against buckling and concrete confinement. To avoid drilling holes and threading cross-links through the core of the old column, the perimeter tie is normally supplemented at most with an octagonal closed tie outside the old column, providing antibuckling restraint to longitudinal bars which are close to, but not exactly at the corner. An octagonal tie may be replaced by short corner ties at 45° to the perimeter, engaging in 90°-135° hooks the two bars adjacent to the corner bar. A diamond-shaped tie can be placed only if the size of the enlarged column is at least twice that of the old one and is unnecessary if the jacket does not have mid-side bars to be restrained. To facilitate placement, closed ties may come in two pieces (two L-shaped ones, or a U-shaped piece and a straight one), with some hooks bent to 135° in shop and others in situ after placement (see Fig. 5-2 for examples). Tie hooks around bundled bars are more difficult to construct and normally have a larger diameter bent to accommodate the bundled bars.

If the jacket does not surround the old column (one-, two-, or three-sided jackets), the reinforcement of the existing column will have to be exposed and the added ties of the jacket may be welded on the old ties, or bent around the old vertical bars.

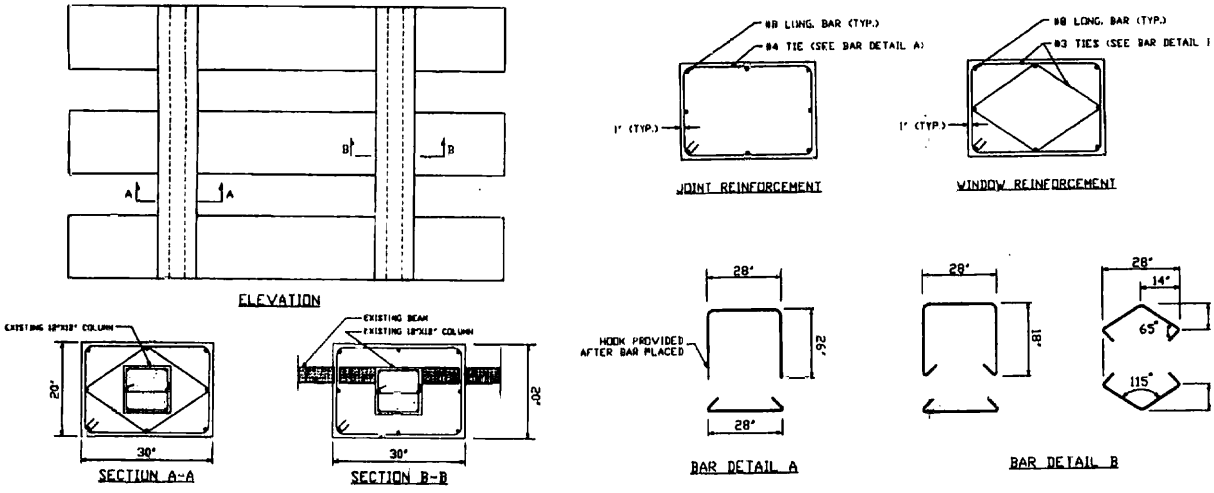

Fig. 5-2: Jackets constructed around columns in 2:3 scale 2-storey, 1-bay test frame by Stoppenhagen et al (1995).

The jacket should extend into the beam-column joint region, with ties placed there through horizontal holes drilled in the beams. (Drilling of beams is not an easy task and requires locating their reinforcement). If beams frame into up to three faces of the joint, the ties may come in two pieces: a U-shaped piece and a straight one. The two pieces may be lap-welded after they are put in place and the two ends of one of the pieces bent by 90°. Alternatively, the ends of the straight piece may be bent in shop at 135° and those of the U-shaped one in situ (Fig. 5-2). Ties to be placed around joints with beams framing on all four sides may need to come either in four straight pieces with one end bent to 135° in the shop and the other in situ after placement, or in four L-shaped pieces with their ends lap-welded after placement through the holes drilled in the beams. It should be reminded at this point that past experience has shown that interior joints with all four faces confined by beams of width not much less than the side of the column, are much less vulnerable than exterior joints, even when they are unreinforced. So the labourious task of placing ties in such joints is not essential. It is worth mentioning that, in order to avoid placing new ties through the beams, Alcocer 1992 and Alcocer and Jirsa 1993 constructed a steel cage around the joint, consisting of four heavy steel angles at the corners of the jacketed column, welded to two horizontal collars, one at the top

Copyright fib, all rights reserved. This PDF copy of fib Bulletin 24 is intended for use and/or distribution only by National Member Groups of fib.

surface of the slab and the other right beneath the soffit of the beams framing, into the joint. The four angles were dimensioned to provide, through their flexural stiffness, a joint confinement equivalent to that of the ties that should had been placed through the joint. This alternative is consistent with the ACI-318 concept of joint ties as a means of confining the joint core and not as joint horizontal shear reinforcement. It is noteworthy that, although thejacketed 3D beam-column subassemblages tested by Alcocer 1992, Alcocer and Jirsa 1993 developed their ultimate strength by joint shear failure, the steel cage proved effective in confining the joint core and preventing it from disintegrating and losing resistance, even at storey drifts of 4%.Guidance documents for the construction of concrete jackets – and construction practice alike – provide for measures assuring the shear connection of the old and the new concrete at their interface. The most commonly recommended and followed measure is the intermittent lap-welding of the (corner) bars of the jacket to the (exposed for this purpose) longitudinal bars of the old column through Z- or U-shaped steel inserts (see Fig. 5-3 for the steps involved in the implementation of this measure and for application examples). It should be emphasized that positive connection of steels of different grades (and hence of different chemical composition) promotes their corrosion. Therefore, such connection of the old and new longitudinal bars through welding to intermediate pieces of steel should be avoided.

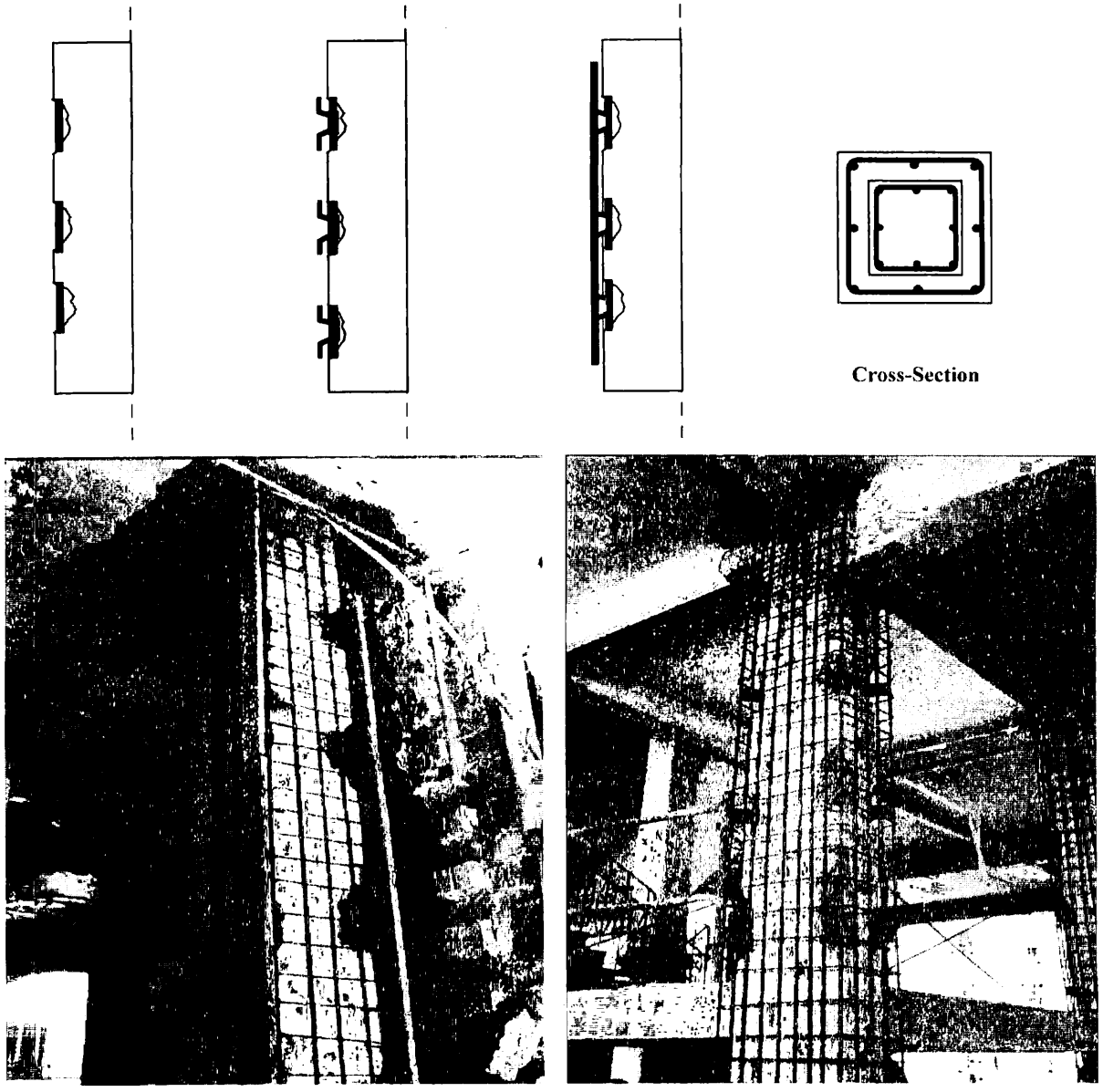

Fig. 5-3: Concrete jackets with U-shaped rebars or steel plates welded to old and new corner bars for shear connection

Copyright fib, all rights reserved. This PDF copy of fib Bulletin 24 is intended for use and/or distribution only by National Member Groups of fib.

An alternative measure includes roughening of the surface of the old element and provision of dowels over this surface, at a spacing in the order of 0.5m. Dowels are epoxy-grouted in holes drilled in the old element and protrude into the overlay of new concrete for almost its full thickness. As this thickness is usually small, to improve the anchorage of the dowel into the new concrete its end is often bent into a 90°-hook. There is some experimental evidence that dowels or steel inserts in the plastic hinge region may precipitate disintegration of the concrete of the overlay around them.

The recommended and commonly applied provision of either welded steel inserts between the new and old corner bars or epoxy-grouted dowels originates from concerns of the '70s or '80s about the participation of the jacket concrete in carrying the column axial force due to gravity loads. The original intent was to transfer part of this load from the old column to the jacket, through shear forces in the welded steel inserts and in the dowels. The concern about gravity load capacity was certainly motivated by the fact that in the past concrete jackets were applied mainly – if not exclusively – to heavily damaged columns, often with partly disintegrated core. The concern about sharing column axial load between the jacket and the old column is also reflected in past recommendations to use props, wedges and even jacks under the beams framing into the column, in order to unload it as much as possible prior to jacketingFor undamaged or moderately damaged columns the above concerns about sharing the axial load are not warranted. Moreover, recent experimental evidence (Elwood and Moehle, 2001) has demonstrated that concrete columns subjected to large post-ultimate drifts that cause heavy damage in the concrete core retain a large part of their gravity load capacity. So, given the collateral negative effects of the afore-mentioned devices for shear connection (potential triggering of rebar corrosion by the welded steel inserts, early localisation of concrete damage around such inserts or dowels) and the additional cost and time requirements of these measures, it seems both prudent and cost-effective not to employ such devices and rely only on friction for the transfer of shear at the interface. Friction is assisted by the compression stress developing at the interface, because the old member restrains the shrinkage of the concrete overlay in the radial and circumferential directions. (Restraint of jacket shrinkage induces compressive stresses in the radial direction in both the old and the new concrete and in the circumferential direction in the old member, plus tensile stresses in the circumferential direction in the jacket and its circumferential tie; this amounts to additional confinement of the old element, even prior to any lateral loads and deflections).

Friction is enhanced if the interface is rough, but is not clear that the time-consuming and costly artificial roughening of this interface is essential. The 2:3 scale two-storey, one-bay frame of Fig. 5-2 by Stoppenhagen et al (1995), in which sizeable concrete jackets were constructed around the heavily damaged columns of the original test frame with the interface just roughened, sustained storey drifts of 1.25% (which, if they are due to the columns alone, are translated to a drift ratio of the clear column length of over 4%) without loss of lateral force resistance of the columns and with apparent monolithic behaviour of the jacketed column. Similarly, monolithic behaviour of the jacketed columns and beams was apparently achieved in the 3D subassemblages of Alcocer 1992 and Alcocer and Jirsa 1993, even though no positive measures were taken to improve the shear capacity of the interface.

More experimental work is needed to clarify this issue. If indeed shrinkage of the concrete of the overlay results in confinement of the old member and enhances friction at the interface, then the more expensive and difficult to apply nonshrink mortars should not be used instead of conventional cast-in-situ concrete or shotcrete for the overlay.

If the aim of the concrete jacket is limited to increasing shear strength and deformation capacity of the member (the latter through the confinement and the antibuckling action developed on the old member) and to remedy deficiencies in lap splices without any increase in flexural strength, then the jacket does not need to continue through the slab into the next storey. The necessary magnitude of the gap between the jacket and the face of the joint or the slab in that case, remains a controversial issue. A large gap (in the order of 50 mm) is often advocated there, to avoid: a) increasing indirectly the flexural capacity of the member and hence the shear force demands in the member and in the joint; and b) concentration of flexural deformation demands in a very small length of the member, in the order of a few mm. Regarding the second issue, test results on members with a concrete-, steel- or FRP-jacket which stops almost at the face of the joint do not point to any negative effects of this plane or zone of weakness on deformation capacity of the retrofitted member. It seems that a gap of a few mm there acts just as a pre-existing large crack, while the concrete of the compression

Copyright fib, all rights reserved. This PDF copy of fib Bulletin 24 is intended for use and/or distribution only by National Member Groups of fib.

zone within this gap is effectively confined by the adjacent concrete beyond the length of the gap. Anyway, FRP- or steel-jackets, to be covered in following sections, lend themselves better than concrete jackets for shear strengthening and enhancement of deformation capacity without flexural strengthening.

Confined boundary elements are created in old shear walls by adding jackets to the ends of the wall section. Hoops of such a concrete jacket come in two pieces: one straight piece, driven through a hole drilled in the web, and a U-shaped piece placed around the edge of the wall and lap-welded to the other piece. Additional shear strength is provided by a concrete overlay of the web with horizontal and vertical bars.

5.3.4.3 Strength, stiffness and deformation capacity of members with concrete jackets

Complete information on concrete members strengthened with concrete jackets and tested under monotonic or axial load was found for only 15 tests:

1) Three double-ended short columns by Bett et al (1988), strengthened (mainly in shear) through a 66mm-thick shotcrete jacket. Longitudinal bars of the jacket were not connected to the footing of the column and hence did not contribute to its flexural strength. The interface of the old and new concrete was mechanically roughened, and in two of the three specimens was provided with cross-ties of 9.5mm diameter at 228mm centers at column mid-side through holes drilled in the old column. The cross-ties acted also as dowels at a cross-sectional area ratio of 0.1% with respect to the interface.
2) Four double cantilever columns by Rodriguez and Park (1994), with a 75mm-thick cast-in-place jacket, the longitudinal bars of which were anchored into the base of the specimen, contributing to flexural strength enhancement. The interface between the old and the new concrete was roughened, but not crossed by dowels.
3) Two tests on simple cantilever columns by Gomez and Appleton (1998), strengthened with a 30mm-thick jacket, with longitudinal bars extending into the base for anchorage by 20 bar diameters and with the old-to-new concrete interface just roughened.
4) Three column specimens by Ersoy et al (1993), subjected to eccentric compression without transverse load. The vertical reinforcement of the 35mm-thick jacket was well anchored into the base and was also welded to the corner bars of the old column through Z-shaped rebar pieces, supplementing the shear connection provided by roughening of the interface.
5) One test by Yamamoto (1992) on a double cantilever column strengthened with a 30mm-thick jacket. Longitudinal bars of the jacket were well anchored into the base, but special provisions for roughening the interface with the old concrete were not taken.
6) Two three-storey tall walls with rectangular cross-section and bar bells at the two ends by Iliya and Bertero (1980). In the first storey web thickness was doubled from 102mm to 204mm with cast-in-situ concrete and well-anchored vertical reinforcement was added to the barbells.

The results of these tests were analysed under the following assumptions:

a) The member was considered as monolithic, with full composite action between old and new concrete.
b) The concrete strength of the new (jacket) concrete was considered to apply over the full section of the member, including the base within which the longitudinal bars, new or old, are anchored. This assumption is considered reasonable even under field conditions, as the compressive zone of the composite member, as well as anchorage of the new bars, are controlled by the new concrete.
c) The longitudinal reinforcement of the jacket (if anchored into the base) was considered as top and bottom reinforcement of the section (i.e. for the calculation of the tension and compression steel ratios, $\rho_1=\rho_2$ and of the fixed-end rotation due to bar slippage in the anchorage zone), the reinforcement of the old column was considered as vertical web reinforcement and assumed as uniformly distributed between the top and bottom reinforcement of the section (although generally it was not). The new longitudinal reinforcement which did not extend into the base for anchorage in the three tests by Bett el al (1988) was ignored and the effective depth d was measured to the old reinforcement.

The geometric and mechanical characteristics of the 15 specimens before and after strengthening are shown in Tables 5-3 and 5-4 respectively. Table 5-4 presents also the available test results of the strengthened specimens.

Reference	Test	h_w mm	L_s mm	b mm	h mm	d mm	$\rho_1=\rho_2$ %	ρ_v %	f_y MPa	f_{yv} MPa	ϕ_L mm	ϕ_h MPa	s_h mm	f_{yw} MPa	steel type	f_c MPa	tested before retrofit
Bett et al (1988)	1-2.	460	460	300	300	268	0.950	0.620	462	462	19	6	203	413	1	31	No
Bett et al (1988)	1-3.	460	460	300	300	268	0.950	0.620	462	462	19	6	203	413	1	31	No
Bett et al (1988)	1-1R	460	460	300	300	268	0.950	0.620	462	462	19	6	203	413	1	31	Yes
Rodriguez, Park (1994)	SS1	1425	1425	350	350	295	0.769	0.507	325	325	20	6	265	350	1	29.5	Yes
Rodriguez, Park (1994)	SS2	1425	1425	350	350	295	0.769	0.507	325	325	20	6	265	350	1	27.2	No
Rodriguez, Park (1994)	SS3	1425	1425	350	350	295	0.769	0.507	325	325	20	6	265	350	1	27.2	No
Rodriguez, Park (1994)	SS4	1425	1425	350	350	295	0.769	0.507	325	325	20	6	265	350	1	25.9	Yes
Gomez, Appleton (1998)	P2R	1000	1000	200	200	180	0.565	0	480	0	12	6	150	480	1	53.2	Yes
Gomez, Appleton (1998)	P3R	1000	1000	200	200	180	0.565	0	480	0	12	6	50	480	1	58.2	Yes
Ersoy et al (1993)	RBM	1000	1000	160	160	155	0.880	0	300	0	12	4	100	260	1	33.1	Yes
Ersoy et al (1993)	RBR	1000	1000	160	160	155	0.880	0	300	0	12	4	100	260	1	34.5	Yes
Ersoy et al (1993)	SBR	1000	1000	160	160	155	0.880	0	300	0	12	4	100	260	1	40.3	No
Yamamoto (1992)	No.5	500	500	250	250	235	0.610	0	358	0	13	4	125	439	1	21.1	No
Iliya, Bertero (1980)	SW7R2	1181	6622	254	2388	2261	0.380	0.135	510	482	19	6	152	582	1	40.8	Yes
Iliya, Bertero (1980)	SW8R2	1181	6622	254	2388	2261	0.380	0.135	510	482	19	6	152	582	1	40.8	Yes

Table 5-3: Concrete jacket tests – Original specimens (last two: walls; rest: columns)

Copyright fib, all rights reserved. This PDF copy of fib Bulletin 24 is intended for use and/or distribution only by National Member Groups of fib.

Reference	test	cyclic	h_w mm	L_s mm	b mm	h mm	d mm	$\rho_1=\rho_2$ %	ρ_v %	f_y MPa	f_{yv} MPa	ϕ_L mm	steel type	hoop legs	ϕ_h mm	s_h mm	f_{yw} MPa	f_c MPa	ν	θ_y %	θ_u %	M_y kNm	ϕ_y 1/m	ϕ_u 1/m
Bett et al (1988)	1-2.	No	460	460	432	432	334	0.036	0.300	462	462	19	1	2	6	63	462	32.3	0.05	1.00	>2.5	153	-	-
Bett et al (1988)	1-3.	No	460	460	432	432	334	0.105	0.300	462	462	19	1	2	6	63	462	32.3	0.05	0.90	>2.3	147	-	-
Bett et al (1988)	1-1R	Yes	460	460	432	432	334	0.105	0.300	462	462	19	1	2	6	63	462	32.3	0.05	1.25	>2.6	143	-	-
Rodriguez, Park (1994)	SS1	Yes	1425	1425	550	550	512	0.260	0.830	502	325	16	1	2	10	95	340	32.9	0.10	0.60	3.6	428	-	-
Rodriguez, Park (1994)	SS2	Yes	1425	1425	550	550	512	0.260	0.830	502	325	16	1	2	10	95	340	34.0	0.10	0.60	3.1	498	-	-
Rodriguez, Park (1994)	SS3	Yes	1425	1425	550	550	503	0.150	0.980	491	369	12	1	4	10	72	330	19.4	0.10	0.50	2.8	400	-	-
Rodriguez, Park (1994)	SS4	Yes	1425	1425	550	550	503	0.150	0.980	491	369	12	1	4	10	72	330	25.2	0.10	0.70	2.8	342	-	-
Gomez, Appleton (1998)	P2R	Yes	1000	1000	260	260	240	0.330	0.670	480	480	12	1	2	6	75	480	58.2	0.18	0.70	5.1	63	-	-
Gomez, Appleton (1998)	P3R	Yes	1000	1000	260	260	240	0.330	0.670	480	480	12	1	2	6	50	480	49.6	0.18	0.80	6.8	68	-	-
Ersoy et al (1993)	RBM	Yes	1000	1000	230	230	226	0.430	0.850	300	300	12	1	2	8	100	260	30.6	0.35	-	-	58	0.021	0.1340
Ersoy et al (1993)	RBR	Yes	1000	1000	230	230	226	0.430	0.850	300	300	12	1	2	8	100	260	30.7	0.35	-	-	56	0.020	0.0920
Ersoy et al (1993)	SBR	Yes	1000	1000	230	230	226	0.430	0.850	300	300	12	1	2	8	100	260	33.0	0.35	-	-	67	0.022	0.0610
Yamamoto 1992	No.5	Yes	500	500	310	310	265	0.390	0.800	358	358	13	1	2	4	50	447	27.6	0.14	0.75	>8	54	-	-
Iliya, Bertero (1980)	SW7R2	Yes	1181	6622	2388	254	2261	0.590	0.270	510	482	21	1	2	6	152	582	51.4	0.03	0.42	>.8	7250	-	-
Iliya, Bertero (1980)	SW8R2	Yes	1181	6622	2388	254	2261	0.590	0.270	510	482	21	1	2	6	21	582	49.6	0.03	0.25	1.0	7600	-	-

Table 5-4: Concrete jacket tests – Jacketed specimens (dimensions and reinforcement of jacketed member)

Copyright fib, all rights reserved. This PDF copy of fib Bulletin 24 is intended for use and/or distribution only by National Member Groups of fib.

Copyright fib, all rights reserved. This PDF copy of fib Bulletin 24 is intended for use and/or distribution only by National Member Groups of fib.

Quantity	No. of data	Mean	Median	Coef. of variation (%)
$M_{y,exp}/M_{y,pred.eq(5\text{-}8)}$	15	0.97	0.88	35
$\theta_{y,exp}/\theta_{y,pred.eq(5\text{-}2)}$	12	0.99	0.86	31
$(M_{y,exp}L_s/3\theta_{y,exp.})/(M_{y,pred.}L_s/3\theta_{y,pred.})$	12	1.02	0.99	29
$\theta_{u,exp}/\theta_{u,pred.eq(5\text{-}9)}$	6	1.08	1.00	32
$\theta_{u,exp}/\theta_{u,pred.eq(5\text{-}12)\text{-}(5\text{-}26)}$	6	1.02	0.95	55

Table 5-5: Mean, median and coefficient of variation of ratio of experimental-to-predicted quantities, assuming monolithic member. Jacketed specimens.

All 15 specimens provide values of the yield moment, M_y, but only 12 of them gave also values of the chord rotation at yielding, θ_y, as the 3 specimens by Ersoy et al (1993) were tested under pure bending with axial force and gave only curvature data (at yielding and ultimate). Only 6 of these 12 specimens reached failure: the tests by Bett et al (1988) and by Yamamoto (1992) did not reach failure, while in the two shear walls failure took place in the two upper unstrengthened storeys.

Table 5-5 compares the experimental results with the predictions of the expressions quoted in 2.2.1 for monolithic members. Equation numbers in Table 5-5 refer to that part of the report.

The comparison leads to the following conclusions:

- When the simplifying assumptions (a) to (c) above are made, the strength and the deformations of the jacketed member at yielding is overestimated by the models applying for monolithic members by about 10%. Compared to that of the large database of monolithic elements, the scatter of the prediction is higher for the yield moment M_y, but lower for the yield chord rotation and the effective stiffness at yielding ($M_yL_s/3\theta_y$). Therefore the yield moment and chord rotation of the jacketed member may be estimated by applying modification factors k_m=0.9 and k_y=0.9 in Eqs. (5-27), (5-28) on the values of M_y and θ_y estimated from Eqs. (5-2) and (5-8) for monolithic members, assuming that the entire column has the concrete strength of the jacket and that the vertical bars of the old column work as if they were uniformly-distributed intermediate vertical reinforcement. This gives an effective stiffness of the jacketed column equal to that of the monolithic member. It should be noted that if the vertical bars of the old column are neglected, the yield chord rotation θ_y will not change much, but the yield moment M_y and the effective stiffness will be underpredicted by about 10% and 20%, respectively. Moreover, this assumption has adverse effects on the prediction of ultimate deformation, θ_u, so overall it is worse than the assumption of including the old bars as intermediate reinforcement of the column cross-section.
- The expressions developed for the ultimate chord rotation θ_u of monolithic members (Eqs. (5-9), (5-11), (5-12) to (5-26)) work on average well for jacketed columns considered as monolithic. The scatter of the prediction(s) is much smaller than that for the full database, but this is mainly due to the small present sample size. Although not shown in Table 5-5, for the three specimens by Bett et al (1988) which did not fail, the empirical expressions, Eqs. (5-9), (5-11) predict that they would have just failed, whereas the set of expressions, Eqs. (5-12)-(5-26), based on rational mechanics predict that they would have escaped failure with a slim margin. The overall conclusion is that all expressions developed for the value of ultimate chord rotation θ_u of monolithic members may be applied to jacketed members according to Eq. (5-29) with a modification factor k_u of about 1.0.

Strength and deformation capacities of jacketed members may be calculated neglecting the fact that the axial load due to gravity loads is originally applied on the old column alone and that the jacket is constructed without removing this axial load from the old column. This is a reasonable simplification, as after the column yields, it does not retain any memory about the original conditions of application of the axial load and the latter is carried by the compression zone, which normally lies within the jacket, as if it had been applied to the full column section from the beginning of loading.

It is worth mentioning again, in closing, the tests performed by Alcocer 1992 and Alcocer and Jirsa 1993, on four 2:3-scale 3D beam-column subassemblages retrofitted with column (and joint) jackets, or – in one test – with beam and column jackets. The retrofit subassemblages developed a cyclic lateral force resistance at storey drift of 4% between 3.5

Copyright fib, all rights reserved. This PDF copy of fib Bulletin 24 is intended for use and/or distribution only by National Member Groups of fib.

and 6 times that of the unretrofitted subassemblage. Beam hinging took place in the retrofitted specimens, with a large part of the slab (reinforcement) fully contributing to the tension flange of the beam. Joint shear was critical, but did not lead to a drop in resistance even under bi-directional load cycles. No bond problems were observed along the part of the beam or column bars through the joint, although its length was limited to 18 bar diameters (or 10 equivalent bar diameters for the bar bundles) and to 23 bar diameters in the beams.

5.3.4.4 Recommendations for dimensioning and verification of jacketed members in practical retrofit design

On the basis of the information presented above, the following recommendations may be made for dimensioning and verification of RC members (in particular columns or walls) retrofitted with concrete jackets, with longitudinal reinforcement fully anchored beyond the member end:

- The jacketed member may be considered as monolithic. A roughened interface is considered sufficient for full composite action between new and old concrete. For simplicity, concrete strength may be taken as that of the jacket; nonetheless, large differences in strength between the old and the new concrete should be avoided. The axial load may be considered to act on the full, composite section.
- The longitudinal reinforcement of the jacketed column is mainly that of the jacket; the existing longitudinal reinforcement in the old column should be considered at its actual location between the tension and compression reinforcement of the composite member (i.e. should be included in longitudinal reinforcement distributed in the "web"), taking into account appropriately any differences in yield strength. For walls, old reinforcement near the edges may be taken into account as reinforcement of the tension and compression flanges, as appropriate; old web reinforcement may be included in the web reinforcement of the composite member; in both cases differences in yield stress between new and old reinforcement should be appropriately taken into account.
- Only the transverse reinforcement in the jacket should be taken into account for confinement. For the calculation of shear resistance, the old transverse reinforcement may be considered only in walls, provided it is well anchored in the (new) boundary elements.
- The yield moment and the flexural capacity of the member should be taken as 90% of that of the monolithic member considered according to 1 and 2 above (k_m=0.9).
- The shear strength of the member may be taken equal to that of the monolithic member considered according to 1 to 3 above. It should exceed the shear force corresponding to development of the member flexural capacity, with adequate margin to take into account flexural overstrength due to steel strain hardening and concrete confinement (e.g. by 25%).
- Member deformations at flexural yielding (e.g. the chord rotation at yielding) may be taken as 90% of those of the monolithic member according to 1 to 3 above (k_y=0.9). This results in a member secant-to-yield stiffness equal to that of the monolithic member.
- Flexure-controlled ultimate deformations (e.g. the ultimate chord rotation, θ_u) may be taken equal to that of the monolithic member considered according to 1 to 3 above (k_u=1.0). This calculation should be based on the less ductile of the two types of longitudinal steel used in the composite member.
- At beam-column joints horizontal ties should be provided in the jacket at the appropriate amount and detailing, as required for the shear strength of the joint between the retrofitted column and the beam(s). Anchorage of beam and column (jacket) bars within that joint should satisfy the corresponding detailing rules for joints in new structures.
- Fulfillment of the strong-column weak-beam rule should be considered as appropriate, when selecting the dimensions and reinforcement of the column jacket.

5.3.5 Retrofitting using externally bonded Fibre Reinforced Polymers (FRP)

5.3.5.1 Introduction

Externally bonded (eb) fibre reinforced polymers (FRPs) in the form of continuous carbon (C), glass (G) or aramid (A) fibres bonded together in a matrix made of epoxy, vinylester or polyester, are being employed extensively throughout the world in retrofitting reinforced

Copyright fib, all rights reserved. This PDF copy of fib Bulletin 24 is intended for use and/or distribution only by National Member Groups of fib.

concrete structures. Early applications have been mainly for strengthening against non-seismic actions. Nonetheless, their high strength-to-weight ratio, immunity to corrosion and easy handling and installation are making FRP jackets the material of choice in an increasingly large number of seismic retrofitting projects, despite the relatively high material costs.

The literature on FRP-strengthened RC elements is vast: several journal or conference papers cover a variety of aspects on seismic retrofitting, the most important ones being shear strengthening and increase of confinement. The basic concepts involved in using FRPs as strengthening materials of concrete structures are covered in a review article of Triantafillou (1998a). Progress in various strengthening methods, questions associated with the long-term durability of FRP, as well as the development of design guidelines and codes for non-seismic applications were addressed in a review paper by Neale (2000). Presently the most comprehensive and up-to-date overview – albeit without emphasis on seismic retrofitting – is the one in (*fib*, 2001). A recent survey of the literature on seismic retrofitting with FRPs may be found in a review article by Triantafillou (2001).

Given that continuity and anchorage of FRPs in a joint beyond a member end is difficult to achieve, the main uses of FRPs in seismic retrofitting of existing RC elements are the following:

- The shear capacity of sub-standard elements (columns, shear walls, etc.) can be enhanced, by providing externally bonded FRPs with the fibres in the hoop direction.
- A ductile behaviour of flexural plastic hinges at beam or column ends can be achieved through added confinement in the form of FRP jackets, with the fibres placed along the beam or column perimeter.
- The flexural strength of RC columns can only be developed when debonding of the reinforcement in lap splices is prevented. Such debonding occurs once vertical cracks develop in the cover concrete and progresses with increased dilation and cover spalling. The associated rapid flexural strength degradation can be prevented or limited with increased lap confinement, again with fibres along the column perimeter.

This section focuses on the seismic retrofitting of RC members (mainly columns, but also beams, shear walls and beam-column joints) using FRPs. Following a brief review of key properties of FRP materials, some basic retrofitting issues (shear strengthening, increase of confinement) are summarised and a brief summary of application techniques is given. Next, more information on the behaviour and design of shear-strengthened or confined (with FRP) members is provided. Finally, a brief description of some recent developments related to seismic strengthening of beam-column joints is presented.

A presentation of the entire body of research and design issues in this field is not feasible within the scope of this section. The intent rather is to provide a representative overview, to underline the basis of design methods and to provide an extensive, but not exhaustive, bibliography on the subject.

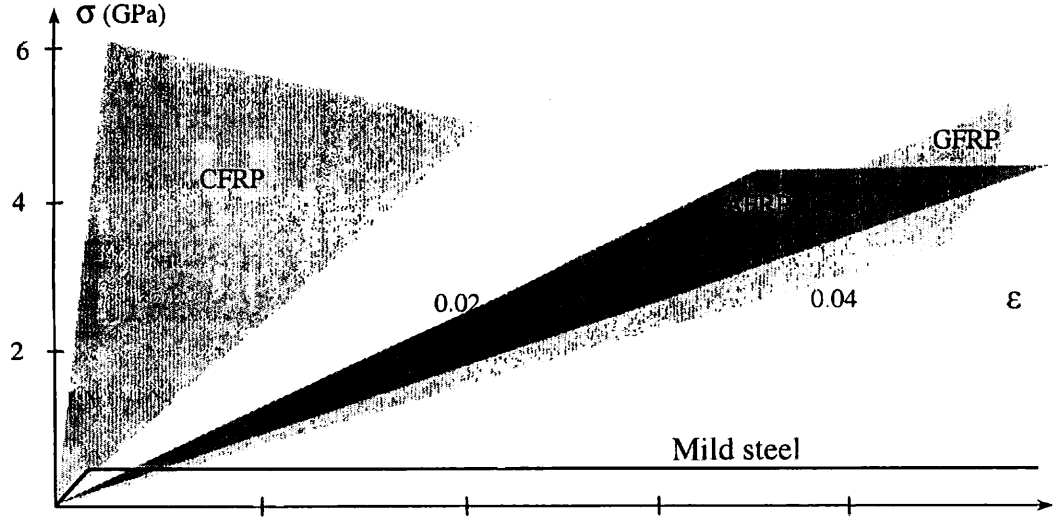

Fig. 5-4: Uniaxial tension stress-strain diagrams for different unidirectional FRPs and steel. CFRP = carbon FRP, AFRP = aramid FRP, GFRP = glass FRP (fib 2001).

Copyright fib, all rights reserved. This PDF copy of fib Bulletin 24 is intended for use and/or distribution only by National Member Groups of fib.

Material	Elastic modulus (GPa)	Tensile strength (MPa)	Ultimate tensile strain (%)
Carbon			
High strength	215-235	3500-4800	1.4-2.0
Ultra high strength	215-235	3500-6000	1.5-2.3
High modulus	350-500	2500-3100	0.5-0.9
Ultra high modulus	500-700	2100-2400	0.2-0.4
Glass			
E	70	1900-3000	3.0-4.5
S	85-90	3500-4800	4.5-5.5
Aramid			
Low modulus	70-80	3500-4100	4.3-5.0
High modulus	115-130	3500-4000	2.5-3.5

Table 5-6: Typical properties of fibres (fib 2001).

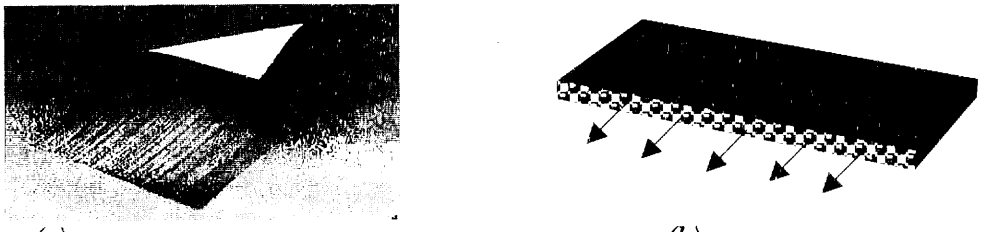

(a) *(b)*

Fig. 5-5: (a) FRP sheet made of unidirectional fibres. (b) Stresses carried by the fibres.

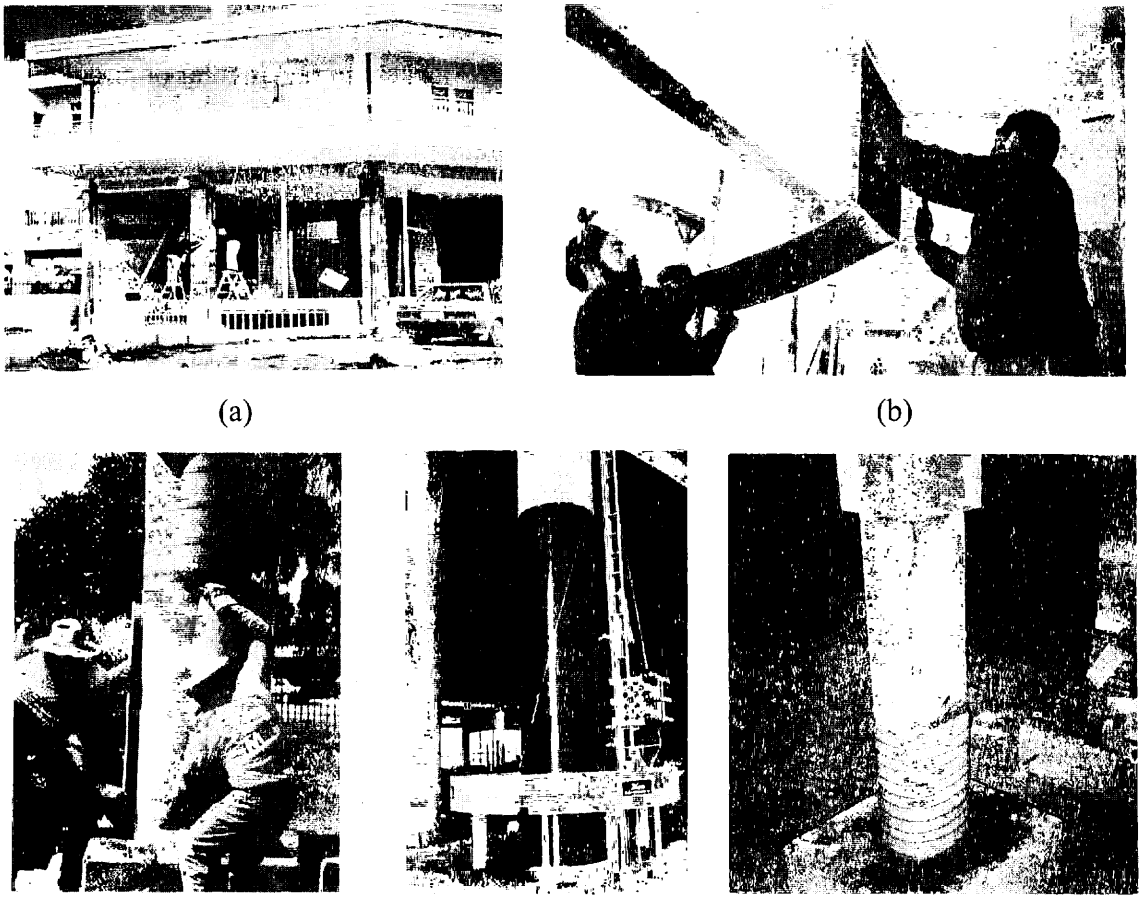

(a) (b)

(c) (d) (e)

Fig. 5-6: Retrofitting with: (a) and (b) FRP sheets; (c) prefabricated shells; (d) automated wrapping; (e) prestressed FRP jackets through the use of expansive mortar.

Copyright fib, all rights reserved. This PDF copy of fib Bulletin 24 is intended for use and/or distribution only by National Member Groups of fib.

5.3.5.2 Materials and their application

The combination of unidirectional fibres, which constitute the primary load-carrying elements, with a polymeric matrix results in a material that behaves as linear elastic to failure, without a yield plateau. Hence, a fairly complete characterization of this material is obtained by defining the elastic modulus and the tensile strength in the direction of the fibres (Fig. 5-5). Both parameters can be estimated by the so-called "rule of mixtures", which, for typical FRP materials, can be simplified as:

$$P_f \approx P_{fib} V_{fib} \tag{5-30}$$

where P_f = property of FRP (elastic modulus E_f or tensile strength f_{ft}), P_{fib} = corresponding property of fibres and V_{fib} = volume fraction of fibres in the FRP (in the order of 40-65%). A summary of basic mechanical properties for various types of fibres is given in Table 5-6 and, in a more schematic form, in Fig. 5-4 (*fib* 2001).FRP jackets may be applied either as *wet lay-up* systems (Fig. 5-6 a,b) or as *prefabricated* systems. Wet lay-up systems include: a) dry sheets or fabrics impregnated with resin in-situ, b) pre-impregnated sheets or fabrics or tows (untwisted bundles of continuous fibres) installed with or without additional resin and c) dry tows impregnated with resin during winding. Prefabricated systems are typically factory-made curved or shaped elements, or split shells that can be fitted around columns (Fig. 5-6c).

Techniques for seismic retrofitting with FRP comprise manual application of the aforementioned systems or automated wrapping of fibre tows (Fig. 5-6d), which may be either unstressed or prestressed during application. Another option to achieve prestressing is by filling prefabricated FRP jackets placed around RC members with expansive mortar or concrete (e.g. Saadatmanesh et al. 1997, Shimbo et al. 1997), see Fig. 5-6e.

5.3.5.3 Shear strengthening of RC components

(1) Beams, columns and walls

Shear capacity, a strength issue, can be added by FRP jackets to rectangular or circular RC columns or shear walls, in a way similar to adding shear strength through internal stirrup reinforcement.

A number of experimental studies have been carried out to investigate the shear strengthening of flexural members with FRP jackets. In these studies, various researchers have shown that the shear strength of RC members can be increased as the thickness of the jacket increases (e.g. Priestley and Seible 1995, Fujisaki et al. 1997, Masukawa et al. 1997, Sirbu et al. 1998, Matsuzaki et al. 2000). Typical lateral force-displacement curves for an as-built shear-critical and a companion retrofitted column are compared in Fig. 5-7 (Priestley and Seible, 1995), which demonstrates that brittle shear failure is suppressed and stable hysteretic behaviour may lead to high ductility levels.

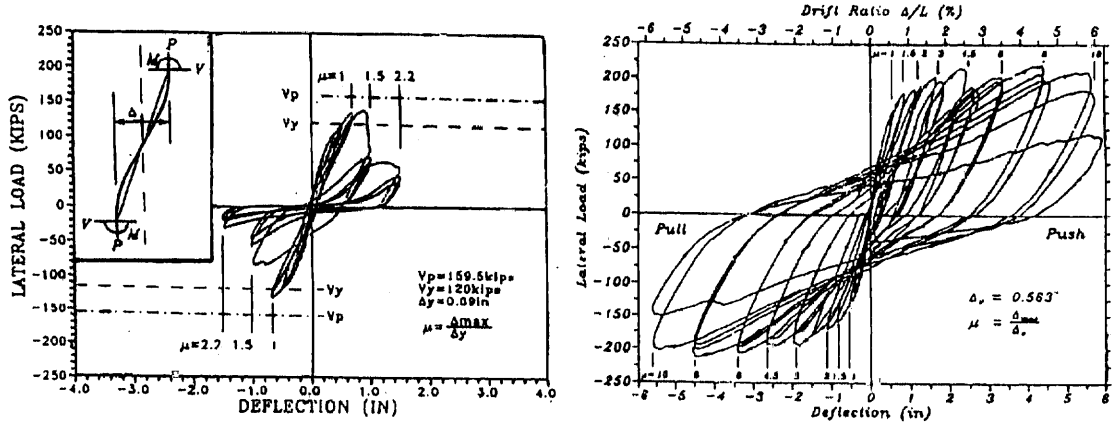

(a) (b)

Fig. 5-7: Lateral force-displacement response of shear-critical rectangular columns: (a) as-built; (b) retrofitted with GFRP jacket (Priestley and Seible 1995).

Copyright fib, all rights reserved. This PDF copy of fib Bulletin 24 is intended for use and/or distribution only by National Member Groups of fib.

Detailed investigations on shear strengthening of RC members have been relatively limited and, to a certain degree, controversial. Quite a few researchers have idealised the FRP materials in analogy with internal steel stirrups, assuming that the contribution of FRP to shear capacity (V_{fd}, in analogy to V_{wd}) emanates from the capacity of fibres to carry tensile stresses at a more or less constant strain, which is equal either to the FRP ultimate tensile strain, ε_{fu}, or to a reduced value. Priestley and Seible (1995) suggested that the FRP contribution to the shear capacity of columns be calculated by assuming an FRP strain equal to 0.004; Japanese researchers (e.g. JCI 1998) proposed a fixed fraction of ε_{fu}, which varied from 20% to 60% of ε_{fu} for AFRP (aramid FRP) and from 2/3 to 100% for CFRP (carbon FRP).

In more recent studies, Triantafillou (1998b) and Triantafillou and Antonopoulos (2000) introduced the concept of the effective strain, $\varepsilon_{f,e}$, defined as the strain in the FRP when the strengthened member reaches its shear capacity, and demonstrated that this strain depends on a number of factors, including: (a) the FRP failure mode, which may be characterized by tensile fracture or by debonding, depending on the type of jacket (closed jackets and low elongation capacity fibres are more likely to fracture than to debond, compared with partially wrapped open jackets and high strain capacity fibres); (b) the axial rigidity of the jacket along the perimetre, $E_f t_f$, where E_f = elastic modulus of FRP and t_f = thickness of jacket ($\varepsilon_{f,e}$ decreases as $E_f t_f$ increases); and (c) the strength of concrete ($\varepsilon_{f,e}$ increases with the tensile strength of concrete).

In design format, the following equations may be adopted:

$$V_{fd} = 0.9\varepsilon_{fd,e} E_f \rho_f b_w d(\cot\theta + \cot\alpha)\sin\alpha \tag{5-31}$$

where: $\varepsilon_{fd,e}$ = design value of effective FRP strain; b_w = minimum width of cross section over the effective depth; d =effective depth of cross section; ρ_f = FRP reinforcement ratio equal to $2t_f \sin\alpha / b_w$ for continuously bonded shear reinforcement of thickness t_f (b_w = minimum width of the concrete cross section over the effective depth), or to $(2t_f/b_w)(b_f/s_f)$ for FRP reinforcement in the form of strips or sheets of width b_f at a spacing s_f (Fig. 5-8); E_f = elastic modulus of FRP in the principal fibre orientation; θ = angle of diagonal crack with respect to the member axis; and α = angle between principal fibre orientation and longitudinal axis of member (Fig. 5-8).

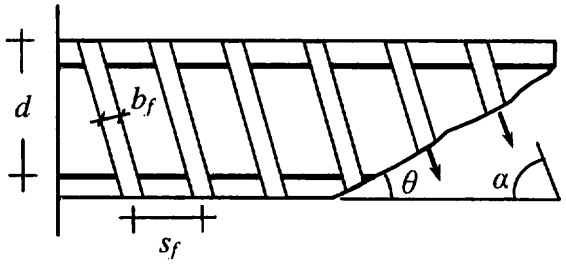

Fig. 5-8: Orientation of FRP strips and definition of dimensions.

The design value of the effective FRP strain, $\varepsilon_{fd,e}$, may be obtained in terms of the characteristic value, $\varepsilon_{fk,e}$, which is related to the mean value $\varepsilon_{f,e}$ (see *fib*, 2001, for details). A synthesis and evaluation of the published experimental results on shear strengthening of RC members with FRP sheets or fabrics reported in the literature up to early 1999 resulted in the best fit power-type expressions given next (Triantafillou and Antonopoulos 2000). Adoption of these equations in cases other than the ones given below (e.g. for GFRP jackets) should be done with caution.

- Fully wrapped (i.e. closed) or properly anchored (in the compression zone) CFRP jackets (fracture of the jacket is dominant):

$$\varepsilon_{f,e} = 0.17\left(\frac{f_{cm}^{2/3}}{E_f \rho_f}\right)^{0.30} \varepsilon_{fu} \tag{5-32 a}$$

- Side or U-shaped (i.e. open) CFRP jackets (fracture of the jacket may be preceded by debonding):

Copyright fib, all rights reserved. This PDF copy of fib Bulletin 24 is intended for use and/or distribution only by National Member Groups of fib.

$$\varepsilon_{f,e} = \min\left[0.65\times10^{-3}\times\left(\frac{f_{cm}^{2/3}}{E_f\rho_f}\right)^{0.56}, 0.17\left(\frac{f_{cm}^{2/3}}{E_f\rho_f}\right)^{0.30}\varepsilon_{fu}\right] \quad (5\text{-}32\text{ b})$$

- Fully wrapped (i.e. closed) or properly anchored AFRP jackets (fracture of the jacket is dominant):

$$\varepsilon_{f,e} = 0.048\left(\frac{f_{cm}^{2/3}}{E_f\rho_f}\right)^{0.47}\varepsilon_{fu} \quad (5\text{-}32\text{ c})$$

In the above equations f_{cm} is in MPa and E_f is in GPa. Furthermore, $\varepsilon_{f,e}$ should be limited to a maximum value (ε_{max}) in the order of 0.006, to ensure that the shear integrity of concrete is maintained sufficiently, so that other mechanisms, such as aggregate interlock, may be activated too.

The above concept of non-constant effective FRP strain (but decreasing with increasing FRP stiffness or decreasing concrete strength) was adopted recently in design guidelines by both ACI (ACI-440 2001) and JSCE (2001), with slightly different formulation.

According to a less empirical approach, the design value of the effective FRP strain, $\varepsilon_{fd,e}$, can be related to the maximum FRP strain (design value) at the ultimate limit state in shear, $\varepsilon_{fd,max}$. Assuming that the FRP jacket is properly anchored (e.g. closed jackets) and a linearly increasing opening of the shear crack, this relationship is $\varepsilon_{fd,e} \approx 0.5\varepsilon_{fd,max}$, with $\varepsilon_{fd,max} = f_{jd}/E_f$, where f_{jd} = design tensile strength of FRP jacket and E_f = elastic modulus of jacket. Note that f_{jd} is, in general, less than the uniaxial tensile strength f_{fd}. This reduction is attributed to several reasons, including: (a) the multiaxial state of stress in the FRP (e.g. at corners of low radius); and (b) the quality of execution (potential local ineffectiveness of some fibres due to misalignment and overstressing of others; damaged fibres at sharp corners or local protrusions etc). In the case of open jackets (e.g. U-shaped) the tensile capacity of the FRP is typically not exhausted, due to debonding; this can be described by an appropriate bond stress-slip model. For instance, an appropriate modification of the model by Neubauer and Rostásy (1997) results in $\varepsilon_{fd,max}$ being approximately equal to $0.40(f_{ctm}/E_f t_f)^{1/2}$, where f_{ctm} = mean tensile strength of concrete in MPa, E_f in MPa and t_f in mm. The value of 0.006 may still be assumed as a limiting one for $\varepsilon_{fd,max}$, to ensure that the shear integrity of concrete (e.g. aggregate interlock) is maintained sufficiently.

The material above refers mainly to RC members of rectangular (or nearly rectangular) cross sections, which are mainly of interest for buildings. If the cross section is circular (as is usually the case in bridge piers), the contribution of FRP to shear capacity is controlled by the tensile strength of the FRP jacket, but is limited to a maximum value corresponding to excessive dilation of the concrete due to aggregate interlock at inclined cracks. By limiting concrete dilation, that is the radial strain (which is equal to the FRP hoop strain) to a maximum value, say, ε_{max}, one may show that for inclined cracks forming an angle θ with the column axis, the FRP contribution to shear capacity is as given below (assuming fibres perpendicular to the member axis):

$$V_{fd} = 0.5\varepsilon_{fd,e}E_f\rho_f A_c \cot\theta \quad (5\text{-}33)$$

where A_c= column cross-sectional area and ρ_f = FRP volumetric ratio. Eq. (5-33) assumes that at shear failure all the FRP material crossing an inclined crack is strained uniformly at $\varepsilon_{fd,e}$. Experimental evidence suggests that $\varepsilon_{fd,e}$ is in the order of 0.004 (Priestley and Seible, 1995).

Testing of shear walls strengthened with FRP jackets has been very limited. A recent study (Lombard et al. 2000) focused on flexural strengthening of RC walls and hence shear failure is not relevant, whereas some researchers have tested RC columns with wing walls strengthened in shear (Masuo 1999, Iso et al. 2000). From the limited data available in the literature it may be deduced that FRP jackets perform more or less the same as in beams or columns: they act as horizontal reinforcement with a strain that decreases as the thickness and/or the Elastic Modulus (along the perimeter) of the jacket increases.

(2) Beam-column joints

Shear strengthening of RC joints is a challenging task, which poses major practical difficulties. As an alternative to conventional RC or steel jackets, which require considerable

Copyright fib, all rights reserved. This PDF copy of fib Bulletin 24 is intended for use and/or distribution only by National Member Groups of fib.

labour and artful detailing, FRP materials have been used successfully as strengthening materials of exterior beam-column joints with deficiency in shear strength (Pantelides et al. 1999, Gergely et al. 2000).

In a recent study, Antonopoulos and Triantafillou (2003) conducted a comprehensive experimental programme, which comprised the investigation of several design parameters through 2/3-scale testing of 18 exterior joints. Parameters under consideration included: thickness of FRP, distribution of FRP between the beam and the column, column axial load, internal joint (steel) reinforcement, initial damage, carbon versus glass fibres, sheets versus strips, effect of transverse beams. A typical result is shown in Fig. 5-9, which illustrates that even very thin jackets (e.g. two 0.12 mm thick CFRP sheets in the beam direction and two in the column direction) may substantially increase the shear capacity. This experimental study was followed by development of an analytical model (Antonopoulos and Triantafillou 2002) for the shear capacity of FRP-strengthened joints (through stress and strain analysis), which was found in excellent agreement with test results. Concepts for the use of FRP in shear strengthening of joints are illustrated in Fig. 5-10.

Another application of FRP related to combined strengthening of joints, as well as of critical regions of beams and/or columns is illustrated in Fig. 5-11. This concept has been studied in the experimental work of Castellani et al. (1999) and Prota et al. (2001), who demonstrated that an increased resistance to bar slippage within the joint, as well as increased shear resistance in the connection region is possible.

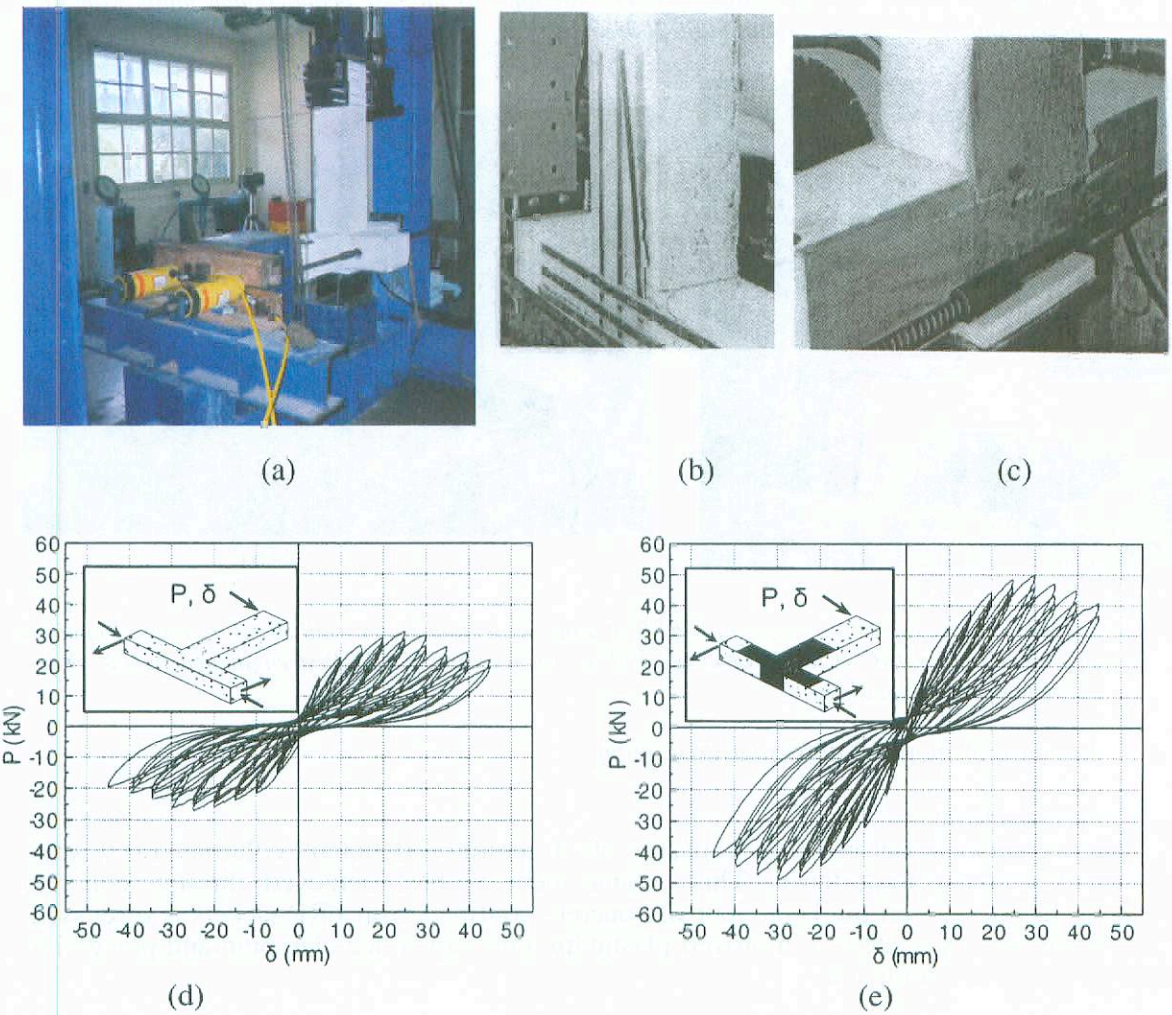

Fig. 5-9 Strengthening of beam-column joints: (a) Testing; (b) Poor performance (debonding) of rigid CFRP strips; (c) Satisfactory performance of flexible CFRP sheets (strain capacity of FRP achieved fully); (d) Lateral force-displacement response of control joint; and (e) Response of joint strengthened with CFRP sheets (two layers in the vertical and two in the horizontal direction).

Copyright fib, all rights reserved. This PDF copy of fib Bulletin 24 is intended for use and/or distribution only by National Member Groups of fib.

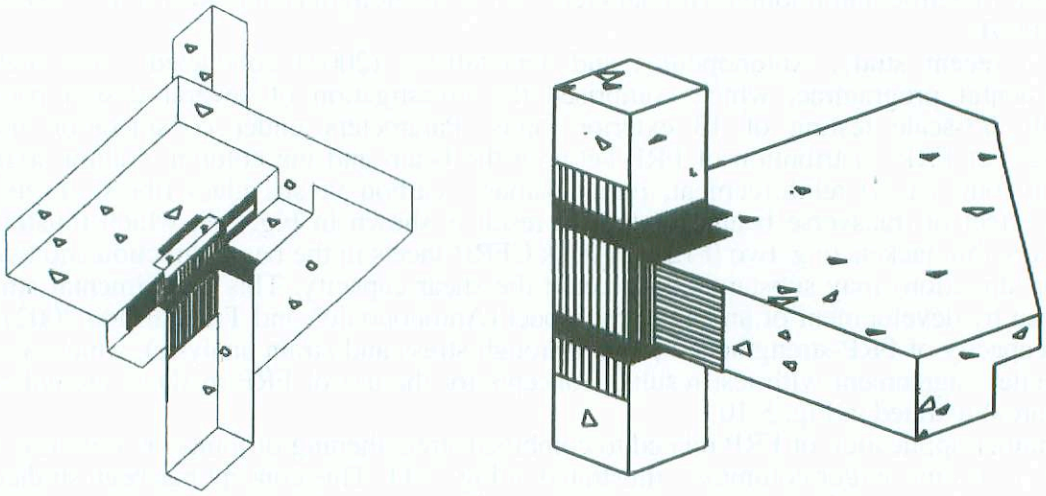

(a) (b)

Fig. 5-10: Concepts for shear strengthening of (a) exterior and (b) interior beam-column joints with FRP sheets (Antonopoulos and Triantafillou 2003).

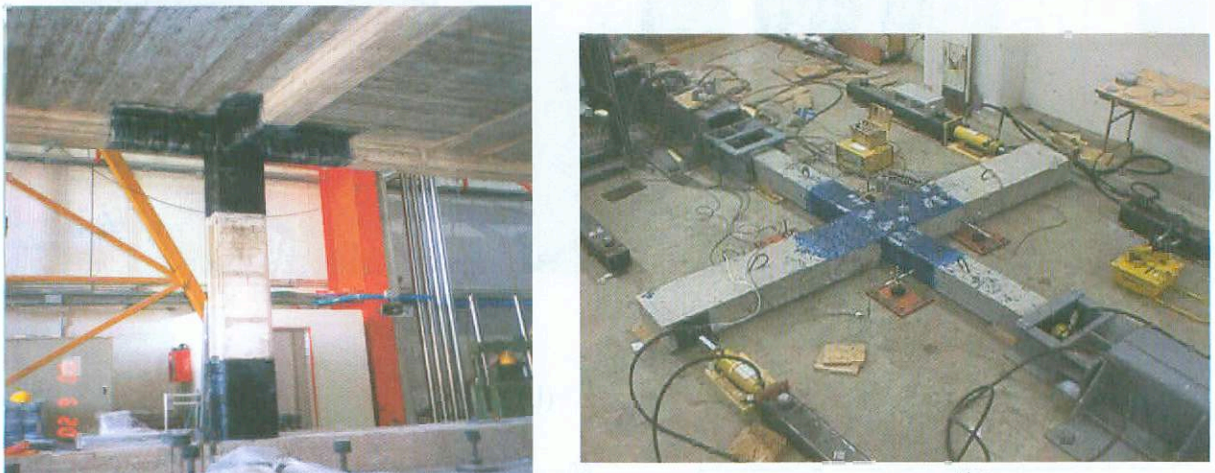

(a) (b)

Fig. 5-11: (a) View of local strengthening with CFRP of a full scale dual frame-wall structure tested, repaired and re-tested at JRC (Castellani et al. 1999). (b) Testing of CFRP-strengthened beam-column connection (Prota et al. 2001)

5.3.5.4 Increase of member deformation capacity

(1) Introduction

Enhancement of deformation capacity of structurally deficient columns in seismic regions is of outmost importance. This enhancement is best achieved through concrete confinement. In this section the behaviour of concrete confined with FRP jackets is discussed. Then key design issues related to improved plastic hinging, lap splice clamping and prevention of rebar buckling are highlighted.

(2) Behaviour of FRP-confined concrete

Concrete is a restraint-sensitive material, which means that its response under axial loading depends heavily on the lateral restraint provided through confinement (e.g. Pantazopoulou 1995). Let us examine a cylindrical concrete column with diameter D, wrapped with an FRP jacket having thickness t_f and Modulus of Elasticity E_f in the circumferential direction, which typically coincides with the principal fibre direction. Axial

Copyright fib, all rights reserved. This PDF copy of fib Bulletin 24 is intended for use and/or distribution only by National Member Groups of fib.

loading will cause shortening of the column and lateral expansion, which, in turn, will cause the FRP jacket to extend in the circumferential direction and develop confinement pressure onto the concrete. Assuming that the stress in the FRP is σ_f, the confinement stress, σ_r, exerted on the concrete in the radial direction equals:

$$\sigma_r = \frac{2t_f}{D}\sigma_f = \frac{2t_f}{D}E_f\varepsilon_f \tag{5-34}$$

where ε_f is the circumferential FRP strain. The confinement stress reduces the shear stress components of the triaxial stress tensor in the concrete and suppresses microcracking and crack initiation/propagation.

One approach to examine the behaviour of FRP-confined concrete is to look at its volumetric response, shown in Fig. 5-12 (e.g. *fib* 2001). The volumetric strain in this figure is equal to the sum of the three principal strains, tensile strains and dilation considered negative. It is interesting to observe from the volume strain versus axial strain curve that for the CFRP jacket the volumetric strain first decreases, as expected, then reverts to zero and beyond a certain level of axial strain the ever-increasing confinement pressure curtails the volumetric expansion and inverts its direction. The position of the point where the confinement action starts becoming effective (that is, when the branches depart from the unconfined one) depends on the stiffness of the confining device: the GFRP-confined concrete (jacket of equal thickness) departs later than the other two. This is the point where sufficient lateral pressure develops to prevent the lateral dilation of concrete from increasing unrestrained (this is not the case with steel confinement jackets, where yielding is associated with unstable volumetric expansion).

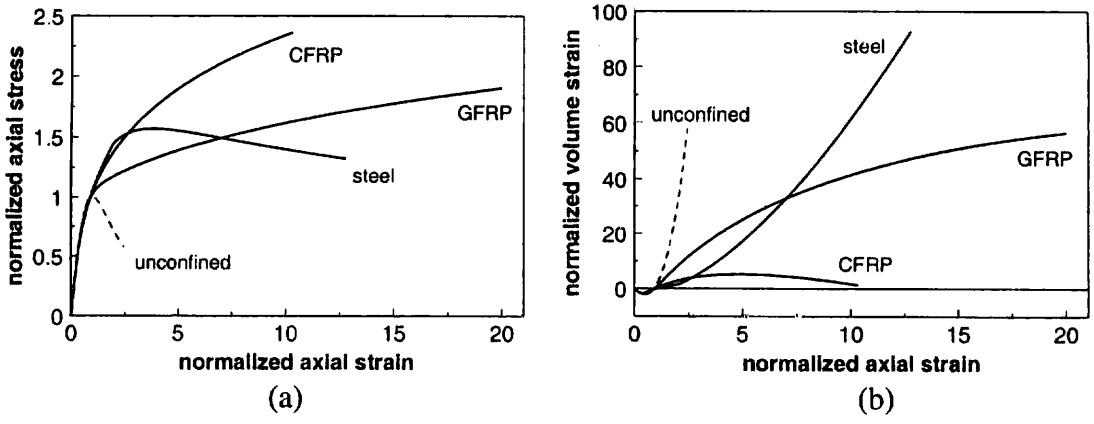

Fig. 5-12: (a) Stress-strain and (b) volumetric response of FRP-confined concrete.

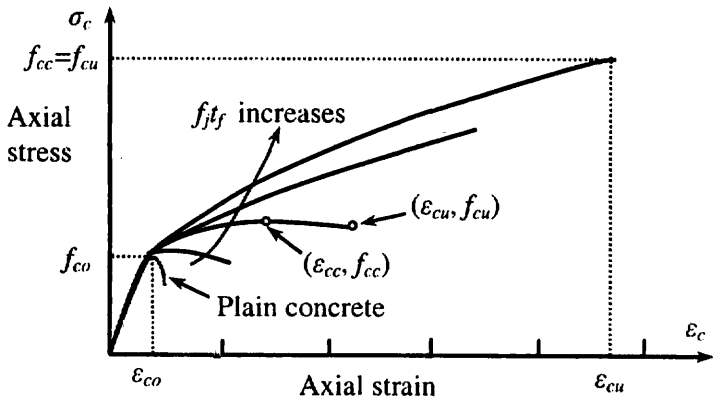

Fig. 5-13: Axial stress-strain response of FRP-confined concrete versus plain concrete.

The stress-strain response of FRP-confined concrete is illustrated in Fig. 5-13. The figure displays a nearly bilinear response with a sharp softening and a transition zone at a stress level

Copyright fib, all rights reserved. This PDF copy of fib Bulletin 24 is intended for use and/or distribution only by National Member Groups of fib.

near the strength of unconfined concrete. After this stress the tangent stiffness changes a little, until the concrete reaches its ultimate confined strength f_{cc} when the jacket reaches tensile failure at a stress $\sigma_f = f_j$ (and a corresponding strain ε_{ju}) which is, in general, less than the uniaxial tensile strength f_f. This reduction is attributed to the triaxial state of stress in the FRP (due to axial loading and confining action, but also due to bending, e.g. at corners of low radius) and to the quality of execution.

If confinement is provided by applying the FRP through automated or manual winding with the fibres in a prestressed state, an additional confining stress, given by Eq. (5-34) with σ_f replaced by the prestress level, must be added to that caused by column shortening.

Analytical and experimental studies of the stress-strain response of FRP-confined concrete have been conducted by several researchers (e.g. Fardis and Khalili 1981, Priestley and Seible 1995, Hosotani et al. 1997, Karbhari and Gao 1997, Miyauchi et al. 1997, Watanabe et al. 1997, Harmon et al. 1998, Samaan et al. 1998, La Tegola and Manni 1999, Saafi et al. 1999, Spoelstra and Monti 1999, Wang et al. 2000, Xiao and Wu 2000, Lam and Teng 2001). Most of the FRP-confinement models give the stress at ultimate strain f_{cu} and the associated strain ε_{cu} as functions of f_{co} and ε_{co}, respectively, the confining (lateral) stress at ultimate, σ_l (= $2t_f E_f \varepsilon_{ju}/D = 2t_f f_j/D$) and the jacket ultimate strain ε_{ju}. The effectiveness of confinement depends heavily on the jacket characteristics and increases as the stiffness and the ultimate strain increase.

The confinement model by Spoelstra and Monti (1999), combining simplicity with accuracy, is:

$$f_{cu} = f_{co}\left(0.2 + 3\sqrt{\frac{2t_f f_j}{Df_{co}}}\right) \tag{5-35 a}$$

$$\varepsilon_{cu} = \varepsilon_{co}\left(2 + 1.25\,\frac{E_c}{f_{co}}\,\varepsilon_{ju}\sqrt{\frac{2t_f f_j}{Df_{co}}}\right) \tag{5-35 b}$$

If the cross-section of the column is rectangular, confinement is less effective. Confining stress is transmitted then to the concrete through the four corners of the cross section and increases with the corner radius R (Fig. 5-14). The confinement effectiveness factor, α_f, is just the ratio of the confined (shaded) area of the section to the total in Fig. 5-14.

$$\alpha_f = \left(1 - \frac{(h-2R)^2 + (b-2R)^2}{3bh}\right) \tag{5-36}$$

(b, h = external dimensions of concrete section). For a more detailed treatment of the application of FRP confinement models to concrete, the interested reader is referred to *fib* (2001).

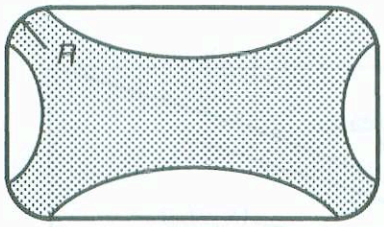

Fig. 5-14: Effectively confined area (defined by parabolas) in FRP-confined rectangular column.

(3) Improved plastic hinge behaviour

Plastic hinge confinement is crucial, as the unconfined compression strength of concrete is insufficient to enable the development of large displacement or chord rotation ductility factors μ_θ. Experimental results (e.g. Kobatake et al. 1993, Saadatmanesh et al. 1996, Masukawa et al. 1997, Seible et al. 1997, Sexsmith et al. 1997, Feng and Bahng 1999, Fujii et al. 1999, Fukuyama et al. 1999, Matsuzaki et al. 1999, Seible et al. 1999, Zhang et al. 1999, Saiidi et al. 2000, Sheikh et al. 2000) have demonstrated that enhancement of the ductility capacity is easily achieved by properly designed FRP jackets (Fig. 5-15).

Copyright fib, all rights reserved. This PDF copy of fib Bulletin 24 is intended for use and/or distribution only by National Member Groups of fib.

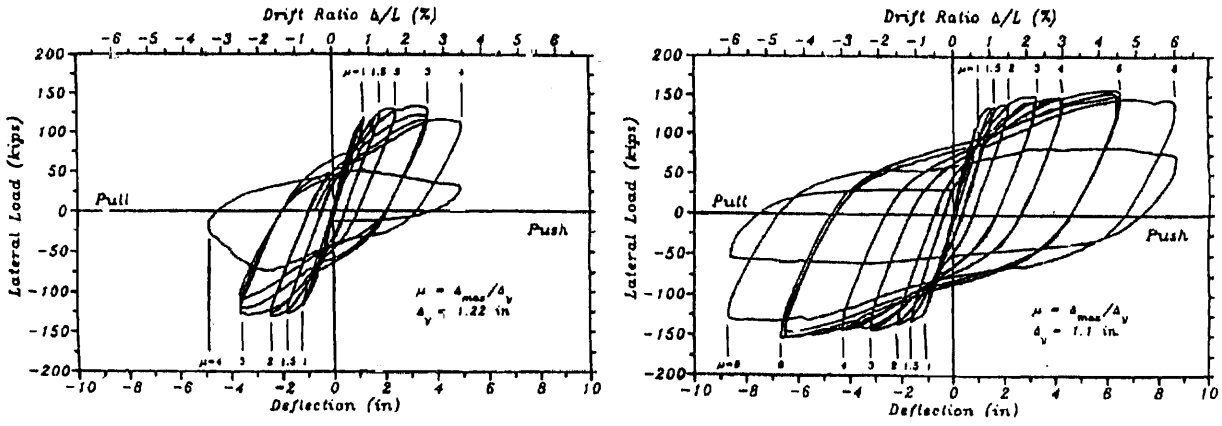

(a) (b)

Fig. 5-15: Lateral force-displacement response of flexure-dominated rectangular columns: (a) as-built; (b) retrofitted with GFRP jacket at the plastic hinge region (Priestley and Seible 1995).

Eqs. (5-9) to (5-26) may be used, along with eq. (5-34) to select the jacket thickness for a specified ductility factor μ_θ, provided that eqs. (5-35), (5-36) (or equivalent alternatives) are used instead of eqs. (5-21) and (5-20) or (5-22) respectively. It should be noted, though, that eqs. (5-23) to (5-26) have been fitted to specimens without FPR wraps, using eqs. (5-21), (5-22). Therefore, their validity has to be checked. Alternative expressions may be used, fitted to tests on FRP-wrapped specimens. It is emphasized, though, that these alternative expressions have to be consistent with the model to be applied for FRP-confined concrete (e.g. Eqs. (5-34) to (5-36)).

Japanese researchers have followed a different approach towards assessing the displacement ductility factor of FRP-confined columns. According to this approach, the ductility factor may be related to the shear capacity, V_u, and the shear force at the flexural strength, $V_{fu}=M_u/L_s$ of the member after retrofit according to empirical equations of the type:

$$\mu_\theta = \alpha + \beta \frac{V_u}{V_{fu}} \tag{5-37}$$

where constants α, β depend on the type (that is the deformability) of the fibres (Mutsuyoshi et al. 1999).

Another method for relating ductility to the FRP material characteristics was proposed by Monti et al. (2001). Key element in this method is the definition of the "upgrading index" I:

$$I = \frac{r_{tar}}{r_o} \frac{\mu_{\theta,tar}}{\mu_{\theta,o}} \tag{5-38}$$

where r_{tar} = resistance (strength) of desired upgrading (target), r_o = initial resistance (before retrofitting), $\mu_{\theta,tar}$ = target ductility and $\mu_{\theta,o}$ = initial ductility. The upgrading index is related to a number of characteristics of the member before retrofitting (longitudinal reinforcement, axial load, concrete strength), as well as to the strength and ultimate strain of confined concrete. The last two properties (f_{cc}, ε_{cu}) may be related to the FRP jacket thickness and deformation capacity through an appropriate confinement model (e.g. Eqs. (5-35), leading to the optimum jacket design for a given value of I.

In a recent study, Tastani and Pantazopoulou (2002) proposed an empirical (based on data fit) simple lower-bound expression relating the available displacement or chord-rotation ductility factor to confining pressure σ_l provided by FRP:

$$\mu_\theta = 1.3 + 12.4\left(\frac{\sigma_l}{f_c} - 0.1\right) \geq 1.3 \tag{5-39}$$

For rectangular columns subjected to flexure in the axis parallel to the side of width b_w, the lateral confining stress equals $a_w \rho_w f_{yw} + 2a_f\, t_f\, f_f / b_w$, where a_w in the first term is the effectiveness coefficient of stirrups (with a volumetric ratio ρ_w and yield stress f_{yw}). Hence, for a given jacket material, Eq. (5-39) may be used to estimate the FRP thickness required to achieve the displacement or chord-rotation ductility factor μ_θ.

Copyright fib, all rights reserved. This PDF copy of fib Bulletin 24 is intended for use and/or distribution only by National Member Groups of fib.

(4) Lap-splice clamping

A number of experimental studies (Ma and Xiao 1997, Saadatmanesh et al. 1997, Seible et al. 1997, Restrepo et al. 1998, Osada et al. 1999, Chang et al. 2001, Haroun et al. 2001, Saatcioglu and Elnabelsy 2001) have demonstrated that FRP jackets are quite effective in preventing lap-splice failures (e.g. Fig. 5-16). Whilst this effectiveness is maximum for circular columns, it is reduced considerably for rectangular ones, by a factor in the order of 50% (Seible et al. 1997, Saatcioglu and Elnabelsy 2001). Lap-splice clamping requires sufficient lateral pressure onto the splice region to prevent the concrete prisms that adhere to the lapped reinforcement to slip relative to each other. Tests have shown that the onset of lap-splice relative slippage starts when the dilation strains are between 0.001-0.002. Adopting the lower limit of dilation strain, that is 0.001, a rough estimate of the FRP jacket thickness as a function of the lateral stress required to keep the lap splice from debonding (through frictional restraint) in circular columns may be obtained as (Seible et al. 1997):

$$t_f = \frac{D(\sigma_l - \sigma_h)}{2E_j \times 0.001} \tag{5-40}$$

where σ_l represents the clamping stress over the lap splice length L_s,

$$\sigma_l = \frac{A_s f_{sy}}{\left[\frac{p}{2n} + 2(d_b + c)\right] L_s} \tag{5-41}$$

and σ_h is the hoop stress in the stirrups at a strain of 0.001, which can be ignored, or the active pressure from the grouting between the FRP and the column, if provided. In Eq. (5-41) p = perimeter line in the column cross section along the inside of longitudinal reinforcement, n = number of spliced bars along p, A_s and f_{sy} = area and yield stress, respectively, of longitudinal reinforcement, c = concrete cover to the longitudinal rebars and d_b = bar diameter.

One possible extension of the above formulation to rectangular columns (which are of interest for buildings) could be made here by replacing D by b_w (as in the previous section) and by reducing the effectiveness of FRP jacketing through the use of a coefficient equal to the ratio of $A_{s,c}/A_s$, where $A_{s,c}$ = area of longitudinal reinforcement inside the effectively confined part of the cross section.

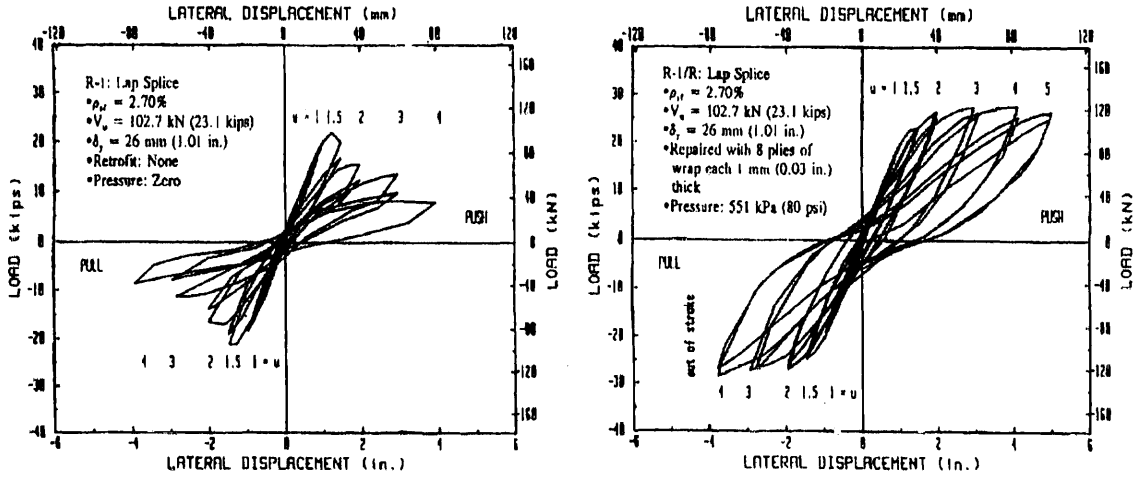

(a) (b)

Fig. 5-16 Lateral force-displacement response of flexure-dominated rectangular columns with base lap-splices: (a) as-built; (b) retrofitted with FRP jacket at the lap-splice region (Saadatmanesh et al. 1997).

(5) Rebar buckling

To prevent column rebar buckling in the plastic hinge region, Priestley et al. (1995) proposed the following equation for the required volumetric transverse reinforcement ratio ρ_f

Copyright fib, all rights reserved. This PDF copy of fib Bulletin 24 is intended for use and/or distribution only by National Member Groups of fib.

of FRP (= $4t_f/D$ in circular columns):

$$\rho_f = \frac{4t_f}{D} = \frac{0.45 n f_s^2}{E_{ds} E_f} \tag{5-42}$$

where:

$$E_{ds} = \frac{4E_s' E_i}{\left(\sqrt{E_s'} + \sqrt{E_i}\right)^2} \tag{5-43}$$

and n = number of longitudinal rebars, f_s = longitudinal steel stress at a strain of 0.04, E_s' = secant modulus of steel from f_s to f_u (ultimate stress) and E_i = initial elastic modulus of the longitudinal steel reinforcement. For rectangular cross sections, a confinement effectiveness coefficient could be applied along the lines of the previous section, resulting in increased FRP thickness requirements.

5.3.6 Steel jackets

5.3.6.1 Role and construction of steel jackets

This technique (exemplified in Figure 5-17 for columns, as well as for beams, where it first developed as a means of their flexural strengthening in the span) both is more expensive than concrete jackets. It is, however, fast and effective if there is need for immediate use of the building after a damaging earthquake, or where there is a danger of collapse of the structure.

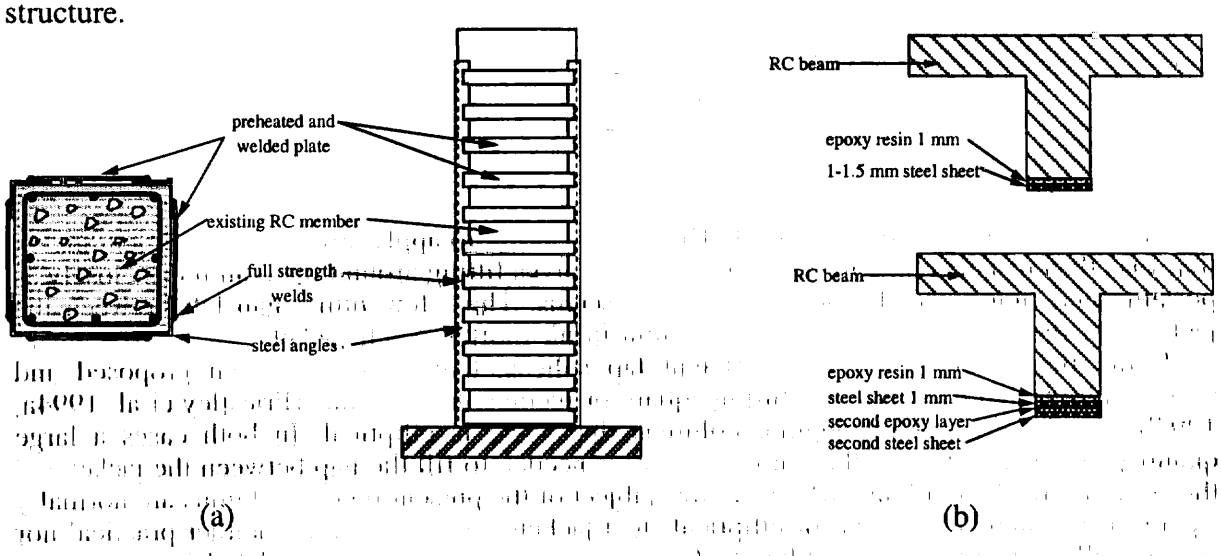

Fig. 5-17: Use of steel plates in repair of (a) columns and (b) beams

The role of thin-walled steel jackets fitted around columns is similar to that of FRP wraps: to increase shear strength, improve deficient lap splices and enhance ductility through confinement. From the point of view of mechanical behaviour, their main difference with FRP wrapping is that, as steel is isotropic, it has significant stiffness and strength in the member longitudinal direction as well, which unavoidably affects the flexural stiffness and strength of the member. The extent of this influence depends on how the steel jacket is connected to the concrete member and to the ones framing into it. In this respect it should be noted that steel jackets are normally not intended for flexural strength enhancement: their continuation beyond the member end, although not so difficult as that of FRP jackets, is not easy. Moreover, even if they can transmit forces beyond the member end by bolting or welding to other steel elements through the slab and by bearing against the concrete surface, they are not so effective in resisting cyclic flexural stresses in composite action with the concrete member inside, as their thin wall may buckle. Therefore, they are applied on the concrete surface so that they develop stresses mainly in the circumferential direction and their effect on member flexural strength and stiffness is minimized.

Although surface-bonded steel plates have been used for strengthening of RC members for almost half a century and their technology is simple and familiar to the construction industry,

Copyright fib, all rights reserved. This PDF copy of fib Bulletin 24 is intended for use and/or distribution only by National Member Groups of fib.

they are being replaced fast by surface-bonded FRPs, which, although more costly, are much lighter and easier to apply. It is also noteworthy that through a combination of work in the shop and in the field, the technique of steel jacketing can be applied faster than concrete jackets. So, as it is based on materials and technology readily available near most sites, it is often applied as a non-engineered measure to deficient or slightly (or even moderately) damaged buildings and columns during the immediate post-earthquake period, for building re-occupancy even during the aftershock period. Detailed assessment and retrofit design may take place in the following period and the steel jackets may be removed when the retrofit is implemented, or stay in place (as in the columns of Fig. 5-18).

Fig. 5-18. Examples of steel jackets built-up in situ of corner angles and horizontal straps

Thin-walled steel jackets are most efficient and easier to apply around circular columns. In that case they usually come in two semi-circular halves fitting around the column as closely as possible and field-welded along two vertical seems. The - few mm - gap left between the jacket and the column is grouted with a nonshrink mortar. Such jackets are so efficient in confining the concrete and any deficient lap splices, that they have been proposed and successfully tested even for retrofitting square or rectangular columns (Priestley et al, 1994a, 1994b). In the case of rectangular columns the jacket is elliptical. In both cases a large quantity of concrete (rather than mortar grout) is needed to fill the gap between the jacket and the column. In RC buildings, which are the subject of the present report, columns are normally square or rectangular: circular or elliptical steel jackets around them are neither practical nor aesthetically appealing. So circular steel jackets are not covered in any detail here; anyway, their role, behaviour and modeling for confinement of concrete and enhancement of laps splices or shear strength is rather similar to that of FRP wraps around circular columns and may be covered as in Section 5.3.5. (The main difference with FRP wraps is the isotropy of steel and its implications for confinement effectiveness and flexural stiffness and strength).

Around square or rectangular columns steel jackets are built up of four corner angles, on which continuous thin steel plates or thicker horizontal steel straps or batten plates are welded. Within the limitations placed by the heavy weight of the resulting segments, continuous thin plates may be are welded in the shop to the corner angles into larger L-shaped pieces, corresponding to half the perimeter of the column to be fitted around, and fillet-welded in the field (see Fig. 5-21). The (10 to 20 mm-wide) gap between the plate and the external surface of the column is grouted with nonshrink mortar. When there is a need for thick steel plates, it is advisable to use several thin layers instead, to minimise interfacial shear stresses (see Fig. 5-17 b).

A lighter and easier to install version of the steel jacket may consist of angles epoxy-bonded to the four corners of the column, on which horizontal straps or batten plates are field-welded. Fig. 5-17 a presents a schematic of this technique and Fig. 5-18 shows two applications to real buildings. In the second case, drawn from a slightly damaged building, a cast-in-place concrete jacket is added at the end around the column; a steel cage has been built-up before around the old column to confine it and enhance its ductility and axial load

Copyright fib, all rights reserved. This PDF copy of fib Bulletin 24 is intended for use and/or distribution only by National Member Groups of fib.

capacity during the immediate post-earthquake period and is being integrated in the jacketed column. Normally these straps or batten plates are pre-heated in the field to 200° – 400°C just prior to welding, so that when they cool down the jacket exerts some positive confinement on the column. This effect is gradually lost due to concrete creep, therefore it is not taken into account in design. Depending on the intended role of the jacket, the gap between the column and the straps or batten plates (which is normally narrower than when continuous steel plates are used) may be grouted with non-shrink mortar or left unfilled.

5.3.6.2 Confinement action of rectangular steel jackets

Unless restrained in the direction normal to the column perimeter by bolts anchoring them to the column, the thin steel plates or straps in-between the angles do not exert any confining pressure along the sides, as they are flexible and bulge outwards. Then, regardless of whether it consists of continuous thin steel plates partly shop-welded to the corner angles, or of straps or batten plates field-welded to them, the jacket exerts to the column confining forces only at the corners; confininig action is according to the mechanism shown in Fig. 5-14 for FRP wraps. For jackets consisting of continuous steel plates, Eq. (5-36) applies for the calculation of the confinement effectiveness factor, with R replaced by the width, c, of the contact area of the corner angle and the column (c = leg width of the steel angle). For jackets consisting of steel straps or batten plates welded to corner angles, Dritsos and Pilakoutas (1992) proposed calculating the confinement effectiveness factor, α, as:

$$\alpha = \left(1 - \frac{s_c}{2b}\right)\left(1 - \frac{(h-2c)^2 + (b-2c)^2}{3bh}\right) \tag{5-44}$$

where s_c is the clear spacing, s_n, of straps or batten plates, reduced by twice the corner angle width, c, according to a postulated 45° dispersion of confining action from the strap into the corner angle:

$$s_c = s_n - 2c \tag{5-45}$$

Confinement action offered by the steel jacket may be calculated as if the jacket (continuous or in straps) were internal hoops and ties, using as geometric steel ratio ρ_x or ρ_y in each transverse direction of the column the cross-sectional ratio of the jacket relative to a vertical section through the column.

Sakino and Sun (2000) used the results of 87 concentric compression tests on square columns with steel jackets to develop and verify expressions for the effect of confinement by the jacket on the stress-strain response of concrete. Enhancement of ultimate strength is by a factor K, defined through the following expression in terms of the thickness t_j and the yield strength f_{yj} of the jacket material:

$$f_{cc} = Kf_c = \left(1 + 45\frac{f_{yj}}{f_c}\frac{t_j^2}{b^2}\right)f_c \tag{5-46 a}$$

Factor K presumably includes the effect of the confinement effectiveness factor α of Eq. (5-44). The effect on the strain at ultimate strength, ε_{cc} is given by the following expression:

$$\varepsilon_{cc} = \varepsilon_{co}(1 + 4.7(K-1)) \tag{5-46 b}$$

That on the extreme fibre strain at section ultimate strength (not at section ultimate curvature) is given by:

$$\varepsilon_{cu} = \varepsilon_{co}(1.375 + 0.1K) \tag{5-46 c}$$

According to Sakino and Sun (2000) the member ultimate moment computed on the basis of the confined concrete strength and extreme fibre strain of Eqs. (5-46 a), (5-46 c) is further increased due to steel strain-hardening and concrete confinement beyond the member end; the

Copyright fib, all rights reserved. This PDF copy of fib Bulletin 24 is intended for use and/or distribution only by National Member Groups of fib.

increase is by 10% for values of the axial load ratio $\nu = N/A_c f_c$ less than 0.3, or by a factor equal to $1.1 + 0.8(\nu - 0.3)^2$ for higher values of ν.

The friction that develops at the interface of the corner angles and the column, owing to the confining forces developed there when the concrete column is heavily stressed and approaching ultimate conditions, enhances the composite action of the column with the steel jacket and mobilizes the jacket in the longitudinal direction, even when it is not continued into the joint beyond the member end. This effect increases the stiffness and possibly the strength of the steel-jacketed column. The magnitude of this increase is uncertain and cannot be taken into account in design calculations. Nonetheless, this effect may be considered as a second line of defense against loss of axial-load-capacity of the retrofitted column in the post-ultimate range of behaviour. Measures are often taken, though, against possible adverse effects of an enhancement of column flexural strength. Such adverse effects include the increase in shear force demand on the column and the joint, or the shear and moment input in the foundation, beyond the limits estimated on the basis of the considered strength of the plastic hinge. A few-mm gap is often provided between the end of the jacket and the end of the column (face of the joint or top of the foundation) to prevent the jacket from bearing (at large column drifts) against the face of the elements to which the column is connected and developing compressive forces that may inadvertently enhance column flexural strength.

It has been emphasized at the beginning of this Section that, due to their tendency to bow out under the action of the concrete pressure, rectangular thin-walled steel jackets are not very efficient in confining rectangular columns. The confinement effectiveness of such jackets is further reduced by their Poisson expansion due to any longitudinal compressive stresses that may develop in the jacket through its partial or full composite action with the concrete column inside (see last paragraph). If there is full composite action in the longitudinal direction, the large Poisson ratio of steel will delay development of any confinement action until concrete approaches ultimate strength and its Poisson ratio becomes larger than that of steel. Steel jackets consisting of a cage of angles at the corners with welded transverse straps or butten plates do not suffer from reduction of confinement effectiveness due to Poisson effects. Such effects are minimized also if the continuous thin-walled steel plate is replaced by corrugated sheets with the corrugation in the transverse direction of the member, welded along the corners of the section (see Fig. 5-19 for the proposed application of this concept to beam-column connections by Ghobarah et al 1997 and Biddah et al, 1997). Due to the very low extensional stiffness of the corrugated sheet in the axial direction of the member, confinement is not reduced by Poison effects. More importantly, the large out-of-plane rigidity of the corrugated sheet almost eliminates outward bulging of the jacket and results in values of the confinement effectiveness factor, α, close to 1.0. The effectiveness of the scheme to increase the flexural deformation capacity of columns has been demonstrated by Ghobarah et al (1998).

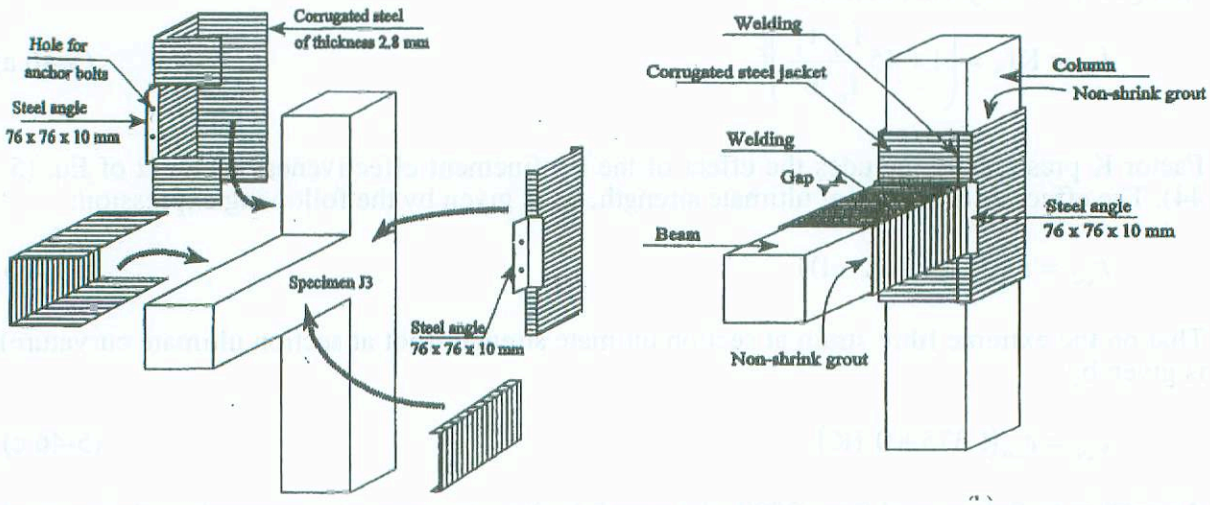

Fig. 5-19: Corrugated steel jacketing of beam-column connection: (a) proposed assembly; (b) assembled jacket (Ghobarah et al 1997).

Copyright fib, all rights reserved. This PDF copy of fib Bulletin 24 is intended for use and/or distribution only by National Member Groups of fib.

5.3.6.3 Shear strengthening by steel jackets

Unlike steel jackets intended for enhancement of column deformation capacity or of deficient lap splices, which are normally applied over only the plastic hinge or the lap splice region, steel jackets intended for shear strengthening extend over the full height of the column. The few-mm gap mentioned at the end of the paragraph above is then provided between the jacket and the face of the members into which the column frames, to minimize shear force demands due to flexural strength enhancement.

Fuse et al. (1992) strengthened a shear-critical 250-mm square column with a column-high steel jacket for several values of jacket thickness and gap-width between the column and the jacket. Shear strength increased so that the retrofitted columns yielded in flexure at a value of chord rotation of about 2% and reached a maximum strength by 0% to 23% higher than the theoretical ultimate moment, consistent with the above-mentioned argument by Sakino and Sun (2000). Interestingly, the enhancement in strength was not accompanied by improvement in hysteretic energy dissipation compared to the unretrofitted column.

On the basis of the results of 24 tests of steel-jacketed square columns with shear-span ratio less than 1.5 failing in shear, Sakino and Sun (2000) verified that the conventional expressions for shear resistance of RC members apply to steel-jacketed columns, provided that: a) the contribution of the steel jacket to shear strength, with its total thickness $2t_j$ used instead of the familiar term A_{sw}/s for hoops or ties, is added to that of transverse reinforcement; and b) account is taken for the contribution of confinement of the concrete by the jacket in preventing or delaying shear failure by diagonal compression in the web.

A similar confirmation for 13 shear-critical retrofitted columns may be found in Aveles et al (1996), although in that case comparison was with the predictions of the Compression-Field-based expression in the Canadian Concrete Code, rather than with those of the empirical Arakawa expression used in Japan.

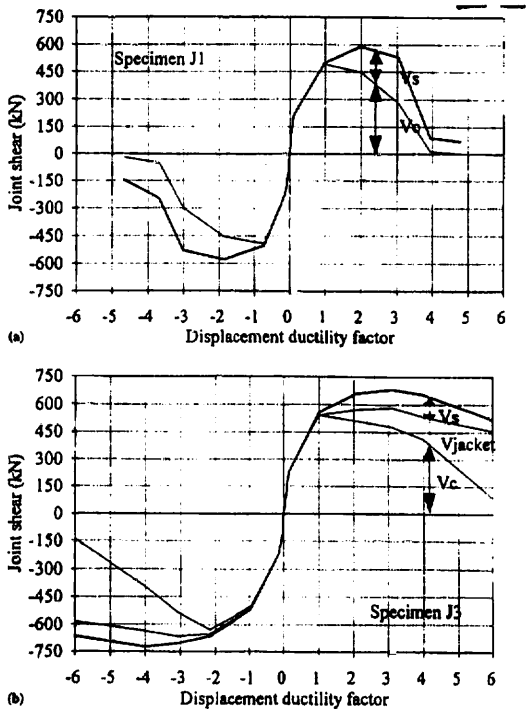

Fig. 5-20: Joint shear force vs connection ductility factor (ductility = 1 at joint shear cracking) for: a) unretrofitted connection; and (b) connection retrofitted with corrugated steel sheets (Biddah et al, 1997).

The tests of Biddah et al (1997) and Ghobarah et al (1997) on shear deficient beam-column connections retrofitted with corrugated steel jacket (see Figs. 5-19, 5-20) have demonstrated the effectiveness of such jackets for shear strengthening of the joint and the members framing into it. In this particular case strengthening of the joint is effected not only through the direct contribution of the shear force capacity of the sheet ($2t_jh_bf_{yj}$, where h_b is the beam depth)

Copyright fib, all rights reserved. This PDF copy of fib Bulletin 24 is intended for use and/or distribution only by National Member Groups of fib.

against the horizontal shear force in the joint, V_{jh}, but also by improving confinement of the concrete core and allowing it to retain most of its contribution to joint shear capacity up to post-ultimate-strength drift levels, at which such a contribution is completely lost in joints with only internal steel ties (see Fig. 5-20, Biddah et al, 1997).

Aboutaha et al (1996a, 1999) tested several large-scale shear-critical columns retrofitted with specimen-long steel jackets employing continuous thin-wall plates welded to corner angles Fig. 5-21). Tested specimens represented typical non-ductile building columns designed and constructed in the 1960's in the U.S.A with inadequate lap splices in the longitudinal reinforcement. Different configurations of 6.3 mm thick steel jackets were applied, with and without adhesive anchor bolts to seven full-scale specimens subjected to cyclic loading. The test results show significant increase in the ductility of the reinforced concrete members, whilst minimum change in the initial stiffness of the members was observed. The ductile flexure-dominated response of the retrofitted models enabled their full flexural capacity to be developed, hence significant increase in strength was also recorded. Measurements during the tests have shown that the jacket is inactive, until the concrete column develops a major diagonal crack. The relative movement of the two pieces of the column on either side of such a crack causes the column to bear against the jacket and activate it. From that point on, the jacket resists all the additional shear force and controls the width of the original diagonal crack, as well as development of new ones and disintegration of the concrete core due to cycling of the shear.

Aboutaha et al (1999) concluded that, in order to play this role, the steel jacket has to remain elastic. To this end, they recommend it be proportioned to resist shear with only 50% of its yield stress. Under this condition they propose a model for shear resistance of the jacketed column in which the contribution of the jacket to shear resistance is calculated with an expression analogous to Eq. (5-31) for the shear resisted by FRP wraps, applied with angle α with respect to the column axis equal to 90° and the product $\varepsilon_{fd,e}E_f$ replaced by 50% of the yield stress of the steel jacket. The contribution to shear resistance of internal column ties is added; also that of concrete V_c, if the angle θ of concrete compression struts to the column axis is taken equal to 45°. As the jacket prevents cyclic degradation of the shear resistance of the concrete column, the reduction of V_c with the magnitude of cyclic ductility demand, μ_θ, may be neglected. It should be noted that this recommendation is not consistent with that of Sakino and Sun (2000), namely that the full yield strength of the steel jacket be used in the calculation of shear resistance. The end effect of this discrepancy is small, though, as for practical values of the jacket thickness its contribution to shear strength is so large, that the recommendation of Aboutaha et al (1999) – namely to consider the jacket as 50% effective in shear – can be implemented without undue penalties for the jacket.

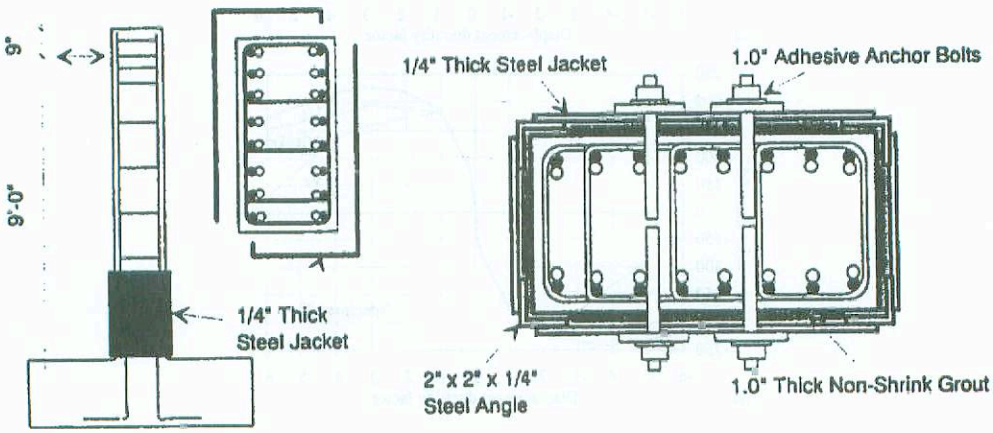

Fig. 5-21: Steel jacket used by Aboutaha el al (1996 a,b) for retrofitting concrete column with insufficient lap splices

5.3.6.4 Clamping of lap splices by steel jackets

Abouhata et al (1996 a, b) performed a systematic experimental study of rectangular columns with deficient lap splices (24 bar diameters) in the plastic hinge zone. As shown in Fig. 5-21, the partial-height steel jacket, consisting of 6.3mm thick continuous plates fillet-welded to corner angles, is anchored to the old column through epoxy-grouted bolts arranged

Copyright fib, all rights reserved. This PDF copy of fib Bulletin 24 is intended for use and/or distribution only by National Member Groups of fib.

along lines parallel to the column axis. The bolts anchor the long sides of the jacket to the column and are parallel to the direction of loading.

Test results have shown that very high cyclic deformation capacity of the retrofitted column (to drift ratios above 5%) can be achieved, provided that:

- The jacket exceeds by about 50% the length of the lap splice region (exceedance of this length by 20% was found insufficient);
- The jacket is back-anchored into the column by at least two (horizontal rows) of bolts on each side normal to the direction of loading: one (row or bolt) above the top of the splice region and another at about one-third of that region from the bottom. Intermediate (rows of) bolts between these two heights are not necessary for effective clamping of the lap splices;
- The number of bolts in each horizontal row increases as the aspect ratio of the column cross-section increases and the concrete strength, f_c, decreases. According to the recommendations by Aboutaha et al (1996), no bolts are needed if f_c exceeds 35 MPa or 28 MPa, respectively, in cross-sections with aspect ratio 2:1 or 1.5:1, respectively. In elongated sections with low concrete strength two bolts are needed per row, at third-point of the long side of the section.
- Aboutaha et al (1996) proposed also an extension of Paulay's friction-based model for the clamping action of confinement on lap splices. The extended model is based on:
- A postulated shear transfer area over the lap splice, defined by strips with width not exceeding 1.5 bar diameters ($1.5d_b$) on either side of each spliced bar and length equal to the lap length, l_s; the surface-area of the shear transfer area for one spliced bar is equal to: $A_{sf}=l_s\min(3d_b, s_b)$, with s_b denoting the spacing between lapped longitudinal bars.
- A postulated friction coefficient μ_f of 1.4 with clamping action of anchor bolts, or of 1.0 without;
- An assumed clamping action of anchor bolts due to a bond stress v_b of $0.042\sqrt{f_c}$ (units MN, m) developing along their entire embedment length, l_{ab};
- Clamping action of tie-legs which are normal to the potential splitting plane (and parallel to the anchor bolts) and enclose the lap-splices, based on the full yield force, $\Sigma A_{st}f_{yt}$, of these tie legs.
- Clamping action of the (two) sides of the steel jacket which are parallel to the above-mentioned tie-legs and anchor bolts, based on the full yield stress of the steel jacket in tension.

This is expressed by the following verification inequality:

$$v_{sf}b \le 2t_j f_{yj} + \sum \frac{A_{st}f_{yt}}{s_t} + \frac{v_b \pi d_b l_{ab} n_{ab}}{l_s} \tag{5-47}$$

In Eq. (5-47) v_{sf} is the shear stress demand over the shear transfer area along the splice length of a single bar:

$$v_{sf} = \frac{1.25A_{sl}f_{yl}}{\mu_f A_{sf}} \tag{5-48}$$

in which A_{sl} amd f_{yl} denote the cross-sectional area and the yield stress of a single lap-spliced bar and factor 1.25 accounts for strain hardening in that bar. Other variables in Eq. (5-47) are: b = column width parallel to the potential splitting plane and normal to the tie-legs and anchor bolts; s_t = spacing of tie-legs in the direction of the member axis; n_{ab} = number of anchor bolts over the entire area of lap-splicing, bl_s. All other variables in Eqs. (5-47), (5-48) have been defined before.

Ghobarah et al (1998) and Biddah et al (1997), respectively, tested one column with lap splices of 40 bar diameters and deficient transverse reinforcement and one beam-column connection with inadequate anchorage of beam bottom bars in the joint. Both found that the local confinement effected by corrugated steel jacketing of the column or the joint, respectively, prevented pre-emptive bond failure.

It is noted, in closing, that Aboutaha et al (1996) found that discrete collars built-up of channel sections fitted around the column and bolted at its corners, are not as effective as jackets consisting of corner angles and continuous steel plates welded on them.

Copyright fib, all rights reserved. This PDF copy of fib Bulletin 24 is intended for use and/or distribution only by National Member Groups of fib.

5.3.6.5 Deformations of steel-jacketed columns at yielding and ultimate

A column retrofitted with a steel jacket is expected to yield and ultimately fail in flexure, without any adverse effects of lap splices or shear on their force and deformation capacity, as determined by flexure. If there is a small gap between the end of the jacket and the end of the column at the face of the adjoining members, the yield moment of the jacketed column will be effectively that of the old column. The deformations of the column at yielding will be slightly smaller, depending on the extent of the steel jacket over the length of the column and on the mobilization of the jacket into composite action with the old column. The effect of partial-height rectangular jackets on chord rotation and secant stiffness at yielding is small and may be neglected. Therefore in Eqs. (5-27), (5-28) k_y and k_m may be taken equal to 1.0.

Provided that the gap between the end of the jacket and the end of the column at the face of the adjoining members is small, the ultimate chord rotation of a steel-jacketed column may be estimated in principle on the basis of the ultimate curvature of the confined concrete core and the column plastic hinge length. However such procedure has not been verified yet against the limited available tests on columns with rectangular steel jacket and its applicability is doubtful without calibration.

Sakino and Sun (2000) have fitted the following empirical expression to the post-ultimate strength chord rotation at 95% of the peak resistance in 27 tests on columns retrofitted with full-height rectangular steel jackets:

$$\theta_u = \frac{\max\left(1,\ \frac{f_c(\mathrm{MPa})}{36}\right)\min\left(0.18\frac{M}{Vh}+0.06,\ 0.36-0.02\frac{M}{Vh}\right)}{v^{1.1}\left(\frac{b+2t_j}{t_j}\right)^{0.8}} \tag{5-49}$$

The shear span ratio, M/Vh, of the 27 specimens ranges between 1.0 and 2.0, with all specimens with M/Vh=1.0 failing in shear. Eq. (5-49) fits well the data with a coefficient of variation of 27%. Nonetheless, its applicability may be limited by the very small size of the databank and the narrow range of the control variables (e.g., it gives very high values for near-zero values of the axial load ratio v and near-zero values for very low thickness of the steel jacket).

5.3.6.6 Analysis of data on strength, stiffness and deformation capacity of members with steel jackets

Cyclic test results on steel-jacketed concrete members are limited in the international literature. Most of them have been gathered in Table 5.7, where the measured strength (in terms of yield moment M_y and shear resistance V_R – determined as the ratio of M_y to shear span, L_s) and the measured chord rotation at yielding, θ_y, and at the end of the test are compared to predicted values.

As the steel jacket does not extend into the column base, the measured yield moment M_y of the retrofitted column is compared to the value computed for the unretrofitted specimen inside the jacket according to Eqs. (5-3)-(5-8) in Section 5.3.2.

The measured chord rotation at yielding, θ_y, is also compared to the value computed for the unretrofitted specimen by means of Eq. (5-2), with yield curvature φ_y from Eqs. (5-3)-(5-7).

Shear resistance, V_R, determined as measured M_y over L_s, is compared to the sum of the value obtained from Eqs. (4-13), (4-14) at the peak value of displacement attained during the test, plus 40% of the ideal contribution of the jacket to shear resistance. This 40%-value is tried here as an alternative proposal to the 50% suggested by Aboutaha et al (1999) on the basis of their test results.

Finally, the final value of chord rotation, be it at specimen failure (conventionally defined as loss of 20% of maximum resistance at the peak of the cycle) or at the end of a test not carried to failure, is compared to the flexure-controlled ultimate chord rotation of the unretrofitted specimen, computed from Eq. (5-9) with confinement effectiveness factor, α (see Eq. (5-10)), equal to 0, as appropriate for members with no properly closed stirrups.

Reference	test	L_s mm	b mm	h mm	d mm	$\rho_1=\rho_2$ (%)	ρ_v (%)	f_{yl} MPa	d_{bl} mm	d_{blv} mm	stirr. legs	d_{bw} mm	s mm	f_{yw} MPa	P_w (%)	f_c MPa	v	Type of jacket	t_j mm	f_{yj} MPa	θ_y (%)	θ_u (%)	$\theta_{u,nf}$ (%)	M_y kNm	V_y kN
Aboutaha et al. (1996) *	FC17	2743	458	458	420	0.96	0.00	414	25	0	2	10	400	276	0.086	18.2	0	W-SJ	6	400	1.20		5.00	708	258
Aboutaha et al. (1996)	FC11	2743	915	458	420	0.96	0.00	414	25	0	5	10	400	276	0.107	19.7	0	W-SJ	6	400	1.30	3.20		671	245
Aboutaha et al. (1996)	FC12	2743	915	458	420	0.96	0.00	414	25	0	5	10	400	276	0.107	22.5	0	W-SJ	6	400	1.50	5.50		647	236
Aboutaha et al. (1996)	FC9	2743	915	458	420	0.96	0.00	414	25	0	5	10	400	276	0.107	20.0	0	W-SJ	6	400	1.25	3.00		610	222
Aboutaha et al. (1999)	SC10	1220	458	915	875	0.48	0.96	414	25	25	2	10	400	276	0.086	16.5	0	W-SJ	6	400	1.00	4.00		1276	1046
Aboutaha et al. (1999)	SC11	1220	458	915	875	0.48	0.96	414	25	25	2	10	400	276	0.086	16.3	0	C-PSJ	6	400	0.85	2.00		896	734
Aboutaha et al. (1999) **	SC5	1220	915	458	420	0.96	0.00	414	25	0	5	10	400	276	0.107	15.5	0	Collars	?	?	1.40	3.20		570	467
Aboutaha et al. (1999)	SC6	1220	915	458	420	0.96	0.00	414	25	0	5	10	400	276	0.107	15.6	0	W-SJ	6	400	1.50	5.00		787	645
Aboutaha et al. (1999)	SC7	1220	915	458	420	0.96	0.00	414	25	0	5	10	400	276	0.107	20.3	0	B-SJ	6	400	1.00		6.50	652	534
Aboutaha et al. (1999)	SC8	1220	915	458	420	0.96	0.00	414	25	0	5	10	400	276	0.107	19.2	0	U-PSJ	6	400	1.00		7.00	652	534
Ghobarah et al. (1997)	S2	2550	510	610	580	0.23	0.23	440	15	15	4	6.4	150	490	0.166	24.0	0.08	G-SJ	3.5	280	1.18	6.30		383	150
Fuse et al. (1992)	C-11	500	250	250	220	1.60	1.92	396	16	16	2	4	100	396	0.100	27.6	0.25	G-SJ	1.6	291	0.45		1.75	90	180
Fuse et al. (1992)	C-12	500	250	250	220	1.60	1.92	396	16	16	2	4	100	396	0.100	29.0	0.25	G-SJ	1.6	291	0.45		2.50	90	180
Fuse et al. (1992)	C-21	500	250	250	220	1.60	1.92	396	16	16	2	4	100	396	0.100	26.3	0.25	G-SJ	3.2	265	0.45		1.90	90	180
Fuse et al. (1992)	C-22	500	250	250	220	1.60	1.92	396	16	16	2	4	100	396	0.100	27.5	0.25	G-SJ	3.2	265	0.45		2.10	90	180
Harries et al. (1996)	R1	750	300	500	460	0.98	0.10	437	25	10	2	10	225	447	0.233	36.3	0	G-SP	4.75	353	1.00	2.00		244	325
Harries et al. (1996)	R2	750	300	500	460	0.98	0.10	437	25	10	2	10	225	447	0.233	44.2	0	B-SP	4.75	353	0.96	2.40		264	352
Harries et al. (1996)	R3	750	300	500	460	0.98	0.10	437	25	10	2	10	225	447	0.233	44.3	0	B-SP	4.75	366	0.87	2.63		294	392
Aboutaha,Machado (1999) #	STHSRC1	1829	305	508	468	0.98	0.65	414	25	25	2	10	150	414	0.343	83.0	0	ST	8	352	1.20	7.50		306	167
Aboutaha,Machado (1999) #	STHSRC2	1829	305	508	468	0.98	0.65	414	25	25	2	10	150	414	0.343	83.0	0.12	ST	8	352	1.70		7.00	651	356
Aboutaha,Machado (1999) #	STHSRC3	1829	305	508	468	0.98	0.65	414	25	25	2	10	150	414	0.343	83.0	0.16	ST	8	352	1.80		8.00	735	402

L_s: shear span, b: section width, h: section depth, d: effective depth, ρ_1, ρ_2: tensile and compressive long. reinf. ratio, ρ_v: intermediate long. bars reinf. ratio, f_{yl}: yield strength long. reinf., d_{bl}: long. bar diameter, d_{blv}: intermediate long. bar diameter, d_{bw}: trans. reinf. diameter, s: trans. reinf. spacing, f_{yw}: yield strength trans. reinf., ρ_w: trans reinf. ratio, f_c: concrete strength, v: normalised axial load, t_j: steel jacket thickness, f_{yj}: steel jacket yield strength, θ_y: drift at yield, θ_u: ultimate drift, $\theta_{u,nf}$: ultimate drift of non-failed specimens, M_y: yield moment, $V_y = M_y/L_s$

Type of jacket : W-SJ : welded steel jacket, B-SJ : bolted steel jacket, G-SJ : grouted steel jacket, C-PSJ : C-shaped partial steel jacket, U-PSJ : U-shaped partial steel jacket, B-SP : bolted steel plates, G-SP : grouted steel plates, ST : steel tube

* reported strength value unrealistically high

** missing data for thickness and yield strength of steel jacket

\# reported elastic and yield deformations may have been affected by flexibility of specimen base

Table 5-7: Steel jackets: dimensions, reinforcement and jackets of test specimens, and key test results.

Copyright fib, all rights reserved. This PDF copy of fib Bulletin 24 is intended for use and/or distribution only by National Member Groups of fib.

Copyright fib, all rights reserved. This PDF copy of fib Bulletin 24 is intended for use and/or distribution only by National Member Groups of fib.

Quantity	No of data	Mean	Median	Coefficient of variation (%)
$M_{y,exp}/M_{y,pred.eq(5-8)}$	20	0.97	0.99	17.5
$\theta_{y,exp}/\theta_{y,pred.eq(5-2)}$	18	1.19	1.23	36
$(M_{y,exp}L_s/3\theta_{y,exp.})/(M_{y,pred.}L_s/3\theta_{y,pred.})$	17	0.88	0.80	31
$\theta_{u,exp}/\theta_{u,pred.eq(5-9)}$ failed specimens	12	0.90	0.79	43
$\theta_{u,exp}/\theta_{u,pred.eq(5-9)}$ non-failed specimens	9	1.12	0.95	35
$V_{y,exp}/V_{u,pred.eq(4-13)\ or\ (4-14)}$ failed specimens	11	0.56	0.55	42 (Eq. 4-13) or 46 (Eq. 4-14)
$V_{y,exp}/V_{u,pred.eq(4-13)\ or\ (4-14)}$ non-failed specimens	9	0.58	0.58	26 (Eq. 4-13) or 29 (Eq. 4-14)

Table 5-8: Mean, median and coeficient of variation of ratio of experimental quantities to predicted ones for concrete member alone (jacket considered only for shear, at 40%) .Steel jacketed specimens.

Comparison of the measured V_R and of the final chord rotation values to the ones predicted at shear-controlled or flexure-controlled failure, respectively, takes place separately for the groups of specimens carried to failure (those for which values are given in the column of experimental θ_u) and for those stopped before that (for which values are given in the column of experimental $\theta_{u,nf}$).

Statistics of the ratio of the experimental to the predicted value (mean, median, coefficient of variation) of the strength and deformation quantities referred to above are listed in Table 5-8. With the reservation of the small size of this data, the conclusions drawn from these statistics are the following:

- The steel jacket does not affect the yield moment of the column.
- The steel jacket adds to the shear strength of column at least equal to 40% of the shear force corresponding to yielding of the two sides of the jacket which are parallel to the direction of loading. With this 40% value, in none of the jacketed columns carried to (flexure-controlled) failure is the calculated shear resistance less than the measured value. Therefore, 40% of the ideal shear strength of the jacket is a conservative lower bound to the contribution of the steel jacket to shear strength.
- The jacket does not increase the elastic stiffness of the member (equivalently, it does not reduce its chord rotation at yielding). As a matter of fact, the jacketed columns in the tests of Table 5-7 exhibit an average elastic stiffness lower than the ideal value of the unretrofitted column without the jacket. This is clearly hard to rationalize. The most plausible guess is that of artificial flexibility of the test specimen or setup.
- The deformation capacity of the retrofitted columns that failed was on average about equal to the predicted value of the unretrofitted and poorly detailed column inside the jacket, as this value is controlled by flexure. It is reminded that the limited data on columns with "old" or "non-conforming" type of detailing suggest that such columns have an average deformation capacity 15% lower than similar columns with the same geometry and with reinforcement of the same amount but of proper detailing, which compares well with the mean of 0.9 and the median of 0.79 of the failed specimens in Table 5-7. The retrofitted columns that did not fail were carried to displacement demands above the theoretical capacity of the unretrofitted column. It seems, therefore, that the jacket improves slightly (through confinement or other means) the deformation capacity of the column, at least to the point of preventing shear failure and effecting a flexure-controlled one. Nonetheless, certain factors and phenomena possibly having to do with the interaction and the connection between the jacket and the column inside it, limit the effectiveness of the technique in enhancing deformation capacity.

A tentative conclusion on the basis of the limited experimental data summarized in Table 5-7 is that a steel jacket can be used to improve shear resistance and suppress failure of lap splices, without increasing much the strength, stiffness and deformation capacity of the original column, as these are controlled by flexure.

5.3.6.7 Recommendations for dimensioning and verification of steel-jacketed RC members in practical retrofit design

On the basis of the information presented above, the following recommendations may be made for dimensioning and verification of RC members (in particular columns or walls) retrofitted with steel jackets not continued to the member end:

Copyright fib, all rights reserved. This PDF copy of fib Bulletin 24 is intended for use and/or distribution only by National Member Groups of fib.

1) With a 25 to 50 mm gap provided between the end of the jacket and the member end (face of the joint or top of the foundation), the yield moment and flexural capacity of the jacketed member is that of the end section of the original member.
2) The shear capacity of the jacketed (part of the) member may be estimated as that of the original member plus the contribution of the jacket to shear resistance, $V_j=\eta\ A_j f_{yj} h$, where A_j = total cross-sectional area of steel jacket parallel to the direction of the shear, per unit length of the member (for a continuous thin plate or corrugated sheet, A_j is the total jacket thickness on the two column sides parallel to the shear force, while for a cage of corner angles and straps welded on them, A_j the total cross-sectional area of the straps per unit length of member); f_{yj} = yield strength of jacket steel; h = member cross-sectional depth parallel to the shear force; and η = jacket efficiency factor, with values between 0.4 and 1.0 (close to 0.4 for continuous thin plates or corrugated sheets, higher than 0.5 for straps or batten plates welded to corner bars). The shear capacity of the retrofitted column should exceed the shear force corresponding to development of the member flexural capacity, with adequate margin to take into account flexural overstrength due to steel strain hardening and concrete confinement (e.g. by 25%).
3) The thickness t_j of a continuous thin plate or corrugated sheet required for clamping deficient lap splices may be obtained according to the procedure proposed by Aboutaha et al (1996), as outlined in Sect. 2.2.5.4. More specifically: a) Eqs. (5-47), (5-48) may be applied, with symbols and variables as in the second half of Sect.5.3.6.4; b) the steel jacket length should exceed by about 50% that of the lap-splice; and c) if f_c is less than 28 or 35 MPa, respectively, on the long side of cross-sections with aspect ratio greater than 1.5:1 or 2:1, the steel jacket should be back-anchored into the column just above the splice region and at about one-third of the height of that region from the column bottom, with two bolts at each height at third-point of the column side.
4) The (secant-to-yield) stiffness of the retrofitted member may be taken equal to that of the original column (neglecting the effect of any deficient lap splices).
5) Flexure-controlled deformation capacity of the retrofitted member may be taken equal to that of the original member (again neglecting the effect of deficient lap splices, as this is corrected by the retrofitting). The positive effect of concrete confinement on concrete ultimate strain (see Eqs. (5-20), (5-22)) and ultimate curvature of the end section (Eq. (5.14)) may be taken into account, but can also be neglected in view of the lack of strong experimental confirmation. Nonetheless, for jackets other than corrugated sheets, the reduced effectiveness of confinement should also be taken into account (see Eq. (5-36), applicable for continuous thin plates with R = leg-width of corner angle, or Eqs. (5-44), (5-45) for cages of corner angles and cross-straps). It should be emphasized, though, that the available empirical expressions for plastic hinge length, L_{pl}, (e.g. Eqs. (5-23)-(5-26)) have been fitted to RC members without retrofitting and, unless verified for steel-jacketed members, should be used with great caution. Eq. (5-49) is another alternative, that should also be used with caution due the limited databank on which it was based and its very narrow scope.

5.4 Member-level retrofitting techniques – selective effect

As noted in Section 3.3.1.1, selective intervention techniques blend well with displacement-based approaches. With reference to Fig. 3-3, the possible intervention scenarios present different solutions, either by targeting the elastic stiffness of the structure, K_y, its strength, F_y, or its ductility, μ. Which solution is more economical and feasible depends on the case studied, considering both the structure characteristics and the displacement spectra for different damping levels. This view provides more degrees of freedom to the designers of intervention schemes. This argument serves to contrast methods of retrofitting that affect more than one response parameter simultaneously, with those intended for a controlled and selective effect on one parameter only, as described below.

5.4.1 Stiffness-only scenarios

RC structures subjected to small earthquakes may suffer significant stiffness reduction due to heavy cracking of concrete members. However, if concrete crushing and buckling of reinforcement bars do not occur, the flexural strength of the members will not necessarily be

Copyright fib, all rights reserved. This PDF copy of fib Bulletin 24 is intended for use and/or distribution only by National Member Groups of fib.

adversely affected. Hence, an effective intervention targeting stiffness of cracked members reinstatement without changing their strength is the more economical and logical approach.

A structure may have an irregular stiffness distribution, due to incorrect design approach, architectural constraints or due to the use of a more lenient code at the time of its construction. To upgrade such a structure in order to improve its behaviour or to make it comply with new modern code design criteria, a selective intervention that will enable the designer to concentrate uniquely on the parameter in question is required. Otherwise, if repair or retrofitting methods which affect not only the stiffness of the members but also their flexural capacity are applied, then a complete structural redesign is needed, resulting in a more costly and time-consuming solution.

5.4.2 Strength-only scenarios

New code design philosophy requirements or an increase in seismic loads can lead to a requirement for structural upgrading. If the structure had been designed according to conventional direct design principles, then altering the sequence of plastic hinge formation to achieve a predetermined failure mode (in harmony with the capacity design concept) becomes imperative. This will require an increase in strength of strategically located members. However, if the serviceability limit states are still met with the existing stiffness distribution, an increase in this parameter is not required. Furthermore, if the stiffness distribution is in accordance with code prerequisites, changes could result in code violation, thus full dynamic analysis and redesign would be required.

Adverse torsional effects caused by stiffness eccentricity are widely known and relatively well addressed in seismic codes, where they are considered in simplified approaches whenever possible. In contrast, strength eccentricity is not mentioned. In a study by Xian [1992], it was shown that the inelastic response is altered by this factor, resulting in an increase in ductility demand. Such a situation may arise, for instance, in a dual structural system, where in order to achieve stiffness symmetry, structural walls are used to balance the eccentric stiffness distribution. Since the relationship between strength and stiffness of both systems is by no means similar, even though their relative stiffness are in equilibrium, the strength distribution may be eccentric. Only a selective strength-only intervention can be effective in addressing such deficiency.

5.4.3 Ductility-only scenarios

This is probably the most common situation where selective intervention is required. Problems with lack of ductility supply may arise if the members are poorly detailed due to inappropriate design, inadequate construction or lack of sufficient code requirements, as was the case of old building regulations. The effects of such deficiency can be extremely hazardous since ductility plays a critical role in guaranteeing that a structure can deform without significant loss of strength, thus avoiding collapse.

Traditionally, for such cases, use of concrete jacketing is a popular solution, due to its ease of application and comparatively low cost. However, these retrofitting schemes, described above, are normally applied only at the lower floors of a building, where higher levels of ductility demand are expected, thus causing changes in the global behaviour of the structure that can be extremely disadvantageous. As a consequence of the large stiffness increase due to jacketing, the structure will attract higher seismic loads that the unstrengthened storeys may not withstand. Moreover, changing stiffness distribution in elevation may cause an increase in higher modes contribution to the deformed shape, rendering design according to simplified static analysis totally inadequate. Therefore, in the event of an earthquake, the retrofitted structure may suffer severe damage in its upper storeys, or even total collapse, as has already been observed in post-earthquake field investigations.

5.4.4 Design expressions for selective effects

5.4.4.1 Introduction

Extensive parametric analyses have been undertaken (Pinho, 2000) for the three repair/retrofitting tools of stiffness-only, strength-only and ductility-only interventions,

Copyright fib, all rights reserved. This PDF copy of fib Bulletin 24 is intended for use and/or distribution only by National Member Groups of fib.

leading to the development of design guidelines and expressions, as below. Whereas the figures and formulations are given for RC walls, they apply easily to columns, or indeed any flexure-dominated member. To evaluate the three fundamental design response parameters, the definitions described in Fig. 5-22 [Paulay & Priestley, 1992] is adopted. This elasto-plastic bilinear approximation for the force-displacement monotonic response of a reinforced concrete member has its principal application in design, where knowledge of the real inelastic behaviour of the member is not generally required. It is, therefore, most suitable for the objectives of the present work which, as mentioned earlier, focus on the development of practical analytical tools for redesign of RC structures.

The slope of the idealised linear elastic response, $K = S_y/\Delta_y$, is used to quantify stiffness. It is based on the effective secant stiffness to the real load-displacement curve at a load of about $0.75S_y$. An acceptable approximation is to calculate this point based on the first yield of reinforcement [Paulay & Priestley, 1992]. The yield value of the equivalent elasto-plastic response, i.e. the ideal or yield strength of the member, can thus be estimated as being S_y=1.33S'_y. Finally, a convenient quantity to evaluate the member ductility capacity is the ultimate displacement ductility, defined as $\mu_\Delta = \Delta_u / \Delta_y$, where Δ_u corresponds to member deformation at failure. The latter is evaluated when one of three ultimate criteria is attained; ultimate strain in the tensioned reinforcement bars, ultimate compression strain in the concrete or member resistance equal to $0.85S_y$. In the following sections, these definitions are used to calculate the design response parameters of the walls.

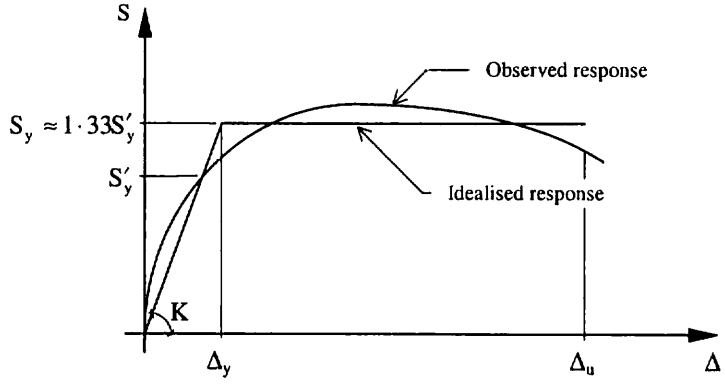

Fig. 5-22: Typical load-displacement relationship for a reinforced concrete element [Paulay & Priestley, 1992].

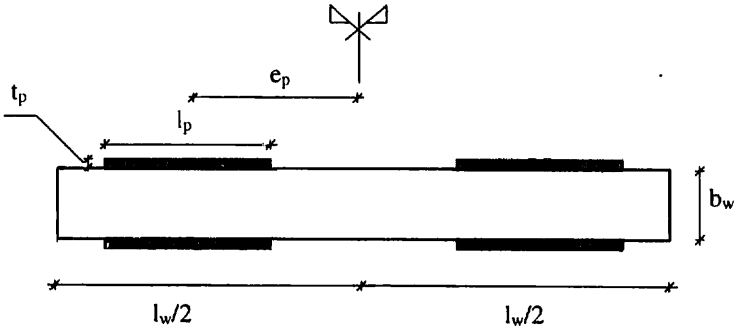

Fig. 5-23: Plate position and section dimensions for stiffness-only intervention

5.4.4.2 Stiffness-only intervention

A variable F_K, defined as the ratio between the upgraded/repaired and original/damaged stiffness of the member, is used to quantify the outcome of the intervention:

$$F_K = \frac{K^{upgraded}}{K^{original}} \tag{5-50}$$

The parameters needed to fully describe such a scheme are the height of the steel plates (h_p), their thickness (t_p), width (l_p) and distance to the geometric centre of the member cross section (e_p), as depicted in Fig. 5-23.

Copyright fib, all rights reserved. This PDF copy of fib Bulletin 24 is intended for use and/or distribution only by National Member Groups of fib.

(1) Height of the plate

For efficient stiffness-only intervention, the height of the plate should be greater than or equal to the expected flexural plastic hinge length. This will guarantee that the steel plates cover the area where severe cracking of the concrete is likely to occur.

In Fig. 5-24a the curvature distribution at maximum response of a RC flexural wall is illustrated and inelasticity is observed up to a height of about 40% of the full height of the wall (h_w). A stiffness improvement vs. height of steel plates plot resulting from the analysis of the same wall with different stiffness-only configurations is shown in Fig. 5-24 b. It is observed that increasing the height of the plates to values close to $0.5h_w$ has an important effect on the success of the intervention. However, from this point onwards, the effect of this parameter diminishes, as expected.

In the design expressions and curves derived, the plates are considered to be spanning the whole height of the column or wall. This is the most logical approach since, as shown in Fig. 5-24 b, it will provide maximum efficiency. Nevertheless, if a different solution is sought, Fig. 5-24 b can be consulted for guidance.

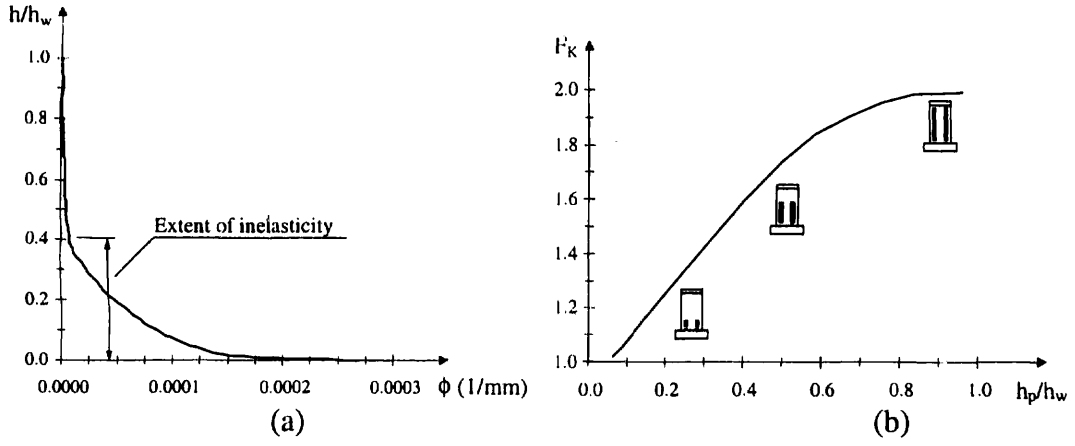

Fig. 5-24: (a) Curvature at maximum response; (b) Stiffness improvement vs. height of steel plates.

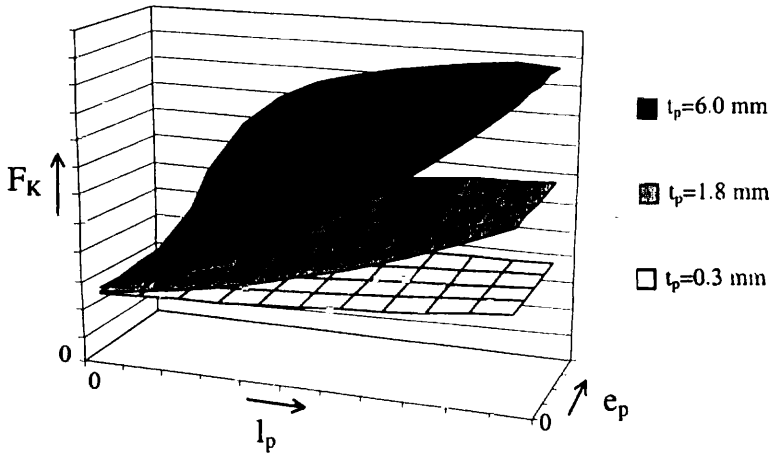

Fig. 5-25: Influence of plate dimensions and position in the wall

(2) Plate position and section dimensions

In Fig. 5-25, the influence of thickness, width and position of the steel plates on the stiffness parameter F_K is demonstrated. It is observed that increasing the dimensions of the steel plates and their distance from the symmetry axis of the column or wall will increase the effect of the intervention. This is expected since larger plates and eccentricity will increase the moment of inertia of the section and the effectiveness of crack arrest. However, the significance of such effect varies considerably with the values of these geometric parameters.

When steel plates are located close to the geometric centre of the section ($e_p \rightarrow 0$), the significance of their dimensions relative to this distance is great. Thus, wider plates will

Copyright fib, all rights reserved. This PDF copy of fib Bulletin 24 is intended for use and/or distribution only by National Member Groups of fib.

induce a higher stiffness improvement since they will cause an important geometric eccentricity effect. As the plates are placed further away from the wall symmetry axis, the narrower plates ($l_p \rightarrow 0$) will be more beneficial since it will be possible to achieve larger eccentricities. Hence, highest increases in the value of F_K are obtained in the range of smaller values of l_p. Such effect is clearly observed in Fig. 5-25, particularly for the surface corresponding to t_p=6.0 mm. Moreover, because flexural cracking is concentrated at the wall edges, having a thicker but narrower plate shifted to the sides is a more efficient way of gaining stiffness.

A non-dimensional parameter S_K, suitable for the characterisation of this intervention is derived. This includes both the wall and plates properties that are most likely to influence the intervention results, and is defined by:

$$S_K = constant \times \frac{A_p}{A_w} \times \frac{e_p}{l_w} = 100 \times \frac{4 t_p l_p}{b_w l_w} \times \frac{e_p}{l_w} = 400 \frac{t_p l_p e_p}{b_w l_w^2} \tag{5-51}$$

where A_p and A_w represent the total cross section area of the plates and wall, respectively.

From extensive analysis and comparison with tests, the values of F_K are plotted against the corresponding S_K in Fig. 5-26, where it is shown that a bi-linear polynomial fit to the data provides excellent results, with high coefficients of correlation (R^2). Further studies were carried out to include two additional parameters – reinforcement ratio (ρ_s) and normalised axial force (ν).

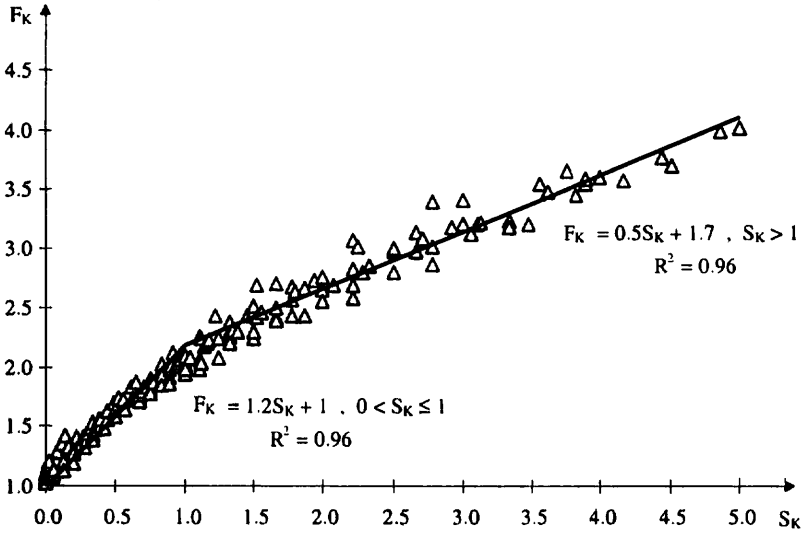

Fig. 5-26: Polynomial fit to stiffness-only results.

The former is defined by Eq. (5-51), where A_s represents the total area of longitudinal reinforcement in the wall, and was considered in the range of $0.4 \leq \rho_s \leq 4$ (%), as is generally adopted in design applications. The variable ν is defined by Eq. (5-53), where N stands for axial force and f_c' is the concrete compressive strength. For the purpose of this study, the value of ν was varied in the range of $0 \leq \nu \leq 0.10$, similar to commonly observed values in practice.

$$\rho_s = \frac{A_s}{b_w l_w} \tag{5-52}$$

$$\nu = \frac{N}{b_w l_w f_c'} \tag{5-53}$$

The final design expressions for this intervention is expressed as follows:

$$0 < S_K \leq 1 \qquad F_K = (1.2 S_K + 1)(1.1 - 3.2 S_K \nu) \rho_s^{-0.1 \ln(S_K) - 0.4} \tag{5-54}$$

$$S_K > 1 \qquad F_K = (0.5 S_K + 1.7)[1.1 - (0.16 S_K + 3)\nu] \rho_s^{0.01 S_K - 0.4} \tag{5-55}$$

Copyright fib, all rights reserved. This PDF copy of fib Bulletin 24 is intended for use and/or distribution only by National Member Groups of fib.

Both the design curves and expressions derived by regression analysis have a maximum coefficient of variation of 15% compared with results obtained by finite element analyses of a wide variety of walls. These results confirm that the parameters defined to characterise the selective intervention and the derived design expressions (or curves) appropriately account for all variables that most influence the effectiveness of this repair scheme.

5.4.4.3 Strength-only intervention

The variable F_S, defined as the ratio between the upgraded and original strength of the member, is used to quantify the effect of the intervention:

$$F_S = \frac{S^{upgraded}}{S^{original}} \tag{5-56}$$

In Fig. 5-27, a description of the relevant characteristics of this repair method is given. These are the distance of the external steel plates or re-bars to the edge of the wall (d_p), their cross section area (A_p) and yield strength (f_y^p).

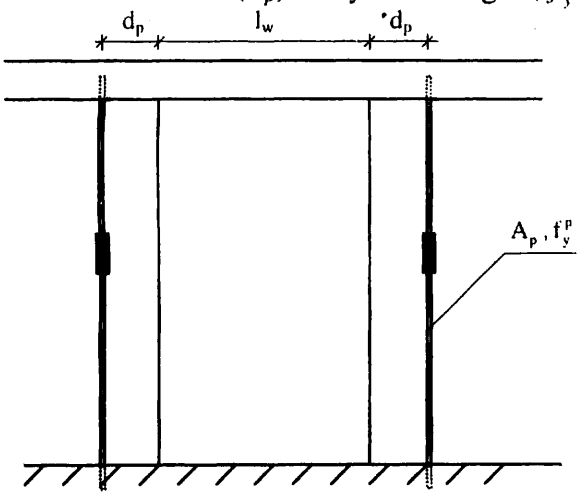

Fig. 5-27: Strength-only intervention parameters.

(1) Interaction delay mechanism (IDM)

The most critical parameter in this intervention is the value of the design gap (g_{IDM}) adopted in the delay mechanism. This value should be such that the strength-only intervention does not begin interacting with the structure too early, thus affecting the member stiffness, or too late, by which time significant damage may have occurred (Fig. 5-28). Moreover, when the mechanism starts contributing to the flexural resistance at a late stage, two levels of ductility are created; a difficult situation to address in the light of current definitions of ductility.

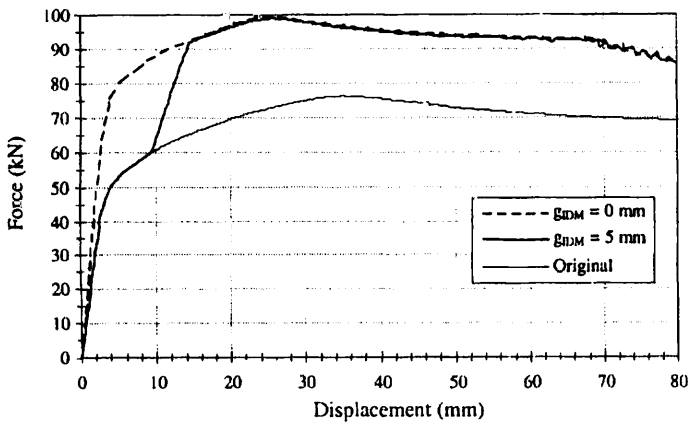

Fig. 5-28: Influence of g_{IDM} on the response of the strengthened wall.

Copyright fib, all rights reserved. This PDF copy of fib Bulletin 24 is intended for use and/or distribution only by National Member Groups of fib.

If an idealised bilinear load-displacement relationship is considered, then a simple way of evaluating the design gap for the IDM may be derived. This should be designed to allow the mechanism to contribute to the flexural resistance at a point somewhere between the first yield strength (S'_y) and the global yield strength (S_y) of the wall. In this manner, the original stiffness will be maintained and the dynamic characteristics of the member will remain unaltered.

An estimate of the vertical displacement at the edges of the wall for these two loading stages is required for the determination of the design gap. This may be achieved by calculating the rotation (θ) and the neutral axis depth (c) at the top of the wall. If these values are known, then the vertical displacement in the external plates or re-bars (Δ^v_p) is given by:

$$\Delta^v_p = (d_p + l_w - c)\theta \tag{5-57}$$

From section analysis the value of curvature at the point of first yield (ϕ'_y) and the corresponding neutral axis depth (c'_y) can easily be determined at the foundation level. At this loading stage, it is also possible to assume the latter (c'_y) as constant throughout the height of the wall, whilst the curvature varies linearly. Finally, taking into consideration the relationship between S_y and S'_y, suggested earlier, an upper and a lower bound on the design gap of the delay mechanism is defined by:

$$(d_p + l_w - c'_y)\phi'_y \frac{h_w}{2} \le g_{IDM} \le (d_p + l_w - c'_y)\phi'_y \frac{h_w}{1.5} \tag{5-58}$$

Alternatively, simplified methods of seismic design in which a behaviour factor is used to obtain the design load, i.e. the ideal or global yield strength of a reinforced concrete member (S_y), can also be used to obtain the upper bound on the IDM gap value. In this way, the design of the strength-only mechanism would be consistent with the member original design philosophy. By describing the curvature at the base of the wall as:

$$\phi_d = \frac{M_d}{E_c I_e} = \frac{F_d h_w}{E_c I_e} = \frac{F_e h_w}{q E_c I_e} \tag{5-59}$$

where F_e represents the elastic horizontal load, q stands for behaviour factor and I_e is the equivalent moment of inertia of the cross section at first yield in the extreme fibre, and substituting (Eq.5-59) in (5-58), the following alternative expression can be used to define the value of g_{IDM}:

$$(d_p + l_w - c'_y)\phi'_y \frac{h_w}{2} \le g_{IDM} \le \frac{F_e h_w^2}{2 q E_c I_e}(d_p + l_w - c_d) \tag{5-60}$$

It is important to note that these expressions are derived from principles which apply to monotonic loading only. Under cyclic loading regimes, cumulative plastic deformations may lead to uncertainties regarding the vertical elongation of the wall. These factors cannot be addressed by the expressions suggested above. Further, because these expressions are derived assuming linear curvature distribution at point of first yield, their application in design situations where such an assumption is not valid (for instance, high axial load), will produce slightly inaccurate results.

(2) Distance to the member edge

The external steel plates or re-bars contribute to the flexural strength at the location of their longitudinal axes. A force criterion can thus be used to define the strength increase due to the intervention. The distance to the member edge of the external strengthening mechanism should also be considered when designing these intervention schemes. The use of large re-bars very close to the wall will cause a significant decrease in ductility since the gain in extensional deformation capacity caused by the intervention is not balanced on the compressive side. Hence, the concrete will be subjected to higher compressive strains and eventually the member will fail earlier due to concrete crushing.

In Fig. (5-29), the analytical response of two identical RC walls with different configurations of strength-only intervention is shown. Although both walls exhibit identical strength enhancement, their ductility is completely different. Larger distances between the external mechanism and the wall lead to significantly less reduction in ductility than the opposite scenario. Hence, such configuration should be applied in the upgrading of members

Copyright fib, all rights reserved. This PDF copy of fib Bulletin 24 is intended for use and/or distribution only by National Member Groups of fib.

in which available ductility does not comply with the demands arising from a 'short-distance' strength-only intervention. Moreover, its applicability is still feasible, particularly if there are infill panels on both sides, since the external mechanism can be located at a greater distance embedded in the infill panel without adverse architectural effects.

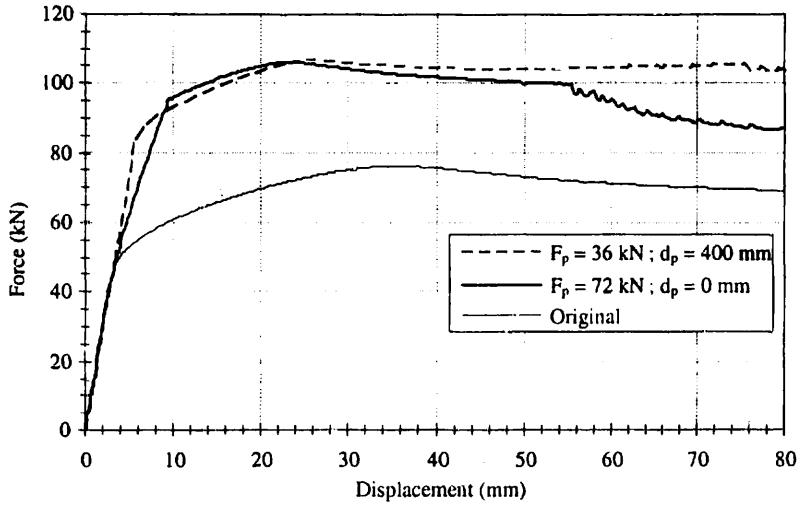

Fig. 5-29: Influence of d_p on the response of the strengthened wall.

(3) Design expressions

A single parameter that enables a clear representation of the factors influencing the effectiveness of this scheme is derived. In this case, both the member and external plates material properties are of importance, and were included in the strength-only selective intervention parameter S_S, defined as

$$S_S = constant \times \frac{A_p f_y^p}{A_s f_y} \times \frac{d_p + l_w/2}{l_w} = 10 \frac{A_p}{A_s} \frac{f_y^p}{f_y} \frac{d_p + l_w/2}{l_w} \tag{5-61}$$

where f_y represents the yield strength of the longitudinal reinforcement of the wall.

In Fig. 5-30, the polynomial fit to the results of the parametric investigations without axial load is shown. A global correlation factor of 0.97 indicates the adequacy of the linear regression used.

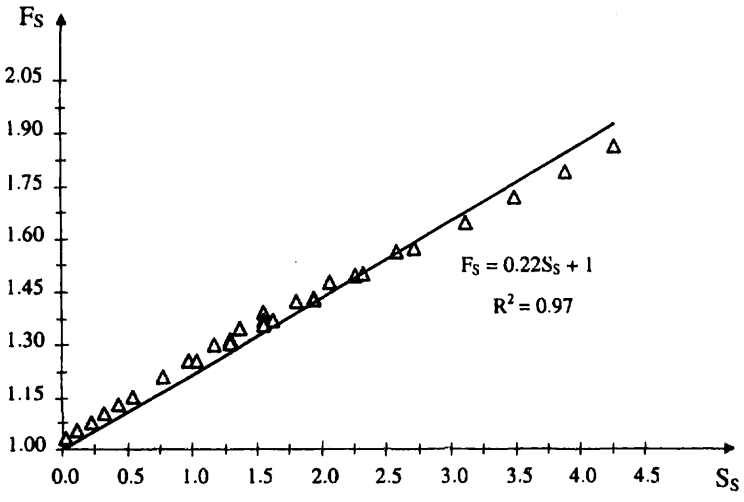

Fig. 5-30: Polynomial fit to strength-only results.

The final design expression, which includes the variables discussed above alongside the influence of axial load, is given as:

Copyright fib, all rights reserved. This PDF copy of fib Bulletin 24 is intended for use and/or distribution only by National Member Groups of fib.

$$F_S = \left(1 + 0.22 S_S\right)\left(1 - 0.65 S_S^{0.4} v\right) \tag{5-62}$$

The results obtained by Eq. (5-62) compare well with the values given by finite element analysis of several different RC walls, giving a maximum coefficient of variation of 4%.

5.4.4.4 Ductility-only intervention

It is not be feasible to address this intervention scheme in a manner similar to the procedure adopted for the two previous cases. Relating the physical characteristics of this intervention to the global ductility increase is neither practical nor effective. The uncertainties in the definition of yield and failure criteria would not allow the development of a simple and accurate design procedure. Instead, an approach similar to that widely used in the design of reinforced concrete members confined with internal steel hoops is followed. In this procedure, the concrete stress-strain relationship is changed by the application of a confinement factor dependent on the configuration of the stirrups and dimensions of the section. Accordingly, the ductility-only selective intervention parameter (k_D), described by Eq. (5-63), is defined as the ratio between the externally confined and unconfined concrete compressive strength, respectively f'_{cc} and f'_c.

$$k_D = \frac{f'_{cc}}{f'_c} \tag{5-63}$$

(1) Design expression

This intervention technique requires the definition of three geometric variables, namely the thickness of the plates (t_p), their height (h_p) and spacing (s_p), together with the bolt prestressing force (P_b) as shown in Fig. 5-31.

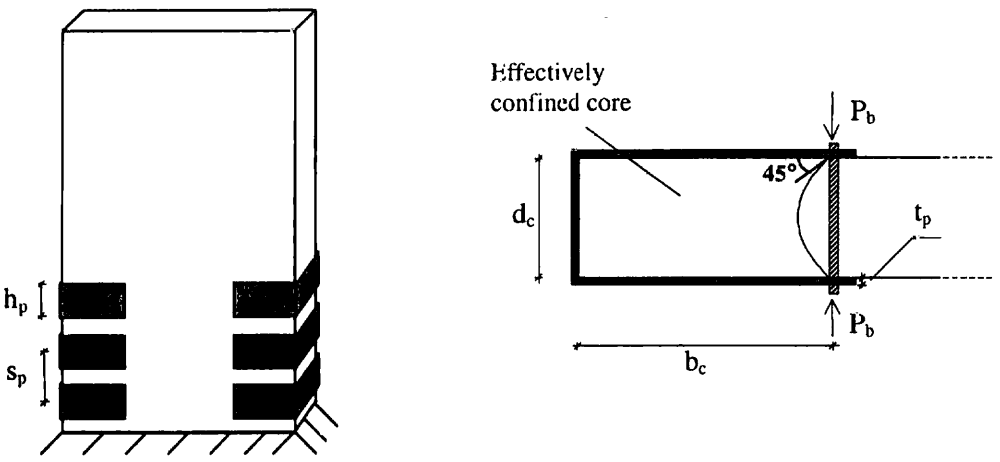

Fig. 5-31: Ductility-only intervention parameters.

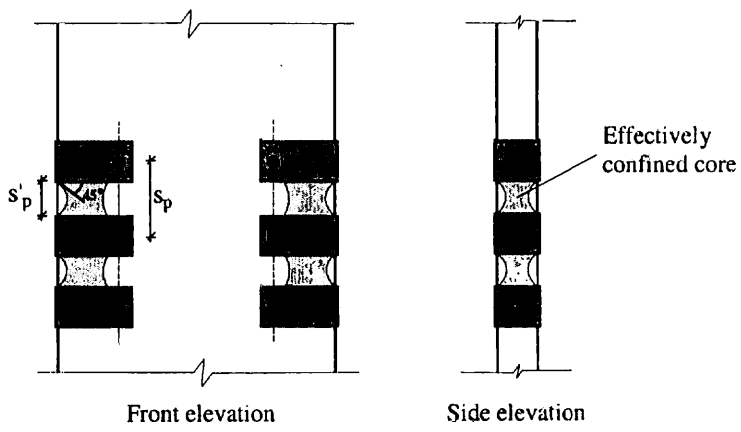

Fig. 5-32: Effectively and ineffectively confined core.

Copyright fib, all rights reserved. This PDF copy of fib Bulletin 24 is intended for use and/or distribution only by National Member Groups of fib.

A simplified methodology to evaluate k_D based on the approach proposed by Mander *et al.* [1988], is followed. Although the latter was initially developed for circular or rectangular internal steel hoops, an adaptation to the ductility-only technique is undertaken below. The discontinuities between plates and, more importantly, those caused by the presence of a bolt as the fourth closing side of the external confinement system, were studied by the use of formulations for soil and rock mechanics [Poulos & Davis, 1974]. The analysis of the path of the compression confinement stresses between plates and bolts leads to the conclusion that an arching effect similar to that suggested by Mander *et al.* [1988], can be used to obtain the limits of the effectively confined concrete core in this intervention. Hence, the following assumptions are made:

- the U-shape steel plates are stiff enough to avoid being pushed outwards due to lateral confinement pressure, therefore reduction in plan of the effectively confined concrete core due to arching occurs only in the vicinity of the closing bolt (as in Fig. 5-31);
- in elevation, reduction of effectively confined concrete core occurs due to arching effects between consecutive external plates and bolts, as shown in Fig. 5-32;
- the arching effects are modelled as second-degree curves with an initial tangent of 45°;
- the prestressed bolt is capable of fully transmitting the lateral confining pressure to the steel plates, thus representing adequately a closed hoop behaviour of the whole assembly, albeit locally.

Consequently, the effectively confined concrete core area (A_e) at the most unfavourable location (midway through two consecutive plates) is given by:

$$A_e = \left(b_c d_c - \frac{d_c^2}{6}\right)\left(1 - \frac{s_p + s'_p}{4b_c}\right)\left(1 - \frac{s'_p}{2d_c}\right) \tag{5-64}$$

and the confinement effectiveness coefficient becomes:

$$k_e = \frac{A_e}{A_{cc}} = \frac{\left(1 - \frac{d_c}{6 \cdot b_c}\right)\left(1 - \frac{s_p + s'_p}{4b_c}\right)\left(1 - \frac{s'_p}{2d_c}\right)}{(1 - \rho_{cc})} \tag{5-65}$$

with ρ_{cc} representing the ratio of longitudinal reinforcement to the confined concrete core area (A_{cc}).

The prestressed bolt is designed to act as the fourth side of the external hoop, capable of transmitting the lateral stresses to the steel plates. To guarantee equilibrium of confining stresses, the bolt should be designed so as to assure that its axial capacity equals that of the opposite plate. This may involve the use of a prestressing force such that

$$f_y^p A_p = f_y^b A_b + P_b \tag{5-66}$$

where A_b and A_p represent the cross section area of the bolt and steel plate, respectively, whilst their yield strength values are f_y^b and f_y^p respectively.

Since k_e takes into account all the discontinuities present in this scheme, and the bolt is designed to ensure a closed hoop behaviour of the whole assembly, the effective section area ratios of transverse reinforcement (ρ_x and ρ_y) can be defined by:

$$\rho_x = \frac{2A_p}{d_c s_p} = \frac{2h_p t_p}{d_c s_p} \tag{5-67}$$

$$\rho_y = \frac{2A_p}{b_c s_p} = \frac{2h_p t_p}{b_c s_p} \tag{5-68}$$

By virtue of force equilibrium between the lateral confinement stress resultants and the tension forces in the plates, the effective lateral confining stresses (f'_{lx} and f'_{ly}) are determined by:

Copyright fib, all rights reserved. This PDF copy of fib Bulletin 24 is intended for use and/or distribution only by National Member Groups of fib.

$$f'_{lx} = k_e \rho_x f_y^p \tag{5-69}$$

$$f'_{ly} = k_e \rho_y f_y^p \tag{5-70}$$

Finally, by using the general solution curves described in the work of Mander *et al.* [1988], the ductility-only selective intervention parameter k_D can be determined, and the stress-strain relationship of the concrete is then adjusted to incorporate the effect of the intervention. As mentioned earlier, this approach is equivalent to methods currently used in the design of reinforced concrete members confined with internal steel hoops. Hence, its application in design situations is equally practical and straightforward.

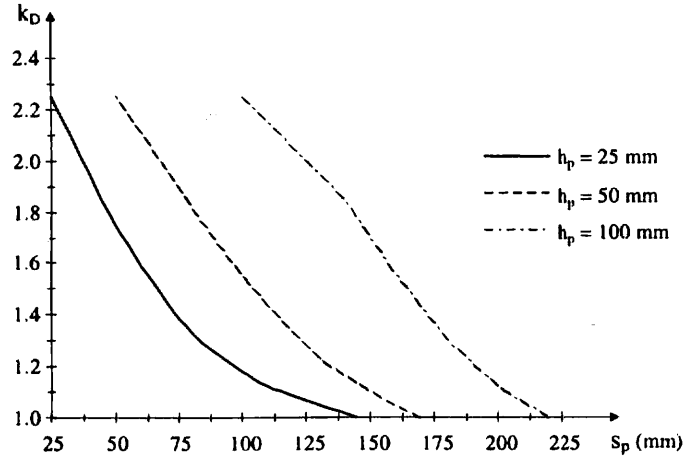

Fig. 5-33: Influence of s_p in the ductility-only intervention parameter.

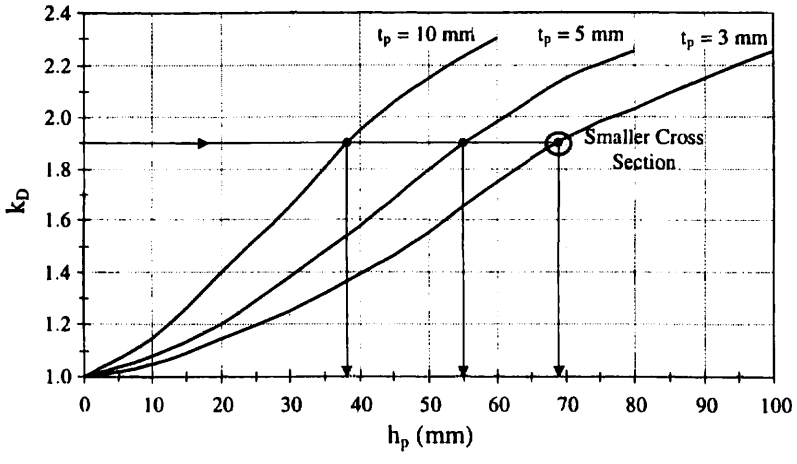

Fig. 5-34: Effect of t_p and h_p in the ductility-only intervention parameter.

(2) Thickness, height and spacing of the steel plates

In Fig. 5-33, it is observed that the smaller the spacing, the higher the confinement level achieved by the intervention. Nonetheless, in order to avoid changes in stiffness, a sensible spacing should be left between plates to minimise crack arrest.

In addition to the decrease in spacing of the plates, an increase in the effect of this selective scheme can also be obtained by means of greater height or thickness of the plates. However, results from analyses on retrofitted walls in which these two parameters are varied lead to the conclusion that the most effective way of enhancing ductility with this type of external intervention is by increasing the height of the plates, not their thickness.

In Fig. 5-34, it is shown that if, for instance, a target confinement ratio is set as $k_D = 1.9$, then using thickness of 10, 5 and 3 mm, will result in heights of 38, 55 and 69 mm, leading to a steel plate section area of 380, 275 and 207 mm^2, respectively. Therefore, using wide plates

Copyright fib, all rights reserved. This PDF copy of fib Bulletin 24 is intended for use and/or distribution only by National Member Groups of fib.

closely spaced is the most efficient way of achieving a confinement factor that will satisfy a target ductility. This, however, may affect stiffness.

5.5 Structure-level retrofitting techniques

Global intervention methods may represent a more cost-effective strategy than universal upgrading of the existing components, especially if the disruption of occupancy and the demolition and replacement of partitions, architectural finishes and other non-structural components are considered (Fardis, 1998). This is particularly true for structures where no transverse load path is available, or in the case of high flexibility systems. In such cases the methods described below may indeed provide a feasible strengthening solution.

5.5.1 Addition of new RC walls

5.5.1.1 Introduction

One of the most common methods used for strengthening of existing structures is the provision of additional shear walls. These are extremely efficient in controlling global lateral drifts, thus reducing damage in frame members. It should be born in mind, though, that due to the large cross-sectional dimension of the walls, their own deformation capacity (expressed in terms of chord rotations, curvatures or storey drifts), is inherently smaller than that of slender frame members.

Configuration and dimensioning of new walls. Connection to existing members

The most convenient way to introduce new shear walls is by infilling fully or partly strategic bays of the existing frame. If the wall takes up the full width of a bay, then it incorporates the beams and the two columns, the latter acting as its boundary elements. In that case only the web of the new wall needs to be added, sometimes by shotcreting against a light formwork or a partition wall to be encapsulated within the core of the web. In the latter case, shotcrete is normally used for increase adherence between the existing and added material. Precast panels may also be used to reduce time and disruption.

Full continuity between different levels of the wall increases strength, whilst proper anchorage of re-bars to delimiting beams and closely spaced mesh provides high deformation abilities. Special connectors need to be attached to the existing beams and columns all around the infilled panel, to fasten the new web to the frame members. Both the fastening of these connectors to the existing members and their extension into the new concrete should be proportioned for the transfer of the web shear and of the tensile capacity of the web reinforcement to the frame members. Poor detailing and lack of proper load-path between old and new members may lead to global ductility reduction or brittle failure of infill panels.Test results by Kahn and Hanson (1979) on single-bay one-storey 1:2 scale frames infilled with a cast-in-place or precast web panels to form a squat wall, show the sensitivity of the strength and dissipation capacity of shear-critical walls to the details of the shear connection between the frame and a thinner infilling panel. Frosch et al (1996) infilled a two-storey single bay 2:3 scale frame with smaller-size precast concrete panels and used steel pipes embedded in the frame members as shear lugs at the interface. In addition to acting as dowels, steel pipes through the depth of the beams allowed passage of continuous vertical wall reinforcement.

Preferably the new wall should be sufficiently thick to encapsulate the existing beams and columns. In that case holes and slots should be drilled through the slab, for the vertical bars to pass from one storey to the next. The concrete filling these slots acts as a shear key between the new wall and the slab. Obviously, new walls thick enough to encapsulate the frame members should be cast from the top through the holes and slots cut into the slab for the passage of vertical steel. Regardless of whether the new wall encapsulates the existing beams or not, it may have to encapsulate the existing columns for another reason: existing columns normally do not have sufficient deformation capacity, due to lack of confining reinforcement, short lap splices, etc. Then a cast-in-place or a shotcrete jacket needs to be constructed around them, with new longitudinal and transverse steel (see Fig. 5-35 (a) for an example). The jacket needs to be continuous from storey to storey through the slab, for continuity of longitudinal bars, etc. Sometimes it is also connected to the existing column through epoxy-grouted

Copyright fib, all rights reserved. This PDF copy of fib Bulletin 24 is intended for use and/or distribution only by National Member Groups of fib.

dowels, installed in it at about 0.5m centres. Nonetheless, as already noted in the section on concrete jackets of columns or walls, such dowels are not essential and sometimes they may have adverse local effects for the integrity of the concrete overlay.

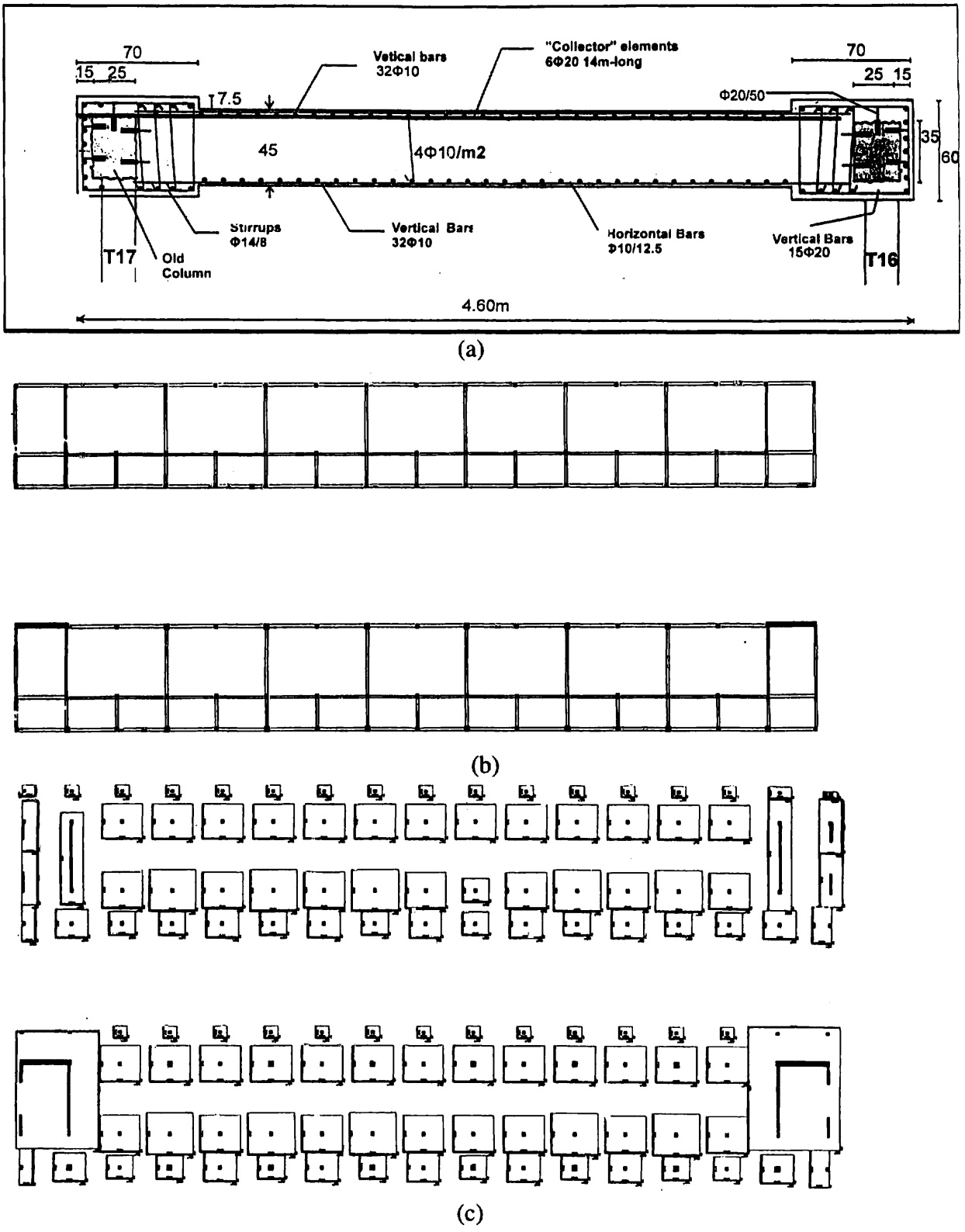

Fig. 5-35: 3-storey building strengthened in long direction by adding two RC walls: (a) cross-section of added wall; (b) plan of framing, before (top) and after retrofitting (bottom); c) foundation plan, before (top) and after retrofitting (bottom).

Copyright fib, all rights reserved. This PDF copy of fib Bulletin 24 is intended for use and/or distribution only by National Member Groups of fib.

Added walls are typically designed and detailed as in new structures, i.e. for flexural plastic hinging only at their base. To this end, in the plastic hinge zone at the base they are provided with boundary elements at the ends of the section, well-confined and detailed for flexural ductility. They are also capacity-designed in shear throughout their height (see also the discussion on dimensioning of collectors at the end of this section) and overdesigned in flexure above the plastic hinge region, to ensure that inelasticity or pre-emptive failure will not take place elsewhere in the wall before plastic hinging at the base and that the new wall will remain elastic above the plastic hinge zone.

Application of this technique to a single or a few previously damaged storey(s), may cause hazardous strength irregularities. This was shown by the response of a three-storey building repaired with shear walls at the first storey only, after being damaged by the 1968 Tokachi-oki earthquake. As reported by Nakano (1995), the structure suffered heavy damage at the second storey, when subjected to a subsequent event, in 1994.

The transfer of inertia forces from the floors to the new walls needs to be assured. A wall created by infilling a bay of a frame can be considered as adequately connected to the floor diaphragms if it encapsulates existing beams and columns, or if web panels are adequately fastened around their perimeter to the frame members and the floor slab is monolithically connected with the existing beams. In general, though, "collector" elements may need to be placed and proportioned for the transfer of floor inertia loads to the new walls. As these walls are often placed at the perimeter of the building with their long dimension parallel to it, collectors can be in the form of steel ties along the perimeter, with one end embedded into the web of the new wall at floor level. These ties can be fastened to the side of the perimeter beams and should be long enough to collect the inertia forces from the diaphragm see (Fig. 5-36 for an example). Fastening to the side of the beams can be effected by welding the tie on steel plates anchored to the web of the perimeter beam. The collectors and their anchorage onto the perimeter beams may be covered with a thin shotcrete layer for protection. They should be dimensioned for seismic action effects which are based on capacity-design considerations and account also for higher-mode effects. The magnification factor to be applied on the seismic loads transferred from the floor to the new wall according to the analysis for the seismic action, should be at least equal to that provided by Eurocode 8 for the derivation of the design shear force of new walls of Ductility Class H. That factor depends on the ratio of the wall (overstrength) flexural capacity at the base to the wall bending moment there from the analysis, as well as on a semi-empirical correction accounting for higher-mode effects after plastic hinging at the base. Nonlinear response-history analyses of dual (wall-frame) systems have shown that such higher-mode effects on peak floor forces are much larger than on storey shears (which are the cumulative effect of floor forces).

5.5.2 Foundation issues for added walls

Every new wall should normally be provided with a corresponding foundation element. A serious problem to be solved is the transfer of the large overturning moment of the new wall to the foundation. So, a drawback of the method is the need for strengthening the foundations to resist these increased overturning moments. This type of work is usually costly and quite disruptive thus rendering the application of this technique unsuitable for buildings without an existing adequate foundation system.

Even when the new wall is created by infilling a bay of a frame, in which case the new foundation element encapsulates the ones of the two columns of the bay, the vertical load transferred to the soil is disproportionately low in comparison to the wall overturning moment. This will result in large uplifting and large rocking rotations of the foundation element, which reduce the overturning moment well below the value calculated assuming a constant foundation impedance. Rocking of the wall at the base will increase considerably lateral drifts at floor levels and will reduce the effectiveness of the new wall in protecting existing elements from large deformation demands. More specifically, although the wall may continue acting as a stiff vertical spine preventing formation of a storey mechanism, it will induce high chord rotation demands on the beams of the system, especially on those directly framing into the wall within its plane (such chord rotations will be about equal to the rotation of the base of the wall with respect to the ground). These beams may be unable to resist such demands, especially if they are not retrofitted too.

Copyright fib, all rights reserved. This PDF copy of fib Bulletin 24 is intended for use and/or distribution only by National Member Groups of fib.

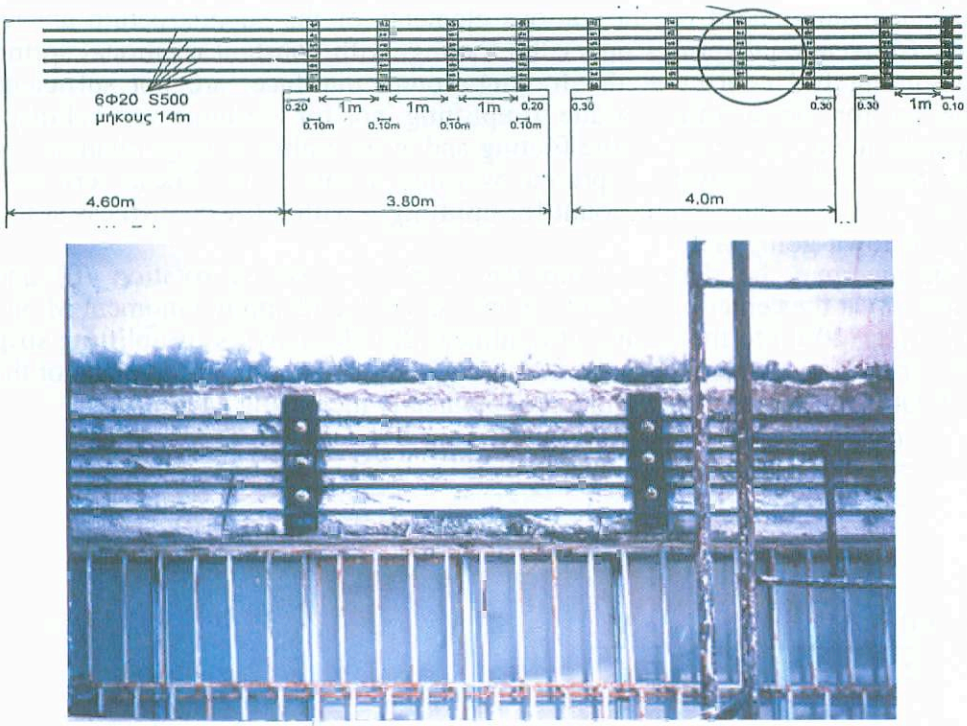

Fig. 5-36: Collector element for concrete walls of Fig. 5-35, fastened to side of perimeter beams.

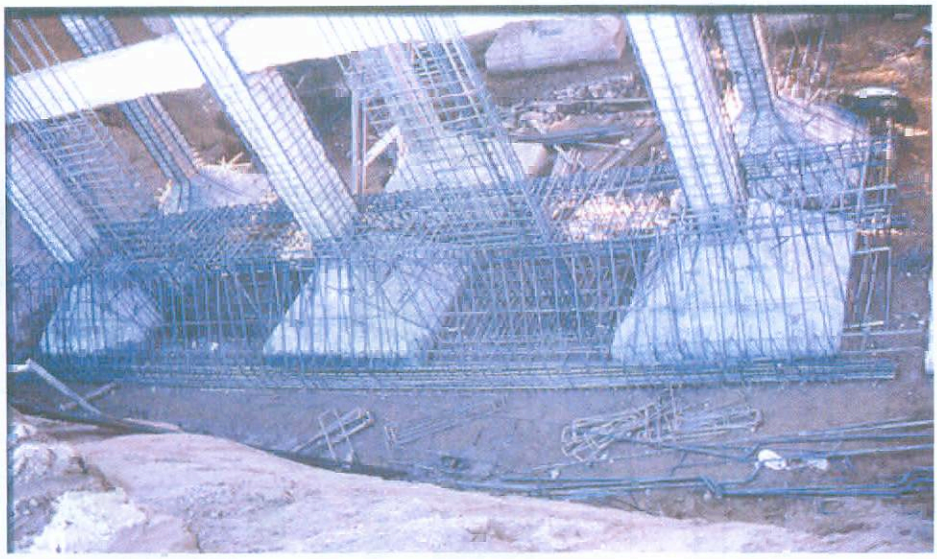

Fig. 5-37: New wall founded on foundation beam encapsulating footings of neighbouring columns

To allow the wall to play its intended role, it is essential to reduce the uplift and rocking of its foundation element. This can be achieved by one or more of the following: a) by increasing the size of the new footing in plan, in order to increase its weight and the impedance of the underlying soil and/or to encapsulate footings of neighbouring columns and mobilize their vertical load against the uplift (see Fig. 5-35(c) for an example); b) by connecting the new foundation element to neighbouring ones through stiff and strong grade- or tie-beams (see Fig. 5-37 for an example); or c) by providing micropiles or other tension anchors as hold-down devices for the new foundation element. Implementation of any of these solutions is quite costly and disruptive and acts as a disincentive against adding new walls to buildings which do not have already a stiff and strong (almost storey-high) foundation beam around the perimeter, to which a new wall could be conveniently connected.

Unless rocking of the new wall is effectively prevented by means such as those listed under b) and c) above, it should be appropriately modeled in the analysis, so that its effects on

Copyright fib, all rights reserved. This PDF copy of fib Bulletin 24 is intended for use and/or distribution only by National Member Groups of fib.

the seismic demands placed on the various elements of the superstructure are realistically estimated. Conventional springs under the footing, with constant rotational spring stiffness derived assuming full contact at the footing-ground interface, are not sufficient, as they account neither for spring softening due to uplifting, nor for the large vertical displacements caused by uplifting at the center of the footing and at the uplifting edge relative to the down-going one. Such effects may be captured by using a pair of nonlinear vertical springs at opposite ends of the footing that account for uplifting – with a lower stiffness at the uplifting relative to the down-going end.

Such springs may be derived from the relations between rotation (θ) and vertical displacement (z) at the center of the footing on one hand, and applied moment M on the other, fitted by Cremer (2001) to the results of nonlinear 2D FE analyses of uplifting strip footings over elastic or inelastic ground. If B denotes the width of a footing in the plane of the rocking, the secant relations between θ or z and a monotonically increasing M are:

$$\theta = \frac{\theta_o}{2 - \frac{M}{M_o}} \tag{5-71}$$

$$z = \frac{B\theta_o}{2}\left[\frac{\frac{M}{M_o} - 1}{2 - \frac{M}{M_o}} + \ln\left(2 - \frac{M}{M_o}\right)\right] \tag{5-72}$$

In Eqs. (5-71), (5-72) M_o denotes the moment at which uplifting starts and $\theta_o = M_o/K_{\theta o}$ the associated (elastic) rotation, derived from M_o through the elastic rotational impedance $K_{\theta o}$ of a footing with full contact with elastic ground.

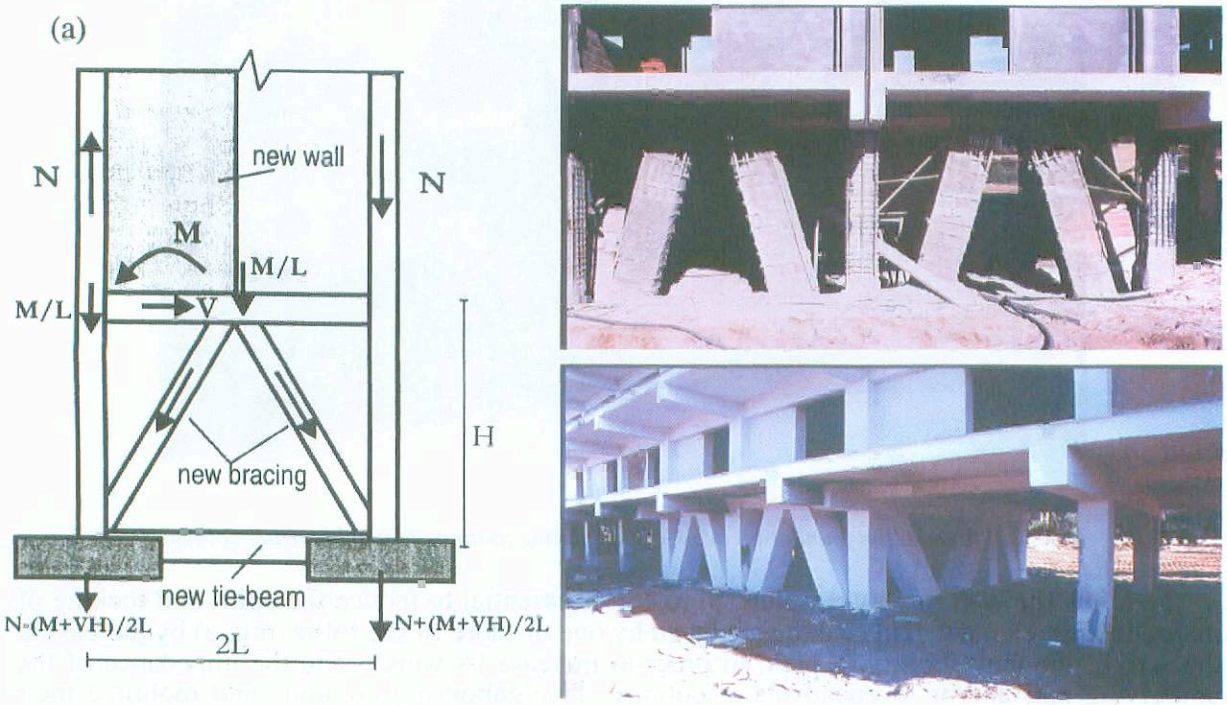

Fig. 5-38: Foundation of new wall through diagonal concrete braces: (a) transfer of wall forces to ground; (b) shotcreting of braces and of columns jackets; (c) retrofit completed.

The vertical load N at the base of the (new) wall is typically very low relative to the bearing capacity of the (concentric) footing, N_u, and then the value of M_o on elastic ground is approximately equal to:

Copyright fib, all rights reserved. This PDF copy of fib Bulletin 24 is intended for use and/or distribution only by National Member Groups of fib.

$$M_o \approx 0.25BN \tag{5-73}$$

A more accurate approximation for higher values of N is:

$$M_o \approx 0.25BN\exp\left(-2.5\frac{N}{N_u}\right) \tag{5-73 a}$$

The secant relation between the force F=M/B at the two nonlinear vertical springs at the ends of the footing and the associated vertical displacements there are:

At the uplifting edge ($\delta_1>0$):

$$\delta_1 = \frac{B\theta_o}{2}\left(\frac{\frac{FB}{M_o}}{2-\frac{FB}{M_o}} + \ln\left(2-\frac{FB}{M_o}\right)\right) \tag{5-74 a}$$

and for the downwards displacement ($\delta_2>0$) at the opposite end:

$$\delta_2 = \frac{B\theta_o}{2}\left(1-\ln\left(2-\frac{FB}{M_o}\right)\right) \tag{5-74 b}$$

giving tangent stiffnesses:

$$\frac{dF}{d\delta_1} = \frac{2K_{\theta o}}{B^2}\frac{\left(2-\frac{FB}{M_o}\right)^2}{\frac{FB}{M_o}} \tag{5-75 a}$$

and

$$\frac{dF}{d\delta_2} = \frac{2K_{\theta o}}{B^2}\left(2-\frac{FB}{M_o}\right) \tag{5-75 b}$$

If the axial load N is low in comparison to N_u, there is very little hysteresis in cyclic loading, and Eqs. (5-74) and (5-75) may be applied also for nonlinear response-history analysis, considering the springs as nonlinear elastic ones.

An ingeneous system that has been used in Greece (Tsicknias and Pittas, 1992) to mitigate the problem of the transfer of the overturning moment of new walls to the soil without large uplift and base rotations, is to construct a new wall over half the bay width L of the frame and to replace the new wall at the bottom storey with a Chevron concrete bracing (i.e. one consisting of two braces meeting at beam midspan) and a tie-beam connecting the existing spread footings of the two columns of the bay (Fig. 5-38 a). Then the overturning moment M at the base of the new wall, i.e. at the floor level above the Chevron bracing, is resolved into a couple of vertical forces equal to 2M/L. One of these forces is applied to the joint of the Chevron bracing at beam midspan and is transferred to the two tied footings, through tension or compression forces in the two braces. The end result is a couple of concentric vertical forces on the existing footings, each force equal to ±M/L, and an axial force in the tie-beam. The axial load N in the existing footing prevents uplift until the moment M at the base of the wall reaches a value: M=NL, which is much larger than the uplift resistance of a footing enlarged to accommodate the new wall along with the existing column. The base rotation, equal to the difference in the settlement of the two footings divided by their distance L, is also much less, and the effectiveness of the new wall in limiting lateral drifts is increased. Implementation of this scheme normally requires also (shotcrete) jacketing of the ground storey beam and the two columns to accommodate the internal forces associated with the action of the Chevron bracing and also the connection of the beam and columns with the braces, the tie-beam and the possible enlargement of the two existing footings (Fig. 5-38).

5.5.3 The special case of external buttresses

To reduce or eliminate disruption to the use of a building, external buttresses may be constructed to increase the lateral resistance of the structure as a whole. An example of such a scheme is shown in Fig. 5-39. The aesthetic quality of buttresses is questionable, but various

Copyright fib, all rights reserved. This PDF copy of fib Bulletin 24 is intended for use and/or distribution only by National Member Groups of fib.

options exist to improve it, such as introducing openings in the buttress web or covering the whole intervention scheme is an attractive cladding.

Such an intervention scheme, in common with the construction of RC walls, within the original perimeter of the building plan requires a foundation system. In the scheme shown in Fig. 5-39, the foundation scheme would possibly be eccentric footings (eccentric with respect to the axis of the buttress to avoid excavation under the building). The actions on the footings depend on whether the buttress is designed to act in both pulling and pushing or just in pushing (pushing when the structure bears against the buttress and pulling when it sways away from it). The tension forces that need to develop at the interface while pulling are normally high, hence it is might be more practical to have wider buttresses on either sides pushing only.

The two most intricate problems in strengthening by building a set of external buttresses are as follows:

- The buttress stability may be critical since it is not actually loaded vertically downwards in the same way that the structure is. The vertical action on the buttress is its own weight only. This increases the possibility of uplifting of the foundations and reduces considerably the effectiveness of the buttresses.
- The connections between the buttress on the one hand and the building on the other is far from straightforward. To insure full interaction and load sharing when the structure is subjected to lateral actions, the buttress should be connected to the floors and columns at all levels. The connection area will be subjected to unusual levels of stresses that require special attention. Moreover, providing positive connection between the buttress and the columns and slabs requires construction work that may lead to some internal disruption.

Notwithstanding, this is an effective solution that is used in practice, where the buttresses are designed using capacity design principles and displacement-based approaches.

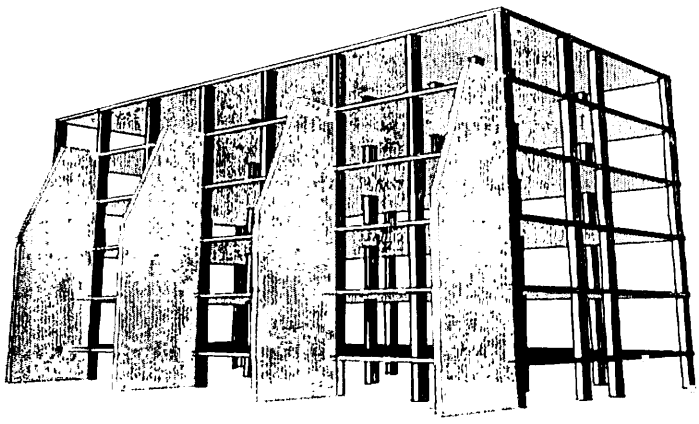

Fig. 5-39: External buttress strengthening of an RC building

5.6 Strengthening by adding a (steel) bracing system

5.6.1 Introduction

Adding diagonal braces within most or all storeys of selected bays of a reinforced concrete frame is an effective means of global strengthening. This has been shown in practice, as a series of RC buildings retrofitted with steel bracing have been reported to withstand the 1985 Michoacán earthquake with practically no structural damage (Del Valle, 1980; Foutch *et al.*, 1988).

Installation of a bracing is not as disruptive as that of shear walls. However, connection between existing concrete elements and braces may be cumbersome.

Architectural constraints are likely to condition the positioning of the braces due to the effects these have on available openings. For convenience the bracing is usually - but not exclusively - placed at the facades. Then its installation causes minimal disruption of occupancy.

Copyright fib, all rights reserved. This PDF copy of fib Bulletin 24 is intended for use and/or distribution only by National Member Groups of fib.

The most commonly used material for the braces is structural steel. An advantage of a steel bracing system is that normally no intervention to foundations is needed, or such an intervention is minimal.

Addition of a steel bracing system to a concrete structure increases considerably its lateral force resistance, but not so much its lateral stiffness. Therefore it is not an effective retrofit technique for stiff concrete structures, such as wall or dual systems or masonry-infilled frames. Deformation (drift) capacity of a relatively flexible but non-ductile concrete frame may be considerably enhanced, though, by adding a steel bracing system, provided that early brittle failure of braces and their connections or of nonductile (e.g. shear-critical) concrete elements is avoided.

Sometimes a system of concrete braces, combined with shotcrete jacketing of the beams and columns around the braced bays, is preferred over steel bracing. Obviously such a system is not as easy to install as a steel bracing, but it is much stiffer, especially if the braces are post-tensioned to prevent cracking under the peak axial tension demands.

The special case of bracing with post-tensioned system is overviewed at the end of this section.

Passive energy dissipation devices may also be used in conjunction with the bracing to efficiently increase dynamic damping (Okada *et al.*, 1992; Martinez-Romero, 1993). However, if the bracing system increases the stiffness of the frame considerably, the efficiency of the damping mechanism is compromised since these normally require large levels of displacement to be cost-effective (Fardis, 1998). A thorough review of passive devices installed within steel bracing systems is included in the work by Martinez-Rueda (1997).

5.6.2 Concentric steel bracing systems

5.6.2.1 Configuration and conceptual design issues

Concentric bracing systems are most convenient for retrofitting concrete frames. Such systems contribute to the lateral-load resistance of the structure through the horizontal projection of the axial force (mainly axial tension) developing in their inclined members (braces).

Appropriate (concentric) bracing systems are those with:

- Diagonal bracings, in which there is a single diagonal per braced bay of the frame
- X-diagonal (or cross-diagonal) bracings, with braces along both diagonals of a braced bay.
- V- or inverted-V bracings (termed chevron bracings in the USA), in which a pair of inclined braces is connected to a single point near or at mid-span of horizontal member (beam or slab) of the bay of the frame.

K-bracings, in which the inclined braces are connected to a point within the clear height of a column, should not be used.

Sometimes diagonal braces extend over more than one storey or bay of the existing frame.

Retrofit design should rely mainly on the tension diagonal for lateral load resistance and energy dissipation; it should also take appropriate measures against loss of diagonals in their post-buckling stage. (It is reminded that in seismic design of new steel braced frames, compression diagonals are normally neglected in the analysis for the seismic action and consequently for lateral load resistance, with the exception of V-braced systems, as there both tension and compression braces are considered for lateral load resistance).

For given RC frame geometry, V-braced systems offer the advantages of: a) reduced unbraced length of braces and b) earlier mobilisation of their strength and dissipation capacity (braces yield at a storey drift ratio equal to their yield strain times the brace inclination to the vertical, which is lower in V-braced systems). On the other hand the horizontal member to which the two braces connect should (be designed to) resist, as a transverse (vertical) load, the balance between the vertical components of the tension and compression braces. (For this purpose the post-buckling force of the compression brace is normally conservatively assumed equal to 30% of the yield force or one-third of the buckling load). Unless properly strengthened through horizontal steel elements attached to its top and bottom flanges, an existing RC beam normally cannot resist the bending action due to this unbalanced force. The unbalanced force applied to the frame member after buckling of the compression brace is the reason for avoiding K-braced systems, as in such systems the unbalanced force will be applied

Copyright fib, all rights reserved. This PDF copy of fib Bulletin 24 is intended for use and/or distribution only by National Member Groups of fib.

within the clear height of the existing RC column and may cause its failure.

If the sense of V-bracings is reversed in adjacent storeys, i.e. if an inverted-V is used in one storey and a V-bracing in the storey above (forming an X over two storeys), then the braces in consecutive storeys are almost continuous and unbalanced transerve forces on the horizontal RC member cancel each other. Then this member, along with the new steel elements attached to it, has to resist essentially only the flexural action produced by a concentrated moment (couple) applied at its midspan by the braces (the braces exert their resultant horizontal forces – sum of horizontal projections of tension and compression force in the braces – at the top and bottom of the horizontal member, i.e. at an eccentricity with respect to its axis).

The arrangement of single diagonal braces in different bays (or groups of adjacent bays) of the frame should be such that the retrofitted frame has similar lateral resistance and stiffness for the two senses of action of the earthquake within the plane of the bracings. It is worth reminding that, for exactly that purpose, codes for earthquake-resistant design of new steel structures include the requirement that the total horizontal projection of the cross-sectional area of all tension diagonals is about the same for both senses of action of the earthquake in the plane of the bracing. (For new braced steel frames Eurocode 8 restricts the difference of the values of this horizontal projection for the two senses of action to less than 10% of their average value). Obviously in X- or V-braced systems this symmetry requirement is automatically satisfied.

For convenience of fabrication of steel bracings, the cross-sections of the braces may be selected to be the same in several storeys, or even in all the storeys of the retrofitted frame. It should be born in mind that if these braces are dimensioned on the basis of the lateral force resistance requirements in upper storeys, then in lower storeys the balance between lateral force resistance requirements and capacity of the bracing system will be taken by flexural action in the original frame, possibly with some of its members acting compositely with the new steel horizontal and vertical members surrounding the braces. If, on the other hand, braces are dimensioned on the basis of the lateral force resistance requirements in lower storeys, then the overstrength in upper storeys may lead to undesirable concentration of inelasticity and energy dissipation demands in the lower storeys. It is worth reminding that to avoid such a situation codes for earthquake-resistant design of new steel structures normally limit the maximum difference in overstrength among all bracings in the structure. For example, Eurocode 8, Part 1, does not allow a maximum overstrength ratio in the entire steel braced frame (defined as ratio of brace force capacity to demand from the analysis) that exceeds by more than 25% the minimum value of this ratio anywhere in the structure.

Although there have been proposals for connection of the diagonal braces to the frame only through steel sleeves (collars) added around the top or bottom of the columns and anchored to the concrete slab (Ignatiev, 1998), diagonals braces should be supplemented with a frame ("rim") of horizontal and vertical steel members firmly attached to the delimiting concrete members – columns and beams or slab. The role of the horizontal steel member(s) of the rim is two fold: 1) To assist the concrete frame resist the load effects (moments and shears) from the frame action developing along with the truss action, as well as from the truss action itself (axial forces – action as horizontal chord of the truss). 2) To act as collector element, for the transfer of inertia forces from the slabs into the bracing system. In order to play this second role, horizontal elements need to be continuously fastened to the adjacent horizontal concrete members (top and bottom surface of beam or slab). The role of the vertical steel members of the rim is mainly similar to that listed above under 1) for the horizontal members (i.e. to assist existing columns to provide their share of lateral load resistance, as frame members and vertical chords of the truss). Moreover, and depending on how they are attached to the existing columns, the vertical steel members of the rim may work as a backup system for gravity loads in case (some) concrete columns cannot sustain the imposed storey drifts and fail. To play their role(s), the vertical steel members do not have to be continuously fastened to the existing concrete columns; they only need to be made continuous from storey to storey (be it via threaded rods or other elements passing through the concrete slab). New vertical steel elements may consist of four angles at the corners of the concrete column, connected into a lattice through inclined steel straps or plates along the sides of the column, welded to the angles (cf. the application to the Park Espana building in Mexico City in Foutch et al, 1989); the four angles at the corners may also be connected through horizontal batten plates along the sides of the column (as in Masri and Goel, 1996 and Goel and Masri, 1996).

Copyright fib, all rights reserved. This PDF copy of fib Bulletin 24 is intended for use and/or distribution only by National Member Groups of fib.

Steel straps, continuously fastened to the sides of the concrete column, may also be used as vertical elements of the rim.

5.6.2.2 Recommendations for design and dimensioning

Experience from past earthquakes shows that concentrically braced steel frames may fail in a nonductile manner, due to premature cracking and fracture of the braces and their connections during the post-buckling stage. Therefore, the key to good performance of a concentrically braced system (be it for a new steel structure or for retrofitting of an old concrete frame) is its ability to withstand post-buckling cyclic deformations without premature fractures. This is achieved through appropriate design and detailing of the braces to control their buckling and post-buckling behaviour and the associated adverse effects (distortion and local buckling of the member, early failure of welds, etc.) that may jeopardize or reduce the full tensile capacity of the member after it is straigthened back during the next half-cycle of the response.

Local buckling in compression braces precipitates fracture, due to concentration of strains and their accumulation with cycling. This may be the most important factor limiting the ductility and energy dissipation capacity of the bracing system. Design of the braces should include measures against their local buckling. This amounts to using for them 'compact' sections, with width-to-thickness ratios of their parts below a certain limit. For braces used in seismic design or retrofitting, this limit should be considerably lower (e.g. by 50%) than what is considered appropriate for monotonic loads. For new designs of steel or composite buildings, Eurocode 8 requires using steel sections of: a) "class" 1 in structures with values of the behaviour factor q at least 4.0 (so called Ductility Class High - H structures), b) "class" 1 or 2 in buildings designed for a q-factor value between 2.0 and 4.0, or c) "class" 1, 2 or 3 in those designed for a q value between 1.5 and 2.0. (Section "classes" are defined in Eurocode 3, Part 1, depending on the shape of the section and its width-to-thickness ratio).

Regardless of whether compression braces are taken into account in the analysis for the retrofit design (as in V-bracings), or neglected (as may be the case in diagonal or X-braced systems), their slenderness should be limited. In US retrofitting practice an upper limit of 80 has been recommended for the slenderness ratio of braces (Wyllie, 1996, 1998). A more rational choice may be the upper limit of 2 imposed by some seismic design codes for new steel structures (e.g. Eurocode 8, Part 1) on the non-dimensional slenderness $\bar{\lambda}$, defined as the square root of the ratio of the member yield force, f_yA, to its critical buckling load, N_{cr}. If the compression braces of X-braced systems are neglected for resistance against the seismic action (e.g. in the analysis), it is worth remembering that for such a situation codes for earthquake-resistant design of new steel structures, such as Eurocode 8, set a lower limit of 1.3 on the non-dimensional slenderness $\bar{\lambda}$ of braces. This limit aims to reduce the axial force of compression braces in the pre-buckling stage and prevent overloading of frame members (columns and beams) with seismic action effects (much) higher than those from the analysis and developing inelastic action and damage before yielding of the tension diagonals – which are the intended means of energy dissipation.

The effective unbraced length of braces should be calculated on the basis of realistic assumptions for their end restraint conditions. For X-braces welded to a common gusset plate at their midpoint(s), FEMA 356 recommends taking an effective unbraced length equal to half the total (diagonal) length of the brace, including the gusset plates. (It is noteworthy that in the cyclic tests performed by Bush et al 1991a, 1991b on a 2/3-scale two-storey, two-bay RC frame retrofitted with X-bracings continuous over two storeys, braces buckled at a load consistent with an effective length equal to 50% of the unbraced length between connections with gusset plates at intersections with other members, and not of their total diagonal length). For other types of braces welded to gusset plates, it is recommended to take an effective unbraced length equal to the total (diagonal) length of the brace for out-of-plane buckling, or 80% (90% for bolted connections) of that length for in-plane buckling.

Gusset plates connected to braces susceptible to out-of-plane buckling are recommended in FEMA 274 to have clear length at least equal to twice their thickness, to limit restraint of brace plastic rotations in the post-buckling stage.

Before moving to the subject of seismic analysis and design of the retrofitting, it is emphasised that the existing RC frame, possibly considered to act compositely with the steel horizontal and vertical members added around bracings, should provide the entire required

Copyright fib, all rights reserved. This PDF copy of fib Bulletin 24 is intended for use and/or distribution only by National Member Groups of fib.

resistance against (factored) gravity loads, without any contribution from the braces (including those of V-braces, which should not be considered to provide an intermediate support at beam mid-span).

There are two possible approaches for the seismic analysis of an RC frame structure retrofitted with steel bracing and for the verification of the retrofitted structure (including the elements of the bracing system): a) The conventional force-based approach of current seismic codes for new structures, using a global behaviour factor q (or response modification factor R) for the reduction of the elastic response spectrum of the design seismic action and of the elastic forces derived therefrom; b) An approach based on nonlinear analysis (typically static, of the pushover type) of the retrofitted structure for the design seismic action, with deformation-based verification of the bracing elements intended for energy dissipation and appropriate force- or deformation-based verification of all other elements (including those of the existing RC frame).

The first approach is, in principle, simpler. The main difficulty lies in the selection of an appropriate value for the q or R factor. The values given in current force-based seismic design codes for new braced steel structures may be used as a guide. These values may even be fully adopted, if it is decided to provide the entire lateral load resistance through the bracing system. (In code terminology, this implies entrusting only the elements of the bracing system as "primary" elements that provide the earthquake resistance and considering the elements of the existing RC structure as "secondary", entitled only to support the gravity loads).

It is reminded, in this connection, that Part 1 of Eurocode 8 provides the following q-factor values for concentric braced steel or composite frames: for systems with diagonal bracings: q=4; for V-braced systems q=2.5 for Ductility Class (DC) High (H) or q=2 for DC Medium (M) - the main difference between DC H and M in this case being that only steel sections of (compactness) class 1 may be used in DCH, while also section class 2 is allowed for DC M. Adoption of these (relatively low) q-factor values implies following all relevant rules of Eurocode 8 for concentric braced frames. These include the already mentioned rules of :

- Neglecting compression diagonal in the analysis (except in V-braced systems);
- Limiting the non-dimensional slenderness $\bar{\lambda}$ to a maximum of 2 and for X-bracings, in addition, to a minimum value of 1.3;
- Restricting the difference between the values of the total horizontal projection of cross-sectional areas of all tension diagonals for the two senses of earthquake action in the plane of the bracing (+ or -), to 10% of the average of these two values;
- Limiting the maximum (over the system) value of the ratio of brace force capacity to demand from analysis ("overstrength ratio") to 1.25 times the minimum value of this ratio in the entire system;
- Verification of horizontal and vertical members against buckling for an axial compression equal to 1.2 times the sum of: a) the axial force due to gravity loads, plus b) the axial force due to the seismic action from the analysis, amplified by the minimum value of the aforementioned overstrength factor over all diagonals in the system; this axial force should be considered to act simultaneously with the member bending moment from the analysis for the seismic action.
- Verifying horizontal members connected to V-braces for the (unbalanced) transverse force resulting from the full axial resistance of the tension brace and from 30% of the buckling load of the compression brace.
- Verifying vertical members connected to single compression diagonals (neglected in the analysis) for the effects of the full buckling load developing in such diagonals.

In the alternative approach, i.e. the one based on nonlinear (static) analysis, all members of the retrofitted system (including those of the existing RC frame and the compression braces) should be included in the model.

In a static (pushover) analysis compression braces may be modelled as elastic-perfectly plastic up to their ultimate deformation, with a yield force equal to a small fraction of their buckling load (20% of this load is recommended in FEMA 273 and 356). Nonetheless, the last bullet point above should be considered for the members connected to compression braces.

According the FEMA 356, the ultimate (shortening) deformation of compression braces is normally between 8 and 10 times their deformation at buckling load (the value of 10 applies for compact – class 1 – circular tubes, and in the in-plane direction of braces consisting of double angles or channels; in the out-of-plane direction of such braces a value of 9 applies, the same as for I sections; a value of 8 applies for concrete-filled tubes or for compact rectangular

Copyright fib, all rights reserved. This PDF copy of fib Bulletin 24 is intended for use and/or distribution only by National Member Groups of fib.

cold-formed tubes). After this ultimate deformation, the resistance of compression braces should be neglected. The same document (FEMA 356) recommends as limiting acceptable deformation of compression braces a value of about 60% of the above ultimate values at the "Life Safety" performance level, or of about 80% of it at the "Collapse Prevention" level.

Again according to FEMA 356, tension braces may be considered with their full tensile capacity up to a ductility factor (ratio of peak extension to extension at yield) of 12, and with 80% of that capacity beyond that and up to a ductility factor of 15 (beyond which they are considered to break). Exhaustion of the ductility factor of 12 (corresponding to peak resistance) is considered acceptable for tension braces at the Collapse Prevention performance level, while an acceptable value of 8 is recommended for the "Life Safety" level. Nonetheless, for other than short-duration seismic actions likely to induce more than one half-cycle of large inelastic excursions, verification of the retrofitting should not rely on the limiting deformations of the tension braces, if those of the compression braces are exhausted.

The members of the RC frame should also be verified by comparing the peak deformation demands from the nonlinear analysis with the corresponding acceptable deformations. These latter values should be estimated from their conservatively factored ultimate deformations, taking into account their seismic detailing or lack thereof and whether they have been retrofitted or not with new steel elements (as, e.g., is the case with the horizontal and vertical elements delimiting the braced bays of the frame).

As the global stiffening effect of a steel bracing is rather limited, it is likely that significant lateral displacements may have to develop before full utilization of the bracing. (It is reminded that steel braces yield at a storey drift ratio equal to their yield strain times the brace inclination to the vertical, i.e. normally at drift ratios of 0.3% to 0.5%). If the (nonlinear) analysis of the retrofitted structure shows that some of the existing RC columns may suffer considerable damage and approach or exceed their (limited) deformation capacity under the predicted peak deformation demands, then it is recommended to provide with bracing the bays of the frame on both sides of the vulnerable columns and to dimension the vertical steel members attached to, or built around, these columns for the full gravity load of the column (against collapse of the latter due to the imposed seismic deformations).

Still within the second analysis and design approach (where the existing RC frame is included in the model for the nonlinear analysis, along with the bracing system) the RC frame should be verified for the load effects of the frame action, according to the results of the analysis. If the intent of the retrofit design is to concentrate inelastic action and energy dissipation only in the (tension) braces, then the existing RC frame, acting compositely with the new horizontal and vertical steel elements, should provide some overstrength against the results of the analysis for the frame action. It is reminded that, with this intention, Eurocode 8, Part 1, requires frame members of new braced steel buildings to be dimensioned for the seismic action effects from the analysis amplified by the minimum value of the afore-mentioned overstrength factor in all diagonals of the system, plus the simultaneously acting gravity loads, the sum multiplied by an additional safety factor of 1.2.

In closing this long discussion on design recommendations, a few words are in order regarding dimensioning of vertical steel elements of the rim around braced bays. If such elements are not continuously fastened to the existing concrete columns, their action is neither independent of, nor composite with, these columns, and is hard to model and quantify. Often these elements consist of four angles at the corners of the column, welded into a lattice with horizontal batten plates or inclined or horizontal straps arranged along the four sides of the column. The angles at the four corners need to be dimensioned to resist – through tension on one side of the column and tension or compression on the other – the combination of bending moment and axial tension resulting from the analysis at the top and bottom sections of the column; any axial compression from the analysis for the seismic action may be entrusted to the RC column. The straps of the lattice, or the horizontal batten plates, should then be designed to resist the shear force accompanying the moment at the column ends – through tension and compression in inclined straps of the lattice, or by bending and shear in the horizontal batten plates. To reduce uncertainty regarding the interaction of the existing column and the new steel element(s) placed around it without continuous fastening, it is recommended to design the latter for compatibility of their elastic flexural deformations with those of the existing column up to yielding. This may be achieved by selecting the inclination and cross-section of the straps in the lattice, or the spacing and cross-section of the horizontal batten plates, so that the elastic stiffness of the steel element built-up around the column is

Copyright fib, all rights reserved. This PDF copy of fib Bulletin 24 is intended for use and/or distribution only by National Member Groups of fib.

equal to the secant-to-yield stiffness of the concrete column it encloses (for both members with assumed fixity at floor levels).

5.6.3 Eccentric bracing systems

With one exception (Bouwkamp, 2000), steel bracing systems proposed and applied so far for retrofitting are concentric. In new steel or composite (steel-concrete) structures, connection of the diagonal braces with the frame members at a short distance from a beam-column connection, or from another brace-beam connection, produces a zone where a large amount of energy can be dissipated through cyclic bending and/or shear in a controlled manner. This zone is often termed "seismic link". In retrofit applications "seismic links" cannot be provided in the new horizontal and vertical steel members, as the adjacent stiff concrete elements prevent large localised deformations in any designated "seismic link" zones along them. In the reference quoted above as an exception, an (inverted) Y-braced frame was used for retrofitting: the inverted Y-bracing was connected to the bottom of a new horizontal I beam fastened to the soffit of the existing concrete beam, through a vertical steel beam stub intended to dissipate energy in shear as seismic link (stem of the Y-bracing, see Fig. 5-40). The new I beam above the "link", another I beam at the bottom of the inverted Y-bracing and two steel plates attached to the inside face of the concrete columns to complete the steel frame, were all fastened to the surrounding frame members through adhesive anchors pre-installed in the concrete with the help of a template.

The two approaches outlined in Section 5.6.2.2 for the seismic analysis and design of retrofitting with concentric steel braces, apply also for this alternative retrofit concept. If the first approach is adopted, i.e. the one based on linear analysis with forces from the elastic spectrum reduced by the q or R factor of new eccentric braced steel frames, then the "seismic link" region should be dimensioned and detailed according to the rules of seismic design codes for eccentrically braced new steel (or composite) structures. Moreover, the existing RC structure and the other elements of the steel bracing system should possess sufficient overstrength to assure that inelastic energy dissipation will be mainly concentrated in the "seismic links". It is reminded that Eurocode 8, Part 1 gives a value of the behaviour factor q of eccentric braced frames equal to 4 for Ductility Class M, or of 6 for Ductility Class H (default value; value may go up to 8 for highly redundant structures). It also limits the peak inelastic rotation demand (estimated from elastic analysis on the basis of the equal displacement rule) on short or long links to 0.08 rad or 0.02 rad, repectively, and gives rules for the minimum number of intermediate web stiffeners depending on the peak inelastic rotation demand on the link. (A link is considered as short if its clear length is less than 80% of the length, $2M_{pl}/V_{pl}$, beyond which yielding is controlled by flexure instead of shear and long if it exceeds 1.5 times the above transition value of the length). Eurocode 8 requires also dimensioning all parts of the structural system outside the seismic links for overstrength action effects resulting from 1.2 times: a) those due to the gravity loads which act simultaneously with the earthquake, plus b) the seismic action effects corresponding to development of 1.5 times the design capacity of the seismic link with the lowest overstrength – over the requirements of the analysis for the design seismic action – in the system. These latter effects are computed on the basis of the analysis for the seismic action and proportionality.

In the second design approach, namely that based on nonlinear (static) analysis of a model of the entire (retrofitted) structure, seismic links are modelled as elastic-perfectly plastic up to their maximum strength and with a resistance reduced by 20% up to ultimate deformation. For short links (see definition above) with at least 3 intermediate web stiffeners FEMA 356 gives a value of 0.15 rad for the inelastic rotation at link maximum strength and of 0.17 rad at link ultimate deformation; acceptable link inelastic rotation demands according to FEMA 356 are 0.11 rad for the Life Safety performance level and 0.14 rad at the Collapse Prevention one. All these values are multiplied by $0.5(1+N_{wst}/3)$, with N_{wst} = number of intermediate web stiffeners, if $N_{wst} < 3$. The FEMA 356 limits are more liberal than those of Eurocode 8 (0.11 rad vs. 0.08 rad), mainly due to the conservatism inherent in the philosophy for new designs. For the parts of the structural system outside the seismic links, what has been said in Section 2.4.2.2 still applies. Nonetheless, if the intention is to use the seismic links as the only means of energy dissipation in the retrofitted system, then the EC8 rule mentioned at the end of the paragraph above is worth adopting.

Copyright fib, all rights reserved. This PDF copy of fib Bulletin 24 is intended for use and/or distribution only by National Member Groups of fib.

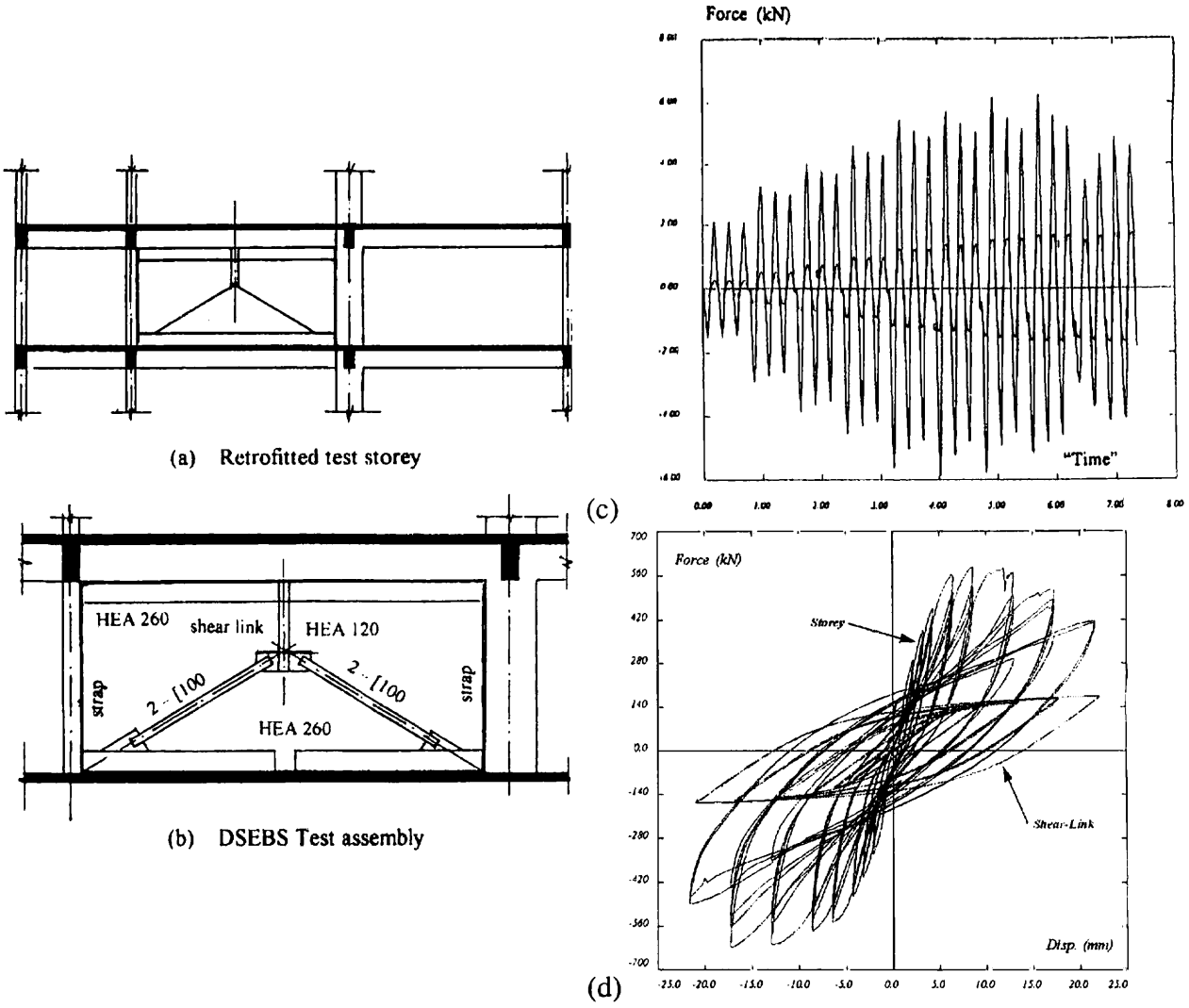

Fig. 5-40: Eccentric bracing with vertical shear link for retrofitting (Bouwkamp, 2000): (a) Overview of bracing, (b) components of bracing; (c) time-history of global lateral force (exterior waveform) and of shear in link; (d) measured force-displacement loops of the entire storey and of the link.

5.6.4 Construction issues and alternatives

Normally there are more construction difficulties in retrofitting with steel bracings, than in the construction of new steel or composite buildings.

Prefabrication of large steel subassemblages, as in new construction, is not feasible. To match the steel members to the exact dimensions of the concrete frame, considerable fabrication or modification of members (e.g. trimming of length) has to take place in situ.

Most of the welding has also to be done in the field, especially if steel members are attached to the inside of the concrete frame or are placed flush against its exterior surface (façade) to reduce eccentricities between the mid-planes of the frame and of the steel bracing. Under these conditions, achievement of high quality full penetration welds is very difficult and weldments may end up being the weak link(s) of the retrofitting.

Another difficulty is associated with the installation of epoxy-grouted fasteners to connect the bracing to the concrete frame (from the technical point of view, this is the best type of connection for full composite action of the steel elements of the rim and the concrete elements of the frame). Normally the holes for the fasteners have to be drilled into the concrete in phases: First, partial-depth holes are drilled using the steel member with its annuli as template; then the steel member is removed, to finish the drilling and clean the holes; the steel member is put back, in order to grout the holes with epoxy, insert the fasteners and secure the steel member in place. In some cases interference with the reinforcement or with the connections between steel members may prevent achievement of full penetration depth for

Copyright fib, all rights reserved. This PDF copy of fib Bulletin 24 is intended for use and/or distribution only by National Member Groups of fib.

some fasteners, or may cause their relocation – which requires drilling new annuli through the steel members in the field.

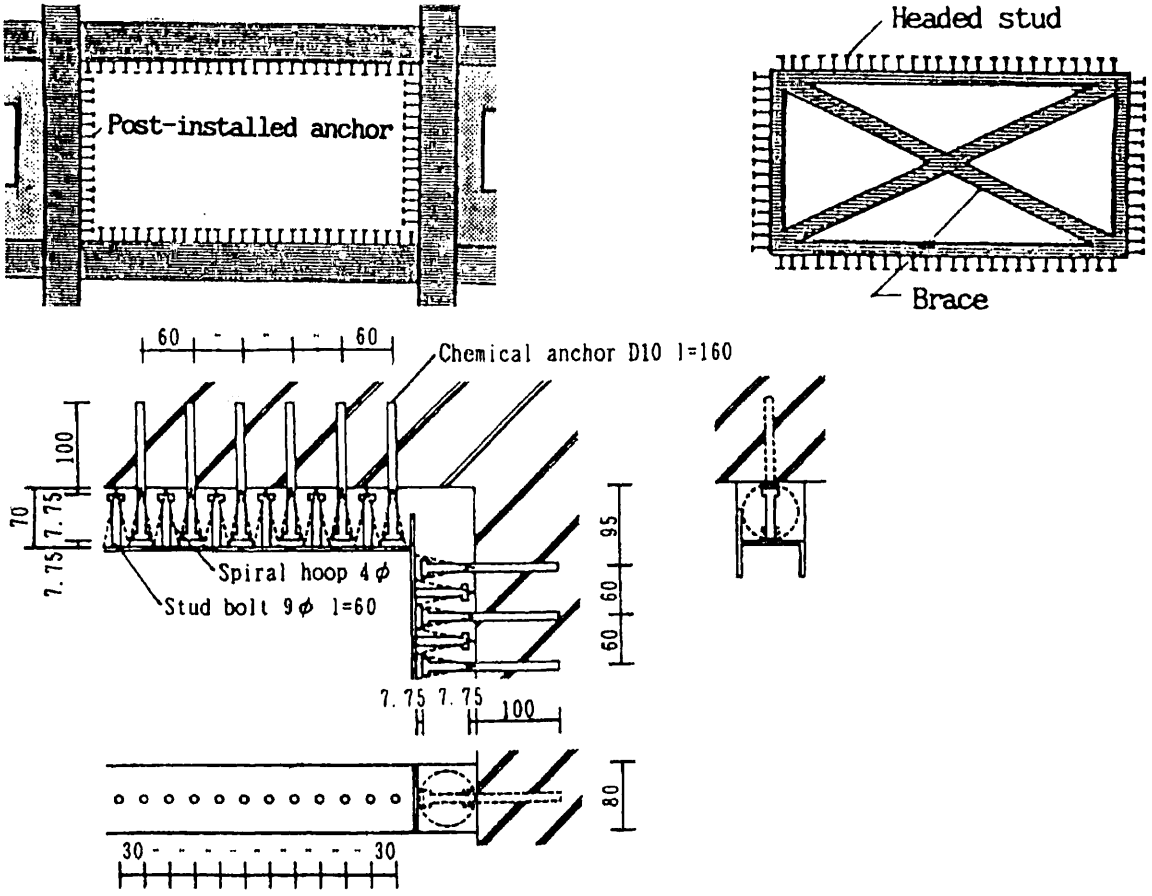

Fig. 5-41: Prefabricated steel bracing according to Yamamoto (1993): (a) post-installed anchors and shear studs for the connection; (b) detail of joint between steel rim and concrete frame.

In Japan, where traditionally retrofitting with steel braces has been very popular, most of the construction difficulties above are circumvented by using pre-fabricated bracing subassemblages, which consist of a heavy rectangular rim with X-, V-, inverted V-, or double K-bracings inside. These subassemblages are placed in the bays of the existing RC frame between adjacent beams and columns (Fig. 5-41 a). To accommodate variations in the dimensions of the RC frame, a tolerance of many cms is provided around the rim. Connection of the prefabricated subassemblages and the surrounding frame members is achieved through a system consisting of: a) mortar filling the gap between the rim and the RC frame; b) closely spaced headed studs, welded to the outside surface of the rim and protruding into the gap; and c) fasteners (normally epoxy-grouted and closely spaced), installed at the interior face of the surrounding frame (spiral reinforcement is often inserted along the mortar joint, between the fasteners and the headed studs).

Fig. 5-41 b, which refers to 1:3 scale test specimens by Yamamoto (1993), shows a typical detail of the rim-to-frame connection. These tests have shown that single-storey single-bay frames retrofitted in this way develop a lateral force resistance equal to the sum of the shear capacity of the frame and of the braces (horizontal projections of yield force of tension brace and of buckling load of compression brace) and can maintain it up to storey drift ratios of more than 3%. If the resistance of the steel braces increases beyond a certain point, the horizontal mortar joint may fail in sliding shear. The horizontal failure plane extends into the column(s) in tension and may precipitate a flexure-shear failure in the column(s) in compression. The lateral force resistance in this case is equal to the sum of: a) the sliding shear resistances of the mortar joint and of the column(s) in tension, and b) the normal shear resistance of the column(s) in compression. The cyclic drift capacity of this failure mode is reduced, but in the tests by Yamamoto (1993) it was still between 2% and 3%.

Copyright fib, all rights reserved. This PDF copy of fib Bulletin 24 is intended for use and/or distribution only by National Member Groups of fib.

5.6.5 Selected experimental results on steel-braced concrete frames

The effectiveness of retrofitting with steel bracing can be meaningfully studied only through tests on larger subassemblages, such as the 1:3 scale two-storey two-bay frame retrofitted in one bay by Masri and Goel (1996) and Goel and Masri (1996) and the 2:3 scale one retrofitted over both bays and storeys by Bush et al (1991a, 1991b).

In the first test the retrofitted specimen exhibited full and stable hysteresis loops up to top drifts of 2%, at which welds failed at the connection of vertical steel elements added around columns to the foundation. Premature fracture of welds upon straightening of buckled braces was also the reason for terminating the test by Bush et al (1991a, 1991b) at a top drift ratio of only 0.6%. Before this drift was reached the brittle concrete columns failed also in shear, despite the significant increase in their capacity due to their confinement by the vertical steel members continuously attached on either side of these columns. The low deformation capacity of this test frame demonstrates the sensitivity of this complex method of retrofitting to minor details in the fabrication and installation of the bracing system and the need for caution in assigning storey drift capacities or q-factor values to so-retrofitted structures.

The reference quoted above for seismic retrofitting with eccentric steel bracing (Bouwkamp, 2000) reports also on the experimental response of a full-scale 3-bay 4-storey masonry-infilled RC frame representative of old European construction, in which an infilled panel in the 2nd storey was replaced by the Y-bracing of Fig. 5-40 a, b, with a shear-controlled ("short") seismic link. The response is summarised in Figs. 5-40 c and d. In the tests storey drifts were applied in sets of three constant-amplitude cycles, with increasing set amplitude up to failure of the 4-storey structure. Failure took place at a "time" of about 5.00, because the masonry infill sheared–off the top of a lightly reinforced 2nd-storey column. After that point global resistance of the frame degraded with cycling of the displacements from 600kN to about 400kN: As demonstrated by its full and stable and hysteresis loops in Fig. 5-40 d, and by the increase in its resistance with cycling in Figs. 5-40 c – the inner waveform – and d (over a yield value of about 100kN), the seismic link performed very well during the entire test up to an inelastic rotation of about 0.036 rad and would have continued to do so at larger displacement cycles, if the test had not been stopped.

5.6.6 Retrofitting with post-tensioned cables

Retrofitting concrete buildings via inclined post-tensioned cables bears strong similarities with steel bracing systems, but also has some important differences. If prestressing of the cables is at a level sufficient to prevent them from becoming slack during the seismic response, then it is a means of keeping active and fully considering for lateral force resistance and stiffness those diagonal braces which are "compressed" (strictly speaking shortened) during the response. Therefore, the initial prestressing level is an important parameter in the retrofit design: if it is high, others may yield early and start accumulating inelastic tensile strains that reduce their bracing effectiveness. Tena-Colunga (1996) reports two applications of the technique in Mexico city with initial prestresss levels of about 20% of yield force. Miranda (1990) and Miranda and Bertero (1990) have proposed an initial prestress of 30% to 35% of the yield force. In their in-depth analytical studies of the technique, Pincheira and Jirsa (1992) proposed and used initial prestress levels of about 75% the yield level. It should be mentioned that, unlike what happens with low initial prestress, at such a high initial prestress level time-dependent losses (mainly due to relaxation of the cables) are very prenounced and - unless the cables are periodically retensioned – a significant part of this initial prestress may not be available in the long-term.

Prestressing cables are most conveniently arranged at the facades of buildings and should extend over several storeys; normally, and most conveniently for anchorage, from the foundation to the top. They consist of strands and, being external, should be enclosed in steel or PVC ducts with appropriate corrosion protection (through grouting, durability and water-tightness of the ducts, etc.).

Pretensioning of the cables induces axial compression in the columns of the building. In mid- to high-rise buildings the axial force level in the columns due to gravity loads may already be high and existing columns may be need to be strengthened against the adverse effects of high axial load levels on their ductility. Teran-Gilmore et al (1996) note that from

Copyright fib, all rights reserved. This PDF copy of fib Bulletin 24 is intended for use and/or distribution only by National Member Groups of fib.

this point of view retrofitting with pretensioned cables is most appropriate for infilled buildings, as the vertical compression due to the initial prestress goes mainly to the infills, rather than to the concrete columns, to the benefit of the resistance and ductility of infill panels against in-plane lateral (shear) forces.

5.7 Effect of intervention scheme on local and global supply and demand

In this section, general guidelines are given with regard to the effect of local intervention schemes on the local and global response of retrofitted structures. Moreover, comments on the problems associated with global intervention techniques and possible measures to be taken are given in a summary form.

In Table 5-9, the shown implications are rather controversial, since various workers in the field have different preferences and different experiences. However, the comments given are useful for relatively inexperienced engineers and may help start the process of assessing the various options and weighing their relative merits. It is emphasised that each repair and/or strengthening task is a special case and generalizations are inherently inaccurate. The procedures described in the various sections of this chapter, however, provide a suite of tools for the engineer to apply more than one approach.

Copyright fib, all rights reserved. This PDF copy of fib Bulletin 24 is intended for use and/or distribution only by National Member Groups of fib.

Technique	Local Effect	Global Effect	Relative Cost	Disruption	Technology	Comments
Resin injection	Reinstates stiffness and strength	No global effect	Low-to-Medium	Low	Medium	Reinstatement approach
RC jackets	Upgrade stiffness and strength and (possibly) ductility.	Changes response characteristics. If applied to columns, it forces hinging to beams	Low, per member	Medium-to-high	Low, unless extensive welding used	Can remedy soft storey response. If in few storeys, can lead to soft storey above
Steel jacket or rings	Ductility and shear strength only; if strong composite action, stiffness increases	Increased global deformation capacity	Medium	Low	Medium	Effective where the main problem is sparse transverse reinforcement; fast implementation
Narrow FRP wrapping	Large increase in ductility; little effect on strength or stiffness	As for steel rings	High	Low	Medium-to-high	Suitable solution if cost is not a controlling factor
Beam-column joint wrapping by FRP	Eliminates shear failure in connections.	Reduces marginally global drift by reducing connection deformation	High	Low	Medium-to-high	As above
Complete FRP jacketing	Very large increase in ductility and shear strength; little increase in stiffness	Preservation of the stiffness distribution with drastic effect on strength distribution	High	Low	Medium-to-high	As above
Selective techniques	Measured and quantifiable increase in any one parameter or a combination of parameters	Tuned structural response to fit with performance objectives	Low	Medium	Medium-to-high (more in analysis and know how than in materials)	Most suitable and objective approach if analysis capabilities and specialized engineering expertise exists
RC walls addition	Could lead to increased force demands in the immediate vicinity	Drastic reduction in deformation demands on all other members. Resolves problems of soft storey.	Medium	High	Low	Most effective solution if disruption is not a problem. Drastic intervention to foundation needed.
Steel bracing	Protects brittle RC members in its vicinity from collapse. May introduce large forces at connections	Increases global ductility and dissipation capacity. May resolve problems of soft storey.	Medium-to-high	Low-to-medium (depending on external or internal application)	Medium	Sensitive to detailing of braces and connections against local buckling and post-buckling fracture.
Infilling of panels	Generates high corner stresses. Increases storey stiffness, hence reduces storey drift	Increases weight hence seismic loads. Reduces period, hence increases higher accelerations. May lead to modified global response if panels are monolithic, leading to cantilever response	Medium	Medium-to-high (depending on external or internal application)	Low	If applied externally and secured fully, it is an effective solution. Possibly by replacing masonry panels by precast concrete units
External buttresses	Generates very high local demand at connection with structure.	As in RC wall addition.	Medium-to-high	Low	Medium	Requires elaborate foundations. Uplifting is a problem.

Table 5-9: Summary of relative consequences of repair techniques

Copyright fib, all rights reserved. This PDF copy of fib Bulletin 24 is intended for use and/or distribution only by National Member Groups of fib.

References

Aboutaha, R.S., Engelhardt, M.D., Jirsa, J.O. and Kreger, M.E. 1999. Rehabilitation of shear critical concrete columns by use of rectangular steel jackets. ACI Structural J., Vol. 96, No. 1, pp. 68-78.

Aboutaha, R.S., Engelhardt, M.D., Jirsa, J.O. and Kreger, M.E. 1996. Retrofit of concrete columns with inadequate lap splices by the use of rectangular steel jackets. Earthquake Spectra, Vol. 12, No. 4, pp. 693-714.

Aboutaha, R.S., Engelhardt, M.D., Jirsa, J.O. and Kreger, M.E. 1996. Seismic Retrofit of R/C columns using steel jackets. ACI Spec. Publ. SP160, "Seismic Rehabilitation of Concrete Structures" (Sabnis, G.M. et al, eds.), American Concrete Institute, Detroit, Mi, pp. 59-72.

Aboutaha, R. and Machado, R.I. 1999. Seismic resistance of steel tubed high strength reinforced – concrete columns. ASCE J. of Structural Eng., Vol. 125, No. 5, pp. 485-494.

ACI 440.2R-01, 2001. Guide for the design and construction of externally bonded FRP systems for strengthening concrete structures, ACI, Detroit, Mi.

Alcocer, S.M. 1992. Rehabilitation of RC frame connections using jacketing. In: *Proc. 10th World Conference on Earthquake Engineering, Madrid*, Balkema, Rotterdam, pp.5235-5240.

Alcocer, S.M. and Jirsa, J.O. 1993. Strength of reinforced concrete frame connections rehabilitated by jacketing. ACI Structural J., Vol. 90, No. 3, pp. 249-261.

Antonopoulos, C. and Triantafillou, T.C. 2002. Analysis of FRP-strengthened RC beam-column joints. Journal of Composites for Construction, ASCE, Vol. 6, No. 1, pp. 41-51.

Antonopoulos, C. and Triantafillou, T.C. 2003. Experimental investigation of FRP-strengthened RC beam-column joints. Journal of Composites for Construction, ASCE, Vol. 7, No. 1, pp. 39-49.

Bertero, V.V., Cowel, A. and Popov, E. 1980. Repair of bond in RC structures by epoxy injection. *Proceedings of the First Seminar on Repair and Retrofit of Structures, Ann Arbor, Michigan*, pp. 234-240, US/Japan Co-operative Earthquake Engineering Research Program, Dept. of Civil Engineering, Univ. of Michigan.

Bett, J., Klingner, R. and Jirsa, J. 1988. Lateral load response of strengthened and repaired reinforced concrete columns. ACI Structural J., Vol. 85, No 5, pp.499-507.

Biddah, A., Ghobarah, A. and Aziz, T.S. 1997. Upgrading of nonductile reinforced concrete frame connections. ASCE J. of Structural Engineering, Vol. 123, No. 8, pp. 1001-1010.

Bouwkamp, J.G. 2000. A ductile steel eccentrically-braced system as seismic retrofit for brick-masonry infilled concrete frames. *Proc. G. Penelis International Symposium on Concrete and Masonry Structures, Aristotle University of Thessaloniki, Dept. of Civil Engineering, Thessaloniki*, pp.179-189.

Bracci, J.M., Reinhorn, A.M. and Mander, J.B. 1995. Seismic resistance of reinforced concrete frame structures designed for gravity loads: Performance of structural system. ACI Structural J., Vol. 92, No. 5, pp.597-609.

Bush, T.D., Jones, E.A. and Jirsa, J.O. 1991. Behavior of RC frame strengthened using structural steel bracing. ASCE J. of Structural Engineering, Vol. 117, No. 4, pp.1115-1126.

Bush, T.D., Wyllie, L.A. and Jirsa, J.O. 1991. Observations on two seismic strengthening schemes for concrete frames. Earthquake Spectra, Vol. 7, No. 4, pp.511-527.

Castellani, A., Negro, P., Colombo, A., Grandi, A., Ghisalberti. G. and Castellani, M. 1999. Carbon fiber reinforced polymers (CFRP) for strengthening and repairing under seismic actions. European Laboratory for Structural Assessment, Joint Research Centre Research Report I.99.41, Ispra, Italy.

CEB 1983. CEB Bulletin 162 - Assessment of concrete structures and design procedures for upgrading (Redesign). Comité Euro-International du Béton, Lausanne.

Chai, Y.H., Priestley, M.J.N. and Seible, F. 1994. Analytical model for steel-jacketed RC circular bridge columns. ASCE, J. of Structural Engineering, Vol. 120, No. 8, pp. 2358-2376.

Chang, K.C., Liu, K.Y. and Chang, S.B. 2001. Seismic retrofit study of RC rectangular bridge columns lap-spliced at the plastic hinge zone. *In: Proc. of the International Conference on FRP Composites in Civil Engineering, Hong Kong*, pp. 869-875.

Crémer, C. 2001. 'Modélisation du comportement non linéaire des fondations superficielles sous séisme. Macro-élément d'interaction sol-structure'. Thèse de doctorat. Spécialités : Mécanique-Génie mécanique-Génie civil. Laboratoire de Mécanique et de Technologie de

Copyright fib, all rights reserved. This PDF copy of fib Bulletin 24 is intended for use and/or distribution only by National Member Groups of fib.

Cachan. ENS Cachan. Paris.

Dritsos, S. and Pilakoutas, K. 1992. Composite technique for repair-strengthening of RC members. *Proc. 2nd International Symposium on Composite Materials and Structures, Peking University Press*, China, pp. 958-963.

EERI, 1996. Theme issue: Repair and rehabilitation research for seismic resistance of structures. Earthquake Spectra Vol. 12, No. 4.

El-Attar, A.G., White, R.N. and Gergely, P. 1997. Behavior of gravity load designed reinforced concrete buildings subjected to earthquakes, ACI Structural J., Vol. 94, No. 2, pp.133-145.

Elnashai, A.S. 1992. Effect of member characteristics on the response of RC structures. *Proc. of the Tenth World Conference on Earthquake Engineering, Madrid*, Vol. 6, pp. 3275-3280, Balkema, Rotterdam.

Elnashai, A.S. and Salama, A.I. 1992. Selective repair and retrofitting techniques for RC structures in seismic regions. *Research Report ESEE/92-2*, Engineering Seismology and Earthquake Engineering Section, Imperial College, London, UK.

Elwood, K.J. and Moehle, J.P. 2001. Shake-table tests on the gravity load collapse of reinforced concrete frames. 3rd US-Japan Workshop on Performance-Based Earthquake Engineering Methodology for Reinforced Concrete Building Structures, Seattle, Washington, USA.

Ersoy, U., Tankut, T. and Suleiman, R. 1993. Behavior of jacketed columns. ACI Structural J., Vol. 90, No 3, pp.288-293.

Fardis, M.N. and Khalili, H.H. 1981. Concrete encased in fiberglass-reinforced plastic. ACI Journal, Vol. 78, No. 6, pp. 440-446.

FEMA, 1989. Establishing programs and priorities for the seismic rehabilitation of buildings. *FEMA Report 174*, Federal Emergency Management Agency, Washington, D.C.

FEMA, 1989. Techniques for seismically rehabilitating existing structures. *FEMA Report 172*, Federal Emergency Management Agency, Washington, D.C.

Feng, M.Q. and Bahng, E.Y. 1999. Damage assessment of jacketed RC columns using vibration tests. Journal of Structural Engineering (ASCE), Vol. 125, No. 3, pp. 265-271.

fib (2001). Externally bonded FRP reinforcement for RC structures. Bulletin 14, prepared by the working party EBR of the Task Group 9.3.

Fiorato, A.E., Oesterle,R.G. and Corley, W.G. 1983. Behavior of earthquake resistant structural walls before and after repair, ACI Structural Journal, Vol. 80, No 5, pp.403-413.

Foutch, D.A., Hjelmstad, K.D, Del Valle Calderon, E., Gutierrez, F. and Downs, R.E. 1989. The Mexico earthquake of September 19, 1985 – Case studies of seismic strengthening for two buildings in Mexico City. Earthquake Spectra, Vol. 5, No. 1, pp.153-174.

Foutch, D.A., Hjelmstad, K.D. and Del Valle Calderón, E. [1988] Seismic retrofit of a RC building: A case study. *Proceedings of the Ninth World Conference on Earthquake Engineering, Tokyo-Kyoto*, Vol. 7, pp. 451-456.

Frosch, R.J., Li, W., Jirsa, J.O. and Kreger, M.E. 1996. Retrofit of non-ductile moment-resisting frames using precast infill wall panels. Earthquake Spectra, Vol. 12, No. 4, pp. 741-760.

Fujii, S., Matsuzaki, K., Nakano, K. and Fukuyama, H. 1999. Japanese state of the art on seismic retrofit by fiber wrapping for building structures: Evaluations. In: Dolan CW, Rizkalla SH & Nanni A (eds) Fiber Reinforced Polymer Reinforcement for Reinforced Concrete Structures. ACI Report SP-188. Detroit, Mi., pp. 895-906.

Fujisaki, T., Hosotani, M., Ohno, S. and Mutsuyoshi, H. 1997. JCI state-of-the-art on retrofitting by CFRM – research. In: Non-Metallic (FRP) Reinforcement for Concrete Structures (Vol 1). Japan Concrete Institute, pp. 613-620.

Fukuyama, H., Suzuki, H. and Nakamura, H. 1999. Seismic retrofit of reinforced concrete columns by fiber sheet wrapping without removal of finishing mortar and side wall concrete. In: Dolan CW, Rizkalla SH & Nanni A (eds) Fiber Reinforced Polymer Reinforcement for Reinforced Concrete Structures. ACI Report SP-188. Detroit, Mi., pp. 205-216.

Fuse, T., Okuta, K., Hiramatsu, K., Ozawa, T. and Hara, N. 1992. Cyclic loading tests of reinforced concrete column strengthened with steel tube. In: *Proceedings 10th World Conference on Earthquake Engineering, Madrid*, Balkema, Rottterdam, pp.5227-5233.

Copyright fib, all rights reserved. This PDF copy of fib Bulletin 24 is intended for use and/or distribution only by National Member Groups of fib.

Gergely, J., Pantelides, C.P. and Reaveley, L.D. 2000. Shear strengthening of RC T-Joints using CFRP composites. ASCE J. of Composites for Construction, Vol. 4, No. 2, pp. 56-64.

Ghobarah, A., Aziz, T.S. and Biddah, A. 1997. Rehabilitation of reinforced concrete frame connections using corrugated steel jacketing. ACI Structural J., Vol. 4, No. 3, pp. 283-294.

Ghobarah, A., Biddah, A. and Mahgoub, M. 1997. Rehabilitation of reinforced concrete columns using corrugated steel jacketing. Journal of Earthquake Engineering, Vol. 1, No. 4, pp. 651-673.

Goel, S.C. and Masri, A.C. 1996. Seismic strengthening of an RC slab-column frames with ductile steel bracing. *Proceedings 11th World Conference on Earthquake Engineering, Acapulco*, Paper No. 506.

Gomes, A.M., Appleton, J. 1998. Repair and strengthening of reinforced concrete elements under cyclic loading. *Proceedings 11th European Conf. Earthquake Engineering, Paris.*

Harries, K.A., Cook, W.D. and Mitchell, D. 1996. Seismic retrofit of reinforced concrete coupling beams using steel plates, ACI Special Publication SP160, "Seismic Rehabilitation of Concrete Structures" (Sabnis, G.M. et al, eds.), American Concrete Institute, Detroit, Mi.

Hamilton, H.R. and Dolan, C. 2000. Durability of FRP reinforcements for concrete. Progress in Structural Engineering and Materials, No. 2, pp. 139-145.

Harmon, T.G., Gould, P.L., Wang, E. and Ramakrishnan, S. 1998. Behavior of confined concrete under cyclic loading. In: Saadatmanesh H & Ehsani MR (eds) *Second International Conference on Composites in Infrastructure, ICCI '98, Tucson, AZ* (Vol 1), pp. 398-410.

Haroun, M.A., Mosallam, A.S., Feng, M.Q. and Elsanadedy, H.M. 2001. Experimental investigation of seismic repair and retrofit of bridge columns by composite jackets. In: *Proceedings of the International Conference on FRP Composites in Civil Engineering, Hong Kong*, pp. 839-848.

Hosotani, M., Kawashima, K. and Hoshikuma, J. 1997. A study on confinement effect of concrete cylinders by carbon fiber sheets. In: Non-Metallic (FRP) Reinforcement for Concrete Structures (Vol 1). Japan Concrete Institute, pp. 209-216.

Ignatiev, N. 1998. Some problems of strengthening of existing buildings with new structural components. 2nd Japan-Turkey Workshop on Earthquake Engineering, on "Repair & Strengthening of Existing Buildings", Japan International Cooperation Agency and Istanbul Technical University – Faculty of Civil Engineering, Volume 1, Istanbul.

Iliya, R. and Bertero, V.V. 1980. Effects of amount and arrangement on wall – panel reinforcement on hysteretic behavior of reinforced concrete walls", Report No. UCB/EERC-80/04, University of California, Berkeley.

Iso, M., Matsuzaki, Y., Sonobe, Y., Nakamura, H. and Watanabe, M. 2000. Experimental study on reinforced concrete columns having wing walls retrofitted with continuous fiber sheets. In: *Proceedings 12th World Conference on Earthquake Engineering, New Zealand*, pp.1865-1871.

Izzuddin, B.A. and Elnashai, A.S. 1989. ADAPTIC, a program for adaptive large displacement elastoplastic dynamic analysis of steel, concrete and composite frames. *Research Report ESEE-89/7*, Engineering Seismology and Earthquake Engineering Section, Imperial College, London, UK.

Japan Concrete Institute, 1998. Technical Report on Continuous Fiber Reinforced Concrete.

Jirsa, J.O. and Stoppenhagen, D.R. 1987. Seismic repair of a reinforced concrete frame using encased columns. PMFSEL Report 87-2, Phil M. Ferguson Structural Engineering Laboratories, University of Texas, Austin.

JSCE (2001). Recommendations for Upgrading of Concrete Structures with Use of Continuous Fiber Sheets, edited by Maruyama K, Japan Society of Civil Engineers.

Kahn, L.F. and Hanson, R.D. 1979. Infilled walls for earthquake strengthening. ASCE J. of the Structural Division, Vol. 105, No. ST2, pp. 283-296.

Karbhari, V.M. and Gao, Y. 1997. Composite jacketed concrete under uniaxial compression – verification of simple design equations. ASCE J. of Materials in Civil Engineering, Vol. 9, No. 4, pp.185-193.

Kobatake, Y., Kimura, K. and Katsumata, H. 1993. A retrofitting method for reinforced concrete structures using carbon fiber. In: Nanni A (ed) Fiber-Reinforced-Plastic (FRP)

Copyright fib, all rights reserved. This PDF copy of fib Bulletin 24 is intended for use and/or distribution only by National Member Groups of fib.

Reinforcement for Concrete Structures: Properties and Applications. Elsevier Science Publishers, pp. 435-450.

Koyluoglu, A.M., Yuva, Y., Askar, G.A., Verzeletti, G. and Pinto. A.V. 1995. Seismic strengthening of R/C joints using adhesively bonded steel plates. Experimental Results. Safety Technology Institute, European Laboratory for Structural Assessment, Report EUR 16276 EN, Joint Research Centre, European Commission.

Kraetzig, W.B., Meyer, I.F., and Stangenberg, F. 1989. Experimentelle Untersuchungen zur Schadigungsevolution und Instandsetzung von Stahlbetonstützen Unter Erdbebenahnlicher Beanspruchung. SFB 151, Berichte Nr. 14, Ruhr–Universität, Bochum.

La Tegola, A. and Manni, O. 1999. Experimental investigation on concrete confined by fiber reinforced polymer and comparison with theoretical model. In: Dolan CW, Rizkalla SH & Nanni A (eds) Fiber Reinforced Polymer Reinforcement for Reinforced Concrete Structures. ACI Report SP-188. Detroit, Mi., pp. 243-253.

Lam, L. and Teng, J.G. 2001. A new stress-strain model for FRP-confined concrete. In: *Proceedings of International Conference on FRP Composites in Civil Engineering, Hong Kong*, pp. 283-292.

Lombard, J.C., Lau, D.T., Humar, J.L., Cheung, M.S. and Foo, S. 2000. Seismic repair and strengthening of reinforced concrete shear walls for flexure and shear using carbon fibre sheets. In: Humar J & Razaqpur AG (eds) Advanced Composite Materials in Bridges and Structures, Montreal: The Canadian Society for Civil Engineering, pp. 645-652.

Ma, R. and Xiao, Y. 1997. Seismic retrofit and repair of circular bridge columns with advanced composite materials. Earthquake Spectra, Vol. 15, No. 4, pp. 747-764.

Mander, J.B., Priestley, M.J.N. and Park, R. 1988. Theoretical stress-strain model for confined concrete. ASCE J. of Structural Engineering, Vol. 114 No. 8, pp. 1804-1826.

Martinez-Rueda, J.E. 1997. Energy dissipation devices for seismic upgrading of RC structures. Ph.D. Thesis, Imperial College, London, UK.

Martinez-Rueda, J.E. and Elnashai, A.S. 1997. Confined concrete model under cyclic load. Materials and Structures, Vol. 30, pp. 139-147.

Masri, A.C. and Goel, S.C. 1996. Seismic design and testing of an RC slab-column frame strengthened by steel bracing. Earthquake Spectra, Vol. 12, No. 4, pp.645-666.

Masukawa, J., Akiyama, H. and Saito, H. 1997. Retrofit of existing reinforced concrete piers by using carbon fiber sheet and aramid fiber sheet. In: Non-Metallic (FRP) Reinforcement for Concrete Structures (Vol 1). Japan Concrete Institute, pp. 411-418.

Masuo, K. 1999. Seismic retrofitting of reinforced concrete columns with wing walls using carbon fiber reinforced plastic walls. In: Dolan CW, Rizkalla SH & Nanni A (eds) Fiber Reinforced Polymer Reinforcement for Reinforced Concrete Structures, ACI Report SP-188. Detroit, Mi., pp. 193-204.

Matsuzaki, Y., Nakano, K., Fujii, S. and Fukuyama, H. 1999. Japanese state of the art on seismic retrofit by fiber wrapping for building structures: Research. In: Dolan CW, Rizkalla SH & Nanni A (eds) Fiber Reinforced Polymer Reinforcement for Reinforced Concrete Structures, ACI Report SP-188. Detroit, Mi., pp. 879-893.

Matsuzaki, Y., Nakano, K., Fujii, S. and Fukuyama, H. 2000. Seismic retrofit using continuous fiber sheets. *Proc., 12th World Conference on Earthquake Engineering, New Zealand*, pp. 2524-2531.

Miranda, E. 1990. Upgrading of a school building in Mexico city. *Proc. 4th US National Conference on Earthquake Engineering, Palm Springs, Ca*, Vol. 1, pp. 109-118.

Miranda, E. and Bertero, V.V. 1990. Post-tensioning technique for seismic upgrading of existing low-rise buildings. *Proc. 4th US National Conference on Earthquake Engineering, Palm Springs, Ca*, Vol. 3, pp. 393-402.

Miyauchi, K., Nishibayashi, S. and Inoue, S. 1997. Estimation of strengthening effects with carbon fiber sheet for concrete column. In: Non-Metallic (FRP) Reinforcement for Concrete Structures (Vol 1). Japan Concrete Institute, pp. 217-224.

Monti, G., Nistico, N. and Santini, S. 2001. Design of FRP jackets for upgrade of circular bridge piers. ASCE J. of Composites for Construction, Vol. 5, No. 2, pp. 94-101.

Mutsuyoshi, H., Ishibashi, T., Okano, M. and Katsuki, F. 1999. New design method for seismic retrofit of bridge columns with continuous fiber sheet – Performance-based design. In: Dolan CW, Rizkalla SH & Nanni A (eds) Fiber Reinforced Polymer Reinforcement for Reinforced Concrete Structures, ACI Report SP-188. Detroit, Mi., pp. 229-241.

Copyright fib, all rights reserved. This PDF copy of fib Bulletin 24 is intended for use and/or distribution only by National Member Groups of fib.

Nakano, Y. 1995. Damage to buildings due to 1994 Sanriku-harukaoki earthquake (in Japanese), Building Disaster, Vol. 211, Japan Building Disaster Prevention Association, pp.6-15.

Neale, K.W. 2000. FRPs for structural rehabilitation: a survey of recent progress. Progress in Structural Engineering and Materials, Vol. 2, pp. 133-138.

Neubauer, U. and Rostásy, F. S. 1999. Bond failure of concrete fibre reinforced polymer at inclined cracks – experiments and fracture mechanics model. In: Dolan CW, Rizkalla SH & Nanni A (eds) Fiber Reinforced Polymer Reinforcement for Reinforced Concrete Structures, ACI Report SP-188. Detroit, Mi. pp. 369-382.

Osada, K., Yamaguchi, T. and Ikeda, S. 1999. Seismic performance and the retrofit of hollow circular reinforced concrete piers having reinforcement cut-off planes and variable wall thickness. In: Transactions of the Japan Concrete Institute, Vol. 21, pp. 263-274.

Pantazopoulou, S. 1995. Role of expansion on mechanical behavior of concrete. ASCE J.of Structural Engineering, Vol. 121, No. 12, pp.1795-1805.

Pantelides, C.P., Gergely, J., Reaveley, L.D. and Volnyy, V. 1999. Retrofit of RC bridge pier with CFRP advanced composites. ASCE J. of Structural Engineering, Vol. 125, No. 10, pp. 1094-1099.

Paulay, T. and Priestley, M.J.N. 1992. *Seismic Design of Reinforced Concrete and Masonry Buildings*, John Wiley & Sons Inc., New York.

Petersson, H. and Popov, E.P. 1977. Constitutive relations for generalised loading. *Journal of the Engineering Mechanics Division, ASCE* **103**(4): 611-627.

Pincheira, J.A. and Jirsa, J.O. 1992. Post-tensioned bracing for seismic retrofit of RC frames. *Proc. 10th World Conf. on Earthquake Engineering, Mardid,* Balkema, Rottterdam, pp.5199-5204.

Pinho, R. 2000. Selective repair and retrofitting of RC structures using selective techniques. Ph.D. Thesis, Imperial College, University of London, London (to be submitted).

Poulos, H.J. and Davis, E.H. 1974. *Elastic Solutions for Soil and Rock Mechanics*, John Wiley & Sons Inc., New York.

Priestley, M.J.N. and Seible, F. 1995. Design of seismic retrofit measures for concrete and masonry structures. Construction and Building Materials, Vol. 9, No. 6, pp. 365-377.

Priestley, M.J.N., Seible, F. and Calvi, G.M. 1996. Seismic Design and Retrofit of Bridges, John Wiley & Sons Inc., New York.

Priestley, M.J.N., Seible, F. and Chai, Y.H. 1992. Seismic retrofit of bridge columns using steel jackets. *Proc. 10th World Conf. on Earthquake Engineering, Madrid,* Balkema, p.5285-5290.

Priestley, M.J.N., Seible, F., Xiao, Y. and Verma, R. 1994. Steel jacket retrofitting of reinforced concrete bridge columns for enhanced shear strength – Part 1: theoretical considerations and test design. ACI Structural J., Vol. 91, No. 5, pp.394-405.

Priestley, M.J.N., Seible, F., Xiao, Y. and Verma, R. 1994. Steel jacket retrofitting of reinforced concrete bridge columns for enhanced shear strength – Part 2: test results and comparison with theory. ACI Structural J., Vol. 91, No. 5, pp.537-551.

Prota, A., Nanni, A., Manfredi, G. and Cosenza, E. 2001. Selective upgrade of beam-column joints with composites. In: *Proceedings of the International Conference on FRP Composites in Civil Engineering, Hong Kong,* pp. 919-926.

Restrepo, J.I., Wang, Y.C., Irwin, R.W. and DeVino, B. 1998. Fibreglass/epoxy composites for the seismic upgrading of reinforced concrete beams with shear and bar curtailment deficiencies. In: *Proceedings 8th European Conference on Composite Materials, Naples*, pp.59-66.

Rodriguez, M. and Park, R. 1994. Seismic Load Tests on Reinforced Concrete Columns strengthened by Jacketing, ACI Structural J., Vol. 91, No 2, pp.150-159.

Saadatmanesh, H., Ehsani, M.R. and Jin, L. 1996. Seismic strengthening of circular bridge pier models with fiber composites. ACI Structural J., Vol. 93, No. 6, pp. 639-647.

Saadatmanesh, H., Ehsani, M.R. and Jin, L. 1997. Repair of earthquake-damaged RC columns with FRP wraps. ACI Structural J., Vol. 94, No. 2, pp. 206-215.

Saafi, M., Toutanji, H.A. and Li, Z. 1999. Behavior of concrete columns confined with fiber reinforced polymer tubes. ACI Materials J., Vol. 96, No. 4, pp.500-509.

Saatcioglu, M. and Elnabelsy, G. 2001. Seismic retrofit of bridge columns with CFRP jackets. In: *Proceedings of the International Conference on FRP Composites in Civil Engineering, Hong Kong*, pp. 833-838.

Copyright fib, all rights reserved. This PDF copy of fib Bulletin 24 is intended for use and/or distribution only by National Member Groups of fib.

Saiidi, S., Sanders, D.H., Gordaninejad, F., Martinovic, F,M. and McElhaney, B.A. 2000. Seismic retrofit of non-prismatic RC bridge columns with fibrous composites. In: *Proceedings 12th World Conference on Earthquake Engineering, New Zealand*, pp. 143-150.

Sakino, K. and Sun, Y. 2000. Steel jacketing for improvement of column strength and ductility. *Proc. 12th World Conf. on Earthquake Engineering, Christchurch, New Zealand*, Paper No. 2525.

Salama, A.I. 1993. Repair of earthquake-damaged RC structures. Ph.D. Thesis, Imperial College, University of London, London.

Samaan, M., Mirmiran, A. and Shahawy, M. 1998. Model of concrete confined by fiber composites. ASCE J. of Structural Engineering, Vol. 124, No. 9, pp. 1025-1031.

Seible, F., Innamorato, D., Baumgartner, J., Karbhari, V. and Sheng, L.H. 1999. Seismic retrofit of flexural bridge spandrel columns using fiber reinforced polymer composite jackets. In: Dolan CW, Rizkalla SH & Nanni A (eds) Fiber Reinforced Polymer Reinforcement for Reinforced Concrete Structures, ACI Report SP-188. Detroit, Mi, pp. 919-931.

Seible, F., Priestley, M.J.N., Hegemier, G.A. and Innamorato, D. 1997. Seismic retrofit of RC columns with continuous carbon fiber jackets. ASCE J. of Composites for Construction, Vol. 1, No. 2, pp. 52-62.

Sexsmith, R., Anderson, D. and English, D. 1997. Cyclic behavior of concrete bridge bents. ACI Structural J., Vol. 94, No. 2, pp. 103-113.

Sheikh, S.A., Iacobucci, R. and Bayrak, O. 2000. Seismic upgrade of concrete columns with fibre reinforced polymers. In: Humar J & Razaqpur AG (eds) *Advanced Composite Materials in Bridges and Structures*. Montreal: The Canadian Society for Civil Engineering, pp. 267-274.

Shimbo, H., Yamada, K., Asai, H., Iwata, M. and Yonekura, A. 1997. Aseismic retrofit of concrete piers with CFRP ring and expansive concrete. In: Non-Metallic (FRP) Reinforcement for Concrete Structures (Vol 1). Japan Concrete Institute, pp. 363-370.

Sirbu, G., Yoshihiro, T., Sato, Y. and Ueda, T. 1998. Shear resisting capacity of a reinforced concrete pier retrofitted with carbon fiber sheet. In: Transactions of the Japan Concrete Institute, Vol. 20, pp. 233-238.

Spoelstra, M.R. and Monti, G. 1999. FRP-confined concrete model. ASCE J. of Composites for Construction, Vol. 3, No. 3, pp. 143-150.

Stoppenhagen, D.R., Jirsa, J.O. and Wyllie, L.A. 1995. Seismic repair and strengthening of a severely damaged concrete frame. ACI Structural J., Vol, 92, No. 2, pp.177-187.

Sugano, S. 1996. State-of-the-Art in techniques for rehabilitation of buildings, *Proc. 11th World Conference Earthquake Engineering, Acapulco*, paper No.2175.

Tankut, A.T. and Ersoy, U. 1992. Behaviour of repaired/strengthened reinforced concrete structural members, *Evaluation and Rehabilitation of Concrete Structures and Innovations in Design, ACI Special Publication – 128*.

Tasai, A. 1992. Effective repair with resin for bond failure of RC members. Proc. *10th World Conf. on Earthquake Engineering, Madrid*, Balkema Rotterdam, pp.5211-5216.

Tassios, T.P. 1983. Physical and mathematical models for re-deign of damaged structures. In *Proceedings, IABSE Symposium: Strengthening of Building Structures – Diagnosis and Therapy, Venice*, pp. 29-77.

Tastani, S. and Pantazopoulou, S.J. 2002. Design of seismic strengthening for brittle RC members using FRP jackets. *Proc. 12th European Conf. on Earthquake Engineering, London*, paper 360.

Tena-Colunga, A. 1996. Some retrofit options for the seismic upgrading of old low-rise school buildings in Mexico. Earthquake Spectra, Vol. 12, No. 4, pp. 883-902.

Teran-Gilmore, A., Bertero, V.V. and Youssef, N.F.G. 1996. Seismic rehabilitation of infilled non-ductile frame buildings using post-tensioned steel braces. Earthquake Spectra, Vol. 12, No. 4, pp.863-882.

Triantafillou, T.C. 1998a. Strengthening of structures with advanced FRPs. Progress in Structural Engineering and Materials, Vol. 1, pp. 126-134.

Triantafillou, T.C. 1998b. Shear strengthening of reinforced concrete beams using epoxy-bonded FRP composites. ACI Structural J., Vol. 95, pp. 107-115.

Triantafillou, T.C. 2001. Seismic retrofitting of structures using FRPs. Progress in Structural Engineering and Materials, Vol. 3, No. 1, pp. 57-65.

Copyright fib, all rights reserved. This PDF copy of fib Bulletin 24 is intended for use and/or distribution only by National Member Groups of fib.

Triantafillou, T.C. and Antonopoulos, C.P. 2000. Design of concrete flexural members strengthened in shear with FRP. ASCE J. of Composites for Construction, Vol. 4, No. 4, pp. 198-205.

Tsicknias, T. and Pittas, M. 1992. Strengthening of buildings with shotcrete braces (in Greek). *Proc. 1st National Conf. on Earthquake Engineering and Engineering Seismology, Athens*, V.B., pp.349-362.

Unjoh, S. and Kawashima, K. 1992. Seismic inspection and seismic strengthening method of reinforced concrete bridge piers. *Proc. 10th World Conference on Earthquake Engineering, Madrid,* Balkema, pp.5279-5285.

Wang, T.Y., Bertero, V.V. and Popov, E.P. 1975. Hysteretic behavior of reinforced concrete framed walls. Report No. EERC 75-23, University of California, Berkeley, Ca.

Wang, Y.C., Restrepo, J.I. and Park, R. 2000. Retrofit of reinforced concrete members using advanced composite materials. University of Canterbury Department of Civil Engineering Research Report 2000-3, New Zealand.

Watanabe, K., Nakamura, H., Honda, Y., Toyoshima, M., Iso, M., Fujimaki, T., Kaneto, M. and Shirai, N. 1997. Confinement effect of FRP sheet on strength and ductility of concrete cylinders under uniaxial compression. In: Non-Metallic (FRP) Reinforcement for Concrete Structures (Vol 1). Japan Concrete Institute, pp. 233-240.

Wyllie, L.A. Jr. 1996. Strengthening strategies for improved seismic performance, *Proc. 11th World Conf. on Earthquake Engineering., Acapulco*, paper No.1424.

Wyllie, L.A. Jr. 1998. Evaluation and strengthening concrete structures for acceptable seismic performance. *Proc. XIIIth FIP Congress, Amsterdam*, Balkema ed., Rotterdam, 2, pp.625-630.

Xiao, Y. and Wu, H. 2000. Compressive behavior of concrete confined by carbon fiber composite jackets. ASCE J. of Materials in Civil Engineering, Vol. 12, No. 2, pp. 139-146.

Yamamoto, T. 1992. FRP Strengthening of RC Columns for Seismic Retrofitting. *Proc.10th World Conf. on Earthquake Engineering, Madrid*, Balkema, pp.5205-5210.

Yamamoto, Y. 1993. Strength and ductility of frames strengthened with steel bracing. In "Earthquake Resistance of Reinforced Concrete Structures", A Volume Honouring H. Aoyama (T. Okada, ed.), pp.467-476.

Yamamoto, Y. and Umemura, H. 1992. Analysis of reinforced concrete frames retrofitted with steel brace. *Proc. 10th World Conf. on Earthquake Engineering, Madrid*, Balkema, pp.5187-5192.

Zhang, A., Yamakawa, T., Zhong, P. and Oka, T. 1999. Experimental study on seismic performance of reinforced concrete columns retrofitted with composite materials jackets. In: Dolan CW, Rizkalla SH & Nanni A (eds) Fiber Reinforced Polymer Reinforcement for Reinforced Concrete Structures, ACI Report SP-188. Detroit, MI, pp. 269-278.

Copyright fib, all rights reserved. This PDF copy of fib Bulletin 24 is intended for use and/or distribution only by National Member Groups of fib.

6 Probabilistic concepts and methods

6.1 Introduction

The multiplicity of design objectives that goes under the name of Performance Based Design (PBD), the new design philosophy which is now firmly established, necessarily implies that an objective measure be associated to the degree of compliance of the final design with each of these objectives.

That a proper, if not the only, measure of compliance is represented by a probability value is long undisputed: objections refer to the complexity introduced in the design process, to the additional expertise required, to the wide margins for subjective choices that remain, by the nature of the approach, in the hands of the designer.

Probabilities are already explicitly indicated in all recent design codes: they qualify the intensity values that are to be used in designing for the considered Performance Levels (PL).

If this is certainly a progress over previous practice, when intensity levels were fixed empirically by tradition and updated following the occurrence of earthquakes, the present approach is still quite limited and inadequate with respect to the goals of PBD. A deterministic design or assessment, made on the basis of a probability-qualified seismic action goes less than half-way towards the goal of a reliability-based design or assessment. In effect, such a procedure cannot provide any estimate of the total probability of exceedance of the PL of interest, since it does not account, as it should, for seismic intensities which may be higher, or lower, or indeed equal to the design one. Intuitively, the total probability must depend on the characteristics of the hazard (i.e., on the variation of the function: $\Pr\{I \geq i\}$ with the value of the intensity $I = i$), which is a site-specific feature, and on the sensitivity of the structure to variations of I. If this latter is expressed by the probability density function (PDF): $f_c(i) \cdot di$, which gives the probability of exceeding the capacity C of the structure with respect to a given PL when the seismic intensity is in the interval: $(i \leq I \leq i + di)$, the total probability is the continuous summation of the product:

$$P_f = \int_{all\ I's} \Pr\{I > i\} \cdot f_c(i)\, di \tag{6-1}$$

where each elementary integrand is the probability of failure given that the intensity lies in the interval $(i \leq I \leq i + di)$.

Eq. (6-1), with P_f understood as the probability of exceedance of any specified PL characterized by a random capacity C, provides an objective measure of performance.

Implementation of eq. (6-1) into a viable design or assessment procedure is admittedly a major task. It is appropriate to note, though, that for what concerns the design of new buildings the motivation for such a rigorous approach is less pressing than for the assessment of existing ones. The rather sophisticated design procedures and detailing rules incorporated in current codes are in fact capable of ensuring without undue additional cost ample reserves of energy dissipation capacity, such that properly designed structures can resist earthquakes of much stronger intensity than the design one.

The case of existing structures, though, is almost at the opposite end: these structures have quite often basic weaknesses for what concerns the path of internal forces under lateral actions, and contain a number of brittle elements whose failure may well precipitate the global one. If the performance of these structures has to be assessed without undue conservatism, less conventional procedures need to be adopted, in which the use of realistic mechanical models is coupled with an explicit treatment of all sources of uncertainty.

Reliability-based seismic assessment methods are discussed in this Chapter.

Copyright fib, all rights reserved. This PDF copy of fib Bulletin 24 is intended for use and/or distribution only by National Member Groups of fib.

The State-of-the Art on the subject is reviewed in recent papers (Pinto, 2001)(Ellingwood, 2001)(Der Kiureghian, 1996), where it appears that while theoretically rigorous approaches are still under development and are likely to result in complex procedures unsuited for practical use, simple but effective approximate proposals are emerging which seem to have the potential for professional application; two of these will be illustrated in this chapter. As both approaches require non-linear dynamic analysis of the structure, care is needed in the definition of the seismic input. This aspect is discussed in the following section.

6.2 Seismic motion for reliability assessments

There are two basic choices for selecting the time-histories needed for non linear analyses: use of recorded or of artificial accelerograms.

It is generally agreed that the former are the ones appropriate when an absolute measure of risk is sought. Difficulties with the use of recorded accelerograms are two-fold. First, even when records are classified for narrowly defined ranges of magnitude (M) and distance (D), and they belong to similar stiff soil sites, the resulting from sample to sample variability of the response is quite significant, which obliges to make use of a large number of samples if sharp estimates of the mean and the standard deviation of the response are sought.

Secondly, risk analysis procedures generally require a certain amount of scaling of the original intensity of the records, and this practice meets with objections from engineering seismologists, who rightly point out that different (M, D) ranges produce motions with different characteristics, which makes it improper to scale for instance a record from a certain (M, D) range to the mean intensity of a group of records belonging to a different range.

Both of these arguments can be answered in a way that their relevance in actual risk computations is greatly reduced.

As regards the first one, it will be shown while presenting the SAC-FEMA 6.4.1 method that a precise estimate of the response variability is not necessary, since the overall value of risk is not much sensitive to this quantity. Hence, a small number of records, of the order of between 5 and 10, is adequate for the purpose. For what concerns the second question, at least a partial answer comes from the extensive statistical investigation reported in (Shome et al., 1998). There it is shown that, provided one chooses as intensity measure of the records their respective response spectrum ordinate at the fundamental period of the structure under study, $S_a(T)$, records can be scaled without introducing bias in the estimate of both the median and the standard deviation of the (inelastic) response. This is demonstrated by scaling the intensity of groups of records from widely different (M, D) ranges to the same $S_a(T)$, either many times higher or lower than the original average value proper to each group. The result is that, for the same $S_a(T)$, the average (median value in the study) responses and their associated variabilities from different groups are equal, to an extent which is fully acceptable for all practical purposes. The statement is particularly strong if the response is measured in terms of ductility μ.

As expected, normalisation of all records to the same $S_a(T)$ reduces the variability δ of the response: this is an advantage, since reducing δ involves a reduction of the statistical uncertainty in the estimate of the median. The reduced δ, however, should be seen as a conditional quantity, the condition being the chosen value of $S_a(T)$.

This fact needs not to be a drawback. If the final objective is the evaluation of risk, the variability of S_a is specifically accounted for by the hazard function $H(S_a) = \Pr(S_a > s_a)$. If only the variability of the response (unconditional with respect to S_a) is sought, then one needs to perform a (reduced) number of analyses so as to obtain a functional relationship between the response μ and S_a of the form: $\mu = a \cdot S_a^b \cdot \varepsilon$, where ε is an error term with

Copyright fib, all rights reserved. This PDF copy of fib Bulletin 24 is intended for use and/or distribution only by National Member Groups of fib.

median 1 and a dispersion δ_ε obtained from the regression. The unconditional δ can then be approximately retrieved as: $\delta = \delta_\mu = \sqrt{b^2\delta_{S_a}^2 + \delta_\varepsilon^2}$ where $\delta_{S_a}^2$ is the dispersion of the S_a value about the median value, evaluated on the basis of the $5 \div 10$ records available.

The term *artificial* accelerograms is used here to mean accelerograms whose elastic response spectrum approximates a given spectrum, for instance an idealised uniform hazard spectrum adopted by a seismic design code. The use of such a spectrum as a basis for risk analysis can obviously only serve to check whether the existing structure that is being assessed has a risk larger or smaller than that of a new one that would be designed in the same region according to the same spectrum.

For a consistent reliability approach, it is necessary that the given spectrum be qualified in terms of probability of exceedance of its ordinates, for instance 50% fractile, and that a distribution function for the maximum of the response process (e.g. extreme type I) be postulated. With this information, and two additional assumptions : duration and form of non-stationarity, the underlying stochastic process can be traced back and samples of this process can be easily generated. If the scatter produced by these samples about the given spectral ordinates is negligible, a result that existing generation procedures can provide, one might consider in approximation that the average values of the maximum responses obtained from a small number of simulated samples represent the same fractile characterising the ordinates of the originating spectrum.

In other words, the responses obtained from spectrum-matching accelerograms are (x%) fractile values, conditional on the specific intensity characterising the spectrum. Since the spectral shape is fixed, the intensity measure can be indifferently chosen as the anchoring value of the PGA, or as a spectral ordinate at any period.

6.3 Modelling of mechanical randomness

This section summarises for convenience the main inelastic mechanisms which cause a RC structure subjected to a strong shaking to undergo a progressive deterioration before reaching its final state of collapse. Modelling of these mechanisms is dealt with extensively in Chapter 3; here only some of the more basic expressions are presented, for use in the ensuing reliability analysis. Alternative and additional expressions may be introduced, if deemed more appropriate, with the general procedures remaining unaffected.

A paragraph is also devoted to a simple model for describing uncertainty in spatially distributed mechanical parameters.

6.3.1 Resistance of beam-column joints

Damage to the joints can take one or more of the following forms: a) slippage of the bars (usually those of the beams) through the joint, due to loss of bond, b) bi-diagonal fine cracking of the joint panel, c) large diagonal cracks, and d) diagonal compressive failure. Phenomena a) and b) are important, since they do not allow development of the moment capacities of the beams and columns, and decrease substantially the overall stiffness of the structure, respectively. These states of damage, however, are not by themselves considered as ultimates ones, though they may contribute to anticipating the actual collapse.

Phenomena c) and d) occur frequently in non-confined joints, especially exterior ones, either L-shaped or T-shaped, when horizontal joint reinforcement is missing or too light, and/or the transverse dimension of the joint is too small. Since these failures cut the transmission of moments between the elements framing into the joint, they involve a sudden drop of resistance of the whole structure, especially when they take place at the lower floors, and is therefore quite reasonable to equate their occurrence to that of a collapse.

The expression provided in (New Zealand Nat. Soc. for Earthq. Eng., 1996) for the

Copyright fib, all rights reserved. This PDF copy of fib Bulletin 24 is intended for use and/or distribution only by National Member Groups of fib.

resisting shear force of an exterior joint without horizontal (tie) reinforcement is:

$$V_R = k\sqrt{f_c'}\left(1 + \frac{N}{A_g k\sqrt{f_c'}}\right)^{1/2} bh \quad (f_c' \text{ in MPa}) \tag{6-2}$$

where f_c' is the estimated compressive strength of concrete, A_g the gross cross-section of the column, b, h the dimensions of the face of the joint normal to the beam axis, and N is the axial force value consistent with the maximum external acting shear force. For the factor k the following values are recommended: $k = 0.4$ when the beam longitudinal bars are anchored by bending the hooks into the joint core, $k = 0.25$ when the bars are anchored by bending the hooks into the columns above or below. No quantitative indication is given in (New Zealand Nat. Soc. for Earthq. Eng., 1996) regarding the scatter characterizing eq. (6-2), although it is commented that the k values are based on very limited experimental evidence. A CoV of the order of 0.30 – 0.35 might probably be adequate.

The eq. (6-2) refers to mechanism c), i.e. exceedance of principal tensile stress. According to (Priestley, 1997), joint failure due to diagonal tension takes place progressively and hence is less brittle than mechanism d). This latter can thus be more critical in the case of joints with high shear stress level and high normal forces. A failure criterion based on principal compressive stress is suggested in (Priestley, 1997):

$$p_c = \frac{N}{2A_g} + \sqrt{\left(\frac{N}{2A_g}\right)^2 + \tau^2} < 0.5 f_c' \tag{6-3}$$

6.3.2 Shear strength of beams and columns

Past codes have been traditionally rather conservative for what concerns dimensioning for shear, so that shear-critical elements are not found frequently in old framed buildings. Inelastic cycling, however, is known to produce a degradation of shear capacity, and to lead to failures of the shear type even for elements which under static forces would fail in flexure. If this phenomenon occurs in one or more beams, it is usually considered as a local failure event, since it does not impair the functioning of the whole system and can be repaired with relative ease. Shear failure of a column, instead, can imply loss of vertical load carrying capacity, and is obviously a more grave (and irreversible) state of damage, such that it can be defined as an ultimate one for the structure.

Predictive equations for shear strength of concrete columns have been proposed in (Priestley, 1997) and adopted in (New Zealand Nat. Soc. for Earthq. Eng., 1996). The expression is of the form:

$$V = V_c + V_s + V_n \tag{6-4}$$

where the three additive terms represent the contribution of concrete, of shear reinforcement and of normal force, respectively, and are given by:

$$\begin{aligned} V_c &= K\sqrt{f_c'}0.8A_g \\ V_s &= A_n f_y \frac{d'}{s}\text{cotg}\,30^\circ \\ V_n &= N\tan\alpha \end{aligned} \tag{6-5}$$

where A_n is the total transverse area of reinforcement, d' is the distance between the peripheral hoops, s is the stirrup spacing, and α is the angle between the column longitudinal axis and a line connecting the compression centres at the top and bottom sections

Copyright fib, all rights reserved. This PDF copy of fib Bulletin 24 is intended for use and/or distribution only by National Member Groups of fib.

of the column. The factor K takes into account the effect of the ductility demand in reducing the shear carried by the concrete. Its value is 0.29 for μ-values up to 2, then decreases linearly down to 0.1 for $\mu = 4$, and remains constant.

The scatter between experimental values and those predicted by eq. (6-4) is quite modest, the indicated values of the CoV being about 0,13; however, the number of specimens used in establishing this CoV was rather limited.

6.3.3 Ultimate member chord rotation

Ultimate drifts of members are traditionally expressed by means of the plastic hinge model, which assumes all inelastic behaviour to be uniformly distributed within the length of this ideal "hinge". Denoting by L_s and L_{pl} the shear span of the member ($L_s = M/V$) and the plastic hinge length, respectively, and by ϕ_y and ϕ_u the yield and the ultimate curvature of the sections within the plastic hinge length, the ultimate drift is given by the well-known expression

$$\theta_u = \phi_y \frac{L_s}{3} + (\phi_u - \phi_y) L_{pl} (1 - 0,5 \frac{L_{pl}}{L_s}) \tag{6-6}$$

The scatter between the predictions obtained from eq. (6-6) and the actual experimental values arises from several sources, the major one being obviously the determination of L_{pl}. In (Panagiotakos and Fardis, 2001) an expression has been derived for L_{pl} which provides the best fit between the values from eq. (6-6) and a large number (several hundred) of test results on beams and beam-colums subjected to monotonic and cyclic loading to failure. The expression for cyclic loading is:

$$L_{pl} = 0,12 L_s + 0,014 a_{sl} d_b f_y \tag{6-7}$$

where f_y is in MPa, d_b is the diameter of compression longitudinal reinforcement and a_{sl} is a zero-one variable for absence or presence of bar pullout from the anchorage zone beyond the section of maximum moment. With the use of eq. (6-7) into eq. (6-6), the ratio of experimental and predicted values of θ_u has a mean value of $1,23$, a median value of $0,99$ and a CoV of $0,83$.

When using eq. (6-6) for assessment purpose, in addition to the variability of L_{pl} one has also to consider that of the material properties, the most influential one being the ultimate compressive strain of concrete in the quantification of ϕ_u. Extensive numerical investigations on the variability of strength and ductility of reinforced concrete sections are reported in (Kappos et al., 1999) where, for example, curvature ductility $\mu_\phi = \phi_u/\phi_y$ is studied as function of the basic (random) material properties: f'_c, f_y, ε_{su} and ε_{cu}. The dominant contribution to the Cov of μ_ϕ comes of that of ε_{cu}, which is estimated to be in the order of 0,35.

An alternative approach is to look directly at the rotation capacity, defined as the ultimate rotation at one end of an element in antisymmetric bending. Only empirical expressions are available to provide this quantity as a function of the many parameters that have a major influence on it.

The expression given in (Panagiotakos and Fardis, 2001), which has been elaborated from a large database of several hundred tests is:

$$\theta_u(\%) = \alpha_{st}\alpha_{cyc}\left(1 + \frac{a_{sl}}{2.3}\right)(0.2^{\nu})\left(\frac{\max(0.01, \omega_2)}{\max(0.01, \omega_1)} f'_c\right)^{0.275} \times$$
$$\times \left(\frac{L_s}{h}\right)^{0.45} \cdot 1.1^{100\alpha\rho_{sx}\frac{f_{yh}}{f'_c}} \cdot 1.3^{100\rho_d} \tag{6-8}$$

Copyright fib, all rights reserved. This PDF copy of fib Bulletin 24 is intended for use and/or distribution only by National Member Groups of fib.

where α_{st} is a coefficient for steel quality, equal to: 1.5 for hot-rolled ductile steel, 1.25 for heat-treated tempcore steel, 0.8 for cold-worked brittle steel; α_{cyc} is a coefficient equal to 1 for monotonic and 0.6 for cyclic loading; a_{sl} is a coefficient for bars slippage, equal to 1 if it is expected, zero otherwise; ν is the axial force ratio; ω_1 and ω_2 are the mechanical reinforcement ratios of tension and compression reinforcement; α is the confinement effectiveness factor as given in (Comite Eurointernational du Beton, 1993); ρ_{sx} is the geometric ratio of transverse reinforcement; f_{yh} is the yield stress of the transverse reinforcement; ρ_d is the geometric ratio of bi-diagonal reinforcement. The CoV associated with the ratio between the experimental values and the values obtained from eq. (6-8) is 0.47.

The chord rotation capacity corresponds to the likely loss of integrity of the element: if the capacity is attained even in a single column of a storey, the structure may be considered as failed, similar to the case of the failure due to shear.

6.3.4 Weak storey failure

Experience has repeatedly shown that when in one or more storeys the lateral capacity to lateral demand ratio is significantly lower than in the adjacent ones, a concentration of inelastic deformation demand takes place in these storeys, and storey collapses are likely to occur. This phenomenon is obviously related to the one previously considered, but here the emphasis is in the global stability of the storeys, which may be triggered at a ground motion intensity level lower than that required to exhaust the capacity of a single element. By definition, the phenomenon is assumed to occur when the curve of the maximum (over the storeys of the building) interstory drift versus the intensity of the action becomes almost flat. If the analysis of the response is performed dynamically, the intensity producing instability is obtained as the one which produces in one storey a flattening of the curve representing maximum (in time) drift versus intensity of the motion.

6.3.5 Uncertain parameters

Reducing the number of the non-linear structural analyses is a goal common to all methods of seismic reliability. With this objective in mind, a commonly adopted approach is to partition the vector of structural variables into two sub-vectors. The first one: $\mathbf{x}$, is of relatively small dimensions and contains the variables which have a significant influence on the response, as for instance the stiffnesses, the ratios of the yield strengths between adjacent elements, etc., and in general all variables a change of whose values would reasonably require performing a new analysis. The second sub-vector: $\mathbf{y}$, of much larger dimensions, is composed of variables of local nature, as for instance the shear strengths of all columns, the strength of the joints, etc., and in general of all variables which are suitable for detecting a state of failure of the structure, but whose own state is not such as to affect significantly the global dynamic response of the structure. The distinction between the components of $\mathbf{x}$ and of $\mathbf{y}$ is to some extent arbitrary and relies more on engineering judgement than on theoretical arguments: experience shows that it often leads to acceptable approximations.

It is difficult to discuss in general terms the selection of the structural parameters which are influential on the maximum response and are characterized by a significant amount of uncertainty. Since the response of a structure is essentially conditioned by its stiffness and yield strength, one should restrict the attention to those basic variables which can affect these two global parameters. For what concerns the stiffness, it depends on the geometry of the elements and on the amount of their reinforcement: the former is often known with sufficient precision, the latter normally much less so. The cracked stiffness, however, assuming that the model can account for differential cracking of the elements, is not too sensitive to the amount of reinforcement. Until significant yielding of the elements takes place, therefore, one could in many cases leave the estimation of the

Copyright fib, all rights reserved. This PDF copy of fib Bulletin 24 is intended for use and/or distribution only by National Member Groups of fib.

global stiffness to the computer code, with little, if any, consideration of uncertainty.

In moment resisting frame structures, it is customary to distinguish two basic modes of ductile type of failure, called beam-sway and column-sway mechanisms, respectively. Formation of one or the other mechanism depends, as it is well known, on the relative flexural strengths of the beams and the columns framing into the joints. It has been proposed in a recent draft code (New Zealand Nat. Soc. for Earthq. Eng., 1996) to use the following index:

$$S_i = \frac{\sum(M_{bl} + M_{br})}{\sum(M_{ca} + M_{cb})} \tag{6-9}$$

in order to judge whether, at a given horizontal level, plastic hinges occur in beams or columns. eq. (6-9) considers the ratio between the sum of the beam resisting moments at the left and right of the joint, for all joints of the ith floor, and the sum of the resisting moments above and below the joints at the same floor, see Fig. 6-1. If, for instance, S would be larger than one at two consecutive floors: i and $i+1$, formation of a storey mechanism would be likely to occur.

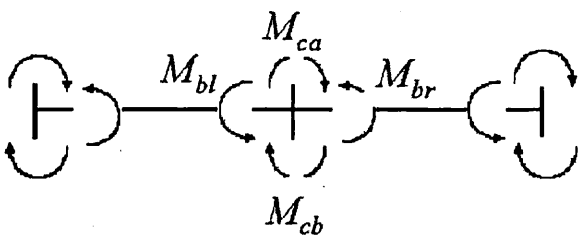

Figure 6-1: Meaning of symbols in eq.(6-9)

The use of the indices $S_i (i = 1, ...n)$ for modelling the uncertainty in the steel strength and in the reinforcement ratio in the beams and columns, instead of using separately the strength of each beam and column, is not only convenient for reducing the number of random variables to be included in the analysis, but it may also correspond to the type of information that can be gathered or guessed with a reasonable amount of effort.

It is recognized that modelling the parameter uncertainty through the S_i's may not be appropriate in some cases, as for instance, when failure of the structure depends on a small number of isolated critical members, and it is certainly not appropriate for structures other than moment resisting frames. Modelling the system randomness is a structure specific task and, for a given structure, it depends on the type of information available.

6.4 Assessment methods

A certain amount of literature exists dealing with probabilistic studies on RC structures. Rather than aiming to provide methods for use in practice, many of these studies consist of detailed and extensive investigations aimed at assessing the reliability of structures designed according to some deterministic code. The unique character of this type of studies makes their computational demand a rather secondary issue. One notable recent contribution in this field is the work by Dymiotis et al. (Dymiotis et al., 1999) on probabilistic assessment of RC frames, in which particular attention is devoted to the contribution to risk from the randomness of the mechanical parameters and from the uncertainty in the structural model. The procedure has been applied to the assessment of a RC frame designed to Eurocode 8 and to the probabilistic calibration of the force-reduction factors provided therein. The assessment methods to be described in this chapter belong

Copyright fib, all rights reserved. This PDF copy of fib Bulletin 24 is intended for use and/or distribution only by National Member Groups of fib.

to a different category of approaches, whose defining properties is that of being usable, in terms of competence and amount of work, by ordinary, though knowledgeable, engineers.

Two recently proposed methods in this category are presented herein. They have in common the fact of using accelerograms and non-linear analyses to calculate response probabilities: a feature that makes them eligible for the category of "simulation" approaches. This may not be inappropriate, provided the difference is noted that they are both extremely sparing in the number of records they require, compared with that of even the more efficient classical simulation approaches. The paradox is only apparent and the explanation is easy to give: these so-called "economic" simulation methods are valid within the (perhaps wide) sub-class of structural problems where the response is dominated by a single mode, and failure mechanisms, even if they are multiple, as in the present case, are all activated by the same single mode.

The first method is the so-called "2000 SAC/FEMA" method developed by Cornell et al. (Cornell et al., 2002) with specific reference to steel moment-resisting frames. Applications of this method to RC structures are not to be found in the literature yet: an example application to a 3D existing building is given in this section. This pilot application shows that the assumptions and simplifications on which the method is based are valid and provide consistent results for RC structures as well. The method requires only elementary notions of probability, and yields the total risk, i.e. the mean annual rate ($\simeq$ annual probability) of exceedance of a given PL. The method has been also cast in a partial safety factors format, for use in the design of new structures.

The second method has been developed in (Giannini et al., 2003) with direct reference to RC structures, addressing their peculiar failure mechanisms. The direct outcome of a single application is the value of P_f given a measure of intensity of the seismic action. Repeating the analysis for parametrically varying values of the intensity the fragility function is obtained, which can then, if required, be multiplied by the hazard function and integrated to calculate the risk. The probabilistic background required for the use of the method is even less than for the "2000 SAC/FEMA". An application to an existing RC frame is provided.

6.4.1 2000 SAC/FEMA method

This method provides the basis for the FEMA-350 Guidelines (Cornell et al., 2002) for seismic design and assessment of steel moment resisting frames. For use in practice, the Guidelines are set in the conventional format of partial safety factors affecting separately loads and resistances (referred to as "demand" and "capacity" in the Guidelines). These factors, however, originate from a full probabilistic treatment of the design/assessment problem, whereby the annual probability of exceeding specified levels of response is computed.

The method uses the following assumptions. The hazard at the site is defined in terms of the acceleration spectral ordinate corresponding to a period close to the fundamental period of the structure: $S_a(T)$. The spectral ordinate S_a is the intensity factor of the accelerograms (recorded accelerograms) used for the dynamic response analyses. The response of the structure, given the input, is deterministic, i.e. the uncertainty in the mechanical parameters which might affect the response is disregarded. Failure occurs when the maximum demand D over the duration of the seismic excitation exceeds the corresponding capacity C . In the original formulation, which is intended for steel frames, the two scalar response variables D and C represent maximum interstorey drift. In principle, however, D and C may refer to any other suitable couple of scalar variables of either deformation or of strength: the limitation remains that failure is defined in terms of single modes only.

As it will be seen, a fundamental advantage of the method lies in its mathematical

Copyright fib, all rights reserved. This PDF copy of fib Bulletin 24 is intended for use and/or distribution only by National Member Groups of fib.

simplicity and in the comparatively light computational effort it requires. These characteristics would permit, when necessary, to extend its present limits concerning structural determinism and single mode of failure without excessive impairment of the efficiency. Possible ways for dealing with these problems will be discussed subsequently.

6.4.1.1 Description of the basic method

In essence, the method aims at providing a closed form (and easy to compute) expression for the classical time-invariant reliability formulation, i.e.:

$$P_f = \int_0^\infty [1 - F_D(\alpha)]\, f_C(\alpha)\, d\alpha \tag{6-10}$$

in which $F_D(\cdot)$ is the cumulative distribution function (CDF) of the annual maxima of the demand, and $f_C(\cdot)$ the PDF of the capacity.

The starting point is to express the hazard at the site in the form

$$H(S_a) = \Pr(S_a \geq s_a, 1 \text{ year}) = k_0 s_a^{-k} \tag{6-11}$$

The form of eq. (6-11) is in several cases the direct result of the hazard analysis, when the more usual expressions for the attenuation laws and for the activity of the seismic regions are adopted. If the actual expression of $H(S_a)$ differs from eq. (6-11), then the latter should be fitted to the actual one in the region of the s_a values having a probability of exceedance close to the final value of P_f (this may require an iteration, if the order of magnitude of P_f is not known in advance).

The second step of the procedure is the passage from the probability of S_a to the probability of the response, or demand, D.To make this passage analytically simple, it is assumed that the median value of D : $\hat{D}$ can be approximately expressed as a function of S_a as:

$$\hat{D} = a\,(s_a)^b \tag{6-12}$$

The two constants a and b are to be determined by means of a (small, of the order of $5 \div 6$) number of nonlinear dynamic analyses using recorded accelerograms. Again for better accuracy, eq. (6-12) should be obtained using values of S_a whose probability brackets the value P_f . The same non-linear dynamic analyses provide an estimate of the dispersion of D about its median value (for the s_a values in the range considered in the analyses). The demand D is assumed to be log-normally distributed about the median, with standard deviation of the natural logarithms ('dispersion') equal to β_D (For values of $\beta_D = \sigma_{\ln D} \lesssim 0.3$, β_D is practically equal to the CoV of D . Hence the r.v. D can be expressed as:

$$D = \left(a\, s_a^b\right) \varepsilon \tag{6-13}$$

where ε is a log-normal r.v. with unit median, and dispersion equal to β_D. Eq. (6-13) can be inverted to give:

$$s_a = \left(\frac{D}{a\varepsilon}\right)^{\frac{1}{b}}$$

Using this expression and eq. (6-11), the probability $\Pr(D > d) = 1 - F_D(d)$ is obtained

Copyright fib, all rights reserved. This PDF copy of fib Bulletin 24 is intended for use and/or distribution only by National Member Groups of fib.

by first conditioning it to the r.v. ε as follows:

$$\Pr(D > d) = \int_0^\infty \Pr(D > d|\,\varepsilon)\, f_\varepsilon(\varepsilon)\, d\varepsilon =$$
$$= \int_0^\infty \Pr\left[S_a > \left(\frac{d}{a\varepsilon}\right)^{\frac{1}{b}}\right] f_\varepsilon(\varepsilon)\, d\varepsilon = k_0 \left(\frac{d}{a}\right)^{-\frac{k}{b}} \int_0^\infty \left(\frac{1}{\varepsilon}\right)^{-\frac{k}{b}} f_\varepsilon(\varepsilon)\, d\varepsilon =$$
$$= k_0 \left(\frac{d}{a}\right)^{-\frac{k}{b}} e^{\frac{1}{2}\frac{k^2}{b^2}\beta_D^2} \tag{6-14}$$

Eq. (6-14) can be read as saying that the probability of D exceeding any given value d is given by the product of the probability that the hazard exceeds the value necessary to produce $D = d$ assuming the $S_a - D$ relationship as deterministic, times the factor $e^{\frac{1}{2}\frac{k^2}{b^2}\beta_D^2}$. In this latter three parameters appear with the same weight: the slope k of the hazard curve (for S_a values having a probability of exceedance roughly equal to P_f), the exponent b of the demand as function of S_a, and the "dispersion" β_D of the input-output relationship. Realistic values of these parameters might be: $k = 3$, $b = 1$, and $\beta_D = 0.3$, in which case the value of the multiplicative factor would result: $\exp\left[\frac{1}{2}\left(\frac{3}{1}0.3\right)^2\right] \simeq 1.5$. Obviously the same factor would be equal to 1 for $\beta_D = 0$.

This example allows to conclude that the variability of the response, given the input, though certainly influential, is not such as to alter the order of magnitude of the total exceedance probability, which is dominated by the hazard.

The third and final step consists in the probabilistic definition of the r.v. expressing the capacity C, and then in carrying out the integration of eq. (6-10) analytically. The assumptions on the capacity are two: C is independent from D , and is log-normally distributed: $C = LN\left(\hat{C}, \sigma_{\log C} = \beta_C\right)$. The integral in eq. (6-10), taking into account of eq.(6-14) becomes:

$$P_f = \int_0^\infty \left[k_0 \left(\frac{\alpha}{a}\right)^{-\frac{k}{b}} e^{\frac{1}{2}\frac{k^2}{b^2}\beta_D^2}\right] f_C(\alpha)\, d\alpha$$

where $f_C(\cdot)$ is the log-normal PDF of C . Integration of the previous expression gives:

$$P_f = k_0 \left(\frac{1}{a}\right)^{-\frac{k}{b}} e^{\frac{1}{2}\frac{k^2}{b^2}\beta_D^2} \int_0^\infty \alpha^{-\frac{k}{b}} f_C(\alpha)\, d\alpha =$$
$$= k_0 \left(\frac{1}{a}\right)^{-\frac{k}{b}} e^{\frac{1}{2}\frac{k^2}{b^2}\beta_D^2} \hat{C}^{-\frac{k}{b}} e^{\frac{1}{2}\frac{k^2}{b^2}\beta_C^2} = H\left[S_a\left(\hat{C}\right)\right] e^{\frac{1}{2}\frac{k^2}{b^2}\left(\beta_D^2+\beta_C^2\right)} \tag{6-15}$$

Similarly to eq. (6-14), this last expression can be read as saying that the unconditional probability of failure, or total risk, is given by the product of the probability that the hazard exceeds the value necessary to produce a demand D equal to the median capacity $\hat{C}$, as if the $S_a - d$ relationship were deterministic, times a factor which now contains in addition the dispersion β_C of the capacity. Using the same values as before for k, b and β_D, and a value $\beta_C = 0.3$ for the capacity, the value of the multiplicative factor becomes

$$\exp\left[\frac{1}{2}\frac{3^2}{1}\left(0.3^2 + 0.3^2\right)\right] \simeq 2.25$$

which again confirms that the order of magnitude of P_f is dictated by the hazard, and not by the uncertainties/randomnesses in both input-output relationship and in the capacity.

Copyright fib, all rights reserved. This PDF copy of fib Bulletin 24 is intended for use and/or distribution only by National Member Groups of fib.

Eq. (6-15) is written in a form appropriate for the assessment of an existing structure. When used for design purposes, P_f is supposed to be a requirement. Denoting by P_0 the target value of P_f, eq. (6-15) can be rearranged so as that the median values of C and D appear, each multiplied by its respective partial safety factor.

To achieve this result, eq. (6-15) is first rewritten as:

$$P_0 = k_0 \left(\frac{\hat{C}}{a}\right)^{-\frac{k}{b}} \exp\left[\frac{1}{2}\frac{k^2}{b^2}\left(\beta_C^2 + \beta_D^2\right)\right]$$

Upon elevation of all terms to the exponent $-\frac{b}{k}$ one gets:

$$a\left(\frac{P_0}{k_0}\right)^{-\frac{b}{k}} = \hat{C}\exp\left[-\frac{1}{2}\frac{k}{b}\left(\beta_C^2 + \beta_D^2\right)\right]$$

which can be cast in the form:

$$\hat{D}\left(P_0\right)\gamma = \hat{C}\phi \tag{6-16}$$

where account has been taken that the left-hand term represents, according to eq. (6-11) and (6-12), the median demand produced by an S_a value with exceedance probability equal to P_0, and γ and ϕ are defined as

$$\begin{aligned}\gamma &= \exp\left[\frac{1}{2}\frac{k}{b}\beta_D^2\right]\\ \phi &= \exp\left[-\frac{1}{2}\frac{k}{b}\beta_C^2\right]\end{aligned}$$

For completeness of the presentation, a mention should be made to a further step introduced in the 2000 SAC/FEMA procedure. It consists in the realization that the uncertainties attributed to D and C with the CoV's β_D and β_C reflect only a portion of the total uncertainty related to the two variables. It remains to account for the part of the uncertainty that derives from incomplete knowledge, be it due to the simplifications of the mechanical models adopted, and/or from the limited statistical basis used for evaluating D and C. For what concerns the hazard, also, it is customary to take into account of the uncertainty related to the different possible choices on the elements entering the analysis (boundaries of seismic regions, upper bounds of the magnitudes, etc.) by providing, in addition to the median estimate of the hazard function: $\hat{H}(s_a)$, other "fractile" functions, from which the mean estimate: $\bar{H}(s_a)$ and a dispersion: β_H , can be deduced.

In the assumption that the uncertainty in the hazard has a log-normal distribution, the mean curve is related to the median through:

$$\bar{H}\left(s_a\right) = \hat{H}\left(s_a\right)\exp\left(\frac{1}{2}\beta_H^2\right)$$

The SAC/FEMA approach consists in the following.

- For what concerns the hazard, reference is made to the *mean* function, in which the uncertainty β_H appears explicitly.

Copyright fib, all rights reserved. This PDF copy of fib Bulletin 24 is intended for use and/or distribution only by National Member Groups of fib.

- For what concerns D and C, the epistemic part of the uncertainty is introduced by multiplying each of the two r.v.'s: $D = \hat{D} \cdot \varepsilon_D$ and $C = \hat{C} \cdot \varepsilon_C$ by a further log-normal r.v.:

$$D = \hat{D}\varepsilon_D\varepsilon_{DU} \qquad C = \hat{C}\varepsilon_C\varepsilon_{CU}$$

where ε_{DU} and ε_{CU} have unit means and logarithmic standard deviations β_{DU} and β_{CU}

If the same steps as those previously described to calculate the integral in eq. (6-10) are repeated keeping however ε_{DU} and ε_{CU} as free variables, one arrives at the following expression for P_f :

$$P_f = \bar{H}\left[S_a\left(\hat{C}\right)\right] \exp\left[\frac{1}{2}\frac{k^2}{b^2}\left(\beta_C^2 + \beta_D^2\right)\right] \varepsilon_{DU}^{\frac{k}{b}} \varepsilon_{CU}^{\frac{k}{b}} \tag{6-17}$$

which shows that now P_f has become a (lognormal) r.v., function of the two r.v.'s ε_{DU} and ε_{CU}. Using the distributions of these latter the parameters of the distribution of P_f can be evaluated, as well as any desired fractile value. Median and logaritmic standard deviations are:

$$\hat{P}_f = \bar{H}\left[S_a\left(\hat{C}\right)\right] \exp\left[\frac{1}{2}\frac{k^2}{b^2}\left(\beta_C^2 + \beta_D^2\right)\right] \tag{6-18}$$

$$\beta_{P_f} = \left|\frac{k}{b}\right| \left[\left(\beta_C^2 + \beta_D^2\right)\right]^{1/2} \tag{6-19}$$

where it is noted that $\hat{P}_f$ is the same as eq. (6-15) but for the use of the *mean* estimate of hazard, instead of the *median*.

Fractile values of P_f are given by the expression

$$P_f^* = \hat{P}_f \exp\left(\kappa\beta_{P_f}\right) \tag{6-20}$$

in which κ is a standardized Gaussian variate associated with the desired probability of non exceedance. For example, $\kappa = 1$ is associated with a probability level of 84%.

6.4.1.2 Remarks and possible extensions of the method

The SAC/FEMA method has been subjected to extensive numerical checking on different typologies of steel frames. Obviously, its effectiveness is better when the response is predominantly contributed by the first mode (due to the choice of $S_a(T_1)$ as intensity parameter) and when failure is controlled by a single scalar variable, as for instance the max interstorey drift.

The method does not deal directly with uncertainties related to mechanical parameters which may have an influence on the response. The significance of this feature is probably minor in the case of steel structures, whose structural systems are generally simpler, more standardized and easier to ascertain than those made of reinforced concrete.

Experience with the use of this method for existing reinforced concrete structures is quite limited as yet: a pilot application is presented in detail at the end of this section. The two most notable differences with respect to steel are: the usually higher degree of uncertainty (lack of knowledge) on the characteristics of the structure (dimensions of the elements, amount and details of the reinforcement, etc.), and the multiplicity of the possible failure modes (shear failures, joints failures, crushing of concrete, etc.), whose relative importance varies from case to case. As a minimum, this last feature requires

Copyright fib, all rights reserved. This PDF copy of fib Bulletin 24 is intended for use and/or distribution only by National Member Groups of fib.

monitoring a quite large number of possibly critical elements/mechanisms, and calculating P_f for each of them.

How to deal then with these independently calculated probabilities is no simple matter. A major simplifying assumption providing an upper bound to the global P_f , and whose validity may in some cases be well established, is to consider failures as independent events. This assumption is at the base of the method to be presented in the following section which is specifically aimed at reinforced concrete structures.

Consideration of the uncertainty in the mechanical parameters (in addition to that affecting the capacity of the elements) is possible at the cost of a considerable increase in the computations. The obvious idea is to compute P_f conditional on parametrically varying values of the components of the uncertain vector $(\mathbf{x})$, so as to obtain $P_f \approx P_f(\mathbf{x})$ from a discrete number of points in the $\mathbf{x}$-space. Details on this approach and a worked-out example are presented in the following section 6.4.2.

6.4.1.3 Example application

The "2000 SAC/FEMA" approach has been applied for assessing the seismic safety of a four storey, reinforced concrete building shown in Fig. 6-2 (Lupoi et al., 2002). The building is located in Catania (Italy), an area which was not classified as seismic, as it is now, at the time the building was built; therefore the structure has not been designed according to any seismic code. This is a representative example of a large number of structures which are potentially unsafe and whose seismic risk has to be evaluated.

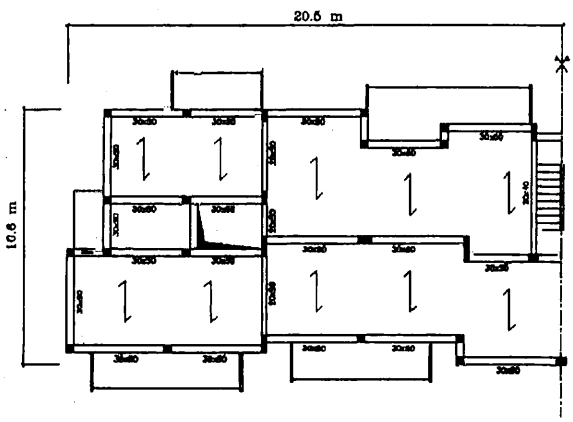

Figure 6-2: Plan view of the second floor

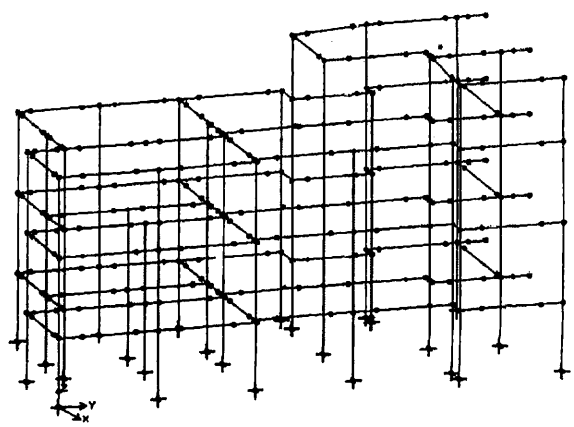

Figure 6-3: 3-D F.E. model

A 3-D model of the building has been set up (Fig. 6-3), employing state-of-the-art fiber frame elements (Taucer et al., 1991) to represent columns and beams. Concrete and steel behaviour is described by non-linear, cyclic constitutive laws.

The initial (uncracked) fundamental period T_f of the structure is equal to 0.51 *sec*; the damping ratio ξ has been assumed equal to 5%.

The failure mechanisms investigated are those described in section 6.3. The contributions of all columns have been taken into account to evaluate the partial P_f's due to shear and drift failures; 38 "critical" joints, selected on the basis of the results of a push-over analysis carried out initially, have been monitored to assess the joint-failure partial P_f.

The demand. A number of 21 earthquake records have been selected from the PEER database for soil class types A and B, with magnitude varying between 5.5 and 7.5 and distance between 25 and 75 Km. The number of records is larger than the one indicated as the minimum necessary ($\sim 5 \div 6$); it has been adopted here for the purpose of examining the actual variability of the demand with the intensity S_a.

Copyright fib, all rights reserved. This PDF copy of fib Bulletin 24 is intended for use and/or distribution only by National Member Groups of fib.

For each record a non-linear dynamic analysis has been carried out and the maximum value of the demand $D(t)$ on each element and mechanism has been recorded: $D = \max\{D(t)\}$.

The *joint demand* is expressed as the principal tensile stress σ_t, and is evaluated through the expression:

$$\sigma_t = \frac{N_c}{2A_c} - \sqrt{\left(\frac{N_c}{2A_c}\right)^2 + \left(\frac{V_j}{b_j \cdot h_j}\right)^2} \tag{6-21}$$

where N_c is the axial force acting on the column, A_c is the column area, V_j is the shear acting inside the joint and $b_j \cdot h_j$ is the joint resisting shear area. The shear V_j is computed as:

$$V_j = \frac{M_l}{z_l} + \frac{M_r}{z_r} - V_c \tag{6-22}$$

where M_l,M_r and z_l,z_r are moments and internal lever arms acting on the left and right beams to the joint, respectively, and V_c is the column shear, The dimensions b_j and h_j have been evaluated as described in (Paulay and Priestley, 1992).

For what concerns the *shear demand*, it is noted that the largest value of the shear V attained during the analysis does not necessarily represent the worst condition for the column, because the shear resistance varies with the axial force N, as shown by eq. (6-4,6-5), and this latter varies with time. An objective measure is obtained normalizing the shear force at time t to the median shear resistance at the same time, which is therefore adopted as the shear demand: $V(t)/\hat{V}_{res}(t)$.

The *chord-rotation demand* is simply the column drift and it is evaluated as:

$$\delta = \frac{u_j - u_i}{L_c} \tag{6-23}$$

where u_j and u_i are the top and bottom horizontal displacements of the columns, respectively, and L_c is the column length.

The $\hat{D} - s_a$ relation for each element and mechanism is derived evaluating the parameters a and b in eq.(6-12) by means of a regression on the dynamic analyses results. For this particular application, all the 21 records selected have been utilised to obtain $\hat{D} - s_a$ relation. As an example, in figure 6-4 the "experimental" points (D, S_a) from the 21 analyses and the resulting $\hat{D} - s_a$ relations are shown for the three different mechanisms considered in three different elements.

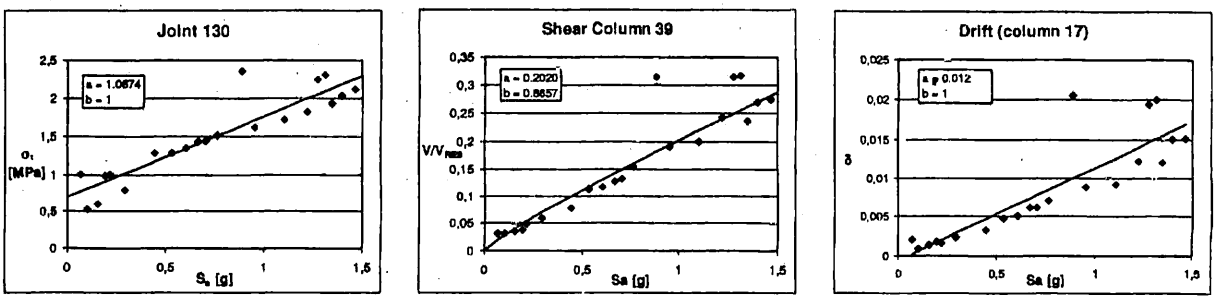

Figure 6-4: Experimental points and $D - s_a$ relations

The dispersion in the demand β_D has been evaluated as the mean square error of the results of analyses. In order to investigate the variability of β_D with S_a, β_D has been computed for three different intervals of S_a; the value of β_D corresponding to the interval

Copyright fib, all rights reserved. This PDF copy of fib Bulletin 24 is intended for use and/or distribution only by National Member Groups of fib.

which includes $S_a(\hat{C})$, i.e. the spectral acceleration for which the element attains its *median* capacity, has been used in the evaluation of P_f through eq. (6-15). In Table 6-1 the β_D values for the three mechanisms of different elements are given as examples. It is observed that the dispersion in the maximum inter-storey drift is consistently larger than that in the other two responses.

S_a	Joints	Shear	Drift
0.0 - 0.5	0.222	0.206	0.578
0.5 - 1.0	0.194	0.340	0.524
1.0 - 1.5	0.094	0.158	0.441

Table 6-1: β_D's for different intervals of S_a

The capacity. The statistics for the capacity have been estimated on the basis of available literature data, reported in section 6.3.

The *joint capacity*, expressed in terms of principal tensile stress, is given by eq. (6-2). Assuming for the concrete compression strength a normal distribution characterized by a mean value equal to $36.64 N/mm^2$ and a CoV of 0.18, the latter value suggested in (Kappos et al., 1999), the statistics of the capacity are estimated through the following expressions:

$$\hat{C} = 0.42 \cdot \mu_{\sqrt{f_c}} \quad ; \quad \sigma_C = 0.42 \cdot \sigma_{\sqrt{f_c}} \quad ; \quad \beta_C \cong \frac{\sigma_C}{\hat{C}} \tag{6-24}$$

which yield: $\hat{C} = 2.5 N/mm^2$ and $\beta_C = 0.09$.

In addition to the principal tensile stress criterion, the one based on principal compressive stress given by eq. (6-3) has also been considered.

The *column shear capacity* is given by the expression in eq.(6-4). For this capacity to be compared with the shear demand, $V/\hat{V}_{res}$, it must also be normalized: $C = V_{res}/\hat{V}_{res}$. Therefore, the median value of the capacity is equal to unity: $\hat{C} = 1$. The CoV is estimated in (Priestley et al., 1994) and it is taken equal to: $\delta_C = \beta_C = 0.13$.

The *drift capacity* is given by the expression in eq.(6-8) as function of material and geometrical parameters; the CoV of that expression is estimated in (Panagiotakos and Fardis, 2001) equal to: $\beta_C = 0.275$.

The hazard. A standard probabilistic seismic hazard analysis (PSHA) (Cornell, 1968) was performed, using the attenuation laws proposed in (Sabetta and Pugliese, 1996), developed for Italy; the seismic parameters for each seismological area have been evaluated on the basis of the Italian Catalogue of Earthquakes. The hazard curve has been approximated with the expression in eq.(6-11), yielding the following values for the coefficients k and k_0 : $k = 1.398$, $k_0 = 0.0049$.

Risk Evaluation. The probability of failure for each monitored element $P_f(el)$ has been evaluated by means of the expression in eq.(6-15); in Table 6-2 the values for the most critical elements in each mechanism are given. The $P_f(el)$'s of all elements belonging to a failure mechanism j have been combined in the assumption of a serial arrangement, to obtain the mechanism partial P_f^j. Finally, the P_f^j's of the three mechanisms investigated are combined with the same assumption to obtain the total probability of failure, P_f. These values are shown in Table 6-3. It can be noted that the failure of joints is by far the most critical mechanism. The value of P_f for the joint failure in the table above refers

Mech.	Joint no. 130	Shear col. 39	Drift col. 17
$P_f(el)$	$2.42 \cdot 10^{-3}$	$3.86 \cdot 10^{-4}$	$8.17 \cdot 10^{-6}$

Table 6-2: Probabilities of failure of single elements

Copyright fib, all rights reserved. This PDF copy of fib Bulletin 24 is intended for use and/or distribution only by National Member Groups of fib.

Mech.	Joint	Shear	Drift	**Total**
P_f	$3.2 \cdot 10^{-2}$	$3.8 \cdot 10^{-3}$	$1.6 \cdot 10^{-5}$	$3.6 \cdot 10^{-2}$

Table 6-3: Partial and total annual probabilities of failure

to the tensile mechanism (eq. (6-2)); if this type of failure is assumed as representative of actual collapse, then it would be the main contributor to the total P_f.

The value of P_f for the joint compressive failure mechanism (eq. (6-3)) resulting from the analyses is $8.3 \cdot 10^{-4}$. It is noted that depending on which mechanism is assumed as representative of collapse, the critical mechanism changes from joint tensile failure to shear failure.

A closer examination of the element's P_f shows that the exponential factor in eq.(6-15) varies from 1.008 to 1.037 for the joint mechanism, from 1.013 to 1.509 for the shear mechanism and from 1.53 to 3.30 for the drift mechanism. This is a furtrher confirmation of the already mentioned dominance of the hazard on the final value of P_f.

6.4.2 EFA Method

The EFA (Efficient Fragility Analysis) method, developed in (Giannini et al., 2003), aims at the determination of the P_f of the structure conditional on one parameter defining the intensity of the motion, i.e., the fragility function. The evaluation of the fragility and of the following integral of the product of the fragility by the hazard function are carried out numerically. The accelerograms used can indifferently be either recorded ones or spectrum-compatible. In the first case the scaling factor would be, as in section 6.4.1, the spectral ordinate at the fundamental period (T_1) of the structure; in the second case the peak ground acceleration (PGA, a_g) could be used as well, since the spectral shape is the same for all the simulated records, and hence S_a and a_g differ by a constant factor.

The different significance of using real or spectrum-compatible accelerograms is discussed in section 6.2.

The procedure can account for all modes of failure typical of RC structures for which probabilistic strength/ultimate deformation capacity models can be set up. Similarly to the previous method in section 6.4.1, the structural response, given the input, is deterministic. However, since the method is computationally efficient, the randomness of a reduced number of influential mechanical parameters can be accommodated as indicated in the following without sacrificing its practical applicability. With regard to the general features of the method, it may be mentioned that a version of it has been developed (Giannini et al., 2003), in which the load-response ($Q - q$) relationship is obtained via a pushover analysis. For each value of q the conditional probability of failure: $P_f(q)$ is evaluated. The structure is then idealised as an equivalent sdof system for which the CDF of the maximum response to a given process is rapidly obtained by simulation. Finally, by multiplying the function $P_f(q)$ by the probability of the response: $f_q(q)dq$ and integrating, the unconditional risk is obtained.

It is believed, however, that the advantages of the " static" procedure in terms of computing time are not enough to compensate for the poorer accuracy and for the conceptual/numerical difficulties encountered in pushover analysis beyond peak resistance. Hence, only the fully dynamic version of the method is presented herein.

6.4.2.1 Description of the method

In the basic method the structure is considered as deterministic. Possible uncertainty in these parameters (the components of sub-vector $\mathbf{x}$, as discussed in section 6.3.5) is dealt with as indicated in the following.

Given one sample accelerogram from a group, all scaled to the same intensity S_a or PGA, a dynamic analysis is carried out. Let the maximum action effect in the s-th critical

Copyright fib, all rights reserved. This PDF copy of fib Bulletin 24 is intended for use and/or distribution only by National Member Groups of fib.

element/mechanism be denoted by $D_{s,k}$. By comparing this value with the corresponding resistance, R_s , the probability of failure of the element/mechanism is evaluated as

$$P_{f,s,k} = F_{R_s}(D_{s,k})$$

where $F_{R_s}(\cdot)$ is the CDF of the capacity of the mechanism. Failures according to different mechanisms can at least in approximation be considered as independent events, hence the probability of failure for the serial system representing the structure, due to the k-th accelerogram, is simply:

$$P_{f,k} = 1 - \prod_s (1 - P_{f,s,k}) \tag{6-25}$$

The analysis is then repeated with different accelerograms and the probability of failure unconditional with respect to sample variability is given by:

$$P_f \simeq \frac{1}{N} \sum_{k=1}^{N} P_{f,k} \tag{6-26}$$

where the number N of the samples must be large enough to provide stable estimates of P_f and of its sample standard deviation.

In eq. (6-26) the dependence of P_f on the intensity of seismic action is omitted: the fragility function is obtained by calculating P_f for a convenient number of S_a or PGA values.

For what concerns the uncertainty in the structural parameters, there are two ways, widely referred to in the literature (for a review, see for instance (Pinto, 2001)), to account for the dependence of P_f on $\mathbf{x}$. The first one is the *Response Surface* approach, which consists in a least square fitting of a polynomial function to the values of P_f calculated in an appropriate sub-region of the $\mathbf{x}$-space. A second order polynomial is normally used, some terms of which can be dropped from the start based on intuitive reasoning. If n is the dimension of the $\mathbf{x}$-space, the number of coefficients needed for a full 2nd order polynomial is: $(1+n+n^2)$. With reference to framed structures, according to the discussion in section 6.3.5, the components of $\mathbf{x}$ may be the n-th storey indices: for a building of, say, 5 storeys, the coefficients would then be 31.

This number represents the required minimum number of experiments, each one providing a value of P_f. In order to improve the smoothness of the surface, however, the method makes use of a redundant number of experiments. A plan which is considered appropriate for general application involves the assignment of two values for each variable (for instance a reference value of $\mathbf{x} \pm 1\sigma$) and consideration of all their possible combinations (2^n factorial terms), plus the so-called star scheme in which in turn all variables remain at their reference values except one, which is assigned a value of $\pm\alpha\sigma$ from the reference value, with α comprised between 2 and 3. The total number of experiments in this so-called central-composite plan is $(2^n + 2n)$, which gives 42 for $n = 5$.

Denoting by $\mathbf{x}^*$ the reference value of $\mathbf{x}$, the full quadratic expression of P_f is given by:

$$P_f(\mathbf{x}) = P_f(\mathbf{x}^*) + \sum_{i=1}^{n} a_i \cdot (x_i - x_i^*) + \sum_{i=1}^{n}\sum_{j=1}^{n} b_{ij} \cdot (x_i - x_i^*)(x_j - x_j^*) \tag{6-27}$$

The unconditional probability of failure is finally obtained by computing the expected

Copyright fib, all rights reserved. This PDF copy of fib Bulletin 24 is intended for use and/or distribution only by National Member Groups of fib.

value of P_f:

$$P_f = \mathrm{E}_{\mathbf{x}}\left[P_f\left(\mathbf{x}\right)\right] =$$

$$= P_f\left(\mathbf{x}^*\right) + \sum_{i=1}^{n} a_i \cdot \left(\bar{x}_i - x_i^*\right) + \sum_{i=1}^{n}\sum_{j=1}^{n} b_{ij} \cdot \mathrm{E}_{\mathbf{x}}\left[\left(x_i - x_i^*\right)\left(x_j - x_j^*\right)\right] =$$

$$= P_f\left(\mathbf{x}^*\right) + \sum_{i=1}^{n} a_i \cdot \left(\bar{x}_i - x_i^*\right) + \sum_{i=1}^{n}\sum_{j=1}^{n} b_{ij} \cdot \left[\sigma_{ij} + \left(x_i - x_i^*\right)\left(x_j - x_j^*\right)\right] \tag{6-28}$$

where σ_{ij} denotes the covariance of x_i and x_j. If the reference value $\mathbf{x}^*$ is taken as the mean value $\bar{\mathbf{x}}$, eq. (6-28) simplifies into:

$$P_f = P_f\left(\mathbf{x}^*\right) + \sum_{i=1}^{n}\sum_{j=1}^{n} b_{ij} \cdot \rho_{ij}\sigma_i\sigma_j \tag{6-29}$$

with obvious meaning of the symbols.

The alternative way to account for the dependence of P_f on $\mathbf{x}$ is similar to the one just examined, and consists in expanding P_f in series about a reference value, and truncating the series at the quadratic terms. The form is the same as that in eq. (6-27), with the coefficients a_i and b_{ij} now being given by:

$$a_i = \frac{\partial P_f}{\partial x_i} \qquad b_{ij} = \frac{1}{2}\frac{\partial^2 P_f}{\partial x_i \partial x_j} \tag{6-30}$$

The derivation of P_f with respect to $\mathbf{x}$ is performed numerically, and obviously the unconditional expression of P_f is also given by equations (6-28) or (6-29). The first approach is in principle more accurate since the coefficients are obtained from a larger number of experiments. This allows also to determine in eq. (6-27) an "error term", in the form of an additive, zero mean Gaussian random variable ε, that might be used to treat P_f in eq.(6-29) still as a random variable.

6.4.2.2 Example application

This method has been applied for assessing the seismic safety of the frame shown in Fig. 6-5.

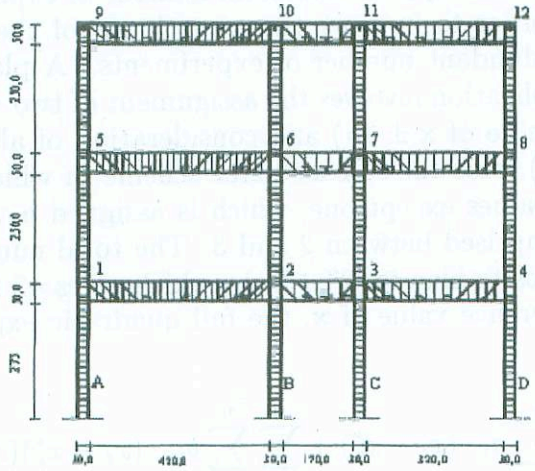

Figure 6-5: Geometry and reinforcement of the example frame

Design and detailing of the frame reflect the practice in Europe during the post-war years from the 50's to the mid-70's. The structure is intended to resist vertical loads only;

Copyright fib, all rights reserved. This PDF copy of fib Bulletin 24 is intended for use and/or distribution only by National Member Groups of fib.

smooth, low-grade bars are used for the reinforcement, and proper anchoring of them is disregarded. A 2/3 scale model of the frame with identical materials and details of the one studied here has been constructed and tested under cyclic loading up to collapse at the University of Pavia (Calvi et al., 2001).

Materials. For the purpose of the assessment, based on the tests on concrete and steel specimens carried out in Pavia, the following data have been assumed for the materials:

Concrete	compressive strength	$f_c = 2,0 \cdot 10^4$ KN/m^2
	tensile strength	$f_t = 0,1 f_c = 2,0 \cdot 10^3$ KN/m^2
	deformation at peak stress	$\varepsilon_{cc} = 0,003$
	initial elastic modulus	$E_c = 2,7 \cdot 10^7$ KN/m^2
Steel	yield strength	$f_y = 3,5 \cdot 10^5$ KN/m^2
	ultimate strength	$f_{su} = 4,5 \cdot 10^5$ KN /m^2
	deformation at the onset of strain hardening	$\varepsilon_{sh} = 0,0035$
	initial elastic modulus	$E_s = 1,6 \cdot 10^8$ KN/m^2

The indicated values are considered as mean ones, and are used as input for the analysis of the response. Those mechanical properties which enter into the considered failure mechanisms will be probabilistically characterized later on.

Seismic Action. The safety of the structure is measured against a seismic action defined in terms of an elastic response spectrum, scaled by the value of the peak ground acceleration: PGA. The spectral shape is the one given by the Eurocode 8 (ENV 1998-1, 1994) for intermediate soils. Ten spectrum-matching accelerograms have been generated for the purpose of the dynamic analyses.

Failure mechanisms. All four mechanisms leading to collapse described in section 6.3 have been considered in the example. Joint failures and shear failures, however, dominated over the remaining two: exhaustion of deformation capacity and storey instability, to an extent that consideration of these two latter could be omitted entirely. Lack of reinforcement in the joints, in particular, was the critical factor in determining failure of the frame in almost all cases. The strength of the joints was assumed to be given by eq. (6-2), with a CoV of 0.30, while eq. (6-4) was used for shear strength, also with a CoV of 0.30, which is higher than the value indicated in (Priestley et al., 1994), a choice made rather arbitrarily to test the relative sensitivity of P_f with respect to the two mechanisms.

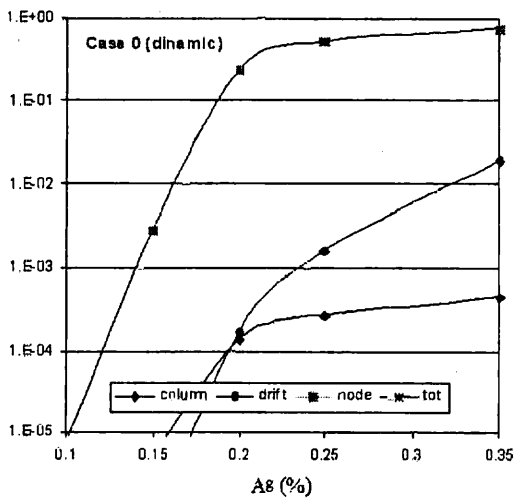

Figure 6-6: P_f due to separate mechanisms, and global.

Uncertain structural parameters. Uncertainty in the actual distribution of strengths between elements has been described through the storey index defined in eq. (6-9). As

Copyright fib, all rights reserved. This PDF copy of fib Bulletin 24 is intended for use and/or distribution only by National Member Groups of fib.

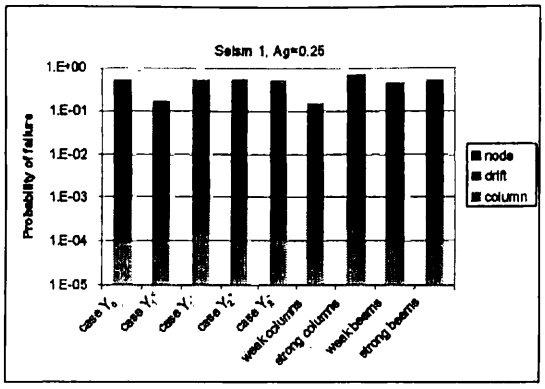

Figure 6-7: P_f as function of the relative beam-column strength.

discussed in the paper, for framed structures this index is considered effective for detecting the tendency of a structure towards either a beam-sway or a column-sway mechanism. In the example, five cases have been considered. Case Y_0 represents the situation of the indexes at the various floors as determined from the design drawings. Cases Y_1^+ and Y_1^- refer to variations of the index at the first floor, cases Y_2^+ and Y_2^- to variations at the second floor. Possible variations at the third floor were considered to be uninfluential and hence ignored. The variations were implemented by attributing to the yield strength of the steel a variation of ±30%. Specifically, at each floor, the first case represents an increase of 30% in the beams and a decrease of 30% in the columns, and viceversa for the second case.

Evaluation of P_f. With this approach a value of P_f is calculated for each accelerogram, based on the maximum values of the response at all potentially critical elements/mechanisms. Averaging the P_f values obtained for an increasing number of accelerograms, the procedure stops when the value of P_f stabilizes within a given tolerance. In the example considered seven accelerograms were found to provide a sufficiently accurate estimate of P_f. The fragility curves in Fig. 6-6 give P_f separately for the three mechanisms and for the combination of them: joint failure is dominant in contributing to failure of the frame.

The variation of P_f for the different cases of the storey indexes is shown in Fig.6-7, for a fixed value of the seismic intensity. The contribution from the beam-column joints is seen to be little sensitive to the parameter. This is because even a large variation of it is not such as to produce in this case a change of the critical mechanisms from joint failure to column-sway failure.

References

P.E. Pinto. Reliability methods in earthquake engineering. *Progr. Struct. Eng. Mater.*, 3 (1):76–85, March 2001.

B.R. Ellingwood. Eaarthquake risk assessment of building structures. *Reliability Engineering and System Safety*, 74(3):251–262, December 2001.

A. Der Kiureghian. Structural reliability methods for seismic safety assessment: a review. *Engineering Structures*, 18(6):412–424, 1996.

N. Shome, A.C. Cornell, P. Bazzurro, and I.E. Carballo. Earthquakes, records and nonlinear responses. *Earthquake Spectra*, 14(3):469–500, 1998.

(NZNSEE) New Zealand Nat. Soc. for Earthq. Eng. The assessment and improvement of the structural performance of earthquake risk buildings. Draft for General Release, 1996.

Copyright fib, all rights reserved. This PDF copy of fib Bulletin 24 is intended for use and/or distribution only by National Member Groups of fib.

M.J.N. Priestley. Displacement-based seismic assessement of reinforced concrete buildings. *J. of Earthq. Eng.*, 1(1):157–192, 1997.

T. Panagiotakos and M.N. Fardis. Deformations of reinforced concrete members at yielding and ultimate. *ACI Structural Journal*, 98(2):135–148, 2001.

A.J. Kappos, M.K. Chryssanthopoulos, and C. Dymiotis. Uncertainty analysis of strength and ductility of confined rc members. *Eng. Struct., Elsevier*, 21(3):195–208, 1999.

(CEB) Comite Eurointernational du Beton. *CEB/FIP Model Code 1990.* T. Telford, London, 1993.

C. Dymiotis, A. Kappos, and M. K. Chryssanthopoulos. Seismic reliability of RC frames with uncertain drift and member capacity. *Jnl. of Struct. Eng., ASCE*, 125(9):1038–1047, 1999.

C.A. Cornell, F. Jalayer, R.O. Hamburger, and D.A. Foutch. The probabilistic basis for the 2000 SAC/FEMA steel moment frame guidelines. *Journ. of Struct. Eng. ASCE*, 128(4):526–533, 2002.

R. Giannini, P.E. Pinto, and G. de Felice. Seismic reliability of r.c. structures. *Submitted to: Earthquake Engng. Struct. Dyn.*, 2003.

G. Lupoi, A. Lupoi, and P.E. Pinto. Seismic risk assessment of r.c. structures with the "2000 SAC/FEMA" method. *Journal of Earthquake Engineering*, 6(4):499–512, 2002.

F. Taucer, E. Spacone, and F.C. Filippou. *A Fiber Beam-Column Element for Seismic Response Analysis of Reinforced Concrete Structures.* Earthq. Eng. Research, University of California, Berkeley, December 1991. Report no. UCB/EERC-91/17.

T. Paulay and M.J.N. Priestley. *Seismic Design of Reinforced Concrete and Masonry Buildings.* J. Wiley & Sons, 1992.

M.J.N. Priestley, R. Verma, and Y. Xiao. Seismic shear strenght of reinforced concrete buildings. *Journ. of Struct. Eng. ASCE*, 120(8):2310–2329, August 1994.

C.A. Cornell. Engineering seismic risk analysis. *Bull. the Seismological Soc. of Am.*, 58 (5):1583–1606, 1968.

F. Sabetta and A. Pugliese. Estimation of response spectra and simulation of nonstationary earthquake ground motions. *Bull. Seism. Soc. Am.*, 86(2):337–352, 1996.

GM. Calvi, S. Pampanin, M. Moratti, J. Ward, G. Magenes, A. Pavese, and A. Rasulo. Seismic vulnerability assessment of existing concrete buildings. experimental tests on a three-story r.c. frame. Technical report, University of Pavia, Pavia, Italy, 2001.

Copyright fib, all rights reserved. This PDF copy of fib Bulletin 24 is intended for use and/or distribution only by National Member Groups of fib.

7 Case studies

7.1 Introduction

This Chapter includes a number of case studies of seismic assessment – and sometimes retrofit – of concrete buildings, representative of existing construction in the seismic regions of the South of Europe. The two case studies in Sections 7.2, 7.3 refer to two real buildings – a four-storey and an eight-storey one – damaged in two of the strong earthquakes that hit Turkey in the second half of the '90s and retrofitted afterwards. Both case studies include detailed assessment of the not yet retrofitted buildings and evaluation of the retrofitted ones. Four analysis and assessment procedures are applied: according to FEMA 273/356, using linear dynamic (modal), nonlinear static (pushover) and – for verification of the pushover analysis – nonlinear time-history analysis, and the composite spectrum method (CSM) of ATC-40. The two real-life applications give the opportunity to evaluate different analysis approaches (via comparison to each other and to the response observed in the main shocks and aftershocks).

The case studies in Section 7.5 refer to two regular planar frames representative of Italian construction of the '60s: a two-storey five-bay frame and a seven-storey two-bay one. The case studies represent a very detailed and in-depth evaluation of the various analysis methods, linear or nonlinear, proposed for seismic assessment of existing RC buildings: from linear dynamic (response spectrum) at one extreme to nonlinear time-history analysis at the other, with pushover analysis in-between. Various pushover approaches are studied, including those of FEMA 273 and 356, ATC-40 and of the N2 method (Fajfar and Fischinger, 1988), with alternative lateral load patterns and under force or displacement control.

The case study in Section 7.6 refers to a 4-storey dual (frame-wall) concrete building typical of Greek construction of the '60s or '70s. The building is assessed according to the FEMA 273 (ATC 1997) and 356 (ASCE 2000) linear and nonlinear static procedures and the displacement-based approach of the New Zealand draft Guidelines and Priestley (1997). Selected conclusions are evaluated on the basis of nonlinear time-history analyses.

7.2 Case study 1: Four-storey building in Dinar

7.2.1 Introduction

The four-storey building shown in Fig. 7-1 was moderately damaged after the 1995 Dinar earthquake (Wasti et al., 2001) in Turkey. It was retrofitted by adding new shear walls extending along the full building height, as indicated by cross hatches in Fig. 7-2 on the ground storey plan. Before seismic retrofitting, the structural system of the building was a reinforced concrete frame with concrete slabs and individual footings connected by foundation tie beams in both directions. A typical floor area was 310 m^2, the storey heights were 3.80 m at the ground level and 3.50 m at the three layers above. The most common column size was 0.25 m by 0.6 m and all beam sizes were 0.25 m by 0.7 m. There were cantilevering floors of 1 m above the ground level on the front and the backsides of the building (Figs. 7-1 and 7-2). The ground storey had a smaller number of brick-masonry partition walls than the upper storeys, which created a storey-weakness.

During the 1 October 1995 Dinar earthquake, all of the 23 columns in the ground storey were damaged: in two of them the damage was severe due to shear failures at both ends, in three it was moderate and in 18 light. Out of 37 beams, two were severely, three were moderately and one was lightly damaged in combined shear and flexural modes. All of the nine brick partition walls were severely damaged at the ground storey.

Severe damage in all partition walls and distributed damage in all columns at the ground storey indicated lack of lateral stiffness and strength. Less damage in beams indicated stronger beams than columns. Furthermore, decrease of damage in the above storeys, perhaps due to substantial increase in the amount of partition walls, was the sign of a weak ground storey. The concrete core specimens from the building revealed a mean concrete strength of 12 MPa. The spacing of transverse reinforcement in columns ranged from 200 to 250 mm.

In the seismic retrofitting of the building, two U-shaped shear walls were added to the existing system and the corner columns were improved as shown in Fig. 7-2. The column at the end of line B was severely damaged. Since it was to planned to be incorporated in one of the new shear walls, its concrete was completely removed and it was recast with the new wall.

Copyright fib, all rights reserved. This PDF copy of fib Bulletin 24 is intended for use and/or distribution only by National Member Groups of fib.

The other severely damaged column was the third one from the left on line B. It was jacketed with a concrete overlay in the ground storey.

The seismic performance of the existing and of the retrofitted building were evaluated by 3-D linear and 2-D nonlinear models, as presented comparatively in the following.

Fig. 7-1: Four storey damaged building in Dinar

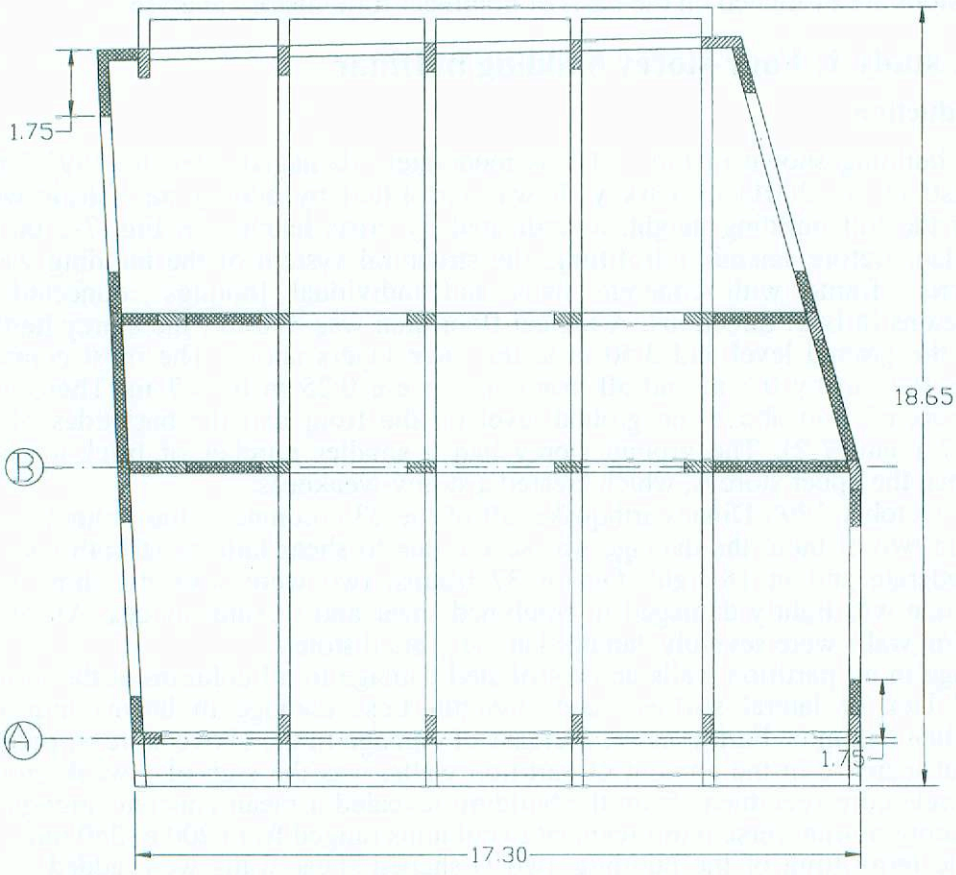

Fig 7-2: Retrofitting scheme applied to the ground storey plan of the four storey building in Dinar. Cross-hatching indicates the added shear walls

Copyright fib, all rights reserved. This PDF copy of fib Bulletin 24 is intended for use and/or distribution only by National Member Groups of fib.

Column axis	DCR-before retrofitting X	DCR-before retrofitting Y	DCR-after retrofitting X	DCR-after retrofitting Y
2A	4.0	3.6	1.5	1.3
3A	3.8	3.2	1.6	1.2
4A	3.9	2.9	1.7	1.0
5A	3.9	2.7	2.1	0.7
3B	4.0	4.9	1.2	1.5
4B	4.0	4.5	1.4	1.7
3C	3.8	3.4	1.2	0.8
4C	3.9	3.2	1.5	0.8
2D	1.7	5.4	1.1	1.5
3D	2.0	5.3	1.3	1.5
4D	2.6	5.3	2.0	1.5

Table 7-1: Demand-capacity ratios in columns before and after retrofitting

7.2.2 Linear dynamic procedure

Three-dimensional linear models were prepared for the existing frame and for the retrofitted frame-wall system. The contribution of brick partition walls were ignored in the linear models. As expected, components of the existing frame did not satisfy the acceptability criterion, whereas the retrofitted system components were all acceptable on the basis of the m-factors given in ASCE (2000) for primary components at Life-safety performance level (Tables 3-1 to 3-3). In the columns of the retrofitted system where forces were delivered by yielding beams, seismic force demands were reduced by a factor of 2 (ASCE, 2000). In-situ material strengths were used in capacity evaluation.

A comparison of bending moment demand-capacity ratios (DCR) for the first storey columns, which were not part of the added walls (Fig. 7-2) is given in Table 7-1. DCR values in Table 7-1 show that the seismic action effects in columns before retrofitting were reduced drastically after the frame system is retrofitted by the added walls, although the capacities of many of columns were still exceeded, some of them about twice. The nonlinear evaluation procedure that followed revealed that this exceedance this did not present a serious problem.

In calculating the flexural capacities of columns, axial forces due to the earthquake action were not obtained from the linear spectral analysis, but calculated from the shear capacities of connecting beams after they develop plastic hinges at the ends. Beam shear forces act in alternate directions at the two sides of a joint that undergoes rotation. Column axial forces calculated from beam shear capacities are considerably lower than the axial forces (compression or tension) obtained from linear spectral analysis. Otherwise the interaction of elastic axial forces with bending moments leads to severe underestimation of column flexural capacities when the axial force is tensile.

7.2.3 Nonlinear static (pushover) analysis

Two-dimensional models that include frames A and B indicated on Fig. 7-2 were prepared for the existing and the retrofitted systems. Since the computer program Drain 2DX (Prakash et al., 1993) only considers flexural hinge formation, member and connection shear forces were traced in response calculations to verify that their shear capacities are not exceeded. No strain hardening of the existing members was taken into account, whereas 5% strain hardening ratio was assumed for the new walls.

Infill walls were modeled by a pair of equivalent diagonal inelastic strut elements with elasto-plastic behaviour in compression and no resistance in tension. The infill walls in Dinar were made of hollow bricks of 0.13 m thickness, laid with cement-lime mortar, considered as non-load-bearing. Specimens of similar bricks were transported to the METU laboratory in Ankara, and prism specimens prepared with similar mortar were tested in compression, to give a mean gross compressive strength of 1 MPa and a Modulus of Elasticity of 700 MPa with slight variations. The elastic stiffness considered in compression is based on the strut width a as defined in FEMA 273/356 and on the measured Modulus of Elasticity. The force capacity of the strut was calculated from the shear strength of the wall panel at the onset of

Copyright fib, all rights reserved. This PDF copy of fib Bulletin 24 is intended for use and/or distribution only by National Member Groups of fib.

diagonal cracking (Sucuoglu and McNiven, 1991). A shear strength value of 0.06 MPa was obtained for typical infill masonry panels employed in the analytical model of the building.

Stiff shear walls comprising the strengthening system tend to rotate about their base under lateral loads, when their foundation consists of individual strip footings. In analytical models, rotational springs can be provided under new shear walls to account for the compliance of the wall foundation (ASCE, 2000). The soil properties employed in rotational foundation stiffness herein were determined by using the boring log data obtained from Dinar at the related sites. Analysis of several borehole data at the upper 5 m indicated mean values of 1.8 t/m^3 for the mass density, 0.40 for Poisson ratio and 200 m/s for the shear wave velocity of soil.

Uplifting and the resulting vertical displacement at the wall centrelines were not considered in the model due to software limitations, although it is known that the uplifting phenomena increase the deformation demands in the beams framing into new walls.

A lateral force distribution proportional to the respective first mode shapes was applied to the models of the existing frame and the retrofitted frame-wall system. Each of these models was analyzed for two different cases: The existing frame was considered as bare and as infilled; the retrofitted frame-wall system was considered with fixed-base and with rotational springs under the added walls. Accordingly, the contribution of the brick-masonry infills and of the rocking wall foundations on the system response could be assessed separately.

The results of the pushover analysis are presented in Fig. 7-3. It can be observed that masonry infills increased the lateral strength and stiffness of the existing bare frame by 15% and 20%, respectively. The existing frame approximately possessed the lateral strength required by the governing 1975 Turkish Seismic Code at the time of its construction; however it was lacking in deformation capacity. Allowing for foundation rocking at the bases of the added walls in the retrofitted system reduced system lateral stiffness and strength in the linear and non-linear response ranges. Retrofitting of the existing frame by added shear walls increased both strength and deformation capacity significantly.

Three important stages are marked on the pushover curves in Fig. 7-3. These were identified as first yield, global yield and severe damage. The plastic hinge mechanisms in the retrofitted system at these three stages are shown in Fig. 7-4. Although first yield started early, yielding occurred in beams connected to shear walls and in the top storey columns which have low axial loads. Global yielding occurred with hinge formation at the base of the larger added wall and excessive rotations at the beam ends connecting to the shear walls. Severe damage was defined by wide-spread development of plastic hinges throughout the system. On the other hand, the existing frame formed a soft storey mechanism at the ground storey shortly after the global yielding stage.

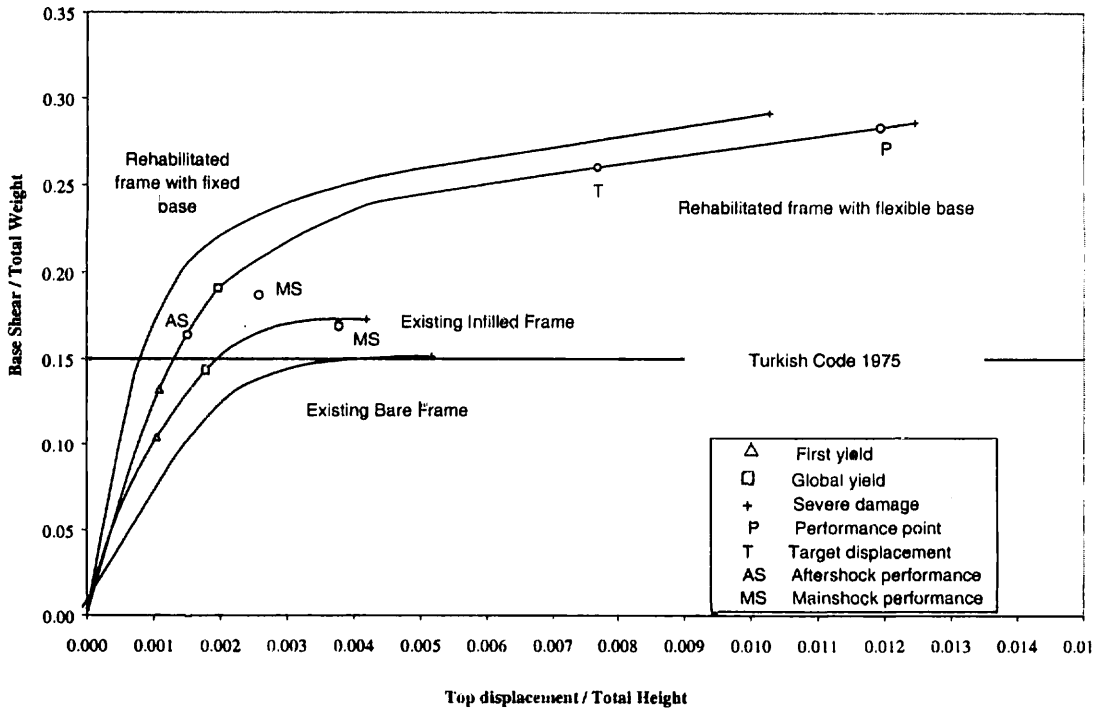

Fig. 7-3: Normalized capacity curves for the four storey building in Dinar, obtained by pushover analysis

Copyright fib, all rights reserved. This PDF copy of fib Bulletin 24 is intended for use and/or distribution only by National Member Groups of fib.

The elastic vibration periods of the existing and retrofitted systems were calculated as 0.6sec and 0.56sec, respectively, with the corresponding code spectral displacements of 89 mm and 82 mm. When these values and the first modal participating factors at the roof level were employed to calculate the target roof displacement normalized with respect to building height, target values of 0.88% and 0.79% were obtained for the existing and the retrofitted systems, respectively. It is shown in Fig. 7-3 that the deformation capacity of the existing system is dramatically less than 0.88%, whereas the retrofitted system achieves a top drift ratio of 0.79%, long before the severe damage stage. At this deformation level, a life safety performance can be assigned globally to the retrofitted building.

The acceptance criteria of FEMA-356 in terms of plastic hinge rotation, θ_{pl}, were applied to all components of the retrofitted system at the target displacement level. Plastic rotation demands are presented in Table 7-2 for the first storey beams and columns and for the added walls. All members shown in Fig. 7-2 are numbered from left to right in the Table. Only the maximum non-zero plastic rotation demands are given.

Member	Member Number							
Type	1	2	3	4	5	6	7	8
Beam	0.0083	0.0044	0.0108	0.0060	0.0	0.0	0.0	0.0
Column	0.0042	0.0050	0.0031	0.0050	0.0032	0.0031	0.0032	0.0043
Wall	0.0028	0.0045						

Table 7-2: Plastic rotation demands of members in the first storey of Case 1 building (rad)

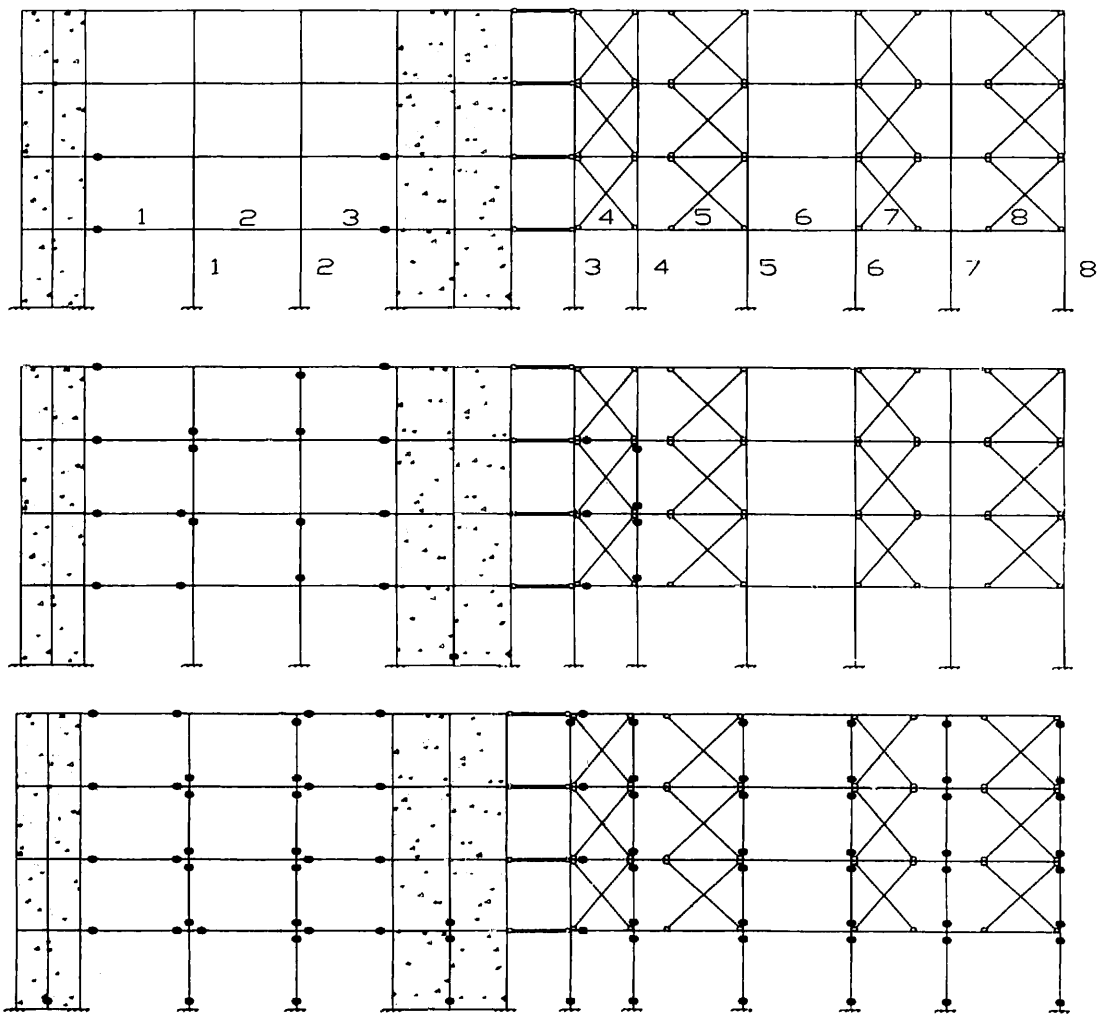

Fig. 7-4: Plastic hinge mechanisms in the retrofitted 4-storey building in Dinar at the first yield, global yield and severe damage stages during the pushover analysis

Copyright fib, all rights reserved. This PDF copy of fib Bulletin 24 is intended for use and/or distribution only by National Member Groups of fib.

The acceptable plastic rotation for beams with non-conforming (ASCE, 2000) transverse reinforcement was a minimum of 0.005 rad at the life safety performance level. Expectedly, beams 1 and 3 framing into the new walls developed high plastic rotations that exceed acceptable values. Large plastic rotation demands at such beam sections are inevitable; this should not be considered as a serious deficiency, as long as beams respond in the flexural failure mode. Accepting these weak links as "fuses" (Holmes, 2000), presents a more rational solution than increasing their flexural capacity to reduce plastic rotation demands. Increasing their rotation capacity on the other hand, is rather difficult for field application. For non-conforming columns, the acceptable plastic rotation is 0.005 rad at life safety performance level for low axial loads, which reduces to 0.002 rad when 40% of the axial capacity is exceeded. The normalized axial load levels (axial force/f_cA_c) under combined gravity and seismic loading do not exceed 0.20, except in columns number 4 and 5, where they are about 0.40. However, shear stresses in these columns are very low. The added shear walls are under no axial load and are detailed as the primary lateral load resisting elements. The calculated plastic rotation demands were much lower than the accepted value of 0.008 rad. These two walls undertake, together, 79%, 76% and 73% of the total base shear force at the first yield, global yield and collapse stages, respectively.

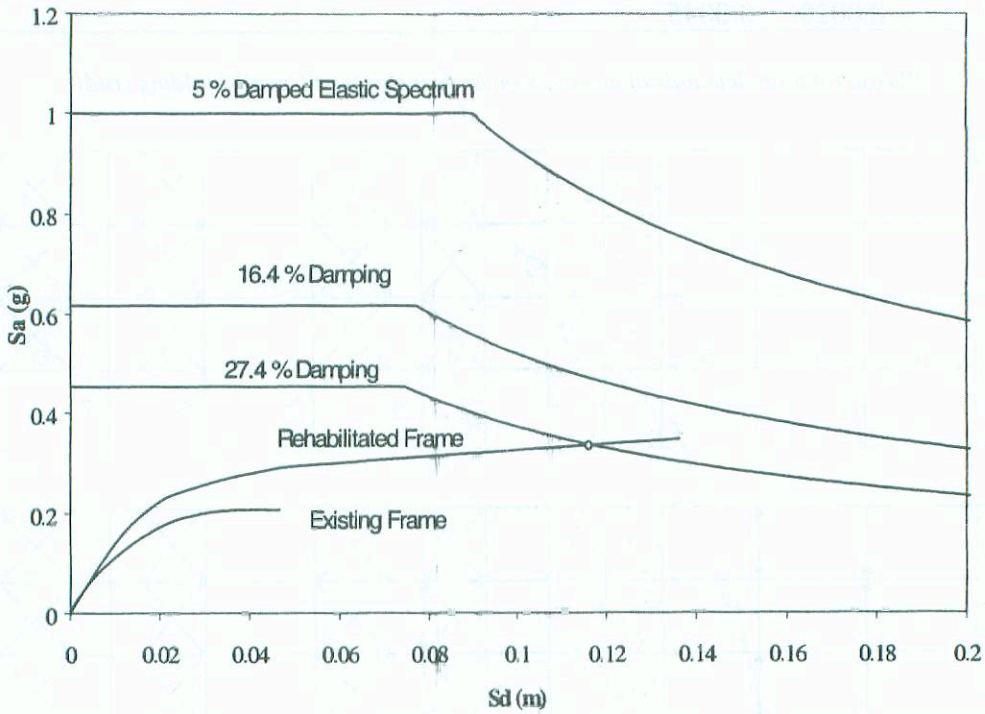

Fig. 7-5: Application of capacity spectrum method to the fourstorey building using the Turkish Seismic Code design spectrum

7.2.4 Performance evaluation with the capacity spectrum method

Seismic demand and capacity of the four-storey building was expressed in the Acceleration-Displacement Response Spectrum (ADRS) format, by using the procedure outlined in ATC-40 (1996). Seismic demand was determined in accordance with the Turkish Code (1998), which yields very similar spectral requirements with ATC-40, as shown in Fig. 7-1. Structural behaviour types were selected as types C and B for the existing and retrofitted systems, respectively. These types correspond to a poor existing building (type C) and a building whose primary elements are combinations of existing and new elements (type B), where both buildings were subjected to a short duration shaking such as the Dinar earthquake ground motion. The first mode participation factor and the modal mass coefficient were 1.29 and 0.85 for the existing and 1.31 and 0.84 for the retrofitted frames, respectively.

Seismic demand and capacity spectra of the building are shown in Fig. 7-5 in the ADRS format. The existing building is estimated to possess an energy dissipation capacity at the

Copyright fib, all rights reserved. This PDF copy of fib Bulletin 24 is intended for use and/or distribution only by National Member Groups of fib.

ultimate stage equivalent to 16.4% viscous damping, for which the reduced demand spectrum did not intersect with its capacity spectrum. This result verified that the existing building is not capable of satisfying the code seismic action requirements. The estimated energy dissipation capacity of the retrofitted building was higher, equivalent to 27.4% viscous damping. Capacity and demand intersect at a performance point where the base shear coefficient is equal to 0.28 and the ratio of roof displacement to total height was 0.805%. This value was larger than the target value of 0.79% calculated in line with the FEMA-356 rules. At this performance, the building was still considered to satisfy the life safety performance level in ATC-40, although the performance displacement is very close to the displacement demand.

7.2.5 Nonlinear dynamic analysis

Nonlinear time-history analyses were conducted for the existing and the retrofitted buildings under the NS component of the Dinar mainshock ground motion. The normalized top displacement time histories obtained by Drain 2DX are shown in Figs 7-6 a and 7-6 b. The points at maximum dynamic displacements are marked on Fig. 7-4 along the respective capacity curves. It can be inferred that the existing frame (with masonry infills) did not collapse but performed slightly better than collapse, which conformed with the observed damage. On the other hand, the retrofitted system performance at a roof displacement ratio of 0.26% can be classified as immediate occupancy under the same ground excitation.

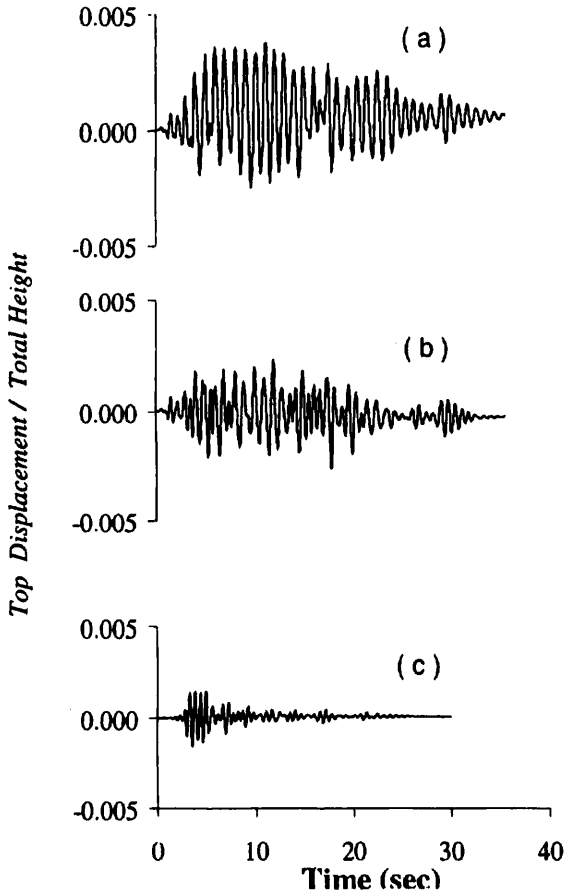

Fig. 7-6: Normalized roof displacement time histories of the four-storey building
a) Existing building under Dinar mainshock, NS component
b) Retrofitted building under Dinar mainshock, NS component
c) Retrofitted building under Dinar aftershock, NS component

Copyright fib, all rights reserved. This PDF copy of fib Bulletin 24 is intended for use and/or distribution only by National Member Groups of fib.

7.2.6 Aftershock test in Dinar

On 4 April 1998, a magnitude 4.6 aftershock occurred on the Dinar fault (Gülkan et al., 1998). This aftershock produced at the Dinar station a strong ground motion with a PGA of 0.13g and a mean elastic response spectrum shown in Fig. 7-1 a. Since the retrofitting of 35 buildings had been completed in Dinar before the aftershock, it was considered as a live testing of the retrofitted building stock for performance evaluation. The observations on 35 buildings following the aftershock indicated the presence of minor hairline cracking along the interfaces between the newly cast concrete infills and the existing frame members in some buildings, and hairline plaster cracking of masonry infill walls in some other buildings. The four storey building presented herein exhibited minor shear cracking of the masonry piers between windows at the second storey which spanned the cantilevering facade (Fig. 7-2 and 7-3) and vertical hairline cracks at the face of joints of first storey beams with the shear walls.

A time-history analysis was performed on the nonlinear model under the NS component of the 1998 aftershock. The results shown in Fig. 7-6 c indicate a performance at a base shear ratio of 0.18 and a roof displacement ratio of 0.15%, which was slightly beyond the first yield stage (Fig. 7-4). Plastic hinges with very small plastic rotations (maximum 0.0014 rad.) formed at the ends of beams connecting to shear walls at all four storeys. This was somewhat beyond the observed damage, possibly due to underestimation of actual strength capacities in the model. These results confirmed the operational performance level of the building following the aftershock.

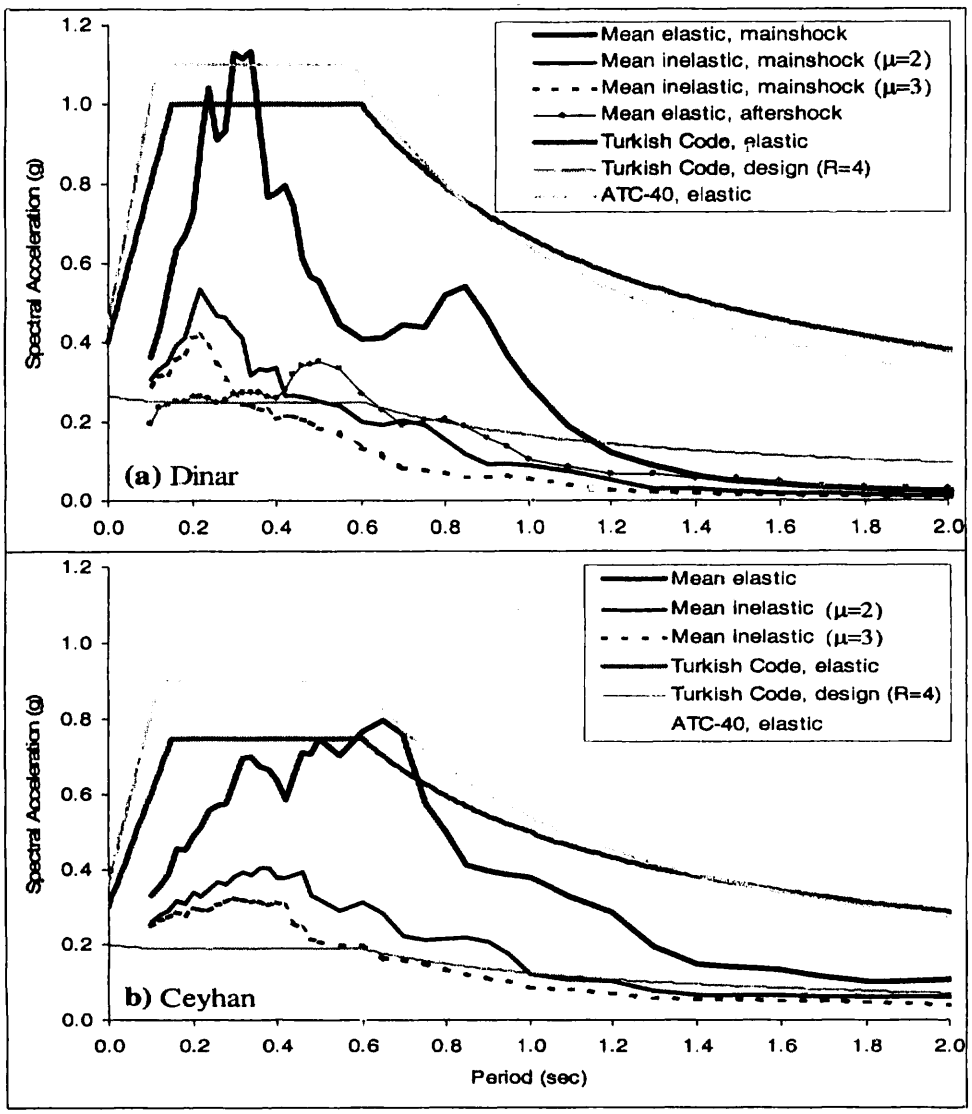

Fig. 7-7: Acceleration response spectra of the Dinar and Ceyhan earthquake ground motions and the related code spectra

Copyright fib, all rights reserved. This PDF copy of fib Bulletin 24 is intended for use and/or distribution only by National Member Groups of fib.

Fig. 7-8: Eight-storey damaged building in Ceyhan

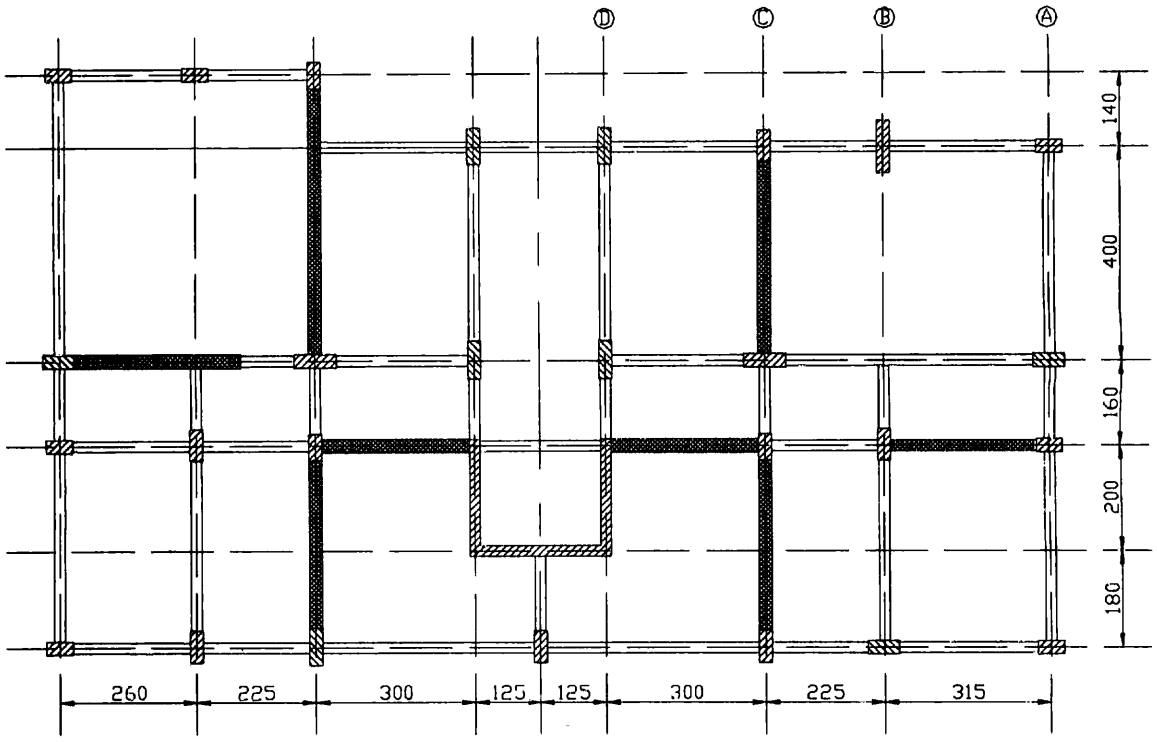

Fig. 7-9: Retrofitting scheme applied to the ground storey plan of the eight-storey building in Ceyhan

Copyright fib, all rights reserved. This PDF copy of fib Bulletin 24 is intended for use and/or distribution only by National Member Groups of fib.

7.3 Case study 2: Eight-storey building in Ceyhan

7.3.1 Introduction

The building shown in Fig. 7-8 experienced moderate damage during the June 25, 1998 Adana-Ceyhan earthquake (Sucuoglu et al., 2000). Damage was mostly observed in beams in the first five levels and in the columns and the U-shaped shear wall around the elevator shaft in the first level. The shear walls indicated with darker shading on Fig. 7-9 were added for seismic retrofitting. Door openings were allowed in both of the new walls axes that were connected to the edges of the U-shaped wall.

The structural system of the existing building was regular and almost symmetrical in the long direction. Its foundation consisted of two-way continuous footings at a depth of 1 m from the ground. The beam sizes were 200 mm by 600 mm, the concrete slab thickness 140 mm, and column sizes varied between 250 mm by 500 mm and 250 mm by 700 mm. A typical floor area was 227 m^2 at the upper storeys and 195 m^2 at the ground storey. The storey height was 3.0 m for all storeys. The characteristic concrete strength was estimated as 14 MPa from the core samples taken from walls and beams.

During the Adana-Ceyhan earthquake, four of the 24 columns at the first storey were moderately damaged and the other 20 were undamaged. Two of the three existing concrete wall segments were lightly damaged and one was moderately damaged. Most of the 55 beams and 36 infill walls were moderately damaged. Similar beam and infill wall damage patterns were repeated from the first to fifth storeys above the ground level.

In the majority of connections, the strong column-weak beam condition was satisfied. The longitudinal reinforcement ratio in columns was between 1% and 2%, and the beams were lightly reinforced. The spacing of transverse reinforcement was 200 mm in all frame members. Although the beam damage distribution over the five storeys indicated a tendency toward a favourable beam mechanism, the infill wall damages was an indication of the lack of lateral stiffness and strength.

7.3.2 Linear dynamic procedure

The results obtained from three-dimensional models prepared for both the existing and the retrofitted systems were employed for testing the acceptability of seismic action demands. Design earthquake actions were reduced by a factor of 2 for the vertical elements of the existing and the retrofitted systems where the equivalent seismic forces were delivered by yielding beams (ASCE, 2000). DCR values for maximum bending moments are compared in Table 7-3 for the 16 ground storey columns, which preserved their original status during

Column axis	DCR-before retrofitting X	DCR-before retrofitting Y	DCR-after retrofitting X	DCR-after retrofitting Y
1A	1.5	1.6	0.4	0.4
1B	1.0	2.3	0.3	0.6
1D	1.3	4.0	0.3	0.4
1F	1.2	4.8	0.3	0.4
1H	4.0	0.5	0.5	0.2
1I	1.9	1.6	0.4	0.5
2A	1.7	1.7	0.5	0.5
2D	2.4	1.6	0.3	0.5
2F	2.4	1.7	0.4	0.5
3H	1.1	2.3	0.6	0.5
3I	1.5	2.8	0.4	0.8
5A	5.9	1.5	0.3	0.4
5B	3.1	3.4	0.5	0.3
5E	1.1	1.4	0.3	0.3
5H	2.4	3.2	0.3	0.5
5I	1.3	1.3	0.3	0.4

Table 7-3: Demand-capacity ratios in first storey columns before and after retrofitting

Copyright fib, all rights reserved. This PDF copy of fib Bulletin 24 is intended for use and/or distribution only by National Member Groups of fib.

retrofitting. The columns were labeled from A to I (right to left) and from 1 to 5 (top to bottom) in Fig. 7-9.

It may be observed that the columns, which were assessed to fail in the existing state, were relieved substantially after retrofitting. All components of the retrofitted frame/wall system that were relieved by the addition of new walls were found to satisfy the force-controlled acceptance criteria of FEMA-356.

7.3.3 Nonlinear static (pushover) analysis

Two different two-dimensional nonlinear structural models were prepared for representing the existing and the retrofitted state of the building. Both models included one half of the building in the nearly symmetrical direction (axes A to D on Fig. 7-9). Masonry infill walls were not considered, because their number was small. The foundation flexibility was also ignored, due to both the rigidity of the existing two-way continuous foundation system and the negligible contribution of the continuous foundation flexibility after global yielding of the structural system. First-mode-proportional lateral load distributions were applied to each model.

The capacity curves of the two models are shown in Fig. 7-10. It is observed that the existing system did not possess the lateral resistance required by the 1975 Turkish Code. The added shear walls increased lateral strength and deformation capacities by 72% and 75%, respectively.

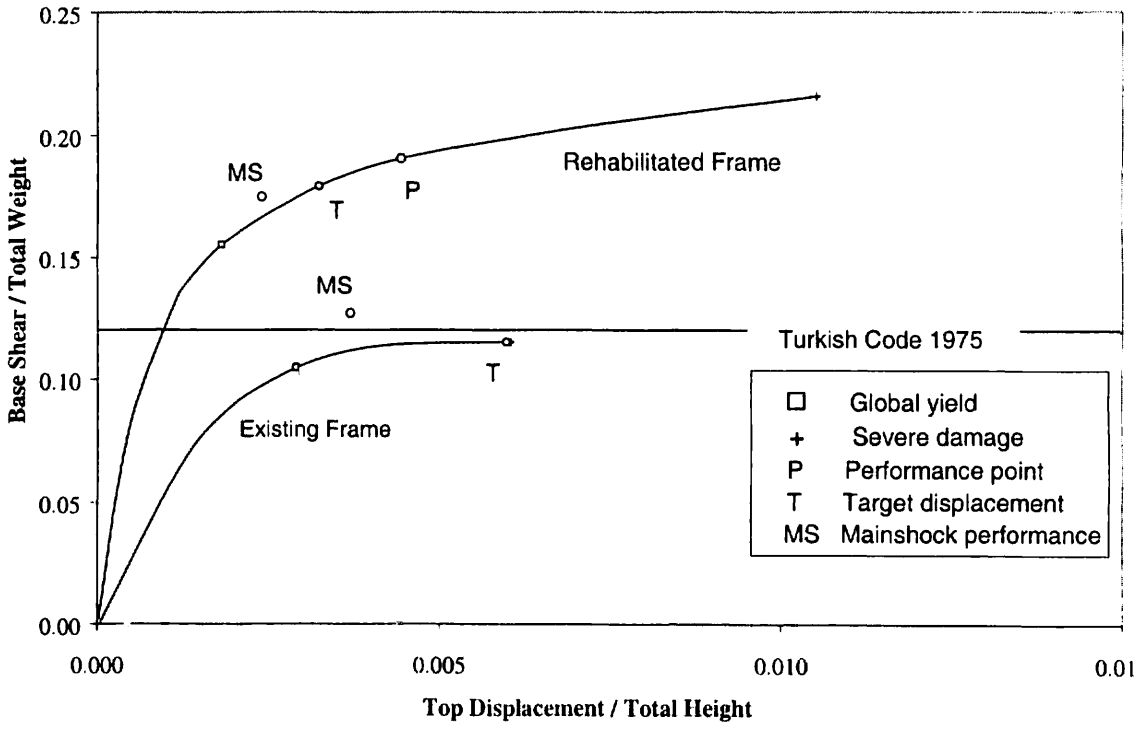

Fig. 7-10: Normalized capacity curves for the eight-storey building in Ceyhan

The global yield and severe damage stages are marked on Fig. 7-10 and the associated plastic hinge mechanisms for the retrofitted system are shown in Fig. 7-11. In the existing system, global yield occurred by the yielding of the U-shaped shear wall at the base and by yielding of all beams connected to this wall. A combination of distributed beam mechanism and a storey mechanism between first and fourth level lead to the severe damage stage accompanied with considerable deformability. On the other hand, the system behaviour was completely controlled by the added coupled shearwalls in the global yield and severe damage stages of the retrofitted system as indicated on Fig. 7-11, with further enhanced deformability.

Effective vibration periods of 0.95 and 0.57 sec., and code level spectral displacements of 102 and 60 mm were combined to calculate target roof displacements of 116 and 77 mm for the existing and retrofitted systems, respectively. These displacements are normalized with

Copyright fib, all rights reserved. This PDF copy of fib Bulletin 24 is intended for use and/or distribution only by National Member Groups of fib.

respect to the building height as 0.60% and 0.32%. The existing building may be considered to satisfy collapse prevention and the retrofitted building life safety performance levels, respectively, in view of Fig. 7-10.

Table 7-4 gives the plastic hinge rotations in 1st-storey members of the retrofitted system at target displacement. All members are numbered from left to right in Fig. 7-11.

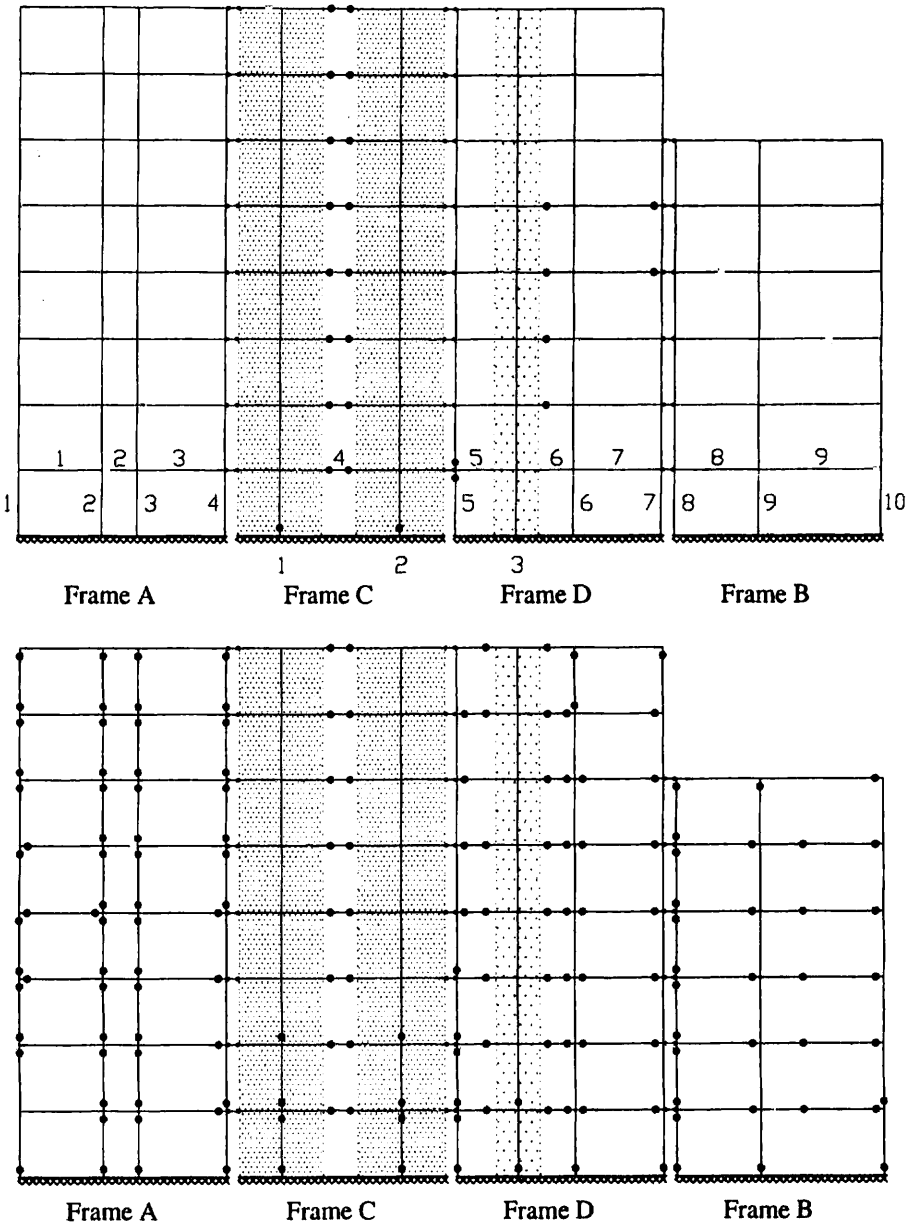

Fig. 7-11: Plastic hinge mechanisms in the retrofitted building at the global yield and severe damage stages during the pushover analysis

Member Type	Member numbers 1	2	3	4	5	6	7	8	9	10
Beams	0.0	0.0	0.0	0.0072	0.0019	0.0027	0.0015	0.0008	0.0009	
Columns	0.0	0.0	0.0	0.0	0.0031	0.0033	0.0033	0.0032	0.0032	0.0006
Walls	0.0018	0.0017	0.0014							

Table 7-4: Plastic rotations of members in the first storey of Case-2 building (rad.)

All beams, columns and walls displayed plastic rotations less than the acceptable values, including the coupling beam number 4 in frame C, which is assigned a plastic rotation limit of 0.008 rad. On the other hand the three shear walls that received 70% of the total base shear

Copyright fib, all rights reserved. This PDF copy of fib Bulletin 24 is intended for use and/or distribution only by National Member Groups of fib.

force at the target displacement performed at the immediate occupancy level. They dominated the seismic response of the retrofitted system.

7.3.4 Performance evaluation with the capacity spectrum method

The capacity-spectrum method was applied to the eight-storey building with a procedure similar to that applied to the four-storey building. The Acceleration Displacement Response Spectrum representation of the demand and capacity spectra is shown in Fig. 7-12. A performance point was not obtained for the existing system, whereas a performance point was obtained for the retrofitted one, at an equivalent damping ratio of 26%. At the performance point, spectral acceleration and displacement values were determined as 0.27 g and 87 mm, which corresponded to a base shear coefficient of 0.191, a roof displacement of 105 mm and a roof displacement ratio of 0.44%. This roof displacement was significantly higher than the target roof displacement of 77 mm; nonetheless it indicated a life safety performance.

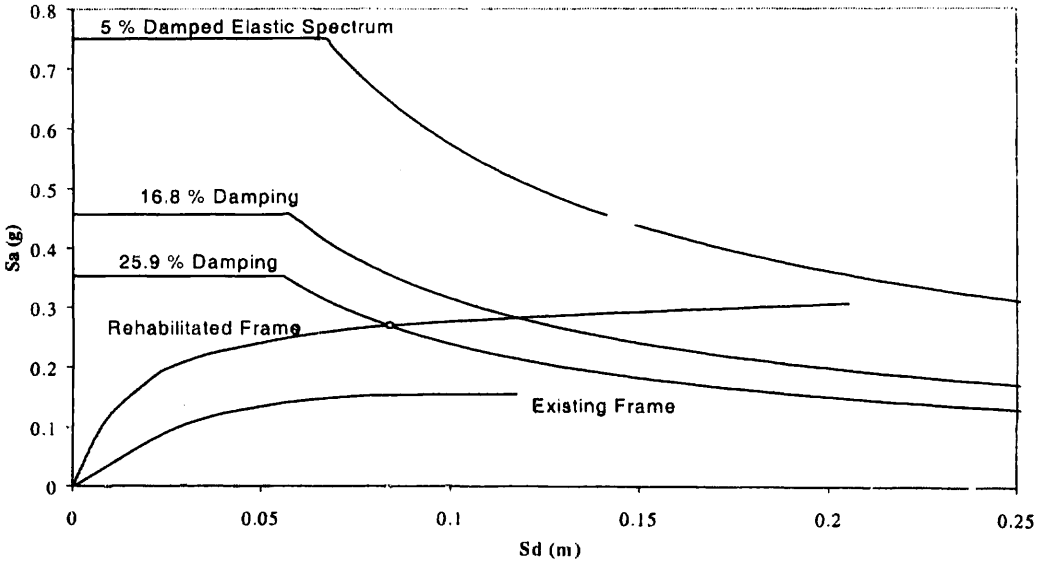

Fig. 7-12: Application of the capacity spectrum method on the eight-storey building using the Turkish Seismic Code design spectrum

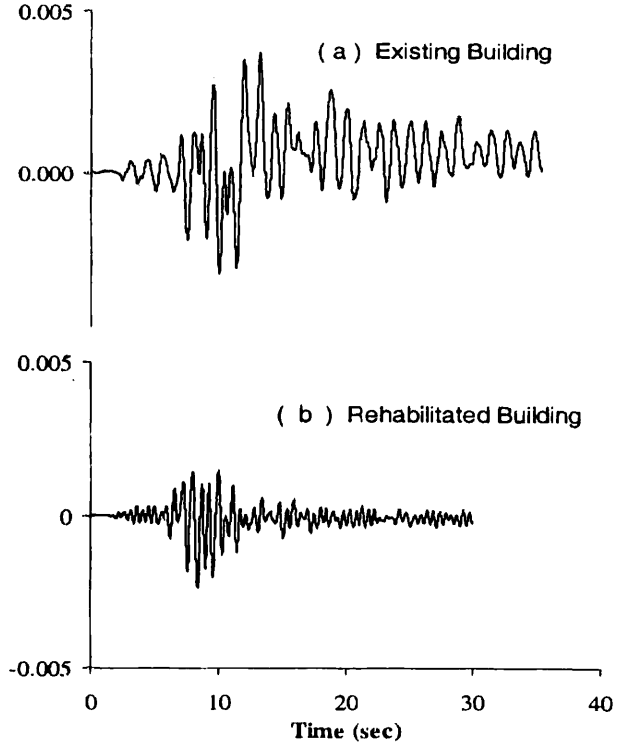

Fig. 7-13: Normalized roof displacement time histories for the eight-storey building under the NS component of Ceyhan strong motion record

Copyright fib, all rights reserved. This PDF copy of fib Bulletin 24 is intended for use and/or distribution only by National Member Groups of fib.

7.3.5 Nonlinear time history analysis

Nonlinear dynamic responses of the existing and retrofitted systems were calculated under the NS component of Ceyhan earthquake by the Drain 2DX program and shown in Fig. 7-13. The time history analysis produced maximum roof displacement ratios of 0.37% and 0.24% for the existing and the retrofitted systems, respectively. The maximum response points are marked on Fig. 7-10 for comparison with the target displacement and performance points on the capacity curves. It is noteworthy that the existing system performed well at the life safety level, which was confirmed by the observed damage after the earthquake. The retrofitted system also exhibited the same performance level under the same ground excitation. However it was accompanied with a well controlled damage distribution (Fig. 7-11).

Building Cases	Effective period (s)	Code spectrum		Earthquake ground motion	
		Target	CSM	Target	Time history
4-storey, existing	0.60	>Collapse	No performance	0.0036	0.0038
4-storey retrofitted	0.56	0.0079	0.0106	0.0032	0.0026
8-storey, existing	0.95	0.0060	No performance	0.0049	0.0037
8-storey, retrofitted	0.57	0.0032	0.0044	0.0030	0.0024

Table 7-5: Comparison of normalized roof displacements from different nonlinear methods

7.4 Discussion of results of case studies 1 and 2

Different nonlinear analysis methods were employed (ATC 1997, ASCE 2000, ATC 1996) for evaluating the seismic performances of two actual buildings in Turkey, both in their existing and retrofitted states. Since performance-based-evaluation mainly depends on peak response displacements, it is worthwhile to compare maximum displacements from different methods. The comparison is presented in Table 7-5 in terms of roof displacement ratios.

When the results of CSM and the FEMA-273/356 target displacement method in the respective columns of Table 7-5 are compared, it may be observed that both methods predict collapse for the existing buildings under the same code spectra. It must be considered that the target roof drift of 0.6% for the eight-storey existing building is very close to its ultimate displacement capacity. However the same consistency does not apply for the retrofitted buildings, where composite-spectra performance displacements overestimate the target displacements by about one-third in both cases. It is apparent that the equivalent damping ratios proposed by the composite spectrum method are insufficient for reducing the elastic code spectra to realistic levels.

In the last two columns of Table 7-5, target displacements are compared with the dynamic response displacements under spectral and signal definitions of the same ground motions, respectively. Although the results can be accepted as reasonably close, target displacements are usually larger than the maximum nonlinear dynamic displacements. Considering the ultimate simplicity of the target displacement method relative to the nonlinear time-history analysis, such a conservatism may be deemed tolerable.

The linear dynamic procedure, combined with the force-based component acceptance criteria for the existing buildings, leads to similar decisions with those of nonlinear static procedures, such that both building performances are unacceptable (X-direction in Table 7-1 and Y-direction in Table 7-3). For the retrofitted buildings, the linear procedure does not accept the force-based performance of the four-storey building, since linear elastic demands exceed force capacities. Nonetheless, a displacement-based performance can be acceptable, since the DCR values for the retrofitted building in Table 7-1 only slightly exceed the m-factors proposed for columns in FEMA-356. In fact, the corresponding plastic rotations are acceptable according to the nonlinear static procedure (Table 7-2). On the other hand, both procedures accept the performance of the eight-storey retrofitted building. This is expected, as the plastic rotations given in Table 7-4 are very small.

Copyright fib, all rights reserved. This PDF copy of fib Bulletin 24 is intended for use and/or distribution only by National Member Groups of fib.

7.5 Case study 3: Frames typical of old Italian design

7.5.1 Introduction

The object of this section is the seismic assessment of two 2D R.C. frames (a low and a high rise one), belonging both to multistorey buildings designed and built according to the Italian Seismic Code of 1960 in a high seismic hazard region.

Structural performance has been evaluated, for different PGA (peak ground acceleration) values, applying the *Capacity Spectrum Method* (according to ATC-40), the *Displacement Coefficient Method* (of FEMA 273, 356) and the *N2 Method* (Fajfar and Fischinger 1988). Results have been compared with those of Linear Response Spectrum Analyses, of simple approaches like Equal Energy and Equal Displacement assumptions (which give the well-known relationships $q = \sqrt{2\mu - 1}$ and $q=\mu$, respectively) and with those derived via nonlinear dynamic analyses, using both natural and synthetic accelerograms.

These methods have been applied using different capacity curves, obtained via either displacement- or force-controlled pushover analyses, with different lateral load profiles. Global and local responses in terms of displacements, interstorey drifts, plastic rotations, plastic hinge distributions and storey shears, as well as material deformations, are then computed from different pushover analyses, imposing top displacements equal to the maximum dynamic one.

7.5.2 Case study frames

The reference structures are planar frames belonging to a real multistorey building. Both structures were designed and built according to 1960 Italian Seismic Code, in a high seismicity region. Design was made at working stresses; this implies that maximum design stress in reinforcement is about half the yield value. Columns were not dimensioned for shear. Static lateral forces are applied, equal to the storey mass times a constant floor acceleration of 0.10 g (base shear coefficient: 0.1).

The first frame (Fig. 7-14 a) has five bays and two floors and is representative of the behaviour of low rise structures. The second frame (Fig. 7-14 b) has two bays and seven floors and is representative of high rise structures.

The dynamic properties for the two frames are listed in Table 7-6. They have been computed assuming uncracked sections. The first two mode shapes for the two floors structure and the first three ones for the high rise frame are shown in Fig. 7-16, respectively.

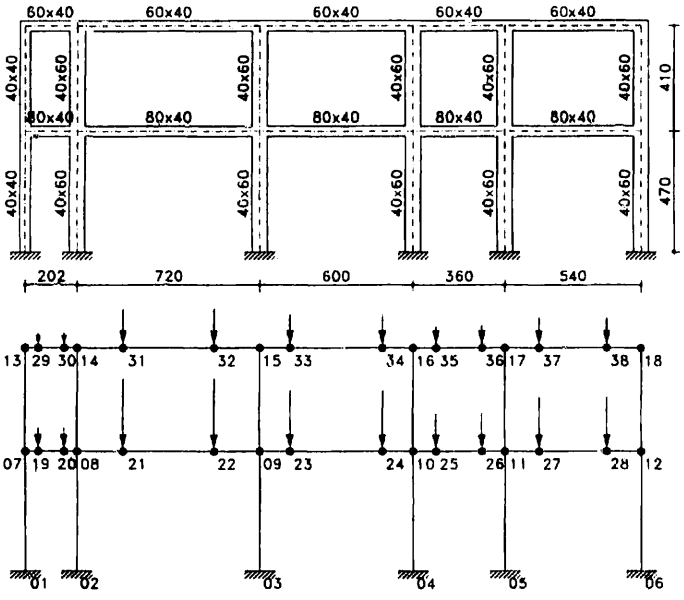

Elem.	Reinf.	Elem.	Reinf.
01-07	4Ø20	09-10	Top: 5Ø20
02-08	6Ø20		Bott: 10Ø20
03-09	6Ø20	10-11	Top: 4Ø20
04-10	6Ø20		Bott: 8Ø20
05-11	6Ø20	11-12	Top: 4Ø20
06-12	6Ø20		Bott: 7Ø20
07-13	4Ø20	13-14	Top: 2Ø16
08-14	6Ø20		Bott: 4Ø16
09-15	6Ø20	14-15	Top: 4Ø20
10-16	6Ø20		Bott: 8Ø20
11-17	6Ø20	15-16	Top: 5Ø20
12-18	6Ø20		Bott: 10Ø20
07-08	Top: 6Ø20	16-17	Top: 4Ø20
	Bott: 11Ø20		Bott: 7Ø20
08-09	Top: 7Ø20	17-18	Top: 3Ø20
	Bott: 13Ø20		Bott: 6Ø20

Fig. 7-14 a: Low frame: geometry, model and reinforcement.

Copyright fib, all rights reserved. This PDF copy of fib Bulletin 24 is intended for use and/or distribution only by National Member Groups of fib.

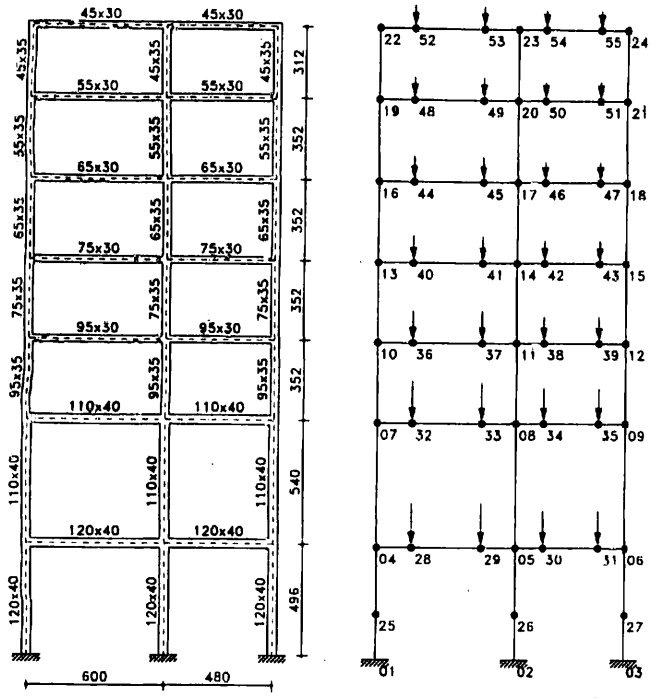

Elem.	Reinf.	Elem.	Reinf.
01-25	46Ø16	17-20	8Ø16
02-26	46Ø16	18-21	8Ø16
03-27	46Ø16	19-22	6Ø16
25-04	18Ø16	20-23	6Ø16
26-05	22Ø16	21-24	6Ø16
27-06	18Ø16	04-05	Top: 2Ø12+18Ø16
04-07	18Ø16	05-06	Bott: 2Ø12+8Ø16
05-08	22Ø16	06-07	Top: 2Ø12+18Ø16
06-09	18Ø16	07-08	Bott: 2Ø12+8Ø16
07-10	18Ø16	08-09	Top: 2Ø12+18Ø16
08-11	20Ø16	09-10	Bott: 2Ø12+8Ø16
09-12	18Ø16	13-14	Top: 2Ø12+11Ø16
10-13	14Ø16	14-15	Bott: 2Ø12+5Ø16
11-14	18Ø16	16-17	Top: 2Ø12+9Ø16
12-15	14Ø16	17-18	Bott: 2Ø12+8Ø16
13-16	12Ø16	19-20	Top: 2Ø10+8Ø12
14-17	14Ø16	20-21	Bott: 2Ø10
15-18	12Ø16	22-23	Top: 2Ø10+7Ø12
16-19	8Ø16	23-24	Bott: 2Ø10

Fig. 7-14 b: High frame: geometry, model and reinforcement.

	low frame		
Mode	T_m [s]	Γ_m [m^{-1}]	α_m [%]
1	0.412	14.7	92.3
2	0.129	4.2	7.7

	high frame		
mode	T_m [s]	Γ_m [m^{-1}]	α_m [%]
1	1.82	19.5	76.6
2	0.67	8.3	14
3	0.37	4.4	4
4	0.24	4.2	3.6
5	0.19	3.0	1.8

Table 7-6: Modal characteristics (T_m=period, Γ_m=participation factor, α_m=mass participation factor): (left) low frame, (right) high frame.

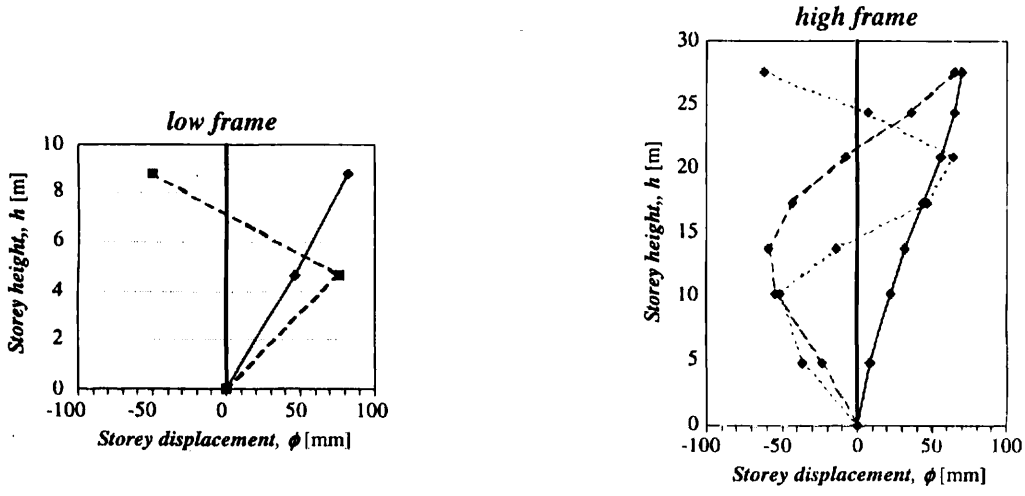

Fig. 7-15: Mode shapes: (left) low frame, (right) high frame.

Copyright fib, all rights reserved. This PDF copy of fib Bulletin 24 is intended for use and/or distribution only by National Member Groups of fib.

7.5.3 Nonlinear dynamic analysis

Nonlinear dynamic analyses were conducted for both structures. The structural response from those analyses is assumed as the "real" one. A nonlinear fibre model was used, with the software *Fiber* (Petrangeli et al, 1999). The steel model (Brisighella, 1988) and the model for concrete are shown in Fig. 7-17. Both confined and unconfined concrete are separately modeled.

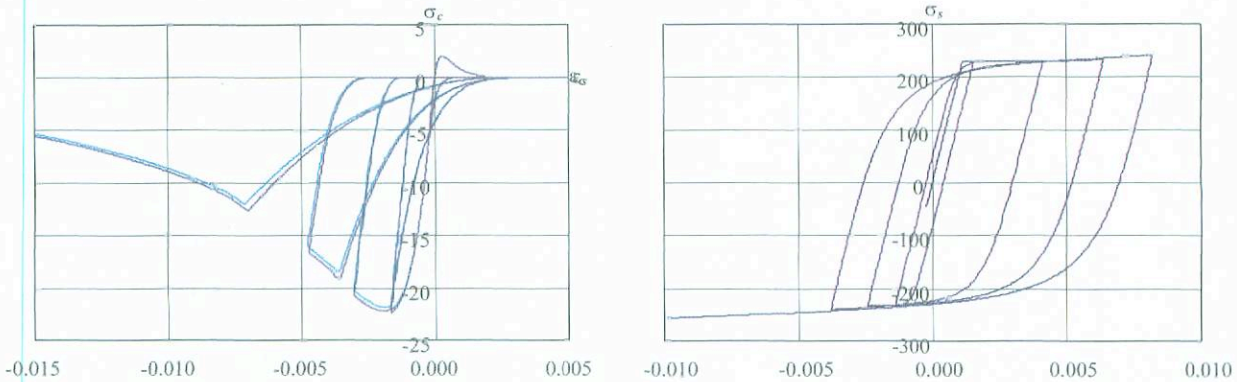

Fig. 7-17: (left) Steel and (right) concrete constitutive models.

The accelerograms used, both natural and synthetic are:

- 9 artificial ones generated with the *SIMQKE* program (Gasparini, 1976). The accelerograms are compatible with the soil type B spectrum in ENV 1998-1-1:1994, with a duration of 20 s, peak ground acceleration (*pga*) equal to 0.05 g, 0.10 g, 0.20 g and 0.30 g for the high rise structure and 0.05 g, 0.10 g, 0.30 g, 0.40 g and 0.50 g for the low rise one.
- 32 natural accelerograms, selected among those listed by Miranda (1993). They are from the Loma Prieta (1989, 7.1 M_S) and the Whittier-Narrows (1989, 6.1 M_L) events, recorded on different soil types (rock, alluvium and soft). For the sake of conciseness, only the results relative to the high rise frame for the Loma Prieta event, recorded over alluvium at Hollister station at an epicentral distance of 48km, are shown (pga=0.17 g). The elastic response spectrum of this record has a trend similar to the EC8 one for periods longer than the high frame elastic period (Fig. 7-18). Other cases are reported in (Albanesi, 2001).

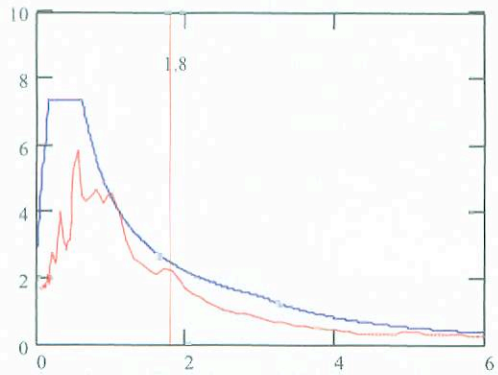

Fig. 7-18: Loma Prieta (Hollister) response spectra vs ENV 1998-1-1:1994 (soil type B, pga=0.30 g).

7.5.4 Nonlinear static (pushover) analysis

Both structures have been analyzed with the pushover technique, with both displacement and force control, also considering different load profiles. Since the frames are not symmetric with respect to the central axes, pushover analysis was conducted for both senses of action, positive or negative. These analyses have been made with the same 2D model and software used for the dynamic analyses, to avoid discrepancies due to different models.

Copyright fib, all rights reserved. This PDF copy of fib Bulletin 24 is intended for use and/or distribution only by National Member Groups of fib.

The analyses were up to a top displacement of 200 mm and 600 mm, respectively, for the low and high rise structure. These values are about 2% of the total height and coincide with the limit proposed by ATC-40 (1996) for the life safety performance level.

Capacity curves, expressed as base shear vs. top displacement, computed with both force- and displacement-controlled pushover analysis and with load profile proportional to the first mode (Fig. 7-19) are compared with the maxima of response from nonlinear dynamic analyses (Fig. 7-20).

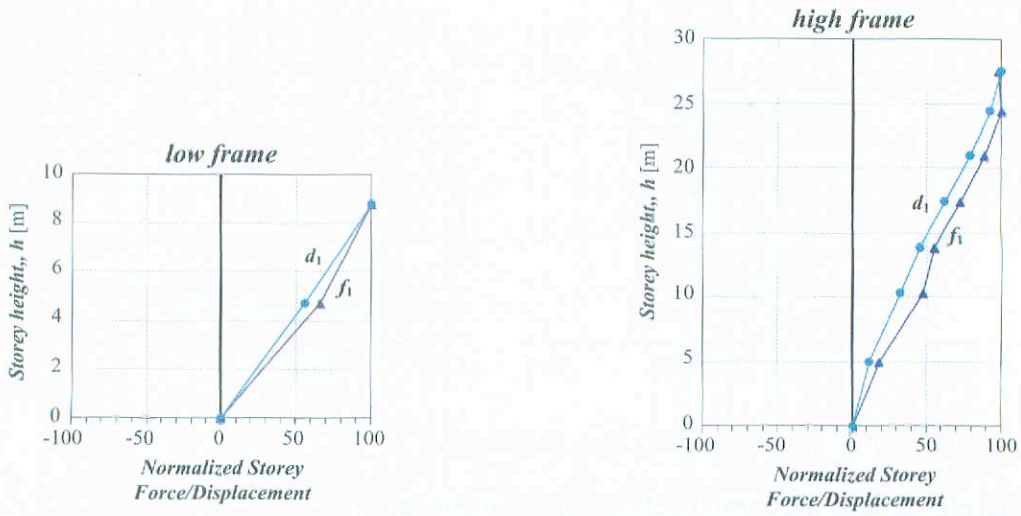

Fig. 7-19: Initial first mode storey force, f_1, and displacement, d_1, profiles, used in pushover analyses for low frame (left) and high frame (right).

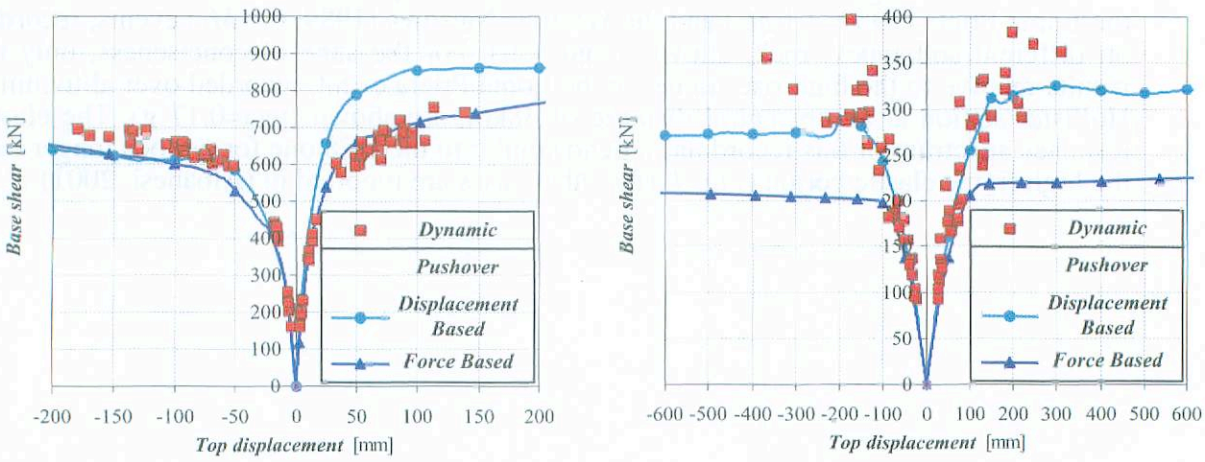

Fig. 7-20: Comparison of capacity curves from pushover analysis with force- or displacement-control to dynamic response of low frame (left) or high frame (right).

For the low rise frame results from pushover analyses are accurate with respect to peak dynamic response, both in the elastic and in the plastic range. For the high rise frame the picture is different: pushover analyses are accurate in the linear range, while they underestimate the peak inelastic dynamic response, being less accurate with increasing excursion in the plastic range. In this latter case results from dynamic analyses have considerable scatter about the mean.

Results of the analyses are sensitive to the applied load profile. Fig. 7-21, 7-22 show the different load profiles used for the low and high rise frames, respectively. The profiles are:

- Uniform load profile (*Uniform*), where constant floor acceleration is assumed (force at each level proportional to the floor mass, $F_i \propto m_i$)
- Equivalent static forces according to the Italian Seismic Code (*NTI*):

Copyright fib, all rights reserved. This PDF copy of fib Bulletin 24 is intended for use and/or distribution only by National Member Groups of fib.

$$F_{1i} = \frac{w_i h_i}{\sum_{j=1}^{N} w_j h_j} V_{b1} \tag{7-1}$$

In eq. (7-1) w_i= weight at i-th level, h_i= distance between w_i and the base, V_{b1}= base shear in first mode and N= number of floors.

- Load profile compatible with the first mode (*1st mode*):

$$F_{1i} = \frac{w_i \phi_i^{(1)}}{\sum_{j=1}^{N} w_j \phi_j^{(1)}} V_{b1} \tag{7-2}$$

in which $\phi_i^{(1)}$= first mode at i-th level;

- Non-linear load profile as suggested by *FEMA-273, 356* (*FEMA*):

$$F_{1i} = \frac{w_i h_i^k}{\sum_{j=1}^{N} w_j h_j^k} V_{b1} \tag{7-3}$$

in which k is a coefficient dependent on the first period, T_e:

$$k = \begin{cases} 1.0 & T_e \le 0.5s \\ 1.0 + 0.5(T_e - 0.5) & 0.5s < T_e < 2.5s \\ 2.0 & T_e \ge 2.5s \end{cases} \tag{7-4}$$

- Non-linear load profile resulting from the *SRSS* combination of modal floor forces (*Freeman, 1978*):

$$F_i = \sqrt{F_{mi}^2} = \sqrt{\sum_{m=1}^{N} \left(\Gamma_m \phi_i^{(m)} a_m m_i\right)^2} \tag{7-5}$$

in which m_i= mass at the i-th level, $\phi_i^{(m)}$= m-th mode shape at the i-th level, a_m= spectral pseudo-acceleration of the m-th mode and Γ_m= participation factor of the m-th mode:

$$\Gamma_m = \frac{\mathbf{1}^T \mathbf{M} \boldsymbol{\phi}^{(m)}}{\boldsymbol{\phi}^{(m)T} \mathbf{M} \boldsymbol{\phi}^{(m)}} \tag{7-6}$$

in which $\boldsymbol{\phi}^{(m)}$ is the shape of the m-th mode, $\boldsymbol{M}$ the diagonal matrix of the floor masses and $\mathbf{1}=[1, 1, \ldots, 1]^T$ the unity vector.

- Load profile corresponding to an equivalent modal shape (*Valles*):

$$F_i = \frac{m_i \phi_{eq,i}}{\sum_{j=1}^{N} m_j \phi_{eq,j}} V_b \tag{7-3}$$

in which ϕ_{eq} is the equivalent fundamental mode defined by:

$$\phi_{eq,i} = \sqrt{\sum_{m=1}^{N} \left(\phi_i^{(m)} \Gamma_m\right)^2} \tag{7-4}$$

Copyright fib, all rights reserved. This PDF copy of fib Bulletin 24 is intended for use and/or distribution only by National Member Groups of fib.

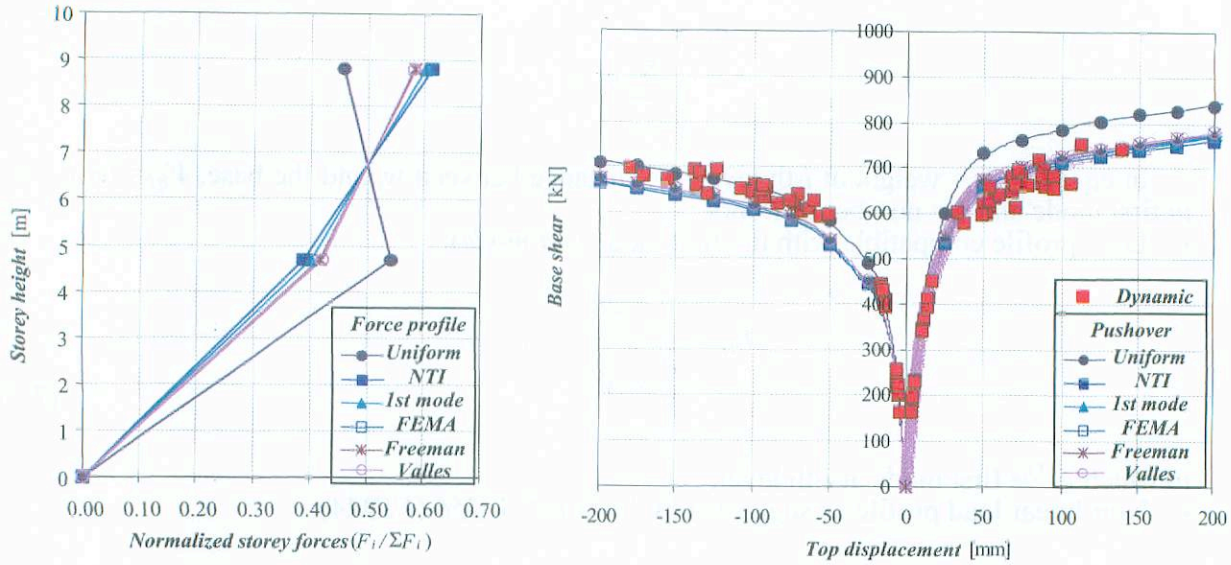

Fig. 7-21: Low frame: (left) force profiles for pushover analysis and (right) capacity curves for different force profiles compared with peak dynamic responses.

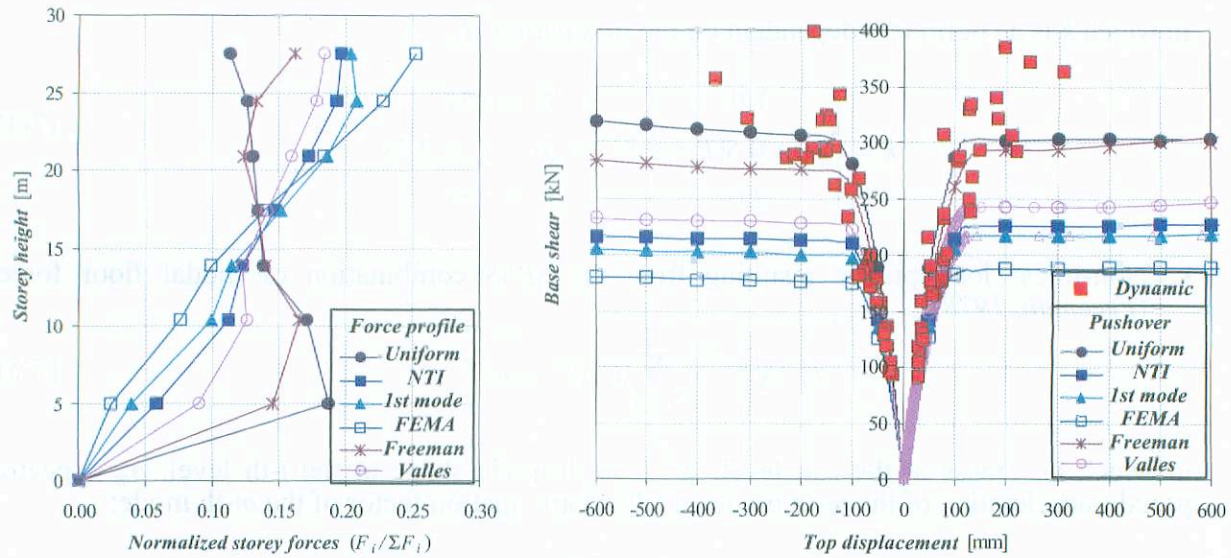

Fig. 7-22: High frame: (left) force profiles for pushover analysis and (right) capacity curves for different force profiles compared with dynamic response.

The resulting capacity curves are compared with the peak response computed via dynamic analyses in Fig. 7-21 b and Fig. 7-22 b.

The capacity curves of the low rise frame are weakly sensitive to the load profile. As a matter of fact, load profiles do not show important differences, and there is almost no difference among the curves computed with the load profile of the first mode and those determined with multimodal load distributions, which also account for higher modes. For instance the *FEMA* distribution (k=1) coincides with the *NTI*. One can also observe a good matching of the maxima of responses (expressed in terms of base shear and top displacement) determined via dynamic and pushover analyses. As a general remark, for regular structures with low to medium periods (less than about 1.2 sec), under usual earthquakes (i.e. with large spectral values in the 0.1-0.6 sec range) conventional pushover analysis is adequate.

Capacity curves for the high rise frame (Fig. 7-22 b) show a strong dependence on load profile. As a matter of fact, higher modes are important and this influences the shape of load

Copyright fib, all rights reserved. This PDF copy of fib Bulletin 24 is intended for use and/or distribution only by National Member Groups of fib.

profiles. For equal base shear top displacement grows with increasing resultant of applied loads. This observation partly justifies the different shapes shown by the capacity curves corresponding to the different load profiles.

A constant (in time) load profile implies assuming a constant distribution of inertial forces during the earthquake. This assumption is reasonable if the structural response is weakly influenced by higher modes and if the structure has a unique yielding mechanism. In such cases constant load profiles lead to a good estimation of displacements and deformations. Constant load profiles have, however, inherent approximations and may even lead to inaccurate results for long period structures with localized yielding mechanisms.

For the high rise frame higher modes are important. This is partly taken into account by *Freeman (1978)*. The other approaches are essentially based on the first mode are not very accurate for the base shear if the ductility demand is high (Fig. 7-22 b). For the low rise frame this problem is not present, since the response is dominated by the first mode.

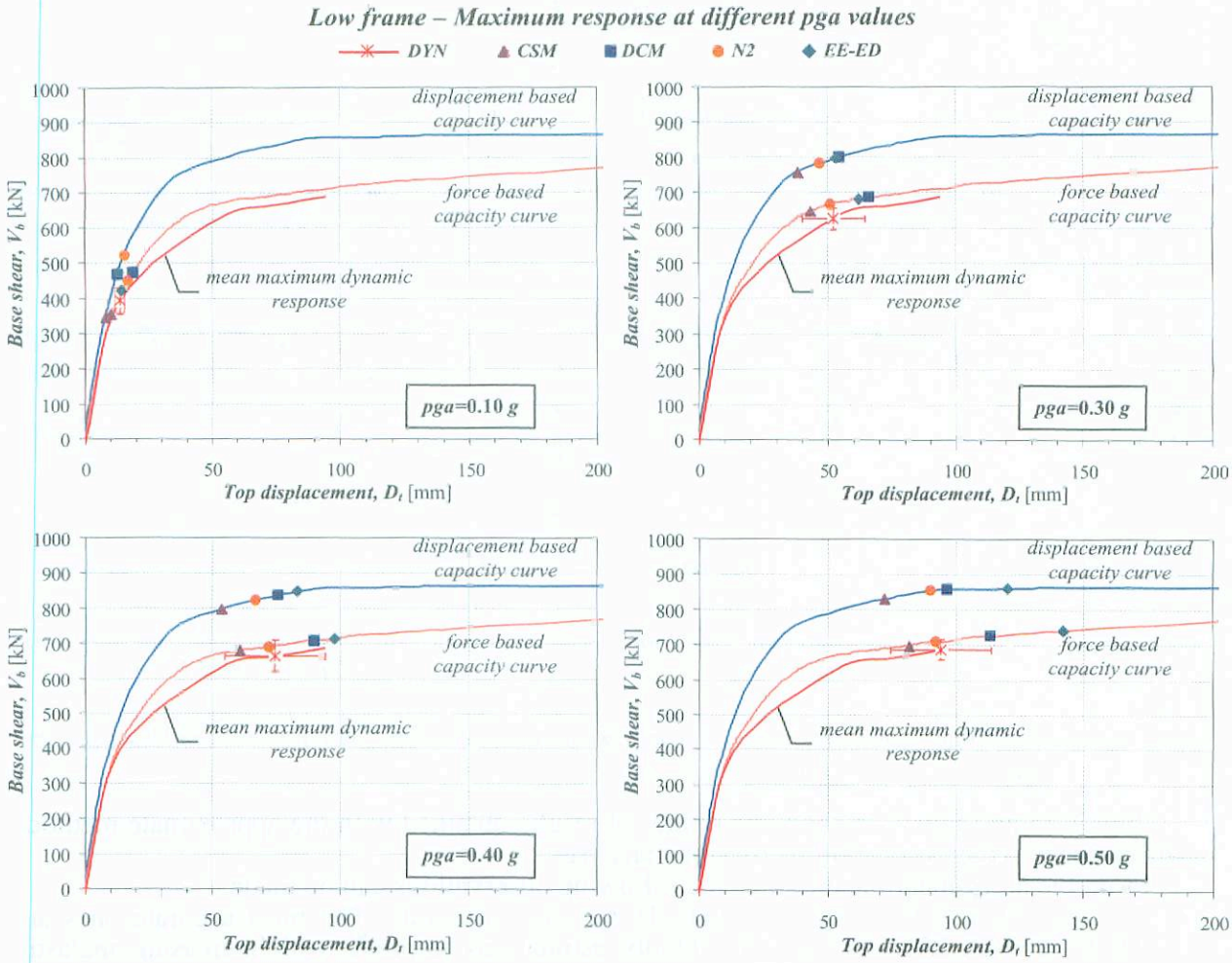

Fig. 7-23: Low frame: comparison between maximum responses from pushover and nonlinear dynamic analyses at different pga values.

7.5.5 Evaluation of global response

Top displacement for the different *pga* values have been computed applying nonlinear static methods, i.e. the Capacity Spectrum Method (ATC-40), the Displacement Coefficient Method (FEMA-273/356) and the N2 Method (Fajfar and Fishinger, 1988). Results have been compared with those of Linear Response Spectrum Analyses (*RSA*), with those of simple approaches like Equal Energy ($q = \sqrt{2\mu - 1}$) and Equal Displacement ($q=\mu$) assumptions and with those derived via nonlinear dynamic analyses.

These methods have been applied with different capacity curves, obtained via pushover analyses with lateral displacement (*D*), or force (*F*) control. The different load profiles of

Copyright fib, all rights reserved. This PDF copy of fib Bulletin 24 is intended for use and/or distribution only by National Member Groups of fib.

Section 7.5.4 have been considered only for the high rise frame, since for the low rise frame the differences are negligible. The performance points computed with all the methods have been compared at increasing earthquake intensity. In Figs 7.23, 7.24 a comparison is shown between these results and the mean results from dynamic analyses.

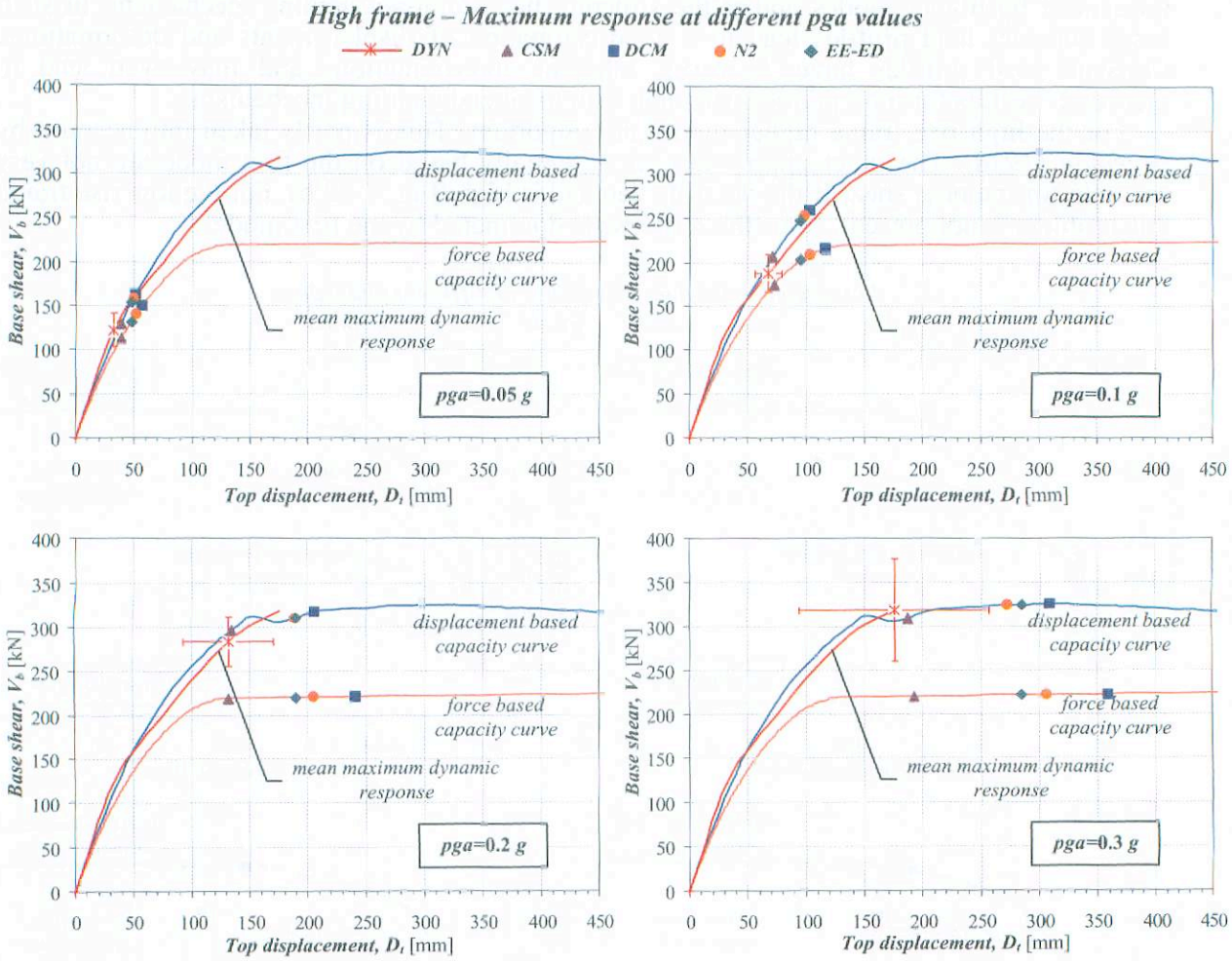

Fig. 7-24: High frame: comparison between maximum responses from pushover and nonlinear dynamic analyses at different pga values.

Fig. 7-25 and Fig. 7-26 show the scatter of results obtained with the approximate methods with respect to the average of the dynamic analyses.

From the afore-mentioned figures the following observations can be made:

- For the low rise frame all the methods are rather accurate. The most accurate ones are *DCM* (FEMA 273/356) and *N2*. Oddly estimations improve with increasing inelastic excursion.
- For the high rise frame the methods overestimate the real response. Only *CSM* shows a reasonable agreement, while *DCM* and *N2* are less precise than *EE-ED*.
- Nonlinear static methods (with pushover based on the first mode) do not take into account higher modes. For the high rise frame this causes the base shear to be underestimated with increasing inelastic excursion. The estimations obtained with different methods are practically coincident, because of the flat capacity curves beyond yielding.
- For the low frame the *CSM* underestimates the expected displacement and overestimates the base shear, while for the high frame it has the opposite effects. This implies underestimation of period shift in the nonlinear range for the low frame and overestimation for the high, which in turn implies that the period corresponding to the performance point is the lower limit for the low frame and the upper one for the high frame while for the high frame it has the opposite effects.

The different capacity curves do not influence much the conclusions of the *CSM*. This can be

Copyright fib, all rights reserved. This PDF copy of fib Bulletin 24 is intended for use and/or distribution only by National Member Groups of fib.

explained if one notices that for the low rise frame capacity curves are similar, independently of their definition and for the high rise frame the response lies in the region of the spectrum where the equal displacement rule applies well.

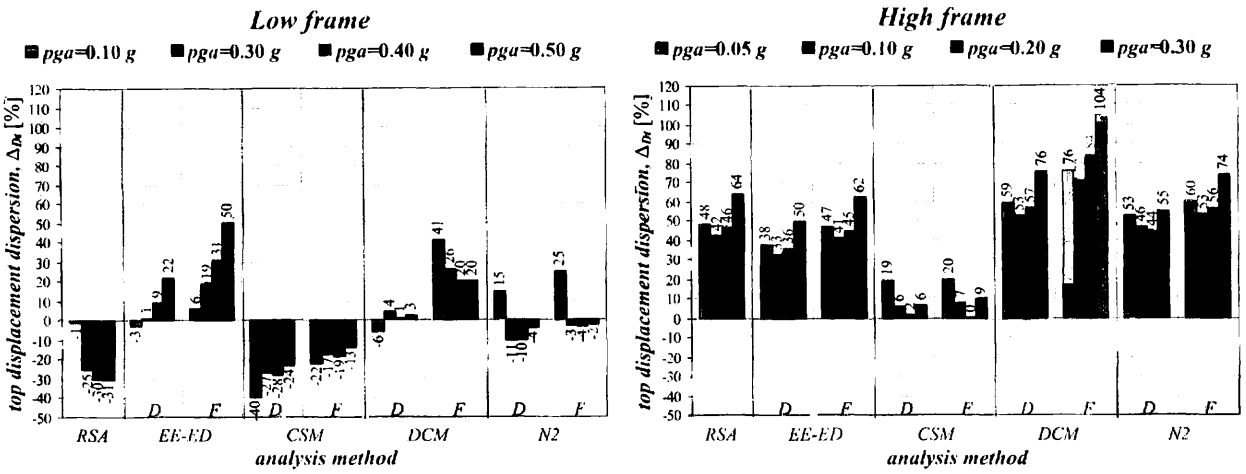

Fig. 7-25: Difference [%] in peak top displacement from different simplified methods, relative to mean nonlinear dynamic analyses results. Low frame (left), high frame (right).

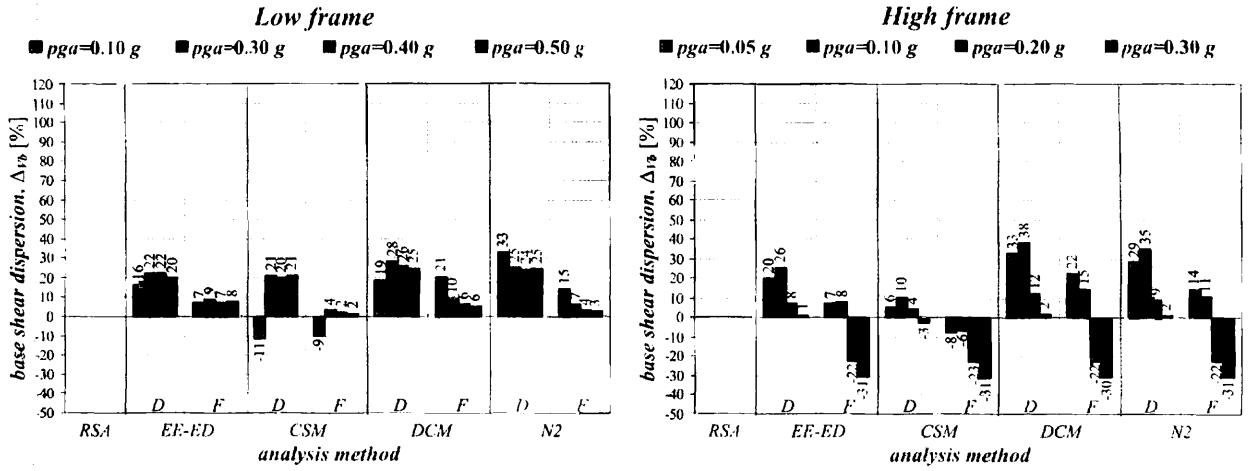

Fig. 7-26: Difference [%] in maximum base shear (V_b) from different simplified methods, relative to mean nonlinear dynamic analyses results. Low frame (left), high frame (right).

For the high rise frame the effect of the load profile has also been investigated. The response variables are top displacement and base shear; the percent difference between the above methods and the response from the nonlinear dynamic analysis are shown in Fig. 7-27. The different results obtained with the same *pga* and method are due to the different capacity curves.

As for the displacement estimation, the load profile influences only the results of *CSM* and *N2*. The estimated displacement decreases and global accuracy increases, if one passes from a first mode to a multimodal to - finally - a uniform profile.

In term of base shear, the differences between the methods (with the same load profile) tend to become uniform with increasing *pga*. This depends on the low value of strain hardening considered after yielding. In the elastic range the *FEMA* 273/356 distribution seems the most accurate, whereas in the nonlinear range the *Freeman* (1978) and *Uniform* profiles show an advantage.

It is worth noticing that using *CSM* the response of the nonlinear dynamic analyses is between the *1st mode* or *FEMA* results and the uniform or multimodal (*Freeman, 1978*) ones. In particular unimodal results are the upper limit for top displacement and the lower limit for base shear (V_b), while the opposite applies for the uniform or multimodal results.

Copyright fib, all rights reserved. This PDF copy of fib Bulletin 24 is intended for use and/or distribution only by National Member Groups of fib.

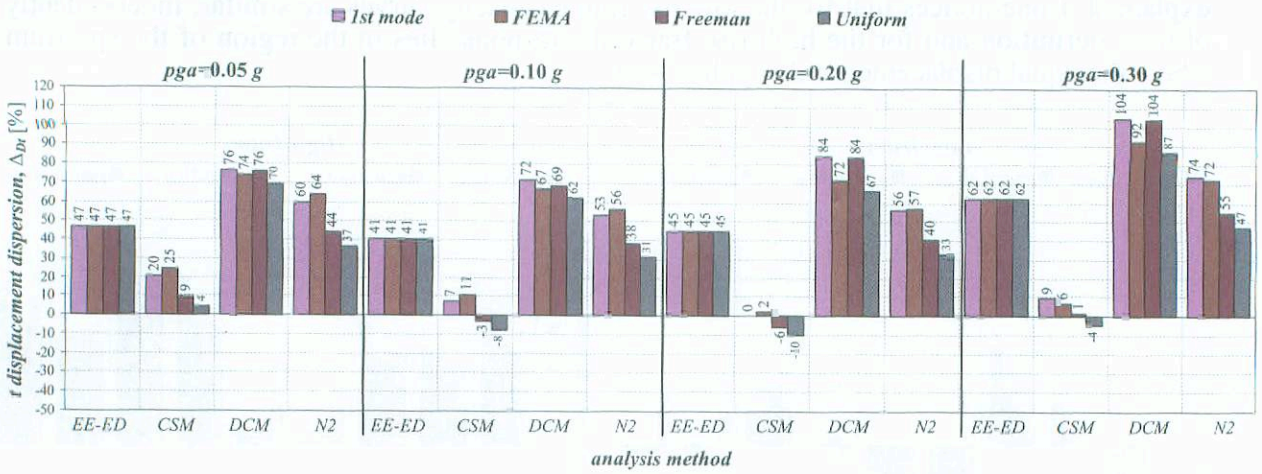

Fig. 7-27: Difference [%] of peak top displacement from different simplified methods and load profile for high frame relative to non linear dynamic analyses results.

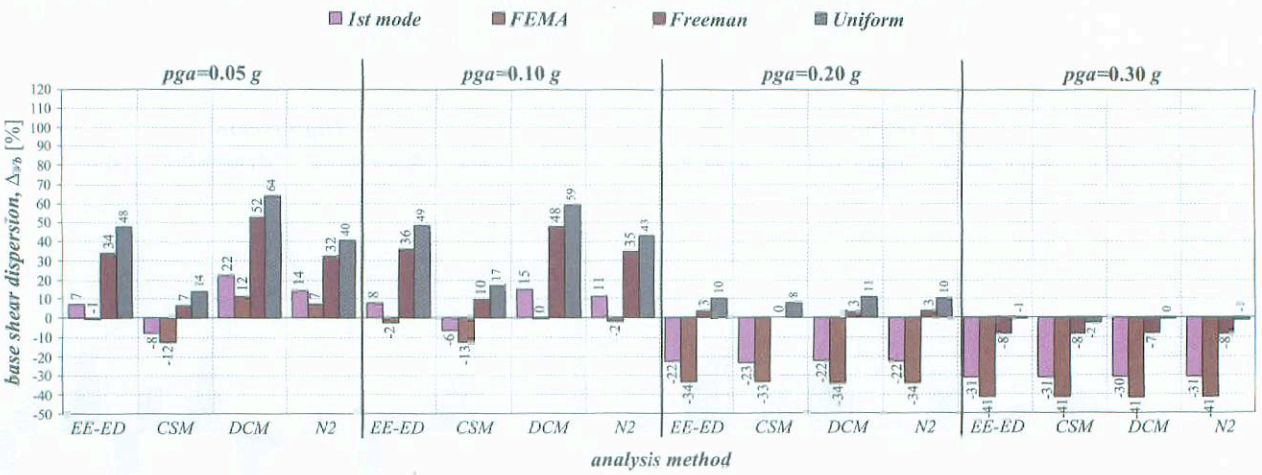

Fig. 7-28: Difference [%] of maximum base shear (V_b) from different simplified methods and load profile for high frame relative to non linear dynamic analyses results.

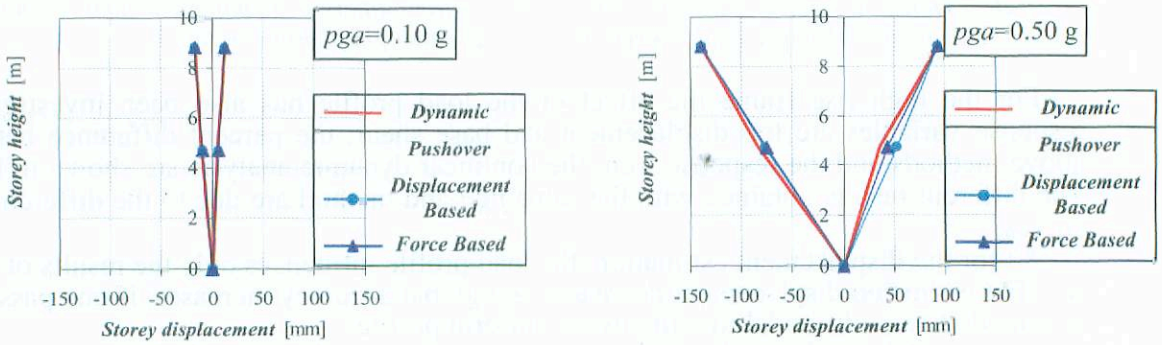

Fig. 7-29: Low frame: comparison between displacement profiles from dynamic analyses and pushover analyses with displacement- or force-control.

7.5.6 Local versus global response evaluation

For a given maximum top displacement, pushover analysis gives local responses, such as interstorey drifts, as well as element hinge end rotations.

Copyright fib, all rights reserved. This PDF copy of fib Bulletin 24 is intended for use and/or distribution only by National Member Groups of fib.

Results are compared for equal top displacement for the different methods of analyses considered. For conciseness, only the results for the minimum and maximum *pga* values are shown.

Fig. 7-29 and 7-30 show the trend of the displacement profiles. The results for different analyses are similar for the low rise frame, whereas they appear rather different for the high rise frame, the difference being more for the higher seismic intensity. For the high rise frame the mean dynamic profile is bounded by the ones from pushover analysis.

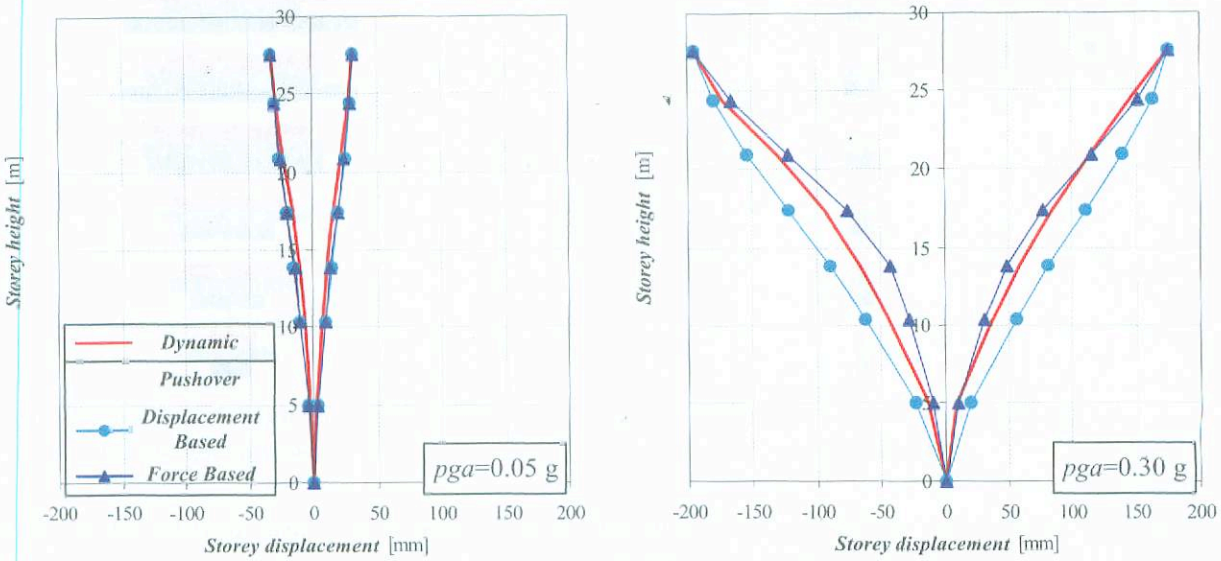

Fig. 7-30: High frame: comparison between displacement profiles from dynamic analyses and pushover analyses with displacement- or force-control.

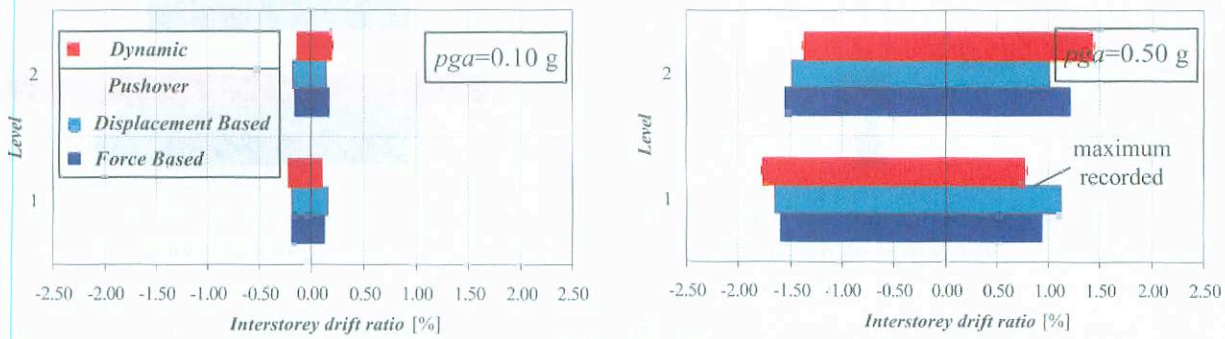

Fig. 7-31: Low frame: comparison between interstorey drift ratios from dynamic analyses and pushover analyses with displacement- or force-control.

Figs. 7-31, 7-32 compare the interstorey drift ratio from dynamic analysis at the time the maximum top displacement occurs, with those of pushover analysis with displacement- or force-control, for the high frame. Displacement-controlled pushover analyses underestimate the results at upper floors and overestimate them elsewhere. Force-controlled ones have the opposite result. If the peak interstorey drift ratios (thin bars in Fig. 7-31, 7-32) during dynamic response are considered, the maximum between the values from the force-controlled and the displacement-controlled analysis at each floor corresponds approximately to dynamic analysis values, with the exception of the top floor, where dynamic response is much higher than pushover estimates.

Fig. 7-33 to 7-35 show peak beam and column plastic hinge rotations, for the same top displacement. Unlike the cases before, these results, are not accurate either for the low frame or the high one, when the plastic excursions are significant. Differences are even higher if one

Copyright fib, all rights reserved. This PDF copy of fib Bulletin 24 is intended for use and/or distribution only by National Member Groups of fib.

considers the maxima obtained from dynamic analyses (thin bars in Fig. 7-33 to Fig. 7-35), mainly for the high rise frame. The check with component acceptability limits would lead to very different conclusions in terms of assessment.

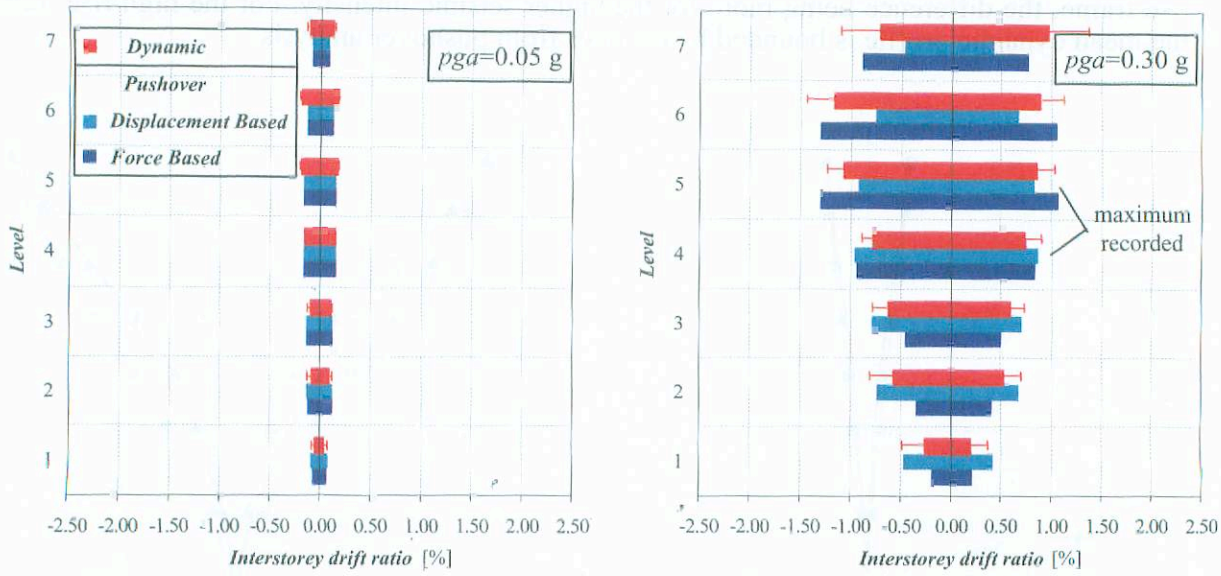

Fig. 7-32: High frame: comparison between interstorey drift ratios from dynamic analyses and pushover analyses with displacement- or force-control.

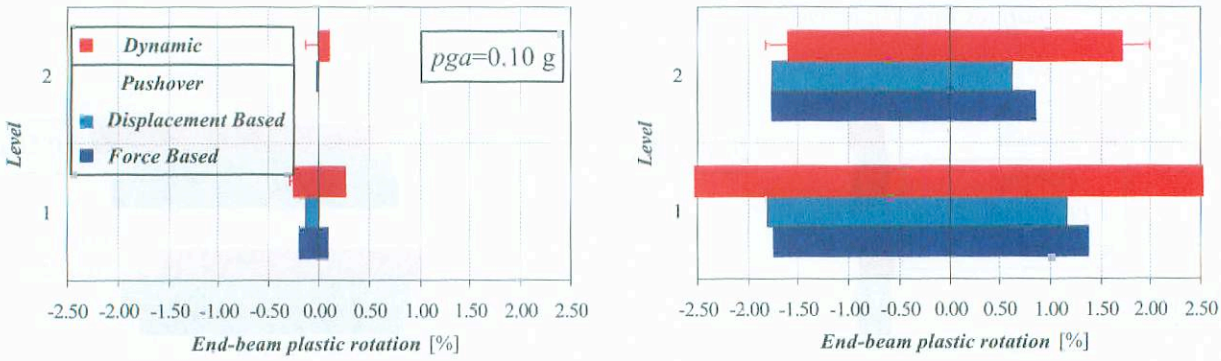

Fig. 7-33: Low frame: comparison between beam plastic hinge rotations from dynamic analyses and pushover analyses with displacement- or force-control.

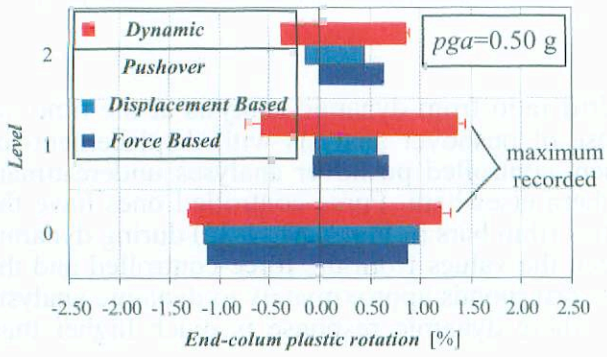

Fig. 7-34: Low frame: comparison between column plastic hinge rotations from dynamic analyses and pushover analyses, with displacement- or force-control.

Copyright fib, all rights reserved. This PDF copy of fib Bulletin 24 is intended for use and/or distribution only by National Member Groups of fib.

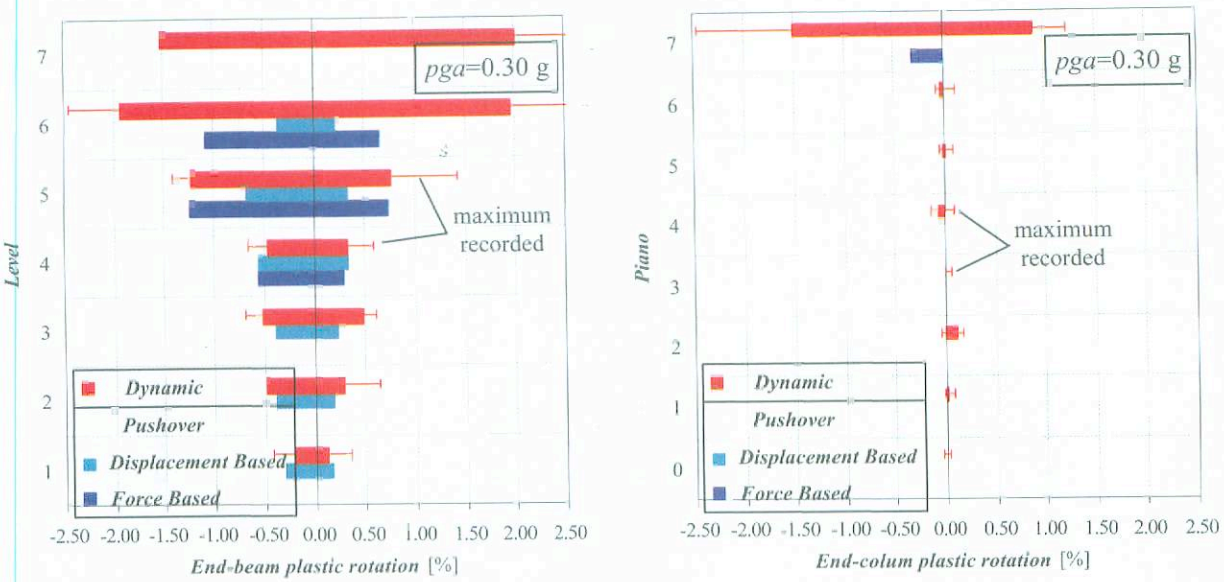

Fig. 7-35: High frame: comparison between beam and column plastic hinge rotations from dynamic analyses and pushover analyses with displacement- or force-control.

The distribution of plastic hinges is shown in Figs. 7-36 and 7-37). For the low frame, pushover analyses yield results consistent with those of the nonlinear dynamic. Notice that plastic hinges first form at beam ends and then spread to the column. For the high frame, the predictions are rather different with respect to the dynamic analyses. The latter show plastic hinges forming in almost all beams, starting from the higher level, and in some of the central columns. The soft storey mechanism forms at the sixth level. Pushover analyses underestimate the numbers of plastic hinges in both beams and columns.

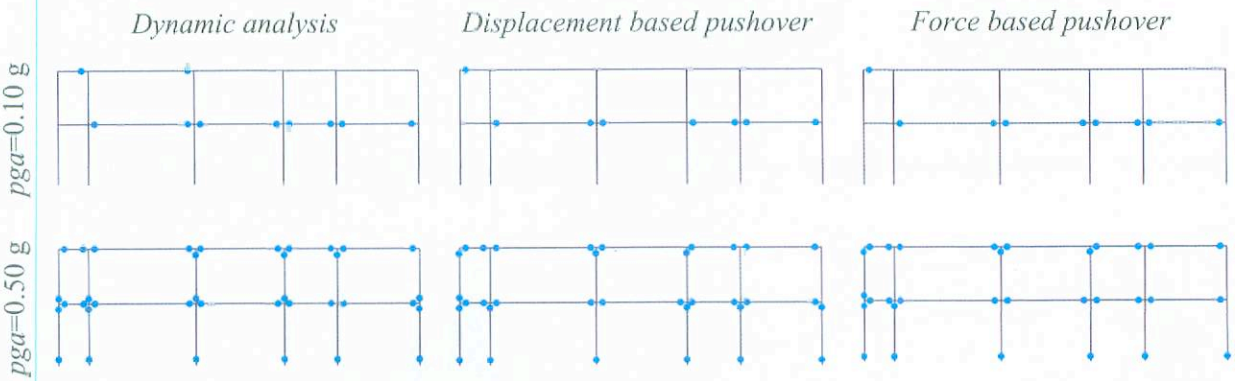

Fig. 7-36: Low frame: comparison between plastic hinge distributions from dynamic analyses and from nonlinear static methods with displacement and force-controlled pushover analyses.

Concrete and steel fibre demands in terms of ratios of strain, ε_c or ε_s, to compressive strain at concrete ultimate strength or steel at yielding, ε_{cc} or ε_{sy}, calculated via dynamic analyses (Fig. 7-39) are compared with those estimated via pushover analyses with displacement- (Fig. 7-40) or force- (Fig. 7-41) control. In each node concurrent elements are numbered in counterclockwise sequence, as shown in Fig. 7-42.

Copyright fib, all rights reserved. This PDF copy of fib Bulletin 24 is intended for use and/or distribution only by National Member Groups of fib.

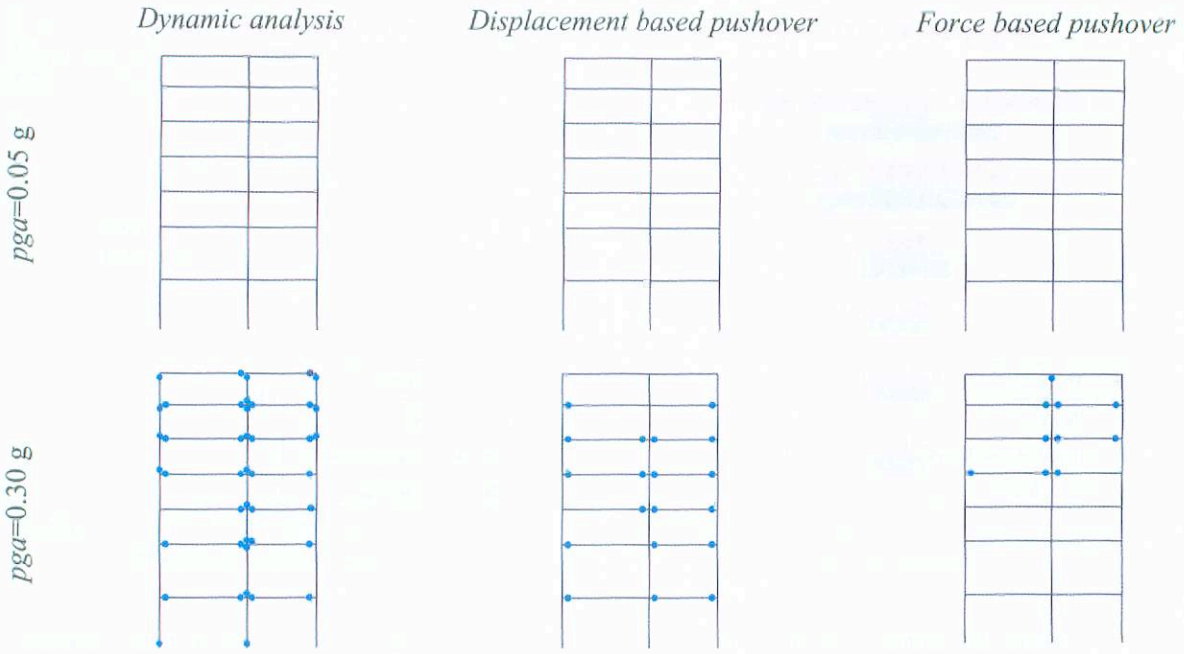

Fig. 7-37: High frame: comparison between plastic hinge distributions from dynamic analyses and from nonlinear static methods with displacement and force-controlled pushover analyses.

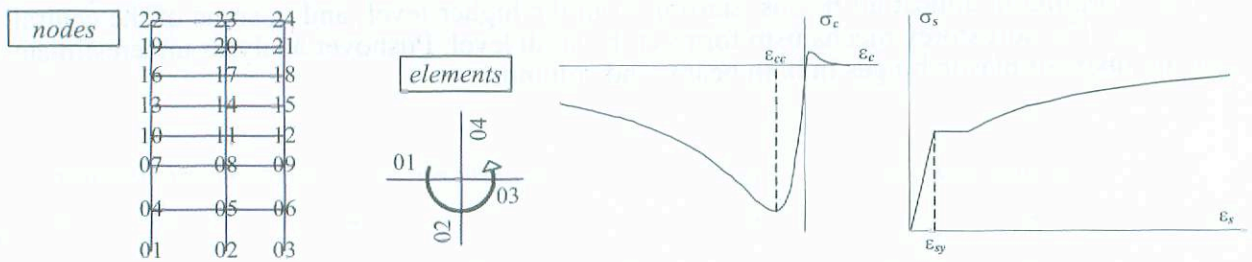

Fig. 7-38: Nodal and element identification numbers adopted to identify fibre strains in the high frame.

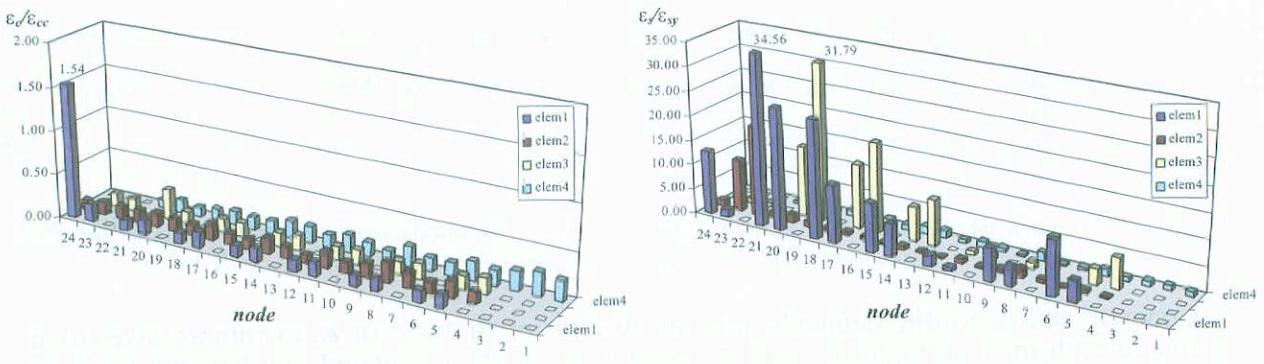

Fig. 7-39: High frame: concrete (left) and steel (right) strains from dynamic analyses.

Copyright fib, all rights reserved. This PDF copy of fib Bulletin 24 is intended for use and/or distribution only by National Member Groups of fib.

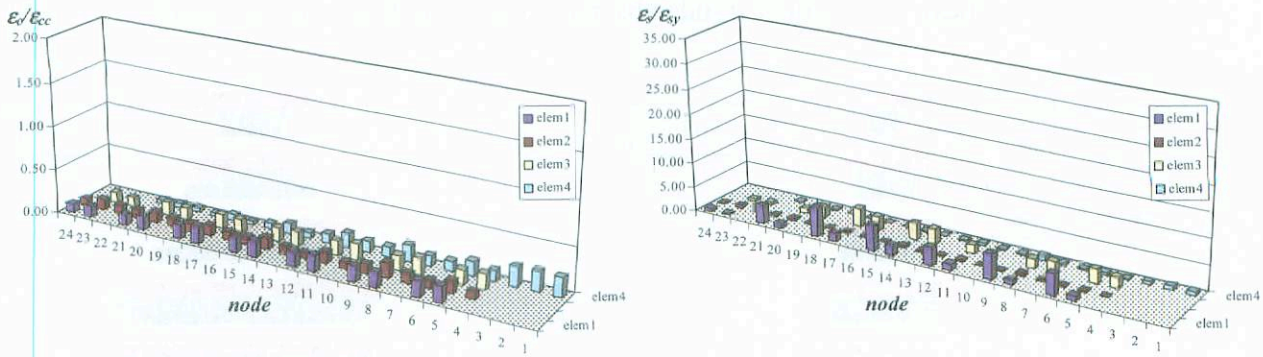

Fig. 7-40: High frame: concrete (left) and steel (right) strains obtained from pushover analyses with displacement-control.

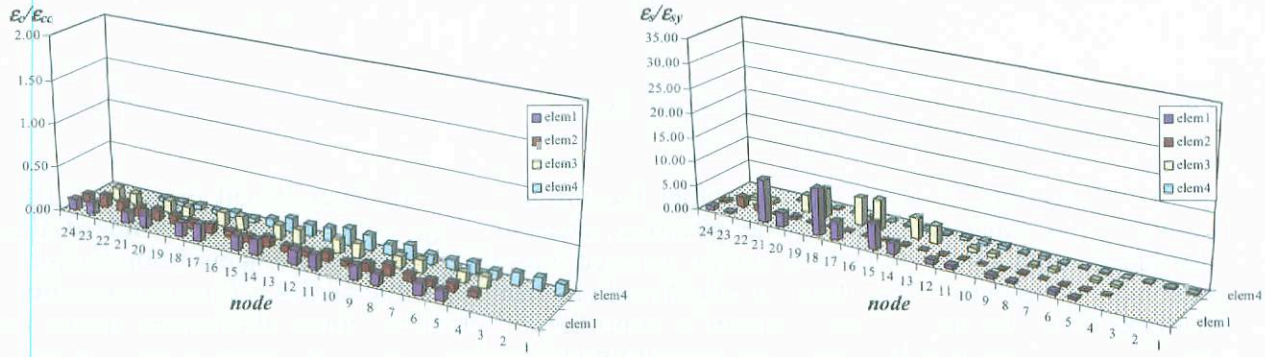

Fig. 7-41: High frame: concrete (left) and steel (right) strains obtained from pushover analyses with force-control.

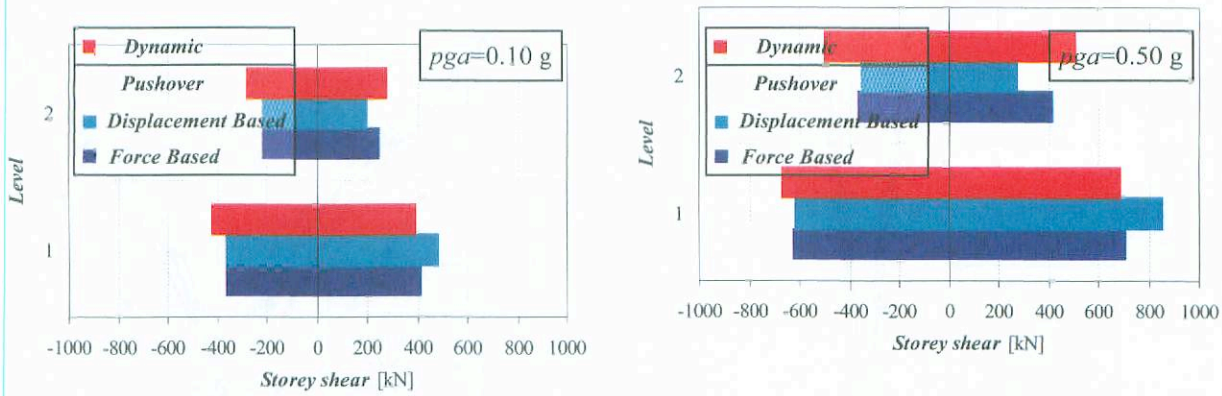

Fig. 7-42: Low frame: comparison between storey shears obtained from dynamic analyses and displacement and force based pushover analyses.

Storey shears are compared in Fig. 7-42 and Fig. 7-43 (dynamic storey shears are the peak values during the analyses).

In pushover analyses with imposed force profiles, ratios among seismic forces at each level are constant, in clear contrast with the real behaviour: in fact, once plastic behaviour is attained, the above ratios depend on seismic intensity. This is particularly important for the high frame and may therefore in this case yield false results. For the high frame the pattern of redistribution of the seismic forces at the different levels is noteworthy: the higher the seismic input, the weaker the relation between columns of the same vertical line. Beams in fact

Copyright fib, all rights reserved. This PDF copy of fib Bulletin 24 is intended for use and/or distribution only by National Member Groups of fib.

experience increasing plastic excursions and the structure gets stiffer at lower levels (with respect to higher ones), with similar trends observed in seismic forces at each level.

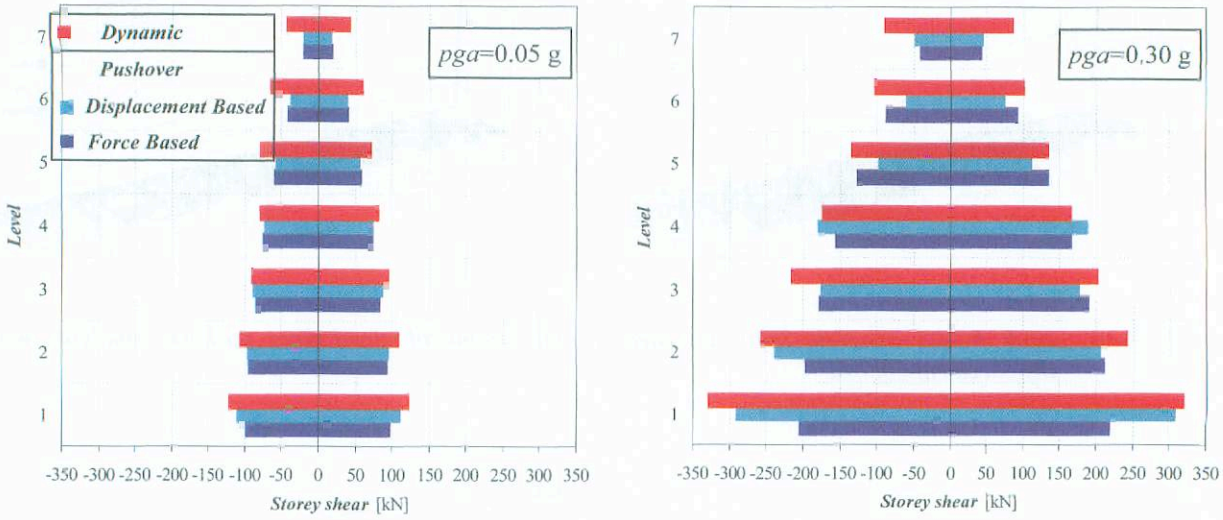

Fig. 7-43: High frame: comparison between storey shears from dynamic analyses and displacement- or force-controlled pushover analyses.

As in Section 7.5.5, we now consider the influence of the lateral load profile used to compute the capacity curve in the pushover analysis. Fig. 7-44 shows the trend of the displacement profile with varying *pga*, compared with the peak displacements from dynamic analyses. No load profile matches the deformations from dynamic analyses for every *pga* but, with possible exception of the uniform load profile, all profiles capture the correct shape. In the advanced plastic field (*pga*=0.30 *g*) multimodal pushover analyses (*Valles* and *Freeman 1978*) are the closest to dynamic analysis in this respect.

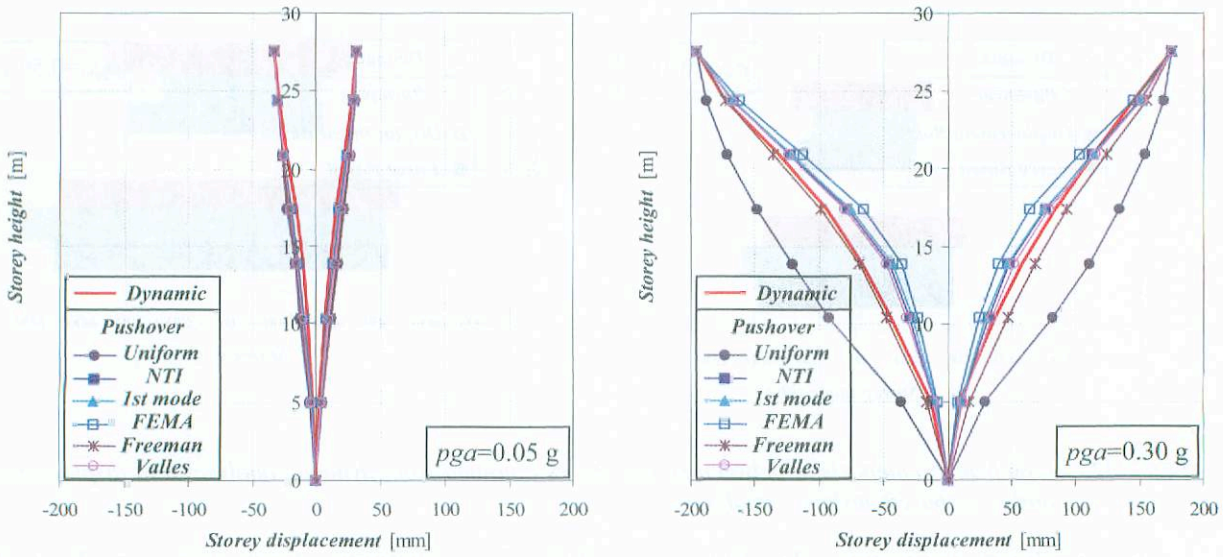

Fig. 7-44: High frame: comparison between displacement profiles from dynamic analyses and force controlled pushover analyses with different load profiles.

Interstorey drifts are compared in Fig. 7-45. The conclusions drawn for displacements apply.

Copyright fib, all rights reserved. This PDF copy of fib Bulletin 24 is intended for use and/or distribution only by National Member Groups of fib.

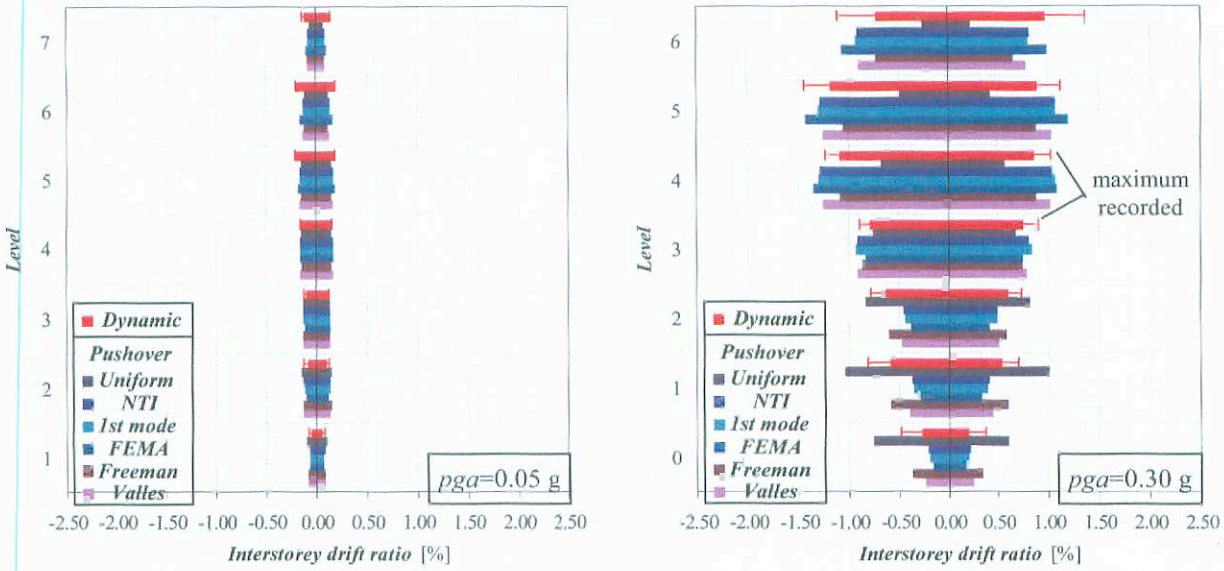

Fig. 7-45: High frame: comparison between interstorey drifts obtained from dynamic analyses and force-controlled pushover analyses with different load profiles.

Fig. 7-46 refers to peak plastic hinge rotations at beam and column ends. Results have the same trend as previously observed. The very high rotations observed at the upper storeys of the high frame cause local beam failure.

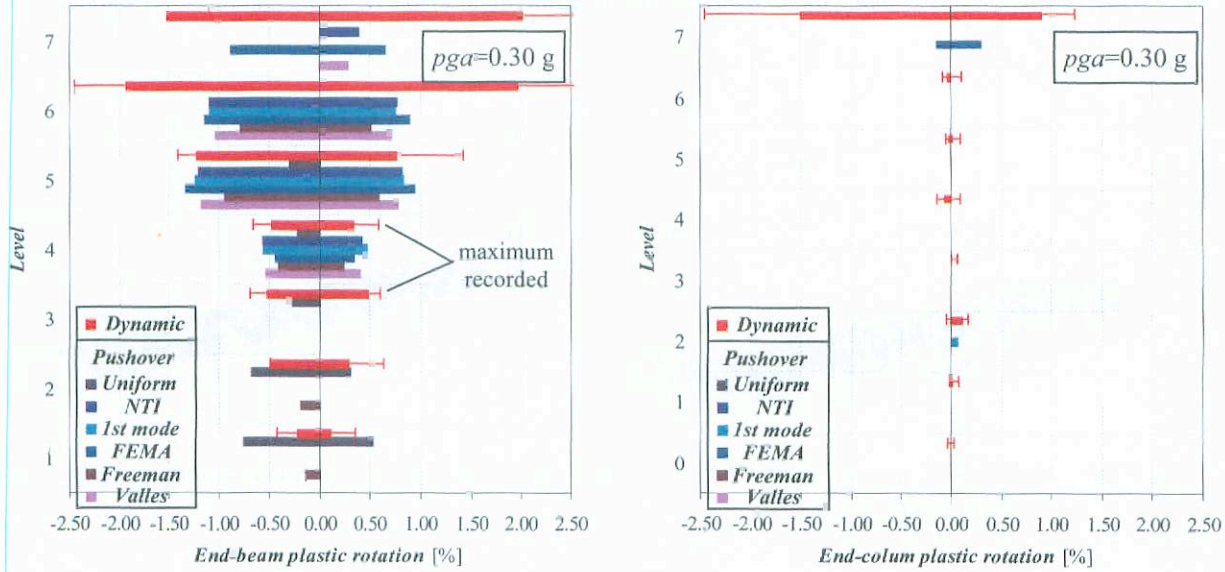

Fig. 7-46: High frame: (left) beam plastic rotations and (right) column plastic rotations from dynamic analyses and force-controlled pushover analyses with different load profiles.

The distributions of plastic hinges from pushover and dynamic analyses are shown in Fig. 7-47. Pushover analyses strongly underestimate the number of plastic hinges. A multimodal load profile does not improve accuracy.

Fig. 7-48 to Fig. 7-53 show concrete and steel fibre demands in terms of ratios between strain demand and concrete compressive strain at ultimate strength or steel strain at yielding, estimated via the different force-controlled pushover analyses. These results confirm the previous observations.

Copyright fib, all rights reserved. This PDF copy of fib Bulletin 24 is intended for use and/or distribution only by National Member Groups of fib.

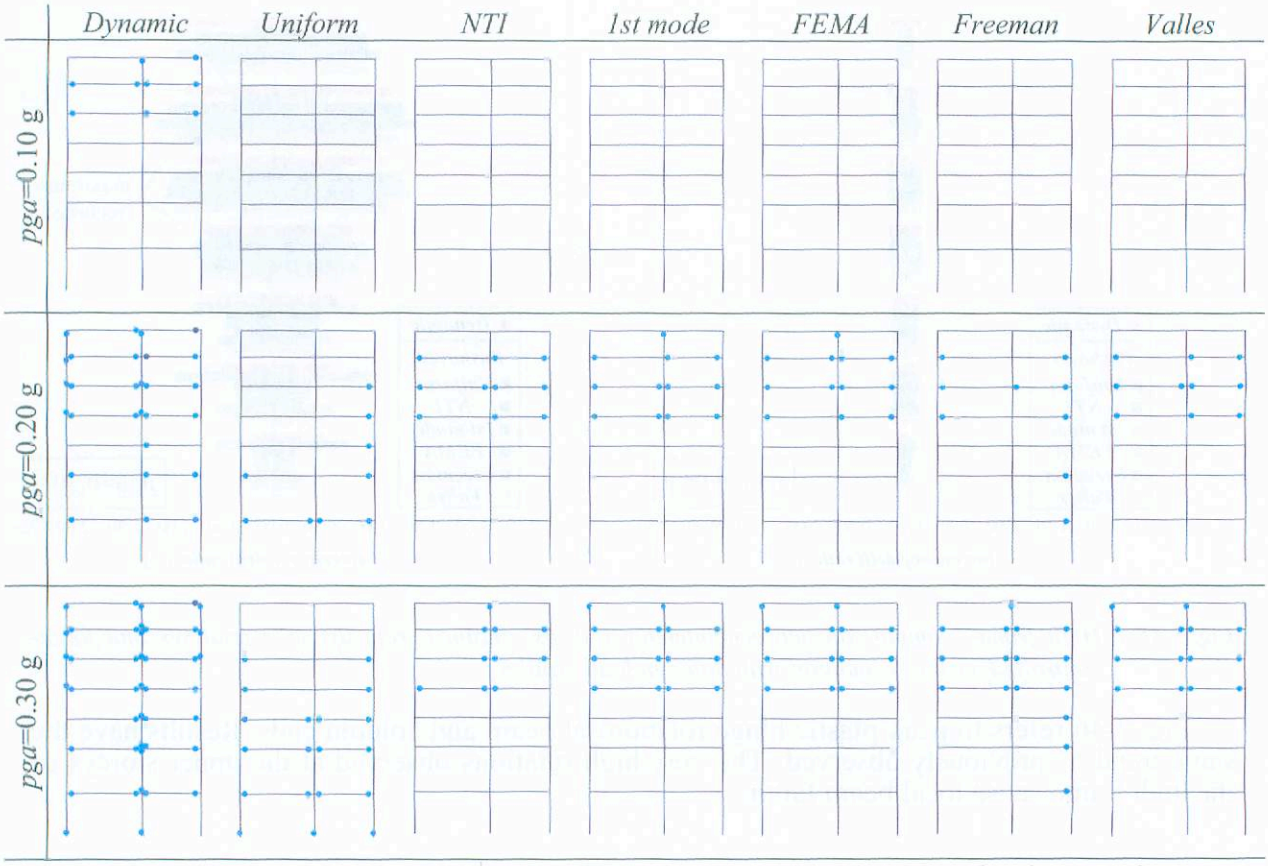

Fig. 7-47: High frame: comparison of distributions of plastic hinges from dynamic and pushover analysess.

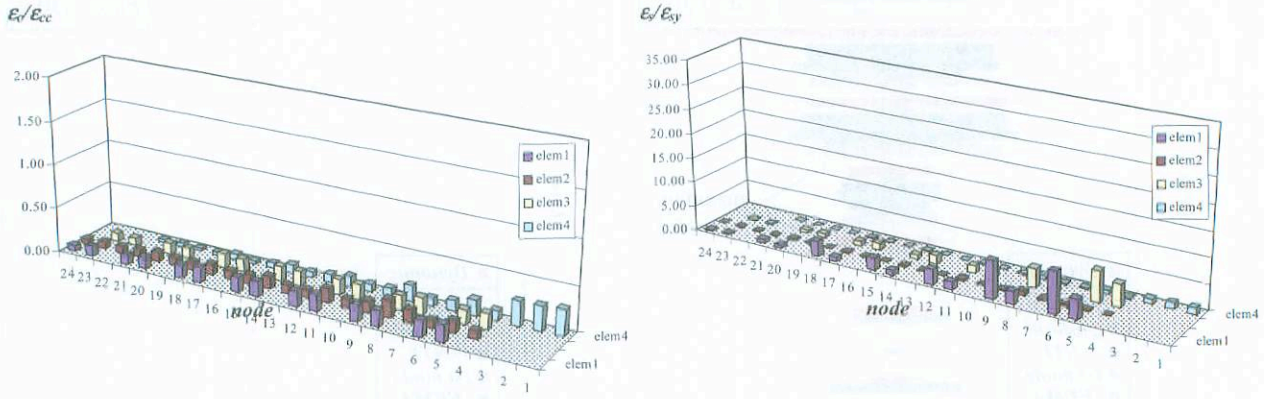

Fig. 7-48: High frame: concrete (left) and steel (right) strains from force-controlled pushover analysis with Uniform load profile.

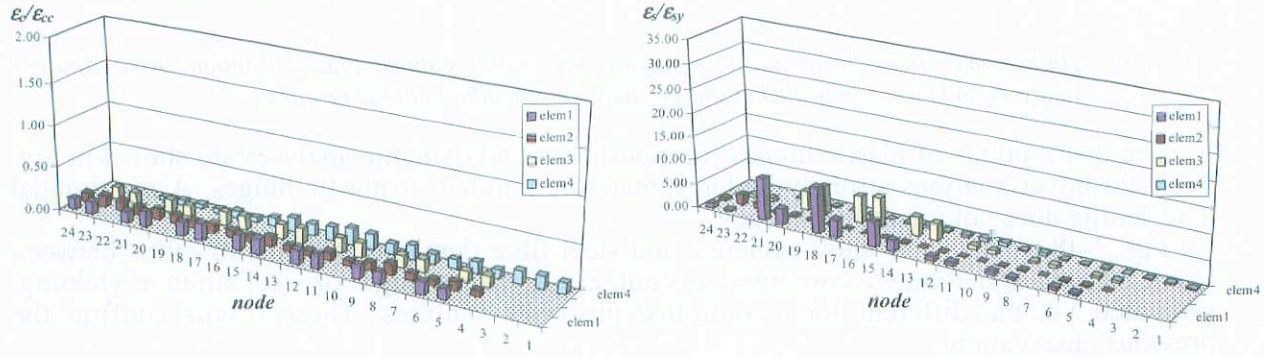

Fig. 7-49: High frame: concrete (left) and steel (right) strains from force-controlled pushover analysis with NTI load profile.

Copyright fib, all rights reserved. This PDF copy of fib Bulletin 24 is intended for use and/or distribution only by National Member Groups of fib.

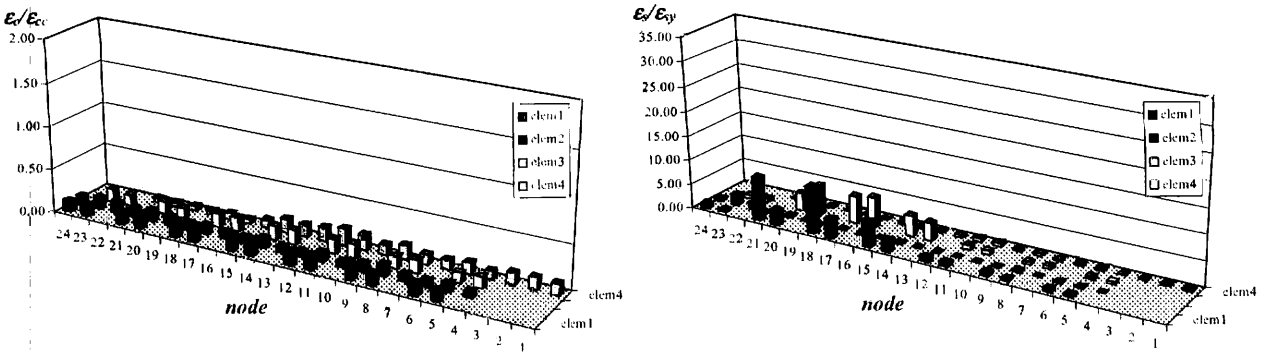

Fig. 7-50: High frame: concrete (left) and steel (ight) strains from force-controlled pushover analysis (1st mode load profile)

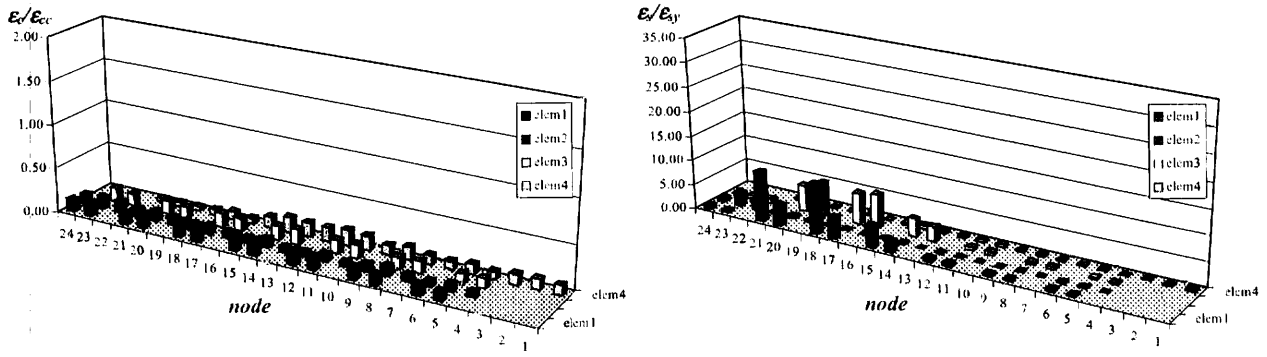

Fig. 7-51: High frame: concrete (left) and steel (right) strains from force-controlled pushover analysis (FEMA 273/356 load profile).

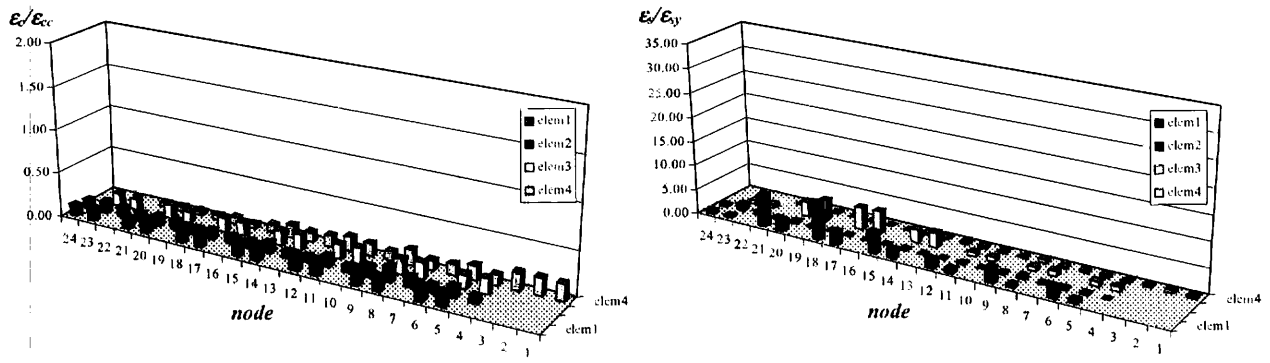

Fig. 7-52: High frame: concrete (left) and steel (right) strains from force-controlled pushover analysis (Freeman 1978 load profile).

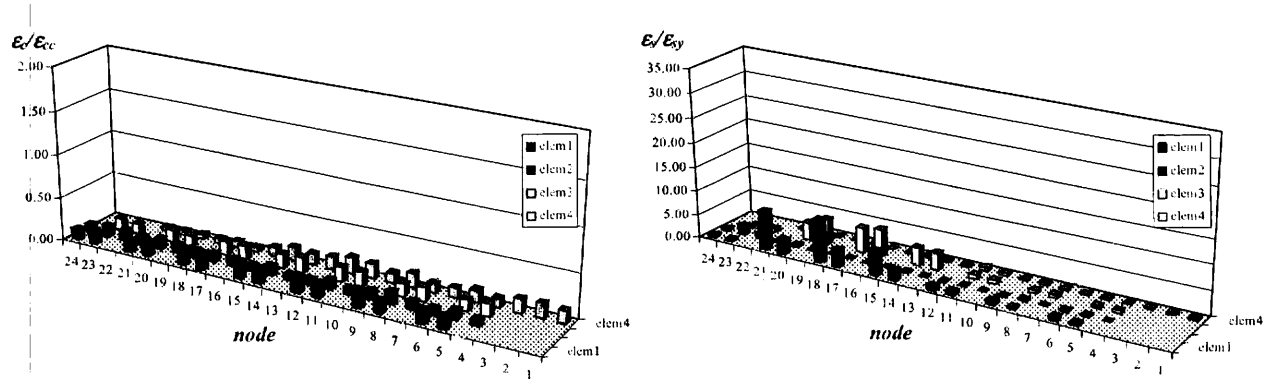

Fig. 7-53: High frame: concrete (left) and steel (right) strains from force-controlled pushover analysis (Valles load profile).

Copyright fib, all rights reserved. This PDF copy of fib Bulletin 24 is intended for use and/or distribution only by National Member Groups of fib.

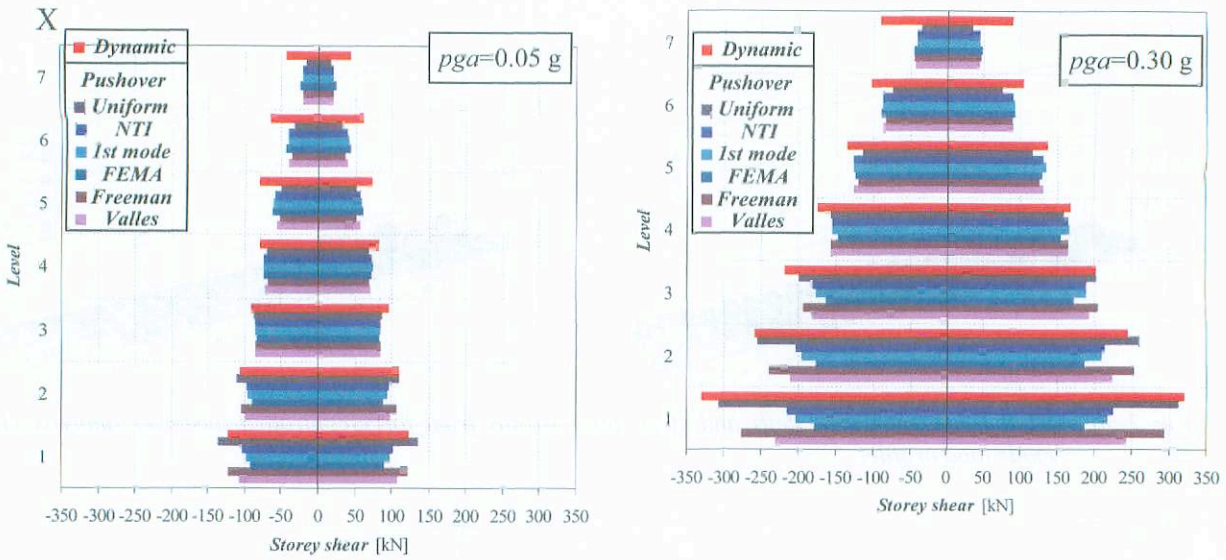

Fig. 7-54: High frame: comparison of storey shears from dynamic analyses and force-controlled pushover analyses with different load profiles.

Storey shears are also underestimated (Fig. 7-54) both at high and low inelasticity and pga levels; the uniform and multimodal profiles give the best approximations to the peak floor shears.

7.5.7 Structural response with natural accelerograms

For the high rise frame, local response evaluations are compared with dynamic analyses for the natural accelerogram of Loma Prieta at Hollister station (*pga*=0.17 g). Results shown in the following figures confirm the observations drawn from the analyses with artificial accelerograms (section 7.5.6).

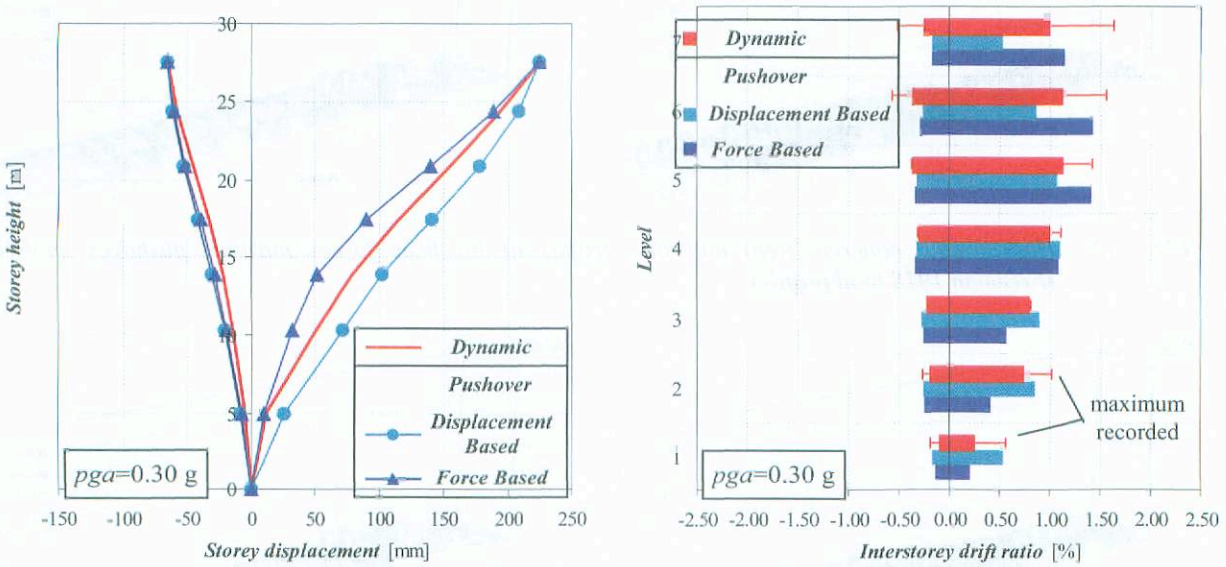

Fig. 7-55: High frame: comparison of displacement profiles and interstorey drift ratios from dynamic analyses and displacement- or force-controlled pushover analyses.

Copyright fib, all rights reserved. This PDF copy of fib Bulletin 24 is intended for use and/or distribution only by National Member Groups of fib.

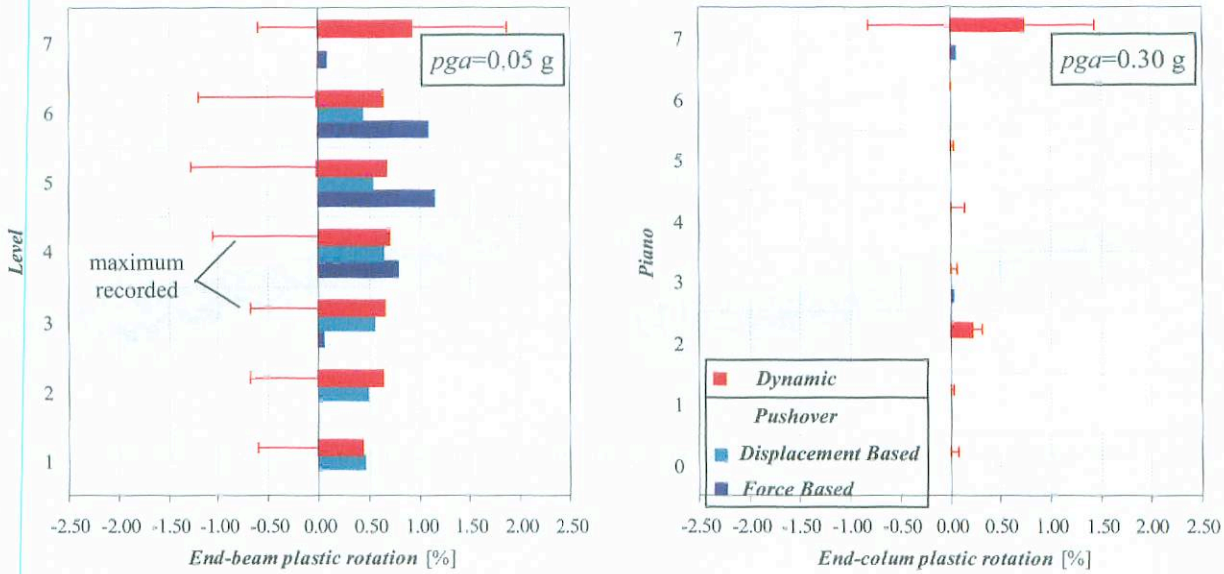

Fig. 7-56: High frame: (left) beam plastic rotations and (right) column plastic rotations from dynamic analyses and from displacement- or force-controlled pushover analyses.

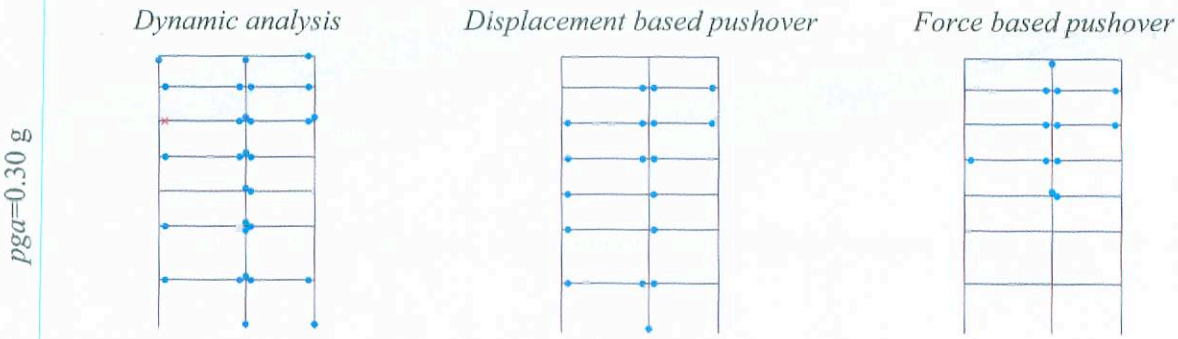

Fig. 7-57: High frame: comparison of plastic hinge distributions from dynamic analyses and displacement- or force-controlled pushover analyses.

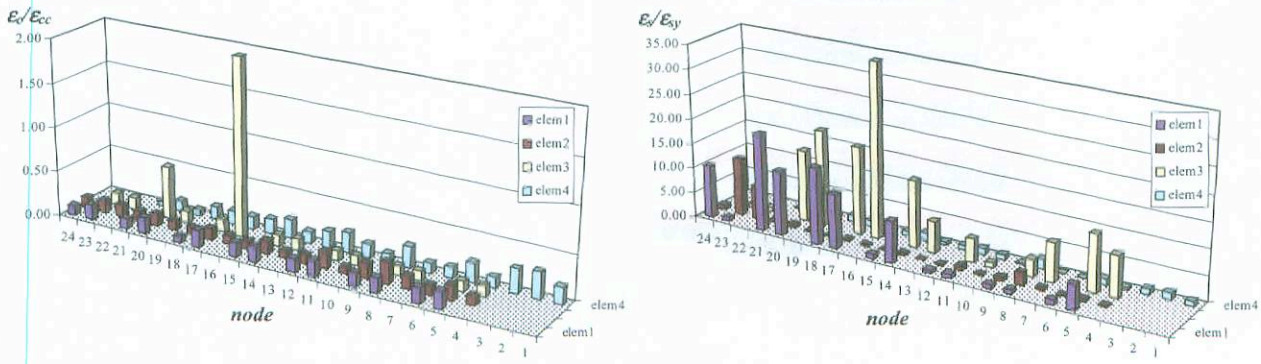

Fig. 7-58: High frame: concrete (left) and steel (right) strains from dynamic analyses.

Copyright fib, all rights reserved. This PDF copy of fib Bulletin 24 is intended for use and/or distribution only by National Member Groups of fib.

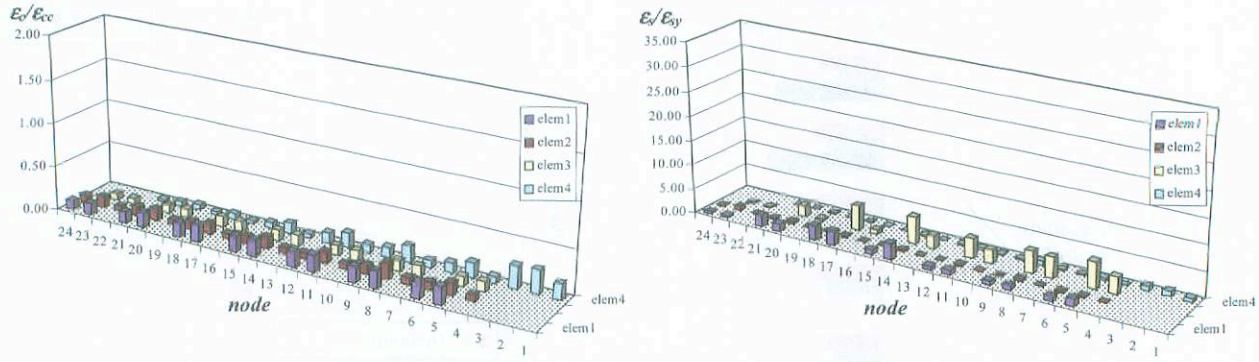

Fig. 7-59: High frame: concrete (left) and steel (right) strains obtained from displacement-controlled pushover analyses.

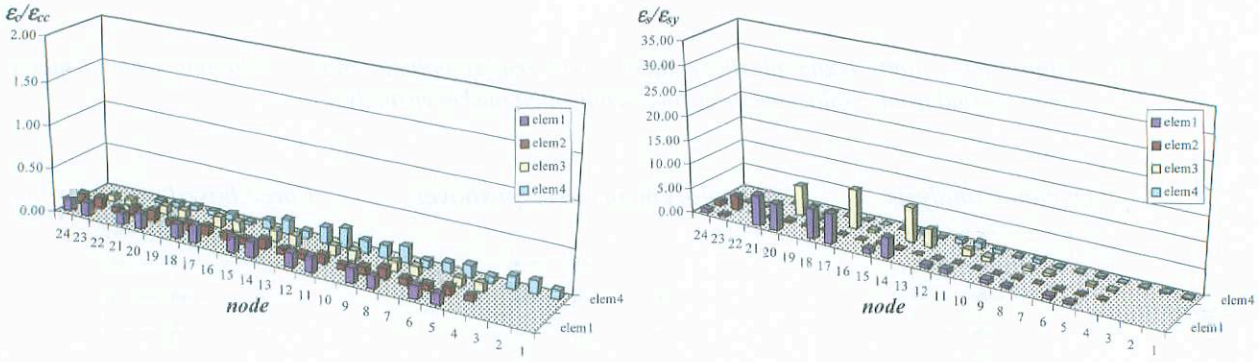

Fig. 7-60: High frame: concrete (left) and steel (right) strains obtained from force-controlled pushover analyses.

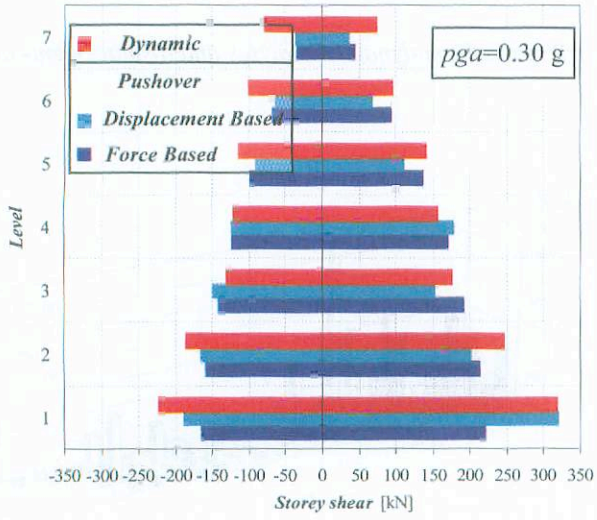

Fig. 7-61: High frame: comparison of storey shears from dynamic analyses and displacement- or force-controlled pushover analyses.

Copyright fib, all rights reserved. This PDF copy of fib Bulletin 24 is intended for use and/or distribution only by National Member Groups of fib.

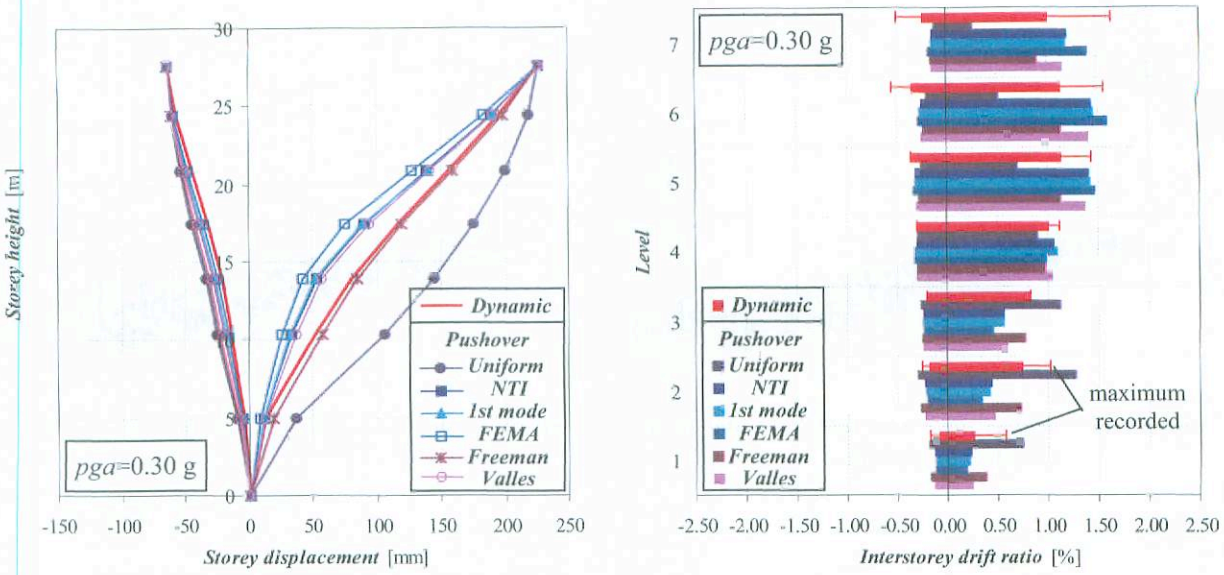

Fig. 7-62: High frame: comparison of (left) displacement profiles and (right) interstorey drift ratios from dynamic analyses and from force-controlled pushover analyses with different load profiles.

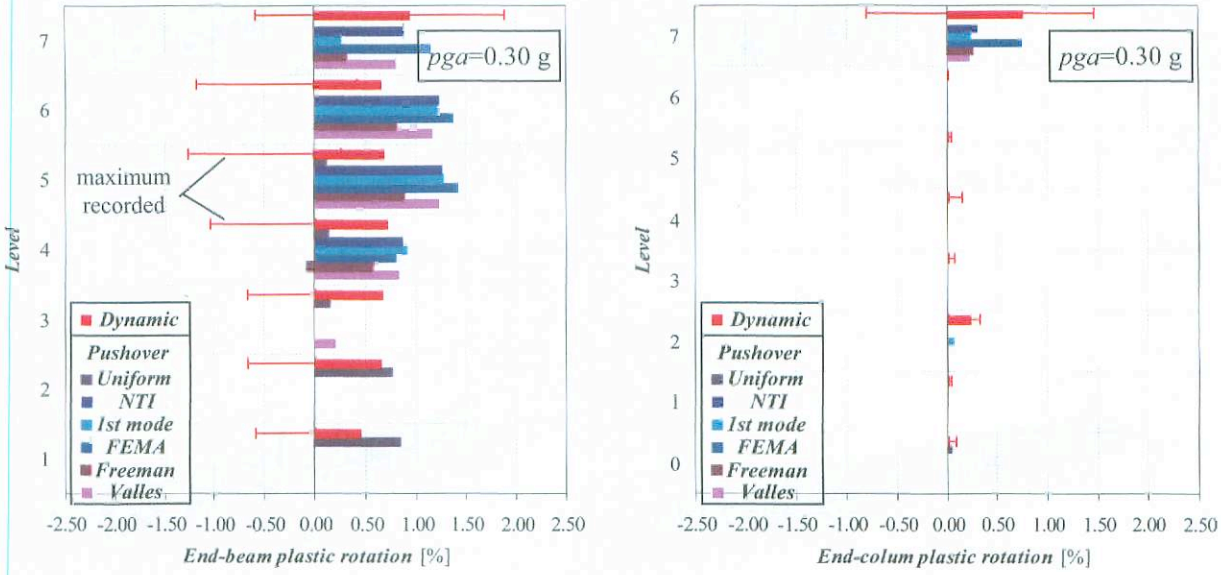

Fig. 7-63: High frame: comparison of (left) beam plastic rotation and (right) column plastic rotations from dynamic analyses and from force-controlled pushover analyses with different load profiles.

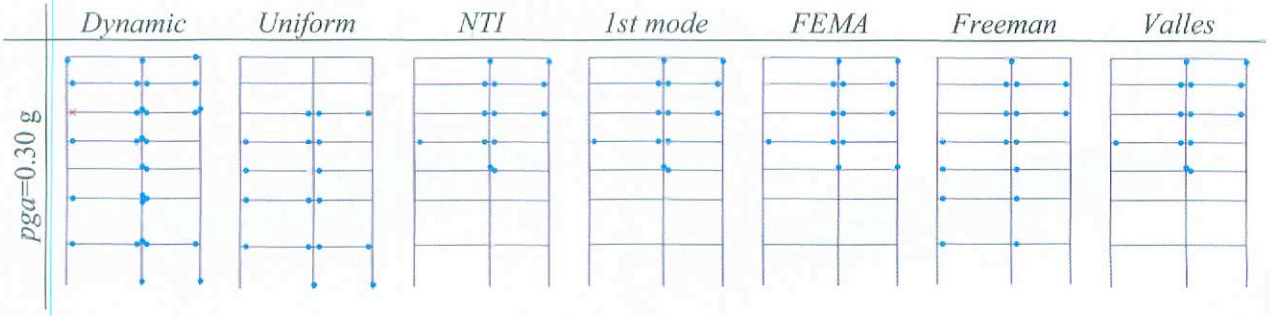

Fig. 7-64: High frame: comparison of distributions of plastic hinges from dynamic analyses and from force-controlled pushover analyses with different load profiles.

Copyright fib, all rights reserved. This PDF copy of fib Bulletin 24 is intended for use and/or distribution only by National Member Groups of fib.

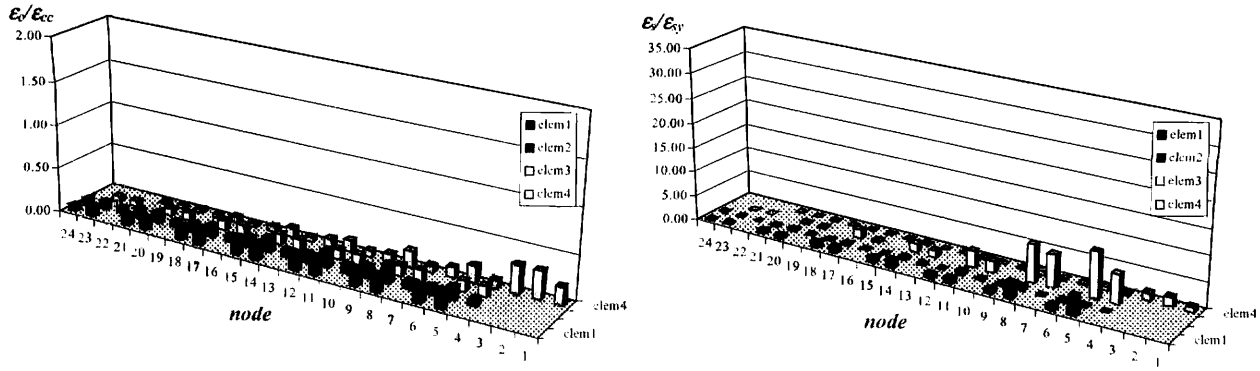

Fig. 7-65: High frame: concrete (left) and steel (right) strains from force-controlled pushover analysis with Uniform load profile.

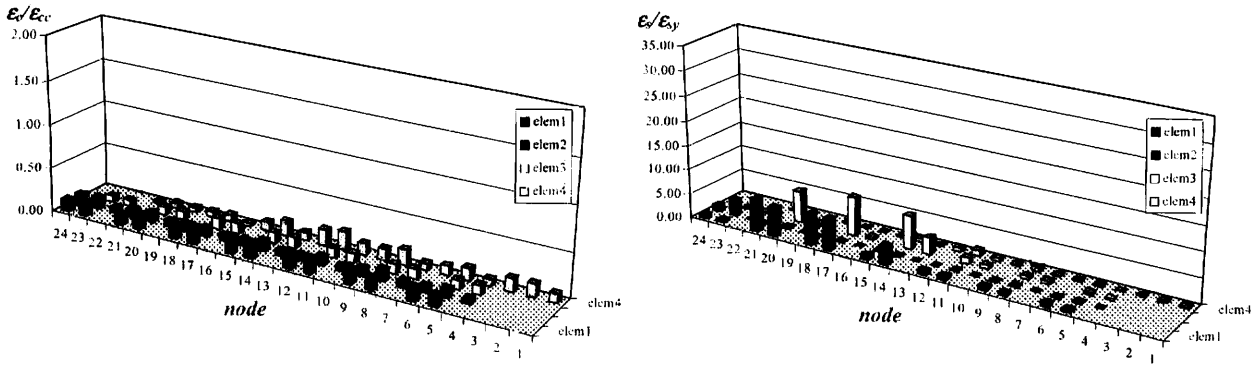

Fig. 7-66: High frame: concrete (left) and steel (right) strains from force-controlled pushover analysis with NTI load profile.

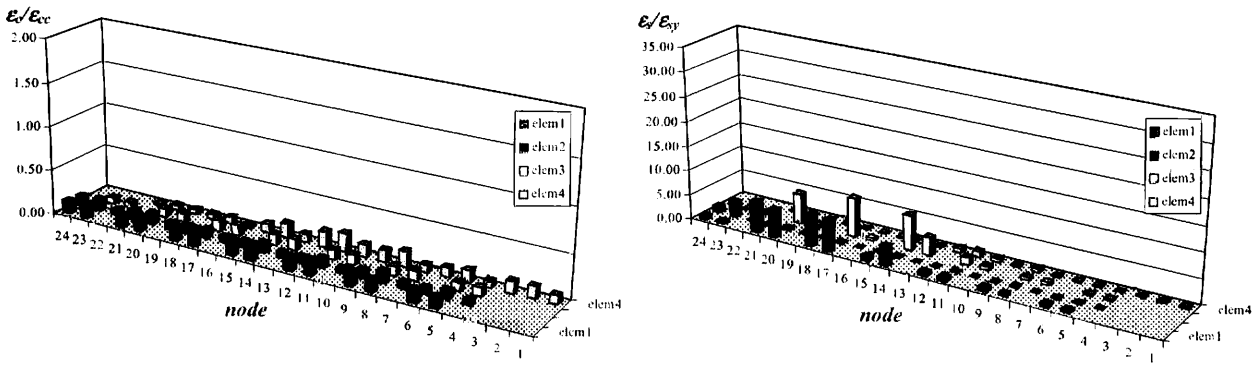

Fig. 7-67: High frame: concrete (left) and steel (right) strains obtained from force-controlled pushover analysis with 1st mode load profile.

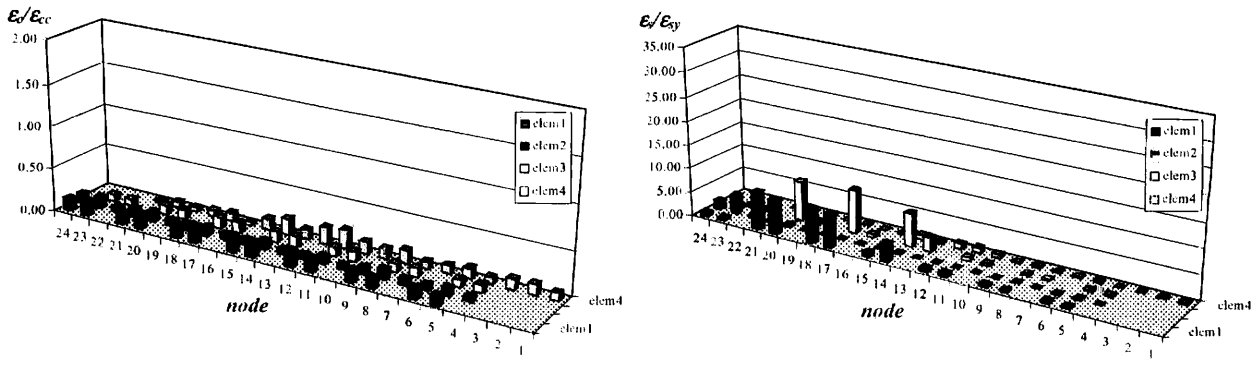

Fig. 7-68: High frame: concrete (left) and steel (right) strains from force-controlled pushover analysis with FEMA 273/356 load profile.

Copyright fib, all rights reserved. This PDF copy of fib Bulletin 24 is intended for use and/or distribution only by National Member Groups of fib.

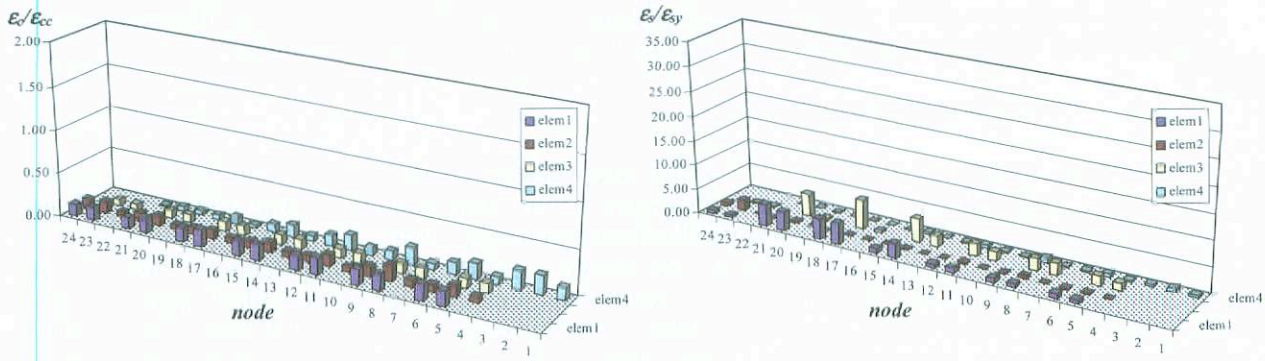

Fig. 7-69: High frame: concrete (left) and steel (right) strains from force-controlled pushover analysis with Freeman (1978) load profile.

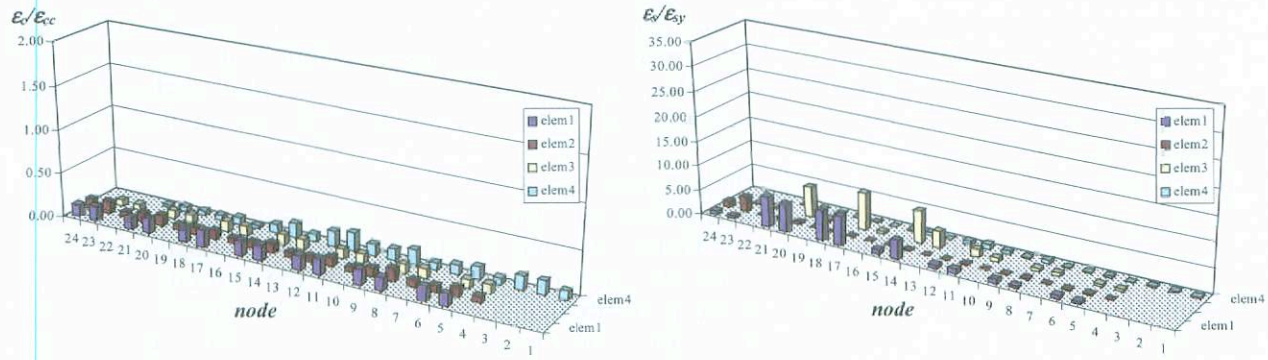

Fig. 7-70: High frame: concrete (left) and steel (right) strains from force-controlled pushover analysis with Valles load profile.

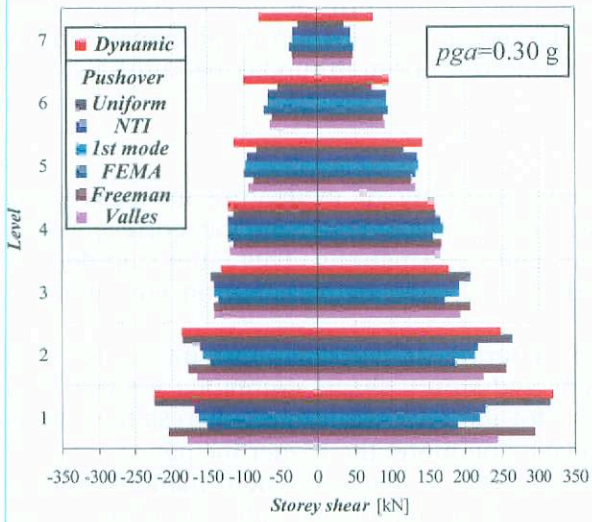

Fig. 7-71: High frame: comparison of storey shears from dynamic analyses and force-controlled pushover analyses with different load profiles.

7.5.8 Conclusions

Global and local responses of two planar RC real frames, a low and a high rise one, were determined via a nonlinear static procedure based on different types of pushover analysis and compared to the results of nonlinear dynamic response analyses. The model of the structure is the same for static and dynamic analysis: fibre finite elements.

Both structures have been analyzed with displacement- and force-controlled pushover techniques, also considering different load profiles.

Copyright fib, all rights reserved. This PDF copy of fib Bulletin 24 is intended for use and/or distribution only by National Member Groups of fib.

Pushover analysis of the low rise frame gives accurate results with respect to peak dynamic responses, both in the elastic and plastic range; for the high rise frame pushover analyses become less accurate with increasing excursion in the plastic range.

7.5.8.1 Global response evaluation

The capacity curves of the low rise frame are weakly sensitive to the load profile. Capacity curves for the high rise frame show instead a strong dependence on the adopted pushover technique (force- or displacement-controlled) and on load profile.

For the low rise frame all methods are rather accurate. The most accurate ones are the FEMA 273/356 method (mean dispersion, with displacement/force-controlled pushover equal to 3.5%/26.7% in top displacement and 24.5%/10.7% in base shear) and *N2* (10%/8.5% in top displacement and 26.7%/7.2% in base shear). For the high rise frame the methods overestimate the real top displacement. Only the composite spectrum method shows a reasonable agreement (8.2%/9% in top displacement and 5.7%/17% in base shear) while the FEMA 273/356 method and *N2* are even less precise than the traditional equal-energy/equal-displacement approaches. Nonlinear static methods with unimodal pushover do not take into account higher modes and, for the high rise frame, lead to underestimation of base shear with increasing inelastic excursion. In particular, the composite spectrum method underestimates the displacement, while it overestimates the base shear in the low frame; for the high frame it has the opposite effects.

Load profile influences mostly the capacity spectrum method and *N2*: in fact, in these methods the capacity curve has a significant influence on the estimation of the equivalent viscous damping and of the behaviour factor (defined as the ratio between elastic and yield strength). For the high frame, since the effective period, T_{eff}, lies in the velocity-controlled region of the spectrum, estimation of the performance point via the FEMA 273/356 approach depends only on T_{eff}, which slightly varies for the different capacity curves considered. Multimodal (*Freeman*) and *Uniform* profiles seem the most accurate both in the elastic and nonlinear ranges, in particular if applied with the capacity spectrum method (top displacement dispersion is less then 10%).

When using the capacity spectrum method, the nonlinear dynamic response is bounded between the unimodal (*1st mode* or *FEMA*) results and the uniform or multimodal (*Freeman*) ones. In particular unimodal profile results are the upper limit for top displacement and the lower limit for base shear. The opposite applies for uniform or multimodal load profiles.

7.5.8.2 Local response evaluation

Accuracy of static methods depends on their capability of evaluating the peak global responses and, given these (in particular peak top displacement), on the correspondance between top response and local quantities: forces and deformations. This latter step does not depend on the method (composite spectrum, FEMA 273/356 or N2), but on how pushover analysis is carried out.

Static and dynamic results were compared in terms of deformations, interstorey drift, plastic hinge rotations, plastic hinge distributions and storey shears computed with different pushover analysis approaches. Results are similar for the low rise frame, whereas they appear rather different for the high rise one, the difference being more, the higher the pga is.

For the high rise frame, no lateral load profile is able to match the deformations from the nonlinear dynamic analysis for all seismic intensities. Especially inaccurate, for what concerns the load profile, is uniform load, which systematically overestimates the displacement distribution along the height; the other load profiles give at least qualitatively correct distributions. In the advanced inelastic range multimodal profile pushover analyses (*Valles* and *Freeman*) are the most accurate ones.

Maxima of beam and column plastic rotations are instead not accurate when the plastic excursions are significant, independently of the applied load profile: differences can be even 100%.

Pushover analyses underestimate the number of plastic hinges both in beams and in columns and are not able to capture the soft storey mechanism which forms at the sixth level. Multimodal load profiles do not improve results in this respect.

Storey shears are also underestimated both at upper and lower floors. For the low frame

Copyright fib, all rights reserved. This PDF copy of fib Bulletin 24 is intended for use and/or distribution only by National Member Groups of fib.

the underestimation in less then 30%. For the high frame, the underestimation is about 10% and 30-40% at the base with unimodal displacement and force-controlled pushover analyses, respectively, about 50% at the top floor and less then 20% at the other levels with both methods. The uniform and multimodal lateral load profiles give the best approximations: in particular, with the *Freeman* (1978) profile the difference is even less then 18% over the whole height, with the exception of the top floor.

7.6 Case study 4: Assessment of RC building typical of old Greek design

7.6.1 Introduction

The focus in this case-study is on a four-storey RC building designed to the old Greek codes (1954 Concrete Code, 1959 Seismic Code) applicable until 1984. The building has a dual lateral load resisting system consisting of frames and shear walls and a regular configuration. It was designed for a base shear equal to 6% of its service load, without any particular provisions for ductility. It is analysed and assessed herein using alternative procedures of varying complexity, namely

- The FEMA 273 (1997) and FEMA 356-ASCE (2000) static procedures (linear and nonlinear)
- Displacement-based assessment, as suggested by the NZ draft guidelines and by Priestley (1997)
- Nonlinear dynamic analysis for a large number of input accelerograms

In addition to applying the aforementioned alternative procedures, the FEMA-ASCE methodology was applied using different modelling assumptions for the R/C members, i.e. a lumped plasticity approach (SAP 2000) and a distributed plasticity approach (IDARC-5), as well as different procedures for calculating the available strength and ductility capacities of the members.

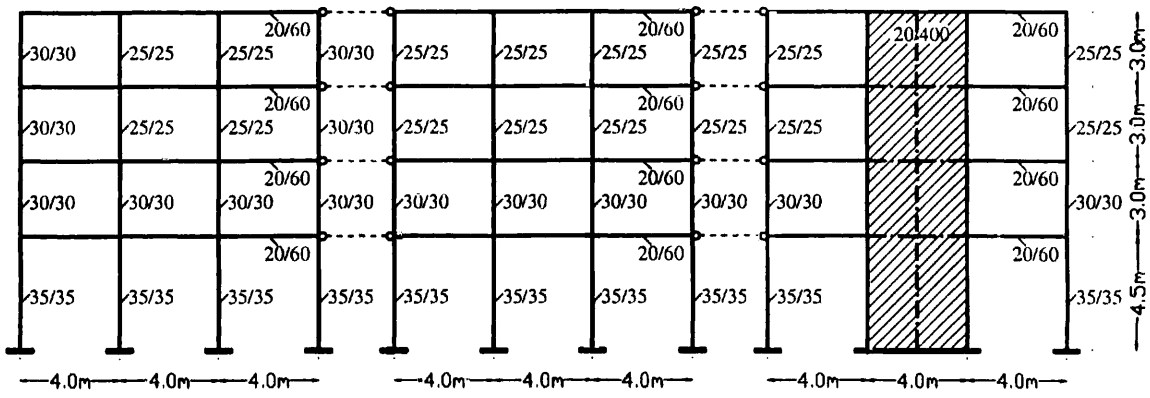

Fig. 7-72: Geometry of the assessed structure (cross-sectional dimensions in (cm))

7.6.2 Description of the assessed building

Due to its regular configuration the building was modelled in all cases as a plane structure, i.e. a series of frames and dual systems, as shown in Figure 7-72.

The building is situated in zone II of the current (2000) Greek Seismic Code, which is characterised by a Eurocode 8 type spectrum for soil B, with a PGA equal to 0.16g. According to the old (1959) Code, the base shear for this zone and soil was equal to 6% its *total* service load (G+Q), rather than the reduced load (G+0.3Q) that is used to specify seismic loading according to the modern code. In order to establish a common basis for the alternative assessment procedures applied in the following, the Eurocode 8 seismic load combination involving the reduced live load ($G+\psi_2 Q \pm E$) was used. The same live load is also included in the seismic mass calculation.

The materials used were B225 concrete, for which a mean cube strength of 22.5 MPa was

Copyright fib, all rights reserved. This PDF copy of fib Bulletin 24 is intended for use and/or distribution only by National Member Groups of fib.

specified, hence a mean cylinder strength of about 18.4 MPa and a characteristic cylinder strength of 10 to 11 MPa. The longitudinal steel reinforcement consisted of StIII deformed bars, with a specified strength of 420 MPa (f_{yk}=420MPa) while ties were made of StI smooth bars with a specified strength of 220 MPa. The assessment was based on the assumption that the above values were appropriate for the structure, i.e. the case of sub-standard materials was not addressed.

The design to the old codes was carried out using the working stress method, with a 30% increase of allowable stresses when the seismic load combination (G+Q±E) is considered. Had the building been designed to the current code provisions, the base shear would have been equal to 11.4% of its reduced service load (G+0.3Q), to be compared with about 1.5 times the value according to the old code (i.e. 9%) when proper adjustment for ULS vs. working stress design and the different service load is made. This means that the building is not particularly deficient in terms of strength according to the current standard (base shear 21% lower than the required one). It is noted, though, that no provision for simultaneous application of the two horizontal components was made in the old code, nor of accidental eccentricity effects; hence the final strength level of members is not fully captured by the base shear comparison, particularly so for columns and walls, for which capacity design procedures are applied according to the current code.

The analysis of the building for the seismic combination was carried out using a standard plane frame model; this is quite common practice in Greece since the early 80's, but before then hand calculations were commonly used, based on distributing the storey shear to the vertical elements according to their relative rigidities, considering them (including walls) fixed against rotation at floor levels. However, the design of the wall in the building studied (see Fig. 7-72) was governed by minimum provisions for flexure with axial loading, hence weaknesses in previously prevailing analysis would not have affected it.

Ductility provisions, such as the use of closely spaced hoops and ties with 135° hooks in plastic hinge regions were not included in the old codes; anchorage and splicing did not conform to current practice either. Ties in both critical and non-critical regions of beams generally consisted of 8 mm smooth bars (f_{yk}=220 MPa) with 90° hooks, at a spacing of 200 mm. Column ties were either 8 or 6 mm smooth bars at a spacing of 200 mm; this satisfied the old code provisions. Confined boundary elements were not provided at wall edges.

7.6.3 Assessment using the ASCE (2000) - FEMA 273/356 procedures

7.6.3.1 Introduction

Given the relatively small height of the building and its regular configuration, it is appropriate to use the static methods adopted in FEMA 273/274 (1997a, b) and FEMA 356-ASCE (2000), i.e. the linear static and the nonlinear static (pushover) analyses. An additional condition for the elastic method to be applicable, namely that the demand/capacity ratios, DCR, (ratios of force demand from the seismic load combination to the expected strength of the member) do not exceed 2.0 in any member, is violated in some members; nonetheless it was deemed appropriate to apply the procedure anyway, to be able to compare its results with those from other procedures.

The performance requirement selected for the assessment of the building was "life safety", which is the standard requirement for buildings. The corresponding seismic action was the Eurocode 8 type spectrum for soil B with a PGA equal to 0.16g, which is the full seismic action currently used for the design of new buildings in seismic zone II of Greece.

Regarding the so-called "knowledge factor", reflecting the degree of uncertainty involved in the assumed values of structural properties (geometry, material strengths, reinforcement areas and placement), both values prescribed in FEMA 273 and 356 (0.75 and 1.0) were used in the elastic analysis case; inelastic analysis is only permitted when the requirements for considering the knowledge factor equal to 1.0 are met.

In assessing the structure to the FEMA procedures all members were modelled assuming reduced effective values for the flexural rigidities (EI_{ef}), shear rigidities (GA_{ef}) and axial rigidities (EA_{ef}), depending on member type (beam, column, or wall) and the level of axial load and/or cracking, according to Table 6-4 in FEMA (1997a). This is cumbersome, as it is not known beforehand whether seismically loaded columns are under tension or compression and iterations may be required. At the second stage of this case study, wherein the FEMA 356-ASCE (2000) document was used, column stiffness depended only on axial stress under

Copyright fib, all rights reserved. This PDF copy of fib Bulletin 24 is intended for use and/or distribution only by National Member Groups of fib.

gravity loads, hence no iteration is needed. Flexural checks (with or without axial loading) were carried out on a deformation-control basis (using mean values of strengths), whereas shear checks in all members were carried out on a force-control basis (using characteristic values of strengths).

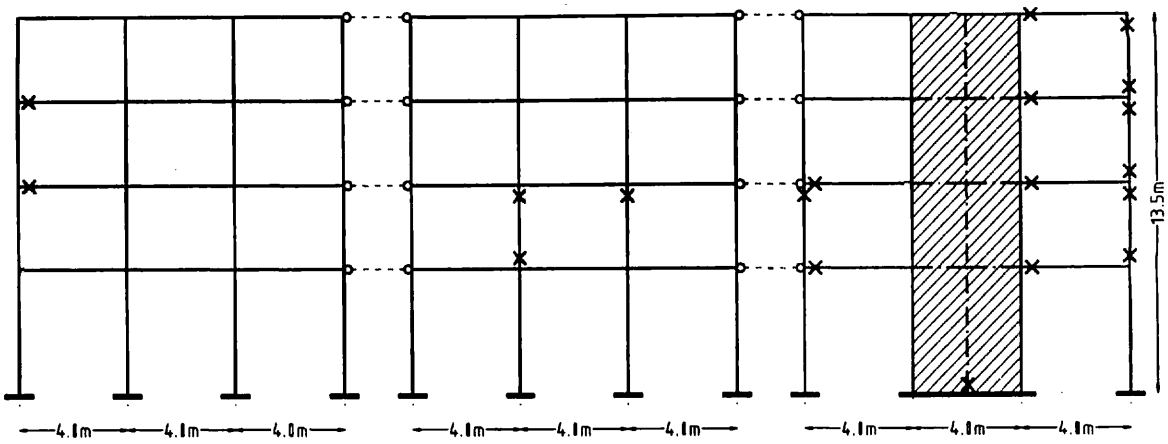

Fig. 7-73: Results of linear static procedure (loads applied from left to right): flexural checks

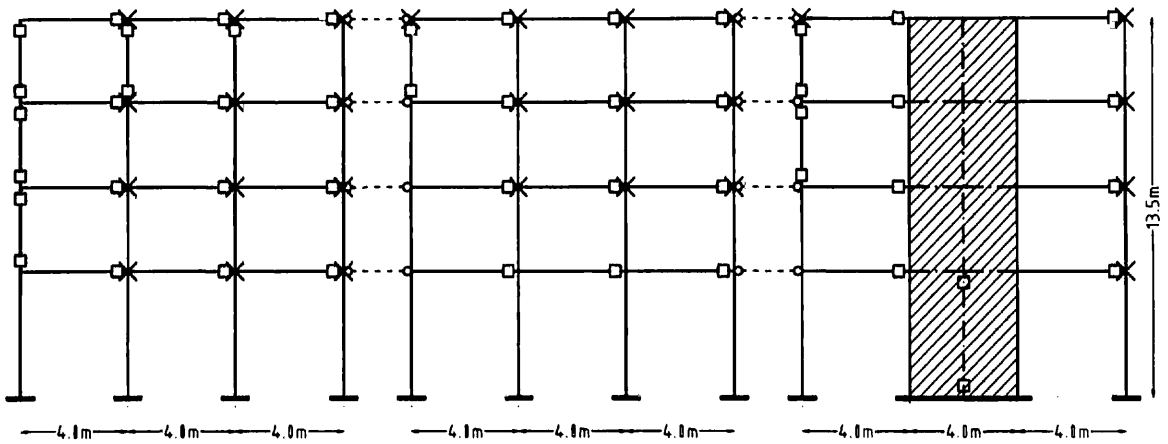

Fig. 7-74: Results of linear static procedure (loads applied from left to right): shear checks

7.6.3.2 FEMA 273 linear static procedure

The elastic base shear for the building is 40% of its service load (G+0.3Q), given that its fundamental natural period is 0.57 sec (calculated using the aforementioned effective rigidities). The base shear for elastic analysis using the FEMA formula involving the C_i coefficients results in a value of 46% the weight, due to the higher than unity coefficient C_2 accounting for the effect of stiffness degradation and strength deterioration on maximum displacement; the structure was classified as "framing type 1" for assessing this coefficient.

Bending moments in members were calculated by directly combining the elastic seismic moments with those from gravity loading (G+0.3Q), while shear and axial forces were calculated using limit analysis. Shears from this procedure were always higher (sometimes significantly so) than those resulting from the alternative procedure allowed by FEMA 273, wherein elastic seismic shears V_E are divided by the C_i factors prior to being combined with the gravity shears $V_{G+0.3Q}$.

Member strengths were estimated using the Eurocode 2 and 8 provisions. Flexural strengths were calculated on the basis of mean values of material strengths (f_{cm}=18.4 MPa, f_{ym}=1.25f_{yk}=525 MPa, following the FEMA recommendation), whereas shear strengths were calculated using characteristic strengths; the "concrete contribution" (V_c) within the plastic hinge zones of beams was taken as 30% of its value outside these zones. For comparison purposes, shear strengths were also calculated using the FEMA 273 equations (similar to

Copyright fib, all rights reserved. This PDF copy of fib Bulletin 24 is intended for use and/or distribution only by National Member Groups of fib.

those used in ACI 318); it is noted that in this case the concrete contribution is conservatively taken equal to 0 whenever the shear demand exceeds twice the value of the shear force under gravity loading. It was found that when V_c=0 in the FEMA equation, the shear strength calculated on the basis of Eurocodes was slightly higher, whereas when V_c>0 the FEMA shear strength was substantially higher. Shear strengths of beam-column joints was assessed using the shear stress limits in FEMA.

The results of flexural checks in the case of a knowledge factor equal to 1.0 are summarised in Fig. 7-73; violation of the acceptance criterion is denoted by an "x" at the corresponding member end. Several violations are detected, particularly in the dual system; violations are recorded in all types of members (beams, columns, wall). Many more failures were detected in the case that a knowledge factor equal to 0.75 was assumed.

The results of the shear checks for knowledge factor equal to 1.0 case are summarised in Fig. 7-74; violation of the acceptance criterion is denoted by an open square at the corresponding column end and by an "x" at the corresponding joint (when a joint failure is predicted). Numerous failures are predicted in all types of members, including beam-column joints. In columns, shear failures were predicted only where axial loading was reduced due to the seismic action (left columns in Fig. 7-74). Again, many more failures were detected in the case of knowledge factor equal to 0.75.

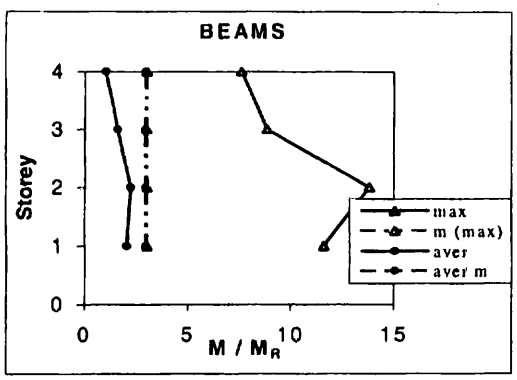

(a)

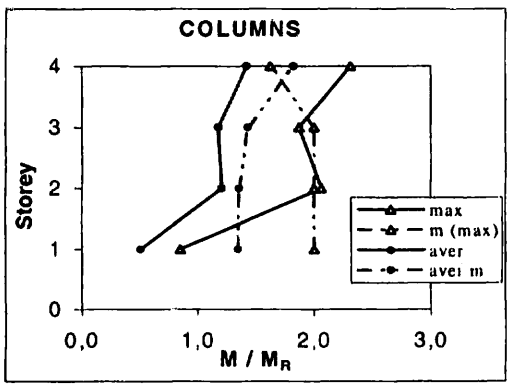

(b)

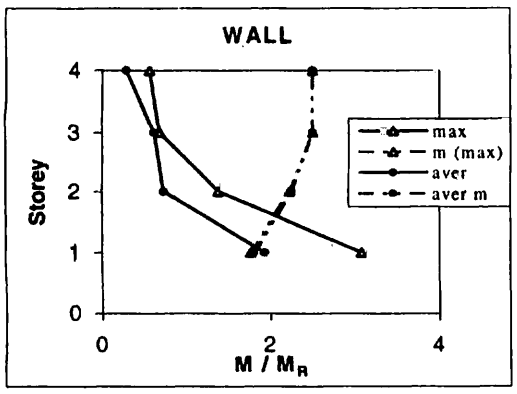

(c)

Fig. 7-75: Flexural checks at each storey, based on linear elastic analysis according to FEMA 273.

Copyright fib, all rights reserved. This PDF copy of fib Bulletin 24 is intended for use and/or distribution only by National Member Groups of fib.

The amount by which flexural criteria are violated or not can be seen in Fig. 7-75, where the ratios of required to available flexural capacity (M/M_R) are plotted for beams, columns and walls, along with the corresponding m-factors (allowable values of the previous ratios, see Tables 3-1 to 3-3). Both maximum and average (over the storey) values are indicated in *all* cases, to provide a clearer picture of the demands. While on average the ratios do not exceed the corresponding m-values (the only exception being the wall base where there is a slight violation), maximum values can exceed the allowable m, significantly in some cases. Values up to about 13 are recorded in some beams, whereas in columns and walls the ratios are generally less than about 3. As is common in dual systems, demand in walls is higher at the base, whereas maximum column demands occur in the upper storeys. Based on the results of Fig. 7-75, the condition of demand to capacity ratio less than 2 imposed by FEMA 273 with regard to the applicability of the linear procedures is clearly not met by the structure; it is noted that such a requirement would preclude the use of linear procedures in most if not all dual systems, wherein beam-to-wall connections tend to attract relatively high seismic actions (and plastic hinges form early in the response). Even higher demand to capacity ratios are recorded when a knowledge factor of 0.75 applies.

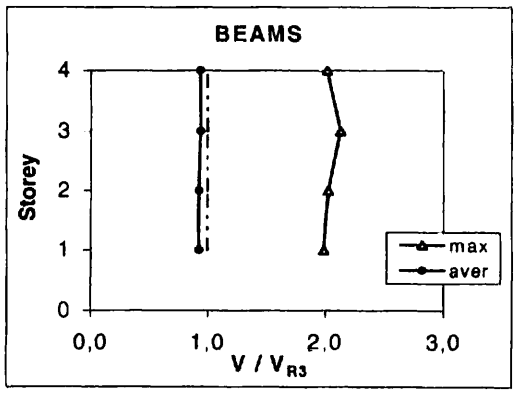

(a)

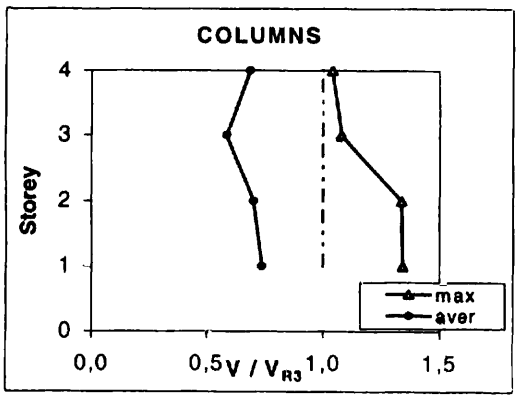

(b)

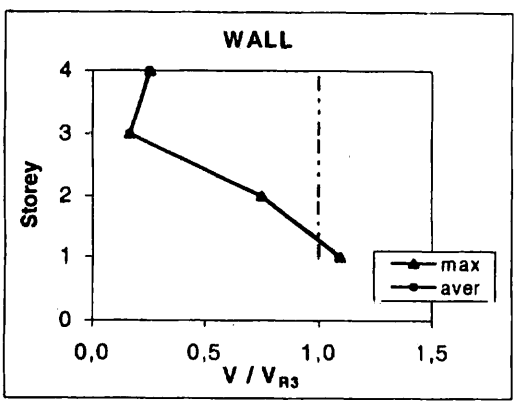

(c)

Fig. 7-76: Shear checks at each storey, based on linear elastic analysis according to FEMA 273.

Copyright fib, all rights reserved. This PDF copy of fib Bulletin 24 is intended for use and/or distribution only by National Member Groups of fib.

The amount by which shear criteria are violated or not can be seen in Fig. 7-76, where the ratios of required to available flexural capacity (V/V_R) are plotted for beams, columns and walls. The acceptance criterion is not met whenever the ratio exceeds 1.0 (force-controlled check). Again, while on average the V/V_R ratios do not exceed 1.0 (the only exception being the wall base where there is a slight violation), maximum values can exceed unity, significantly in the case of beams.

On the basis of the results presented herein, the FEMA 273 linear static procedure suggests that the structure does not satisfy the selected performance criteria and retrofit is required, mainly with respect to shear capacity, but also with respect to flexural capacity of some members. It is noted that no recourse was made here to the possibility of classifying some members as "secondary", for which less strict performance criteria apply.

7.6.3.3 FEMA 273 nonlinear (pushover) procedure

For practical application of pushover-based assessment two options are available on the modelling side, namely:

- lumped plasticity (point hinge) models;
- distributed plasticity models, using various assumptions regarding the spread of inelasticity along the member.

Both approaches were used in the present study. The pushover procedure prescribed by the FEMA (1997) recommendations was first applied using the distributed plasticity model of IDARC (Valles et al. 1996) that assumes linear variation of the member flexibility between the end sections and the zero moment point. The effective rigidity of the end sections is calculated from the corresponding moment (M) – curvature (φ) diagrams. These diagrams were found both from rigorous analysis (fibre models) and on the basis of the plastic deformation values given in FEMA 273 as a function of the shear stress, the reinforcement ratio, and the axial loading (in columns/walls). Since the FEMA values are for plastic rotations, the corresponding plastic curvatures were derived using the standard equivalent plastic hinge length approach (as described in Penelis and Kappos, 1997). The M-φ hysteresis model has a trilinear envelope and follows (in time-history analysis) the refined hysteresis rules described in Valles et al. (1996). For the purposes of this study, the trilinear envelope was reduced to a bilinear one, as required by FEMA 273. The IDARC model ignores the effect of axial load on the yield moment, hence a number of iterations (i.e. a number of pushover analyses) were required to derive the axial loads on the basis of which the M-φ curves of vertical members were defined. Column axial loads under combined gravity and seismic loading are generally not constant; so for defining appropriate yield moment values the axial loads at the stage when the structure reaches the target displacement were considered.

Member strengths were generally based on the amount of reinforcement provided in each critical section (with due allowance for slab reinforcement); an additional assessment was carried out wherein the effect of inadequate anchorage of beam bars at the bottom of end supports (a rather common feature in old buildings) was modelled by considering half the corresponding ("positive") yield moment.

The target displacement $\square_t$ for the pushover analysis was calculated using the so-called "coefficient method" prescribed in FEMA 273. This is not necessarily the most accurate method for predicting the target displacement and other methods, particularly those based on inelastic spectra, might be more appropriate (Kappos & Petranis, 2001). However, since the goal was to apply the FEMA procedure along with other proposals, it was deemed appropriate to use the FEMA method. Then for the EC8 Soil B spectrum for 0.16g, a target displacement of 45 mm was estimated.

Different patterns of the lateral load were used, as required by FEMA 273 (1997); one was the "triangular" one, and the other the "uniform" one. Fig. 7-77 shows the corresponding pushover curves; as expected, the uniform distribution gives a higher prediction of the structure's strength (due to delayed yielding in the lower storeys, compared to the triangular distribution). Also shown in the figure is the curve resulting from the assumption of reduced yield moments at the bottom of end supports due to inadequate anchorage. The effect on strength is very minor, while there is a small increase in the ductility of the structure due to lower reinforcement ratios and shear stresses in the beams. In all curves the point where a clear reduction in stiffness is detected corresponds to yielding at the wall base.

Copyright fib, all rights reserved. This PDF copy of fib Bulletin 24 is intended for use and/or distribution only by National Member Groups of fib.

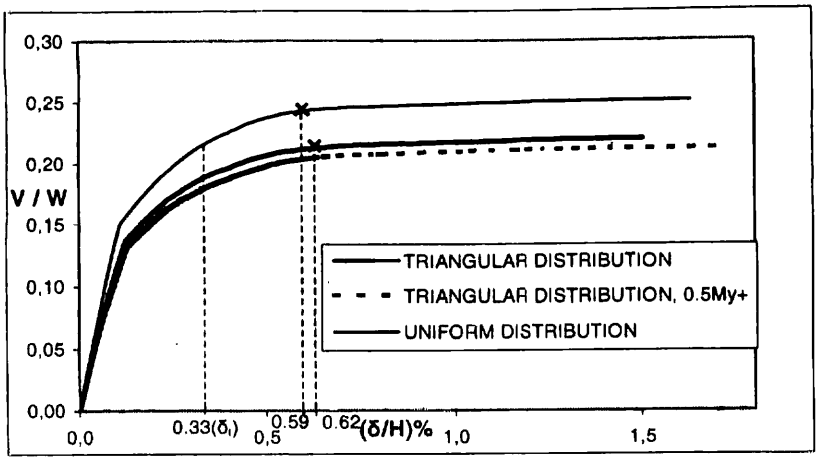

Fig. 7-77: Base shear vs. top displacement diagrams from pushover method (FEMA 273)

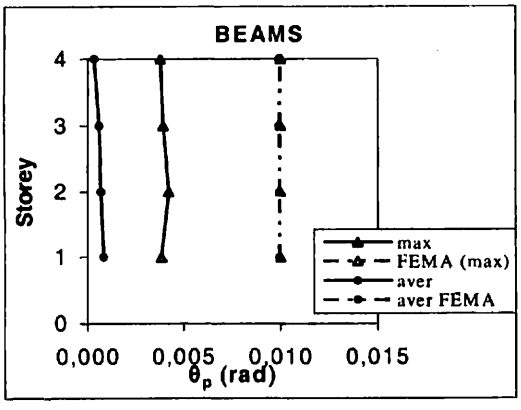

(a)

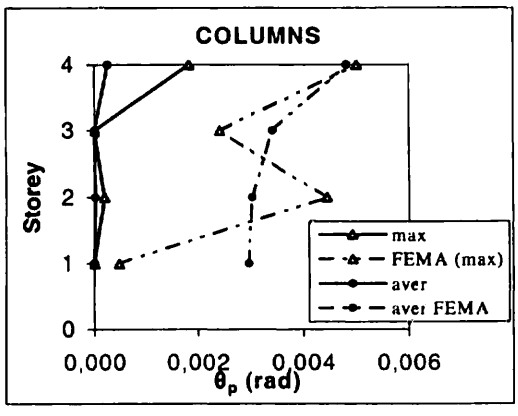

(b)

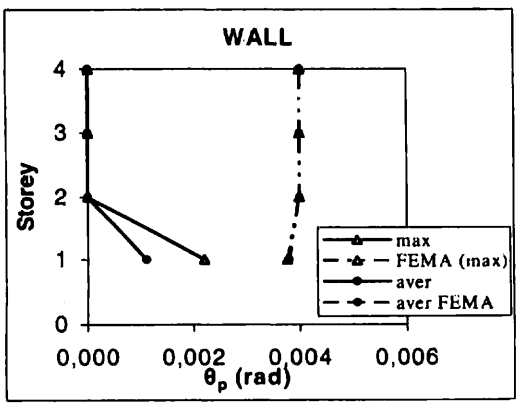

(c)

Fig. 7-78: Flexural checks at each storey from pushover method according to FEMA 273 (triangular loading)

Copyright fib, all rights reserved. This PDF copy of fib Bulletin 24 is intended for use and/or distribution only by National Member Groups of fib.

As shown in Fig. 7-77, the target displacement (corresponding to a top drift of 0.33%) is very close to the apparent "global yield" of the building, while the point where failure of the wall base is indicated by the analysis corresponds to a top drift of $\delta/H \approx 0.6\%$, about twice the target displacement. IDARC does not directly model member failure, hence the pushover curve continues up to the displacement specified with the input, but subsequent to wall failure the response of the structure is clearly not conservatively predicted (actually further member 'failures' occur after the 0.6% drift level).

Checking of the flexural capacity of RC members revealed that all plastic rotations were within the limits specified in the FEMA 273 tables for primary members at the life safety performance level. Plastic hinges formed mainly in the beams and also at the wall base and a few columns in upper storeys. Figure 7-78 shows the required (full lines) and the available (dotted lines) plastic rotations (max values and storey average) for each member type. It is seen that the most critical case is at the base of the ground storey wall. The available θ_p of the ground storey columns is very small (due to high axial stress), but at the target displacement considered there is no yielding of these elements. Similar results were found in all cases shown in Fig. 7-77. It is worth mentioning that when half the positive moment capacity was assumed at beam ends, plastic rotation demands were higher there, but still within allowable limits (which were slightly higher than in the full M_y^+ case).

Fig. 7-79 summarises shear checks for the building (for the triangular distribution of loading), which is again a force-based approach, only that this time shear forces are calculated from the analysis, rather than from "capacity design" (limit analysis). An open square indicates violation of shear criteria in a member, while "x" indicates violation in a beam-column joint. Both types of violations are recorded, but to a much lesser extent than for linear analysis (cf. Figure 7-74). Most violations occur in the beams and joints of the dual system. Similar results were obtained for the uniform distribution of loading, while for half the positive moment capacity at the beam ends, less violations were found due to lower shears developed.

The results from the pushover-based procedure show a more optimistic picture of the structure's ability to meet the selected performance criteria. Given that the FEMA deformation limits are generally on the conservative side for "non-conforming" (i.e. low ductility) members, it appears that the linear procedure underestimates the flexural capacity of the members and indicates inadequacies where they actually do not exist, as shown by the nonlinear method. As far as shear is concerned, the only difference between the linear and the nonlinear procedure is the way maximum shears are estimated. The advantage offered by the latter method (pushover analysis) is that shear demands are typically lower than those resulting from limit analysis, which is the recommended option in the linear approach (the formulas based on the C_i-based modification of V_E lack adequate verification and are not recommended). The combination of a force-based approach for shear with the use of lower estimates of material properties appears to be rather conservative and suggests a need for shear strengthening of several members (mostly of beams) in the building.

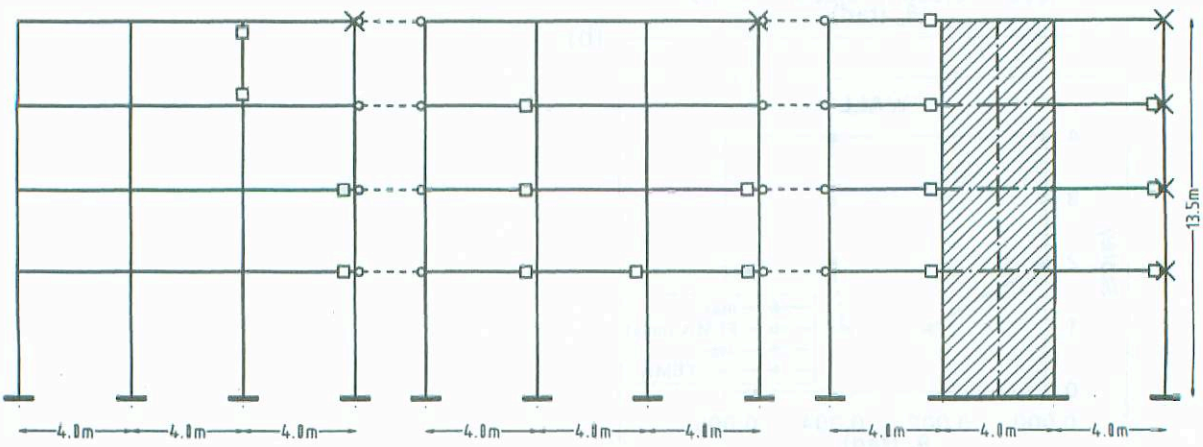

Fig. 7-79: Results of nonlinear static procedure according to FEMA 273 ("triangular" loading): shear checks

Copyright fib, all rights reserved. This PDF copy of fib Bulletin 24 is intended for use and/or distribution only by National Member Groups of fib.

On a more specific issue, consideration of inadequate anchorage of bottom bars at beam supports did not indicate a consistently worse behaviour of the building, since the increased positive rotation demands were still within the allowable limits, whereas lower shears in this case led to a more favourable behaviour with respect to shear capacity. In fact, the low reinforcement ratios in all members (typical in Greek buildings, particularly the old ones), had a generally favourable effect on both the plastic rotation and shear capacities.

Last and not least the importance of the presence of a relatively large R/C wall has to be pointed out. This was the main reason why the fundamental period of the building remained rather low (0.57 sec) even though cracking of members was accounted for, and led to a small target displacement.

7.5.3.4 Selected results from assessment based on FEMA 356/ASCE(2000) procedures

The 4-storey building assessed based on the FEMA 273/4 linear or nonlinear static procedures was then re-assessed using the ASCE (2000) Prestandard for Seismic Rehabilitation, also known as FEMA 356. The two documents are generally similar and the results of the assessment were also similar. Hence, only some key points where differences are worth pointing out will be discussed hereunder.

The modelling approach used in this part of the study was based on lumped plasticity models, as implemented in the SAP2000 Nonlinear code (Computers & Structures Inc., 1999). This approach is indeed favoured in the FEMA procedures, which directly refer to plastic hinge rotations rather than to other, more local, quantities like curvatures or strains. The advantage of the SAP model over that used in IDARC is that it accounts explicitly for the difference between the initial and the residual strength of a member and also that interaction curves (M_y-N) can be introduced for the yield moments of column elements. On the other hand, the point-hinge formulation is less accurate than the distributed plasticity one and the hysteresis rules (in time-history analysis) are simple elastoplastic ones. Moreover, the M-θ_{pl} curves specified for each plastic hinge are based on rough estimates of both the strength and rotation parameters. Indeed, in SAP2000 flexural strengths are calculated to ACI 318 procedures, instead of the actual bending moments, hardening ratios are not explicitly defined, and (importantly) default plastic rotation capacities are average values from the FEMA Tables, not directly related to the actual shear and axial stress present in the member.

To overcome the aforementioned limitations, full fibre model analyses of all critical sections were carried out and their results were used for defining the M-θ curves at each potential plastic hinge. The plastic hinge length used for translating the plastic curvatures into rotations was calculated using two alternative proposals, that by Priestley (1997) and that by Panagiotakos & Fardis (2001). It was found that the second procedure resulted in lengths that were in the case of beams up to 12% higher than those from the former, while for columns differences were between –7% and 4%. In addition (for comparison purposes) the θ_{pl} values from the ASCE (2000) tables, corresponding to the shear and axial stresses at the level of the target displacement determined for each member from preliminary pushover analyses were also used.

A further difference between the FEMA 273 and FEMA 356/ASCE (2000) procedures is that, for linear methods, the coefficient C_2 is taken equal to unity, resulting in a 10% lower base shear in the ASCE linear procedure. Moreover, the introduction of the "effective mass factor" C_m leads to a further reduction in the calculated base shear (C_m=0.8 was assumed for the building, due to the presence of the relatively large R/C wall). The combination of the previous factors resulted in a base shear equal to 34% the service load, compared to 46% in the case of FEMA 273. This is a clear indication that for a broad class of buildings the linear procedures of the ASCE (2000) Prestandard will offer a less conservative assessment than the corresponding FEMA 273 procedures.

Regarding strength evaluation, the FEMA 273 and 356 procedures are generally similar. A minor difference is that in the latter "lower bound" material strength f_{LB} is clearly defined as that based on the mean minus one standard deviation value, and can be calculated assuming that $f_{LB}=f_m/1.5$. This mainly affected the shear strength calculation wherein a lower bound concrete strength of 12.3 MPa was used in the ASCE/FEMA 356 method, compared to the value of 10.4 MPa (estimated lower 5% characteristic strength) used in the FEMA 273 method. In both methods the same values of 220 MPa for the yield strength of ties and of 525 MPa ($1.25f_{yk}$) for the longitudinal steel bars were used.

Copyright fib, all rights reserved. This PDF copy of fib Bulletin 24 is intended for use and/or distribution only by National Member Groups of fib.

As a result of the above differences, less shear criteria violations were recorded using the Prestandard procedure, particularly in the exterior frame (left of Fig. 7-72). However, for a knowledge factor equal to 0.75 most of the members were predicted to fail in shear. Flexural check results for beams and the wall were similar to those depicted in Fig. 7-73, but no column failure was predicted according to the ASCE (2000) Prestandard.

Fig. 7-80 depicts the V/W vs. δ/H curves calculated from pushover analysis for different load distributions (uniform, triangular) and different assumptions regarding the estimation of the strength and rotational capacity of R/C members ('refined', i.e. from fibre model analysis and 'FEMA' based on the ASCE-FEMA 356 tables). There is a difference in the predicted strength, depending on the loading profile used, the uniform loading resulting in a higher strength and initial stiffness than the triangular one. The two methods for modelling the M-θ characteristics lead to differences only in the post-yield range, the FEMA procedure resulting in higher global strength increase, mainly due to the different way strain-hardening was modelled in each case. The ultimate deformation predicted by each method is generally similar (about 0.6%), the FEMA values leading to higher predicted top drift in the triangular loading case. These predictions are very close to the values in Fig. 7-77, calculated using the distributed plasticity model and the FEMA 273 assumptions, despite the different inelastic model used in each case (different way axial loading is accounted for, different numerical procedure used by IDARC and SAP). With respect to strength, the analyses summarised in Fig. 7-80 predict a somewhat smaller apparent yield strength than in Fig. 7-77, mainly due to differences in the assumption on slab reinforcement contributing to the negative yield strength of beams, and in the way the wall web reinforcement was modelled to calculate the corresponding strength. Despite these differences, the two sets of analyses predict similar ultimate strengths (about 0.25W for uniform loading, about 0.21W for triangular loading).

Assessment based on the pushover curves of Fig. 7-80 and the FEMA 356 recommendations led to essentially the same conclusions as when FEMA 273 was used (Figs. 7-78, 7-79). No flexural failures were predicted (the most critical check was at the wall base), but there were some violations of shear strength criteria in beams and joints, particularly in the dual system.

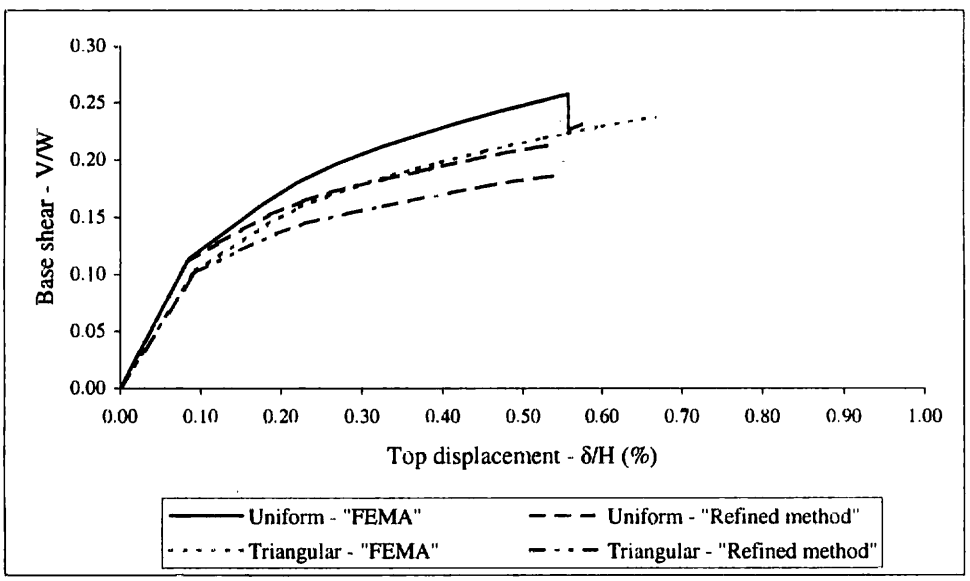

Fig. 7-80: Base shear vs. top displacement diagrams from pushover method (FEMA 356)

7.6.4 Displacement-based assessment according to the NZ draft guidelines and Priestley (1997)

The NZ draft guidelines displacement-based procedure was applied as recommended by Priestley (1997), with minor adjustments, as noted in the following. Material strengths used in the first part of the procedure (involving the evaluation of flexural and shear strengths) were determined as $1.1f_{yk}$ for steel and $1.5f_{ck}$ for concrete, assuming that 'nominal' and 'characteristic' strengths are identical. The resulting values were 460 and 18 MPa,

Copyright fib, all rights reserved. This PDF copy of fib Bulletin 24 is intended for use and/or distribution only by National Member Groups of fib.

respectively; the former is less than the value (525 MPa) used in the FEMA procedures, while the latter is practically the same.

Full moment-curvature analyses were carried out for all critical sections of R/C members, wherefrom both strength and ductility of members was calculated. Flexural strength was taken to correspond to either ε_c=0.004 (rather than 0.005) in the compressed concrete, or ε_s=0.02 in the tension steel. Shear strength was calculated using the Priestley model:

$$V_n = V_c + V_s + V_p \tag{7-9}$$

where

$$V_c = 0.8A_{gross}\,k\sqrt{f_{ca}} \quad \text{(shear carried by concrete, k decreases with curvature ductility)}$$

$$V_s = \frac{A_v f_{yh}(h-c)}{s}\cot\theta \quad \text{(shear carried by ties)}$$

$$V_p = N \tan a \quad \text{(shear carried by axial loading)}$$

The V_n value calculated as above was reduced on the basis of the ¾ factor recommended by Priestley (1997) when shear strength is compared with shear at flexural strength of columns.

Shear strength of beam-column joints was calculated using the procedure based on the principal stresses developed in the joint, calculated as a function of the axial stress (σ_a) and the joint shear stress (v_j) from

$$\sigma_1 = \frac{\sigma_a}{2} \pm \sqrt{\left(\frac{\sigma_a}{2}\right)^2 + v_j^2} \tag{7-10}$$

In sub-standard joints (no shear reinforcement), when the tensile stress σ_1 exceeds $0.29\sqrt{f_{ca}}$ (where $f_{ca}=1.5f_{ck}$) joint diagonal cracking is expected to develop and the requirement for avoiding shear failure is that the compression stress σ_2 does not exceed $0.45f_{ca}$ (for two-way joints). However, even when the latter limit is not exceeded, joint shear strength decreases with the plastic drift; Priestley (1997) suggests that deterioration starts at about storey 1% drift and joint shear reduces to 50% its initial value at 5% drift.

For the joint shear v_j, the most unfavourable situation was considered, assuming that both the top and bottom bars developed their flexural overstrength ($\gamma_n f_{ya}$) with γ_n=1.25, and accounting for slab reinforcement when calculating the negative flexural capacity, hence

$$V_{jh} = (A_{s1}+A_{s2})\gamma_n f_{ya} - V_{col} \tag{7-11}$$

where A_{s1} includes slab reinforcement present within 900 mm on each side of a web. This is an overestimation of V_{jh}, particularly when ductility requirements are low. It is also pointed out that due to inadequate anchorage within the joint, some of the bars (particularly the bottom ones) will not develop their full yield strength (see $0.5M_y^+$ scenario in the previous section). A further issue is that use of $\sigma_2=0.29\sqrt{f_{ca}}$ at exterior joints corresponds to the worst case scenario for bar anchorage (beam bars bent outwards with respect to the joint). In typical old buildings in Greece beam bars at exterior joints are neither bent upwards nor downwards, they just terminate with straight (short) anchorage lengths. In old construction in Italy or Portugal such bars are indeed bent inwards.

On the basis of the aforementioned strengths, the 'sway potential index' may be calculated as:

$$S_p = \frac{\sum_{i=1}^{j}\left(\Sigma M_{(Bn,i)}\right)}{\sum_{i=1}^{j}\left(\Sigma M_{(Cn,i)}\right)} \tag{7-12}$$

Copyright fib, all rights reserved. This PDF copy of fib Bulletin 24 is intended for use and/or distribution only by National Member Groups of fib.

where the numerator represents the sum of the beam flexural strengths and the denominator the sum of the column strengths at a storey. The values of S_p for the structures studied varies from 0.24 at the ground storey to 0.48 at the top storey, i.e. well below the limit of 85% defining the development of a beam mechanism. The reason for the low values is the presence of the 4 m wall that contributes between 70% and 87% of the total strength of vertical members. The low values of the sway potential index should not be interpreted as an indication that plastic hinging is expected exclusively in the beams. A check of relative beam and column strength at each joint of the building gave a prediction of the plastic mechanism as shown in Fig. 7-81. Quite a few column hinges appear, but due to the presence of the wall no column sway mechanism forms. On the basis of the aforementioned plastic mechanism the corresponding ultimate base shear V_b is estimated at 1650 kN.

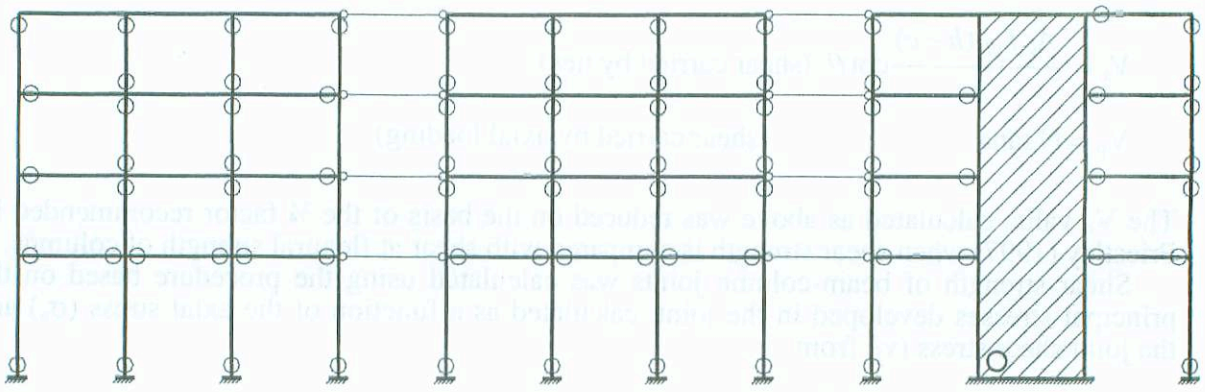

Fig. 7-81: Predicted plastic mechanism based on relative strength at each joint

Section	μ_φ	k	V_c	V_s	V_p	V_n	$0.75V_n$	V_{req}	avail/req
1	7.26	0.050	15.21	112.80	0.00	128.00	96.00	81.50	1.18
2	7.15	0.050	15.21	111.40	0.00	126.61	94.96	84.49	1.12
3	7.05	0.050	15.21	108.87	0.00	124.08	93.06	86.70	1.07
4	7.21	0.050	15.21	106.68	0.00	121.89	91.42	104.39	0.88
5	7.10	0.050	15.21	110.30	0.00	125.51	94.13	96.47	0.98
6	3.78	0.171	51.97	92.98	0.00	144.95	108.71	142.41	0.76
7	3.63	0.176	53.66	92.14	0.00	145.79	109.34	144.29	0.76
8	3.44	0.183	55.80	90.87	0.00	146.67	110.00	157.07	0.70

Table 7-7: Critical shear verifications for beams

The next step is the estimation of the plastic rotation capacity of members and the corresponding displacement of the structure. It was found that, in this respect, the most critical members were the wall and the interior columns of the middle frame (second frame in Fig. 7-81) due to their high axial stress. The plastic rotation θ_p at the wall base (using the ε_c=0.004 criterion) was found to be 0.0042 rad, with a corresponding displacement at the equivalent height (h_{eq}=0.75h_n for dual systems) Δ_p=42 mm. The yield displacement was estimated to be 39 mm, based on an assumed storey drift at yield equal to $2/3\varepsilon_y h_{eq}/l_w$ (where l_w is the length of the wall). The total displacement (at h_{eq}) is then Δ_u=81 mm, and the displacement ductility factor μ=2. Displacement capacities based on column deformability were slightly lower, hence the values resulting from the wall capacity were subsequently used.

The development of the available ductility may be prevented by the shear capacity of members that, as indicated in eq. (7-9), is a function of curvature ductility. Table 7-7 shows the most critical shear verifications, those referring to the beams; the curvature ductility ratios in the second column of the table are the maximum ones (for negative bending). Sections 1 to 3 (left frame in Fig. 7-81) can develop their full flexural ductility, whereas for sections 4 and 5 (middle frame) the ductility ratios are limited (to 5.5 and 6.5, respectively) because shear

Copyright fib, all rights reserved. This PDF copy of fib Bulletin 24 is intended for use and/or distribution only by National Member Groups of fib.

failure precedes the development of full ductility capacity. This causes no real problem since the estimated ductility requirements for these beams at the target displacement are below the reduced values. Sections 6 to 8 corresponding to the ends of the beams that frame into the wall in the dual structure (right of Fig. 7-81) are clearly prone to shear failure since they can not resist the shear demand even if μ_φ does not exceed one (the max value of k in equation 2 is 0.2 for beams). On the other hand, all vertical members (columns, wall) were found to be able to develop their full flexural ductility; it is noted that a major contributor to their shear strength was the axial load component (V_p), which is zero in the case of beams.

It is seen that, as in the other assessment procedures, shear capacity of beams leads to violations of acceptance criteria, the difference being that the model used in the NZ displacement-based assessment leads to less shear failures being predicted than in the FEMA procedures. In the case of beam-column joints, principal stress checks (eq. 7-10) show that cracking will occur in all joints ($\sigma_1>0.29\sqrt{f_{ca}}$), but compression stress σ_2 generally remains below the $0.45f_{ca}$ limit, even when a further reduction factor of 0.75 is applied. The exceptions were the interior joints of the middle frame, where the reduced limit ($0.34f_{ca}$) was exceeded; at the 2nd storey the stress was higher than the full value of the limit ($0.45f_{ca}$). Joint shear strength criteria were satisfied in all exterior joints (contrary to what was found in the FEMA procedure summarised in Fig. 7-79).

The equivalent damping corresponding to μ=2 and a beam mechanism is 26% (Priestley 1997), while for a column mechanism it is 15%; based on the hybrid mechanism shown in Fig. 7-81, which is closer to the beam type, a ratio of 23% was assumed. However, to account for possible premature shear failure of beams in the dual system (right end of Fig. 7-81) and some predicted joint failures in the middle frame that reduces the energy dissipation capacity of the beams (without causing a complete joint sidesway mechanism), a further reduction of 30% in hysteretic damping was deemed necessary; a value of 18% was finally assumed.

The effective period of the structure can be determined from the secant stiffness at the ultimate displacement, $K_{eff}=V_b/\Delta_u$=1650/0.081=20370 kN/m; taking the effective mass as $m_{eff}=0.85M_{tot}$ (SEAOC 1999), the effective period is 1.03 sec (quite longer than the 'elastic' effective period of 0.57 sec used in the FEMA procedures in the previous section).

The response spectrum used was that of EC8 soil B and a PGA of 0.16g; the resulting displacement spectrum for 18% damping is shown in Figure 7-82, and it is seen that the displacement corresponding to an effective period of 1 sec is 33 mm, well below the ultimate displacement of 81 mm, calculated on the basis of the plastic mechanism. It is concluded that the structure will be able to reach the target displacement, however shear failure of the beams framing into the wall will occur at this stage.

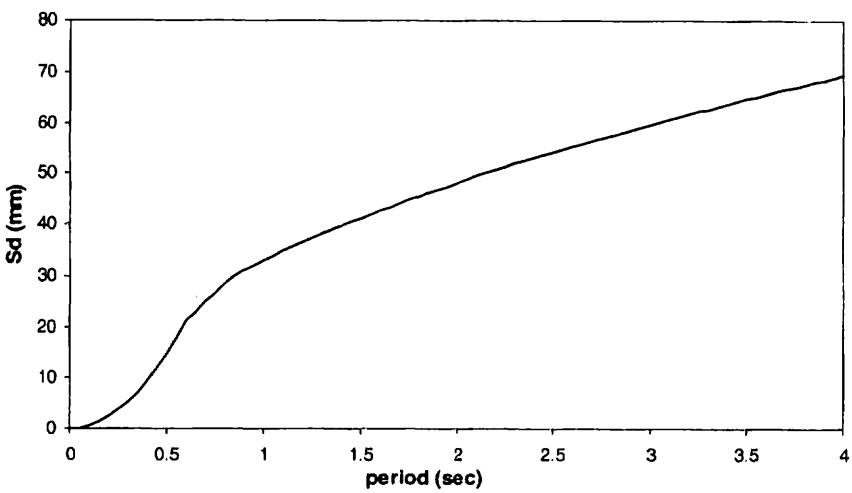

Fig. 7-82: Displacement spectrum for ξ=18%, corresponding to the EC8-B spectrum for 0.16g

7.6.5 Selected results from time-history analysis

The four-storey structure was also analysed for a large number of input accelerograms typical of the site conditions in two Greek cities, Thessaloniki and Volos. A few selected

Copyright fib, all rights reserved. This PDF copy of fib Bulletin 24 is intended for use and/or distribution only by National Member Groups of fib.

results are presented herein; more details can be found in Kappos et al. (2002).

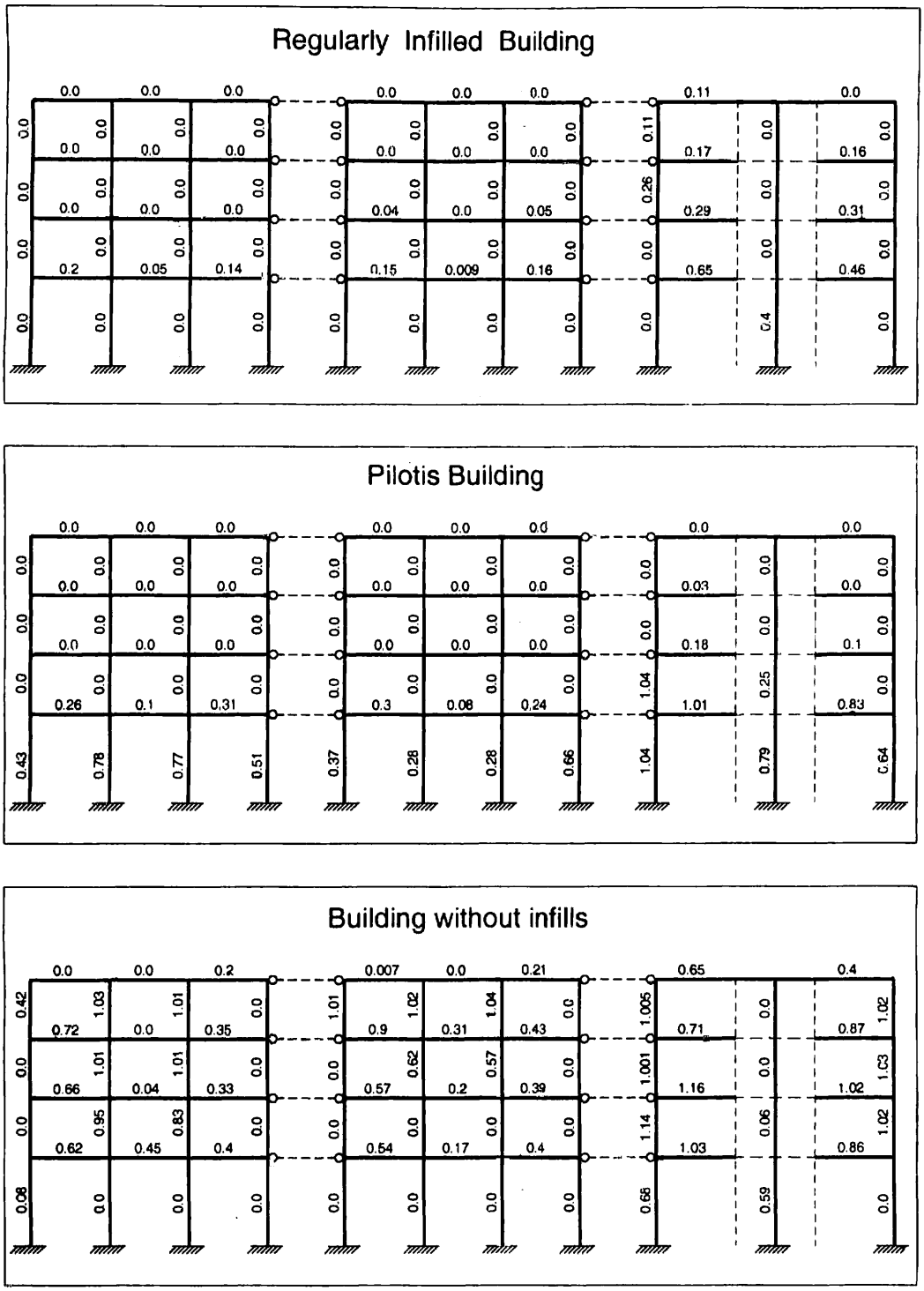

Fig. 7-83: Calculated ratios of required to available plastic rotation for 4-storey 'old' R/C building in an alluvia site with PGA=0.17g.

Fig. 7-83 summarises the ratios of required to available plastic rotation (from fibre model analysis) for all members, when subjected to the most critical motion (alluvia site, with a PGA=0.17g), which for practical purposes can be deemed as representative of the seismic action used in the previous assessments (Sections 7.6.3 and 7.6.4). In addition to the bare structure analysed in the previous studies, two more versions were considered in the time-history analyses, characterised by different arrangements of masonry infill panels along the

Copyright fib, all rights reserved. This PDF copy of fib Bulletin 24 is intended for use and/or distribution only by National Member Groups of fib.

height of the building (regular and irregular, i.e. creating a soft ground storey). Masonry infills were modelled using the refined inelastic panel element developed by Kappos et al. (1998), based on cyclic test results on masonry-infilled R/C frames.

Some differences as well as some similarities with the pushover-based assessment can be noted from the results in Fig. 7-83. The main similarity is that the most critical part of the building is found to be the dual system, where the highest ductility demands were recorded in both the pushover and time-history analyses; the beams framing into the wall are identified as critical elements by both procedures. However, as shown in the bottom part of Fig. 7-83 (which depicts the case of the bare structure, i.e. the one directly comparable to the previous assessments) the end columns of the dual structure are also critical members, with potentially inadequate ductility (ratios up to 1.14), whereas at the wall base the demand to capacity ratio is well below 1.0. In fact, an interesting difference between the pushover and the time-history procedures is that the latter predicts higher demands at the upper storeys of the structure, a conclusion supported also by other studies (e.g. Kappos & Petranis 2001).Still referring to Fig. 7-83, some notable differences between the bare, infilled and pilotis (soft-storey) structure should be noted. The irregularity in the latter renders the ground storey members the critical ones, with failure predicted for some of them, whereas the demands are low along the entire height of the regularly infilled structure. These and other (Kappos et al. 1998) results clearly point to the need to account for the effect of elements such as masonry infills in assessment, otherwise even refined procedures based on inelastic analysis may lead to unrealistic results that can be either overconservative or unconservative.

References

Albanesi, T. 2001. Metodi statici equivalenti per la valutazione della risposta sismica di strutture intelaiate in c.a.. Tesi di Dottorato di Ricerca, Università degli Studi "G. D'Annunzio" - Chieti.

Albanesi, T., Nuti, C. & Vanzi, I. 2000. A simplified procedure to assess the seismic response of nonlinear structures. Earthquake Spectra, Vol. 16, No. 4, pp. 715-734.

ASCE (American Society of Civil Engineers) 2000. Prestandard and commentary for the seismic retrofitting of buildings. Report No. FEMA-356, Washington DC, USA.

Applied Technology Council (ATC) 1996. Seismic evaluation and retrofit of concrete buildings. Report No. ATC-40, Redwood City, California, USA.

Applied Technology Council (ATC) 1997. NEHRP guidelines for the seismic retrofitting of buildings. Report No. FEMA-273, Washington, DC, USA.

Applied Technology Council. 1996. Seismic evaluation and retrofit of concrete buildings. Report ATC-40, Redwood City, California.

Brisighella, L. 1988. Behavior and analysis of R.C. structures under alternate actions including inelastic response. CEB Group, GTC/22, Roma, June,1988.

CEN Eurocode 8, 1994. Design Provision for Earthquake Resistance of Structures. *ENV* 1993-2, Comite European de Normalization, Brussels.

Computers and Structures Inc. 1999. SAP2000: Three dimensional static and dynamic finite element analysis and design of structures, Berkeley, California.

Fajfar, P. & Fischinger, M. 1988. N2 - a method for non-linear seismic analysis of regular buildings. Proc., 9th World Conf. on Earthquake Engrg., Tokyo-Kyoto, Japan, No. 5, pp. 111-116.

FEMA 1997a. NEHRP guidelines for the seismic rehabilitation of buildings. FEMA-273, Washington D.C.

FEMA 1997b. NEHRP commentary on the guidelines for the seismic rehabilitation of buildings. FEMA-274, Washington D.C.

Freeman, S.A. 1978. Prediction of response of concrete buildings to severe earthquake motion. Douglas McHenry International Symposium on Concrete and Concrete Structures, ACI SP-55, American Concrete Institute, Detroit, pp. 589-605.

Gasparini, D. 1976. SIMQKE: a program for artificial motion generation, user's manual and documentation. Technical Report, Dept. of Civil Engineering, M.I.T., Cambridge, Massachussets.

Copyright fib, all rights reserved. This PDF copy of fib Bulletin 24 is intended for use and/or distribution only by National Member Groups of fib.

Gülkan P, Sucuoglu H, Erberik MA, Akkar S. 1998. Dinar aftershock tests retrofitted buildings. EERI Newsletter; Vol. 32, No. 9, pp. 6-8.

Holmes, W.T. 2000. Risk assessment and retrofit of existing buildings. Proceedings, 12th World Conf. Earthquake Eng., Paper no. 2826, Auckland, New Zealand.

Kappos, A.J. and Petranis, C. 2001. Reliability of pushover analysis - based methods for seismic assessment of R/C buildings. Earthquake Resistant Engineering Structures III, WIT Press, pp. 407-416.

Kappos, A.J., Pitilakis, K.D., Morfidis, K. and Hatzinikolaou, N. 2002. Vulnerability and risk study of Volos (Greece) metropolitan area. 12th European Conference on Earthquake Engineering (London, UK, Sep. 2002), CD ROM Proceedings (Balkema), Paper 074.

Kappos, A.J., Stylianidis, K.C., and Michailidis, C.N. 1998. Analytical models for brick masonry infilled R/C frames under lateral loading. Journal of Earthquake Engineering, Vol. 2, No. 1, pp. 59-88.

Ministry of Public Works and Settlement, 1975, revised in 1997. Specifications for buildings constructed in disaster areas. Ankara, Turkey.

Miranda, E. & Bertero, V.V. 1994. Evaluation of strength reduction factors for earthquake-resistant design. Earthquake Spectra, Vol. 10, No. 2, pp. 357-379.

Miranda, E. 1993. Evaluation of site-dependent inelastic seismic design spectra. J. Struct. Engrg., ASCE, Vol. 119, No. 5, pp. 1319-1338.

Panagiotakos, T. B.; Fardis, M. N. 2001. Deformations of reinforced concrete members at yielding and ultimate. ACI Structural Journal, Vol. 98, No. 2, pp. 135-148.

Penelis G.G. and A.J. Kappos 1997. Earthquake-resistant Concrete Structures, E & FN SPON (Chapman & Hall): London.

Petrangeli, M., Pinto, P.E. & Ciampi, V.A. 1999. Fibre Element for cyclic bending and shear. Part I and II. Journal of Engineering Mechanics, ASCE, Vol. 125, No. 9, pp. 994-1009.

Prakash V, Powell GH, Campbell S. 1993. Drain-2DX base program description and user guide. SEMM Report No. 93/17, University of California, Berkeley, California, USA.

Priestley, M.J.N. 1997. Displacement-based seismic assessment of reinforced concrete buildings, Journal of Earthquake Engineering, Vol. 1, No. 1, pp. 157-192.

SEAOC Ad Hoc Committee 1999. Tentative Guidelines for Performance-based Seismic Engineering. App. I of: Recommended lateral force requirements and Commentary, SEAOC, Sacramento, Calif.

Seneviratna, G.D.P.K. & Krawinkler, H. 1996. Modification of seismic demands for MDOF systems. Proc., 11th World Conf. on Earthquake Engrg., Acapulco, Messico, Elsevier Science Ltd., Oxford, U.K., Paper No. 2129.

Sucuoglu H, Gür T, Gülkan P. 2000. The Adana-Ceyhan earthquake of 27 June 1998: seismic retrofit of 120 R/C buildings. 12th Word Conf. on Earthquake Eng., Auckland, NZ.

Sucuoglu H., McNiven HD. 1991. Seismic shear capacity of reinforced masonry piers. Journal of Struct. Eng. ASCE, Vol. 117, pp. 2166-2186.

Valles, R. E.; et al. 1996. IDARC2D version 4.0: a computer program for the inelastic damage analysis of buildings, Rep. NCEER-96-0010, State Univ. of New York at Buffalo.

Wasti T, Sucuoğlu H, Utku M. 2001. Seismic retrofitting of moderately damaged R/C buildings after the 1 October 1995 Dinar earthquake. Journal of Earthquake Engineering, Vol. 5, No. 2, pp. 131-151.

ISSN 1562-3610
ISBN 2-88394-064-9

Seismic assessment and retrofit of reinforced concrete buildings

Contents

1 Introduction
2 Performance objectives and system considerations
3 Review of seismic assessment procedures
4 Strength and deformation capacity of non-seismically detailed components
5 Seismic retrofitting techniques
6 Probabilistic concepts and methods
7 Case studies

fédération internationale du béton
the international federation for structural concrete
created from the merger of CEB and FIP